SEIZURE FORECASTING AND DETECTION: COMPUTATIONAL MODELS, MACHINE LEARNING, AND TRANSLATION INTO DEVICES

EDITED BY: Sharon Chiang, Vikram Rao, Gregory Worrell and Maxime O. Baud

PUBLISHED IN: Frontiers in Neurology

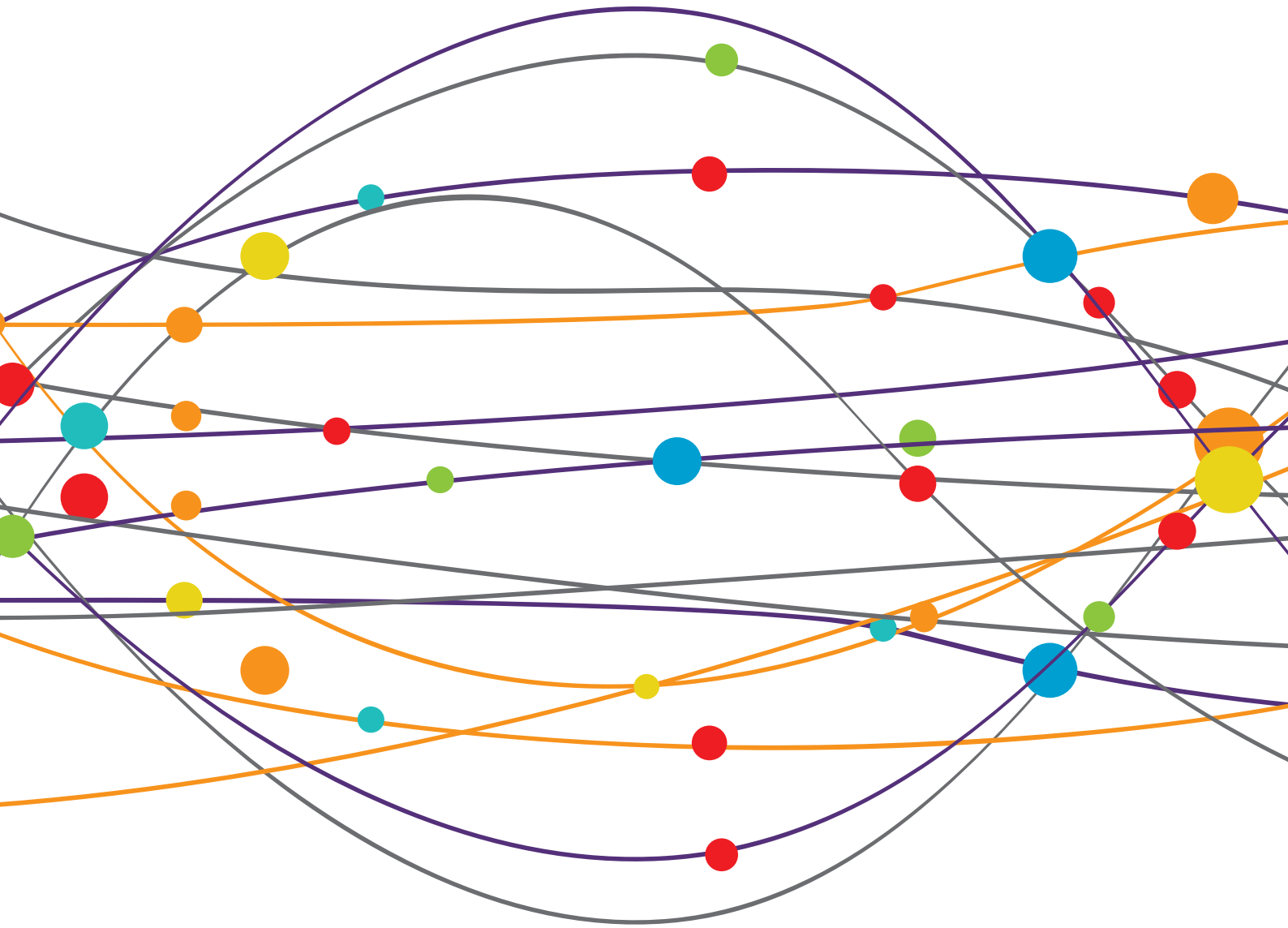

frontiers Research Topics

ISSN 1664-8714
ISBN 978-2-88974-872-3
DOI 10.3389/978-2-88974-872-3

About Frontiers

Frontiers is more than just an open-access publisher of scholarly articles: it is a pioneering approach to the world of academia, radically improving the way scholarly research is managed. The grand vision of Frontiers is a world where all people have an equal opportunity to seek, share and generate knowledge. Frontiers provides immediate and permanent online open access to all its publications, but this alone is not enough to realize our grand goals.

Frontiers Journal Series

The Frontiers Journal Series is a multi-tier and interdisciplinary set of open-access, online journals, promising a paradigm shift from the current review, selection and dissemination processes in academic publishing. All Frontiers journals are driven by researchers for researchers; therefore, they constitute a service to the scholarly community. At the same time, the Frontiers Journal Series operates on a revolutionary invention, the tiered publishing system, initially addressing specific communities of scholars, and gradually climbing up to broader public understanding, thus serving the interests of the lay society, too.

Dedication to Quality

Each Frontiers article is a landmark of the highest quality, thanks to genuinely collaborative interactions between authors and review editors, who include some of the world's best academicians. Research must be certified by peers before entering a stream of knowledge that may eventually reach the public - and shape society; therefore, Frontiers only applies the most rigorous and unbiased reviews.
Frontiers revolutionizes research publishing by freely delivering the most outstanding research, evaluated with no bias from both the academic and social point of view. By applying the most advanced information technologies, Frontiers is catapulting scholarly publishing into a new generation.

What are Frontiers Research Topics?

Frontiers Research Topics are very popular trademarks of the Frontiers Journals Series: they are collections of at least ten articles, all centered on a particular subject. With their unique mix of varied contributions from Original Research to Review Articles, Frontiers Research Topics unify the most influential researchers, the latest key findings and historical advances in a hot research area! Find out more on how to host your own Frontiers Research Topic or contribute to one as an author by contacting the Frontiers Editorial Office: frontiersin.org/about/contact

SEIZURE FORECASTING AND DETECTION: COMPUTATIONAL MODELS, MACHINE LEARNING, AND TRANSLATION INTO DEVICES

Topic Editors:
Sharon Chiang, University of California, San Francisco, United States
Vikram Rao, University of California, San Francisco, United States
Gregory Worrell, Mayo Clinic, United States
Maxime O. Baud, University Hospital Bern, Switzerland

Citation: Chiang, S., Rao, V., Worrell, G., Baud, M. O., eds. (2022). Seizure Forecasting and Detection: Computational Models, Machine Learning, and Translation Into Devices. Lausanne: Frontiers Media SA.
doi: 10.3389/978-2-88974-872-3

Table of Contents

frontiers in Neurology

EDITORIAL
published: 16 March 2022
doi: 10.3389/fneur.2022.874070

Editorial: Seizure Forecasting and Detection: Computational Models, Machine Learning, and Translation Into Devices

Sharon Chiang[1]*, *Maxime O. Baud*[2,3], *Gregory A. Worrell*[4] and *Vikram R. Rao*[1]

[1] Department of Neurology and Weill Institute for Neurosciences, University of California, San Francisco, San Francisco, CA, United States, [2] Department of Neurology, Sleep-Wake-Epilepsy Center and Center for Experimental Neurology, Inselspital Bern, University Hospital, University of Bern, Bern, Switzerland, [3] Wyss Center for Bio- and Neuro-Technology, Geneva, Switzerland, [4] Department of Neurology, Mayo Clinic, Rochester, MN, United States

Keywords: epilepsy, seizure detection, seizure prediction, seizure forecasting, computational models, machine learning, artificial intelligence

Editorial on the Research Topic

Seizure Forecasting and Detection: Computational Models, Machine Learning, and Translation Into Devices

For the 50 million people with epilepsy worldwide, seizures are seemingly unpredictable events that can be associated with significant morbidity and mortality. Reliable methods to identify and anticipate seizures could enable powerful new therapeutic strategies. Owing to the paroxysmal nature of seizures and the challenges associated with long-term monitoring of brain activity, however, such methods have been elusive—until now. Recent advances in computational methods and device technology have reshaped the epilepsy landscape and made accurate detection and forecasting of seizures a reality. This Research Topic was launched with the aims of highlighting the latest of these advances and portraying the current state of seizure detection and forecasting through the viewpoints of patients and researchers. The 18 articles in this special issue comprise three Perspectives, three Reviews, and 12 Original Research articles.

This collection begins with a first-person account from Moss et al. of one family's experience with drug-resistant epilepsy, including their appraisal of current seizure detection devices; challenges encountered related to privacy, stigma, and comfort; and the need for greater collaboration between patients and researchers, Grzeskowiak and Dumanis survey a large sample of caregivers and adults living with epilepsy to assess directly their perspectives on seizure forecasting, including the optimal forecast horizon, the types of information that would be most useful for day-to-day planning, and the potential risks of forecasting tools. Hubbard et al. and Brinkmann et al. review the current status, technical challenges, and performance characteristics of contemporary seizure detection devices. Both groups highlight the critical need for research on several fronts: robustly designed clinical validation studies; algorithms to detect seizure types in addition to convulsive seizures (CS); better incorporation of meaningful clinical outcomes—such as morbidity, mortality, and quality of life—into algorithm evaluation; and more emphasis by developers on patient-centered considerations prior to beta-testing of new algorithms.

Several research groups whose work is included in this issue have already made substantial progress toward these goals. Glaba et al. and Kjaer et al. describe promising new algorithms that leverage physiological measurements to detect seizure types other than CS, including absence seizures, using electroencephalography (EEG),

OPEN ACCESS

Edited and reviewed by:
Fernando Cendes,
State University of Campinas, Brazil

***Correspondence:**
Sharon Chiang
Sharon.Chiang@ucsf.edu

Specialty section:
This article was submitted to Epilepsy, a section of the journal Frontiers in Neurology

Received: *11 February 2022*
Accepted: *15 February 2022*
Published: *16 March 2022*

Citation:
Chiang S, Baud MO, Worrell GA and Rao VR (2022) Editorial: Seizure Forecasting and Detection: Computational Models, Machine Learning, and Translation Into Devices. Front. Neurol. 13:874070. doi: 10.3389/fneur.2022.874070

and focal seizures, using subcutaneous EEG, accelerometry, and electromyography. Although collection of these types of physiological data is essential for seizure detection, patient privacy and unobtrusiveness of devices are also paramount considerations in algorithm and technology development. In this context, Manzouri et al. quantify and compare the relative energy efficiency and performance of several common machine learning methods, including random forests, recurrent (e.g., long short-term memory), and convolutional neural networks. Hyperdimensional computing, reviewed in an accessible tutorial by Schindler and Rahimi, is proposed as a powerful approach to develop energy-efficient seizure detection algorithms. Similar considerations of efficiency and performance are relevant for devices being developed for seizure detection. Frankel et al. report on a prospective feasibility study of Epilog by Epitel, Inc., a wearable 10-channel EEG system for long-term recordings. The authors recruited expert EEG readers and evaluated their ability to detect seizures using Epilog with or without a clinical decision support system. Onorati et al. conducted the first prospective multi-center study of a multimodal CS detection system, based on a wrist-worn device combining accelerometers and electrodermal activity sensors, and they report excellent sensitivity and a low false alarm rate.

Seizure detection algorithms also promise improvements to epilepsy diagnostic evaluations. As discussed by Parasuram et al. computational methods that accommodate spatial and temporal features of EEG may be more useful for identifying the ictal onset zone compared to methods relying on temporal features alone. Li et al. provide promising evidence that deep neural networks can identify seizures that are occult on scalp EEG but visible in intracranial EEG. These neural networks can also achieve high prediction accuracy for other tasks, including ictal onset zone lateralization and discrimination between ictal, preictal, and interictal periods.

Seizure detection and seizure forecasting represent complementary strategies for mitigating morbidity in epilepsy. Whereas, seizure detection provides a means to alert caregivers to seizures when they occur, seizure forecasting aims at reducing uncertainty by quantifying the likelihood of seizures in the future (1–3). The niche endeavor of forecasting seizures already has a decades-long history (4, 5), but has only recently gained traction among clinicians and patients, as the recent development of devices and algorithms makes it a plausible near-reality. Brinkmann et al. review variables that can be incorporated into seizure forecasting algorithms, including cycles of brain activity that help determine seizure risk (6, 7). Karoly et al. delve into these seizure cycles and debunk several common misconceptions related to seizure forecasting. For example, the authors clarify that cycles in epilepsy cannot be explained solely by behavioral patterns, medications, or catamenial effects, and they argue that long timescale rhythms in epilepsy may reflect systemic physiological processes that are cyclical and that manifest across a range of human diseases (Karoly et al.). This view agrees with the identification of multidien rhythms of epileptic brain activity as free-running, and thus likely endogenous in nature (8, 9).

The feasibility of seizure prediction on a population scale hinges on the development of minimally- and non-invasive devices. In a study of 11 patients with wearable devices, Stirling, Grayden et al. demonstrate that seizure likelihood can be forecasted with better than chance-level accuracy by using algorithms that incorporate data on heart rate, sleep, and step counts. Stirling, Maturana et al. show that seizure prediction is also possible with subcutaneous EEG (10) by using a state-based approach involving a two-step combination of logistic regression and random forests. Despite growing interest in potential applications of subcutaneous EEG (11), scalp EEG remains far more widely available, so Truong et al. use scalp EEG data and a Bayesian convolutional neural network to predict seizures in three patients. Attia et al. describe the design and architecture of the Mayo Epilepsy Personal Assistant Device, a cloud-based mobile platform integrated with an implanted intracranial neurostimulation device that is being used in an ongoing trial of neurostimulation in ten patients with bilateral mesial temporal lobe epilepsy. This special issue concludes with a cautionary note from Bosl et al. who draw upon experience from seizure detection efforts to highlight both the promise of seizure forecasting and the need for tempered optimism in a burgeoning field.

The 18 articles featured in this issue provides a status update and insight into representative lessons learned thus far in the years since the goals set by colleagues Mormann et al. (4) and Freestone et al. (5). In summary, we offer the reader the following insights on the current status of seizure detection and forecasting and several important priorities that emerge from this special issue:

1. **Emphasis on multimodal techniques:** There is no single perfect data stream; seizure detection and forecasting approaches will benefit from increased focus on statistical methods that accommodate multimodal data.
2. **Focus on understanding patient priorities and patient-researcher partnerships:** Patient perspectives are crucial to aid understanding of essential algorithm and device design aspects early in the development cycle, and to ensure that patient priorities maintain primacy in algorithm/device development (12).
3. **Interpretability and explainability in machine learning:** Machine learning methods may identify insights that humans cannot. Interpretability and explainability of predictions are active areas of research. We anticipate that the coming years will see translation of emerging computational techniques to enhance explainability into the area of seizure detection/forecasting.
4. **Expansion of seizure detection to other seizure types:** Current seizure detection methods achieve excellent performance using EEG. Detection algorithms with non-EEG signals have attained high sensitivity and specificity for certain types of seizures (convulsions), but remain limited for detection of other seizure types. Communicating the nuanced limitations of these methods to the patient community is just as critical as research on algorithms to detect non-convulsive seizure types. Developing technology

to quantitatively measure patient behavior and consciousness may help advance seizure classification.

5. **Need for increased studies evaluating reproducibility/generalizability:** Studies are emerging which seek to evaluate the reproducibility and generalizability of seizure detection/forecasting algorithms, and additional development will be needed to translate these algorithms into real-world settings. Expanding the sensing, data storage, and streaming capabilities of the next generation of devices will facilitate seizure detection/forecasting algorithm development.
6. **Computational efficiency vs. performance:** Given the importance to patients of non-stigmatizing devices, designing computationally efficient algorithms, balancing computational efficiency vs. performance, and developing minimally-invasive devices are research priorities.
7. **Individualized algorithm development:** Patients are heterogeneous in their seizure patterns and semiologies, as well as in the salient variables and non-linear functions relating these variables. A patient whose seizures may not be detected/forecasted by one algorithm and/or set of variables may be well-predicted by another. It is likely that multiple methods will need to be combined and tailored based on patient-specific factors.
8. **No prediction or detection method is perfect:** Seizure forecasts reduce uncertainty but do not eliminate it. The hope is that quantified uncertainty will translate into improved quality of life for people with epilepsy, but, although reasonable, this leap of faith will require direct testing in the clinical setting.

AUTHOR CONTRIBUTIONS

SC, MOB, GAW, and VRR: manuscript concept, design, and final revision. All authors contributed to the article and approved the submitted version.

FUNDING

SC was supported by the National Institute of Neurological Disorders and Stroke, National Institutes of Health (5R25NS070680-12). GAW was supported by the National Institutes of Health UH2/UH3 NS95495.

REFERENCES

1. Proix T, Truccolo W, Leguia MG, Tcheng TK, King-Stephens D, Rao VR, et al. Forecasting seizure risk in adults with focal epilepsy: a development and validation study. *Lancet Neurol.* (2021) 20:127–35. doi: 10.1016/S1474-4422(20)30396-3
2. Karoly PJ, Cook MJ, Maturana M, Nurse ES, Payne D, Brinkmann BH, et al. Forecasting seizure likelihood with wearable technology. *Epilepsia.* (2020) 61:776–86. doi: 10.1111/epi.16485
3. Kuhlmann L, Karoly P, Freestone DR, Brinkmann BH, Temko A, Barachant A, et al. Epilepsyecosystem.org: crowd-sourcing reproducible seizure prediction with long-term human intracranial EEG. *Brain.* (2018) 141:2619–30. doi: 10.1093/brain/awy210
4. Mormann F, Andrzejak GR, Elger EC, Lehnertz K. Seizure prediction: the long and winding road. *Brain.* (2007) 130(Pt 2):314–33. doi: 10.1093/brain/awl241
5. Freestone DR, Karoly PJ, Cook MJ. A forward-looking review of seizure prediction. *Curr Opin Neurol.* (2017) 30:167–73. doi: 10.1097/WCO.0000000000000429
6. Baud MO, Kleen JK, Mirro EA, Andrechak JC, King-Stephens D, Chang EF, et al. Multi-day rhythms modulate seizure risk in epilepsy. *Nat Commun.* (2018) 9:88. doi: 10.1038/s41467-017-02577-y
7. Karoly PJ, Goldenholz DM, Freestone DR, Moss RE, Grayden DB, Theodore WH, et al. Circadian and circaseptan rhythms in human epilepsy: a retrospective cohort study. *Lancet Neurol.* (2018) 17:977–85. doi: 10.1016/S1474-4422(18)30274-6
8. Rao VR, Leguia GM, Tcheng TK, Baud MO. Cues for seizure timing. *Epilepsia.* (2021) 62(Suppl. 1):S15–31. doi: 10.1111/epi.16611
9. Baud MO, Ghestem A, Benoliel JJ, Becker C, Bernard C. Endogenous multidien rhythm of epilepsy in rats. *Exp Neurol.* (2019) 315:82–7. doi: 10.1016/j.expneurol.2019.02.006
10. Duun-Henriksen J, Baud M, Richardson MP, Cook M, Kouvas G, Heasman JM, et al. A new era in electroencephalographic monitoring? Subscalp devices for ultra-long-term recordings. *Epilepsia.* (2020) 61:1805–17. doi: 10.1111/epi.16630
11. Pathmanathan J, Kjaer TW, Cole AJ, Delanty N, Surges R, Duun-Henriksen J. Expert perspective: who may benefit most from the new ultra long-term subcutaneous EEG monitoring? *Front Neurol.* (2021) 12:817733. doi: 10.3389/fneur.2021.817733
12. Chiang S, Picard RW, Chiong W, Moss R, Worrell GA, Rao VR, et al. Guidelines for conducting ethical artificial intelligence research in neurology: a systematic approach for clinicians and researchers. *Neurology.* (2021) 97:632–40. doi: 10.1212/WNL.0000000000012570

Conflict of Interest: MOB reports personal fees and grants from the Wyss Center for neurotechnology in Geneva, and has a patent application pending under the Patent Cooperation Treaty (62665486). MOB holds shares with Epios, Ltd., a medical device company based in Geneva. GAW declares intellectual property disclosures related to brain state classification algorithms licensed to Cadence Neuroscience Inc. VRR has served as a consultant for NeuroPace, Inc., manufacturer of the RNS System.

The remaining author declares that the research was conducted in the absence of any commercial or financial relationships that could be construed as a potential conflict of interest.

Publisher's Note: All claims expressed in this article are solely those of the authors and do not necessarily represent those of their affiliated organizations, or those of the publisher, the editors and the reviewers. Any product that may be evaluated in this article, or claim that may be made by its manufacturer, is not guaranteed or endorsed by the publisher.

frontiers in Neurology

PERSPECTIVE
published: 13 May 2021
doi: 10.3389/fneur.2021.675728

Prediction of Seizure Recurrence. A Note of Caution

William J. Bosl[1,2,3]*, *Alan Leviton*[1,2] *and Tobias Loddenkemper*[1,2]

[1] Boston Children's Hospital, Boston, MA, United States, [2] Harvard Medical School, Boston, MA, United States, [3] Health Informatics Program, University of San Francisco, San Francisco, CA, United States

Great strides have been made recently in documenting that machine-learning programs can predict seizure occurrence in people who have epilepsy. Along with this progress have come claims that appear to us to be a bit premature. We anticipate that many people will benefit from seizure prediction. We also doubt that all will benefit. Although machine learning is a useful tool for aiding discovery, we believe that the greatest progress will come from deeper understanding of seizures, epilepsy, and the EEG features that enable seizure prediction. In this essay, we lay out reasons for optimism and skepticism.

Keywords: electroencephalography, machine learning, chaos & non-linearity, dynamical systems, seizure prediction

OPEN ACCESS

Edited by:
Fernando Cendes,
State University of Campinas, Brazil

Reviewed by:
Kais Gadhoumi,
Duke University, United States
Hamid Soltanian-Zadeh,
University of Tehran, Iran

***Correspondence:**
William J. Bosl
william.bosl@childrens.harvard.edu

Specialty section:
This article was submitted to Epilepsy, a section of the journal Frontiers in Neurology

Received: *03 March 2021*
Accepted: *20 April 2021*
Published: *13 May 2021*

Citation:
Bosl WJ, Leviton A and Loddenkemper T (2021) Prediction of Seizure Recurrence. A Note of Caution. Front. Neurol. 12:675728. doi: 10.3389/fneur.2021.675728

INTRODUCTION

In a 2016 Epilepsy Foundation research program survey of people with epilepsy, "unpredictability was selected as a top issue regardless of seizure frequency or severity" (1). Seizure recurrence can be severely limiting (e.g., no driving), (2) socially disruptive and stigmatizing (3), and even life-threatening (4). Consequently, seizure prediction has the potential to improve epilepsy management and, therefore, the quality of life of persons with epilepsy (5).

Successful methods to predict an imminent seizure based on electrographic signatures, and potentially intervene with, for example, "responsive neurostimulation" (RNS) (6–8), would allow alternatives to drugs to minimize seizure recurrence. When a "pro-ictal" (9, 10) or "pre-ictal state" (11, 12) is identified, this mode of therapy provides highly localized stimulation intended to interrupt a seizure. Identification of times of greater and lesser seizure susceptibility will likely benefit patients, as such states may permit urgent care and interventions.

Progress in our understanding of how seizures develop and propagate (13) would lead to the expectation that "it may be possible to provide seizure prediction to a wider range of patients than previously thought" (14). We are not so sure. Before we explain why we expect only limited success anytime soon, we briefly review what is new with seizure prediction and potential electronic interventions for refractory epilepsy.

Clinicians and patients have long known that some seizures can be preceded by warning signs or symptoms (15). By and large, only about a quarter of patients with generalized epilepsy acknowledge an aura (15).

Electrocorticography (ECoG), which records from electrodes placed directly on the exposed surface of the brain, appears to be the best way to gather all the information for surgical removal of a seizure focus (16). ECoG signals are physically identical to EEG signals. Since they are placed directly on the cortex, less noise contaminates the signal and electrodes can be more closely spaced. Otherwise, the raw data from ECoG that might be fed into a machine learning algorithm is the same as with EEG data. The prediction of seizure recurrence now seems possible with scalp electrodes (17–31). Nevertheless, "modest outcomes associated with localization of abnormal

electrophysiology suggest … a fundamental gap in our understanding of how neurophysiologic biomarkers relate to pathophysiology" (32).

Seizure prediction algorithms can be characterized in a variety of ways. One perspective is to consider three independent aspects or axes: (1) the physiological signal to be measured, such as brain electrical activity or heart rate; (2) signal processing methods, which compute various signal features; and (3) machine learning methods, which take signal features as input and attempt to find patterns of features that distinguish seizure activity from non-seizure activity. Advances in signal features and machine learning algorithms continue to advance rapidly and contribute to improved seizure prediction. Signal features that are associated with seizures appear to be patient-specific. Hence, to have any value, machine learning algorithms need signal features from many seizures over a long period of time (33). EEG measures of brain electrical activity continue to be the most common physiological measure associated with seizures, but other measures based on cardiac function, dermal response, or movement are also used (34).

BACKGROUND FOR UNDERSTANDING SEIZURE GENERATION, INHIBITION, AND PROPAGATION

In the next few paragraphs, we review some elements of seizure generation and propagation that might aid in understanding electrographic correlates of seizures.

Epileptogenic Zone

The epileptogenic zone (EZ) is tautologically defined as the brain area indispensable for seizure generation (35). Among patients with focal epilepsy, more than 90% of seizures have discharges in the seizure focus and not elsewhere (36). In some patients, however, complete resection of the presumed EZ did not lead to seizure-freedom (37). Post-surgical recordings of these patients suggest that areas adjacent to the resection were also triggering the epileptic seizures. So was born the concept of "potential seizure-onset zones" (37).

Deeper gray structures (such as the thalamic reticular nucleus) appear to modulate the onset and propagation of other seizure phenomena (e.g., epileptic 2–4 Hz spike-wave discharges) (38). In addition, the epileptogenic zone in patients with pharmaco-resistant seizures can be larger than in people whose seizures are more readily controlled with medication (39).

Seizure Propagation and Networks

Seizure generation is only the beginning. Seizures are propagated "when synchronous connected groups of neurons work in tandem with rapidly changing de-synchronous relationships from the surrounding epileptic network" (40). The balance between inhibition and propagation, and—to a certain extent—underlying structural and functional connectivity, will determine to what extent the seizure does or does not spread (41). One seizure onset pattern is characterized by hypersynchrony and progressive impairment of inhibition leading to seizure propagation (42).

Seizures are currently defined by the area and signal recorded. As identification of these improve, so will seizure definition and seizure detection. Examples are intensive care patients who had a much higher percentage of seizures detected by intracortical depth electrodes than by surface EEG (43). Therefore, higher spatial resolution, and evaluation of additional signal characteristics have the potential to influence our perception of seizures. Hence, seizure prediction hinges on our definition of seizure onset, which is likely to change as detection techniques improve.

Inter-neuronal activity in the cortex can restrain the spread of epileptiform activity (44). As might be expected, seizure propagation is enhanced when local inhibition networks are defective (45).

Although many reports of brain functional connectivity have assumed "temporal stationarity" (i.e., no change with time), brain networks do reorganize almost continuously in response to both internal and external stimuli, resulting in temporal fluctuations of functional connectivity within and between networks across multiple time-scales (46, 47). By "coordinating excitability between brain regions in the epileptic network," changes in functional connectivity between/among networks not only allow propagation of the seizure activity, but might "enhance initiation, evolution, and termination of seizures" (32). The widespread disturbances of structural and functional connectivity that characterize some seizure disorders also appear to contribute to treatment resistance (48).

Epilepsy is considered to be a disorder of neural network organization (49). Research in network science has shown that small changes in network structure can have very large effects on network function, just as small changes in initial conditions can have large effects on time series (50). This suggests that small changes to a non-epileptic neural network may be all that's needed to make the brain epileptic. Similarly, small changes in just the right brain regions may be all that's needed to reduce seizures. Although this has not yet been demonstrated in humans, tools for measuring functional cortical networks are now available (51).

The signal variability of local connectivity among people with epilepsy appears to be significantly higher than in healthy controls (52), bringing excitability of the cortical neurons more often closer to the tipping point of seizures. Although network connectivity in seizure-onset zones can be increased during inter-ictal epochs (32, 53), ictal electrographic patterns appear to be generated by network mechanisms that are different from those sustaining inter-ictal potentials (54). Even brief focal spikes can activate diffuse distant networks (55), supporting the characterization of epilepsy as a network disease (56, 57).

Electrographic Correlates/Patterns /Signatures of Seizures

In one third of patients with a diagnosis of pharmaco-resistant focal epilepsy who are candidates for therapeutic surgery, fast activity at 80–120 Hz associated with very slow transient

polarizing shift, and voltage depression appear to be excellent biomarkers of ictogenesis and reliable indicators of epileptogenic zone boundaries (58). The high rate of co-occurrence probably reflects the restrictive criteria used to select candidates for surgery who have a presumed single-seizure-focus. Others have found spectral power in discreet frequency bands, as well as time- and/or frequency-domain inter-channel correlations to be helpful (14, 59).

Still other seizure onset patterns are characterized by de-synchronization of background activity and the appearance of fast low-voltage rhythms (41, 42), while excessive synchronization correlates with termination of the seizure (60). The seizure evolution pathway appears to differ among patients and tends to be stereotypical for each individual (11, 13, 61). Consequently, for prediction purposes, ictal electrographic signatures need to be individualized for each person for each seizure type (5, 14, 17, 20, 23, 25, 31, 56, 62–72). The buzzword is "patient-specific." Perhaps "big data" should be another buzz-word because analyses of large sample sizes and multiple individual variables will be needed to decide if groups of patients with similar epilepsy types and other physiological or demographic conditions can be viewed as a (relatively homogeneous) group.

Chaos and Chaotic Systems

Unlike its meaning in common parlance, "chaos" does not mean random, but only practically unpredictable. Even though the current state of the system might be known almost infinitely precisely, the smallest error or perturbation limits our ability to predict future states of the system.

Seizures often appear to be surprising. This apparent unpredictability might reflect purely random phenomena, or emergent chaotic phenomena that can arise at any time. If seizures are random, then prediction may be impossible in most cases until the pre-seizure changes begin to occur. If seizures are emergent chaotic phenomena, seizure prediction should be possible, since chaotic systems are deterministic. However, the chaotic nature of the system may limit the pre-seizure prediction time.

Non-linear (or chaotic) systems are composed of parts that can interact in complex ways, even if the parts themselves have simple dynamics or behavior. Non-linear systems are characterized by sensitive dependence on initial conditions, emergent phenomena, spontaneous order or synchronization between components, adaptation, and feedback loops (defined below), all of which result from the complex interaction of the parts. The EEG patterns of epilepsy appear to be non-linear (73, 74), likely reflecting non-linear dynamics of the brain.

Emergence has been defined as "the arising of novel and coherent structures, patterns and properties during the process of self-organization in complex systems" (75). This process of "self-organization" consists of adaptive behaviors between parts that emerge within chaotic systems, leading to a limited number of relatively stable configurations (76). The non-epileptic brain is stable and does not easily move into an ictal (seizure) state. It exhibits a property called "dynamical resistance" to seizures, which refers to a resistance to transitions to a seizure state (77). Resilience, a similar dynamical property, describes a system's ability to maintain normal function when internal errors or external environmental conditions arise (78). The epileptic brain may have reduced dynamical resistance and/or resilience, resulting in "multistable dynamics," (79) which means that it may spontaneously self-organize into a stable ictal state (80, 81). Dynamic networks based on EEG channel synchrony or coherence (amplitude synchrony) of the EEG may also differentiate patients with generalized epilepsy from normal controls (82).

Sensitive dependence on initial conditions is exemplified by the butterfly effect. In the highly non-linear atmospheric system, a small perturbation produced by a butterfly can lead to large changes at a future time, perhaps even a hurricane. In short, an arbitrarily small change in the state of a non-linear system at one time can have a large effect later. This is what makes a deterministic non-linear system practically unpredictable. It is not yet known if seizure occurrence (as opposed to the underlying neural spiking activity) follows a deterministic, chaotic pattern, or if it is simply a purely random process (83, 84).

Nobody is in charge of food distribution for most major cities and yet food gets distributed. This characteristic of complex systems is identified as spontaneous order, which may represent what occurs during the inter-ictal resting state (85). Another perspective is that the ictal and inter-ictal states each represent a stable, or semi-stable, attractor state of the dynamical system. An epileptic brain transitions between these states relatively easily, while this phase shift is very difficult to induce in a non-epileptic brain.

Neural connectivity, information transmission, and processing that are essential functions of the brain, may be altered on a large scale to allow the brain to switch into pathological states such as seizures, suggesting a scale dependent tipping (critical) point between normal physiologic function and pathological spread of electrical activity (86). However, if the neural structure of the brain is near a critical point, small changes in neural network structure may tip the brain into an unstable regime where seizures can occur spontaneously. This kind of spatial sensitivity to small changes has been described for networks (87).

Pre-ictal

If seizure prediction is to become clinically useful, programs that analyze electrical activity need to identify the pre-ictal state as early and reliably as possible before seizure onset. At present, we do not know when the pre-ictal state begins. Knowing when the pre-ictal state begins will allow an assessment of the time needed to detect and interrupt an impending seizure.

Dynamic models of events define different phase transitions (some with and others without an event or characteristic) and then model the probability of transitions from one state to another (88–91). People who work on seizure-prediction algorithms recognize at least three states: a seizure (ictal) state, a pre- or pro-ictal state, and all others. Machine-learning programs are given the task of comparing the electrographic characteristics of variously defined time intervals before a seizure to the electrographic characteristics of times further away (in time)

from seizure onset. The goal is to define a pre-ictal state. To do this effectively, the machine-learning programs need to be provided an abundance of EEG recordings (92), which are becoming increasingly available.

Characteristics of Ictal EEG

One group found that a few hours before a seizure, the "network states become less variable ("degenerate"), and this phase is followed by a global functional connectivity reduction" (93). Others have reported "less chaos" (94, 95) or "increased synchronization" before a seizure (18, 96). One group found that prior to seizure onset, the amplitude of pre-ictal discharges progressively increased as the interval between these discharges gradually decreased (97), while others have found that the cumulative energy profile (98), or measures of spectral entropy, spectral energy, and signal energy can help identify pre-ictal states (17). Still others have emphasized that the best discriminators vary for each individual (99), while another group emphasized the co-occurrence of multiple phenomena in a high potassium hippocampal slice model (loss of neuronal network resilience within the setting of critical slowing down, decreased ability of a network to recover from perturbations, increased high frequency fast activity, and successively decreasing resilience to stimulation (100).

Timing

The goal is to be able to identify the increased seizure propensity sufficiently before the seizure onset. The interval between identification of the likelihood of an impending seizure and the occurrence of the seizure has varied considerably, from under 10 s (17, 23, 24, 72, 81, 101, 102) to intervals of an hour or more (20–22, 36, 93, 103).

Periodicity

Seizures can display multiple types of periodicities (e.g., circadian, multi-day, weekly) in dogs (104) and humans (5, 105–109). Because only some people have seizures that occur with an obvious periodicity, seizure prediction is best viewed as patient-specific (5). Changes in level of epileptogenicity (state transitions) (110, 111) that most likely characterize periodicities are best viewed as contributing information to seizure-forecasts (112). To what extent these periodicities reflect changes in high-frequency oscillations (112), EEG spike potentials (112), brain connectivity, and inhibitory neurons (113) remains to be quantified. Seizure prediction algorithms are most likely to be effective when they include all the variables that provide relevant discriminating information for that patient. Each individual's seizure periodicities, once quantified, may be among those discriminating information.

Warning Signals Before Critical Transitions

The existence of early warning signals before catastrophes (e.g., species extinction, pandemics) (114–117) supports the concept that gradual transitions from stable to unstable conditions can reach a tipping point that heralds the irreversibility of the transition (118). Phase transitions in chaotic systems can happen either gradually or suddenly, depending on the system (119). Indeed, the relatively early aspects of the transition from a non-seizure state to seizure activity can be gradual (54, 120, 121) and widespread (36). "The suitability of typically applied early warning indicators for identifying heightened probability of a seizure remains controversial" (122, 123).

Binary Forecast or Probability Estimate of Seizure Risk

The seizure detection system can provide a binary forecast (impending seizure: yes/no), or a forecast that provides an estimated probability of an impending seizure (91, 124). The probability forecast, though obviously more informative than a binary forecast, will likely be degraded to a binary forecast when algorithms are written to initiate responsive neurostimulation (8). Even binary forecasting systems (high- and low-risk), using only patient-reported seizure data, correctly predicted seizures in about half of 50 patients (125).

Relatively Reliable Prediction

In an international crowdsourcing competition, an appreciable number of the more than 10,000 algorithms submitted by 478 teams were able "to distinguish between 10-min inter-seizure versus pre-seizure data clips" for each of three patients based on 442 days of continuous intracranial electroencephalography recordings from 16 subdural electrodes (14). These results prompted the authors to conclude, "clinically-relevant seizure prediction is possible in a wider range of patients than previously thought possible." While these results are promising, they are limited to three patients. As noted previously, different patients, or different epilepsy types, may have different pre-ictal time periods, ranging from seconds to an hour or more. Much larger patient sample populations will be needed to map out the limits of pre-seizure prediction. As a first step in this direction, crowdsourcing analysis of intracranial EEGs continues on related platforms, such as epilepsyecosystem.org (14, 126).

Not so Reliable Prediction

Despite subsequent expressions of enthusiasm (12, 31, 92, 127, 128), others have found that the EEGs of one third of patients with focal (129) or multifocal (130) epilepsies were not able to provide adequate predictive information about impending seizures. Findings such as these prompt us to offer words of caution about the anticipated capability to predict seizures and intervene effectively to prevent seizure occurrence.

In our acknowledging that some, perhaps many, people with seizures will benefit from machine-learning programs that predict seizure recurrence, we also want to justify the restraint in our enthusiasm. We do so based on the following considerations.

Prediction Performance Metrics

Specification of system parameters, such as prediction period, prediction horizon and data-driven characterization of lead seizures (minimal duration of seizure-free period) each influence prediction performance metrics (131). Consequently, investigators have the opportunity to cherry-pick the system parameters that will variably maximize their metrics. To minimize this, one group proposed a test

metric of the difference between algorithm sensitivity and chance sensitivity given an equal proportion of time spent under warning (132).

Prediction performance metrics may include indicators of sensitivity and specificity (59). Sensitivity is defined as the total number of seizures being accurately predicted divided by the total number of seizures recorded. Specificity is the number of correctly-identified non-events and is usually more difficult to evaluate due to the relatively small number of seizure events during most time intervals (133). Performance indices related to specificity include time in warning (the fraction of time the system makes positive predictions), and false positive error rate (8, 132).

A more general measure of performance that summarizes the tradeoff between sensitivity and specificity is the area under the receiver operating characteristic (ROC) curve (AUC) that discriminates between inter-ictal and pre-ictal data and is the preferred measure for many studies benchmarking multiple seizure forecasting algorithms (59, 132, 134).

The ROC curve is a plot of True Positive Rate (TPR) or sensitivity, vs. the False Positive Rate (FPR), or 1-specificity for varying model parameters. Thus, the area under the ROC curve (AUC) is a measure that accounts for the relative trade-off between sensitivity and specificity. Both are needed for a prediction algorithm to be practical. For example, perfect sensitivity is always possible if specificity is completely sacrificed: always predict a seizure and every seizure will be correctly predicted, 100% of the time. Similarly, always predicting "no seizure" will never falsely predict a seizure and thus have perfect specificity. Clearly, neither of these extremes is useful. Optimizing both sensitivity (predict all seizures) and specificity (no false alarms) is the ideal. The AUC is a measure of this optimal balance (135).

Because of the potential problem of overfitting (136) of the evaluation statistical model, investigators now seek to measure an "optimism corrected AUC," which corrects for/avoids optimism by either: cross-validation with replication (137–139) or leave-pair-out cross-validation (140).

Variations or extensions of this theme include a final "Improvement over Chance" binary metric that compares the measured AUC to a "chance-level AUC" (141), accuracy rates based on ROC curves (142), and an ROC analysis to extrapolate a cut-off value for the most significant predictors of seizure recurrence (143).

Another potential approach to assessing the accuracy of a prediction algorithm is to compare its accuracy to that obtained using surrogate output data that has some of the properties of the true data. An example of this is to randomly permute or shuffle the outcomes labels, thus retaining the same number of positives and negatives as in the original outcomes. (144). After permuting the labels, the predictive accuracy, including sensitivity and specificity, is computed. This process is repeated many times in a Monte Carlo style simulation, and the accuracies for all of the surrogate trials are accumulated to determine how likely the predictive accuracy with the true labels can be attained by random chance. For reasons that are not clear, this type of Monte Carlo simulation, which can be used to estimate the probability of attaining a selected AUC (145) has been used less frequently (146–148).

DISCUSSION

Butterfly Effect/Important Data Missing

The butterfly effect refers to the sensitive dependence of a non-linear system on the accuracy of measurements at a given starting time. Prediction of the future state of a non-linear system is limited by the butterfly effect. For example, even if all of the exact physical equations for atmospheric dynamics are known, predicting the weather more than a few days into the future is limited by how accurately the present weather conditions can be measured at every location from the surface of the earth to the top of the lower atmosphere. If neural function is a non-linear system, then seizure prediction may be limited by the butterfly effect.

The butterfly effect results from the slightest measurement imprecision. This is different from a lack of information about all the important processes involved in seizure generation or a lack of data. We prefer to use the word "missingness" (149, 150) to describe a lack of measured data regarding the processes involved in seizure onset and spread.

Seizure prediction will enable successful intervention only if identifiable pre-ictal signatures occur sufficiently clearly and sufficiently early to enable a predictive model to be constructed. A few reviews of the many applications of signal processing and predictive algorithms present the enormous breadth of this effort (151–154). This approach has begun to be applied to seizure prediction (155, 156) with the recognition that the amount of raw EEG data needed for deep learning approaches might be prohibitively large (157).

One Size Does Not Fit All

An algorithm created for one person is unlikely to predict seizure recurrence in another (5, 11, 13, 14, 17, 20, 23, 25, 31, 56, 61–72). Another potential problem is that although seizure prediction is specific to an epilepsy or seizure type, prediction can be conditioned by myriad patient characteristics. Large amounts of patient data, together with properly used machine learning algorithms, are likely needed to identify the best way to apply seizure prediction for optimal patient benefit. Sufficient amounts of data from many patients may improve the ability of patient-independent algorithms for the benefit of patients and their physicians who would strongly prefer not to have to wait a year to receive benefits from the prediction capability of wearable devices. However, it is also clear that seizure prediction algorithms can learn from patient-specific patterns and improve over time scales from days to months (158–160).

Much of the success of the seizure prediction field is owed to those investigators who have created a valuable database, made it publicly available, and asked others to contribute to this culture of data sharing (161). Many annotated seizure databases exist. Some of the better known ones can be explored further in these references: (71, 125, 161–165).

Research using machine learning algorithms is frequently hampered because of the lack of standards that allow data from

disparate databases to be aggregated (166). A lack of sufficient amounts of publicly-available data is also apparent (154). Because insufficient available human data were (59), a recent Kaggle machine learning competition for seizure prediction relied on canine EEG data. Advances in seizure prediction will be enhanced if the epilepsy research community can collaborate to create a common, aggregated, publicly-available data resource as the genomics community has done for the Human Genome Project (167).

We are cautiously optimistic that many people will benefit from an ability to predict seizure recurrence. We do, however, want to temper optimism that this ability will be available to nearly all patients and all seizures. Very large seizure data sets, with proper clinical annotation, and machine learning algorithms, as well as deeper understanding of the dynamics and neurophysiology of seizures and epilepsy, will be needed to provide a much clearer picture of the limits and possibilities of seizure prediction.

DATA AVAILABILITY STATEMENT

The original contributions presented in the study are included in the article/supplementary material, further inquiries can be directed to the corresponding author/s.

AUTHOR CONTRIBUTIONS

AL and TL conceived of the original idea for this paper. AL wrote the first draft. WB wrote substantial sections on non-linear systems, chaos theory, and EEG processing. All authors contributed to the article and approved the submitted version.

REFERENCES

1. Dumanis SB, French JA, Bernard C, Worrell GA, Fureman BE. Seizure forecasting from idea to reality. Outcomes of the My Seizure Gauge Epilepsy Innovation Institute Workshop. *eNeuro.* (2017) 4:1–5. doi: 10.1523/ENEURO.0349-17.2017
2. Al Zaid EH. Prevalence of patients with epilepsy unfit to drive. *J Fam Comm Med.* (2019) 26:51–6. doi: 10.4103/jfcm.JFCM_177_17
3. Besag FMC, Vasey MJ. Social cognition and psychopathology in childhood and adolescence. *Epilepsy Behav*. (2019) 100:106210. doi: 10.1016/j.yebeh.2019.03.015
4. DeGiorgio CM, Curtis A, Hertling D, Moseley BD. Sudden unexpected death in epilepsy: risk factors, biomarkers, and prevention. *Acta Neurol Scand.* (2019) 139:220–30. doi: 10.1111/ane.13049
5. Amengual-Gual M, Sanchez Fernandez I, Loddenkemper T. Patterns of epileptic seizure occurrence. *Brain Res.* (2019) 1703:3–12. doi: 10.1016/j.brainres.2018.02.032
6. Matias CM, Sharan A, Wu C. Responsive neurostimulation for the treatment of epilepsy. *Neurosurg Clin N Am.* (2019) 30:231–42. doi: 10.1016/j.nec.2018.12.006
7. Singhal NS, Numis AL, Lee MB, Chang EF, Sullivan JE, Auguste KI, et al. Responsive neurostimulation for treatment of pediatric drug-resistant epilepsy. *Epilepsy Behav Case Rep.* (2018) 10:21–4. doi: 10.1016/j.ebcr.2018.02.002
8. Gadhoumi K, Lina JM, Mormann F, Gotman J. Seizure prediction for therapeutic devices: a review. *J Neurosci Methods.* (2016) 260:270–82. doi: 10.1016/j.jneumeth.2015.06.010
9. Lopes da Silva FH, Harding GF. Transition to seizure in photosensitive epilepsy. *Epilepsy Res.* (2011) 97:278–82. doi: 10.1016/j.eplepsyres.2011.10.022
10. Baud MO, Proix T, Rao VR, Schindler K. Chance and risk in epilepsy. *Curr Opin Neurol.* (2020) 33:163–72. doi: 10.1097/WCO.0000000000000798
11. Badawy RA, Freestone DR, Lai A, Cook MJ. Epilepsy: ever-changing states of cortical excitability. *Neuroscience.* (2012) 222:89–99. doi: 10.1016/j.neuroscience.2012.07.015
12. Luckett P, Pavelescu E, McDonald T, Hively L, Ochoa J. Predicting state transitions in brain dynamics through spectral difference of phase-space graphs. *J Comp Neurosci.* (2019) 46:91–106. doi: 10.1007/s10827-018-0700-1
13. Karoly PJ, Kuhlmann L, Soudry D, Grayden DB, Cook MJ, Freestone DR. Seizure pathways: a model-based investigation. *PLoS Comp Biol.* (2018) 14:e1006403. doi: 10.1371/journal.pcbi.1006403
14. Kuhlmann L, Karoly P, Freestone DR, Brinkmann BH, Temko A, Barachant A, et al. Epilepsyecosystem.org: crowd-sourcing reproducible seizure prediction with long-term human intracranial EEG. *Brain.* (2018) 141:2619–30. doi: 10.1093/brain/awy210
15. Perven G, So NK. Epileptic auras: phenomenology and neurophysiology. *Epileptic Disord.* (2015) 17:349–62. doi: 10.1684/epd.2015.0786
16. King-Stephens D, Mirro E, Weber PB, Laxer KD, Van Ness PC, Salanova V, et al. Lateralization of mesial temporal lobe epilepsy with chronic ambulatory electrocorticography. *Epilepsia.* (2015) 56:959–67. doi: 10.1111/epi.13010
17. Sridevi V, Ramasubba Reddy M, Srinivasan K, Radhakrishnan K, Rathore C, Nayak DS. Improved patient-independent system for detection of electrical onset of seizures. *J Clin Neurophysiol.* (2019) 36:14–24. doi: 10.1097/WNP.0000000000000533
18. Li F, Liang Y, Zhang L, Yi C, Liao Y, Jiang Y, et al. Transition of brain networks from an interictal to a preictal state preceding a seizure revealed by scalp EEG network analysis. *Cogn Neurodyn.* (2019) 13:175–81. doi: 10.1007/s11571-018-09517-6
19. Khoa TQ, Huong NT, Toi VV. Detecting epileptic seizure from scalp EEG using Lyapunov spectrum. *Comp Math Methods Med.* (2012) 2012:847686. doi: 10.1155/2012/847686
20. Minasyan GR, Chatten JB, Chatten MJ, Harner RN. Patient-specific early seizure detection from scalp electroencephalogram. *J Clin Neurophysiol.* (2010) 27:163–78. doi: 10.1097/WNP.0b013e3181e0a9b6
21. Yang Y, Zhou M, Niu Y, Li C, Cao R, Wang B, et al. Epileptic seizure prediction based on permutation entropy. *Front Comp Neurosci.* (2018) 12:55. doi: 10.3389/fncom.2018.00055
22. Saab ME, Gotman J. A system to detect the onset of epileptic seizures in scalp EEG. *Clin Neurophysiol.* (2005) 116:427–42. doi: 10.1016/j.clinph.2004.08.004
23. Zandi AS, Javidan M, Dumont GA, Tafreshi R. Automated real-time epileptic seizure detection in scalp EEG recordings using an algorithm based on wavelet packet transform. *IEEE Transact Biomed Eng.* (2010) 57:1639–51. doi: 10.1109/TBME.2010.2046417
24. Salant Y, Gath I, Henriksen O. Prediction of epileptic seizures from two-channel EEG. *Med Biol Eng Comp.* (1998) 36:549–56. doi: 10.1007/BF02524422
25. Alotaiby TN, Alshebeili SA, Alotaibi FM, Alrshoud SR. Epileptic seizure prediction using CSP and LDA for scalp EEG signals. *Comp Intell Neurosci.* (2017) 2017:1240323. doi: 10.1155/2017/1240323
26. Zibrandtsen IC, Kidmose P, Christensen CB, Kjaer TW. Ear-EEG detects ictal and interictal abnormalities in focal and generalized epilepsy - A comparison with scalp EEG monitoring. *Clin Neurophysiol.* (2017) 128:2454–61. doi: 10.1016/j.clinph.2017.09.115
27. Jin K, Nakasato N. Long-cherished dreams for epileptologists and clinical neurophysiologists: automatic seizure detection in long-term scalp EEG. *Clin Neurophysiol.* (2014) 125:1289–90. doi: 10.1016/j.clinph.2013.12.105
28. Hopfengartner R, Kasper BS, Graf W, Gollwitzer S, Kreiselmeyer G, Stefan H, et al. Automatic seizure detection in long-term scalp EEG using an adaptive thresholding technique: a validation study for clinical

routine. *Clin Neurophysiol.* (2014) 125:1346–52. doi: 10.1016/j.clinph.2013.12.104
29. Nemtsas P, Birot G, Pittau F, Michel CM, Schaller K, Vulliemoz S, et al. Source localization of ictal epileptic activity based on high-density scalp EEG data. *Epilepsia.* (2017) 58:1027–36. doi: 10.1111/epi.13749
30. Lam AD, Maus D, Zafar SF, Cole AJ, Cash SS. SCOPE-mTL: a non-invasive tool for identifying and lateralizing mesial temporal lobe seizures prior to scalp EEG ictal onset. *Clin Neurophysiol.* (2017) 128:1647–55. doi: 10.1016/j.clinph.2017.06.040
31. Detti P, de Lara GZM, Bruni R, Pranzo M, Sarnari F, Vatti G. A patient-specific approach for short-term epileptic seizures prediction through the analysis of EEG synchronization. *IEEE Transact Biomed Eng.* (2019) 66:1494–504. doi: 10.1109/TBME.2018.2874716
32. Khambhati AN, Bassett DS, Oommen BS, Chen SH, Lucas TH, Davis KA, et al. Recurring functional interactions predict network architecture of interictal and ictal states in neocortical epilepsy. *eNeuro.* (2017) 4:1–18. doi: 10.1523/ENEURO.0091-16.2017
33. Manzouri F, Heller S, Dumpelmann M, Woias P, Schulze-Bonhage A. A comparison of machine learning classifiers for energy-efficient implementation of seizure detection. *Front Syst Neurosci.* (2018) 12:43. doi: 10.3389/fnsys.2018.00043
34. Tsiouris KM, Tzallas AT, Markoula S, Koutsouris D, Konitsiotis S, Fotiadis DI. A review of automated methodologies for the detection of epileptic episodes using long-term eeg signals. *Healthcare Pol Reform Concepts Methodol Tools Appl.* (3201) 8:1464–96. doi: 10.4018/978-1-5225-6915-2.ch066
35. Rosenow F, Bast T, Czech T, Feucht M, Hans VH, Helmstaedter C, et al. Revised version of quality guidelines for presurgical epilepsy evaluation and surgical epilepsy therapy issued by the Austrian, German, and Swiss working group on presurgical epilepsy diagnosis and operative epilepsy treatment. *Epilepsia.* (2016) 57:1215–20. doi: 10.1111/epi.13449
36. Naftulin JS, Ahmed OJ, Piantoni G, Eichenlaub JB, Martinet LE, Kramer MA, et al. Ictal and preictal power changes outside of the seizure focus correlate with seizure generalization. *Epilepsia.* (2018) 59:1398–409. doi: 10.1111/epi.14449
37. Luders HO, Najm I, Nair D, Widdess-Walsh P, Bingman W. The epileptogenic zone: general principles. *Epileptic Disord.* (2006) 8(Suppl. 2):S1–9.
38. Fan D, Liao F, Wang Q. The pacemaker role of thalamic reticular nucleus in controlling spike-wave discharges and spindles. *Chaos.* (2017) 27:073103. doi: 10.1063/1.4991869
39. Suzuki H, Sugano H, Nakajima M, Higo T, Iimura Y, Mitsuhashi T, et al. The epileptogenic zone in pharmaco-resistant temporal lobe epilepsy with amygdala enlargement. *Epileptic Disord.* (2019) 21:252–64. doi: 10.1684/epd.2019.1075
40. Khambhati AN, Davis KA, Oommen BS, Chen SH, Lucas TH, Litt B, et al. Dynamic network drivers of seizure generation, propagation and termination in human neocortical epilepsy. *PLoS Comp Biol.* (2015) 11:e1004608. doi: 10.1371/journal.pcbi.1004608
41. Jiruska P, de Curtis M, Jefferys JG, Schevon CA, Schiff SJ, Schindler K. Synchronization and desynchronization in epilepsy: controversies and hypotheses. *J Physiol.* (2013) 591:787–97. doi: 10.1113/jphysiol.2012.239590
42. Avoli M, de Curtis M, Gnatkovsky V, Gotman J, Kohling R, Levesque M, et al. Specific imbalance of excitatory/inhibitory signaling establishes seizure onset pattern in temporal lobe epilepsy. *J Neurophysiol.* (2016) 115:3229–37. doi: 10.1152/jn.01128.2015
43. Claassen J, Perotte A, Albers D, Kleinberg S, Schmidt JM, Tu B, et al. Nonconvulsive seizures after subarachnoid hemorrhage: multimodal detection and outcomes. *Ann Neurol.* (2013) 74:53–64. doi: 10.1002/ana.23859
44. Parrish RR, Codadu NK, Mackenzie-Gray Scott C, Trevelyan AJ. Feedforward inhibition ahead of ictal wavefronts is provided by both parvalbumin- and somatostatin-expressing interneurons. *J Physiol.* (2019) 597:2297–314. doi: 10.1113/JP277749
45. Liou JY, Ma H, Wenzel M, Zhao M, Baird-Daniel E, Smith EH, et al. Role of inhibitory control in modulating focal seizure spread. *Brain.* (2018) 141:2083–97. doi: 10.1093/brain/awy116
46. Preti MG, Bolton TA, Van De Ville D. The dynamic functional connectome: state-of-the-art and perspectives. *Neuroimage.* (2017) 160:41–54. doi: 10.1016/j.neuroimage.2016.12.061
47. Iraji A, Deramus TP, Lewis N, Yaesoubi M, Stephen JM, Erhardt E, et al. The spatial chronnectome reveals a dynamic interplay between functional segregation and integration. *Hum Brain Mapp.* (2019) 40:3058–77. doi: 10.1002/hbm.24580
48. Tavakol S, Royer J, Lowe AJ, Bonilha L, Tracy JI, Jackson GD, et al. Neuroimaging and connectomics of drug-resistant epilepsy at multiple scales: from focal lesions to macroscale networks. *Epilepsia.* (2019) 60:593–604. doi: 10.1111/epi.14688
49. Kramer MA, Cash SS. Epilepsy as a disorder of cortical network organization. *Neuroscientist.* (2012) 18:360–72. doi: 10.1177/1073858411422754
50. Cornelius SP, Kath WL, Motter AE. Realistic control of network dynamics. *Nat Commun.* (2013) 4:1942. doi: 10.1038/ncomms2939
51. Carr SJA, Gershon A, Shafiabadi N, Lhatoo SD, Tatsuoka C, Sahoo SS. An integrative approach to study structural and functional network connectivity in epilepsy using imaging and signal data. *Front Integr Neurosci.* (2020) 14:491403. doi: 10.3389/fnint.2020.491403
52. Pedersen M, Omidvarnia A, Curwood EK, Walz JM, Rayner G, Jackson GD. The dynamics of functional connectivity in neocortical focal epilepsy. *NeuroImage Clin.* (2017) 15:209–14. doi: 10.1016/j.nicl.2017.04.005
53. Korzeniewska A, Cervenka MC, Jouny CC, Perilla JR, Harezlak J, Bergey GK, et al. Ictal propagation of high frequency activity is recapitulated in interictal recordings: effective connectivity of epileptogenic networks recorded with intracranial EEG. *Neuroimage.* (2014) 101:96–113. doi: 10.1016/j.neuroimage.2014.06.078
54. Huberfeld G, Menendez de la Prida L, Pallud J, Cohen I, Le Van Quyen M, Adam C, et al. Glutamatergic pre-ictal discharges emerge at the transition to seizure in human epilepsy. *Nat Neurosci.* (2011) 14:627–34. doi: 10.1038/nn.2790
55. Walz JM, Pedersen M, Omidvarnia A, Semmelroch M, Jackson GD. Spatiotemporal mapping of epileptic spikes using simultaneous EEG-functional MRI. *Brain.* (2017) 140:998–1010. doi: 10.1093/brain/awx007
56. Olmi S, Petkoski S, Guye M, Bartolomei F, Jirsa V. Controlling seizure propagation in large-scale brain networks. *PLoS Comp Biol.* (2019) 15:e1006805. doi: 10.1371/journal.pcbi.1006805
57. Laufs H. Functional imaging of seizures and epilepsy: evolution from zones to networks. *Curr Opin Neurol.* (2012) 25:194–200. doi: 10.1097/WCO.0b013e3283515db9
58. Gnatkovsky V, de Curtis M, Pastori C, Cardinale F, Lo Russo G, Mai R, et al. Biomarkers of epileptogenic zone defined by quantified stereo-EEG analysis. *Epilepsia.* (2014) 55:296–305. doi: 10.1111/epi.12507
59. Brinkmann BH, Wagenaar J, Abbot D, Adkins P, Bosshard SC, Chen M, et al. Crowdsourcing reproducible seizure forecasting in human and canine epilepsy. *Brain.* (2016) 139 (Pt 6):1713–22. doi: 10.1093/brain/aww045
60. Fisher RS, Scharfman HE, deCurtis M. How can we identify ictal and interictal abnormal activity? *Adv Exp Med Biol.* (2014) 813:3–23. doi: 10.1007/978-94-017-8914-1_1
61. Jirsa VK, Stacey WC, Quilichini PP, Ivanov AI, Bernard C. On the nature of seizure dynamics. *Brain.* (2014) 137 (Pt 8):2210–30. doi: 10.1093/brain/awu133
62. Amengual-Gual M, Ulate-Campos A, Loddenkemper T. Status epilepticus prevention, ambulatory monitoring, early seizure detection and prediction in at-risk patients. *Seizure.* (2019) 68:31–7. doi: 10.1016/j.seizure.2018.09.013
63. Zabihi M, Kiranyaz S, Jantti V, Lipping T, Gabbouj M. Patient-specific seizure detection using nonlinear dynamics and nullclines. *IEEE J Biomed Health Inform.* (2020) 24:543–55. doi: 10.1109/JBHI.2019.2906400
64. Selvakumari RS, Mahalakshmi M, Prashalee P. Patient-Specific seizure detection method using hybrid classifier with optimized electrodes. *J Med Syst.* (2019) 43:121. doi: 10.1007/s10916-019-1234-4
65. Kuhlmann L, Freestone D, Lai A, Burkitt AN, Fuller K, Grayden DB, et al. Patient-specific bivariate-synchrony-based seizure prediction for short prediction horizons. *Epilepsy Res.* (2010) 91:214–31. doi: 10.1016/j.eplepsyres.2010.07.014
66. Kaleem M, Gurve D, Guergachi A, Krishnan S. Patient-specific seizure detection in long-term EEG using signal-derived empirical mode

decomposition (EMD)-based dictionary approach. *J Neural Eng.* (2018) 15:056004. doi: 10.1088/1741-2552/aaceb1
67. Billeci L, Marino D, Insana L, Vatti G, Varanini M. Patient-specific seizure prediction based on heart rate variability and recurrence quantification analysis. *PLoS ONE.* (2018) 13:e0204339. doi: 10.1371/journal.pone.0204339
68. Sandler RA, Geng K, Song D, Hampson RE, Witcher MR, Deadwyler SA, et al. Designing patient-specific optimal neurostimulation patterns for seizure suppression. *Neural Comp.* (2018) 30:1180–208. doi: 10.1162/neco_a_01075
69. Bhattacharyya A, Pachori RB. A multivariate approach for patient-specific EEG seizure detection using empirical wavelet transform. *IEEE Transact Biomed Eng.* (2017) 64:2003–15. doi: 10.1109/TBME.2017.2650259
70. Qu H, Gotman J. A patient-specific algorithm for the detection of seizure onset in long-term EEG monitoring: possible use as a warning device. *IEEE Transact Biomed Eng.* (1997) 44:115–22. doi: 10.1109/10.552241
71. Shoeb A, Edwards H, Connolly J, Bourgeois B, Treves ST, Guttag J. Patient-specific seizure onset detection. *Epilepsy Behav.* (2004) 5:483–98. doi: 10.1016/j.yebeh.2004.05.005
72. Kharbouch A, Shoeb A, Guttag J, Cash SS. An algorithm for seizure onset detection using intracranial EEG. *Epilepsy Behav.* (2011) 22(Suppl. 1):S29–35. doi: 10.1016/j.yebeh.2011.08.031
73. Lehnertz K. Epilepsy and nonlinear dynamics. *J Biol Phys.* (2008) 34:253–66. doi: 10.1007/s10867-008-9090-3
74. Good LB, Sabesan S, Marsh ST, Tsakalis K, Treiman DM, Iasemidis LD. Nonlinear dynamics of seizure prediction in a rodent model of epilepsy. *Nonlinear Dyn Psychol Life Sci.* (2010) 14:411–34.
75. Goldstein JM. Emergence as a construct: history and issues. *Emergence.* (1999) 1:49–72. doi: 10.1207/s15327000em0101_4
76. Rubinov M, Sporns O, Thivierge JP, Breakspear M. Neurobiologically realistic determinants of self-organized criticality in networks of spiking neurons. *PLoS Comp Biol.* (2011) 7:e1002038. doi: 10.1371/journal.pcbi.1002038
77. Rings T, Mazarei M, Akhshi A, Geier C, Tabar MRR, Lehnertz K. Traceability and dynamical resistance of precursor of extreme events. *Sci Rep.* (2019) 9:1744. doi: 10.1038/s41598-018-38372-y
78. Gao J, Barzel B, Barabasi AL. Universal resilience patterns in complex networks. *Nature.* (2016) 530:307–12. doi: 10.1038/nature16948
79. Lopes da Silva FH, Blanes W, Kalitzin SN, Parra J, Suffczynski P, Velis DN. Dynamical diseases of brain systems: different routes to epileptic seizures. *IEEE Transact Biomed Eng.* (2003) 50:540–8. doi: 10.1109/TBME.2003.810703
80. Freeman WJ, Skarda CA. Spatial EEG patterns, non-linear dynamics and perception: the neo-Sherringtonian view. *Brain Res.* (1985) 357:147–75. doi: 10.1016/0165-0173(85)90022-0
81. Frolov NS, Grubov VV, Maksimenko VA, Luttjohann A, Makarov VV, Pavlov AN, et al. Statistical properties and predictability of extreme epileptic events. *Sci Rep.* (2019) 9:7243. doi: 10.1038/s41598-019-43619-3
82. Schmidt H, Woldman W, Goodfellow M, Chowdhury FA, Koutroumanidis M, Jewell S, et al. A computational biomarker of idiopathic generalized epilepsy from resting state EEG. *Epilepsia.* (2016) 57:e200–4. doi: 10.1111/epi.13481
83. Gao J, Hu J, Tung WW, Blasch E. Multiscale analysis of biological data by scale-dependent lyapunov exponent. *Front Physiol.* (2011) 2:110. doi: 10.3389/fphys.2011.00110
84. Lai YC, Harrison MA, Frei MG, Osorio I. Controlled test for predictive power of Lyapunov exponents: their inability to predict epileptic seizures. *Chaos.* (2004) 14:630–42. doi: 10.1063/1.1777831
85. Yang T, Fang Z, Ren J, Xiao F, Li Q, Liu L, et al. Altered spontaneous activity in treatment-naive childhood absence epilepsy revealed by regional homogeneity. *J Neurol Sci.* (2014) 340:58–62. doi: 10.1016/j.jns.2014.02.025
86. Milton JG. Neuronal avalanches, epileptic quakes and other transient forms of neurodynamics. *Eur J Neurosci.* (2012) 36:2156–63. doi: 10.1111/j.1460-9568.2012.08102.x
87. Motter AE, Albert R. Networks in motion. *Phys Today.* (2012) 65:43–8. doi: 10.1063/PT.3.1518
88. McEwen JA, Anderson GB. Modeling the stationarity and Gaussianity of spontaneous electroencephalographic activity. *IEEE Transact Biomed Eng.* (1975) 22:361–9. doi: 10.1109/TBME.1975.324504
89. Chiang S, Vannucci M, Goldenholz DM, Moss R, Stern JM. Epilepsy as a dynamic disease: a Bayesian model for differentiating seizure risk from natural variability. *Epilepsia Open.* (2018) 3:236–46. doi: 10.1002/epi4.12112
90. Lopes da Silva F, Blanes W, Kalitzin SN, Parra J, Suffczynski P, Velis DN. Epilepsies as dynamical diseases of brain systems: basic models of the transition between normal and epileptic activity. *Epilepsia.* (2003) 44(Suppl. 12):72–83. doi: 10.1111/j.0013-9580.2003.12005.x
91. Principe A, Ley M, Conesa G, Rocamora R. Prediction error connectivity: a new method for EEG state analysis. *Neuroimage.* (2019) 188:261–73. doi: 10.1016/j.neuroimage.2018.11.052
92. Acharya UR, Hagiwara Y, Adeli H. Automated seizure prediction. *Epilepsy Behav.* (2018) 88:251–61. doi: 10.1016/j.yebeh.2018.09.030
93. Tauste Campo A, Principe A, Ley M, Rocamora R, Deco G. Degenerate time-dependent network dynamics anticipate seizures in human epileptic brain. *PLoS Biol.* (2018) 16:e2002580. doi: 10.1371/journal.pbio.2002580
94. Bou Assi E, Nguyen DK, Rihana S, Sawan M. Towards accurate prediction of epileptic seizures: a review. *Biomed Signal Process.* (2017) 34:144–57. doi: 10.1016/j.bspc.2017.02.001
95. Schwartz TH, Hong SB, Bagshaw AP, Chauvel P, Benar CG. Preictal changes in cerebral haemodynamics: review of findings and insights from intracerebral EEG. *Epilepsy Res.* (2011) 97:252–66. doi: 10.1016/j.eplepsyres.2011.07.013
96. Le Van Quyen M, Soss J, Navarro V, Robertson R, Chavez M, Baulac M, et al. Preictal state identification by synchronization changes in long-term intracranial EEG recordings. *Clin Neurophysiol.* (2005) 116:559–68. doi: 10.1016/j.clinph.2004.10.014
97. Chen J, Li L, Wu D, Li X, Xue Q, Wang L, et al. Dynamic preictal discharges in patients with mesial temporal lobe epilepsy. *J Clin Neurophysiol.* (2018) 35:381–7. doi: 10.1097/WNP.0000000000000486
98. Litt B, Esteller R, Echauz J, D'Alessandro M, Shor R, Henry T, et al. Epileptic seizures may begin hours in advance of clinical onset: a report of five patients. *Neuron.* (2001) 30:51–64. doi: 10.1016/S0896-6273(01)00262-8
99. Lin LC, Chen SC, Chiang CT, Wu HC, Yang RC, Ouyang CS. Classification preictal and interictal stages via integrating interchannel and time-domain analysis of EEG features. *Clin EEG Neurosci.* (2017) 48:139–45. doi: 10.1177/1550059416649076
100. Chang WC, Kudlacek J, Hlinka J, Chvojka J, Hadrava M, Kumpost V, et al. Loss of neuronal network resilience precedes seizures and determines the ictogenic nature of interictal synaptic perturbations. *Nat Neurosci.* (2018) 21:1742–52. doi: 10.1038/s41593-018-0278-y
101. Meier R, Dittrich H, Schulze-Bonhage A, Aertsen A. Detecting epileptic seizures in long-term human EEG: a new approach to automatic online and real-time detection and classification of polymorphic seizure patterns. *J Clin Neurophysiol.* (2008) 25:119–31. doi: 10.1097/WNP.0b013e3181775993
102. Rogowski Z, Gath I, Bental E. On the prediction of epileptic seizures. *Biol Cybernet.* (1981) 42:9–15. doi: 10.1007/BF00335153
103. Adames NR, Oberle JR, Cooper JA. The surveillance mechanism of the spindle position checkpoint in yeast. *J Cell Biol.* (2001) 153:159–68. doi: 10.1083/jcb.153.1.159
104. Gregg NM, Nasseri M, Kremen V, Patterson EE, Sturges BK, Denison TJ, et al. Circadian and multiday seizure periodicities, and seizure clusters in canine epilepsy. *Brain Commun.* (2020) 2:fcaa008. doi: 10.1093/braincomms/fcaa008
105. Baud MO, Kleen JK, Mirro EA, Andrechak JC, King-Stephens D, Chang EF, et al. Multi-day rhythms modulate seizure risk in epilepsy. *Nat Commun.* (2018) 9:88. doi: 10.1038/s41467-017-02577-y
106. Christodoulakis M, Hadjipapas A, Papathanasiou ES, Anastasiadou M, Papacostas SS, Mitsis GD. Periodicity in functional brain networks: application to scalp EEG from epilepsy patients. *Annu Int Conf IEEE Eng Med Biol Sci.* (2014) 2014:2805–8. doi: 10.1109/EMBC.2014.6944206
107. Loddenkemper T, Vendrame M, Zarowski M, Gregas M, Alexopoulos AV, Wyllie E, et al. Circadian patterns of pediatric seizures. *Neurology.* (2011) 76:145–53. doi: 10.1212/WNL.0b013e318206ca46
108. Hofstra WA, de Weerd AW. The circadian rhythm and its interaction with human epilepsy: a review of literature. *Sleep Med Rev.* (2009) 13:413–20. doi: 10.1016/j.smrv.2009.01.002

109. Karoly PJ, Goldenholz DM, Freestone DR, Moss RE, Grayden DB, Theodore WH, et al. Circadian and circaseptan rhythms in human epilepsy: a retrospective cohort study. *Lancet Neurol.* (2018) 17:977–85. doi: 10.1016/S1474-4422(18)30274-6
110. Abrishami Shokooh L, Toffa DH, Pouliot P, Lesage F, Nguyen DK. Identification of global and local states during seizures using quantitative functional connectivity and recurrence plot analysis. *Comp Biol Med.* (2020) 122:103858. doi: 10.1016/j.compbiomed.2020.103858
111. Crisp DN, Cheung W, Gliske SV, Lai A, Freestone DR, Grayden DB, et al. Quantifying epileptogenesis in rats with spontaneous and responsive brain state dynamics. *Brain Commun.* (2020) 2:fcaa048. doi: 10.1093/braincomms/fcaa048
112. Stirling RE, Cook MJ, Grayden DB, Karoly PJ. Seizure forecasting and cyclic control of seizures. *Epilepsia*. (2021) 62 Suppl 1:S2–S14. doi: 10.1111/epi.16541
113. Scott JM, Ren S, Gliske SV, Stacey WC. Preictal variability of high-frequency oscillation rates in refractory epilepsy. *Epilepsia*. (2020) 61:2521–33. doi: 10.1111/epi.16680
114. Jarvis L, McCann K, Tunney T, Gellner G, Fryxell JM. Early warning signals detect critical impacts of experimental warming. *Ecol Evol.* (2016) 6:6097–106. doi: 10.1002/ece3.2339
115. Drake JM, Griffen BD. Early warning signals of extinction in deteriorating environments. *Nature.* (2010) 467:456–9. doi: 10.1038/nature09389
116. Gao J, Wang K, Ding T. Detecting early-warning signals for influenza A pandemic based on protein dynamical network biomarkers. *Saudi J Biol Sci.* (2017) 24:724–8. doi: 10.1016/j.sjbs.2017.01.048
117. Chen P, Chen E, Chen L, Zhou XJ, Liu R. Detecting early-warning signals of influenza outbreak based on dynamic network marker. *J Cell Mol Med.* (2019) 23:395–404. doi: 10.1111/jcmm.13943
118. Boettiger C, Hastings A. Tipping points: from patterns to predictions. *Nature.* (2013) 493:157–8. doi: 10.1038/493157a
119. Solé R. *Phase Transitions*. Princeton, NJ: Princeton University Press (2011).
120. Zhang ZJ, Koifman J, Shin DS, Ye H, Florez CM, Zhang L, et al. Transition to seizure: ictal discharge is preceded by exhausted presynaptic GABA release in the hippocampal CA3 region. *J Neurosci.* (2012) 32:2499–512. doi: 10.1523/JNEUROSCI.4247-11.2012
121. Worrell GA, Parish L, Cranstoun SD, Jonas R, Baltuch G, Litt B. High-frequency oscillations and seizure generation in neocortical epilepsy. *Brain.* (2004) 127 (Pt 7):1496–506. doi: 10.1093/brain/awh149
122. Wilkat T, Rings T, Lehnertz K. No evidence for critical slowing down prior to human epileptic seizures. *Chaos.* (2019) 29:091104. doi: 10.1063/1.5122759
123. Maturana MI, Meisel C, Dell K, Karoly PJ, D'Souza W, Grayden DB, et al. Critical slowing down as a biomarker for seizure susceptibility. *Nat Commun.* (2020) 11:2172. doi: 10.1038/s41467-020-15908-3
124. Mader M, Mader W, Gluckman BJ, Timmer J, Schelter B. Statistical evaluation of forecasts. *Phys Rev E Stat Nonlinear Soft Matter Phys.* (2014) 90:022133. doi: 10.1103/PhysRevE.90.022133
125. Karoly PJ, Cook MJ, Maturana M, Nurse ES, Payne D, Brinkmann BH, et al. Forecasting cycles of seizure likelihood. *Epilepsia.* (2020) 61:776–86. doi: 10.1111/epi.16485
126. Reuben C, Karoly P, Freestone DR, Temko A, Barachant A, Li F, et al. Ensembling crowdsourced seizure prediction algorithms using long-term human intracranial EEG. *Epilepsia.* (2020) 61:e7–12. doi: 10.1111/epi.16418
127. Karuppiah Ramachandran VR, Alblas HJ, Le DV, Meratnia N. Towards an online seizure advisory system-an adaptive seizure prediction framework using active learning heuristics. *Sensors.* (2018) 18:1–30. doi: 10.3390/s18061698
128. Kuhlmann L, Lehnertz K, Richardson MP, Schelter B, Zaveri HP. Seizure prediction - ready for a new era. *Nat Rev Neurol.* (2018) 14:618–30. doi: 10.1038/s41582-018-0055-2
129. Alexandre Teixeira C, Direito B, Bandarabadi M, Le Van Quyen M, Valderrama M, Schelter B, et al. Epileptic seizure predictors based on computational intelligence techniques: a comparative study with 278 patients. *Comp Methods Progr Biomed.* (2014) 114:324–36. doi: 10.1016/j.cmpb.2014.02.007
130. Lehnertz K, Dickten H, Porz S, Helmstaedter C, Elger CE. Predictability of uncontrollable multifocal seizures - towards new treatment options. *Sci Rep.* (2016) 6:24584. doi: 10.1038/srep24584
131. Chen HH, Cherkassky V. Performance metrics for online seizure prediction. *Neural Netw.* (2020) 128:22–32. doi: 10.1016/j.neunet.2020.04.022
132. Snyder DE, Echauz J, Grimes DB, Litt B. The statistics of a practical seizure warning system. *J Neural Eng.* (2008) 5:392–401. doi: 10.1088/1741-2560/5/4/004
133. Chaovalitwongse W, Iasemidis LD, Pardalos PM, Carney PR, Shiau DS, Sackellares JC. Performance of a seizure warning algorithm based on the dynamics of intracranial EEG. *Epilepsy Res.* (2005) 64:93–113. doi: 10.1016/j.eplepsyres.2005.03.009
134. Baldassano SN, Brinkmann BH, Ung H, Blevins T, Conrad EC, Leyde K, et al. Crowdsourcing seizure detection: algorithm development and validation on human implanted device recordings. *Brain.* (2017) 140:1680–91. doi: 10.1093/brain/awx098
135. Carter JV, Pan J, Rai SN, Galandiuk S. ROC-ing along: evaluation and interpretation of receiver operating characteristic curves. *Surgery.* (2016) 159:1638–45. doi: 10.1016/j.surg.2015.12.029
136. Lemm S, Blankertz B, Dickhaus T, Müller KR. Introduction to machine learning for brain imaging. *Neuroimage.* (2011) 56:387–99. doi: 10.1016/j.neuroimage.2010.11.004
137. La Rocca M, Garner R, Amoroso N, Lutkenhoff ES, Monti MM, Vespa P, et al. Multiplex networks to characterize seizure development in traumatic brain injury patients. *Front Neurosci.* (2020) 14:591662. doi: 10.3389/fnins.2020.591662
138. Scott JM, Gliske SV, Kuhlmann L, Stacey WC. Viability of preictal high-frequency oscillation rates as a biomarker for seizure prediction. *Front Hum Neurosci.* (2020) 14:612899. doi: 10.3389/fnhum.2020.612899
139. Weil AG, Lewis EC, Ibrahim GM, Kola O, Tseng C-H, Zhou X, et al. Hemispherectomy outcome prediction scale: development and validation of a seizure freedom prediction tool. *Epilepsia*. (2021). doi: 10.1111/epi.16861
140. Sip V, Hashemi M, Vattikonda AN, Woodman MM, Wang H, Scholly J, et al. Data-driven method to infer the seizure propagation patterns in an epileptic brain from intracranial electroencephalography. *PLoS Comput Biol.* (2021) 17:e1008689. doi: 10.1371/journal.pcbi.1008689
141. Proix T, Truccolo W, Leguia MG, Tcheng TK, King-Stephens D, Rao VR, et al. Forecasting seizure risk in adults with focal epilepsy: a development and validation study. *Lancet Neurol.* (2021) 20:127–35. doi: 10.1016/S1474-4422(20)30396-3
142. Kleen JK, Speidel BA, Baud MO, Rao VR, Ammanuel SG, Hamilton LS, et al. Accuracy of omni-planar and surface casting of epileptiform activity for intracranial seizure localization. *Epilepsia*. (2021) 62:947–59. doi: 10.1111/epi.16841
143. Turco F, Bonanni E, Milano C, Pizzanelli C, Steinwurzel C, Morganti R, et al. Prolonged epileptic discharges predict seizure recurrence in JME: insights from prolonged ambulatory EEG. *Epilepsia*. (2021). doi: 10.1111/epi.16875
144. Golland P, Fischl B. Permutation tests for classification: towards statistical significance in image-based studies. *Inf Process Med Imaging.* (2003) 18:330–41. doi: 10.1007/978-3-540-45087-0_28
145. Ambrose PG, Grasela DM. The use of Monte Carlo simulation to examine pharmacodynamic variance of drugs: fluoroquinolone pharmacodynamics against *Streptococcus pneumoniae*. *Diagn Microbiol Infect Dis.* (2000) 38:151–7. doi: 10.1016/S0732-8893(00)00185-1
146. Feldwisch-Drentrup H, Schulze-Bonhage A, Timmer J, Schelter B. Statistical validation of event predictors: a comparative study based on the field of seizure prediction. *Phys Rev E Stat Nonlin Soft Matter Phys.* (2011) 83 (6 Pt 2):066704. doi: 10.1103/PhysRevE.83.066704
147. Struck AF, Rodriguez-Ruiz AA, Osman G, Gilmore EJ, Haider HA, Dhakar MB, et al. Comparison of machine learning models for seizure prediction in hospitalized patients. *Ann Clin Transl Neurol.* (2019) 6:1239–47. doi: 10.1002/acn3.50817
148. Andrzejak RG, Chicharro D, Elger CE, Mormann F. Seizure prediction: any better than chance? *Clin Neurophysiol.* (2009) 120:1465–78. doi: 10.1016/j.clinph.2009.05.019
149. Salgado CM, Azevedo C, Proenca H, Vieira SM. *Missing Data. Secondary Analysis of Electronic Health Records*. Cham: Springer (2016). p. 143–62.

150. Sackett DL. Bias in analytic research. *J Chronic Dis.* (1979) 32:51–63. doi: 10.1016/0021-9681(79)90012-2
151. Yang J, Sawan M. From seizure detection to smart and fully embedded seizure prediction engine: a review. *IEEE Trans Biomed Circuits Syst.* (2020) 14:1008–23. doi: 10.1109/TBCAS.2020.3018465
152. An S, Kang C, Lee HW. Artificial intelligence and computational approaches for epilepsy. *J Epilepsy Res.* (2020) 10:8–17. doi: 10.14581/jer.20003
153. Boubchir L. Editorial commentary on special issue of advances in EEG signal processing and machine learning for epileptic seizure detection and prediction. *J Biomed Res.* (2020) 34:149–50. doi: 10.7555/JBR.34.20200700
154. Rasheed K, Qayyum A, Qadir J, Sivathamboo S, Kwan P, Kuhlmann L, et al. Machine learning for predicting epileptic seizures using EEG signals: a review. *IEEE Rev Biomed Eng.* (2021) 14:139–55. doi: 10.1109/RBME.2020.3008792
155. Pinto MF, Leal A, Lopes F, Dourado A, Martins P, Teixeira CA. A personalized and evolutionary algorithm for interpretable EEG epilepsy seizure prediction. *Sci Rep*. (2021) 11:3415. doi: 10.1038/s41598-021-82828-7
156. Geng D, Alkhachroum A, Melo Bicchi M, Jagid J, Cajigas I, Chen ZS. Deep learning for robust detection of interictal epileptiform discharges. *J Neural Eng*. (2021). doi: 10.1088/1741-2552/abf28e
157. Maier A, Syben C, Lasser T, Riess C. A gentle introduction to deep learning in medical image processing. *Zeitschrift Med Phys.* (2019) 29:86–101. doi: 10.1016/j.zemedi.2018.12.003
158. Karoly PJ, Ung H, Grayden DB, Kuhlmann L, Leyde K, Cook MJ, et al. The circadian profile of epilepsy improves seizure forecasting. *Brain.* (2017) 140:2169–82. doi: 10.1093/brain/awx173
159. Kiral-Kornek I, Roy S, Nurse E, Mashford B, Karoly P, Carroll T, et al. Epileptic seizure prediction using big data and deep learning: toward a mobile system. *EBioMedicine.* (2018) 27:103–11. doi: 10.1016/j.ebiom.2017.11.032
160. Leguia MG, Andrzejak RG, Rummel C, Fan JM, Mirro EA, Tcheng TK, et al. Seizure cycles in focal epilepsy. *JAMA Neurol*. (2021) 78:454–63. doi: 10.1001/jamaneurol.2020.5370
161. Wagenaar JB, Worrell GA, Ives Z, Dümpelmann M, Litt B, Schulze-Bonhage A. Collaborating and sharing data in epilepsy research. *J Clin Neurophysiol.* (2015) 32:235–9. doi: 10.1097/WNP.0000000000000159
162. Lehnertz K, Litt B. The First International Collaborative Workshop on seizure prediction: summary and data description. *Clin Neurophysiol.* (2005) 116:493–505. doi: 10.1016/j.clinph.2004.08.020
163. Klatt J, Feldwisch-Drentrup H, Ihle M, Navarro V, Neufang M, Teixeira C, et al. The EPILEPSIAE database: an extensive electroencephalography database of epilepsy patients. *Epilepsia.* (2012) 53:1669–76. doi: 10.1111/j.1528-1167.2012.03564.x
164. DiLorenzo DJ, Leyde KW, Kaplan D. Neural state monitoring in the treatment of epilepsy: seizure prediction-conceptualization to first-in-man study. *Brain Sci.* (2019) 9:1–18. doi: 10.3390/brainsci9070156
165. Clinic UoPM. *IEEG Portal* (2014). Available from: https://www.ieeg.org (Retrieved February 24, 2021).
166. Lehne M, Sass J, Essenwanger A, Schepers J, Thun S. Why digital medicine depends on interoperability. *NPJ Dig Med.* (2019) 2:79. doi: 10.1038/s41746-019-0158-1
167. Varmus H. Genomic empowerment: the importance of public databases. *Nat Genet.* (2003) 35(Suppl. 1):3. doi: 10.1038/ng1186

Conflict of Interest: TL is part of patent applications to detect and predict clinical outcomes, and to detect, manage, diagnose, and treat neurological conditions, epilepsy, and seizures. TL is co-inventor of the TriVox Health technology and Boston Children's Hospital might receive financial benefits from this technology in the form of compensation in the future. WB is named along with TL on a patent for epileptogenicity that is owned by Boston Children's Hospital.

The remaining author declares that the research was conducted in the absence of any commercial or financial relationships that could be construed as a potential conflict of interest.

frontiers in Neurology

BRIEF RESEARCH REPORT
published: 29 June 2021
doi: 10.3389/fneur.2021.685814

Absence Seizure Detection Algorithm for Portable EEG Devices

Pawel Glaba[1], Miroslaw Latka[1], Małgorzata J. Krause[2], Sławomir Kroczka[3], Marta Kuryło[2], Magdalena Kaczorowska-Frontczak[4], Wojciech Walas[5], Wojciech Jernajczyk[6], Tadeusz Sebzda[7] and Bruce J. West[8]*

[1] Department of Biomedical Engineering, Wroclaw University of Science and Technology, Wroclaw, Poland, [2] Department of Pediatric Neurology, T. Marciniak Hospital, Wrocław, Poland, [3] Department of Child Neurology, Jagiellonian University Medical College, Krakow, Poland, [4] The Children's Memorial Health Institute, Warszawa, Poland, [5] Paediatric and Neonatal Intensive Care Unit, Institute of Medical Sciences, University of Opole, Opole, Poland, [6] Clinical Neurophysiology, Institute of Psychiatry and Neurology, Warszawa, Poland, [7] Department of Pathophysiology, Wroclaw Medical University, Wroclaw, Poland, [8] Office of the Director, Army Research Office, Research Triangle Park, Durham, NC, United States

Absence seizures are generalized nonmotor epileptic seizures with abrupt onset and termination. Transient impairment of consciousness and spike-slow wave discharges (SWDs) in EEG are their characteristic manifestations. This type of seizure is severe in two common pediatric syndromes: childhood (CAE) and juvenile (JAE) absence epilepsy. The appearance of low-cost, portable EEG devices has paved the way for long-term, remote monitoring of CAE and JAE patients. The potential benefits of this kind of monitoring include facilitating diagnosis, personalized drug titration, and determining the duration of pharmacotherapy. Herein, we present a novel absence detection algorithm based on the properties of the complex Morlet continuous wavelet transform of SWDs. We used a dataset containing EEGs from 64 patients (37 h of recordings with almost 400 seizures) and 30 age and sex-matched controls (9 h of recordings) for development and testing. For seizures lasting longer than 2 s, the detector, which analyzed two bipolar EEG channels (Fp1-T3 and Fp2-T4), achieved a sensitivity of 97.6% with 0.7/h detection rate. In the patients, all false detections were associated with epileptiform discharges, which did not yield clinical manifestations. When the duration threshold was raised to 3 s, the false detection rate fell to 0.5/h. The overlap of automatically detected seizures with the actual seizures was equal to ∼96%. For EEG recordings sampled at 250 Hz, the one-channel processing speed for midrange smartphones running Android 10 (about 0.2 s per 1 min of EEG) was high enough for real-time seizure detection.

Keywords: childhood absence epilepsy, EEG, wavelets, detector, portable device

OPEN ACCESS

Edited by:
Sharon Chiang, University of California, San Francisco, United States

Reviewed by:
Kais Gadhoumi, Duke University, United States
Jon Kleen, University of California, San Francisco, United States

***Correspondence:**
Miroslaw Latka
miroslaw.latka@pwr.edu.pl

Specialty section:
This article was submitted to Epilepsy, a section of the journal Frontiers in Neurology

Received: *25 March 2021*
Accepted: *03 June 2021*
Published: *29 June 2021*

Citation:
Glaba P, Latka M, Krause MJ, Kroczka S, Kuryło M, Kaczorowska-Frontczak M, Walas W, Jernajczyk W, Sebzda T and West BJ (2021) Absence Seizure Detection Algorithm for Portable EEG Devices. Front. Neurol. 12:685814. doi: 10.3389/fneur.2021.685814

1. INTRODUCTION

Typical absence seizures are brief (lasting seconds) generalized nonmotor epileptic seizures with an abrupt onset and termination (1, 2). Transient impairment of consciousness and spike-slow wave discharges (SWDs) in electroencephalogram (EEG) are their characteristic manifestations. Typical absence seizures are severe in childhood (CAE) and juvenile (JAE) absence epilepsies but mild or inconspicuous in other syndromes such as juvenile myoclonic epilepsy (JME). Typical absence seizures are predominantly spontaneous, but in about 90% of untreated patients, they may be provoked by hyperventilation. Sleep deprivation, photostimulation, specific geometric

patterns, video games, and even thinking may also precipitate them. The pathophysiology of absence seizures is fundamentally different from other types of seizures, making their diagnosis and treatment unique.

CAE is the most common pediatric epileptic syndrome with an age of onset of around 6–8 years (3). It has a prevalence of 10–15% in childhood epilepsies. In children under the age of 16 years, the incidence rate is 1.3 to 6 per 100,000. The ictal EEG of a CAE seizure demonstrates rhythmic 3 Hz bilateral, synchronous, and symmetrical spike and wave discharges (SWDs) with a median duration of approximately 10 s, which on average appear several times per day. In pyknoleptic cases, hundreds of seizures may occur daily (4). The 2010 Childhood Absence Epilepsy Study showed that only 37% of all enrolled subjects were free from treatment failure on their first medication a year after diagnosis (5).

JAE typically begins between 10 and 16 years of age and is usually a life-long condition. JAE seizures tend to be longer than in CAE (lasting up to 45 s) and non-pyknoleptic (typically occurring less than daily).

While CAE and JAE are distinct epilepsy syndromes, there is considerable overlap between them, and the cut-off age remains controversial. During disease, patients with JAE or patients in the overlap group are more likely to develop generalized tonic-clonic seizures and myoclonic attacks. In the long-term follow-up (mean 26 years, range 3–69), only 58% of the patients with absence seizures were in remission (6).

The diagnosis of absence seizures is laborious since it requires analysis of long video-EEGs (on average around 30 minutes long) to detect seizures and their clinical manifestations (consciousness impairment, motor symptoms) and abnormal EEG background activity.

The appearance of low-cost, portable EEG devices (7) has paved the way for long-term, remote monitoring of patients with absence seizures. The potential benefits of this kind of monitoring include facilitation of diagnosis, personalized drug titration, and determining of duration of pharmacotherapy. The need for automatic and reliable detection of absence seizures has long been recognized (8). Diverse algorithms have been proposed so far to detect seizures in animal models of epilepsy (9–12) or in human EEG (13–21). Herein, we present a novel approach to absence seizure detection, which is applicable both to clinical EEGs and recordings made with portable EEG devices with a small number of channels. The algorithm's efficiency and robustness to motion artifacts enable its implementation on mobile devices.

2. MATERIALS AND METHODS

2.1. EEG Recordings

Wroclaw Medical University's Ethics Committee approved a retrospective analysis of routine anonymized video-EEG recordings of patients (36 with CAE and 28 with JAE) as well as 30 EEGs of age-matched controls. Epilepsy syndrome was established based on history, age at onset, clinical EEG findings, and neuroimaging. EEGs were acquired with Elmiko Digitrack (BRAINTRONICS B.V. ISO-1032CE amplifier) or Grass Comet Plus EEG (AS40-PLUS amplifier) using 200 or 250 Hz sampling frequency. The international 10-20 standard was used to arrange 19 Ag/AgCl electrodes (impedance below 5kΩ). Total EEG duration was equal to 37 and 9 h for the patients and controls, respectively.

We assigned patients' EEG to either training or testing datasets. In the first one, there were 34 recordings (22 CAE and 12 JAE) with 199 seizures (6 ± 4 per patient and averaged seizure duration equal to 12 ± 4 s). In the 30 recordings of the testing dataset (15 CAE and 15 JAE), there were 177 absence seizures (6 ± 5 per patient and averaged duration equal to 12 ± 6 s). An experienced neurologist carried out a visual EEG inspection and marked the seizures with a 1 s accuracy.

Figure 1 provides the rationale for using the longitudinal bipolar montage. The seizure detector was developed and tested for two channels: Fp1-T3 and Fp2-T4.

We used three filters for EEG preprocessing: a second-order infinite impulse response (IIR), 6th-order high-pass Butterworth with a cutoff frequency of 0.5 Hz, and 6th-order low-pass Butterworth with a cutoff frequency of 25 Hz. These filters remove 50 Hz power line noise, EEG baseline drift, and muscle artifacts, respectively.

2.2. Continuous Wavelet Transform

The continuous wavelet transform (CWT) of a signal $s(t)$ is an integral transform:

$$T[s](a,t_0) = \frac{1}{\sqrt{a}} \int_{-\infty}^{+\infty} s(t)\psi^* \left(\frac{t-t_0}{a} \right) dt \tag{1}$$

with the basis functions $\psi(a,t_0) = \psi(t - t_0/a)$, known as wavelets, that are translated and scaled version of the mother function $\psi(t)$ (22). Motivated by the results of the previous study (23), as a mother function, we use the complex Morlet wavelet (24, 25):

$$\psi(t) = \frac{1}{\pi^{1/4}} e^{2\pi i f_c t} e^{-t^2/2} \tag{2}$$

whose Fourier transform $\hat{\psi}(f)$ is given by

$$\hat{\psi}(f) = \sqrt{2}\sqrt[4]{\pi} e^{-2\pi^2 (f-fc)^2}. \tag{3}$$

The real parameter f_c is called the center frequency since it is equal to the maximum point of the wavelet's Fourier power spectrum. The scale a corresponds to the following pseudofrequency:

$$f_a = \frac{f_c}{a}. \tag{4}$$

As we can see in Equations (2, 3), the wavelets are localized both in time and frequency domains. This dual localization makes CWT particularly applicable to the detection of transient events such as absence seizures.

Seizure detection is based on the properties of the instantaneous wavelet power $\left|T[s](a,t_0)\right|^2$ normalized by signal's variance σ^2:

$$w^{(n)}(f_a,t_0) = \left|T[s](a,t_0)\right|^2 / \sigma^2. \tag{5}$$

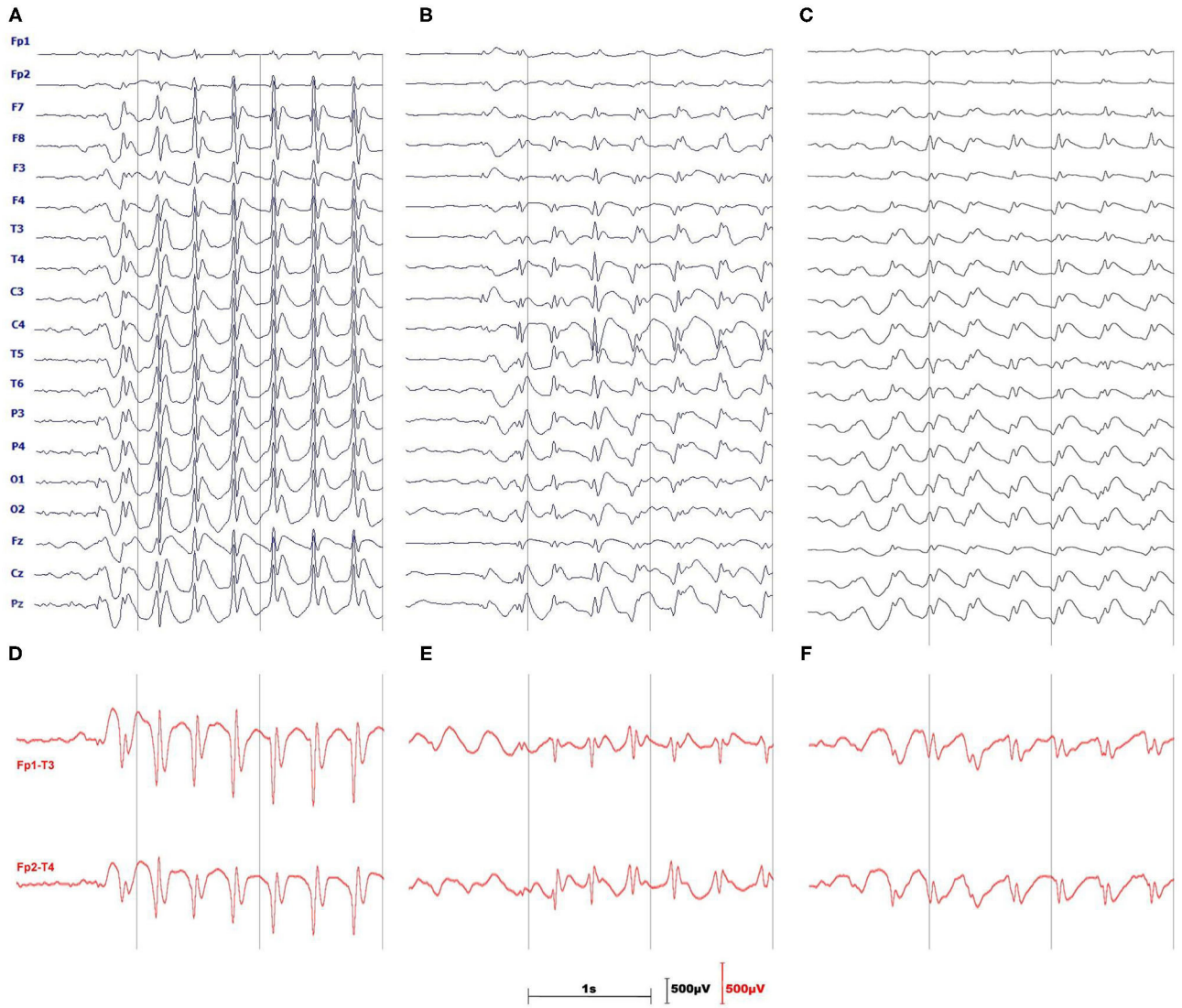

FIGURE 1 | Three monopolar EEGs illustrate the difficulties of absence seizure detection in a single channel. **(A)** is a textbook example of prominent, generalized SWDs. The amplitude of spikes **(B)** or slow waves **(C)** may be small and SWDs may be pronounced only in a handful of channels. **(D–F)** show the advantages of using the longitudinal, bipolar montage which in most cases augments both spikes and slow waves of SWDs.

If we apply the convolution theorem to Equation (1), then it is apparent that the Fourier transform of $T[s](a, t_0)$ is the pointwise product of the Fourier transforms of the signal and wavelet. Thus, it is possible to calculate CWT by taking the inverse Fourier transform of such a product. We used this approach in the MATLAB function, presented in **Supplementary Materials**, which calculates the complex Morlet CWT (25). We included the listing to facilitate the reproduction of the results and avoid confusion related to erroneous normalization of the most popular Python and MATLAB CWT implementations. We will discuss this problem in a forthcoming publication.

For the most commonly used wavelets, such as the complex Morlet, the analytical expression for their Fourier transform is known. Therefore, in the presented function, we calculate only the FFT of the signal and use Equation (3) to obtain the wavelet's FFT spectrum.

The complex Morlet CWT of the preprocessed Fp1-T3 and Fp2-T4 channels was calculated without signal partitioning.

2.3. Detection Algorithm

The detection of an absence seizure (**Figures 2A,E**), defined as an SWD lasting for more than 2 s (26), proceeds in two steps. First, we locate the train of slow waves and then verify that there are epileptic spikes embedded in it. One can see in the scalogram **Figure 2B** that when the wavelet's pseudofrequency is close to that of an absence ($\sim$ 3 Hz), then the wavelet power forms a prominent ridge. We refer to the time interval during which the power exceeds the chosen threshold T_E as the slow-wave

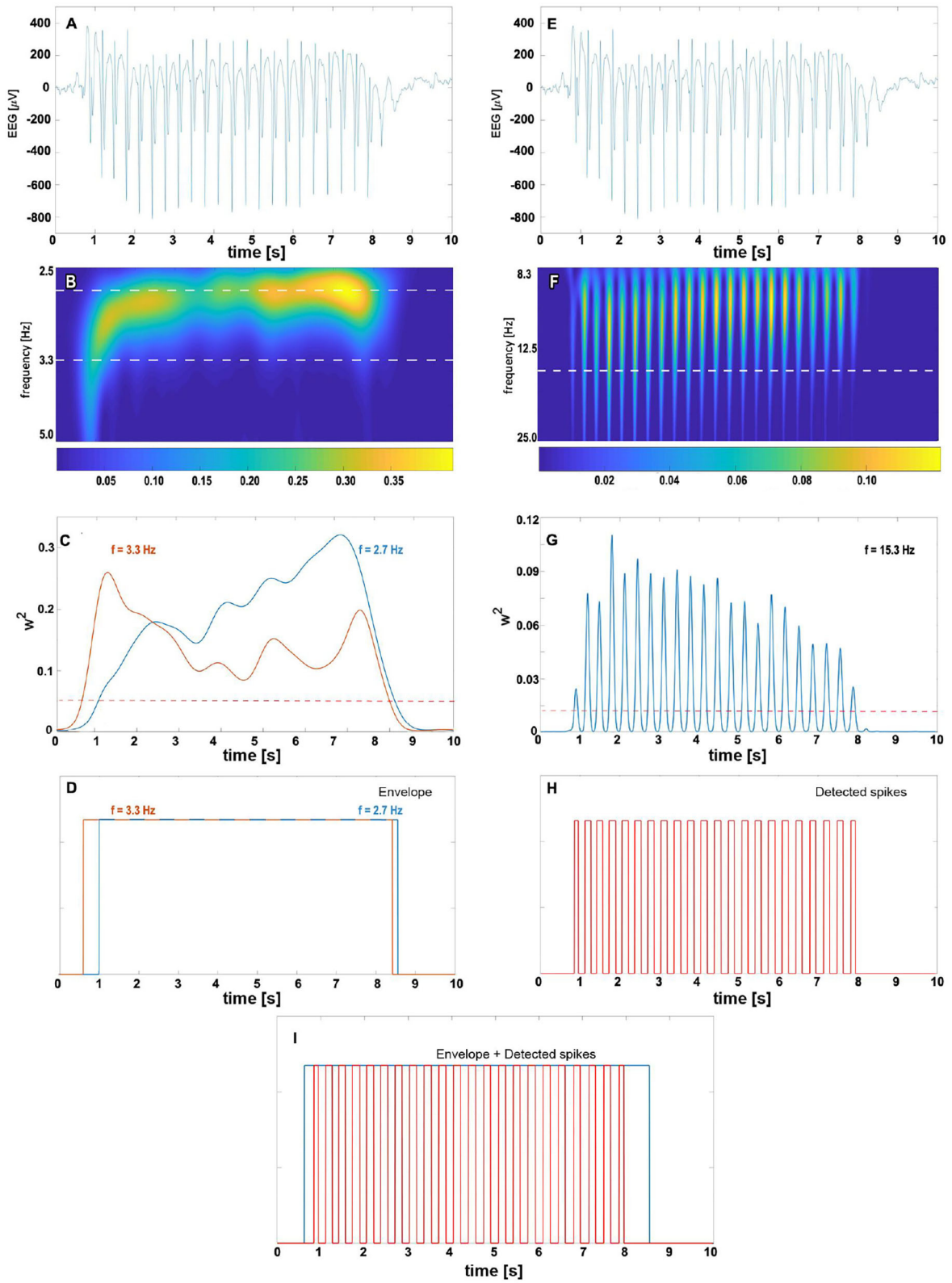

FIGURE 2 | The complex Morlet wavelet analysis of absence slow wave **(B–D)** and spikes **(F–H)**. For clarity, absence EEG is presented at the top of both columns (subplots **A,E**). The density map **(B)** shows the time evolution of normalized wavelet power for pseudo-frequencies in [2.5, 5] Hz range. The 2.7 and 3.3 Hz cuts

(Continued)

FIGURE 2 | (marked with the white horizontal dashed line) are plotted in subplot **(C)** with the blue and orange lines, respectively. We refer to time intervals during which the wavelet power for these frequencies exceeds the predetermined threshold (represented in **(C)** by the red dashed horizontal line) as the slow-wave envelopes. For a given seizure, the total envelope is obtained by merging 2.7 and 3.3 Hz envelopes as shown in **(D)**. The right column shows the complex Morlet analysis with parameters tuned to spike detection. The prominent ridges in wavelet power density map **(F)** and peaks in 15.3 Hz cut **(G)** are manifestations of seizure's spikes. The white horizontal dashed line in **(F)** corresponds to the spike frequency 15.3 Hz obtained in the grid search. The train of unit pulses in **(H)** indicates time intervals during which wavelet power for 15.3 Hz is greater than the spike threshold value (marked in subplot **(G)** with the red dashed horizontal line). An absence is detected whenever the epileptic spikes are found in the slow-wave envelope **(I)**.

envelope. This envelope is a unit boxcar function that takes on one whenever the power is greater than T_E. As the frequency of SWDs is subject-dependent and may even slightly vary during a seizure (15), we construct two envelopes with wavelet frequencies f_{low} and f_{high} (**Figure 2C**) and merge them as shown in **Figure 2D**. The merging amounts to a pointwise application of a logical OR function to both envelopes.

For a suitably chosen pseudofrequency f_{spike}, the wavelet power $w^{(n)}(f_{spike})$ peaks around the position of epileptic spikes (**Figure 2F**). If the percentage of samples PT within the final envelope for which the wavelet power is greater than T_S, we conclude that there are spikes (**Figure 2H**) within the envelope (**Figure 2I**). Such the envelope delineates the absence seizure.

In some cases, $w^{(n)}(f_{spike})$ may also be elevated for high-amplitude artifacts. To reduce the number of false positives, we modified the original algorithm. We do the following amplitude check and disregard all envelopes for which:

- More than 10% of the samples have amplitudes outside the range [−500 μV, 500 μV] (in the differential montage epileptic spikes can have amplitudes of the order of hundreds μV).
- Any sample is outside the range [−1,000 μV, 1,000 μV].

For envelopes shorter than 5 s, we also calculate the variance of $w^{(n)}(f_{spike})$ to detect the wavelet power pulsatility of absence (**Figure 2G**). If such variance is greater than T_V, the detector flags the envelope as a seizure. We refer to such a comparison as the wavelet variance check.

Figure 3 shows the flowchart of the final absence seizure detection algorithm. The proposed algorithm may be used independently for channels Fp1-T3 and Fp2-T4. Alternatively, the seizure envelopes from these two channels may be superposed.

2.4. Determination of Algorithms' Parameters

We determine f_{low}, f_{high}, and T_E by maximizing the overlap of slow-wave envelopes with the absence seizures from a training dataset disregarding possible false detections.

Using these values, we search for the maximum of the following objective function:

$$O(f_{spike}, T_S, PT) = OVR_f - PERR - 0.5 \times FDET - FDET_C \quad (6)$$

to find f_{spike}, T_S, and PT_S – spike detection parameters. In Eq (6), OVR_f is the percentage overlap of slow-wave envelopes with seizures. $PERR$ is the percentage of the number of false positive samples in a given EEG. $FDET$ and $FDET_C$ are the number of false detections for the patients and controls, respectively.

The form of the objective function follows two requirements. The first is that we want to overlap the slow-wave envelope with the seizure as accurately as possible. The second is that in patients, false positives can be associated with epileptiform discharges with no clinical manifestations. Therefore, in Eq (6), the weight assigned to the patients' false detection penalty ($FDET$) is half of that given to the controls. We arbitrarily chose the 1:2 weight ratio.

T_V can be determined in the following way. We calculate the variance of $w^{(n)}(f_{spike})$ for the controls' EEGs. Then, we calculate the mean and standard deviation of the distribution. Finally, T_V is set to the mean increased by three standard deviations (T_V = 0.05).

We determined the slow-wave and spike detection parameters using the exhaustive grid search.

2.5. Software Implementation

The seizure detection software was implemented both in MATLAB (R2018a) and Java. In the latter case, we wrote a desktop version (which can be run on any computer with Java virtual machine) and a mobile version for Android smartphones. In Java software, we used the class FastFourierTransformer from Apache Commons Math Library (version 3.6.1). Testing and performance benchmarking was performed on a desktop PC with AMD Ryzen 7 3700X 8-Core processor running Windows 10 and Samsung S9 mobile phone (4GB of RAM and 2.8 GHz Samsung Exynos 9810 8-Core processor) with Android 10.

3. RESULTS

Using two-step (slow-wave envelope and spike detection) optimization on the training dataset, we obtained the following model parameters f_{low} = 2.7 Hz, f_{high} = 3.3 Hz, T_E = 0.05, f_{spike} = 15.3 Hz, T_S = 0.012, PT_S = 12%. After the parameters were determined, we lowered the value of T_V from 0.05 to 0.008. This change is explained in Discussion section.

The seizure detector had 98.5% and 96.6% sensitivity for the training and testing datasets, respectively (see **Supplementary Tables 1, 2**). The corresponding false detection rates were equal to 0.9/h and 0.4/h. The overlap OVR of the detected and actual seizures was good for both datasets (97% ± 6% and 95% ± 10%). The percentage error $PERR$ that accounts for both false positives and erroneously extended slow-wave envelopes was equal to 0.9% ± 0.7% for both datasets.

Supplementary Table 3 shows that both the amplitude and wavelet variance checks contribute to the false detection reduction.

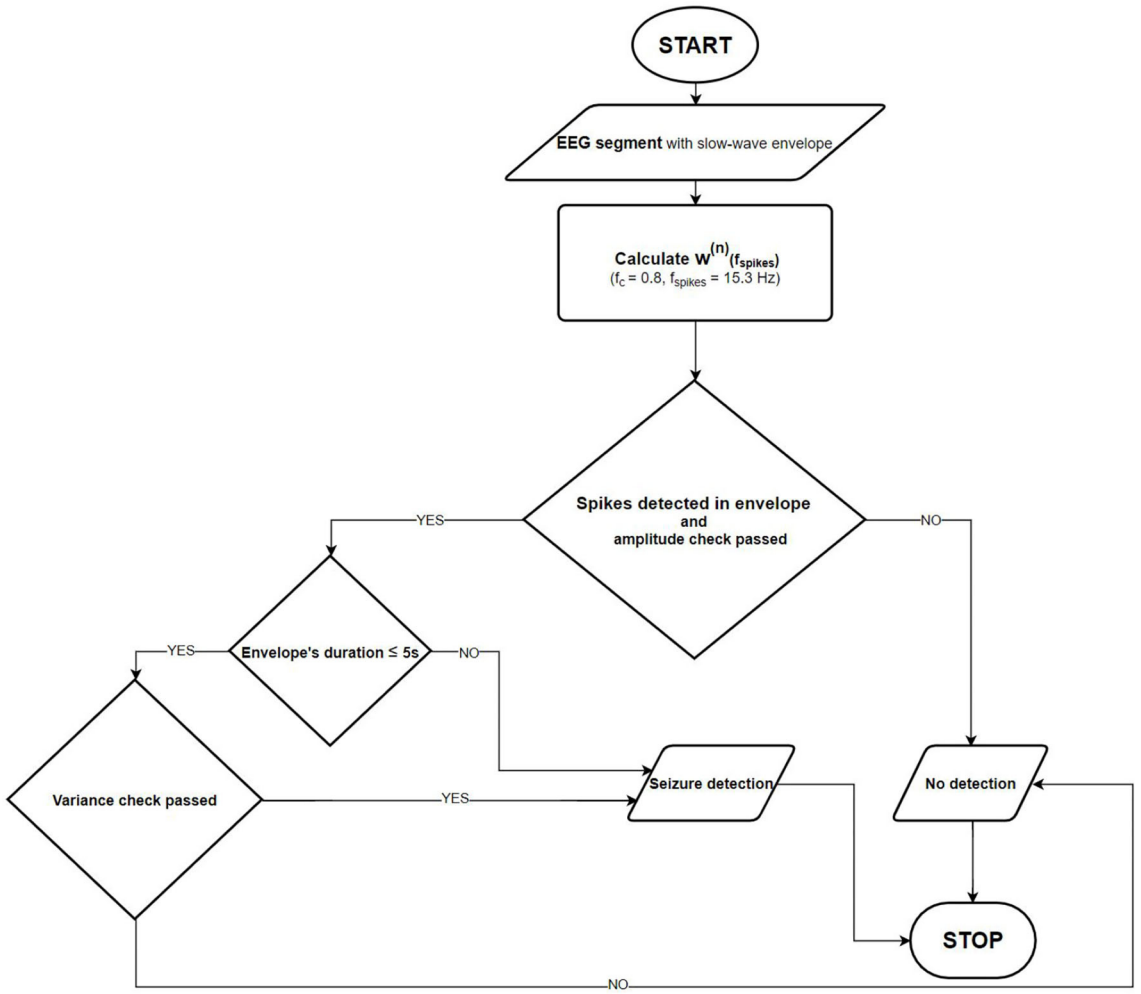

FIGURE 3 | Absence seizure detection flowchart. Once the slow-wave envelope is present in an analyzed EEG segment, the detector checks whether there are epileptic spikes embedded in it. The amplitude and the normalized wavelet power variance checks are also performed to eliminate artifacts.

In **Supplementary Table 4**, we compare the execution times of three absence seizure detector implementations. The execution time is determined by the efficiency of an FFT function, which is used to calculate the continuous wavelet transform. Matlab is renowned for its FFT implementation. Thus, it is not surprising that for the longest segment ($N = 2^{18}$), the Matlab version of the detector ran almost 16 and 19 times faster than the Java software running on Windows 10 and Android 10 (0.18 s vs. 2.79 s and 3.41 s). Interestingly enough, for shorter segments, the detector ran faster on the mid-range Android device than on the PC. Nevertheless, the single-channel Android processing speed of 0.2 s per minute of EEG is adequate for real-time seizure detection.

4. DISCUSSION

It has long been recognized that long-term EEG monitoring is the most reliable method for absence detection (27). Parents notice only about 6% of daytime seizures, and very often, teachers are the ones who recognize the CAE/JEA beginning (28). The 2010 Childhood Absence Epilepsy Study (5) has provided a compelling rationale for using portable EEG devices in the management of CAE/JEA patients. This randomized controlled trial showed that only 37% of all enrolled subjects were free from treatment failure on their first medication a year after diagnosis.

In the last two decades, many researchers have investigated absence seizure detection (13–17, 20). The datasets in these studies were small–the analyzed SWDs came from nine patients (range 2–20). On average, there were 70 seizures longer than 2 s (range 2–158). In all but one algorithm (20), discrete wavelet transform was used for signal preprocessing. Machine learning was used in 3 of 4 detectors. On average, 11 features were extracted from 15 EEG channels.

Kjaer et al. (19) used an experimental EEG setup with 3 electrodes for 24-h EEG monitoring of 6 patients (593 seizures). Their support vector machine detected 98.4% SWD's with 0.23/h false detection rate using 10 features of five-level db4 wavelet EEG decomposition.

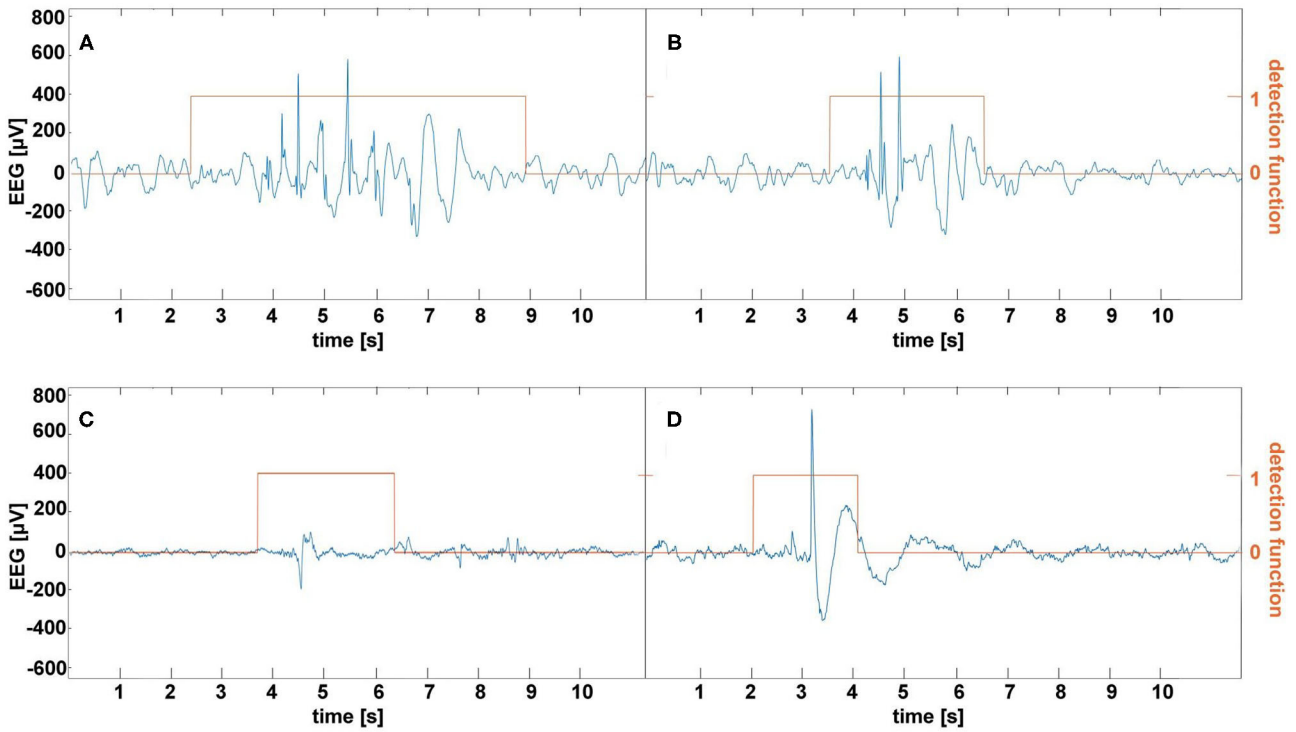

FIGURE 4 | Examples of false absence seizure detection in the EEG of the patients **(A,B)** and controls **(C,D)**. The epileptiform discharges in **(A,B)** were not accompanied by the clinical manifestations. **(C)** shows a rare example of a muscle artifact classified as an absence. A prominent spike-and-wave in **(D)** appeared in a healthy subject's EEG.

The absence seizure detection algorithm presented in this work is unique because it exploits the apparent traits of SWDs and EEG motion artifacts. Despite the simplicity, its 97.6% accuracy matches that of black-box machine learning classifiers.

Our experience indicates that frequent, albeit not excessively long, EEG home monitoring is feasible in pediatric patients as long as an EEG wearable is easy to put on and is comfortable. This study used the bipolar channels Fp1-T3 and Fp2-T4 for seizure detection because they approximately corresponded to the Muse headband electrode placement. On the one hand, this choice seems to be rational given absence seizures are usually well pronounced in the frontal regions (29) and the large spacing between the electrodes augments the characteristic features of SWDs as shown in **Figure 1**. On the other hand, Fp1 and Fp2 channels are prone to muscle and eyeblink artifacts. There were 26 and 8 false detections in the patients and controls, respectively. In the patients, all false detections were associated with epileptiform discharges, which did not yield clinical manifestations. Half of the errors in the control group were caused by the prominent SWDs. We show the examples of misclassified EEG segments in **Figure 4**. We used the stringent value $T_V = 0.05$ for the determination of the model parameters. Once we realized that false detections are not caused by motion artifacts, for classification, we lowered this parameter to 0.008 to maximize the detection sensitivity (for $T_V = 0.05$, the sensitivity was equal to 93% with the false detection rate 0.4/h). Some pediatricians agree that sensitivity of 90% and false detection rate of 1/h are clinically acceptable (19).

Unlike previous studies, the false detection rate was not determined by the motion artifacts. We would like to emphasize that the presented seizure detection was performed on clinical EEGs, which is the main limitation of this study. The question arises as to whether the amplitude and wavelet variance checks would be equally effective in eliminating motion artifacts in EEGs acquired with wearable devices in home settings. It is worth mentioning that the false detection rate can be reduced by using secondary electrodes for artifact cancellation (30) and employing different single-channel artifact detectors (31, 32). As most commercial EEG bands have MEMS accelerometers, one may also explore the possibility of incorporating head acceleration in the artifact removal algorithm. However, the connection between EEG artifacts and head movement is not always apparent (33).

In a recent study, Dan et al. presented an absence seizure detector based on a linear multichannel filter that was precomputed offline in a data-driven fashion based on the spatial-temporal signature of the seizure and peak interference statistics (21). The performance of this detector depends on the number of channels (from 3 to 18) used in the calculations. For the three channels, the accuracy was equal to 95% with a 0.4/h false detection rate. The authors set the minimum seizure length to 3 s (34). It is worth pointing out that for this absence duration threshold, the two-channel detector described in this work had

the false detection rate equal to 0.5/h (18 and 6 false detections for the patients, and controls, respectively.

To the best of our knowledge, we used the most diverse set of CAE/JAE EEGs (37 h of recordings from 64 patients) for development and testing. The overlap of automatically detected seizures with the actual seizures was high (about 96%). The poor overlap in some patients is predominantly caused by a very small amplitude of the epileptic spikes. Consequently, the detector does not classify such SWD trains as absence seizures. At the end of the seizure, the frequency of SWDs can decrease far below the canonical value of 3 Hz. In this case, the slow-wave envelope is shorter than expected. The frequency drop during the seizure leads to its sfragmentation.

For EEG recordings sampled at 250 Hz, the one-channel processing speed for midrange smartphones running Android 10 was high enough (about 0.2 s per 1 min of EEG) for real-time seizure detection. We found that the detection accuracy was highest for a sliding 30 s EEG buffer, which was shifted by 10 s.

Absence seizure manifestations are mild compared to other epileptic syndromes. Consequently, the rationale for using seizure detectors in CAE/JAE patients is different. Emphasis may be shifted from detection alerts to the facilitation of drug titration and side effects elimination. Unobtrusiveness and ease of use are particularly important for pediatric patients, who may be more willing to tolerate regular EEG measurements if they are incorporated into daily routines such as watching cartoons, playing mobile games, or listening to music.

It is worth pointing out that remote seizure monitoring will be one of the elements of personalized CAE/JAE treatment. There is a growing interest in the development of biomarkers of treatment response and side effects (35). These problems are the subject of our research (36).

DATA AVAILABILITY STATEMENT

The raw data supporting the conclusions of this article will be made available by the authors, without undue reservation.

ETHICS STATEMENT

The studies involving human participants were reviewed and approved by Wroclaw Medical University's Ethics Committee. Written informed consent for participation was not required for this study in accordance with the national legislation and the institutional requirements.

AUTHOR CONTRIBUTIONS

ML, PG, and MK: conceptualization and methodology. PG, ML and MJK: investigation original draft preparation. BW, WW, SK, TS, and WJ: review and editing. All authors contributed to formal analysis.

SUPPLEMENTARY MATERIAL

The Supplementary Material for this article can be found online at: https://www.frontiersin.org/articles/10.3389/fneur.2021.685814/full#supplementary-material

REFERENCES

1. Panayiotopoulos CP. *The Epilepsies: Seizures, Syndromes and management*. Oxfordshire (UK): Bladon Medical Publishing (2005).
2. Fisher RS, Cross JH, French JA, Higurashi N, Hirsch E, Jansen FE, et al. Operational classification of seizure types by the International league against epilepsy: position paper of the ILAE commission for classification and terminology. *Epilepsia*. (2017) 58:522–30. doi: 10.1111/epi.13670
3. Covanis A. *Childhood Absence Epilepsy*. Springer-Verlag: Atlas of epilepsies London (2010) p. 1013–23.
4. Schomer DL, da Silva FL. *Niedermeyer's Electroencephalography: Basic Principles, Clinical Applications, and Related Fields*. Oxford University Press (2018).
5. Glauser TA, Cnaan A, Shinnar S, Hirtz DG, Dlugos D, Masur D, et al. Ethosuximide, valproic acid, and lamotrigine in childhood absence epilepsy: initial monotherapy outcomes at 12 months. *Epilepsia*. (2013) 54:141–55. doi: 10.1111/epi.12028
6. Trinka E, Baumgartner S, Unterberger I, Unterrainer J, Luef G, Haberlandt E, et al. Long-term prognosis for childhood and juvenile absence epilepsy. *J Neurol*. (2004) 251:1235–41. doi: 10.1007/s00415-004-0521-1
7. Krigolson OE, Williams CC, Norton A, Hassall CD, Colino FL. Choosing MUSE: validation of a low-cost, portable EEG system for ERP research. *Front Neurosci*. (2017) 11:109. doi: 10.3389/fnins.2017.00109
8. Faust O, Acharya UR, Adeli H, Adeli A. Wavelet-based EEG processing for computer-aided seizure detection and epilepsy diagnosis. *Seizure*. (2015) 26:56–64. doi: 10.1016/j.seizure.2015.01.012
9. Sitnikova E, Hramov AE, Koronovsky AA, van Luijtelaar G. Sleep spindles and spike–wave discharges in EEG: their generic features, similarities and distinctions disclosed with Fourier transform and continuous wavelet analysis. *J Neurosci Methods*. (2009) 180:304–16. doi: 10.1016/j.jneumeth.2009.04.006
10. Ovchinnikov A, Lüttjohann A, Hramov A, Van Luijtelaar G. An algorithm for real-time detection of spike-wave discharges in rodents. *J Neurosci Methods*. (2010) 194:172–8. doi: 10.1016/j.jneumeth.2010.09.017
11. Bauquier SH, Lai A, Jiang JL, Sui Y, Cook MJ. Evaluation of an automated spike-and-wave complex detection algorithm in the EEG from a rat model of absence epilepsy. *Neurosci Bull*. (2015) 31:601–10. doi: 10.1007/s12264-015-1553-5
12. Grubov V, Sitnikova E, Pavlov A, Koronovskii A, Hramov A. Recognizing of stereotypic patterns in epileptic EEG using empirical modes and wavelets. *Phys A Stat Mech Appl*. (2017) 486:206–17. doi: 10.1016/j.physa.2017.05.091
13. Adeli H, Zhou Z, Dadmehr N. Analysis of EEG records in an epileptic patient using wavelet transform. *J Neurosci Methods*. (2003) 123:69–87. doi: 10.1016/S0165-0270(02)00340-0
14. Subasi A. Application of adaptive neuro-fuzzy inference system for epileptic seizure detection using wavelet feature extraction. *Comput Biol Med*. (2007) 37:227–44. doi: 10.1016/j.compbiomed.2005.12.003
15. Xanthopoulos P, Rebennack S, Liu CC, Zhang J, Holmes GL, Uthman BM, et al. A novel wavelet based algorithm for spike and wave detection in absence epilepsy. In: *2010 IEEE International Conference on BioInformatics and BioEngineering*. (Washington, DC: IEEE) (2010). p. 14–19.
16. Petersen EB, Duun-Henriksen J, Mazzaretto A, Kjær TW, Thomsen CE, Sorensen HB. Generic single-channel detection of absence seizures. In: *2011 Annual International Conference of the IEEE Engineering in Medicine and Biology Society*. (Boston, MA: IEEE) (2011). p. 4820–3.
17. Duun-Henriksen J, Madsen RE, Remvig LS, Thomsen CE, Sorensen HB, Kjaer TW. Automatic detection of childhood absence epilepsy seizures: toward a monitoring device. *Pediatr Neurol*. (2012) 46:287–92. doi: 10.1016/j.pediatrneurol.2012.02.018

18. Zeng K, Yan J, Wang Y, Sik A, Ouyang G, Li X. Automatic detection of absence seizures with compressive sensing EEG. *Neurocomputing*. (2016) 171:497–502. doi: 10.1016/j.neucom.2015.06.076
19. Kjaer TW, Sorensen HB, Groenborg S, Pedersen CR, Duun-Henriksen J. Detection of paroxysms in long-term, single-channel EEG-monitoring of patients with typical absence seizures. *IEEE J Transl Eng Health Med*. (2017) 5:1–8. doi: 10.1109/JTEHM.2017.2649491
20. Tenneti SV, Vaidyanathan P. Absence seizure detection using Ramanujan filter banks. In: *2018 52nd Asilomar Conference on Signals, Systems, and Computers*. (Danvers, MA: IEEE) (2018). p. 1913–7.
21. Dan J, Vandendriessche B, Paesschen WV, Weckhuysen D, Bertrand A. Computationally-Efficient Algorithm for Real-Time Absence Seizure Detection in Wearable Electroencephalography. *Int J Neural Syst*. (2020) 30:2050035. doi: 10.1142/S0129065720500355
22. Mallat S. *A Wavelet Tour of Signal Processing*. Burlington, MA: Elsevier (1999).
23. Latka M, Was Z, Kozik A, West BJ. Wavelet analysis of epileptic spikes. *Phys Rev E*. (2003) 67:052902. doi: 10.1103/PhysRevE.67.052902
24. Addison PS. *The Illustrated Wavelet Transform Handbook: Introductory Theory and Applications in Science, Engineering, Medicine and Finance*. Boca Raton, FL; London; New York, NY: CRC Press (2017).
25. Addison PS. Introduction to redundancy rules: the continuous wavelet transform comes of age. *Phil Trans R Soc A*. (2018) 376:20170258. doi: 10.1098/rsta.2017.0258
26. Szaflarski JP, DiFrancesco M, Hirschauer T, Banks C, Privitera MD, Gotman J, et al. Cortical and subcortical contributions to absence seizure onset examined with EEG/fMRI. *Epilepsy Behav*. (2010) 18:404–13. doi: 10.1016/j.yebeh.2010.05.009
27. Browne TR, Dreifuss FE, Penry JK, Porter RJ, White BG. Clinical and EEG estimates of absence seizure frequency. *Arch Neurol*. (1983) 40:469–72. doi: 10.1001/archneur.1983.04210070009004
28. Keilson MJ, Hauser WA, Magrill JP, Tepperberg J. Ambulatory cassette EEG in absence epilepsy. *Pediatr Neurol*. (1987) 3:273–6. doi: 10.1016/0887-8994(87)90067-1
29. Jun YH, Eom TH, Kim YH, Chung SY, Lee IG, Kim JM. Source localization of epileptiform discharges in childhood absence epilepsy using a distributed source model: a standardized, low-resolution, brain electromagnetic tomography (sLORETA) study. *Neurol Sci*. (2019) 40:993–1000. doi: 10.1007/s10072-019-03751-4
30. Nordin AD, Hairston WD, Ferris DP. Dual-electrode motion artifact cancellation for mobile electroencephalography. *J Neural Eng*. (2018) 15:056024. doi: 10.1088/1741-2552/aad7d7
31. Chen X, Liu A, Chiang J, Wang ZJ, McKeown MJ, Ward RK. Removing muscle artifacts from EEG data: multichannel or single-channel techniques? *IEEE Sensors J*. (2015) 16:1986–97. doi: 10.1109/JSEN.2015.2506982
32. Dhindsa K. Filter-bank artifact rejection: high performance real-time single-channel artifact detection for EEG. *Biomed Sig Proc Control*. (2017) 38:224–35. doi: 10.1016/j.bspc.2017.06.012
33. Kline JE, Huang HJ, Snyder KL, Ferris DP. Isolating gait-related movement artifacts in electroencephalography during human walking. *J Neural Eng*. (2015) 12:046022. doi: 10.1088/1741-2560/12/4/046022
34. Tenney JR, Glauser TA. The current state of absence epilepsy: can we have your attention? the current state of absence epilepsy. *Epilepsy Curr*. (2013) 13:135–40. doi: 10.5698/1535-7511-13.3.135
35. Kessler SK, McGinnis E. A practical guide to treatment of childhood absence epilepsy. *Pediatr Drugs*. (2019) 21:15–24. doi: 10.1007/s40272-019-00325-x
36. Glaba P, Latka M, Krause MJ, Kuryło M, Jernajczyk W, Walas W, et al. Changes in interictal pretreatment and posttreatment EEG in childhood absence epilepsy. *Front Neurosci*. (2020) 14:196. doi: 10.3389/fnins.2020.00196

Conflict of Interest: The authors declare that the research was conducted in the absence of any commercial or financial relationships that could be construed as a potential conflict of interest.

frontiers in Neurology

REVIEW
published: 13 July 2021
doi: 10.3389/fneur.2021.690404

Seizure Diaries and Forecasting With Wearables: Epilepsy Monitoring Outside the Clinic

Benjamin H. Brinkmann[1†], Philippa J. Karoly[2†], Ewan S. Nurse[2,3†], Sonya B. Dumanis[4], Mona Nasseri[1,5], Pedro F. Viana[6,7], Andreas Schulze-Bonhage[8], Dean R. Freestone[3], Greg Worrell[1], Mark P. Richardson[6] and Mark J. Cook[2]*

[1] Department of Neurology, Mayo Foundation, Rochester, MN, United States, [2] Department of Medicine, Graeme Clark Institute and St Vincent's Hospital, The University of Melbourne, Fitzroy, VIC, Australia, [3] Seer Medical, Melbourne, VIC, Australia, [4] Epilepsy Foundation, Landover, MD, United States, [5] School of Engineering, University of North Florida, Jacksonville, FL, United States, [6] Institute of Psychiatry, Psychology and Neuroscience, King's College London, London, United Kingdom, [7] Faculty of Medicine, University of Lisbon, Lisboa, Portugal, [8] Faculty of Medicine, Epilepsy Center, Medical Center, University of Freiburg, Freiburg, Germany

OPEN ACCESS

Edited by:
David M. Labiner, University of Arizona, United States

Reviewed by:
Claudio M. T. Queiroz, Federal University of Rio Grande do Norte, Brazil
Enes Akyuz, University of Health Sciences, Turkey

***Correspondence:**
Benjamin H. Brinkmann
brinkmann.benjamin@mayo.edu

†These authors share first authorship

Specialty section:
This article was submitted to Epilepsy, a section of the journal Frontiers in Neurology

Received: *02 April 2021*
Accepted: *10 June 2021*
Published: *13 July 2021*

Citation:
Brinkmann BH, Karoly PJ, Nurse ES, Dumanis SB, Nasseri M, Viana PF, Schulze-Bonhage A, Freestone DR, Worrell G, Richardson MP and Cook MJ (2021) Seizure Diaries and Forecasting With Wearables: Epilepsy Monitoring Outside the Clinic. Front. Neurol. 12:690404. doi: 10.3389/fneur.2021.690404

It is a major challenge in clinical epilepsy to diagnose and treat a disease characterized by infrequent seizures based on patient or caregiver reports and limited duration clinical testing. The poor reliability of self-reported seizure diaries for many people with epilepsy is well-established, but these records remain necessary in clinical care and therapeutic studies. A number of wearable devices have emerged, which may be capable of detecting seizures, recording seizure data, and alerting caregivers. Developments in non-invasive wearable sensors to measure accelerometry, photoplethysmography (PPG), electrodermal activity (EDA), electromyography (EMG), and other signals outside of the traditional clinical environment may be able to identify seizure-related changes. Non-invasive scalp electroencephalography (EEG) and minimally invasive subscalp EEG may allow direct measurement of seizure activity. However, significant network and computational infrastructure is needed for continuous, secure transmission of data. The large volume of data acquired by these devices necessitates computer-assisted review and detection to reduce the burden on human reviewers. Furthermore, user acceptability of such devices must be a paramount consideration to ensure adherence with long-term device use. Such devices can identify tonic–clonic seizures, but identification of other seizure semiologies with non-EEG wearables is an ongoing challenge. Identification of electrographic seizures with subscalp EEG systems has recently been demonstrated over long (>6 month) durations, and this shows promise for accurate, objective seizure records. While the ability to detect and forecast seizures from ambulatory intracranial EEG is established, invasive devices may not be acceptable for many individuals with epilepsy. Recent studies show promising results for probabilistic forecasts of seizure risk from long-term wearable devices and electronic diaries of self-reported seizures. There may also be predictive value in individuals' symptoms, mood, and cognitive performance. However, seizure forecasting requires perpetual use of a device for monitoring, increasing the importance of the system's acceptability to users. Furthermore, long-term studies with concurrent EEG confirmation are lacking currently. This review describes the current

evidence and challenges in the use of minimally and non-invasive devices for long-term epilepsy monitoring, the essential components in remote monitoring systems, and explores the feasibility to detect and forecast impending seizures *via* long-term use of these systems.

Keywords: wearable devices, seizure detection, seizure forecasting, multidian cycles, machine learning, epilepsy

INTRODUCTION

It has long been recognized that seizures occur more frequently than self-reported, though the scale of this underestimation has only recently been appreciated (1–4). This has complicated our ability to provide optimal care and safety strategies (5, 6), and casts uncertainty on the validity of therapeutic strategies and clinical trials results (4).

Wearable sensing devices are increasing in popularity both in the general community and through medical applications such as seizure detection. However, there is insufficient data relating to the clinical utility and reliability of these systems (7). There are also significant concerns around data security, privacy, and data ownership (8), and questions relating to the optimal software, hardware, and data transmission systems. Additionally, there are several separate issues to consider with wearable devices: how the data is acquired, what systems can be used to achieve this acquisition, and how the data may be used to provide more sophisticated feedback to individuals and their caregivers. Wearable devices may also facilitate reliable forecasts of seizure likelihood, providing the potential for people with epilepsy to take fast-acting medications or modify activities in anticipation of an impending seizure (9–11).

Chronically implanted intracranial electroencephalography (EEG) systems have resulted in dramatic insights into the dynamics and underlying rhythms of epileptic activity and seizures (2, 12–19) but are not suitable for widespread use because of issues relating to cost and risk, and are limited in spatial sampling. In addition to unreported seizures, these devices also detect a large number of electrographic seizure patterns without clear behavioral correlates. However, this electrographic epileptic activity is highly relevant to epilepsy management and seizure forecasting, and chronic EEG remains vital to develop and validate standalone wearable systems. These recent studies suggest that the aims of seizure forecasting might be achieved through capturing data, which represent trends and associations in individuals and populations, harnessing the strength of multiple sources, and applying recently developed strategies in machine-learning to combine this information and generate measures of seizure risk. Seizure forecasting using these techniques might ultimately become a useful way for individuals to manage daily activities, and for clinicians to accurately judge the efficacy of therapies.

SEIZURE REPORTING AND DETECTION

An obstacle currently to clinical management of epilepsy is the scarcity of accurate, reliable information available to the physician when diagnosing a seizure disorder and identifying therapeutic options. Because seizure events are infrequent, the physician may not be able to directly observe events, and must rely on the individual, caregivers, and other witnesses to describe events, identify potential precipitants, report their frequency, and discuss the impact on the person's daily life (20). In-hospital diagnostic tests are expensive and may produce a diagnosis of epilepsy, psychogenic non-epileptic events, or syncope, or may be diagnostically inconclusive. Even when a clear diagnosis of epilepsy is established, the limited availability of accurate information hinders effective therapy (1). People with epilepsy may be partly or fully amnestic to seizures (21, 22), individuals may be unable to provide an accurate account of seizure occurrence and severity (23–25), and witness accounts of epileptic and behavioral events are often unreliable (26–28). Changes in seizure frequency and severity, sometimes due to poor medication adherence (29), may increase a person's risk of SUDEP (30), status epilepticus (31), or injury during daily activities. Currently, physicians and caregivers have no way to identify increases in seizure frequency and/or severity between office visits. Many studies confirm that people under-report their seizures for a variety of reasons [summarized by Elger and Hoppe (3)]. A study of an implanted EEG monitoring device for seizure forecasting (2), compared to monthly self-reported seizure diaries to ambulatory intracranial EEG, found vast discrepancies in seizure reports, with some subjects reporting no seizures in months where the device recorded hundreds of clinical and electrographic seizures. Compared to long-term ambulatory EEG monitoring, individuals were found to report less than half of measured seizures (3), and people with epilepsy enrolled in clinical medication trials were aware of their own seizure underreporting in post-study telephone interviews (4).

Objective data characterizing seizure counts (32) and severity (33) could be obtained using devices capable of capturing and storing EEG or other biosignals that indicate seizure occurrence. Invasive, implanted EEG (33) devices with limited capabilities are available currently. The NeuroPace RNS device (16, 34) is clinically available and provides responsive neurostimulation to suppress seizures in focal epilepsy, but also has the ability to record and store limited data segments on the device. Investigational devices like the Medtronic PC+S have a similar capabilities (35, 36) but are used only in limited research applications. The limited data capacity of such devices makes it difficult to evaluate detection sensitivity because there is no way to confirm that *all* seizures have been identified, although identified and stored events can be confirmed as electrographic seizures (specificity). Finally, minimally invasive subscalp EEG

devices are emerging as potential alternatives for continuous EEG recording, providing a balance between signal quality and user acceptability. One subscalp system (24/7 EEG^{TM} SubQ) has been CE-marked for epilepsy monitoring and diagnosis, following a cumulative 490 day trial (nine patients, up to 90 days each) demonstrating its safety and feasibility (37). Automatically assisted, visual identification of electrographic seizures has also been demonstrated in the ultra long-term setting (>6 months) with this system, with excellent sensitivity but low specificity (38).

Non-invasive Seizure Monitoring

Non-invasive, wearable biosensors have the greatest immediate potential to meet the needs of the majority of people with epilepsy. The availability of inexpensive miniaturized electronic components, wireless data telemetry, and rechargeable battery technology has given rise to a large number of lightweight, wearable sensors. Currently, sensors are commercially available to measure continuous, non-invasive photoplethysmography (PPG, to measure the blood volume pulse signal), electromyography (EMG), accelerometry, EEG, electrocardiography (EKG), electrodermal activity (EDA), and skin temperature in a range of form factors. A summary of available sensors is given in **Figure 1** (see also Panels in **Appendix**). Most individuals are familiar with the accelerometers and optical PPG sensors included in consumer electronics like smart watches and fitness monitors. These inexpensive sensors with sophisticated data processing algorithms on cloud-based data management systems are capable of tracking sleep and exercise rates based on accelerometry (39–41), although the accuracy of sleep staging with these devices is unclear. Variable accuracy has been found as well in tracking heart rates from wrist-worn PPG sensors (42). Nevertheless, wearable biosensors remain of interest for epilepsy management, as changes in sleep quality (43), exercise (i.e., heart rate and motion tracking) (44), and stress (i.e., heart rate variability, EDA) (45, 46) may all trigger seizure onset for some people.

Currently, there are two wearable sensors approved by the FDA and EU for detecting convulsive seizures: the first, a wrist-worn smartwatch (Empatica Embrace, Boston MA), uses accelerometry and EDA to detect the subject's movements and maintains a Bluetooth link to the subject's smartphone, where an application telemeters data and detections to cloud servers and issues caregiver alerts for seizures (47). The Empatica Embrace was CE Marked in 2016 and FDA approved in 2018. The second device is attached by an adhesive patch affixed to the subject's bicep and identifies changes in EMG to detect convulsions (BrainSentinel SPEAC, San Antonio TX). This device also has a cloud-based data platform and can send caregiver alerts and was CE Marked in 2013 and FDA approved in 2017 (48). Other CE-Marked devices are available (Biovotion Everion, ByteFlies Sensor Dots, Livassured NightWatch, Epi-Care Free), and studies of performance at detecting seizures are ongoing. Detection of convulsive or motor seizures is relatively easier than other seizure types (49), and studies are beginning to address these other more difficult semiologies, but only with modest success to date (50–52). As detection performance improves, approved devices may become an adjunct measure of seizure activity for anti-seizure medication trials. These would likely initially be used exclusively for the detection of tonic–clonic seizures, as wearable sensors are most performant for this seizure type.

Most commercially available sensors do not have regulatory approval for use in epilepsy, and these sensors span an array of form factors and capabilities. The majority of commercial smartwatches now carry accelerometric and PPG sensors, which could be useful in tracking seizures (53), and smartwatch and smartphone applications have been developed for this purpose. Rigorous testing data is needed, however, and until clear estimates of sensitivity and specificity under a range of conditions are established, wearable systems should not be considered reliable sources of clinically actionable information (54). Apple and FitBit's consumer grade wearables have FDA and CE approval for cardiovascular monitoring currently, and as data accumulates, regulatory approvals for epilepsy could be possible. Devices aimed at the clinical research market are available in a wrist-watch form factor (Empatica E4, Geneactiv), and this form factor is often rated well by people with epilepsy for comfort and ease of use (55). Smart devices in a ring form factor (e.g., Oura and Motiv) can collect accelerometry and finger PPG. The small size of these devices severely limits their battery capacity, and most devices do not incorporate real-time Bluetooth data linkage. Ring devices may be useful for seizure diary applications, or to provide estimates of sleep quality and other factors to forecasting algorithms, but currently are not able to provide physiological data in real time. PPG data quality is adversely affected by subject movement, and wrist and hand-worn PPG sensors may suffer due to limb movements. Recently published results of commercially available wearable sensors in seizure detection are summarized in **Table 1**.

Arm-band style wearable biosensors are available (Biofourmis, BrainSentinel), and many adhesive wearable sensors can be placed on the arm (Byteflies). This is a prime location for measuring EMG, and muscle activity can be used as a proxy for convulsive seizure activity. This placement may also facilitate simultaneous EKG measurement if wires are run through the sleeve to the subject's chest, although this may create maintenance challenges for long-term use. Arm band sensors can be rated lower in comfort and acceptability by subjects (62), and data quality may suffer due to movement or the sensor sliding slightly during wear. Small sensors affixed by adhesive patches (ByteFlies, EpiLog) can conceivably be placed anywhere on the body, although hair and perspiration may interfere with adhesives. Adhesive failure and skin irritation are a barrier to long-term (multiple weeks) and ultra long-term (months to years) use of these devices, although these devices may be suitable for prolonged (up to 7 days) monitoring (e.g., baseline seizure diaries). This category may be the most flexible sensor type, and there are commercially available research-quality sensors for EEG, EMG, EKG, PPG, accelerometry, and EDA (ByteFlies, Epilog). Continuous glucose monitor (CGM) and flash glucose devices, FDA and EU approved for diabetes monitoring, fall in this category of body-worn sensors and have reached a high level of technical maturity and reliability (63, 64).

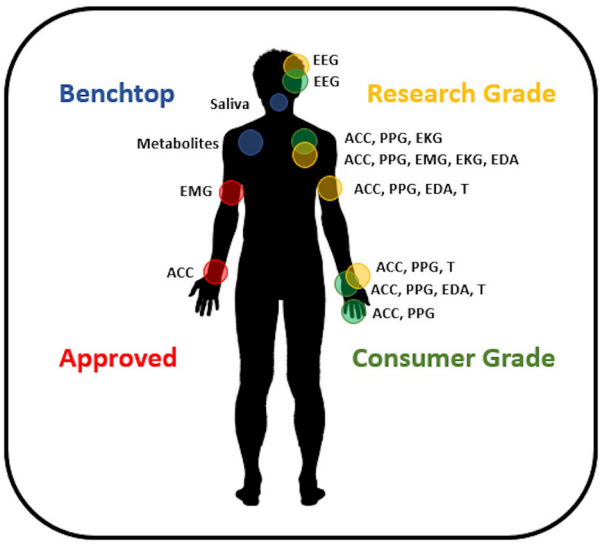

FIGURE 1 | Available wearable devices for seizure management. Approved devices include sensor systems CE Marked and/or FDA approved for epilepsy. Research grade devices are commercially available and provide accurate, high-quality data. Consumer grade devices are commercially available sensors designed around applications where data accuracy is not crucial and may utilize interpolation or estimation methods to provide information to the user. Benchtop devices are innovative sensors under development and not available commercially. EEG, electroencephalography; ACC, accelerometry; PPG, photoplethysmography; EKG, electrocardiography; EMG, electromyography; EDA, electrodermal activity; T, temperature.

In addition to mature, commercially available wearable biosensors, numerous early-stage sensors are under development, which may find application in epilepsy. Sweat sampling sensors are being developed for exercise applications and can non-invasively measure glucose, lactate, sodium, and other metabolites as well as drug or medication levels excreted in sweat. Fluidic sensors with similar technology have been integrated into mouth guards (65) and fabrics (66) to sample saliva and other bodily fluids. Google subsidiary Verily Inc. developed a contact lens with integrated glucose sensors, but abandoned the project in 2018 citing inconsistent monitoring results (67). Known hormonal and metabolic factors that may be altered prior to or immediately following seizures include melatonin (68), cortisol (69), reproductive hormones (70), prolactin and growth hormone (71), lactate, glucose (72), tRNA fragments (73), and others (74), thus providing a range of possible biomarkers for seizure detection. The field is evolving rapidly, and many innovative new sensors will likely become available. Hopefully, new sensor technologies will allow for the detection of a broader range of seizure types, beyond convulsive events.

Behavioral Monitoring

Beyond sensing of basic biosignals, wearable devices and smartphones can be used to track behavior at more complex levels, including activity patterns, movement range, sleep duration and quality, and behavioral indicators of mood, for example, based on analyses of movement speed, social connectivity, or affective tone of speech (75–77). This opens up a window to analyzing behavioral changes occurring over days or weeks, which may correlate with seizure risk as suggested by studies on prodromes and on seizure precipitating factors (78, 79). Beyond passive monitoring, smartphones can be used to track mood changes and cognitive function by actively querying the user (80). Assessments can include pop-up questionnaires at predefined times, as well as specific test batteries assessing general cognitive capabilities like attention or working memory, thus capturing high level dynamic brain states. The use of a smartphones also allows for behavioral intervention, which is becoming a prominent adjunct therapy (81).

DESIGNING AND CONNECTING SEIZURE MANAGEMENT SYSTEMS: DECREASING BARRIERS TO USE

Despite a general willingness of people with epilepsy, caregivers, and healthcare professionals to use seizure monitoring devices (55), there are significant user requirements that impede long-term use. Johansson et al. concluded that on average 19% (range 6–24%) of data recorded from wearables in free-living environments may be missing due to a combination of technical and human factors (82). Cohen et al. found in a long-term study of wearables in Parkinson's and Huntington's disease that app-based reminders ("push notifications") are useful tools in increasing continued device adherence (83), which could provide similar outcomes in seizure monitoring.

The aesthetics and comfort of devices are significant considerations in improving long-term adherence with wearable devices. Bruno et al. found that smartphone and watch-based devices were acceptable to over 70% of people with epilepsy; however, leg, upper-arm, chest, and head-based systems had <50% acceptance. Ring-style wearables had over 60% approval (84). Interestingly, there is a strong discrepancy between the views of people with epilepsy and caregivers for wristband and ring-style wearables, although why this is so is unclear (55). Performance characteristics are significant as well, and Patel et al. (85) showed a strong preference among people with epilepsy and caregivers for excellent sensitivity and text message alerts over comfort, battery life, and other features. Unfortunately, Patel et al. do not separate their responses between people with epilepsy and their caregivers, making it unclear if there are differences in view between these two groups. Furthermore, it is not clear that device users' reported preferences are truly predictive of their behavior. Janse et al. showed significant differences between the preferences of people with epilepsy and caregivers in device form factors, device accuracy, and seizure forecast range (10). Charging the batteries of wearable devices presents a considerable adherence challenge, as devices are ideally worn continuously through both sleep and wakefulness (55). It is estimated that 38–60% of users claim to be satisfied with recharging a device at least daily (55, 85). Battery charging depends on frequency of data sampling and telemetry. Many commercial fitness tracker devices

TABLE 1 | Sensitivity and false alarm rates for detection of seizures with wearable biosensors.

Study	Device	Signal(s)	Environment	Seizure type	Patients (seizures)	Sensitivity (%)	False alarms per day
Beniczky (56)	IctalCare EDDI	EMG	EMU	GTCS	71 (32)	93.8	0.67
Halford (57)	BrainSentinel SPEAC	EMG	EMU	GTCS	199 (46)	76	2.52
					149 (29)[a]	100[a]	1.44[a]
Onorati (49)	Empatica E4	ACC,EDA	EMU	GTCS	69 (22)	94.5[b]	0.2[b]
Vandencasteele (58)	180° eMotion Faros	EKG	EMU	CP (FT)	11 (47)	70	51.6
	Empatica E4	PPG				32	43.2
Johansson (59)	Shimmer3, custom device	ACC	EMU	TCS	8 (10)[c]	100[b]	1.2[b]
Heidberg (51)	Empatica E3	ACC, EDA	EMU	Multiple	8 (55)	89.1[d]	18.1[e]
Jeppesen (60)	ePatch	EKG	EMU	Focal, GTCS	43 (125)[f]	93.1[f]	1.1[f]
Vandenncasteele (61)	ByteFlies	EEG (behind ear)	EMU	Multiple	54 (182)	69.1	0.49[g]

Studies before 2015 or reporting earlier results for a device in an identical setting were excluded. GTCS, generalized tonic clonic seizure; CP, complex partial; FT, fronto-temporal; TCS, tonic clonic seizure; FIA, focal impaired awareness.

[a] *With optimal placement of device over the belly of the bicep.*

[b] *Best performing of three candidate algorithms.*

[c] *Three additional patients and 27 additional seizures reserved for training.*

[d] *Results reported are for the best performing of two algorithms considered using a patient-wise cross validation.*

[e] *Estimated from reported 93.7% specificity, assuming independent 5-min detection windows.*

[f] *Results reported are from the 53% of the cohort who exhibited adequate HR response to seizures.*

[g] *Results reported are from a patient-specific detection algorithm, which performed better than a cross-patient algorithm.*

upload a limited data stream to cloud platforms in near-real time using smartphones connected to the internet, either through broadband WiFi or mobile 4G. This approach is attractive for immediate feedback to people with epilepsy and caregivers but would pose a considerable burden on the battery of both the wearable device and smartphone for clinical quality sensor data on the order of 100s of samples per second.

Computation and Connectivity

Connecting data sources through cloud technologies has the potential to create insights into seizure patterns (86) and even forecast seizure events (9, 87). Measurements of a person's environment, physiology, and behavior through smartphones and wearables can be used to make patient-specific models that help clinicians understand individuals' risk factors (88). The following sections outline common methods for accessing data sources (such as seizure diaries or wearables) through cloud technologies. **Figure 2** presents an overview of how various software interfaces may interact with device data.

Modern on-demand computing services make the collection and distribution of large datasets of potentially unknown size, expanding in response to the users' needs (14, 89). Importantly, data sources should use common formats and definitions for data storage, particularly for imperative entries such as timestamps, seizure type descriptions, and definitions of seizure durations (90). Without accurate timing information, errors can occur between data sources, creating noisy repositories, and inaccurate forecasts. Removing differences between data sources minimizes barriers to integrating heterogeneous data streams and gives the best opportunity for improved care.

Machine learning and artificial intelligence methods are integral to seizure detection and forecasting with wearable biosensors. Machine learning approaches allow algorithms to adaptively learn patterns in data, which may not be apparent to the human observer. Traditional machine learning requires preprocessing raw data to extract features or characteristics of interest, which are then normalized and passed to a classification algorithm for analysis. However, deep learning, or convolutional neural network approaches, provides "end to end" learning, where extraction of salient features is handled by the initial layers of the neural network after repeated presentation of training data (91). Automatic feature extraction is considered a key advantage of deep learning for seizure prediction, because it enables an algorithm to be tailored to particular seizure types or even an individual seizure semiology (or semiologies) (92, 93). Despite this ability for automated feature extraction, the signals recorded must contain some fundamental information relating to seizure events, and hence, appropriate device and sensor selection is still required for utility. For a discussion on factors that may contribute to seizure likelihood, see Section Factors contributing to seizure likelihood. A hurdle for machine learning, and deep learning in particular, is that algorithms typically require a very large number of training seizures in order to learn a generalized representation of the data. Epilepsy databases have facilitated development of machine learning and deep learning methods for seizure detection (94) and forecasting (95–99). This "big-data" approach may improve accuracy in detecting more challenging seizure types.

FORECASTING SEIZURE LIKELIHOOD

People with epilepsy consistently rate the apparent unpredictability of their seizures to be the most disabling aspect of their condition (10, 11), and a reliable system to forewarn individuals or caregivers of impending seizures could allow fast-acting medications to be administered, or simply allow

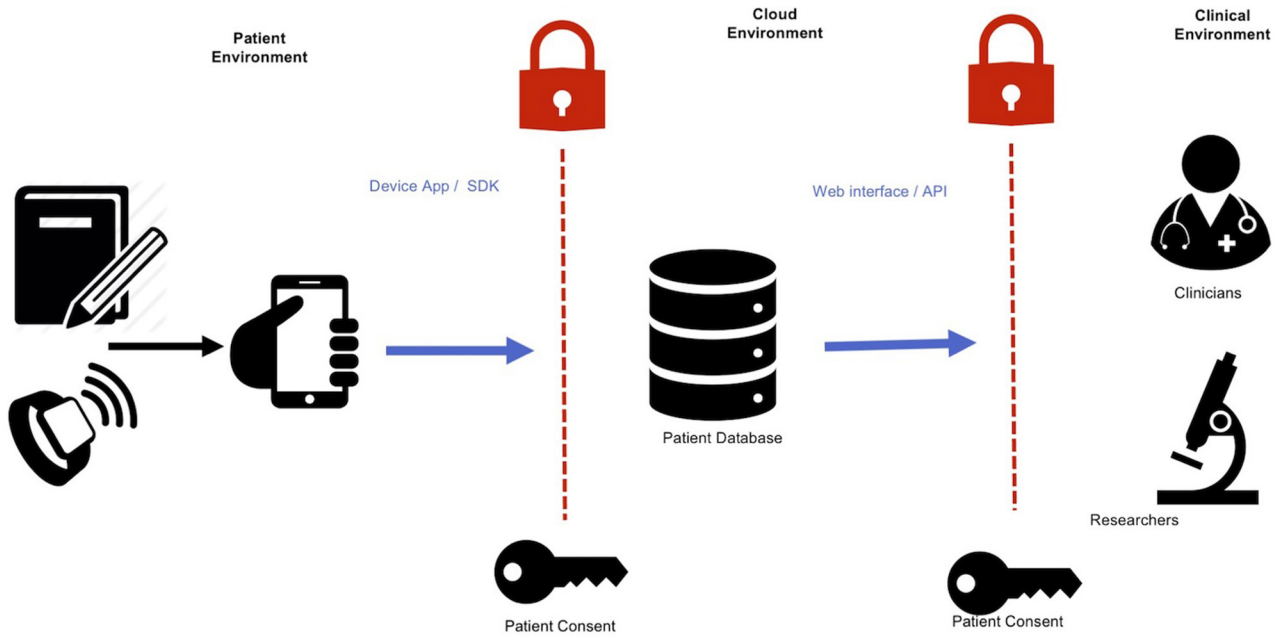

FIGURE 2 | Integrating device data into online accessible databases. An abundance of data relating to physiology, behavior, and environment can be collected with wearable devices and smartwatches. These can then be collected into a single repository in cloud-based data storage. These data can then be accessed by relevant clinicians and researchers through a web interface or programmatic access. Informed permission is necessary for each step of data transfer: from user to the database, and from the database to the clinical environment.

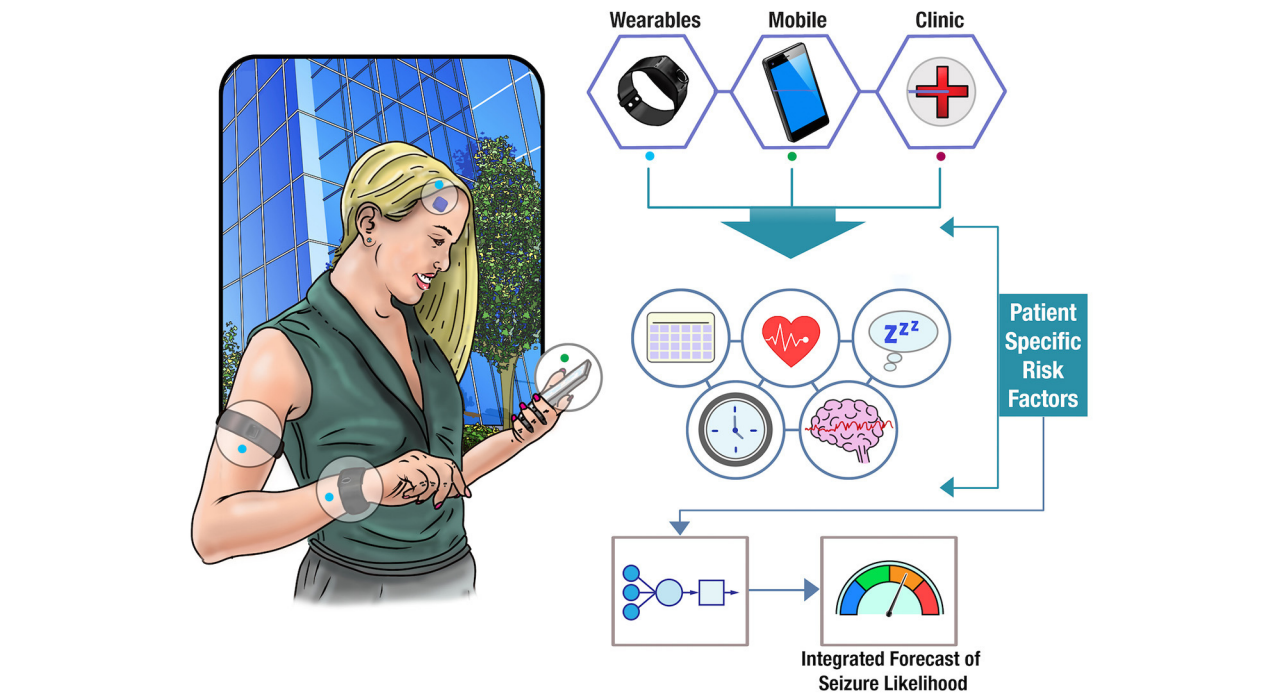

FIGURE 3 | Forecasting seizure likelihood. The schematic shows how data from clinical notes, wearable devices, and mobile apps can be combined to obtain a deeper understanding of patient-specific risk factors. Utilizing cloud computing, these factors can be integrated into an individualized model of seizure likelihood and displayed as a real-time forecast to a user.

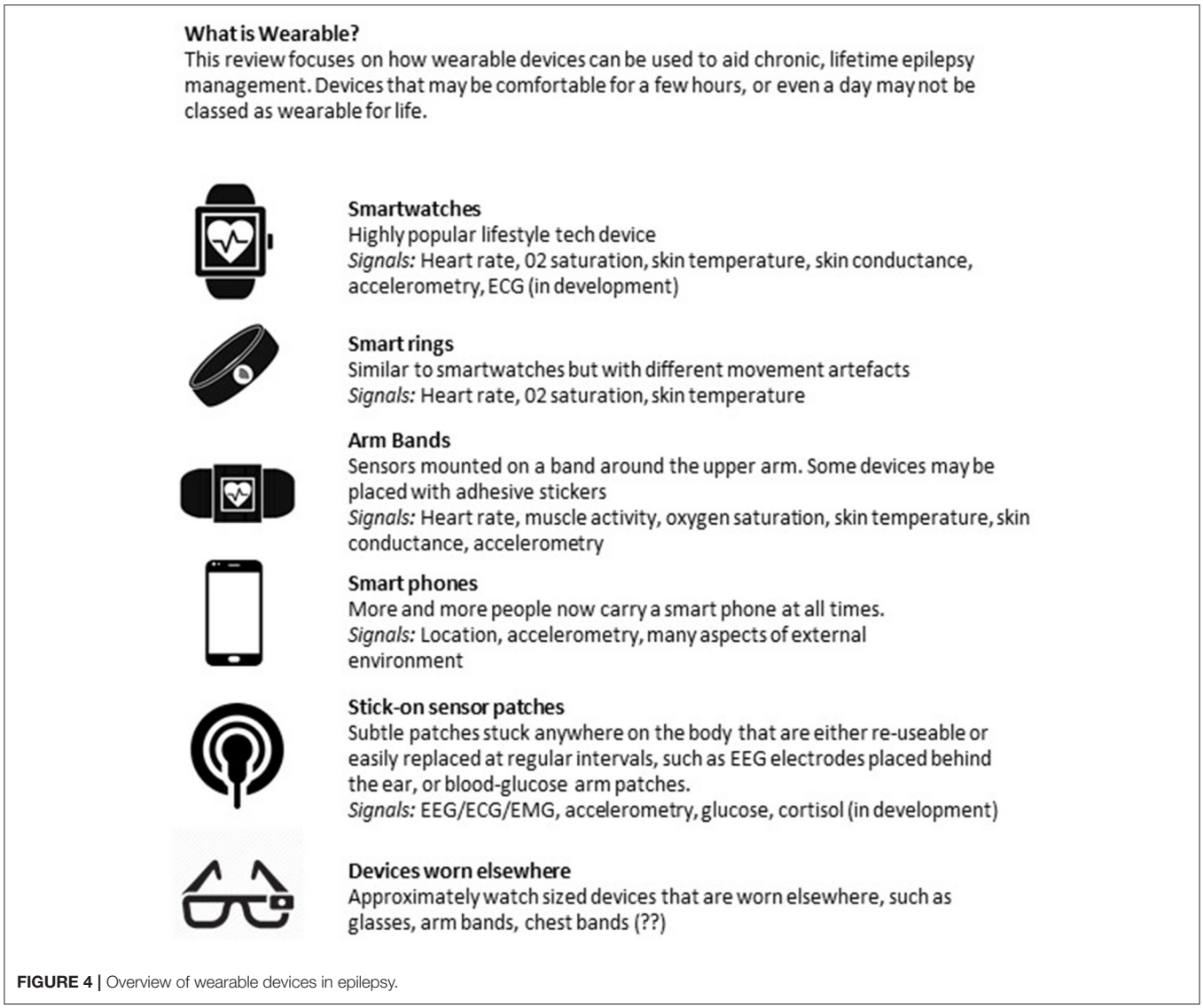

FIGURE 4 | Overview of wearable devices in epilepsy.

a person to take preparatory measures. To date, most devices for use in epilepsy monitoring have been focused on seizure detection, where the main utility from the perspective of people with epilepsy is providing a seizure alert to their clinicians or caregivers. In this context, false alarms have the potential to be disruptive to the life of someone with epilepsy, their families, and caregivers, and can cause people to stop using seizure detection devices (100). However, in seizure forecasting applications, the primary end goal is to inform the individual of their current seizure likelihood. This context reduces the impact of "false alarms," as not every high likelihood alert would be expected to result in a seizure (92). When evaluating forecasts, probabilistic measures can be used instead of only counting "hits" and "misses." Therefore, although the problem of seizure forecasting is more complex than seizure detection from a signal analysis perspective (101), wearable devices may have broader application and wider acceptance in seizure forecasting, which will allow people with epilepsy to plan daily activities and take measures for seizure control. One retrospective validation study of seizure forecasting with wearables recently reported better than chance results in 30 of 69 (43.5%) in-hospital patients studied (102), confirming that forecasting with non-invasive devices is possible for many patients. The ability to record continuous, outpatient data from wearables will enable long-term tracking of risk factors and should improve forecasting performance.

Instead of trying to predict the exact time of an upcoming seizure, it may be more feasible to estimate the probability of someone having a seizure and communicate this risk in a clinically useful manner (12, 92, 103, 104). Accordingly, there is increasing interest within the clinical epilepsy community to develop seizure forecasting devices and applications (9) and understand user requirements (10, 105). In a survey-based study, Schulze-Bonhage et al. reported that probabilistic forecasts were generally considered equally useful to predicting exactly when a

seizure would occur (105). They also found that missed seizures were considered worse than false alarms, and perfect accuracy was not considered a requirement for a forecasting device (105). This survey agrees with reports from individuals enrolled in the human study of a long-term seizure forecasting device (the NeuroVista trial) (2). Subjects in the NeuroVista trial reported on the usefulness of the device (106, 107), despite less than perfect sensitivity and time-in-warning of up to 30% (2). More recently, Janse et al. also showed that seizure forecasting devices were deemed broadly acceptable despite the potential for inaccuracy (up to "inaccurate 30% of the time") (10). Externally worn devices were ranked more highly than subcutaneous or implantable devices (10), reinforcing the potential for development of wearable devices for seizure forecasting applications.

The development of qualitative and clinically useful metrics to evaluate seizure forecasts has been a key priority. Probabilistic measures can be used to evaluate performance (86, 108, 109), but defining an alarm threshold is often deemed necessary to determine clinical utility and the system becomes parameterized by the alarm duration, or "seizure prediction horizon" (110). Nevertheless, evaluation of false alarms is challenging because there is significant individual variability between seizure prediction horizons (2), and the "time-in-warning" is frequently reported as a proxy for a false alarm rate (2, 95, 111). In addition to benchmarking performance, it is important to understand user requirements for a forecasting interface (112). A recent study surveyed people with epilepsy and caregivers about the visual design of seizure forecasts, finding a range of preferences, although graphs that provided some temporal context (i.e., seizure risk plotted over the course of a day or month as opposed to a "gauge") were rated more highly (113). Ultimately, *post-hoc* studies and surveys can only provide an indicative measure of the utility and benefits of a seizure forecasting device. In a prospective setting, some people initially with interest in forecasting devices may find false alarms to be debilitating, whereas others who were initially skeptical about the benefits may find a forecasting device very helpful (107).

Patterns and Rhythms in Seizure Probability

It is now understood that most people with epilepsy exhibit circadian and slower, multiday temporal cycles that modulate their seizure likelihood [see (17) for a recent review]. Recent studies have demonstrated impressive seizure forecasting performance using multiday cycles measured from implantable EEG (114, 115), although prospective validation is needed. Cycles of seizure likelihood can also be measured from self-reported seizure times (116), and for a subset of people, cycles measured from seizure diaries are predictive of the likelihood of electrographic seizures and epileptic activity (116, 117). Machine learning can also be used with historic trends from self-reported seizure diaries, which may be useful to forecast future reported seizures (118, 119). Both cyclic and machine-learning approaches have been shown to accurately forecast seizures (or, more specifically, seizure diary events) in both focal and generalized epilepsies. Despite inaccuracy in individual seizure reporting, long-term patterns and cycles may still be accurately inferred for many individuals (116, 117). Due to the indications for use of who can have implanted EEG for long-term recording, the existence of cycles has largely been validated electrographically in individuals with focal epilepsies. Continuously recorded biomarkers remain important to truly characterize underlying epileptic rhythms, without the inherent limitations and biases of self-reported seizure diary records (120).

Wearable devices and subscalp EEG have the potential to improve seizure diaries by providing objective data and complementary information to help eliminate noise. Objective seizure measures may capture more seizures, enabling cyclic patterns to be detected earlier and characterized more accurately (38). On the other hand, seizure detection with wearable devices currently has a high error rate, and has only been established for convulsive or motor seizures (48–50, 121), although progress is ongoing for other seizure types (51, 52, 93, 122, 123). The distribution of errors with wearables is likely to be different to the error distribution of self-reported seizure diaries. There may also be gaps or poor quality data due to non-adherence or charging issues (124). Wearable seizure detectors may perform better at night, when there are fewer movement artifacts, and when individuals are less likely to self-report seizures (3). Wearable devices also do not suffer from diary fatigue, or other uniquely human biases. Therefore, wearable devices may have the potential to improve the accuracy and completeness of the historic record of individuals' seizure times when used along with a seizure diary. A more accurate seizure count, or a combined forecast from the two data streams (86), may provide a higher performing forecaster for users. A better record of seizure times enables personalized forecasting models to be trained and validated more rapidly and with greater reliability.

Factors Contributing to Seizure Likelihood

Combining multiple sources of information, including cyclic patterns, EEG features, and other environmental factors, may contribute to a stronger forecast of seizure likelihood than any individual signal. There are many data sources that are readily available and have been shown to be associated with seizure likelihood. For example, sleep quality (68), weather (125, 126), mood (78), and stress (45, 46) may all make seizures more likely. These environmental factors can be combined with information from seizure times that capture individuals' daily, weekly, or monthly cycles to deliver an individualized forecast of seizure likelihood (12, 92, 104).

Wearable devices provide an opportunity to augment seizure forecasts with a growing number of physiological signals relevant to seizure likelihood. For instance, changes in heart rate have been often found to precede seizure onset by several minutes (127). Billeci et al. found that heart rate variability could be used to predict seizures up to 15 min before onset with >80% sensitivity, albeit with a relatively high average false positive rate of 0.41 per hour (almost 10 per day) (128). Signals that show some well-defined ictal changes, such as EDA (129–131), heart rate, or EMG (121), also show predictive changes prior to seizure onset (32). For instance, a recent study found predictive value in wearable sensor recordings EDA, blood volume pulse,

accelerometry, and skin temperature (102). Average heart rate has also been found to show similar circadian and multiday cycles to epileptic activity, which are comodulated with seizure risk (132). Long-term datasets that record large numbers of individual seizures over long periods of time in conjunction with continuous wearable monitoring data promise to shed new light on these patterns governing autonomic nervous system and metabolic activity that are co-modulated with seizure onset. The potential of wearable monitoring to track individual seizure triggers may be more powerful when coupled with behavioral and mood data. **Figure 3** illustrates the concept of a multi-modal seizure forecasting system.

There is some early promise that physiological signals derived from peripheral or autonomic systems (i.e., cardiac activity) contain relevant information for predicting seizure onset. **Figure 4** illustrates a number of these systems. Currently, insufficient evidence exists that any stand-alone peripheral signal could be used as a seizure forecast with adequate sensitivity and specificity (105). However, with more data to determine patient-specific trends, and in combination with other predictive signals, wearable monitoring may contribute to an integrated forecast of seizure likelihood. As more prospective, clinical studies of forecasting systems are undertaken, a better understanding of the ideal signals, device specifications, user needs, and performance benchmarks will be elucidated, and forecasting systems may begin to reduce the burden of seizure unpredictability on people living with epilepsy.

CONCLUSION

We are at the edge of a transition in the way that we identify, analyze, and manage seizures and epilepsy. At the moment, however, there is still relatively limited data on which to base decisions about the suitability of various devices currently available, and the types of seizures in which they might be best deployed, particularly for non-motor events. There are challenges ahead regarding the hardware, power, data, and security of the various devices available, though these problems are being solved in numerous mobile device applications. Significant challenges remain around issues related to usability of the systems, and certainly their chronic use. Developing concepts though relating to utilization of multiple modality streams and integrating this information will serve to provide accurate data on which to more effectively manage epilepsy in the clinic and evaluate new therapies. Ultimately, data from a variety of systems will contribute to seizure forecasts and enable people with epilepsy to achieve a greater degree of safety, freedom, and dignity.

AUTHOR CONTRIBUTIONS

BB, EN, and PK performed the literature search and literature revision, drafted the manuscript, reviewed, and edited for important intellectual content. MR, AS-B, GW, DF, MN, and SD participated in the interpretation of data in the literature, reviewed, and edited the manuscript for important intellectual content. MC developed the original concept and design of the manuscript, performed the literature search and analysis of data in the literature, drafted, reviewed, and edited the manuscript. All authors contributed to the article and approved the submitted version.

FUNDING

This work was supported by the Epilepsy Foundation of America's Epilepsy Innovation Institute My Seizure Gauge award.

ACKNOWLEDGMENTS

The authors thank the My Seizure Gauge team for technical and administrative support. Specifically the authors thank at Mayo Clinic Sherry Klingerman, Tal Pal Attia MS, Daniel Crepeau, and Erin Jagodzinski; at Seer Medical Will Hart, Dominique Eden, and Rob Kerr; at King's College London Andrea Biondi MD and Elisa Bruno MD, Ph.D.; at Freiburg University Sebastian Bottcher and Martin Glasstetter; and at the Epilepsy Foundation of America Caitlin Grazkowski Ph.D. and Jackie French MD.

REFERENCES

1. Fisher RS. Bad information in epilepsy care. *Epilepsy Behav.* (2017) 67:133–4. doi: 10.1016/j.yebeh.2016.10.022
2. Cook MJ, O'Brien TJ, Berkovic SF, Murphy M, Morokoff A, Fabinyi G, et al. Prediction of seizure likelihood with a long-term, implanted seizure advisory system in patients with drug-resistant epilepsy: a first-in-man study. *Lancet Neurol.* (2013) 12:563–71. doi: 10.1016/S1474-4422(13)70075-9
3. Elger CE, Hoppe C. Diagnostic challenges in epilepsy: seizure under-reporting and seizure detection. *Lancet Neurol.* (2018) 17:279–88. doi: 10.1016/S1474-4422(18)30038-3
4. Blachut B, Hoppe C, Surges R, Elger C, Helmstaedter C. Subjective seizure counts by epilepsy clinical drug trial participants are not reliable. *Epilepsy Behav.* (2017) 67:122–7. doi: 10.1016/j.yebeh.2016.10.036
5. Langan Y, Nashef L, Sander JW. Case-control study of SUDEP. *Neurology.* (2005) 64:1131–3. doi: 10.1212/01.WNL.0000156352.61328.CB
6. Picard RW, Migliorini M, Caborni C, Onorati F, Regalia G, Friedman D, et al. Wrist sensor reveals sympathetic hyperactivity and hypoventilation before probable SUDEP. *Neurology.* (2017) 89:633–5. doi: 10.1212/WNL.0000000000004208
7. Beniczky S, Wiebe S, Jeppesen J, Tatum WO, Brazdil M, Wang Y, et al. Automated seizure detection using wearable devices: a clinical practice guideline of the International League Against Epilepsy and the International Federation of Clinical Neurophysiology. *Clin Neurophysiol.* (2021) 132:1173–84. doi: 10.1016/j.clinph.2020.12.009
8. Mikk KA, Sleeper HA, Topol EJ. The pathway to patient data ownership and better health. *JAMA.* (2017) 318:1433–4. doi: 10.1001/jama.2017.12145
9. Dumanis SB, French JA, Bernard C, Worrell GA, Fureman BE. Seizure forecasting from idea to reality. Outcomes of the my seizure gauge epilepsy innovation institute workshop. *eNeuro.* (2017) 4:ENEURO.0349-17.2017. doi: 10.1523/ENEURO.0349-17.2017
10. Janse SA, Dumanis SB, Huwig T, Hyman S, Fureman BE, Bridges JFP. Patient and caregiver preferences for the potential benefits and risks of a seizure forecasting device: a best–worst scaling. *Epilepsy Behav.* (2019) 96:183–91. doi: 10.1016/j.yebeh.2019.04.018

11. Schulze-Bonhage A, Kuhn A. Unpredictability of seizures and the burden of epilepsy. In: Schelter B, Timmer J, Schulze-Bonhage A, editors. *Seizure Prediction in Epilepsy: From Basic Mechanisms to Clinical Applications*. Weinheim: Wiley-VCH Verlag (2008). pp. 1–10.
12. Baud MO, Rao VR. Gauging seizure risk. *Neurology*. (2018) 91:967–73. doi: 10.1212/WNL.0000000000006548
13. Karoly PJ, Goldenholz DM, Freestone DR, Moss RE, Grayden DB, Theodore WH, et al. Circadian and circaseptan rhythms in human epilepsy: a retrospective cohort study. *Lancet Neurol.* (2018) 17:977–85. doi: 10.1016/S1474-4422(18)30274-6
14. Brinkmann BH, Wagenaar J, Abbot D, Adkins P, Bosshard SC, Chen M, et al. Crowdsourcing reproducible seizure forecasting in human and canine epilepsy. *Brain.* (2016) 139:1713–22. doi: 10.1093/brain/aww045
15. Kremen V, Brinkmann BH, Kim I, Guragain H, Nasseri M, Magee AL, et al. Integrating brain implants with local and distributed computing devices: a next generation epilepsy management system. *IEEE J Transl Eng Health Med.* (2018) 6:1–12. doi: 10.1109/JTEHM.2018.2869398
16. Bergey GK, Morrell MJ, Mizrahi EM, Goldman A, King-Stephens D, Nair D, et al. Long-term treatment with responsive brain stimulation in adults with refractory partial seizures. *Neurology*. (2015) 84:810–7. doi: 10.1212/WNL.0000000000001280
17. Karoly PJ, Rao VR, Gregg NM, Worrell GA, Bernard C, Cook MJ, Baud MO. Cycles in epilepsy. *Nat Rev Neurol.* (2021) 17:267–84. doi: 10.1038/s41582-021-00464-1
18. Baud MO, Kleen JK, Mirro EA, Andrechak JC, King-Stephans D, Chang EF, et al. Multi-day rhythms modulate seizure risk in epilepsy. *Nat Commun.* (2018) 9:88. doi: 10.1038/s41467-017-02577-y
19. Rao VR, G Leguia M, Tcheng TK, Baud MO. Cues for seizure timing. *Epilepsia.* (2020) 62:S15–31. doi: 10.1111/epi.16611
20. Lees AJ. The strange case of Dr William Gowers and Mr Sherlock Holmes. *Brain.* (2015) 138:2103–8. doi: 10.1093/brain/awv144
21. Tatum IV WO, Winters L, Gieron M, Passaro EA, Benbadis S, Ferreira J, et al. Outpatient seizure identification: results of 502 patients using computer-assisted ambulatory EEG. *J Clin Neurophysiol.* (2001) 18:14–9. doi: 10.1097/00004691-200101000-00004
22. Lanzone J, Ricci L, Assenza G, Ulivi M, Di Lazzaro V, Tombini M. Transient epileptic and global amnesia: real-life differential diagnosis. *Epilepsy Behav.* (2018) 88:205–11. doi: 10.1016/j.yebeh.2018.07.015
23. Nickels KC, Zaccariello MJ, Hamiwka LD, Wirrell EC. Cognitive and neurodevelopmental comorbidities in paediatric epilepsy. *Nat Rev Neurol.* (2016) 12:465. doi: 10.1038/nrneurol.2016.98
24. Samarasekera SR, Helmstaedter C, Reuber M. Cognitive impairment in adults with epilepsy: the relationship between subjective and objective assessments of cognition. *Epilepsy Behav.* (2015) 52:9–13. doi: 10.1016/j.yebeh.2015.08.013
25. Andrade R, Garcia-Espinosa A, Machado-Rojas A, Arteche-Prior M, Díaz-Pedraza A. Unilateral neglect, transient cognitive impairment and intercritical activity in rolandic epilepsy. *Rev Neurol.* (2007) 44:537–40. doi: 10.33588/rn.4409.2005179
26. Erba G, Bianchi E, Giussani G, Langfitt J, Juersivich A, Beghi E. Patients' and caregivers' contributions for differentiating epileptic from psychogenic nonepileptic seizures. Value and limitations of self-reporting questionnaires: a pilot study. *Seizure.* (2017) 53:66–71. doi: 10.1016/j.seizure.2017.11.001
27. Besocke AG, Rojas JI, Valiensi SM, Cristiano E. del Carmen Garcia M. Interview accuracy in partial epilepsy. *Epilepsy Behav.* (2009) 16:551–4. doi: 10.1016/j.yebeh.2009.09.015
28. Thijs RD, Wagenaar WA, Middelkoop HA, Wieling W, van Dijk JG. Transient loss of consciousness through the eyes of a witness. *Neurology.* (2008) 71:1713–8. doi: 10.1212/01.wnl.0000335165.68893.b0
29. Malek N, Heath C, Greene J, A. review of medication adherence in people with epilepsy. *Acta Neurol Scand.* (2017) 135:507–15. doi: 10.1111/ane.12703
30. Williams J, Lawthom C, Dunstan FD, Dawson TP, Kerr MP, Wilson JF, et al. Variability of antiepileptic medication taking behaviour in sudden unexplained death in epilepsy: hair analysis at autopsy. *J Neurol Neurosurg Psychiatry.* (2006) 77:481–4. doi: 10.1136/jnnp.2005.067777
31. Hollinger A, Semmlack S, De Marchis GM, Spiegel R, Hunziker S, Rüegg S, et al. Associations between periodic social events and status epilepticus-An 11-year cohort study. *Epilepsia.* (2018) 59:1381–91. doi: 10.1111/epi.14431
32. Ramgopal S, Thome-Souza S, Jackson M, Kadish NE, Sánchez Fernández I, Klehm J, et al. Seizure detection, seizure prediction, and closed-loop warning systems in epilepsy. *Epilepsy Behav.* (2014) 37:291–307. doi: 10.1016/j.yebeh.2014.06.023
33. Beniczky S, Arbune AA, Jeppesen J, Ryvlin P. Biomarkers of seizure severity derived from wearable devices. *Epilepsia.* (2020) 61:S61–6. doi: 10.1111/epi.16492
34. Morrell M. Brain stimulation for epilepsy: can scheduled or responsive neurostimulation stop seizures? *Curr Opin Neurol.* (2006) 19:164–8. doi: 10.1097/01.wco.0000218233.60217.84
35. Van Gompel JJ, Klassen BT, Worrell GA, Lee KH, Shin C, Zhao CZ, et al. Anterior nuclear deep brain stimulation guided by concordant hippocampal recording. *Neurosurg Focus.* (2015) 38:E9. doi: 10.3171/2015.3.FOCUS1541
36. Herron JA, Thompson MC, Brown T, Chizeck HJ, Ojemann JG, Ko AL. Chronic electrocorticography for sensing movement intention and closed-loop deep brain stimulation with wearable sensors in an essential tremor patient. *J Neurosurg.* (2017) 127:580–7. doi: 10.3171/2016.8.JNS16536
37. Weisdorf S, Duun-Henriksen J, Kjeldsen MJ, Poulsen FR, Gangstad SW, Kjær TW. Ultra-long-term subcutaneous home monitoring of epilepsy−490 days of EEG from nine patients. *Epilepsia.* (2019) 60:2204–14. doi: 10.1111/epi.16360
38. Viana PF, Duun-Henriksen J, Glasstëter M, Dümpelmann M, Nurse ES, Martins IP, et al. 230 days of ultra long-term subcutaneous EEG: seizure cycle analysis and comparison to patient diary. *Ann Clin Transl Neurol.* (2021) 8:288–93. doi: 10.1002/acn3.51261
39. Gruwez A, Bruyneel A-V, Bruyneel M. The validity of two commercially-available sleep trackers and actigraphy for assessment of sleep parameters in obstructive sleep apnea patients. *PLoS ONE.* (2019) 14:e0210569. doi: 10.1371/journal.pone.0210569
40. Toth LP, Park S, Pittman WL, Sarisaltik D, Hibbing PR, Morton AL, et al. Validity of activity tracker step counts during walking, running, and activities of daily living. *Transl J Am Coll Sports Med.* (2018) 3:52–9. doi: 10.1249/TJX.0000000000000057
41. An H-S, Jones GC, Kang S-K, Welk GJ, Lee J-M. How valid are wearable physical activity trackers for measuring steps? *Eur J Sport Sci.* (2017) 17:360–8. doi: 10.1080/17461391.2016.1255261
42. Wang R, Blackburn G, Desai M, Phelan D, Gillinov L, Houghtaling P, et al. Accuracy of wrist-worn heart rate monitors accuracy of wrist-worn heart rate monitors letters. *JAMA Cardiol.* (2017) 2:104–6. doi: 10.1001/jamacardio.2016.3340
43. Shouse MN, da Silva AM, Sammaritano M. Circadian rhythm, sleep, and epilepsy. *J Clin Neurophysiol.* (1996) 13:32–50. doi: 10.1097/00004691-199601000-00004
44. Sevcencu C, Struijk JJ. Autonomic alterations and cardiac changes in epilepsy. *Epilepsia.* (2010) 51:725–37. doi: 10.1111/j.1528-1167.2009.02479.x
45. Temkin NR, Davis GR. Stress as a risk factor for seizures among adults with epilepsy. *Epilepsia.* (1984) 25:450–6. doi: 10.1111/j.1528-1157.1984.tb03442.x
46. Haut SR, Vouyiouklis M, Shinnar S. Stress and epilepsy: a patient perception survey. *Epilepsy Behav.* (2003) 4:511–4. doi: 10.1016/S1525-5050(03)00182-3
47. Regalia G, Onorati F, Lai M, Caborni C, Picard RW. Multimodal wrist-worn devices for seizure detection and advancing research: focus on the Empatica wristbands. *Epilepsy Res.* (2019) 153:79–82. doi: 10.1016/j.eplepsyres.2019.02.007
48. Whitmire L, Voyles S, Cardenas D, Cavazos J. Diagnostic utility of continuous sEMG monitoring in a home setting-real-world use of the SPEAC® system. *Neurology*. (2019) 92(15 Suppl.): 5–12. Available online at: https://n.neurology.org/content/92/15_Supplement/P4.5-012
49. Onorati F, Regalia G, Caborni C, Migliorini M, Bender D, Poh M-Z, et al. Multicenter clinical assessment of improved wearable multimodal convulsive seizure detectors. *Epilepsia.* (2017) 58:1870–9. doi: 10.1111/epi.13899
50. Ulate-Campos A, Coughlin F, Gaínza-Lein M, Fernández IS, Pearl PL, Loddenkemper T. Automated seizure detection systems and their effectiveness for each type of seizure. *Seizure.* (2016) 40:88–101. doi: 10.1016/j.seizure.2016.06.008
51. Heldberg BE, Kautz T, Leutheuser H, Hopfengärtner R, Kasper BS, Eskofier BM. Using wearable sensors for semiology-independent seizure detection

- towards ambulatory monitoring of epilepsy. In: *2015 37th Annual International Conference of the IEEE Engineering in Medicine and Biology Society (EMBC)*. Milano (2015). 5593–6. doi: 10.1109/EMBC.2015.7319660
52. Patterson AL, Mudigoudar B, Fulton S, McGregor A, Poppel KV, Wheless MC, et al. SmartWatch by SmartMonitor: assessment of seizure detection efficacy for various seizure types in children, a large prospective single-center study. *Pediatr Neurol.* (2015) 53:309–11. doi: 10.1016/j.pediatrneurol.2015.07.002
53. Andel J. van, Ungureanu C, Aarts R, Leijten F, Arends J. Using photoplethysmography in heart rate monitoring of patients with epilepsy. *Epilepsy Behav.* (2015) 45:142–5. doi: 10.1016/j.yebeh.2015.02.018
54. Beniczky S, Ryvlin P. Standards for testing and clinical validation of seizure detection devices. *Epilepsia.* (2018) 59:9–13. doi: 10.1111/epi.14049
55. Bruno E, Simblett S, Lang A, Biondi A, Odoi C, Schulze-Bonhage A, et al. Wearable technology in epilepsy: the views of patients, caregivers, and healthcare professionals. *Epilepsy Behav.* (2018) 85:141–9. doi: 10.1016/j.yebeh.2018.05.044
56. Beniczky S, Conradsen I, Henning O, Fabricius M, Wolf P. Automated real-time detection of tonic-clonic seizures using a wearable EMG device. *Neurology.* (2018) 90:e428–34. doi: 10.1212/WNL.0000000000004893
57. Halford JJ, Sperling MR, Nair DR, Dlugos DJ, Tatum WO, Harvey J. Detection of generalized tonic–clonic seizures using surface electromyographic monitoring. *Epilepsia.* (2017) 58:1861–9. doi: 10.1111/epi.13897
58. Vandecasteele K, De Cooman T, Gu Y, Cleeren E, Claes K, Paesschen WV, et al. Automated epileptic seizure detection based on wearable ECG and PPG in a hospital environment. *Sensors.* (2017) 17:2338. doi: 10.3390/s17102338
59. Johansson D, Ohlsson F, Krýsl D, Rydenhag B, Czarnecki M, Gustafsson N, et al. Tonic-clonic seizure detection using accelerometry-based wearable sensors: a prospective, video-EEG controlled study. *Seizure.* (2019) 65:48–54. doi: 10.1016/j.seizure.2018.12.024
60. Jeppesen J, Fuglsang-Frederiksen A, Johansen P, Christensen J, Wüstenhagen S, Tankisi H, et al. O-45 automated seizure detection for epilepsy patients using wearable ECG-device. *Clin Neurophysiol.* (2019) 130:e36. doi: 10.1016/j.clinph.2019.04.360
61. Vandecasteele K, De Cooman T, Dan J, Cleeren E, Van Huffel S, Hunyadi B, et al. Visual seizure annotation and automated seizure detection using behind-the-ear electroencephalographic channels. *Epilepsia.* (2020) 61:766–75. doi: 10.1111/epi.16470
62. Beeler N, Roos L, Delves SK, Veenstra BJ, Friedl K, Buller MJ, et al. The wearing comfort and acceptability of ambulatory physical activity monitoring devices in soldiers. *IISE Trans Occup Ergon Hum Factors.* (2018) 6:1–10. doi: 10.1080/24725838.2018.1435431
63. Christiansen MP, Garg SK, Brazg R, Bode BW, Bailey TS, Slover RH, et al. Accuracy of a fourth-generation subcutaneous continuous glucose sensor. *Diabetes Technol Ther.* (2017) 19:446–56. doi: 10.1089/dia.2017.0087
64. Kropff J, Choudhary P, Neupane S, Barnard K, Bain SC, Kapitza C, et al. Accuracy and longevity of an implantable continuous glucose sensor in the PRECISE study: a 180-day, prospective, multicenter, pivotal trial. *Diabetes Care.* (2017) 40:63–8. doi: 10.2337/dc16-1525
65. Kim J, Imani S, de Araujo WR, Warchall J, Valdés-Ramírez G, Paixão TR, et al. Wearable salivary uric acid mouthguard biosensor with integrated wireless electronics. *Biosens Bioelectron.* (2015) 74:1061–8. doi: 10.1016/j.bios.2015.07.039
66. Gualandi I, Marzocchi M, Achilli A, Cavedale D, Bonfiglio A, Fraboni B. Textile organic electrochemical transistors as a platform for wearable biosensors. *Sci Rep.* (2016) 6:33637. doi: 10.1038/srep33637
67. Brown, Kristen V. *Alphabet's Verily Halts Diabetes-Detecting Contact Lens Project*. Bloomberg (2018). Available online at: https://www.bloomberg.com/news/articles/2018-11-16/alphabet-s-verily-halts-diabetes-detecting-contact-lens-project (accessed May 15, 2019).
68. Hofstra WA. The circadian rhythm and its interaction with human epilepsy: a review of literature. *Sleep Med Rev.* (2009) 13:413–20. doi: 10.1016/j.smrv.2009.01.002
69. Van Campen JS, Hompe EL, Jansen FE, Velis DN, Otte WM, Van De Berg F, et al. Cortisol fluctuations relate to interictal epileptiform discharges in stress sensitive epilepsy. *Brain.* (2016) 139:1673–9. doi: 10.1093/brain/aww071
70. Herzog AG, Klein P, Ransil BJ. Three patterns of catamenial epilepsy. *Epilepsia.* (1997) 38:1082–8. doi: 10.1111/j.1528-1157.1997.tb01197.x
71. Pritchard PB. The effect of seizures on hormones. *Epilepsia.* (1991) 32:S46–50. doi: 10.1111/j.1528-1157.1991.tb05892.x
72. Schauwecker PE. The effects of glycemic control on seizures and seizure-induced excitotoxic cell death. *BMC Neurosci.* (2012) 13:94. doi: 10.1186/1471-2202-13-94
73. Hogg MC, Raoof R, El Naggar H, Monsefi N, Delanty N, O'Brien DF, et al. Elevation in plasma tRNA fragments precede seizures in human epilepsy. *J Clin Invest.* (2019) 129:2946–51. doi: 10.1172/JCI126346
74. Aminoff MJ, Simon RP, Wiedemann E. The hormonal responses to generalized tonic-clonic seizures. *Brain.* (1984) 107:569–78. doi: 10.1093/brain/107.2.569
75. Canzian L, Musolesi M. Trajectories of depression: unobtrusive monitoring of depressive states by means of smartphone mobility traces analysis. In: *UbiComp '15: The 2015 ACM International Joint Conference on Pervasive and Ubiquitous Computing.* Osaka (2015).
76. Stewart CL, Rashid Z, Ranjan Y, Sun S, Dobson RJ, Folarin AA. RADAR-base: major depressive disorder and epilepsy case studies. In: *Proceedings of the 2018 ACM International Joint Conference and 2018 International Symposium on Pervasive and Ubiquitous Computing and Wearable Computers* (ACM). Singapore (2018). p. 1735–43. doi: 10.1145/3267305.3267540
77. Harari GM, Lane ND, Wang R, Crosier BS, Campbell AT, Gosling SD. Using smartphones to collect behavioral data in psychological science: opportunities, practical considerations, and challenges. *Perspect Psychol Sci J Assoc Psychol Sci.* (2016) 11:838–54. doi: 10.1177/1745691616650285
78. Haut SR, Hall CB, Borkowski T, Tennen H, Lipton RB. Clinical features of the pre-ictal state: mood changes and premonitory symptoms. *Epilepsy Behav.* (2012) 23:415–21. doi: 10.1016/j.yebeh.2012.02.007
79. Schulze-Bonhage A, Haut S. Premonitory features and seizure self-prediction: artifact or real? *Epilepsy Res.* (2011) 97:231–5. doi: 10.1016/j.eplepsyres.2011.09.026
80. Haut SR, Hall CB, Borkowski T, Tennen H, Lipton RB. Modeling seizure self-prediction: an e-diary study. *Epilepsia.* (2013) 54:1960–7. doi: 10.1111/epi.12355
81. Haut SR, Gursky JM. Privitera M. Behavioral interventions in epilepsy. *Curr Opin Neurol.* (2019) 32:227–36. doi: 10.1097/WCO.0000000000000661
82. Johansson D, Malmgren K, Murphy MA. Wearable sensors for clinical applications in epilepsy, Parkinson's disease, and stroke: a mixed-methods systematic review. *J Neurol.* (2018) 265:1740–52. doi: 10.1007/s00415-018-8786-y
83. Cohen S, Waks Z, Elm JJ, Gordon MF, Grachev ID, Navon-Perry L, et al. Characterizing patient compliance over six months in remote digital trials of Parkinson's and Huntington disease. *BMC Med Inform Decis Mak.* (2018) 18:138. doi: 10.1186/s12911-018-0714-7
84. Koskimäki H, Kinnunen H, Kurppa T, Röning J. How do we sleep: a case study of sleep duration and quality using data from oura ring. In: *Proceedings of the 2018 ACM International Joint Conference and 2018 International Symposium on Pervasive and Ubiquitous Computing and Wearable Computers* (ACM). Singapore (2018). p. 714–7. doi: 10.1145/3267305.3267697
85. Patel AD, Moss R, Rust SW, Patterson J, Strouse R, Gedela S, et al. Patient-centered design criteria for wearable seizure detection devices. *Epilepsy Behav.* (2016) 64:116–21. doi: 10.1016/j.yebeh.2016.09.012
86. Karoly PJ, Ung H, Grayden DB, Kuhlmann L, Leyde K, Cook MJ, et al. The circadian profile of epilepsy improves seizure forecasting. *Brain.* (2017) 140:2169–82. doi: 10.1093/brain/awx173
87. Ranjan Y, Rashid Z, Stewart C, Kerz M, Begale M, Verbeeck D, et al. RADAR-base: an open source mhealth platform for collecting, monitoring and analyzing data using sensors, wearables, and mobile devices. *JMIR mHealth uHealth.* (2018) 7:e11734. doi: 10.2196/preprints.11734
88. Muse ED, Barrett PM, Steinhubl SR, Topol EJ. Towards a smart medical home. *Lancet Lond Engl.* (2017) 389:358. doi: 10.1016/S0140-6736(17)30154-X
89. Davis KA, Ung H, Wulsin D, Wagenaar J, Fox E, Patterson N, et al. Mining continuous intracranial EEG in focal canine epilepsy: relating interictal bursts to seizure onsets. *Epilepsia.* (2016) 57:89–98. doi: 10.1111/epi.13249

90. Goldenholz DM, Moss R, Jost DA, Crone NE, Krauss G, Picard R, et al. Common data elements for epilepsy mobile health systems. *Epilepsia.* (2018) 59:1020–6. doi: 10.1111/epi.14066
91. LeCun Y, Bengio Y, Hinton G. Deep learning. *Nature.* (2015) 521:436–44. doi: 10.1038/nature14539
92. Freestone DR, Karoly PJ, Cook MJ, A. forward-looking review of seizure prediction. *Curr Opin Neurol.* (2017) 30:167–73. doi: 10.1097/WCO.0000000000000429
93. Nasseri M, Attia TP, Joseph B, Gregg NM, Nurse ES, Viana PF, et al. Non-invasive wearable seizure detection using long–short-term memory networks with transfer learning. *J Neural Eng.* (2021) 18:056017. doi: 10.1088/1741-2552/abef8a
94. Baldassano SN, Brinkmann BH, Ung H, Blevins T, Conrad EC, Leyde K, et al. Crowdsourcing seizure detection: algorithm development and validation on human implanted device recordings. *Brain.* (2017) 140:1680–91. doi: 10.1093/brain/awx098
95. Kuhlmann L, Karoly P, Freestone DR, Brinkmann BH, Temko A, Barachant A, et al. Epilepsyecosystem.org: crowd-sourcing reproducible seizure prediction with long-term human intracranial EEG. *Brain.* (2018) 141:2619–30. doi: 10.1093/brain/awy210
96. Kiral-Kornek I, Roy S, Nurse E, Mashford B, Karoly P, Carroll T, et al. Epileptic seizure prediction using big data and deep learning: toward a mobile system. *EBioMedicine.* (2018) 27:103–11. doi: 10.1016/j.ebiom.2017.11.032
97. Nejedly P, Kremen V, Sladky V, Nasseri M, Guragain H, Klimes P, et al. Deep-learning for seizure forecasting in canines with epilepsy. *J Neural Eng.* (2019) 16:036031. doi: 10.1088/1741-2552/ab172d
98. Eberlein M, Hildebrand R, Tetzlaff R, Hoffmann N, Kuhlmann L, Brinkmann B, et al. Convolutional neural networks for epileptic seizure prediction. In: *2018 IEEE International Conference on Bioinformatics and Biomedicine (BIBM)*. Madrid (2018). 2577–82.
99. Korshunova I, Kindermans P-J, Degrave J, Verhoeven T, Brinkmann BH, Dambre J. Towards improved design and evaluation of epileptic seizure predictors. *IEEE Trans Biomed Eng.* (2017) 65:502–10. doi: 10.1109/TBME.2017.2700086
100. Van Ness PC. Are seizure detection devices ready for prime time? *Epilepsy Curr.* (2019) 19:36–7. doi: 10.1177/1535759719827430
101. Mormann F, Andrzejak RG, Elger CE, Lehnertz K. Seizure prediction: the long and winding road. *Brain.* (2007) 130:314–33. doi: 10.1093/brain/awl241
102. Meisel C, El Atrache R, Jackson M, Schubach S, Ufongene C, Loddenkemper T. Machine learning from wristband sensor data for wearable, noninvasive seizure forecasting. *Epilepsia.* (2020) 61:2653–66. doi: 10.1111/epi.16719
103. Stacey WC. Seizure prediction is possible–now let's make it practical. *EBioMedicine.* (2018) 27:3–4. doi: 10.1016/j.ebiom.2018.01.006
104. Kuhlmann L, Lehnertz K, Richardson MP, Schelter B, Zaveri HP. Seizure prediction—ready for a new era. *Nat Rev Neurol.* (2018) 1:618–30. doi: 10.1038/s41582-018-0055-2
105. Schulze-Bonhage A, Sales F, Wagner K, Teotonio R, Carius A, Schelle A, et al. Views of patients with epilepsy on seizure prediction devices. *Epilepsy Behav.* (2010) 18:388–96. doi: 10.1016/j.yebeh.2010.05.008
106. Gilbert F, Cook M, O'Brien T, Illes J. Embodiment and estrangement: results from a first-in-human "intelligent BCI" trial. *Sci Eng Ethics.* (2019) 25:83–96. doi: 10.1007/s11948-017-0001-5
107. Gilbert F. O'brien T, Cook M. The effects of closed-loop brain implants on autonomy and deliberation: what are the risks of being kept in the loop? *Camb Q Healthc Ethics.* (2018) 27:316–25. doi: 10.1017/S0963180117000640
108. Jachan M, Drentrup HFG, Posdziech F, Brandt A, Altenmüller DM, Schulze-Bonhage A, et al. Probabilistic forecasts of epileptic seizures and evaluation by the brier score. In: Vander Sloten J, Verdonck P, Nyssen M, Haueisen J, editors. *4th European Conference of the International Federation for Medical and Biological Engineering IFMBE Proceedings*. Berlin; Heidelberg: Springer. (2009). p. 1701–5. doi: 10.1007/978-3-540-89208-3_405
109. Schelter B, Feldwisch-Drentrup H, Ihle M, Schulze-Bonhage A, Timmer J. Seizure prediction in epilepsy: from circadian concepts via probabilistic forecasting to statistical evaluation. *Annu Int Conf IEEE Eng Med Biol Soc.* (2011) 2011:1624–7. doi: 10.1109/IEMBS.2011.6090469
110. Winterhalder M, Maiwald T, Voss HU, Aschenbrenner-Scheibe R, Timmer J, Schulze-Bonhage A. The seizure prediction characteristic: a general framework to assess and compare seizure prediction methods. *Epilepsy Behav.* (2003) 4:318–25. doi: 10.1016/S1525-5050(03)00105-7
111. Snyder DE, Echauz J, Grimes DB, Litt B. The statistics of a practical seizure warning system. *J Neural Eng.* (2008) 5:392. doi: 10.1088/1741-2560/5/4/004
112. Stirling RE, Cook MJ, Grayden DB, Karoly PJ. Seizure forecasting and cyclic control of seizures. *Epilepsia.* (2020) 62:S2–14. doi: 10.1111/epi.16541
113. Chiang S, Moss R, Black AP, Jackson M, Moss C, Bidwell J, et al. Evaluation and recommendations for effective data visualization for seizure forecasting algorithms. *JAMIA Open.* (2021) 4:ooab009. doi: 10.1093/jamiaopen/ooab009
114. Proix T, Truccolo W, Leguia MG, Tcheng TK, King-Stephens D, Rao VR, et al. Forecasting seizure risk in adults with focal epilepsy: a development and validation study. *Lancet Neurol.* (2021) 20:127–35. doi: 10.1016/S1474-4422(20)30396-3
115. Maturana MI, Meisel C, Dell K, Karoly PJ, D'Souza W, Grayden DB, et al. Critical slowing as a biomarker for seizure susceptibility. *Nat Commun.* (2020) 11:2172. doi: 10.1101/689893
116. Karoly PJ, Cook MJ, Maturana M, Nurse ES, Payne D, Brinkmann BH, et al. Forecasting cycles of seizure likelihood. *Epilepsia.* (2020) 61:776–6. doi: 10.1101/2019.12.19.19015453
117. Karoly PJ, Eden D, Nurse ES, Cook MJ, Taylor J, Dumanis S, et al. Cycles of self-reported seizure likelihood correspond to yield of diagnostic epilepsy monitoring. *medRxiv.* (2020). doi: 10.1101/2020.10.05.20207407
118. Goldenholz DM, Goldenholz SR, Romero J, Moss R, Sun H, Westover B. Development and validation of forecasting next reported seizure using e-diaries. *Ann Neurol.* (2020) 88:588–95. doi: 10.1002/ana.25812
119. Chiang S, Goldenholz DM, Moss R, Rao VR, Haneef Z, Theodore WH, et al. Prospective validation study of an epilepsy seizure risk system for outpatient evaluation. *Epilepsia.* (2020) 61:29–38. doi: 10.1111/epi.16397
120. Leguia MG, Rao VR, Kleen JK, Baud MO. Measuring synchrony in bio-medical timeseries. *Chaos Interdiscip J Nonlinear Sci.* (2021) 31:013138. doi: 10.1063/5.0026733
121. Beniczky S, Conradsen I, Wolf P. Detection of convulsive seizures using surface electromyography. *Epilepsia.* (2018) 59:23–9. doi: 10.1111/epi.14048
122. Gu Y, Cleeren E, Dan J, Claes K, Van Paesschen W, Van Huffel S, et al. Comparison between scalp EEG and behind-the-ear EEG for development of a wearable seizure detection system for patients with focal epilepsy. *Sensors.* (2018) 18:29. doi: 10.3390/s18010029
123. Van de Vel A, Cuppens K, Bonroy B, Milosevic M, Jansen K, Van Huffel S, et al. Non-EEG seizure detection systems and potential SUDEP prevention: state of the art: review and update. *Seizure.* (2016) 41:141–53. doi: 10.1016/j.seizure.2016.07.012
124. Simblett SK, Biondi A, Bruno E, Ballard D, Stoneman A, Lees S, et al. Patients' experience of wearing multimodal sensor devices intended to detect epileptic seizures: a qualitative analysis. *Epilepsy Behav.* (2020) 102:106717. doi: 10.1016/j.yebeh.2019.106717
125. Rakers F, Walther M, Schiffner R, Rupprecht S, Rasche M, Kockler M, et al. Weather as a risk factor for epileptic seizures: a case-crossover study. *Epilepsia.* (2017) 58:1287–95. doi: 10.1111/epi.13776
126. Payne DE, Dell KL, Karoly PJ, Kremen V, Gerla V, Kuhlmann L, et al. Identifying seizure risk factors: a comparison of sleep, weather, and temporal features using a Bayesian forecast. *Epilepsia.* (2021) 62:371–82. doi: 10.1111/epi.16785
127. Zijlmans M, Flanagan D, Gotman J. Heart rate changes and ECG abnormalities during epileptic seizures: prevalence and definition of an objective clinical sign. *Epilepsia.* (2002) 43:847–54. doi: 10.1046/j.1528-1157.2002.37801.x
128. Billeci L, Marino D, Insana L, Vatti G, Varanini M. Patient-specific seizure prediction based on heart rate variability and recurrence quantification analysis. *PLoS ONE.* (2018) 13:e0204339. doi: 10.1371/journal.pone.0204339
129. Poh M-Z, Loddenkemper T, Reinsberger C, Swenson NC, Goyal S, Sabtala MC, et al. Convulsive seizure detection using a wrist-worn electrodermal activity and accelerometry biosensor. *Epilepsia.* (2012) 53:93–7. doi: 10.1111/j.1528-1167.2012.03444.x

130. Poh M-Z, Loddenkemper T, Reinsberger C, Swenson NC, Goyal S, Madsen JR, et al. Autonomic changes with seizures correlate with postictal EEG suppression. *Neurology*. (2012) 78:1868–76. doi: 10.1212/WNL.0b013e318258f7f1
131. Vieluf S, Amengual-Gual M, Zhang B, El Atrache R, Ufongene C, Jackson MC, et al. Twenty-four-hour patterns in electrodermal activity recordings of patients with and without epileptic seizures. *Epilepsia*. (2021) 62:960–72. doi: 10.1111/epi.16843
132. Karoly PJ, Stirling RE, Freestone DR, Nurse ES, Doyle B, Halliday A, et al. Multiday cycles of heart rate modulate seizure likelihood at daily, weekly and monthly timescales: an observational cohort study. *medRxiv*. (2020). doi: 10.1101/2020.11.24.20237990

Conflict of Interest: PK, EN, DF, and MC are employees of Seer Medical, which provides diagnostic EEG services. BB and GW have licensed IP to Cadence Neuroscience Inc., and have received research devices at no charge from Medtronic Inc. for a study.

The remaining authors declare that the research was conducted in the absence of any commercial or financial relationships that could be construed as a potential conflict of interest.

APPENDIX: PANELS

Panel 1: What Is Wearable?

This review focuses on how wearable devices can be used to aid chronic, lifetime epilepsy management. Devices that may be comfortable for a few hours, or even a day may not be classed as wearable for life. Furthermore, the term "wearable" implies a degree of accessibility that assumes no specialized medical knowledge is required for use.

Smartwatches

Highly popular lifestyle tech device.

Signals: photoplethysmography, O^2 saturation, skin temperature, skin conductance, accelerometry, location (GPS), EKG (in development).

Smart Rings

Similar to smartwatches but with different movement artifacts.

Signals: photoplethysmography, O^2 saturation, skin temperature.

Arm Bands

Sensors mounted on a band around the upper arm. Some devices may be placed with adhesive stickers.

Signals: Heart rate, muscle activity, oxygen saturation, skin temperature, skin conductance, accelerometry.

Stick-On Sensor Patches

Subtle patches stuck anywhere on the body that are either re-useable or easily replaced at regular intervals, such as EEG electrodes placed behind the ear, or blood-glucose arm patches.

Signals: EEG/EKG/EMG, accelerometry, glucose, cortisol (in development).

Smart Phones

Smart phones are not strictly wearable but most wearable devices integrate and present information to users *via* smartphone. Furthermore, more and more people now carry their smart phone at all times, in a pocket or handbag.

Signals: Location, accelerometry, microphone, usage patterns, many aspects of external environment.

Excluded Devices

This review does not consider most scalp EEG electrode caps or headbands to be wearable. Similarly, implantable devices may be eminently suitable for long-term use, but they are not considered "wearable."

PANEL 2: KEY CONSIDERATIONS IN WEARABLE DEVICE DESIGN

- Comfort: devices should be able to be worn without discomfort for extended periods of time, including during sleep and activities such as exercise and bathing.
- Battery life: wearables should be able to record at least 24 h of activity without needing to recharge the device. Recharging time should be limited to a few hours. Connectors should be standard types such as micro-USB or USB-C.
- Accessibility: design of devices and associated phone apps should account for differences in age groups, genders, vision capabilities, and body sizes. Particular care should be given to testing PPG sensors on a variety of skin pigments.
- Appearance: devices should be inconspicuous, or otherwise not immediately identifiable as medical devices.
- Security: data security and individual anonymity are of high concern to users, caregivers, and clinicians. Different regions and jurisdictions will have unique requirements for security compliance, and laws regarding data access and ownership.
- Internet connectivity: Broadband or 4G internet is required to transmit data efficiently. Devices can only store a limited amount of data internally before requiring upload to an associated device (e.g., *via* Bluetooth) or the cloud.
- Integration: interfacing with other devices is essential. Connection with resources such as diaries, smartphone sensors, and location is becoming ubiquitous.

PANEL 3: CASE STUDY: A BUMP IN THE DARK

A 30-year-old man presented with a generalized tonic–clonic seizure after over 12 months of seizure freedom on 500 mg Sodium Valproate once daily. He complained of 6 month history of occasionally feeling poorly rested. An MRI appeared normal, and he was otherwise generally healthy. After two 7-day video-EEG studies (first non-diagnostic), a GTCS was captured lasting 2 min occurring during sleep, of which he had no memory. An additional 500 mg Sodium Valproate was given in the evening and began wearing a wrist-worn accelerometry device to detect nocturnal seizures in the home. Three events were detected within a 2-month period, none of which could be recalled. Carbamazepine was commenced, and he has since been free of seizures for over 6 months.

This case presents a common problem—a seizure diary that provides little information to guide treatment, and non-diagnostic, time-consuming video-EEG studies. Monitoring within the home can provide longitudinal seizure counts with reasonable sensitivity for GTCS events (from both wakefulness and sleep) and provide near real-time alerts to caregivers. Without a wearable device, multiple video-EEG studies may be required to measure the effect of each of the additional medications.

frontiers in Neurology

ORIGINAL RESEARCH
published: 15 July 2021
doi: 10.3389/fneur.2021.704060

Forecasting Seizure Likelihood With Wearable Technology

Rachel E. Stirling[1], David B. Grayden[1,2,3], Wendyl D'Souza[2], Mark J. Cook[2,3], Ewan Nurse[2,4], Dean R. Freestone[4], Daniel E. Payne[1], Benjamin H. Brinkmann[5], Tal Pal Attia[5], Pedro F. Viana[6,7], Mark P. Richardson[6] and Philippa J. Karoly[1,2,3]*

[1] Department of Biomedical Engineering, The University of Melbourne, Melbourne, VIC, Australia, [2] Departments of Medicine and Neurology, St Vincent's Hospital, The University of Melbourne, Melbourne, VIC, Australia, [3] Graeme Clark Institute for Biomedical Engineering, The University of Melbourne, Melbourne, VIC, Australia, [4] Seer Medical, Melbourne, VIC, Australia, [5] Bioelectronics Neurophysiology and Engineering Lab, Department of Neurology, Mayo Clinic, Rochester, MN, United States, [6] School of Neuroscience, Institute of Psychiatry, Psychology and Neuroscience, King's College London, London, United Kingdom, [7] Faculty of Medicine, University of Lisbon, Lisbon, Portugal

The unpredictability of epileptic seizures exposes people with epilepsy to potential physical harm, restricts day-to-day activities, and impacts mental well-being. Accurate seizure forecasters would reduce the uncertainty associated with seizures but need to be feasible and accessible in the long-term. Wearable devices are perfect candidates to develop non-invasive, accessible forecasts but are yet to be investigated in long-term studies. We hypothesized that machine learning models could utilize heart rate as a biomarker for well-established cycles of seizures and epileptic activity, in addition to other wearable signals, to forecast high and low risk seizure periods. This feasibility study tracked participants' (n = 11) heart rates, sleep, and step counts using wearable smartwatches and seizure occurrence using smartphone seizure diaries for at least 6 months (mean = 14.6 months, SD = 3.8 months). Eligible participants had a diagnosis of refractory epilepsy and reported at least 20 seizures (mean = 135, SD = 123) during the recording period. An ensembled machine learning and neural network model estimated seizure risk either daily or hourly, with retraining occurring on a weekly basis as additional data was collected. Performance was evaluated retrospectively against a rate-matched random forecast using the area under the receiver operating curve. A pseudo-prospective evaluation was also conducted on a held-out dataset. Of the 11 participants, seizures were predicted above chance in all (100%) participants using an hourly forecast and in ten (91%) participants using a daily forecast. The average time spent in high risk (prediction time) before a seizure occurred was 37 min in the hourly forecast and 3 days in the daily forecast. Cyclic features added the most predictive value to the forecasts, particularly circadian and multiday heart rate cycles. Wearable devices can be used to produce patient-specific seizure forecasts, particularly when biomarkers of seizure and epileptic activity cycles are utilized.

Keywords: seizure forecasting, cycles (cyclical), seizure cycles, circadian rhythms, multiday rhythms, wearable sensors

OPEN ACCESS

Edited by:
Sharon Chiang, University of California, San Francisco, United States

Reviewed by:
Souptik Barua, Rice University, United States
Kais Gadhoumi, Duke University, United States

****Correspondence:***
Rachel E. Stirling
rachelstirling1@gmail.com

Specialty section:
This article was submitted to Epilepsy, a section of the journal Frontiers in Neurology

Received: *01 May 2021*
Accepted: *17 June 2021*
Published: *15 July 2021*

Citation:
Stirling RE, Grayden DB, D'Souza W, Cook MJ, Nurse E, Freestone DR, Payne DE, Brinkmann BH, Pal Attia T, Viana PF, Richardson MP and Karoly PJ (2021) Forecasting Seizure Likelihood With Wearable Technology. Front. Neurol. 12:704060. doi: 10.3389/fneur.2021.704060

INTRODUCTION

Epilepsy is one of the most common neurological disorders, affecting roughly 1% of the world's population (1) and responsible for 20.6 million disability-adjusted life-years (DALYs) lost, which is comparable to breast cancer in women and lung cancer in men (2). Epilepsy is characterized by an increased predisposition of the brain to generate epileptic seizures, which often result in vast neurobiological, cognitive, psychologic, and social consequences (3). Despite decades of new drug development and surgical treatment, up to one-third of people with epilepsy continue to suffer from recurrent seizures (4, 5). While most people are symptom-free for more than 99.9% of their day-to-day life, epileptic seizures are sudden, potentially catastrophic events that can be life-threatening both for the person with epilepsy and others. Crucially, sudden death in epilepsy (SUDEP), most often following a convulsive seizure, is 27 times more likely than sudden death in control populations, a mortality burden second only to stroke when compared to other neurologic diseases (6, 7). Aside from these risks, living with epilepsy can take a major toll on quality of life and independence, as the unpredictable nature of seizures causes feelings of uncertainty (8) and impacts participation in common day-to-day activities, such as going to work, driving, and social interactions (9).

To address the uncertainty associated with epileptic seizures, researchers across many disciplines have spent years investigating the potential for seizure prediction and forecasting (10). The ability to reduce the uncertainty of when a seizure is about to occur would have tremendous implications for quality of life, and clinical management (10). Timely precautions against seizure-related injury or timed adjustment of treatment according to seizure likelihood (chronotherapy) could also reduce seizure-related harm, hospitalizations, and healthcare-related costs (11).

Until recently, there was no scientific consensus as to whether seizures would be predictable in a prospective setting since most research was based on limited data [from short-duration in-hospital electroencephalography (EEG) recordings] and some presented methodological flaws (12). Access to better quality data [made available in public databases (13, 14) and seizure prediction competitions (15)], more rigorous statistical and analytical methods, and results from a clinical trial of an intracranial EEG seizure advisory system [NeuroVista (16)] have shown promise that seizure prediction devices could be possible in the foreseeable future. Additionally, there is a better understanding of the pre-seizure state and of the mechanisms underlying seizure generation (ictogenesis), with contributions from basic science, network theory, multiscale electrophysiological recordings, and functional neuroimaging (17). Multiple patient-specific seizure precipitants have also been identified, including stress (18, 19), poor sleep (18), exercise (20), diet (21), weather (22, 23), alcohol use (24) and poor drug adherence (25). Many of these factors have shown potential utility in forecasting seizures (18, 23).

Yet perhaps the most significant breakthrough for the field of seizure forecasting has been the characterization of short- and long-term seizure occurrence cycles (11, 26, 27), which typically occur in circadian and multiday (often weekly and monthly) periodicities (27, 28). Similar cycles have been reported in interictal epileptiform activity (IEA) (26), EEG markers of brain critical slowing (29) and heart rate (30), all of which have been linked to seizure timing, suggesting that seizures are co-modulated by underlying biological cycles. An individual's seizure cycles can be utilized to generate seizure forecasts using both self-reporting seizure diaries (31–33) and electrographic seizures (34). However, the discrete nature of seizure events means that the underlying biological cycles may be stronger predictors of seizure occurrence than seizure cycles alone (29, 34, 35). This has already been successfully demonstrated with cycles of IEA in a retrospective seizure forecasting study using an implanted intracranial EEG device (34). Furthermore, algorithms incorporating biological cycles seem to outperform algorithms using more traditional EEG features, such as spectral power and correlation (15).

However, seizure forecasting algorithms typically rely on chronic EEG recordings from invasive, implanted devices, which require surgery (and associated risks), are costly, and may not be an option for many people with epilepsy. Minimally-invasive or non-invasive wearable devices that monitor continuous biomarkers of seizure risk are, therefore, ideal candidates for most people who desire seizure forecasts (9). Currently, some wearable devices are commercially available for seizure *detection* (36), although there are also promising results highlighting the utility of wearables in seizure forecasting. Wearable sensors can be used to detect actigraphy, blood volume pulse, body temperature, cerebral oxygen saturation, electrodermal activity and heart rate, all of which have all shown promise in seizure prediction (37–40). Periodic wearable signals, such as temperature (41) and heart rate (30) may also be used as a biomarker for seizure cycles (35). For example, our recent work in seizure timing and heart rate, measured from a wearable smartwatch, shows that seizures are often phase-locked to underlying circadian and multiday cycles in heart rate (i.e., there is a strong preference for seizures to occur at specific phases of individual-specific heart rate cycles, such as near the peak or trough of a multiday cycle) (30).

To address the need for non-invasive seizure forecasting, this study aimed to develop a wearable device-based seizure forecaster using a long-term dataset from an observational cohort study, Tracking Seizure Cycles. We hypothesized that cycles in heart rate can be leveraged, in addition to other wearable signals (other heart rate features, step count and sleep features), to forecast high and low seizure risk periods. We also investigated the relative contributions of cycles, heart rate, sleep and activity features to forecasting performance.

MATERIALS AND METHODS

Study Design

This retrospective and pseudo-prospective feasibility study was designed using training and testing datasets, followed by pseudo-prospective evaluation using a held-out dataset. We utilized long-term smartphone seizure diaries and a wearable smartwatch to forecast seizure likelihood and elucidate the relationship between seizures and non-invasively measured wearable signals, namely

heart rate, sleep stages, sleep time, and step count. The study was approved by the St Vincent's Hospital Human Research Ethics Committee (HREC 009.19) and all participants provided written informed consent.

Participants

Adults (18 years and over) with a confirmed epilepsy diagnosis and healthy controls were recruited between August 2019 and January 2021. Participants with epilepsy had uncontrolled or partially controlled seizures and were recruited through neurologist referral. All participants provided written informed consent.

Data Collection

Continuous data were collected via smartphone and wearable devices for at least 6 months and up to 20 months. Participants wore a smartwatch (Fitbit, Fitbit Inc., USA) and manually reported seizure times in a freely available smartphone diary app (Seer App, Seer Medical Pty Ltd, Australia). Participants were instructed to report all their clinically apparent events, including generalized and focal seizures (both aware and unaware). The smartwatch continuously measured participants' heart rates (via photoplethysmography) at 5 s resolution (one recording every 5 s). The smartwatch also estimated sleep stage (awake, REM, and light and deep sleep) and step count each minute.

Training, Testing and Held-Out Evaluation Datasets

Participants were required to have 2 months or more of continuous wearable data recordings, at least 80% adherence (i.e., they must have worn the device at least 80% of the time) and a minimum of 20 seizures reported during the recording time to be eligible for seizure forecasting. Eligible participant demographic information is given in **Table 1**.

The training dataset included at least 2 months of continuous recordings (M = 5.4 months, SD = 4 months) and at least 15 seizures (M = 35, SD = 47). The patient-specific training cut-off date was the final day that both of these criteria were met. The testing dataset included participants' continuous recordings (M = 6.6 months, SD = 3.1 months) and seizures (M = 87, SD = 112) reported from their training cut-off date until 1 February 2021. As a further requirement for seizure forecasting, participants must have had at least five lead seizures (at least an hour apart in the hourly forecast and at least a day apart in the daily forecast) reported during the testing period. Any continuous recordings (M = 2.6 months, SD = 0.5) and seizures (M = 13, SD = 14) reported from 1 February 2021 until 25 April 2021 were included in the held-out evaluation cohort, so long as the participant reported at least one seizure during this period. This data was held-out to evaluate the performance of the forecasting algorithm in a pseudo-prospective setting.

Data Preprocessing

The heart rate, step count, and sleep signals were all processed separately. Heart rate features included rate of change in heart rate (RCH) and daily resting heart rate (RHR). Physical activity features included steps recorded in the previous hour and steps recorded on the previous day. Sleep features included total time asleep (not including naps), time in REM, time in deep and light sleep during main sleep, average HR overnight, sleep time deviation from median sleep time over the past 3 months, and wake time deviation from median wake time over the past 3 months. All sleep features were calculated using sleep labels derived from Fitbit's sleep algorithm. Additionally, we included cyclic features, comprising heart rate cycles (circadian and multiday), last seizure time, and second-last seizure time. Compared to the hourly forecast, the daily forecast only included multiday cycles, days since last seizure time, days since second-last seizure time, all sleep features, daily resting heart rate, and steps recorded during the previous day.

To derive heart rate features and heart rate cycles, continuous heart rate signals were initially down-sampled to one timestamp per minute, followed by interpolation of short missing data segments with a linear line (missing segments <2 h) or longer missing data segments with a straight line at the mean heart rate. RCH was used to estimate heart rate variability (HRV), which is defined as the variations in RR intervals and is typically derived using the QRS complex on an electrocardiogram (ECG). RCH was calculated as the mean beats per minute (BPM) in 1 min subtracted from the mean BPM in the previous minute, representing the change in BPM over 2 min. RCH was resampled every hour for the hourly forecast or every day for the daily forecast. Daily RHR was derived as the average of the bottom quintile of BPM where no steps were recorded, thus minimizing the potential for movement artifact.

To compute the heart rate cycles, we used a similar approach to a method used to extract multiday rhythms of epileptic activity (26) [see also (30) for further details]. Briefly, circadian and multiday peak periodicities of heart rate (cycles) were derived using a Morlet wavelet. The heart rate signal was filtered (using a zero-order Butterworth bandpass filter) at the peak periodicities and instantaneous phase of the cycle at each timepoint was estimated using a Hilbert transform. Cycles were used as features for the forecaster if seizures were significantly phase-locked to the cycle [$p < 0.05$, according to Omnibus/Hodges-Ajne test for circular uniformity (42)]. Each cyclic feature (cycle phases and last/second last seizure time) was transformed into two linear features by normalizing the signal from 0 to 2π and computing the sine and cosine.

Forecasting Algorithm

The seizure forecast was presented in hourly and daily formats to assess the accuracy of an hourly forecast compared to a daily forecast. The hourly forecast gave the likelihood of a seizure at the start of the hour, every hour. The daily forecast gave the likelihood of a seizure for the day, shortly after waking from sleep (based on Fitbit's sleep end time).

To forecast the likelihood of a seizure hourly and daily, we used an ensemble of a long short-term memory (LSTM) neural network (43), a random forest (RF) regressor (43), and a logistic regression (LR) classifier (43). An ensemble method was chosen to allow the combination of diverse feature types. **Figure 1** describes the architecture of the model. The training (green), testing (orange) and evaluation (red) cohorts were different

TABLE 1 | Eligible participants' demographic information.

Participant	Type of seizures (Focal, Generalized or Both)	Total seizures during monitoring (frequency/month)	Training recording length (months)	Testing recording length (months)	Evaluation recording length (months)	Sleep scoring (nights)
P1	Focal	57 (5.1)	4.2	4.3	2.7	334
P2	Focal	111 (8.8)	2.0	7.9	2.7	371
P3	Focal	27 (1.5)	12.6	3.1	2.7	549
P4	Focal	24 (1.4)	10.6	4.3	2.7	500
P5	Both	280 (17.0)	2.0	13.3	1.2	459
P6	Focal	246 (36.7)	2.0	2.1	2.6	199
P7	Generalized	28 (1.6)	8.5	5.9	2.7	501
P8	Focal	179 (14.6)	2.5	7.1	2.7	327
P9	Both	392 (19.6)	9.7	7.6	2.7	586
P10	Focal	94 (6.6)	2.4	9.2	2.7	428
P11	Focal	55 (3.9)	3.5	7.8	2.7	399
Summary	**8 focal only, 1 generalized only, 2 both generalized and focal**	**M = 136 (10.6) SD = 123 (10.8)**	**M = 5.5 SD = 4.0**	**M = 6.7 SD = 3.2**	**M = 2.6 SD = 0.5**	**M = 423 SD = 112**

Participants that had more than one seizure during the evaluation period are shown in red.

lengths in each participant, and algorithm retraining occurred weekly during testing and evaluation. The forecast used an LSTM model (which contains 7 days of memory) for all sleep features in order to account for the potential effect of built-up sleep debt on seizure risk (18). All other features (cycles, heart rate features and step counts) then predicted seizure risk using a random forest model. The random forest model was chosen because it achieved the best results during testing using Python's *sklearn* library, when compared to other conventional machine learning models (namely logistic regression, linear discriminant analysis, K-nearest neighbors, naïve bayes and support vector machines). A logistic regression model, which weighs inputs' predictive value, then combined the random forest and LSTM outputs into one seizure risk value per hour or day. This was compared to a rate-matched random model (occasionally referred to as the chance model) using AUC scores. Other metrics were also used to assess forecast performance (see Performance Metrics).

The LSTM model was trained on sleep features computed daily after waking. A weekly history of sleep features was incorporated into each row input, providing a 7×7 matrix for each forecast, representing 7 days and 7 sleep features per day. The LSTM model was composed of a single layer with 64 memory units, followed by two densely connected layers, and a linear activation function. All networks were trained for 100 epochs. We selected the mean squared error loss function as the cost function, using the Adaptive Moment Estimation (Adam) optimizer (44). The LSTM model outputted the likelihood of a seizure for the day based on sleep features and was used as an input to the LR classifier.

The RF regressors with the bootstrap aggregating technique were trained on all physical activity, heart rate, and cyclic features. In the model, the number of decision trees was 1000 and the minimum number of samples required to be at a leaf node was 120. From observation, these model parameters achieved the highest accuracy across the board during training. Most people, particularly participants with low seizure frequency (<2 seizures/month), had a highly imbalanced dataset, with non-seizure hours/days occurring far more frequently than seizure hours/days. RF models typically made more accurate predictions on balanced datasets, so oversampling of seizure hours/days was undertaken before training the RF model. The output of the RF model was the likelihood of a seizure within the following hour or day and was used as an input to the LR classifier.

The LR classifiers were trained on the outputs of the LSTM and RF models. To aid the classifier in distinguishing between non-seizure hours/days and seizure hours/days and to mitigate the low resoltuion of self-reporting, the hour/day immediately preceding and following the hour/day of each seizure were removed in the training dataset. The output of the LR model was the final likelihood of a seizure (risk value); the risk value was represented as a continuous value between 0 for no seizure and 1 for a "guaranteed" seizure within the next hour or day, as appropriate.

The forecaster classified hours and days as either low, medium, or high risk. The medium and high risk cut-off thresholds were computed using the training dataset by optimizing the metrics:

(C1) time spent in low risk > time spent in medium risk > time spent in high risk;
(C2) seizures in high risk > seizures in medium risk > seizures in low risk (29).

If C1 or C2 could not be satisfied, the optimization algorithm maximized the product of the time in low risk and the number of seizures in high risk (C3 and C4):

(C3) maximize the time spent in a low risk state;
(C4) maximize the number of seizures occurring in the high risk state.

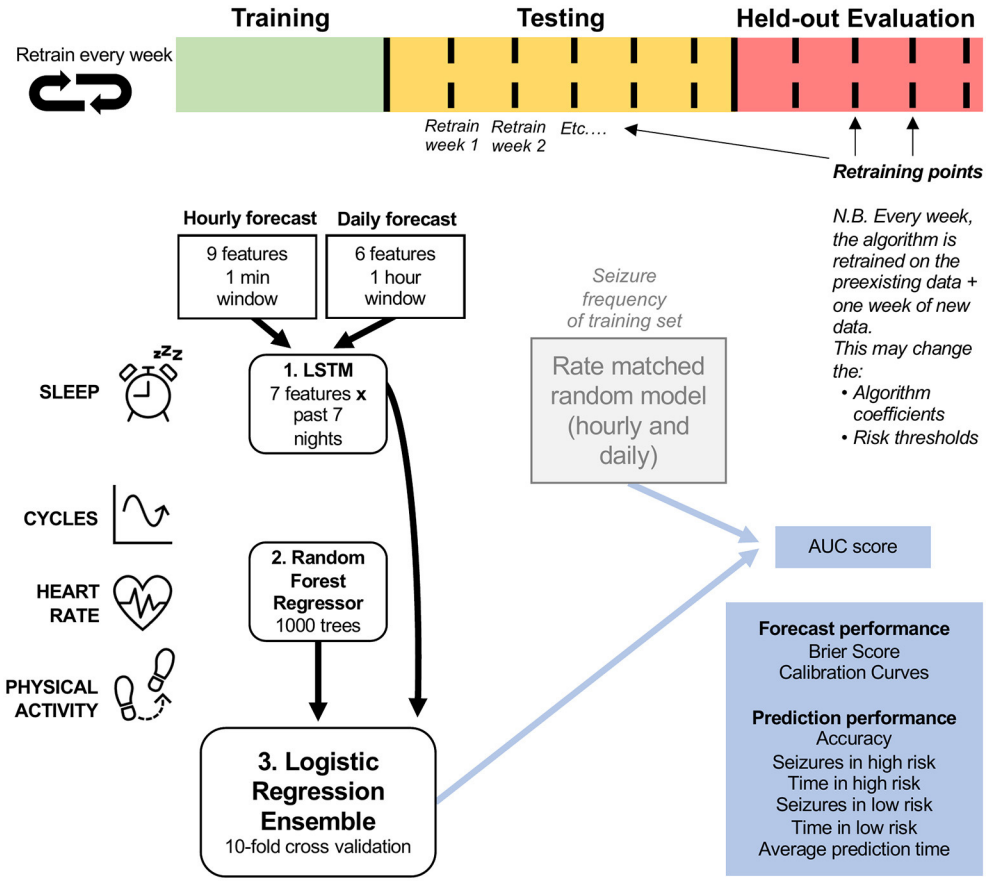

FIGURE 1 | Forecasting model architecture. The logistic regression ensemble (combining LSTM, Random Forest Regressor, and all features) was trained on a training dataset that included at least 15 seizures and at least 2 months of continuous recordings. Two forecasting horizons were compared: hourly and daily forecasts. The LSTM model incorporated sleep features from the past seven nights and the random regressor included all other features (cycles, heart rate, and physical activity features), in addition to the output daily seizure likelihood estimates from the LSTM model. The logistic regression ensemble utilized a 10-fold cross validation approach to forecast seizure likelihood hourly or daily. The forecasting model was assessed (using AUC scores) on a retrospective testing set and a pseudo-prospective held-out evaluation set and compared to a rate-matched random (RMR) model, where seizure frequency was determined by the training set. The algorithm was retrained weekly to imitate a clinical forecast.

Retraining the algorithm was implemented to imitate a clinical seizure forecasting device in which algorithm coefficients and risk thresholds would be regularly updated. Retraining of the seizure forecast occurred on a weekly basis as additional data was collected.

Performance Metrics

To assess the performance of the hourly and daily forecasters, a variety of different metrics were used. During algorithm testing and for pseudo-prospective held-out evaluation, performance of the ensembled model was evaluated using the area under the receiver operating characteristic curve (AUC) and compared to the AUC score of a rate-matched (seizure frequency derived from all seizures that occurred in the training dataset) random forecast. The AUC scores assessed the classifier's ability to discriminate between non-seizure hours/days and seizure hours/days.

Despite the usefulness of the AUC to measure performance, the AUC can change depending on the forecasting horizon (34); in this case, an hourly forecast compared to a daily forecast. This motivated the use of Calibration Curves (CC) to measure how well the predicted likelihood values corresponded to observed probabilities, and the Brier score (or Brier loss) to quantify the accuracy of the predictions. The CC metric provides a visual representation of the forecaster's ability to estimate seizure risk. The ideal CC can be visualized as a diagonal line, where the forecaster's predicted seizure likelihood values are equal to the actual seizure probabilities. Anything above this line would be considered underestimating seizure risk and anything below would be overestimating seizure risk. The Brier score (or Brier Loss) is shown alongside the CC metric, which is often used to assess calibration performance. For the Brier Score, a perfectly accurate forecast would result in a loss score of 0 and a poorly performing forecast would result in a loss closer to 1. We also considered the accuracy of the forecaster, time spent in low, medium and high risk states, and seizures occurring in low, medium and high risk states.

Analyses were executed using Python (version 3.7.9).

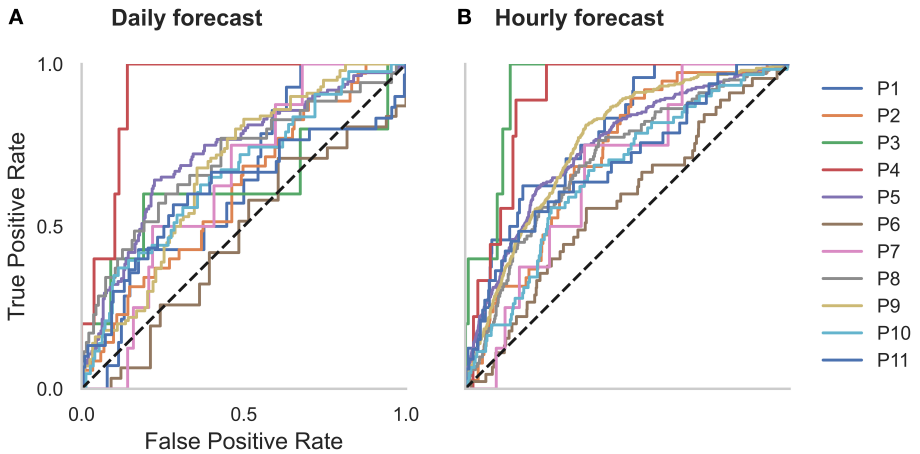

FIGURE 2 | Receiver operator characteristic (ROC) curves for all participants in the **(A)** daily and **(B)** hourly forecast (retrospective testing cohort). The dashed diagonal line represents a balanced random forecast. ROC curves show that hourly forecasts consistently outperformed a balanced random forecaster, and daily forecasts mostly outperformed a balanced random forecaster. Patient-specific forecast performance was assessed by comparing the forecaster's area under the ROC curve (AUC) to the AUC of a rate-matched random forecast (different to the balanced random forecast shown above).

RESULTS

There were 11 out of 39 participants that met the inclusion requirements (see Methods: Study Design and Participants) (**Table 1**). Eligible participants had an average duration of 14.6 months (SD = 3.8) of continuous heart rate and activity monitoring, and an average of 423 nights (SD = 112) that recorded sleep stages and duration. Participant diaries included an average of 136 (SD = 123) seizures reported during the wearable monitoring period. Results from the cohort are given in **Figures 2–6** and **Table 2**. Eight of 11 participants (shown in red in **Table 1**) in the testing cohort were also included in the held-out evaluation cohort, as these people reported more than one seizure during the evaluation period. The results from the prospective evaluation cohort are shown in **Figure 7** and **Table 2**.

Forecast Performance and Metrics

Forecasting performance was quantified to determine which participants would have benefitted from the non-invasive seizure forecast. First, we used the AUC metric to determine forecasting performance. The AUC score quantifies how useful the forecast is, based on the amount of time spent in a high-risk state. An excellent forecast is often considered to have an AUC of >0.9. Of the 11 participants, AUC scores showed that seizures were predicted above chance in all participants using an hourly forecast (M AUC = 0.74, SD = 0.10) and in 10 participants using a daily forecast (M AUC = 0.66, SD = 0.11) (**Figure 2** and **Table 2**).

Both hourly and daily models usually performed well in people with longer recording times. A weak positive correlation was found between total recording length and AUC scores in both the hourly (R^2 = 0.63) and daily (R^2 = 0.59) forecasters (**Supplementary Figure 1**). This suggests that the forecaster improves over time.

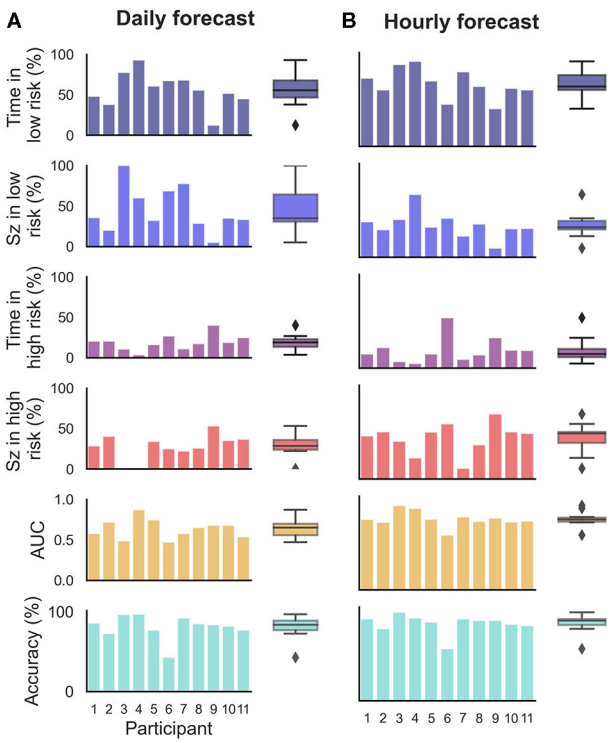

FIGURE 3 | Forecasting and prediction performance metric results in the retrospective testing cohort for the **(B)** hourly and **(A)** daily forecasters. Individual participant bars are shown for each metric. Population box plots are shown on the right of the bars, showing median and upper and lower quartiles for each metric in the hourly and daily forecasters.

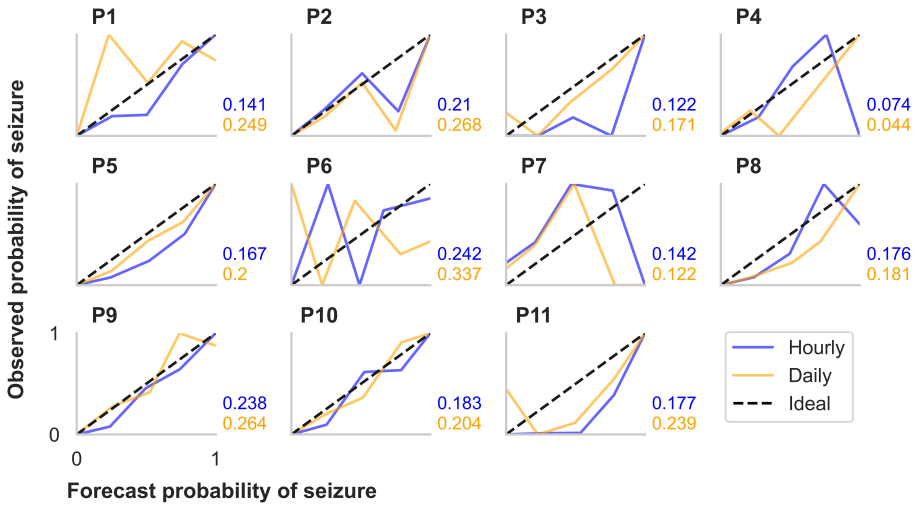

FIGURE 4 | Calibration curves and Brier scores for hourly and daily forecasts summarized for each participant in the retrospective testing cohort. The calibration curves show the relationship between the forecasted likelihood of seizures (x-axes) and the actual observed probability of seizures (y-axes). For the calibration curves, 10 bin sizes were used, so forecast likelihood values were compared to actual probabilities from 0–10%, 10–20%,..., 90–100%. The ideal calibration curve for a hypothetically perfect forecaster is shown in each plot.

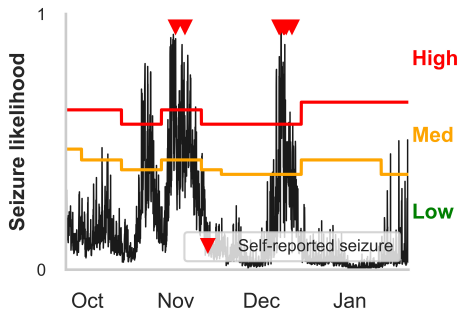

FIGURE 5 | Example hourly forecasts showing high, medium, and low risk states, and medium and high risk thresholds. Predicted seizure likelihood (black line) derived from the hourly forecaster for P4 from the end of September to the end of January. Seizures are marked with red triangles. High, medium and low risk states are indicated by the red, orange and green regions, respectively, and are separated by the medium and high risk thresholds. Note that the medium risk and high risk thresholds—indicated by the orange and red lines, respectively—can change after weekly retraining. The cyclical seizure likelihood is mostly attributable to multiday heart rate cycles.

A relationship was also noticed between seizure frequency and forecasting performance. The model performed worst in the participant with the highest seizure frequency (P6) (0.57 and 0.46 for the hourly and daily forecaster, respectively). P6 had a seizure frequency of 36.7 seizures/month (i.e., more than one per day), which was almost double the next highest participant. Across the whole cohort, a weak negative correlation was found between seizure frequency and AUC scores in both the hourly ($R^2 = -0.58$) and daily ($R^2 = -0.49$) forecasters (**Supplementary Figure 2**). This suggests that participants with lower seizure frequencies (less than once per day) had more accurate predictions using the current model than participants with higher seizure frequencies.

Time spent in high, medium, and low risk, alongside the seizure frequency in high, medium, and low risk, were also considered (**Figure 3**). For the hourly forecast, median forecast accuracy was 86% (min: 56%, max: 95%) and median time in high risk was 14% (min: 5%, max: 45%). For the daily forecast, median forecast accuracy was 83% (min: 43%, max: 97%) and median time in high risk was 18% (min: 6%, max: 29%). Of the 11 participants, the average time spent in high risk (prediction time) before a seizure occurred was 37 min in the hourly forecast and 3 days in the daily forecast. Typically, greater AUC scores implied that the participant spent more time in low risk and most seizures occurred in high risk. For example, P4 spent only 7% of their time in high risk state, but 83% of their seizures occurred whilst in high risk (see **Figure 5** for an example forecast).

Additionally, we evaluated CC metrics and Brier scores (**Figure 4**). Generally, people with more seizures had calibration curves closer to the ideal diagonal line. Hourly and daily forecasts were occasionally found to sit well below the ideal line, suggesting that seizure risk was overestimated in these cases. Brier score loss, another metric to assess forecast calibration performance, varied independently to calibration curve variation. For example, the participants with the highest seizure counts (P5 and P9) had similar calibration curves for both the hourly and the daily forecast; however, Brier loss scores were much greater for P9 than P5. P4 had the lowest Brier loss scores in both the hourly and daily forecast.

Feature Groups on Forecast Performance

To characterize the importance of feature groups on forecasting performance, we analyzed AUC score change with the addition of particular feature groups (**Figure 6**). Physical activity and heart rate feature groups added little predictive value to the daily forecaster. Sleep features appeared to add value to the daily forecaster in some people, but this was not significant across

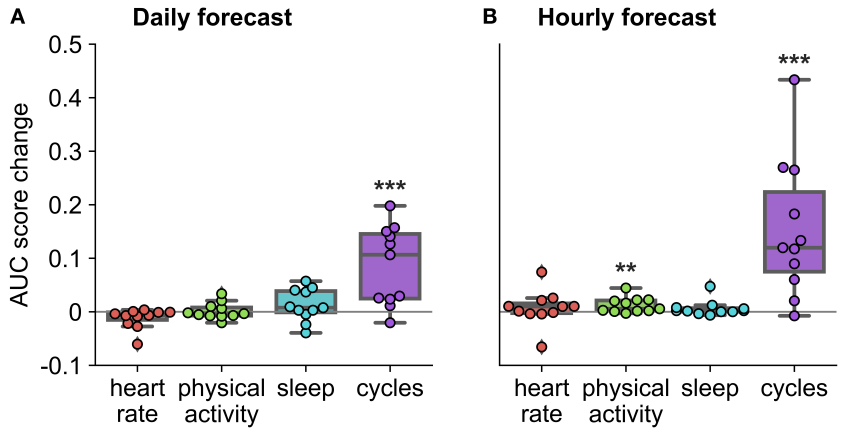

FIGURE 6 | Auxiliary contribution of each feature group on forecasting performance in the retrospective testing cohort. AUC score change represents average change computed over ten runs of the algorithm. Performance of each feature group was characterized by comparing the AUC score of the forecasting algorithm once the feature group was added to the AUC score of the forecasting algorithm without the feature group. For example, in the case of physical activity, we compared the AUC score when the algorithm included all feature groups to the AUC score when the algorithm included only heart rate, sleep, and cycles feature groups. *Indicates that the feature group's contribution was significantly greater than zero across the cohort, using a one-sided *t*-test (***$p < 0.001$ and **$p < 0.01$). **(A)** Daily forecast. **(B)** Hourly forecast.

TABLE 2 | AUC scores of the hourly and daily forecasters for the testing and evaluation cohorts.

		Testing dataset		Evaluation dataset	
		Hourly AUC	**Daily AUC**	**Hourly AUC**	**Daily AUC**
Participant	1	0.79*	0.64*	0.68*	0.42
	2	0.71*	0.61*		
	3	0.93*	0.62*	0.94*	0.69*
	4	0.89*	0.92*		
	5	0.75*	0.72*		
	6	0.57*	0.46	0.55*	0.62*
	7	0.67*	0.64*	0.41	0.45
	8	0.70*	0.70*	0.82*	0.80*
	9	0.76*	0.68*	0.57*	0.45
	10	0.66*	0.66*	0.61*	0.80*
	11	0.69*	0.61*	0.84*	0.45
Mean (SD)		**0.74 (0.1)**	**0.66 (0.11)**	**0.68 (0.18)**	**0.59 (0.16)**

**Indicates performance greater than chance (the rate-matched random forecast).*

the cohort ($p = 0.09$). Physical activity added some predictive value to the hourly forecaster; however, sleep and heart rate features were the weakest predictors in the hourly forecaster. In both the hourly and daily forecaster, the cycles feature group was the strongest predictor across the whole cohort and for most individuals. 10 of 11 participants (all expect P4) had a significant (i.e., seizures were significantly locked onto the cycle in the training dataset) circadian cycle and 10 of 11 (all except P7) people had least one significant multiday cycle. Despite the occasional negative AUC score change with the addition of a feature group, it is important to note that it is unlikely that there is significant positive or negative value added to the forecaster when values are close to 0.

Held Out Evaluation Cohort Performance

The held-out evaluation cohort performed well in most cases (**Figure 7** and **Table 2**). The predictions (based on AUC scores) were above chance in 7 of 8 (88%) people using the hourly forecaster (M = 0.68, SD = 0.18) and 4 of 8 (50%) people using the daily forecaster (M = 0.58, SD = 0.16). It is important to note that the participant, P7, who did not perform better than chance using the hourly forecast model had the lowest seizure count during the evaluation period and was the only participant without a significant multiday heart rate cycle.

DISCUSSION

Summary

People with epilepsy and their caregivers have expressed their interest in non-invasive wearable devices for decades, particularly for seizure forecasting (45) and detection (46). Wearable devices are more acceptable to people with epilepsy than invasive, cumbersome or indiscrete devices (45, 46). Nonetheless, very few studies have investigated the feasibility of non-invasive wearables in seizure forecasting, and although performance in current studies is promising, their datasets are usually short-term (<1 week) (37, 40).

This study demonstrates that features recorded via non-invasive wearable sensors can contribute to accurate seizure forecasts. Individual forecasters performed better than chance with all people when an hourly prediction horizon was used, and with 10 of 11 people when a daily prediction horizon was used. These results indicate that non-invasive seizure forecasting is possible for people with epilepsy with seizure warning periods of up to 24 h.

In the evaluation cohort, predictions were above chance in 7 of 8 people using the hourly forecaster and 4 of 8 people using the daily forecaster. This is contrary to what we expected: that the performance would improve with a longer period on which to

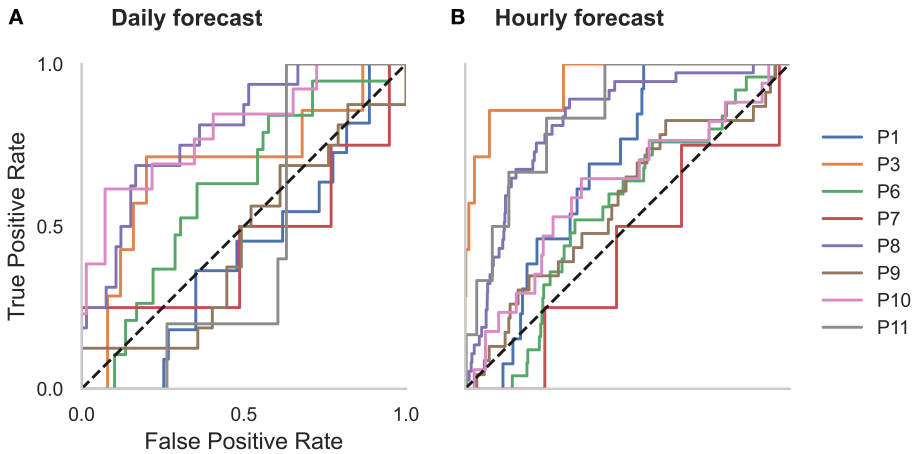

FIGURE 7 | Receiver operator characteristic (ROC) curves for all participants in the **(A)** daily and **(B)** hourly forecast (held-out evaluation testing cohort). The dashed diagonal line represents a balanced random forecast. ROC curves show that hourly forecasts mostly outperformed a balanced random forecaster, and daily forecasts outperformed a balanced random forecaster half of the time. Patient-specific forecast performance was assessed by comparing the forecaster's area under the ROC curve (AUC) to the AUC of a rate-matched random forecast (different to the balanced random forecast shown above).

train the algorithm. The lack of improvement in AUC scores in the evaluation cohort may be attributed to the shorter recording lengths and seizure counts in the evaluation dataset compared to the testing dataset, making it difficult to directly compare the cohorts. Furthermore, the theoretical shift and change that may occur in heart rate cycles over time was not considered in this model. This shift in cycles may be mitigated by consistently retraining the algorithm on a shorter period of data (e.g., the past 4 months, instead of all past data).

Generally, the hourly forecaster resulted in more accurate predictions than the daily forecaster. The superior performance in the hourly forecasts may be attributed to a number of factors, such as the inclusion of circadian heart rate cycles, hourly step count and RCH. The resolution of the daily forecaster would also have played a role in the loss of information. For example, high frequency seizure days (>1 seizure occurred on a day) were weighted equally to low seizure frequency days (1 seizure on a day).

Feature Importance

Overall, cyclic features (heart rate cycles and previous seizure timing) were the strongest predictors of seizures in most cases (**Figure 6**). Most people had a circadian and at least one multiday cycle that aided prediction of seizure risk. This was expected given recent incredibly strong performance of cycles for seizure forecasting (29, 31, 34) and the previously demonstrated utility of heart rate cycles as a biomarker for seizure risk (30). Cycles are now becoming increasingly recognized as a fundamental phenomenon of seizure risk; however, their underlying drivers are still unknown. For recent reviews on cycles in seizure forecasting, refer to Stirling et al. (10) and Karoly et al. (47).

Sleep features appeared to be useful predictors of seizure likelihood for some people using the daily forecaster but were weak predictors in the hourly forecaster. The lack of utility of sleep features in the hourly forecaster may be attributed to the design of the algorithm, as the sleep variable remains constant for all hours of the day after waking, making it difficult for the algorithm to distinguish between non-seizure and seizure hours. In contrast, for some people, sleep was a useful feature in the daily forecaster, which distinguishes seizure-days from non-seizure days. This suggests that sleep does play a role in seizure risk for some people. Sleep features, such as sleep quality, transitions and length, have historically been associated with seizures in many people with epilepsy (18, 23). It is possible that the role of sleep as a seizure precipitant is highly patient-specific, which warrants further investigation in larger cohorts.

Heart rate features—daily RHR and RCH (estimation of HRV)—were not significantly predictive of seizures on a cohort level, but appeared useful in some individuals (**Figure 6**). HRV has been of interest to researchers for decades and is known to reflect autonomic function (48). HRV has also been used to predict seizures minutes in advance, albeit with high false prediction rates (39). It is important to note, however, that we have estimated HRV in the current algorithm using a very basic method, but recent studies have revealed that photoplethysmography-based methods for estimating HRV are available and in the pipeline for wearable devices (49, 50). Daily resting heart rate, on the other hand, is not often associated with seizure risk, but seemed to be a useful feature in some cases. However, daily resting heart rate is likely correlated with multiday rhythms of heart rate and thus may not provide distinct value compared to cyclic features that were derived from heart rate.

Physical activity features were also predictive of seizures in some people, namely in the hourly forecaster (**Figure 6**). Physical activity is beneficial for mental health, quality of life, and cognitive function for people with epilepsy (51). However, people with epilepsy are less likely to engage in physical activity than the general population (52), partially influenced by the inaccurate historical belief that exercise can provoke seizures (53). On the contrary, there is some evidence that increased physical activity is associated with reduced seizure frequency (54,

55). Physical activity is also known to benefit common psychiatric comorbidities of epilepsy, such as anxiety and depression (56), so exercise may indirectly reduce seizure frequency by impacting other seizure precipitants, such as stress and reduced heart rate. We did not explore whether the relationship between physical activity was generally positive or negative in this study, but this should be investigated in future work.

Note that the relative feature contributions found in this work may depend on the specific choice of model and may be taken as an indication of feature importance only. Future work may focus on more rigorous methods for feature importance (57).

Demographic and Clinical Factors

We generally observed that the model performed best for participants with longer recording times, and more consistently over prediction horizons (**Supplementary Figure 1**). This suggests that seizure forecasts utilizing wearable sensors perform better with longer recording times, and are likely to improve over time. We suggest that a clinical forecast requires a minimum amount of data or events before starting to use the forecaster. Future work should investigate the ideal number of events required for the best results, taking into account an individual's seizure frequency, and the optimal number of cycles to observe before incorporating the cycle into the forecaster.

Interestingly, the model tended to perform better in participants with lower seizure frequencies (**Supplementary Figure 2**). This relationship between seizure frequency and forecasting performance was also observed in a prospective forecasting study (16). Although it is well-known that seizure frequency is important to quality of life (58), people with fewer seizures are still subject to anxiety and fear caused by the unpredictability of seizures (8, 59). Therefore, people who have fewer seizures may have the most to benefit from accurate forecaster, as a forecaster may enable them to go about their daily lives without fear of an impending seizure.

Despite less than perfect accuracy in the current model, the results may still meet the user requirements for a practical seizure gauge device. Many people with epilepsy may use a forecasting device despite less than perfect accuracy (45). For example, subjects in a prospective seizure forecasting study found the implanted device useful even though the median sensitivity was only 60% (60). Moreover, shorter time horizons (minutes to hours) seem to be preferable over longer time horizons (days) (45). This is in line with the current results, where the shorter time horizon (hourly) made more accurate predictions than the longer time horizon (daily). Ultimately, prospective seizure forecasting studies with non-invasive wearables are needed to assess user requirements and clinical utility.

Limitations

This study has several limitations. First, self-reported seizure diaries have inherent drawbacks and are known to be inaccurate (61). Not everyone with epilepsy is aware of when they experience a seizure, particularly if they predominantly experience focal aware seizures. Self-reported events also rely on participant or caregiver memory for seizure time recollection, which may cause the forecaster to draw inaccurate conclusions during training. However, self-reported events are non-invasive, easy to capture, and remain the standard data source for medical practice and clinical trials in epilepsy (10). Therefore, seizure diaries remain important for non-invasive seizure forecasting. To improve the accuracy of self-reported events, non-invasive seizure detection devices are available for convulsive seizures, and detection of non-convulsive seizures are in the pipeline (62).

Second, it is worth noting that the accuracy of heart rate and sleep stages measured from smartwatch devices has been investigated compared to electrocardiography and polysomnography, respectively (63–65). These studies collectively show that no significant difference was noted between the heart rate captured using a Fitbit compared to an electrocardiography device during sleep, but some errors did emerge during exercise. Smartwatches are known to be useful in obtaining gross estimates of sleep parameters and heart rate but are not yet suitable substitutes for electrocardiography and polysomnography. This suggests that complex parameters, such as sleep stages and heart rate variability, may need further investigation to understand their role as seizure drivers. Wearable heart rate sensors are also subject to artifacts, although measurement noise was likely to be at a higher frequency than the time scale focused on in the current work.

Third, seizure number and seizure frequency are also limiting factors on whether seizure forecasting is possible. When seizure numbers are low, the forecaster may be unreliable in some cases due to overfitting in the training set. The optimal learning period based on seizure frequency should be investigated in future. Fourth, the ensemble method was complicated because we combined diverse feature types; however, given the main contribution to performance was cyclic features, future work should focus on developing simpler approaches. Cycles may also shift or change over time, thus affecting the accuracy of the forecaster. In a real-world implementation, we may look to remove any past data beyond 1 year or remove the oldest week of data every time a new week is added to account for changes in seizure biomarkers and to reduce memory requirements.

Finally, we attempted to balance our participant recruitment so that it accurately reflected the population of people with refractory epilepsy (variety of adult ages, epilepsy types and seizure frequencies); however, the limited number of participants in this study means that the population may not have been accurately represented in the sample, particularly for people with generalized epilepsy. We also endeavor to explore the relationship between forecasting accuracy and epilepsy type in the future.

CONCLUSION

We assessed the utility of electronic self-reported seizure diaries and non-invasive wearable physiological sensor data to estimate seizure risk in retrospective and pseudo-prospective cohorts. This research has shown that non-invasive wearable sensors in the field of seizure forecasting is not only possible, but feasible and imminent. Prospective analysis and clinical trials should also be undertaken on longitudinal datasets in the future.

DATA AVAILABILITY STATEMENT

The raw data supporting the conclusions of this article will be made available by the authors, without undue reservation.

ETHICS STATEMENT

The studies involving human participants were reviewed and approved by St Vincent's Hospital Human Research Ethics Committee (HREC 009.19). The patients/participants provided their written informed consent to participate in this study.

AUTHOR CONTRIBUTIONS

RS, DG, WD'S, MC, DF, and PK conceived of the presented idea. DF and PK collected the data. RS performed the computations and wrote the manuscript with support from PV, DG, WD'S, MC, and PK. TP, PV, and DP verified the analytical methods, with support and supervision from BB and MR. All authors contributed to the article and approved the submitted version.

FUNDING

This research was funded by an NHMRC Investigator Grant 1178220, the Epilepsy Foundation of America's My Seizure Gauge grant and the BioMedTech Horizons 3 program, an initiative of MTPConnect. The funders were not involved in the study design, collection, analysis, interpretation of data, the writing of this article or the decision to submit it for publication.

SUPPLEMENTARY MATERIAL

The Supplementary Material for this article can be found online at: https://www.frontiersin.org/articles/10.3389/fneur.2021.704060/full#supplementary-material

REFERENCES

1. Abramovici S, Bagić A. Epidemiology of epilepsy. *Handb Clin Neurol.* (2016) 138:159–71. doi: 10.1016/B978-0-12-802973-2.00010-0
2. Murray CJ, Barber RM, Foreman KJ, Ozgoren AA, Abd-Allah F, Abera SF, et al. Global, regional, and national disability-adjusted life years (DALYs) for 306 diseases and injuries and healthy life expectancy (HALE) for 188 countries, 1990–2013: quantifying the epidemiological transition. *Lancet.* (2015) 386:2145–91. doi: 10.1016/S0140-6736(15)61340-X
3. Fisher RS, Acevedo C, Arzimanoglou A, Bogacz A, Cross JH, Elger CE, et al. ILAE official report: a practical clinical definition of epilepsy. *Epilepsia.* (2014) 55:475–82. doi: 10.1111/epi.12550
4. Kwan P, Brodie MJ. Early identification of refractory epilepsy. *New Engl J Med.* (2000) 342:314–9. doi: 10.1056/NEJM200002033420503
5. Chen Z, Brodie MJ, Liew D, Kwan P. Treatment outcomes in patients with newly diagnosed epilepsy treated with established and new antiepileptic drugs: a 30-year longitudinal cohort study. *JAMA Neurol.* (2018) 75:279–86. doi: 10.1001/jamaneurol.2017.3949
6. Devinsky O, Hesdorffer DC, Thurman DJ, Lhatoo S, Richerson G. Sudden unexpected death in epilepsy: epidemiology, mechanisms, and prevention. *Lancet Neurol.* (2016) 15:1075–88. doi: 10.1016/S1474-4422(16)30158-2
7. Thurman DJ, Hesdorffer DC, French JA. Sudden unexpected death in epilepsy: assessing the public health burden. *Epilepsia.* (2014) 55:1479–85. doi: 10.1111/epi.12666
8. Epilepsy Foundation. *Ei2 Community Survey*. Landover, MD: Epilepsy Foundation (2016). Available at: https://www.epilepsy.com/sites/core/files/atoms/files/community-survey-report-2016%20V2.pdf (accessed March 6, 2020).
9. Dumanis SB, French JA, Bernard C, Worrell GA, Fureman BE. Seizure Forecasting from Idea to Reality. Outcomes of the My Seizure Gauge Epilepsy Innovation Institute Workshop. *eNeuro.* (2017) 4:ENEURO.0349-17.2017. doi: 10.1523/ENEURO.0349-17.2017
10. Stirling RE, Cook MJ, Grayden DB, Karoly PJ. Seizure forecasting and cyclic control of seizures. *Epilepsia*. (2020) 62:2–14. doi: 10.1111/epi.16541
11. Baud MO, Rao VR. Gauging seizure risk. *Neurology.* (2018) 91:967–73. doi: 10.1212/WNL.0000000000006548
12. Mormann F, Andrzejak RG, Elger CE, Lehnertz K. Seizure prediction: the long and winding road. *Brain.* (2007) 130:314–33. doi: 10.1093/brain/awl241
13. Klatt J, Feldwisch-Drentrup H, Ihle M, Navarro V, Neufang M, Teixeira C, et al. The EPILEPSIAE Database: An Extensive Electroencephalography Database of Epilepsy Patients. *Epilepsia.* (2012) 53:1669–76. doi: 10.1111/j.1528-1167.2012.03564.x
14. Wagenaar JB, Worrell GA, Ives Z, Dümpelmann M, Litt B, Schulze-Bonhage A. Collaborating and sharing data in epilepsy research. *J Clin Neurophysiol.* (2015) 32:235. doi: 10.1097/WNP.0000000000000159
15. Kuhlmann L, Karoly P, Freestone DR, Brinkmann BH, Temko A, Barachant A, et al. Epilepsyecosystem.org: crowd-sourcing reproducible seizure prediction with long-term human intracranial EEG. *Brain*. (2018) 141:2619–30. doi: 10.1093/brain/awy210
16. Cook MJ, O'Brien TJ, Berkovic SF, Murphy M, Morokoff A, Fabinyi G, et al. Prediction of seizure likelihood with a long-term, implanted seizure advisory system in patients with drug-resistant epilepsy: a first-in-man study. *Lancet Neurol.* (2013) 12:563–571. doi: 10.1016/S1474-4422(13)70075-9
17. Kuhlmann L, Lehnertz K, Richardson MP, Schelter B, Zaveri HP. Seizure prediction — ready for a new era. *Nat Rev Neurol.* (2018) 14:618–30. doi: 10.1038/s41582-018-0055-2
18. Haut SR, Hall CB, Masur J, Lipton RB. Seizure occurrence: precipitants and prediction. *Neurology.* (2007) 69:1905–10. doi: 10.1212/01.wnl.0000278112.48285.84
19. Haut SR, Vouyiouklis M, Shinnar S. Stress and epilepsy: a patient perception survey. *Epilepsy Behav.* (2003) 4:511–4. doi: 10.1016/S1525-5050(03)00182-3
20. Nakken KO. Clinical research physical exercise in outpatients with epilepsy. *Epilepsia.* (1999) 40:643–51. doi: 10.1111/j.1528-1157.1999.tb05568.x
21. Allen CN. Circadian rhythms, diet, and neuronal excitability. *Epilepsia.* (2008) 49:124–6. doi: 10.1111/j.1528-1167.2008.01856.x
22. Chang K-C, Wu T-H, Fann JC-Y, Chen SL, Yen AM-F, Chiu SY-H, et al. Low ambient temperature as the only meteorological risk factor of seizure occurrence: a multivariate study. *Epilepsy Behav.* (2019) 100:106283. doi: 10.1016/j.yebeh.2019.04.036
23. Payne DE, Dell KL, Karoly PJ, Kremen V, Gerla V, Kuhlmann L, et al. Identifying seizure risk factors: A comparison of sleep, weather, and temporal features using a Bayesian forecast. *Epilepsia*. (2020) 62:371–82. doi: 10.1111/epi.16785
24. Frucht MM, Quigg M, Schwaner C, Fountain NB. Distribution of seizure precipitants among epilepsy syndromes. *Epilepsia.* (2000) 41:1534–9. doi: 10.1111/j.1499-1654.2000.001534.x
25. Cramer JA, Glassman M, Rienzi V. The relationship between poor medication compliance and seizures. *Epilepsy Behav.* (2002) 3:338–42. doi: 10.1016/S1525-5050(02)00037-9
26. Baud MO, Kleen JK, Mirro EA, Andrechak JC, King-Stephens D, Chang EF, et al. Multi-day rhythms modulate seizure risk in epilepsy. *Nat Commun.* (2018) 9:88. doi: 10.1038/s41467-017-02577-y
27. Karoly PJ, Goldenholz DM, Freestone DR, Moss RE, Grayden DB, Theodore WH, et al. Circadian and circaseptan rhythms in human

epilepsy: a retrospective cohort study. *Lancet Neurol.* (2018) 17:977–85. doi: 10.1016/S1474-4422(18)30274-6
28. Leguia MG, Andrzejak RG, Rummel C, Fan JM, Mirro EA, Tcheng TK, et al. Seizure cycles in focal epilepsy. *JAMA Neurol.* (2021) 78:454–63. doi: 10.1001/jamaneurol.2020.5370
29. Maturana MI, Meisel C, Dell K, Karoly PJ, D'Souza W, Grayden DB, et al. Critical slowing down as a biomarker for seizure susceptibility. *Nat Commun.* (2020) 11:2172. doi: 10.1038/s41467-020-15908-3
30. Karoly PJ, Stirling RE, Freestone DR, Nurse ES, Doyle B, Halliday A, et al. Multiday cycles of heart rate modulate seizure likelihood at daily, weekly and monthly timescales: an observational cohort study. *medRxiv*. (2020). doi: 10.1101/2020.11.24.20237990
31. Karoly PJ, Cook MJ, Maturana M, Nurse ES, Payne D, Brinkmann BH, et al. Forecasting cycles of seizure likelihood. *Epilepsia.* (2020) 61:776–86. doi: 10.1111/epi.16485
32. Karoly PJ, Ung H, Grayden DB, Kuhlmann L, Leyde K, Cook MJ, et al. The circadian profile of epilepsy improves seizure forecasting. *Brain.* (2017) 140:2169–82. doi: 10.1093/brain/awx173
33. Goldenholz DM, Goldenholz SR, Romero J, Moss R, Sun H, Westover B. Development and validation of forecasting next reported seizure using e-diaries. *Ann Neurol.* (2020) 88:588–95. doi: 10.1002/ana.25812
34. Proix T, Truccolo W, Leguia MG, Tcheng TK, King-Stephens D, Rao VR, et al. Forecasting seizure risk in adults with focal epilepsy: a development and validation study. *Lancet Neurol.* (2021) 20:127–35. doi: 10.1016/S1474-4422(20)30396-3
35. Leguia MG, Rao VR, Kleen JK, Baud MO. Measuring synchrony in bio-medical timeseries. *Chaos.* (2021) 31:013138. doi: 10.1063/5.0026733
36. Ulate-Campos A, Coughlin F, Gaínza-Lein M, Fernández IS, Pearl PL, Loddenkemper T. Automated seizure detection systems and their effectiveness for each type of seizure. *Seizure.* (2016) 40:88–101. doi: 10.1016/j.seizure.2016.06.008
37. Meisel C, El Atrache R, Jackson M, Schubach S, Ufongene C, Loddenkemper T. Machine learning from wristband sensor data for wearable, noninvasive seizure forecasting. *Epilepsia.* (2020) 61:2653–66. doi: 10.1111/epi.16719
38. Moseley BD, Britton JW, So E. Increased cerebral oxygenation precedes generalized tonic clonic seizures. *Epilepsy Res.* (2014) 108:1671–4. doi: 10.1016/j.eplepsyres.2014.09.017
39. Billeci L, Marino D, Insana L, Vatti G, Varanini M. Patient-specific seizure prediction based on heart rate variability and recurrence quantification analysis. *PLoS ONE.* (2018) 13:e0204339. doi: 10.1371/journal.pone.0204339
40. Yamakawa T, Miyajima M, Fujiwara K, Kano M, Suzuki Y, Watanabe Y, et al. Wearable epileptic seizure prediction system with machine-learning-based anomaly detection of heart rate variability. *Sensors.* (2020) 20:3987. doi: 10.3390/s20143987
41. Harding C, Pompei F, Bordonaro SF, McGillicuddy DC, Burmistrov D, Sanchez LD. The daily, weekly, and seasonal cycles of body temperature analyzed at large scale. *Chronobiol Int.* (2019) 36:1646–57. doi: 10.1080/07420528.2019.1663863
42. Ajne B. A simple test for uniformity of a circular distribution. *Biometrika.* (1968) 55:343–54. doi: 10.1093/biomet/55.2.343
43. Swamynathan M. *Mastering Machine Learning With Python in Six Steps: A Practical Implementation Guide to Predictive Data Analytics Using Python*. New York, NY: Apress (2019).
44. Kingma DP, Ba J. Adam: a method for stochastic optimization. *arXiv preprint*. (2014). *arXiv*:1412.6980.
45. Janse SA, Dumanis SB, Huwig T, Hyman S, Fureman BE, Bridges JFP. Patient and caregiver preferences for the potential benefits and risks of a seizure forecasting device: a best–worst scaling. *Epilepsy Behav.* (2019) 96:183–91. doi: 10.1016/j.yebeh.2019.04.018
46. Bruno E, Simblett S, Lang A, Biondi A, Odoi C, Schulze-Bonhage A, et al. Wearable technology in epilepsy: the views of patients, caregivers, and healthcare professionals. *Epilepsy Behav.* (2018) 85:141–9. doi: 10.1016/j.yebeh.2018.05.044
47. Karoly PJ, Rao VR, Worrell GA, Gregg NM, Bernard C, Cook MJ, et al. Cycles in epilepsy. *Nat Rev Neurol.* (2021) 17:267–84. doi: 10.1038/s41582-021-00464-1
48. Lotufo PA, Valiengo L, Benseñor IM, Brunoni AR. A systematic review and meta-analysis of heart rate variability in epilepsy and antiepileptic drugs: HRV in epilepsy. *Epilepsia.* (2012) 53:272–82. doi: 10.1111/j.1528-1167.2011.03361.x
49. Pai A, Veeraraghavan A, Sabharwal A. HRVCam: robust camera-based measurement of heart rate variability. *J Biomed Optics.* (2021) 26:022707. doi: 10.1117/1.JBO.26.2.022707
50. Gadhoumi K, Keenan K, Colorado R, Meisel K, Hu X. A statistical comparative study of photoplethysmographic signals in wrist-worn and fingertip pulse-oximetry devices. In: *2018 Computing in Cardiology Conference (CinC)*. Maastricht: IEEE (2018). p. 1−4.
51. Häfele CA, Freitas MP, da Silva MC, Rombaldi AJ. Are physical activity levels associated with better health outcomes in people with epilepsy? *Epilepsy Behav.* (2017) 72:28–34. doi: 10.1016/j.yebeh.2017.04.038
52. Vancampfort D, Ward PB. Physical activity correlates across the lifespan in people with epilepsy: a systematic review. *Disabil Rehabil.* (2019) 43:1359–66 doi: 10.1080/09638288.2019.1665113
53. Pimentel J, Tojal R, Morgado J. Epilepsy and physical exercise. *Seizure.* (2015) 25:87–94. doi: 10.1016/j.seizure.2014.09.015
54. Eriksen HR, Ellertsen B, Gronningsaeter H, Nakken KO, Loyning Y, Ursin H. Physical exercise in women with intractable epilepsy. *Epilepsia.* (1994) 35:1256–64. doi: 10.1111/j.1528-1157.1994.tb01797.x
55. Lundgren T, Dahl J, Yardi N, Melin L. Acceptance and commitment therapy and yoga for drug-refractory epilepsy: a randomized controlled trial. *Epilepsy Behav.* (2008) 13:102–8. doi: 10.1016/j.yebeh.2008.02.009
56. Arida RM, Scorza FA, da Silva SG, Schachter SC, Cavalheiro EA. The potential role of physical exercise in the treatment of epilepsy. *Epilepsy Behav.* (2010) 17:432–5. doi: 10.1016/j.yebeh.2010.01.013
57. Lundberg S, Lee S-I. A unified approach to interpreting model predictions. *arXiv Preprint*. (2017). *arXiv*:1705.07874.
58. Baker GA, Nashef L, Hout BA. Current issues in the management of epilepsy: the impact of frequent seizures on cost of illness, quality of life, and mortality. *Epilepsia.* (1997) 38:S1–8. doi: 10.1111/j.1528-1157.1997.tb04511.x
59. Arthurs S, Zaveri HP, Frei MG, Osorio I. Patient and caregiver perspectives on seizure prediction. *Epilepsy Behav.* (2010) 19:474–7. doi: 10.1016/j.yebeh.2010.08.010
60. Gilbert F, Cook M, O'Brien T, Illes J. Embodiment and estrangement: results from a first-in-Human "Intelligent BCI" Trial. *Sci Eng Ethics.* (2017) 25:83–96. doi: 10.1007/s11948-017-0001-5
61. Hoppe C, Poepel A, Elger CE. Epilepsy: accuracy of patient seizure counts. *Arch Neurol.* (2007) 64:1595. doi: 10.1001/archneur.64.11.1595
62. Elger CE, Hoppe C. Diagnostic challenges in epilepsy: seizure under-reporting and seizure detection. *Lancet Neurol.* (2018) 17:279–88. doi: 10.1016/S1474-4422(18)30038-3
63. Haghayegh S, Khoshnevis S, Smolensky MH, Diller KR, Castriotta RJ. Accuracy of Wristband Fitbit models in assessing sleep: systematic review and meta-analysis. *J Med Internet Res.* (2019) 21:e16273. doi: 10.2196/16273
64. Haghayegh S, Khoshnevis S, Smolensky MH, Diller KR. Accuracy of PurePulse photoplethysmography technology of Fitbit Charge 2 for assessment of heart rate during sleep. *Chronobiol Int.* (2019) 36:927–33. doi: 10.1080/07420528.2019.1596947
65. Thomson EA, Nuss K, Comstock A, Reinwald S, Blake S, Pimentel RE, et al. Heart rate measures from the Apple Watch, Fitbit Charge HR 2, and electrocardiogram across different exercise intensities. *J Sports Sci.* (2019) 37:1411–9. doi: 10.1080/02640414.2018.1560644

Conflict of Interest: RS, MC, EN, DF, DP, and PK were employed by or have a financial interest in the company Seer Medical Pty. Ltd.

The remaining authors declare that the research was conducted in the absence of any commercial or financial relationships that could be construed as a potential conflict of interest.

frontiers in Neurology

METHODS
published: 20 July 2021
doi: 10.3389/fneur.2021.701791

A Primer on Hyperdimensional Computing for iEEG Seizure Detection

Kaspar A. Schindler[1]* *and Abbas Rahimi*[2]

[1] Department of Neurology, Inselspital, Sleep-Wake-Epilepsy-Center, NeuroTec, Bern University Hospital, University Bern, Bern, Switzerland, [2] IBM Research-Zurich, Ruschlikon, Switzerland

A central challenge in today's care of epilepsy patients is that the disease dynamics are severely under-sampled in the currently typical setting with appointment-based clinical and electroencephalographic examinations. Implantable devices to monitor electrical brain signals and to detect epileptic seizures may significantly improve this situation and may inform personalized treatment on an unprecedented scale. These implantable devices should be optimized for energy efficiency and compact design. Energy efficiency will ease their maintenance by reducing the time of recharging, or by increasing the lifetime of their batteries. Biological nervous systems use an extremely small amount of energy for information processing. In recent years, a number of methods, often collectively referred to as brain-inspired computing, have also been developed to improve computation in non-biological hardware. Here, we give an overview of one of these methods, which has in particular been inspired by the very size of brains' circuits and termed hyperdimensional computing. Using a tutorial style, we set out to explain the key concepts of hyperdimensional computing including very high-dimensional binary vectors, the operations used to combine and manipulate these vectors, and the crucial characteristics of the mathematical space they inhabit. We then demonstrate step-by-step how hyperdimensional computing can be used to detect epileptic seizures from intracranial electroencephalogram (EEG) recordings with high energy efficiency, high specificity, and high sensitivity. We conclude by describing potential future clinical applications of hyperdimensional computing for the analysis of EEG and non-EEG digital biomarkers.

Keywords: brain-inspired computing, intracranial EEG, epilepsy, hyperdimensional space, digital biomarker, personalized medicine

OPEN ACCESS

Edited by:
Sharon Chiang, University of California, San Francisco, United States

Reviewed by:
Amir Aminifar, Lund University, Sweden
Jacopo Tessadori, Italian Institute of Technology (IIT), Italy

***Correspondence:**
Kaspar A. Schindler
kaspar.schindler@insel.ch

Specialty section:
This article was submitted to Epilepsy, a section of the journal Frontiers in Neurology

Received: *28 April 2021*
Accepted: *18 June 2021*
Published: *20 July 2021*

Citation:
Schindler KA and Rahimi A (2021) A Primer on Hyperdimensional Computing for iEEG Seizure Detection. Front. Neurol. 12:701791. doi: 10.3389/fneur.2021.701791

1. INTRODUCTION

At the Sleep-Wake-Epilepsy-Center of the University of Bern, we typically see patients who are not seizure free every 3–6 months. These check-ups often also include recording an electroencephalogram (EEG) with extracranial electrodes for a duration of <1 h. This rate of appointments may be considered typical for a tertiary or quaternary epilepsy center in many parts of the world. However, there is huge potential for improvements for several fundamental reasons. It has, for example, been clearly demonstrated that the patients' accounts of seizure occurrences are not reliable (1). The main explanation is not the occasional patient who does not want to report

seizures to avoid a suspension of the driver's license or other social and professional consequences, but the fact that many patients are actually willing but not able to give an accurate seizure count. Their seizures may occur during sleep, they may lose consciousness during the seizures, and nobody may tell them afterwards that a seizure occurred, or their seizures may impair their memory, as is typically the case in temporal lobe epilepsy. Furthermore, recent landmark studies (2, 3) have proven that epileptiform activity is far from constant, but exhibits fluctuating dynamics with often robust and patient-specific circadian and multidien periodicities, which are severely under-sampled by the typical sporadic appointment-based short-term EEG recordings (4, 5). Devices that could provide more accurate seizure counts and monitor the individual dynamics of epileptiform activity therefore have a large potential to improve and also personalize the care of epilepsy patients. Nonetheless, a decisive aspect of these devices is that they have to be as unobtrusive and non-visible to others as possible to not aggravate the stigmatization that epilepsy patients are often still exposed to—as most impressively described in the recent autobiography by the American author and journalist Kurt Eichenwald (6). There are several, not mutually exclusive, ways to minimize the obtrusiveness of the devices: one might, for example, restrict EEG recordings to night-time (7), or the device might be attached or integrated into personal accessories. Lee et al. (8) developed a strategy to use elastomeric composites with conductive nanomaterials for designing customized, multifunctional electronic eyeglasses that allow for recording EEG, electrooculogram, ultraviolet intensity, and body movements. Steady skin contact of their highly conductive and deformable carbon nanotube/polydimethylsiloxane EEG electrodes was maintained by a spring-coupled pressure device. The electrodes' positions near the ears allowed to accurately track the dynamics of occipital EEG alpha rhythms. Alternatively, EEG electrodes have been integrated into caps or individualized ear pieces (9), or they may be implanted subcutaneously (10, 11) or into the skull (12–14). In all of these cases, however, the devices should be designed to be as small as possible and this is why it is imperative that they are highly energy efficient. Energy efficiency is a hallmark of biological nervous systems and a set of methods, referred to as "brain-inspired computing," has emerged over recent years. These methods aim at replicating principles of biological nervous systems into artificial substrates and thereby allowing the design of a new generation of highly energy efficient hardware. Here, we set out to introduce computing with hyperdimensional (HD) vectors (15), one of the most powerful and elegant of these approaches.

The paper is structured as follows: In section 2, we first give an introduction to the main characteristics of computing with HD vectors. Then we provide a detailed account of how computing with HD vectors has been successfully used to detect epileptic seizures from intracranially recorded EEG signals (iEEG) in section 3. Next, we dedicate section 4 to describing examples of emerging nanotechnology hardware, which is particularly well suited for implementation of computing with HD vectors. We conclude in section 5 by summarizing our main points, giving an outlook on future developments, and important neurologic applications of computing with HD vectors. Finally, we recommend resources for further reading, mainly aimed at clinical neurophysiologists or epileptologists.

2. HYPERDIMENSIONAL COMPUTING

One way to conceive of computation in a very general sense is as the emergence, change, combination, and dissolution of patterns. While in biological systems, computation is considered to mainly rely on self-organization (16, 17), in the case of human artifacts, computation is engineered. In today's typical computer, the patterns used are short bit strings consisting of zeros and ones (18, 19). The central idea of computing with HD vectors, as developed by Finnish neuroscientist Pentti Kanerva, is to use random patterns that are much larger, i.e., in the order of 10,000 (15, 20). These patterns are still made from zeros and ones, but they are identically and independently distributed (i.i.d.), and are referred to as "dense random binary hypervectors" (21). The notion of a "hypervector" is due to the interpretation of these patterns as vectors or points in a very high-dimensional or "hyperspace." Kanerva (15, 20), Plate (22), and Gayler (23) were inspired to design such a novel and unique data type of random HD vectors after studying biological central nervous systems as well as psychological models of human analogy processing. Hence, the notion of computing with HD vectors is inspired by these aspects of brains where information is often represented by very large spatiotemporal distributions of probabilistic neuronal population firing patterns (24).

Crucially, in HD vectors the information is equally distributed across all the bits, which are consequently all of equal importance. The HD vector as a whole and any of its parts represent the same item, though the individual parts in a less reliable manner. As a corollary, there are no most or least significant bits as in classical computing, where bits represent different values depending on their positions within the bit strings. The characteristic that the information is spread across the whole HD vector is often referred to as a holographic or holistic representation (22). The reason why holographic information representation is of fundamental importance is that it yields a very high tolerance to noise. Akin to the situation in biological brains, where very large numbers of neurons may be impaired before there are clinical manifestations (25), many bits—often in the range of 30%—of a HD vector may be randomly flipped before computing with HD vectors fails. To better understand the root causes for this surprising robustness, it is essential to study the hyperdimensional space, which the hypervectors inhabit. Given that the world we live and have evolved in can adequately be described by three spatial dimensions, at least on the scale we have direct sensory access to, it is not surprising that most of us humans do not have an intuitive grasp for hyperdimensional spaces. One such crucial but non-intuitive characteristic of hyperdimensional spaces is called "concentration of measure" (15, 26) and is illustrated in **Figure 1** by the stacked blue median-and-whiskers plot. It describes the distribution of distances between dense binary HD vectors of increasing dimensionality D. The distance between two HD vectors is assessed by the

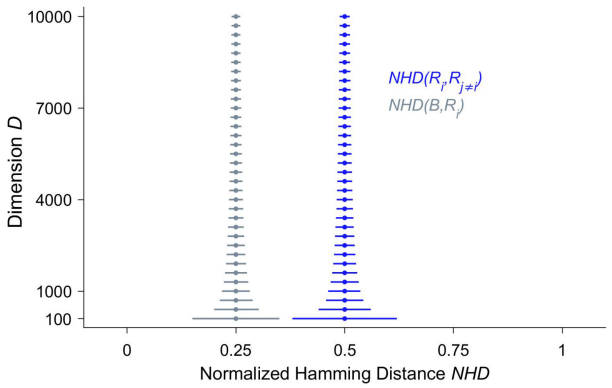

FIGURE 1 | The distributions of normalized Hamming distances (*NHD*) illustrate both the non-intuitive structure of hyperdimensional space and the similarity between a bundled hyperdimensional (HD) vector and its inputs. We have selected three random dense binary HD vectors R_1, R_2 and R_3 and bundled them together to yield the HD vector B, i.e., $B = [R_1 + R_2 + R_3]$. Bundling here denotes the componentwise application of addition followed by the majority rule. Then the pairwise NHD—the number of components where two vectors are different, divided by the dimension D—is computed among the input vectors $NHD(R_i, R_{j\neq i})$ shown in blue, and between B and each of its input vectors $NHD(B, R_i)$, displayed in gray. This procedure is repeated 50,000 times, yielding 150,000 distances for each distribution and for each dimension D, which increases from $D = 100$ to $D = 10,000$ in steps of 300. The dots represent the medians, and the whiskers indicate the 1–99 percentile ranges. One can clearly observe that, with increasing dimension D, the normalized Hamming distances between the random vectors concentrate around 0.5. In other words, the random vectors are almost orthogonal to each other. The distances between the bundled HD vector B and its input vectors is much smaller and concentrates around 0.25. Both of these characteristics become progressively and smoothly—i.e., there is no sensitive dependency—more pronounced with an increasing dimension D.

number of components at which they differ, divided by D, i.e., their normalized Hamming distance. The fundamental, albeit counter-intuitive, observation is that the larger the dimension, the more the distances are concentrated around a normalized Hamming distance of 0.5. Thus, the higher the dimension, the more likely it becomes that two dense binary HD vectors differ in half of their components and are quasi-orthogonal to each other. Put differently, points in hyperdimensional space are surprisingly isolated. If one starts moving away from a point one has to traverse almost half the diameter of the hyperdimensional space until one arrives at other points, but then the number of "neighbors" starts to increase enormously. Compare this to our everyday experience of moving on a 2D plane. Kanerva points out (15), if we double the distance, the "territory" quadruples, but it will never increase billion-fold as it is possible in hyperdimensional space. Hence, in the binary hyperdimensional space, with a common but arbitrarily chosen dimension of $D = 10,000$, there exists an inconceivably large number of different binary i.i.d. HD vectors, which are quasi-orthogonal to each other. Projecting information into a hyperdimensional space therefore not only provides a massive capacity for distinct representations, but these representations are also extremely robust, because most of their neighbors are half the diameter of the whole space away. This inherent robustness is one of the main reasons that lends computing with HD vectors naturally as a computational paradigm for emerging nanoscalable hardware, where noise due to variability of the materials is a central challenge (27–31).

Moreover, it is worthwhile to mention here an interesting recent observation by Singer et al. (32) and Singer and Lazar (33) that corroborates a potential role for computing with HD vectors, or HD computing-like information processing, in biological systems as well. These authors propose that the mammalian cortex in particular might make use of HD projections of sensory information. They point out the similarities between cortical dynamics and reservoir computing (34). Here, the high-dimensional continuous activity, generated and sustained by recurrent artificial neural networks, is perturbed by localized input signals (35, 36). However, only providing a very large number of different and noise-resistant representations does not suffice to furnish an efficient computational substrate. In addition, operations are needed that allow to manipulate these representations. The two main operations for combining HD vectors are called binding and bundling. For the binary dense HD vectors, binding corresponds to the componentwise Exclusive OR function (XOR). Exclusive OR, also referred to as "exclusive disjunction," is a logical operation that outputs "true" only, when the inputs differ. Here, we denote XOR by the circled plus sign ($\oplus$). Importantly, the HD vector C that results from binding the two binary random vectors $A \oplus B$ is again a binary random HD vector that is quasi-orthogonal to both A and B, and hence corresponds to a new, unique, and robust combined representation. The operation XOR has four relevant characteristics. It is both commutative, $A \oplus B = B \oplus A$ and associative, i.e., $(A \oplus B) \oplus C = A \oplus (B \oplus C)$. The neutral element is 0, that is $A \oplus 0 = A$ and finally, XOR is self-inverse, $A \oplus A = 0$. The second main operation is referred to as bundling and is basically a bitwise thresholded sum of HD vectors, yielding 1 if more than half of the components equal 1, otherwise the result is 0. In other words, bundling corresponds to a componentwise majority function. The thresholding or normalization process is essential, because it forces the resulting HD vector to remain in the binary hyperspace. Bundling of three HD vectors is denoted by $[A+B+C]$, where the squared brackets represent thresholding. Note that in the case of an even number of HD vectors to be bundled, the potentially occurring draws are randomly broken. A central distinction between the binding and bundling operations is that while the HD vector resulting from binding is quasi-orthogonal to all of the HD vectors that are bound together, the HD vector yielded by bundling is similar to each of its input HD vectors, i.e., the HD vectors that are bundled together. This characteristic is demonstrated in **Figure 1** by the stacked gray median-and-whiskers plot, representing the distances between the HD vectors R_1, R_2, R_3 and their resulting bundled HD vector B. Therefore, bundling is well suited to represent sets of HD vectors and may function as a memory or in the case of iEEG analysis to construct "prototype" HD vectors that represent brain states of interest.

At this point, it is interesting to re-consider HD computing as being brain inspired and allowing to design cognitive

architectures (37) with mechanisms and characteristics reminiscent of phenomena found in the human brain and mind. For example, the human central nervous system's essential ability to associate novel patterns (17) with already known ones might be part of the neuronal basis of metaphoric thinking, where we try to understand one abstract or not-yet-seen aspect of our world by using a different already familiar or more concrete concept (38, 39). And, on a more philosophical note, as Joseph Campbell so eloquently described in his comprehensive work (40), since the dawn of human consciousness, metaphors have been one of our most powerful tools to create coherent and meaningful stories and myths that help us navigate through our lives (41). Furthermore, one of the most promising modern concepts about consciousness is the theory of integrated information developed by Giulio Tononi et al. (42). This theory starts from the essential properties of phenomenal experience, such as the myriad of unique and different sensory impressions, which are then combined into a coherent ("integrated") whole. These characteristics might be, at least partially, replicated within the framework of computing with HD vectors.

Before we present one way that has already been successfully used to detect epileptic seizures from EEG recorded with intracranial electrodes (iEEG), let us for the sake of completeness mention that instead of binary components (0 and 1) (21), bipolar (23), real (22), or complex (43) ones may be used to design the HD vectors. One frequent alternative choice is $+1$ and -1, in which case the HD vectors are termed bipolar. While these alternatives influence the type of mathematical operations used for binding and bundling and also some aspects of the hardware implementation, the overall principles and characteristics of computing with HD vectors still hold. In other words, for computing with HD vectors the high dimensionality is more important than the type of components and operations used to construct and combine the HD vectors. Furthermore, in addition to the operations of binding and bundling, HD vectors may also be permuted. Permutation is typically implemented as a circular shift of the HD vector's components and geometrically corresponds to a rotation (15). Permutation is most often used to encode sequences, for example the order of letters to classify different languages (44), or the spatiotemporal patterns of electrical muscular activity for hand gesture detection (45). Permutation might turn out to be useful in future studies to better assess the shape of iEEG signals, which has been shown to contain physiologically relevant information (46, 47).

3. SEIZURE DETECTION

After having explained several of the key concepts of computing with HD vectors, we now detail one way this method has been successfully used to detect epileptic seizures from iEEG. The approach starts by first assessing whether an iEEG sampling point is $\geq$ than its preceding one or not. Although this form of symbolization considers only order relations—or, put differently, discards all amplitude information—it has been demonstrated to be helpful for assessing smaller and larger scale iEEG dynamics (48–51). Moreover, it allows for easily building larger

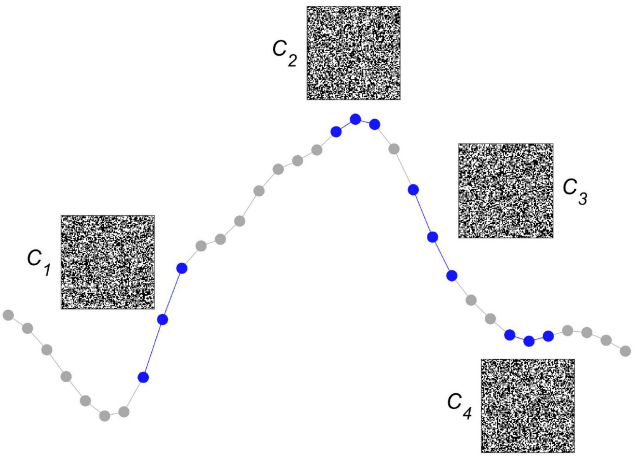

FIGURE 2 | Encoding local intracranial electroencephalogram (iEEG) order relations into hyperdimensional (HD) vectors. We consider whether an iEEG sampling point is $\geq$ or $\not\geq$ than its preceding one. The simple situation of only three sequential iEEG sampling points, used here to demonstrate the method, yields four different possible pairs of order relations (plotted in blue), each of which is associated with a unique quasi-orthogonal binary HD vector of dimension $D = 10,000$. For ease of graphical display, the HD vectors of size 1 x 10,000 are reshaped into squares of size 100 × 100. Each quasi-orthogonal HD vector represents a unique relation, e.g., C_1 represents the relation ($\geq$, $\geq$), C_2 ($\geq$, $\not\geq$),C_3 ($\not\geq$, $\not\geq$), and C_4 ($\not\geq$, $\geq$). These HD vectors are stored in the item memory and stay unchanged during both learning and classification.

symbols by simply considering longer sequences of differences between sampling points. Once the iEEG has been symbolized, the next step is to create an item memory, which we choose to build dense random binary HD vectors of a dimension $D = 10,000$. As is illustrated in **Figure 2**, for the didactic case of very short symbols that take only three consecutive iEEG sampling points into account, each of the four possible symbols is represented by one of the HD vectors $C_{i=1:4}$. The symbols represented by quasi-orthogonal HD vectors behave like classical symbols, they are either identical or completely different. Importantly, these HD vectors, as all the elements of the item memory, will remain unchanged during both learning and classification, they represent the projections of the symbolized iEEG signals into hyperspace.

Next, the *spatial* information contained in the iEEG signals has to be encoded, i.e., *where* a specific-order relation pattern occurs. The corresponding procedure is displayed in **Figure 3**. A second set of HD vectors consisting of HD vectors $E_{i=1:3}$, i.e., one per EEG electrode, is generated and added to the item memory. To compute a spatially composite representation S of the type and location of the occurring symbols, the HD vectors C_i are first bound with the HD vectors E_i and then bundled together, that is, superposed and thresholded. The result is a single binary HD vector of the same dimensionality as its input vectors. Thus, several HD vectors have been combined into one, which correctly implies that some information must have been lost during this process. Therefore, one refers to the resulting HD vector S as a *reduced* representation (43). However, despite the

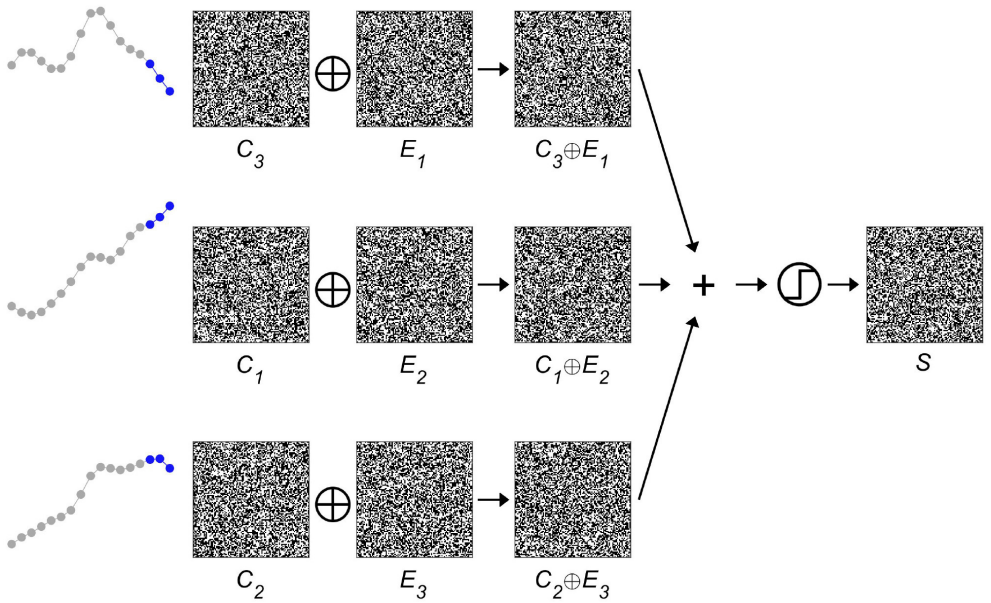

FIGURE 3 | Binding and bundling of hyperdimensional (HD) vectors yield a composite representation *S* of the *spatial* intracranial electroencephalogram (iEEG) characteristics. The item memory consists of two groups of HD vectors. One group, $C_{1:4}$, represents the four possible order relation patterns, the second group, $E_{1:3}$, indicates the three different electrodes. By binding the corresponding pairs of $C_{i\in 1:4}$ and $E_{j\in 1:3}$, one arrives at three HD vectors that denote the type and location of the occurring order relation patterns. Bundling, that is superposing and thresholding, these three vectors produces the single composite *spatial* representation *S*, which is then further processed as a unit.

loss of information, computing with these approximate patterns still performs well in many practical classification tasks. The main reason for this robustness can be traced back to the counter-intuitive structure of hyperdimensional space as described in the previous section, in which HD vectors are extremely resistant toward degradation. Once again, this feature is shared with biological nervous systems, which do most often not create highly precise, but just "good enough" responses when faced with a novel challenge in our ever changing world. Interestingly, and directly related, there exist elegant ways to assess composite HD vectors such as *S*. Given a spatial composite representation *S*, one might for example wonder, which order relation pattern was recorded with electrode 1. This information may be obtained by unbinding HD vector E_1 with *S*. As demonstrated in **Figure 4**, the result of this operation is a noisy or approximate version of C_3. This noisy HD vector can be cleaned up by comparing it with the original HD vectors contained in the item memory, and using the one that has the lowest Hamming distance.

To get from a spatial to a spatiotemporal representation, the procedure shown in **Figure 3** is repeated after shifting to the next sampling point in time, i.e., by using maximal overlap. The resulting set of spatial composite representations computed at timesteps *t*, $S_{t\in 1:15}$ are then bundled to yield a composite representation *ST* across space *and* time as displayed in **Figure 5**. The *ST* vectors generated from the same state are further bundled to produce a prototype HD vector representing a certain brain state. Finally, as illustrated in **Figure 6**, we demonstrate how this method can be applied to seizure detection. We use two iEEG recordings from a patient who suffered from pharmacoresistant temporal lobe epilepsy and underwent pre-surgical examinations at the Sleep-Wake-Epilepsy Center at the University of Bern with intracranial electrodes in order to precisely delineate the seizure onset zone. A total of 60 electrodes was used and the signals were sampled at 512 Hz and band-pass filtered between 0.5 and 120 Hz before analysis. We compared the order relations between 9 consecutive iEEG sampling points, yielding $2^8 = 256$ possible different outcomes. Therefore, in this case the item memory contained 316 random HD vectors, 60 vectors that represented the electrodes, and 256 vectors for the different order relation sequences of length 8. The recording of the first seizure is used to learn two prototype vectors P_{int} and P_{ict} that represent the interictal and the ictal brain states. Learning hereby refers to computing spatiotemporal composite representations, i.e., *ST* vectors, from two reference time periods of 30 s duration. The vectors from a reference time are bundled to produce the prototype HD vector representing the state of interest. For instance, $P_{ict} = [ST_1 + ST_2 + \ldots ST_k]$, where all *k* HD vectors are extracted from the 30 s of the ictal state. Similarly, P_{int} is computed from the interictal reference time. It is noteworthy how simple this type of learning is. There is neither a need for a large number of seizure recordings as training examples nor for any iteration-intensive method, such as back-propagation or gradient descent. In addition, in the following classification step, a query HD vector *Q* is computed in exactly the same way as the two prototypes P_{int} and P_{ict} from the yet unseen second seizure recording. This implies that the same hardware implementation may be used for both learning and classification, another factor helpful for minimizing the energy consumption

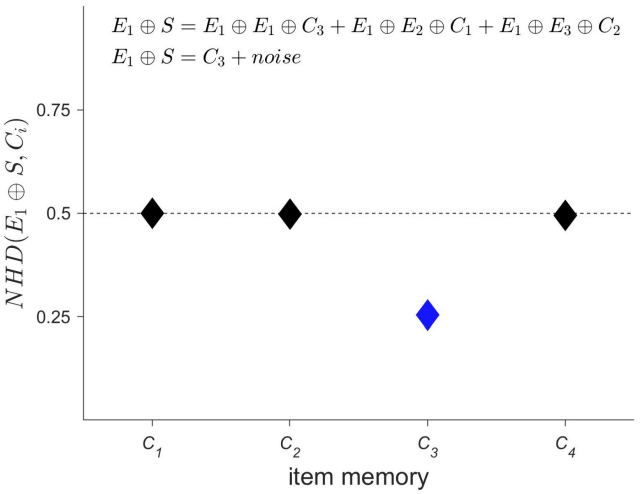

FIGURE 4 | Given a spatial composite representation S, which order relation pattern was recorded by electrode 1? This type of question may be elegantly answered within the framework of hyperdimensional (HD) computing, by binding the HD vector representing electrode 1, i.e., E_1, with the spatial composite representation S. Using the characteristic that XOR is its self-inverse and that binding produces new vectors that are quasi-orthogonal to their input vectors, one can interpret the result of $E_1 \oplus S$ as a noisy version of C_3. This noisy version is then "cleaned up" by measuring its distance to all the HD vectors of the item memory that represent order relation patterns and selecting the most similar one, i.e., C_3 in the present case (displayed in blue). Comparing this result with **Figure 3** shows that the correct pattern has been identified. The ability to compute robustly with approximate patterns is a hallmark of computing with HD vectors and lends it naturally as a computational paradigm for novel nano-scale memory-centric hardware with its intrinsic variability.

and size of an implantable device. This ability to learn from a single pass is also attractive for situations, where intermittent or continuous online learning may be needed. One might, for example, imagine situations, where the iEEG seizure patterns of a patient slightly change over time due to therapeutic interventions or a progression of the epilepsy. In that case, an update and adjustment of the ictal and interictal prototype vectors might be necessary to maintain accurate seizure detection. Coming back to the seizure detection example shown in **Figure 6**, the normalized Hamming distances between Q and both P_{int} and P_{ict} may be used to define thresholds enabling iEEG seizure detection with high sensitivity and specificity.

As indicated at the beginning of this section, symbolization based on order relation patterns combined with HD computing has recently been successfully applied to detecting epileptic seizures from short-term iEEG recordings with high sensitivity, high specificity, and high energy efficiency compared to other state-of-the-art methods (50, 52). These results have been further improved, especially in the latency of seizure detection, by including additional iEEG signal characteristics such as line length and mean amplitude (53) and, notably, could also be replicated for continuous long-term iEEG recordings (51). More specifically, these results surpass those yielded by state-of-the-art methods, including variants of deep learning (54, 55) and support vector machines (56), on the long-term dataset containing 116 seizures of 18 drug-resistant epilepsy patients in 2,656 h of recordings. HD computing trains 18 patient-specific models by using only 24 seizures: 12 models are trained with one seizure per patient, the others with two seizures. The trained models detect 79 out of 92 unseen seizures without false alarms. Importantly, a simple implementation of HD computing on the contemporary Nvidia Tegra X2 embedded device achieves 1.7×–3.9× faster execution and 1.4×–2.9× lower energy consumption compared to the best result from the state-of-the-art methods [see (51) for more details].

We conclude this section by mentioning that, while we have described the use of intra-cranially recorded electric brain signals for HD computing based seizure detection here, it has recently been shown that the method can also be successfully applied to extra-cranially recorded surface EEG signals, which typically contain more movement and muscular artifacts than iEEG (57). In the next section, we focus on viable hardware implementations of HD computing. Particularly, we go beyond the contemporary hardware fabric where HD computing has already shown energy efficiency benefits compared to the other approaches. We provide an overview on how HD computing can benefit from such emerging fabrics.

4. ANALOG IN-MEMORY COMPUTING HARDWARE

We have seen that computing with HD vectors allows to construct highly efficient algorithms, mainly because training is very fast and only uses relatively few steps compared to other approaches such as deep learning, which depends on many iterations to adjust the parameters of its artificial neurons. This single pass, non-iterative type of training is akin to our own neuro-cognitive ability to learn, to keep continuously learning, and to not forget certain events, the latter typically associated with the experience of intense emotions. However, for practical purposes, it is central that not only the algorithms but also the physical substrates into which the algorithms are implemented are efficient, i.e., allow for minimizing energy consumption. Only combining energy efficient algorithms with energy efficient hardware will ultimately enable the design of extremely small devices that can be implanted into the human brain in a minimally invasive way (58, 59), and—once again—biological brains provide inspiration for potential solutions.

John von Neumann, the ingenious Hungarian-American mathematician, physicist and polymath, who among many other achievements also designed the architecture that is still prevalent in most of today's computers (and which are accordingly called von Neumann architectures in his honor), already pointed out some of the major distinctions between biological brains and engineered information processing devices. In his last published and impressively visionary book titled "The Computer and the Brain" (60), he underlines that, although the building elements of biological brains, or "natural automata" as he calls them, are much slower and much less precise than

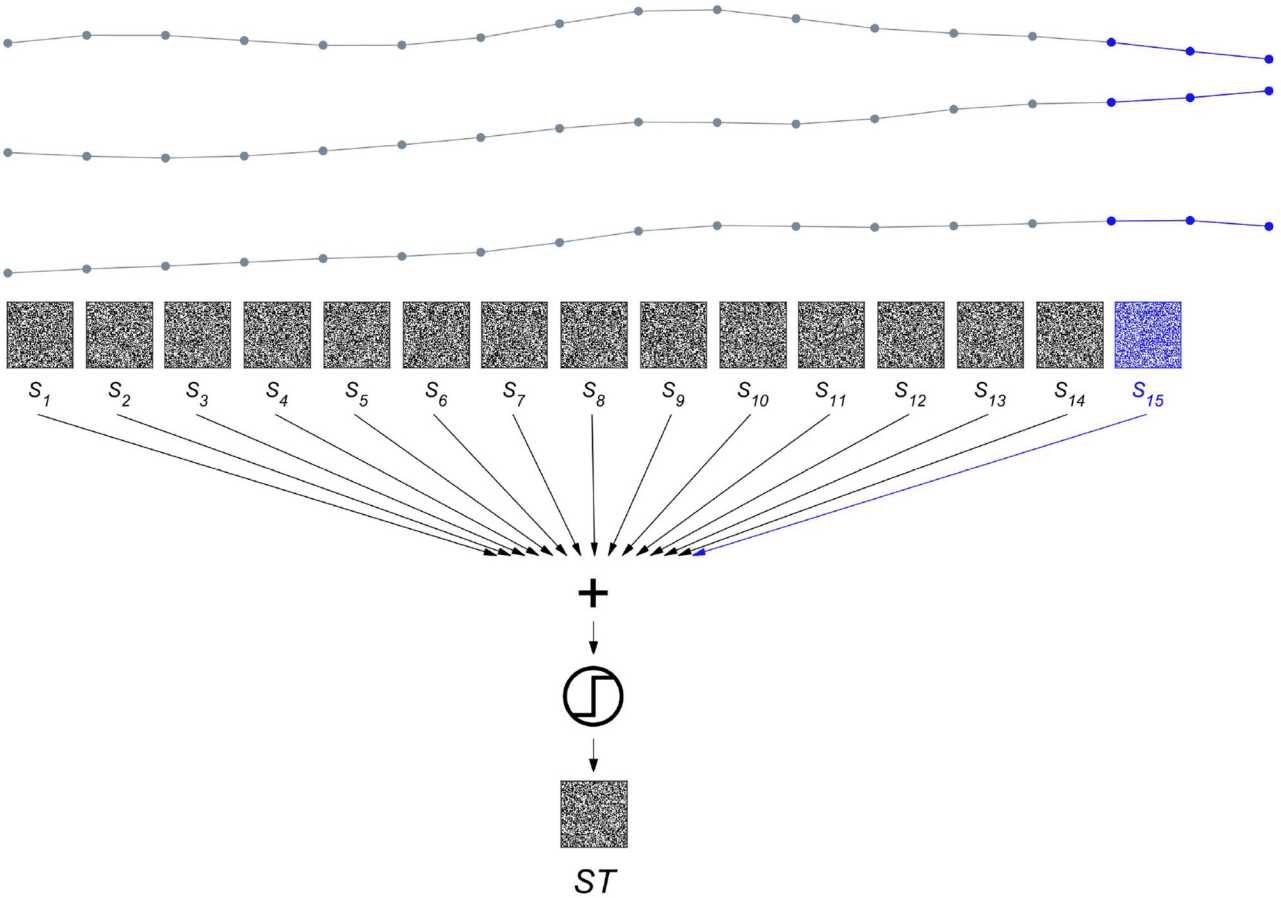

FIGURE 5 | Bundling spatial representations over time produces a spatiotemporal composite representation. The three intracranial electroencephalogram (iEEG) signals are the same as shown in **Figure 3**, but stretched horizontally to enable the display of all the composite spatial representations $S_{t\in 1:15}$. S_{15} plotted in blue is identical to S of **Figure 3**. Each of the HD vectors S_t is aligned with the first of the three sampling points that are compared to yield the order relation patterns. Bundling the 15 composite representation $S_{t\in 1:15}$ produces the spatiotemporal composite representation ST.

their artificial counterparts, they are significantly more energy efficient, work in parallel, and are much more tightly arranged. The latter observation has inspired modern strategies to design non-von Neumann architectures by co-locating memory and computation. As a result, in the non-von Neuman architectures, computations are local and the global interconnects are accessed at a relatively low frequency, as is a hallmark of biological brains molded through evolution, where efficient structures with short communication distances had a selective advantage (61, 62).

In classical von Neumann architectures, data have to be shuffled from memory to the central arithmetic logic unit and back, whereas in brains, information processing and at least some forms of memory formation take place within the same structures, such as the synapses that connect neocortical neurons. Synapses change their electrical resistance depending on their electrical activity, a characteristic that has been replicated in analog memristive devices, such as resistive random access memory (RRAM) and phase-change material (PCM) devices, leading to in-memory computing hardware [see (63) for an overview]. All these emerging nanotechnologies are characterized by a high variability of their components, and they thus rely on computational paradigms that not only compensate but may even embrace randomness. Importantly, it has recently been demonstrated that HD computing can be implemented on large-scale PCM devices arranged into crossbar arrays. It maintained a very high accuracy for various classification tasks with excellent energy efficiency (30). The used HD computing architecture is similar to the one described here for the iEEG seizure detection. **Figure 7** illustrates how the interictal and ictal prototypes can be mapped onto a PCM crossbar array where the Q HD vector is applied for classification. Interestingly, HD computing was used to compensate the intrinsic variabilities of the nanoscale devices on the one hand, but on the other hand these very variabilities were exploited to optimize HD projections (29, 31). This is akin to an intriguing idea put forward in the context of interpreting cortical dynamics as a biological realization of reservoir computing, namely that the variability, diversity, and randomness of neurons may also promote HD projections (36). Furthermore, the aforementioned prototypes (29, 31) achieve shorter communication pathways

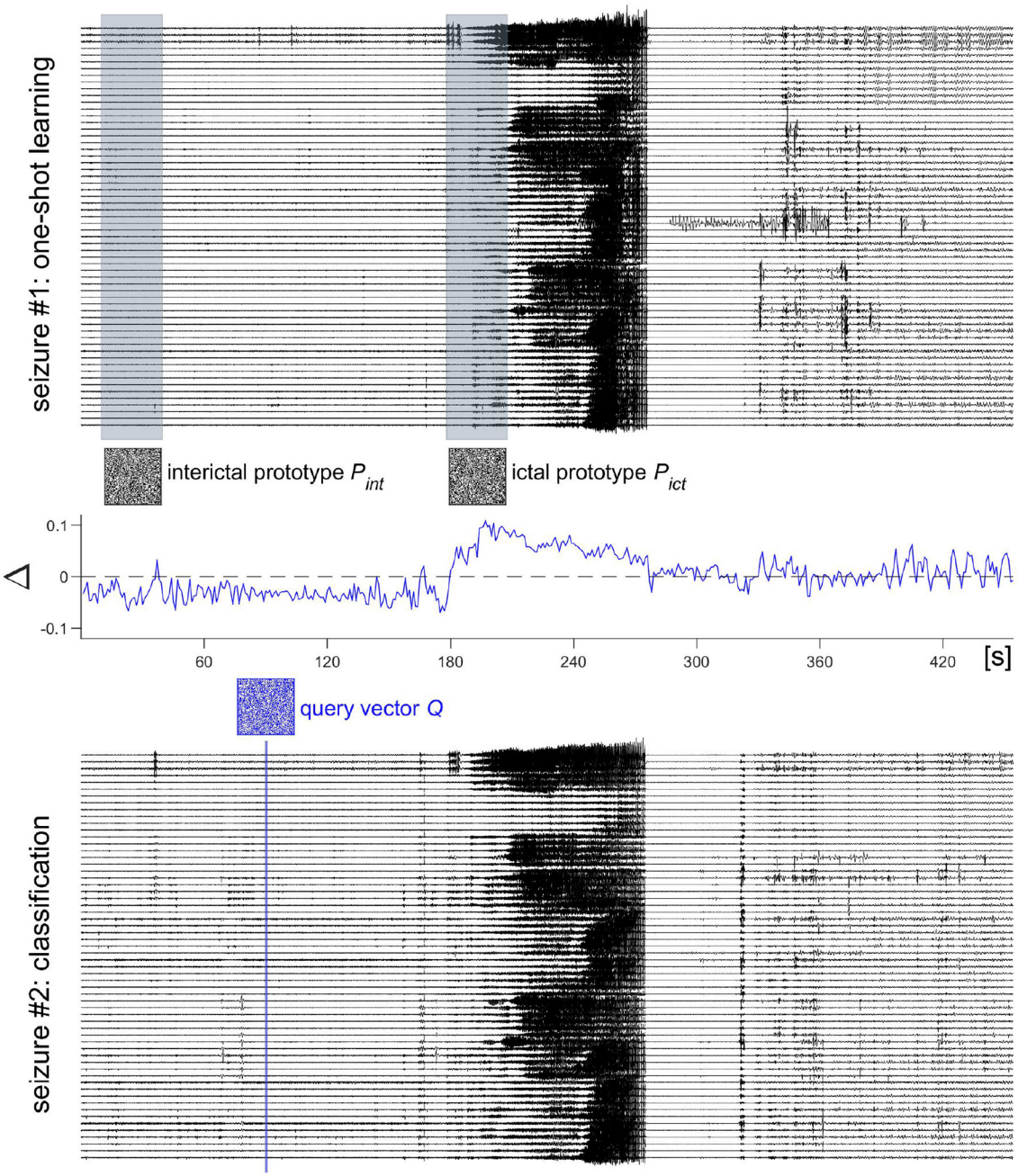

FIGURE 6 | HD computing for intracranial electroencephalogram (iEEG) seizure detection. Two iEEG seizure recordings from a patient with temporal lobe epilepsy are used. The patient was implanted with intracranial electrodes with a total of 60 contacts. From seizure #1, two prototype hyperdimensional (HD) vectors are learnt, P_{int} from an interictal time period and P_{ict} from seizure onset. Both time periods have a length of 30 s and are displayed in gray. Learning consists of splitting the time periods into 30 non-overlapping moving windows of 1 s duration, computing a spatiotemporal composite representation and bundling these 30 representations into the corresponding prototypes. Seizure #2 is then used for classification. From a short moving window, again of a duration of 1 s and displayed in blue, a query HD vector Q is computed and its normalized Hamming distances to the interictal and ictal prototype vectors are measured. The difference $\Delta = NHD(Q, P_{int}) - NHD(Q, P_{ict})$ indicates if the current brain state is closer to the ictal ($\Delta > 0$) or the interictal ($\Delta < 0$) prototype. The amplitude of Δ and its time continuously spent > 0 allow defining thresholds and time periods for iEEG seizure detection with high sensitivity and specificity (50–52).

by using 3D monolithic integration, instead of only 2D, to construct a layered design, similar for example to the neocortex of human brains. To summarize and conclude this section, many of these emerging nano-materials are inherently stochastic and need a computational paradigm that is robust and therein lies the great appeal to invoke computing with HD vectors for

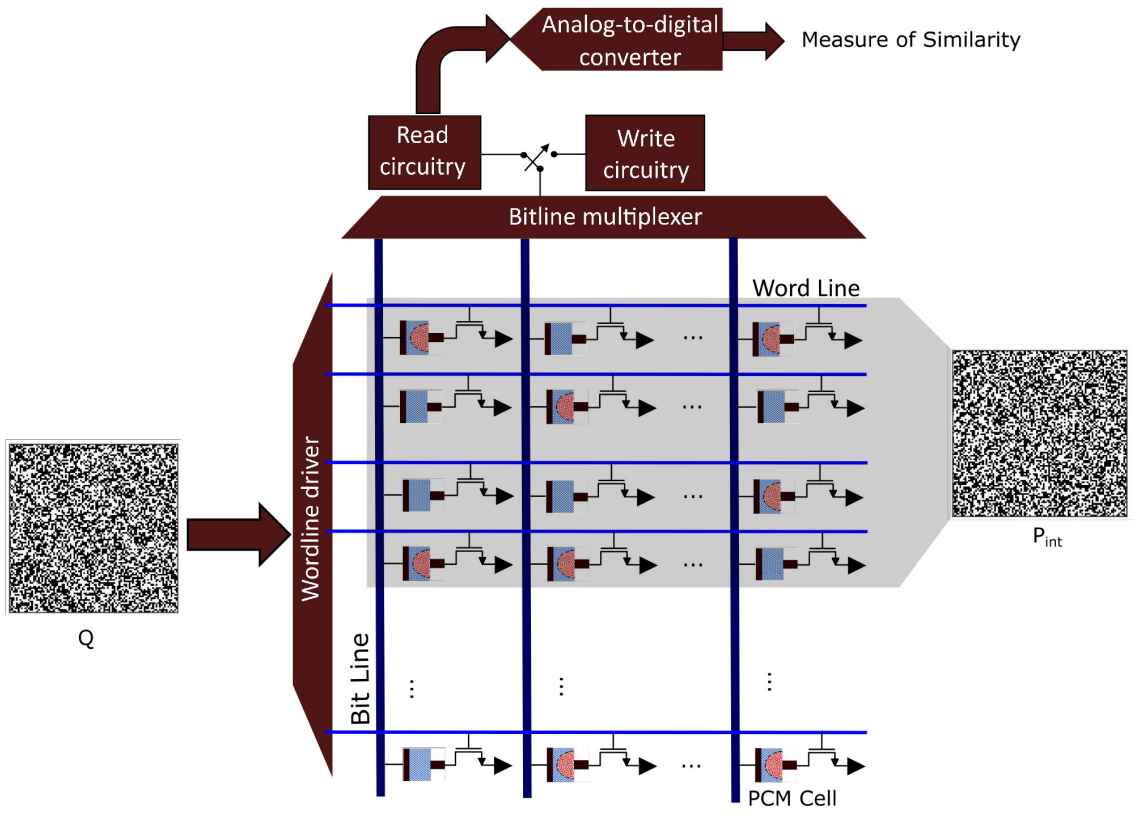

FIGURE 7 | Analog in-memory computing hardware based on phase change material (PCM) devices that are arranged into a crossbar array. In a programming phase, each binary prototype hyperdimensional (HD) vector (P_{int} or P_{ict}) is written into 10,000 PCM cells. This programming is done by applying a write voltage that changes the conductance state of the PCM cells according to the corresponding binary HD vector component. For classification, the query binary HD vector (Q) is applied to the crossbar array, and its similarity is measured with the programmed prototypes.

future miniaturized and thus much better implantable iEEG monitoring systems.

5. CONCLUSIONS AND OUTLOOK

We have presented the key concepts of HD computing and how the method has been successfully used for detecting epileptic seizures from iEEG with high energy efficiency, high specificity, and high sensitivity. We have described how HD computing relies on bit-wise operations, is highly parallel, memory-centric, scalable, and robust thanks to the counterintuitive structure of hyperdimensional space, where points are relatively isolated. Furthermore, computing with HD vectors is transparent and explainable, in the sense that each step during learning or classification is easily understandable. This contrasts to other methods used in artificial intelligence, which are often likened to "black boxes," where even the designers are not able to comprehend the details of why a system arrived at a particular solution. Considering all these characteristics, we regard HD computing as a flexible paradigm ideally suited for a new generation of implantable devices for monitoring electrical brain activity, which will be significantly more energy efficient and will consequently hopefully usher in personalized epileptology on a previously unknown scale.

There are many potential future clinical applications for HD computing based (i)EEG analysis. One compelling recent insight, for example, is how tightly and probably causally connected neurodegeneration is with both the impairment of slow wave sleep (64, 65) and epileptic activity (66–68). Both—slow wave sleep and epileptic activity—might in the future be monitored for ultra long-term time periods, i.e., for months to years, at the patient's home with robust and easy to use (i)EEG devices that make use of computing with HD vectors for a smaller and therefore less obtrusive design. From a neurologic point of view, tracking both sleep and epileptic activity might turn out to be crucial, for the latter might be exacerbated by improving slow wave sleep. This might potentially necessitate the use of drugs or a combination of drugs that simultaneously stabilize sleep and suppress or minimize epileptic activity, such as trazodone (69) together with levetiracetam (70, 71). Ultra long-term monitoring might also provide essential information about whether interictal epileptic activity has a similarly aggravating effect on neurodegeneration as does seizure activity. Such insights are essential for optimizing treatments with drugs like gabapentin

that have been reported to improve slow wave sleep (72) and suppress seizures (73), but increase interictal activity (74).

Another very interesting recent development in epileptology is the growing understanding of how brain–body interactions (75) might give rise to epileptic seizures and epilepsy. In particular, widespread cardiovascular disorders such as arterial hypertension may be associated with or even cause epileptogenic effects (76, 77). Therefore, the multi-modal integration of EEG and non-EEG digital biomarkers (58) is a highly promising approach to monitoring the mutual interactions between the visceral organs and the nervous system. For such multi-modal monitoring, HD computing lends itself naturally as a highly efficient computational paradigm for sensory fusion (78). This type of multi-sensor monitoring may be considered a specific example of "digital phenotyping," a concept recently introduced by Onnela et al. (79) as the moment-by-moment quantification of the individual-level human phenotype *in situ* using data from smartphones and other personal digital devices. Though the main field of investigation for Onnela is psychiatry, digital phenotyping of patients suffering from neurological disorders might inform personalized care as well.

On a more technical side, a very active area of research are memory-augmented neural networks (MANNs), in which a deep neural network is connected to an associative memory for fast and lifelong learning. Computing with HD vectors can reduce the complexity of MANNs by computing with binary vectors (80). This recently proposed method reduced the number of parameters by replacing the fully connected layer of a convolutional neural network with a binary associative memory for EEG-based motor imagery brain–machine interfaces (81). Other interesting developments are the combination of concepts from HD and reservoir computing, which uses recurrent connections in a neural network to create a complex dynamical system (35, 82). Kleyko et al. (83) demonstrated the similarities between the design and manipulation of HD binary vectors and the random projections of input values onto a binary reservoir, its updating, and its nonlinearity. Another recent innovative approach is to combine HD computing with event-driven inputs such as dynamic vision sensors (84). Hersche et al. (85) showed how to embed features extracted from such spiking sensors into binary sparse representations to reduce the complexity of downstream tasks such as regression.

We conclude by providing some recommendations for further reading, in particular intended for clinical neurophysiologists and epileptologists who want to learn more about the mathematical and engineering aspects of computing with HD vectors. In our opinion, the best way to delve deeper into this captivating field is by reading the seminal paper by Pentti Kanerva (15), followed by Tony Plate's book (43). An introduction to computing with HD vectors for robotics, which also includes instructive visualizations to further a more intuitive understanding of hyperdimensional spaces, has been written by Neubert et al. (86). Furthermore, there are two important books that are highly relevant for the use of HD computing to better understand and model biological brains (37) on the one hand, and describe in detail recent and potential future implementations in new types of hardware (87) on the other hand. We hope that this literature will provide a helpful entry point into the fascinating world of HD computing and will thereby promote its medical applications to ultimately improve the care for epilepsy patients.

DATA AVAILABILITY STATEMENT

Publicly available datasets were analyzed in this study. This data can be found here: http://ieeg-swez.ethz.ch/.

AUTHOR CONTRIBUTIONS

KS and AR: conception, writing of manuscript, and design of figures. KS: iEEG data acquisition and analysis, Matlab Code for **Figures 1**–**6**. Both authors significantly contributed to the article and approved the submitted version.

ACKNOWLEDGMENTS

We thank Pentti Kanerva for helpful comments on the manuscript.

REFERENCES

1. Elger CE, Hoppe C. Diagnostic challenges in epilepsy: seizure under-reporting and seizure detection. *Lancet Neurol*. (2018) 17:279–88. doi: 10.1016/S1474-4422(18)30038-3
2. Baud MO, Kleen JK, Mirro EA, Andrechak JC, King-Stephens D, Chang EF, et al. Multi-day rhythms modulate seizure risk in epilepsy. *Nat Commun*. (2018) 9:1–10. doi: 10.1038/s41467-017-02577-y
3. Karoly PJ, Goldenholz DM, Freestone DR, Moss RE, Grayden DB, Theodore WH, et al. Circadian and circaseptan rhythms in human epilepsy: a retrospective cohort study. *Lancet Neurol*. (2018) 17:977–85. doi: 10.1016/S1474-4422(18)30274-6
4. Baud MO, Proix T, Rao VR, Schindler K. Chance and risk in epilepsy. *Curr Opin Neurol*. (2020) 33:163–72. doi: 10.1097/WCO.0000000000000798
5. Baud MO, Schindler K, Rao VR. Under-sampling in epilepsy: limitations of conventional EEG. *Clin Neurophysiol Pract*. (2021) 6:41–9. doi: 10.1016/j.cnp.2020.12.002
6. Eichenwald K. A Mind Unraveled: A Memoir. New York, NY: Ballantine Books (2018).
7. Arnal PJ, Thorey V, Debellemaniere E, Ballard ME, Bou Hernandez A, Guillot A, et al. The Dreem headband compared to polysomnography for electroencephalographic signal acquisition and sleep staging. *Sleep*. (2020) 43:zsaa097. doi: 10.1093/sleep/zsaa097
8. Lee JH, Kim H, Hwang JY, Chung J, Jang TM, Seo DG, et al. 3D printed, customizable, and multifunctional smart electronic eyeglasses for wearable healthcare systems and human-machine interfaces. ACS Appl Mater Interfaces. (2020). 12:21424–32. doi: 10.1021/acsami.0c03110
9. Bleichner MG, Lundbeck M, Selisky M, Minow F, Jaeger M, Emkes R, et al. Exploring miniaturized EEG electrodes for brain-computer interfaces. An EEG you do not see? *Physiol Rep*. (2015) 3:e12362. doi: 10.14814/phy2.12362
10. Weisdorf S, Duun-Henriksen J, Kjeldsen MJ, Poulsen FR, Gangstad SW, Kjaer TW. Ultra-long-term subcutaneous home monitoring of epilepsy-490 days of EEG from nine patients. *Epilepsia*. (2019) 60:2204–14. doi: 10.1111/epi.16360
11. Duun-Henriksen J, Baud M, Richardson MP, Cook M, Kouvas G, Heasman JM, et al. A new era in electroencephalographic monitoring?

Subscalp devices for ultra-long-term recordings. *Epilepsia*. (2020) 61:1805–17. doi: 10.1111/epi.16630
12. Sun FT, Morrell MJ. The RNS System: responsive cortical stimulation for the treatment of refractory partial epilepsy. *Expert Rev Med Devices*. (2014) 11:563–72. doi: 10.1586/17434440.2014.947274
13. Skarpaas TL, Tcheng TK, Morrell MJ. Clinical and electrocorticographic response to antiepileptic drugs in patients treated with responsive stimulation. *Epilepsy Behav*. (2018) 83:192–200. doi: 10.1016/j.yebeh.2018.04.003
14. Quigg M, Skarpaas TL, Spencer DC, Fountain NB, Jarosiewicz B, Morrell MJ. Electrocorticographic events from long-term ambulatory brain recordings can potentially supplement seizure diaries. *Epilepsy Res*. (2020) 161:106302. doi: 10.1016/j.eplepsyres.2020.106302
15. Kanerva P. Hyperdimensional computing: an introduction to computing in distributed representation with high-dimensional random vectors. *Cogn Comput*. (2009) 1:139–59. doi: 10.1007/s12559-009-9009-8
16. Kelso JAS. Dynamic Patterns: The Self-Organization of Brain and Behavior. Cambridge, MA: MIT Press (1997).
17. Buzsáki G. The Brain From Inside Out. New York, NY: Oxford University Press (2019).
18. Gregg J. Ones and Zeros: Understanding Boolean Algebra, Digital Circuits, and the Logic of Sets. New York: IEEE Press (1998).
19. Hillis W. The pattern on the stone: the simple ideas that make computers work. New York: Basic Books. (2015).
20. Kanerva P. Computing with high-dimensional vectors. *IEEE Design Test*. (2019) 36:7–14. doi: 10.1109/MDAT.2018.2890221
21. Kanerva P. Binary spatter-coding of ordered K-tuples. In: *International Conference on Artificial Neural Networks*. (1996), Berlin; Heidelberg: Springer.
22. Plate TA. Holographic reduced representations. *IEEE Trans Neural Netw*. (1995) 6:623–41. doi: 10.1109/72.377968
23. Gayler R. Multiplicative binding, representation operators & analogy. In: Advances in Analogy Research. (1998).
24. Nicolelis M. Beyond Boundaries: The New Neuroscience of Connecting Brains With Machines-and How it Will Change Our Lives. New York, NY: Times Books/Henry Holt and Co. (2011).
25. Dubois B, Hampel H, Feldman HH, Scheltens P, Aisen P, Andrieu S, et al. Preclinical Alzheimer's disease: definition, natural history, and diagnostic criteria. *Alzheimers Dement*. (2016) 12:292–323. doi: 10.1016/j.jalz.2016.02.002
26. Gorban AN, Makarov VA, Tyukin IY. The unreasonable effectiveness of small neural ensembles in high-dimensional brain. *Phys Life Rev*. (2019) 29:55–88. doi: 10.1016/j.plrev.2018.09.005
27. Li H, Wu TF, Rahimi A, Li KS, Rusch M, Lin CH, et al. Hyperdimensional computing with 3D VRRAM in-memory kernels: device-architecture co-design for energy-efficient, error-resilient language recognition. In: 2016 *IEEE International Electron Devices Meeting (IEDM)*. San Francisco, CA: IEEE (2016). p. 16.1.1–16.1.4.
28. Rahimi A, Datta S, Kleyko D, Frady EP, Olshausen B, Kanerva P, et al. High-dimensional computing as a nanoscalable paradigm. *IEEE Trans Circ Syst I Regular Pap*. (2017) 64:2508–21. doi: 10.1109/TCSI.2017.2705051
29. Wu TF, Li H, Huang P, Rahimi A, Rabaey JM, Wong HP, et al. Brain-inspired computing exploiting carbon nanotube FETs and resistive RAM: hyperdimensional computing case study. In: 2018 IEEE International Solid-State Circuits Conference-(ISSCC) San Francisco, CA: IEEE (2018). p. 492–4.
30. Karunaratne G, Le Gallo M, Cherubini G, Benini L, Rahimi A, Sebastian A. In-memory hyperdimensional computing. *Nat Electr*. (2020) 3:327–37. doi: 10.1038/s41928-020-0410-3
31. Rahimi A, Wu TF, Li H, Rabaey JM, Wong HSP, Shulaker MM, et al. Hyperdimensional computing nanosystem: in-memory computing using monolithic 3D integration of RRAM and CNFET. In: Memristive Devices for Brain-Inspired Computing. Elsevier. (2020) p. 195–219.
32. Singer W. Cortical dynamics revisited. *Trends Cogn Sci*. (2013) 17:616–26. doi: 10.1016/j.tics.2013.09.006
33. Singer W, Lazar A. Does the cerebral cortex exploit high-dimensional, non-linear dynamics for information processing? *Front Comput Neurosci*. (2016) 10:99. doi: 10.3389/fncom.2016.00099
34. Tanaka G, Yamane T, Héroux JB, Nakane R, Kanazawa N, Takeda S, et al. Recent advances in physical reservoir computing: a review. *Neural Netw*. (2019) 115:100–23. doi: 10.1016/j.neunet.2019.03.005
35. Maass W, Natschläger T, Markram H. Real-time computing without stable states: a new framework for neural computation based on perturbations. *Neural Comput*. (2002) 14:2531–60. doi: 10.1162/089976602760407955
36. Seoane LF. Evolutionary aspects of reservoir computing. *Philos Trans R Soc B Biol Sci*. (2019) 374:20180377. doi: 10.1098/rstb.2018.0377
37. Eliasmith C. How to Build a Brain: A Neural Architecture for Biological Cognition. Oxford: Oxford University Press (2013).
38. Lakoff G. Metaphors We Live by. Chicago: University of Chicago Press (1980).
39. Lakoff G. Mapping the brain's metaphor circuitry: metaphorical thought in everyday reason. *Front Hum Neurosci*. (2014) 8:958. doi: 10.3389/fnhum.2014.00958
40. Campbell J. The Inner Reaches of Outer Space: Metaphor as Myth and as Religion. Novato, CA: New World Library (2002).
41. Campbell J. *The Power of Myth*. New York, NY: Doubleday (1988).
42. Tononi G, Boly M, Massimini M, Koch C. Integrated information theory: from consciousness to its physical substrate. *Nat Rev Neurosci*. (2016) 17:450–61. doi: 10.1038/nrn.2016.44
43. Plate T. Holographic Reduced Representation: Distributed Representation for Cognitive Structures. Stanford, CA: CSLI Publications (2003).
44. Joshi A, Halseth JT, Kanerva P. Language geometry using random indexing. In: Quantum Interaction. Cham: Springer International Publishing (2017) p. 265–74.
45. Rahimi A, Benatti S, Kanerva P, Benini L, Rabaey JM. Hyperdimensional biosignal processing: a case study for EMG-based hand gesture recognition. In:. 2016 *IEEE International Conference on Rebooting Computing (ICRC)*. San Diego, CA: IEEE (2016). p. 1–8.
46. Schindler K, Rummel C, Andrzejak RG, Goodfellow M, Zubler F, Abela E, et al. Ictal time-irreversible intracranial EEG signals as markers of the epileptogenic zone. *Clin Neurophysiol*. (2016) 127:3051–8. doi: 10.1016/j.clinph.2016.07.001
47. Cole SR, Voytek B. Brain oscillations and the importance of waveform shape. *Trends Cogn Sci*. (2017) 21:137–49. doi: 10.1016/j.tics.2016.12.008
48. Kaya Y, Uyar M, Tekin R, Yildirim S. 1D-local binary pattern based feature extraction for classification of epileptic EEG signals. Appl Math Comput. (2014). 243:209–19. doi: 10.1016/j.amc.2014.05.128
49. Kumar TS, Kanhangad V, Pachori RB. Classification of seizure and seizure-free EEG signals using local binary patterns. *Biomed Signal Proc Control*. (2015) 15:33–40. doi: 10.1016/j.bspc.2014.08.014
50. Burrello A, Schindler K, Benini L, Rahimi A. Hyperdimensional computing with local binary patterns: one-shot learning of seizure onset and identification of ictogenic brain regions using short-time iEEG recordings. *IEEE Trans Biomed Eng*. (2020) 67:601–13. doi: 10.1109/TBME.2019.2919137
51. Burrello A, Cavigelli L, Schindler K, Benini L, Rahimi A. Laelaps: an energy-efficient seizure detection algorithm from long-term human iEEG recordings without false alarms. In: 2019 Design, Automation & Test in Europe Conference & Exhibition (DATE). Florence: IEEE (2019). p. 752–7.
52. Burrello A, Schindler K, Benini L, Rahimi A. One-shot learning for iEEG Seizure detection using end-to-end binary operations: local binary patterns with hyperdimensional computing. In: 2018 *IEEE Biomedical Circuits and Systems Conference (BioCAS)*. Cleveland, OH: IEEE (2018). p. 1–4.
53. Burrello A, Benatti S, Schindler KA, Benini L, Rahimi A. An ensemble of hyperdimensional classifiers: hardware-friendly short-latency seizure detection with automatic iEEG electrode selection. *IEEE J Biomed Health Informatics*. (2020) 25:935–46. doi: 10.1109/JBHI.2020.3022211
54. Truong ND, Nguyen AD, Kuhlmann L, Bonyadi MR, Yang J, Ippolito S, et al. Convolutional neural networks for seizure prediction using intracranial and scalp electroencephalogram. *Neural Netw*. (2018) 105:104–11. doi: 10.1016/j.neunet.2018.04.018
55. Hussein R, Palangi H, Wang ZJ, Ward R. Robust detection of epileptic seizures using deep neural networks. In: 2018 *IEEE International Conference on Acoustics, Speech and Signal Processing (ICASSP)*. Calgary, AB: IEEE (2018). p. 2546–50.
56. Jaiswal AK, Banka H. Local pattern transformation based feature extraction techniques for classification of epileptic EEG signals. *Biomed Signal Proc Control*. (2017) 34:81–92. doi: 10.1016/j.bspc.2017.01.005
57. Asgarinejad F, Thomas A, Rosing T. Detection of epileptic seizures from surface EEG using hyperdimensional computing. In: 2020 42nd Annual International Conference of the IEEE Engineering in Medicine & Biology Society (EMBC). Montreal, QC: IEEE (2020). p. 536–40.

58. Rabaey JM. Human-centric computing. *IEEE Trans Very Large Scale Integr Syst*. (2020) 28:3–11. doi: 10.1109/TVLSI.2019.2956529
59. Neely RM, Piech DK, Santacruz SR, Maharbiz MM, Carmena JM. Recent advances in neural dust: towards a neural interface platform. *Curr Opin Neurobiol*. (2018) 50:64–71. doi: 10.1016/j.conb.2017.12.010
60. Neumann J. The Computer and the Brain. New Haven, CT: Yale University Press (2012).
61. Striedter G. Principles of Brain Evolution. Sunderland, MA: Sinauer Associates (2005).
62. Bassett DS, Bullmore E. Small-world brain networks. *Neuroscientist*. (2006) 12:512–23. doi: 10.1177/1073858406293182
63. Sebastian A, Le Gallo M, Khaddam-Aljameh R, Eleftheriou E. Memory devices and applications for in-memory computing. *Nat Nanotechnol*. (2020) 15:529–44. doi: 10.1038/s41565-020-0756-8
64. Musiek ES, Holtzman DM. Mechanisms linking circadian clocks, sleep, and neurodegeneration. *Science*. (2016) 354:1004–8. doi: 10.1126/science.aah4968
65. Winer JR, Mander BA, Kumar S, Reed M, Baker SL, Jagust WJ, et al. Sleep disturbance forecasts β-Amyloid accumulation across subsequent years. *Curr Biol*. (2020) 30:4291–8.e3. doi: 10.1016/j.cub.2020.08.017
66. Noebels J. A perfect storm: converging paths of epilepsy and Alzheimer's dementia intersect in the hippocampal formation. *Epilepsia*. (2011) 52(Suppl. 1):39–46. doi: 10.1111/j.1528-1167.2010.02909.x
67. Lam AD, Deck G, Goldman A, Eskandar EN, Noebels J, Cole AJ. Silent hippocampal seizures and spikes identified by foramen ovale electrodes in Alzheimer's disease. *Nat Med*. (2017) 23:678–80. doi: 10.1038/nm.4330
68. Vossel KA, Tartaglia MC, Nygaard HB, Zeman AZ, Miller BL. Epileptic activity in Alzheimer's disease: causes and clinical relevance. *Lancet Neurol*. (2017) 16:311–22. doi: 10.1016/S1474-4422(17)30044-3
69. La AL, Walsh CM, Neylan TC, Vossel KA, Yaffe K, Krystal AD, et al. Long-term trazodone use and cognition: a potential therapeutic role for slow-wave sleep enhancers. *J Alzheimers Dis*. (2019) 67:911–21. doi: 10.3233/JAD-181145
70. Schoenberg MR, Rum RS, Osborn KE, Werz MA. A randomized, double-blind, placebo-controlled crossover study of the effects of levetiracetam on cognition, mood, and balance in healthy older adults. *Epilepsia*. (2017) 58:1566–74. doi: 10.1111/epi.13849
71. Xiao R. Levetiracetam might act as an efficacious drug to attenuate cognitive deficits of Alzheimer's disease. *Curr Top Med Chem*. (2016) 16:565–73. doi: 10.2174/1568026615666150813144603
72. Foldvary-Schaefer N, De Leon Sanchez I, Karafa M, Mascha E, Dinner D, Morris HH. Gabapentin increases slow-wave sleep in normal adults. *Epilepsia*. (2002) 43:1493–7. doi: 10.1046/j.1528-1157.2002.21002.x
73. Mattia D, Spanedda F, Bassetti MA, Romigi A, Placidi F, Marciani MG. Gabapentin as add-on therapy in focal epilepsy: a computerized EEG study. *Clin Neurophysiol*. (2000) 111:311–7. doi: 10.1016/S1388-2457(99)00240-0
74. Placidi F, Mattia D, Romigi A, Bassetti MA, Spanedda F, Marciani MG. Gabapentin-induced modulation of interictal epileptiform activity related to different vigilance levels. *Clin Neurophysiol*. (2000) 111:1637–42. doi: 10.1016/S1388-2457(00)00365-5
75. Azzalini D, Rebollo I, Tallon-Baudry C. Visceral signals shape brain dynamics and cognition. *Trends Cogn Sci*. (2019) 23:488–509. doi: 10.1016/j.tics.2019.03.007
76. Gasparini S, Ferlazzo E, Sueri C, Cianci V, Ascoli M, Cavalli SM, et al. Hypertension, seizures, and epilepsy: a review on pathophysiology and management. *Neurol Sci*. (2019) 40:1775–83. doi: 10.1007/s10072-019-03913-4
77. Sarkis RA, Willment KC, Pennell PB, Marshall G. Late-onset unexplained epilepsy: what are we missing? *Epilepsy Behav*. (2019) 99:106478. doi: 10.1016/j.yebeh.2019.106478
78. Chang E, Rahimi A, Benini L, Wu AA. Hyperdimensional computing-based multimodality emotion recognition with physiological signals. In: 2019 IEEE International Conference on Artificial Intelligence Circuits and Systems (AICAS). Hsinchu: IEEE (2019). p. 137–41.
79. Onnela JP, Rauch SL. Harnessing smartphone-based digital phenotyping to enhance behavioral and mental health. *Neuropsychopharmacology*. (2016) 41:1691–6. doi: 10.1038/npp.2016.7
80. Karunaratne G, Schmuck M, Le Gallo M, Cherubini G, Benini L, Sebastian A, Rahimi A. Robust high-dimensional memory-augmented neural networks. *Nat Commun*. (2021) 12:2468. doi: 10.1038/s41467-021-22364-0
81. Hersche M, Benini L, Rahimi A. Binarization methods for motor-imagery brain–computer interface classification. *IEEE J Emerg Select Top Circ Syst*. (2020) 10:567–77. doi: 10.1109/JETCAS.2020.3031698
82. Jaeger H. *The" Echo State" Approach to Analysing and Training Recurrent Neural Networks-With an Erratum Note'*. Bonn, Germany: German National Research Center for Information Technology GMD Technical Report. (2001) 148.
83. Kleyko D, Frady EP, Kheffache M, Osipov E. Integer echo state networks: efficient reservoir computing for digital hardware. *IEEE Trans Neural Netw Learn Syst*. (2020) p. 1-14. doi: 10.1109/TNNLS.2020.3043309
84. Mitrokhin A, Sutor P, Fermüller C, Aloimonos Y. Learning sensorimotor control with neuromorphic sensors: toward hyperdimensional active perception. *Science Robotics*. (2019) 4:eaaw6736. doi: 10.1126/scirobotics.aaw6736
85. Hersche M, Rella EM, Di Mauro A, Benini L, Rahimi A. Integrating event-based dynamic vision sensors with sparse hyperdimensional computing: a low-power accelerator with online learning capability. In: Proceedings of the ACM/IEEE International Symposium on Low Power Electronics and Design. Boston MA: ACM. (2020) p. 169–74.
86. Neubert P, Schubert S, Protzel P. An introduction to hyperdimensional computing for robotics. *Künstl Intell*. (2019) 33:319–30. doi: 10.1007/s13218-019-00623-z
87. Spiga S, Sebastian A, Querlioz D, Rajendran B. *Memristive Devices for Brain-Inspired Computing: From Materials, Devices, and Circuits to Applications-Computational Memory, Deep Learning, and Spiking Neural Networks*. Duxford Cambridge, MA: Woodhead Publishing (2020).

Conflict of Interest: AR was employed by the company IBM (Switzerland).

The remaining author declares that the research was conducted in the absence of any commercial or financial relationships that could be construed as a potential conflict of interest.

frontiers in Neurology

ORIGINAL RESEARCH
published: 29 July 2021
doi: 10.3389/fneur.2021.704170

Epilepsy Personal Assistant Device—A Mobile Platform for Brain State, Dense Behavioral and Physiology Tracking and Controlling Adaptive Stimulation

*Tal Pal Attia[1], Daniel Crepeau[1], Vaclav Kremen[1,2,3], Mona Nasseri[1,4], Hari Guragain[1], Steven W. Steele[5], Vladimir Sladky[1,6], Petr Nejedly[1], Filip Mivalt[1], Jeffrey A. Herron[7], Matt Stead[1,3], Timothy Denison[8], Gregory A. Worrell[1,3] and Benjamin H. Brinkmann[1,3]**

[1] Bioelectronics Neurophysiology and Engineering Laboratory, Department of Neurology, Mayo Clinic, Rochester, MN, United States, [2] Cognitive Systems and Neurosciences, Czech Institute of Informatics, Robotics and Cybernetics, Czech Technical University in Prague, Prague, Czechia, [3] Department of Physiology and Biomedical Engineering, Mayo Clinic, Rochester, MN, United States, [4] School of Engineering, University of North Florida, Jacksonville, FL, United States, [5] Division of Engineering, Mayo Clinic, Rochester, MN, United States, [6] Faculty of Biomedical Engineering, Czech Technical University in Prague, Kladno, Czechia, [7] Department of Neurological Surgery, University of Washington, Seattle, WA, United States, [8] Engineering Sciences and Clinical Neurosciences, Oxford University, Oxford, United Kingdom

OPEN ACCESS

Edited by:
Kette D. Valente,
Universidade de São Paulo, Brazil

Reviewed by:
Matthias Duempelmann,
University of Freiburg Medical Center, Germany
Patricia Rzezak,
University of São Paulo, Brazil

***Correspondence:**
Benjamin H. Brinkmann
brinkmann.benjamin@mayo.edu

Specialty section:
This article was submitted to Epilepsy, a section of the journal Frontiers in Neurology

Received: 01 May 2021
Accepted: 21 June 2021
Published: 29 July 2021

Citation:
Pal Attia T, Crepeau D, Kremen V, Nasseri M, Guragain H, Steele SW, Sladky V, Nejedly P, Mivalt F, Herron JA, Stead M, Denison T, Worrell GA and Brinkmann BH (2021) Epilepsy Personal Assistant Device—A Mobile Platform for Brain State, Dense Behavioral and Physiology Tracking and Controlling Adaptive Stimulation. Front. Neurol. 12:704170. doi: 10.3389/fneur.2021.704170

Epilepsy is one of the most common neurological disorders, and it affects almost 1% of the population worldwide. Many people living with epilepsy continue to have seizures despite anti-epileptic medication therapy, surgical treatments, and neuromodulation therapy. The unpredictability of seizures is one of the most disabling aspects of epilepsy. Furthermore, epilepsy is associated with sleep, cognitive, and psychiatric comorbidities, which significantly impact the quality of life. Seizure predictions could potentially be used to adjust neuromodulation therapy to prevent the onset of a seizure and empower patients to avoid sensitive activities during high-risk periods. Long-term objective data is needed to provide a clearer view of brain electrical activity and an objective measure of the efficacy of therapeutic measures for optimal epilepsy care. While neuromodulation devices offer the potential for acquiring long-term data, available devices provide very little information regarding brain activity and therapy effectiveness. Also, seizure diaries kept by patients or caregivers are subjective and have been shown to be unreliable, in particular for patients with memory-impairing seizures. This paper describes the design, architecture, and development of the Mayo Epilepsy Personal Assistant Device (EPAD). The EPAD has bi-directional connectivity to the implanted investigational Medtronic Summit RC+S™ device to implement intracranial EEG and physiological monitoring, processing, and control of the overall system and wearable devices streaming physiological time-series signals. In order to mitigate risk and comply with regulatory requirements, we developed a Quality Management System (QMS) to define the development process of the EPAD system, including Risk Analysis, Verification, Validation, and protocol mitigations. Extensive verification and validation testing were performed on thirteen canines and benchtop systems. The system is now under a

first-in-human trial as part of the US FDA Investigational Device Exemption given in 2018 to study modulated responsive and predictive stimulation using the Mayo EPAD system and investigational Medtronic Summit RC+S™ in ten patients with non-resectable dominant or bilateral mesial temporal lobe epilepsy. The EPAD system coupled with an implanted device capable of EEG telemetry represents a next-generation solution to optimizing neuromodulation therapy.

Keywords: epilepsy, deep brain stimulation, implantable devices, neuromodulation, seizure detection, seizure prediction, wearables

INTRODUCTION

Drug-resistant epilepsy is one of the most common neurological disorders, affecting almost 1% of the population worldwide (1, 2). Many people living with epilepsy continue to have seizures despite anti-epileptic medication therapy (3, 4), and for them, resective surgery and neuromodulation therapy are the primary therapeutic options. Resective surgery can be attempted if a focal seizure onset zone can be identified, typically via invasive EEG monitoring, and if this area can be removed without causing a functional deficit. Although often effective, brain resection is irreversible, and for many patients, seizures eventually reoccur.

Neuromodulation therapy for epilepsy has grown in prevalence following FDA approvals for responsive neurostimulation (RNS) (5) in 2013 and deep brain stimulation (DBS) (6) in 2018. While these approaches effectively reduce seizures, long-term seizure freedom is rare with these methods. Additionally, optimization of therapeutic parameters, including stimulation amplitude, rate, and pulse width, is a very slow process, and optimal therapeutic effect is only achieved after many years (6, 7). Due to the poor reliability of self-reported seizure diaries (8), physicians may have difficulty knowing how effective a given set of stimulation settings is at suppressing or preventing seizures. Current devices have very limited capability to record and report seizure activity measures (typically EEG activity). However, limited objective measures of seizure rates and epileptiform activity are currently available and have produced profound insights already (9, 10).

Seizure predictions could potentially be used to adjust neuromodulation therapy to prevent the onset of a seizure and prompt medication therapy or to empower patients to avoid sensitive activities during high-risk periods (11, 12). An experimental device (NeuroVista SAS) was preclinically trialed provided clear proof of concept and validation of the value of long-term objective EEG data and seizure forecasts (13–15). However, the device did not progress to approval for clinical use and is no longer available, leaving an unmet need for a next-generation device with long-term EEG and seizure forecasting capabilities. Medtronic Inc. recently designed a novel experimental device with EEG telemetry and therapy modulation capabilities (16). The investigational Medtronic Summit RC+S™ system was developed to telemeter EEG, provide on-device seizure detections, and modulate stimulation therapy based on either on-board EEG analytics or analytics on an associated mobile computer. A full-featured analytics platform is needed to configure sensing and analytics on the device, manage device connectivity and data telemetry, provide distributed analytics for modulation of stimulation, and interact with subjects to deploy such capabilities successfully.

All software and components must be developed in compliance with international engineering standards (in particular ISO 60601) and a design control process compliant with United States federal regulations (specifically Title 21, section 820.20) to use such a system in human subjects. Significant preclinical testing and comprehensive verification and validation testing regimen must be employed to ensure system safety and quality.

As devices become increasingly interconnected and operate in the context of analytical and cloud computational systems, compliance with regulations governing software as a medical device is required, and developing regulations around machine learning (17, 18) must be included to augment the traditional regulatory framework around medical device development. At the core of the design process, user needs, and requirements are translated into system design and implemented with clear documentation and a rigorous process for testing, defect correction, and design updates. The complexity and required skill set for this is often missing in research lab environments, and likely contributes to the many barriers to translation of benchtop discoveries to clinical practice (19).

The EPAD system aims to record objective EEG data during seizures and modulate stimulation therapy based on seizure forecasts, which raises several important issues. First, forecasting algorithms are too compute-intensive to run on an implanted device, requiring data to be telemetered to an associated computer. Second, response times to stimulation require algorithms running with multiple response timescales, as seizure-responsive stimulation must act very quickly to abort a seizure. In contrast, seizure forecasts occur tens of minutes before a seizure allowing more time to adjust stimulation. Third, dynamic adjustment of stimulation requires that algorithm implementations are compliant with regulatory requirements for software development and are confirmed to be safe by extensive testing. The investigational Medtronic Summit RC+S™ neuromodulation device offers a unique combination of near-real-time intracranial EEG telemetry, on-device analytics, and modulated stimulation therapy that could enable therapies not previously possible. The system can be configured using the Medtronic Summit libraries and API in custom software, enabling advanced features. The system is illustrated in **Figure 1**.

FIGURE 1 | The EPAD system—The EPAD system user interface and core logic deployed along with on-tablet seizure detection and forecasting algorithms. EEG data packets from the investigational Medtronic Summit RC+S™ implanted device are decoded, sorted, assembled, compressed, and stored in a cloud-synchronized repository in Multiscale Electrophysiology Format (MEF v.3.0). In addition, dense behavioral inputs from the patient interaction with the EPAD system and data from external wearable devices are synchronized over Wi-Fi or cellular data networks to a cloud-synchronized repository.

The EPAD system user interface and core logic were developed in C#, and compiled python programs were used to deploy on-tablet seizure detection and forecasting algorithms. Data packets containing EEG and accelerometry from the implanted device are decoded, sorted, assembled, and losslessly compressed using Range Encoded Differences (RED) before being stored in a cloud-synchronized repository in Multiscale Electrophysiology Format (MEF v.3.0). Seizure, aura, medication, stimulation changes, and other event annotations are stored in SQL and CSV files. Video files acquired by the tablet's embedded camera during detected or self-reported seizures are synchronized with the EEG and accelerometry data and stored in the cloud repository. Dense behavioral input from the patient is received through interaction with the EPAD system, and data synchronization between devices, tablet, and cloud repository occurs over Wi-Fi or cellular data networks. Data flow between the different parts of the EPAD system is illustrated in **Figure 2**.

This architecture is beneficial for implementation using a mobile-computing middle layer responsible for configuring stimulation and sensing, managing data telemetry from the device to the cloud, and running moderately complex analytical algorithms in near real-time. This architecture allows the system to enable modulated therapy and provide objective EEG and behavioral data to physicians, patients, and caregivers.

DESIGN AND DEVELOPMENT

The EPAD system is designed to be used as part of an investigational device system early feasibility study to examine the safety and potential benefits of a novel closed-loop electrical stimulation therapy to treat drug-resistant epilepsy (DRE). The EPAD system tests the feasibility and potential benefits of three functions that may benefit the management of non-resectable DRE. (1) Seizure diaries arising from chronic electrographic recordings, analytics, and expert review may help physicians better manage patients' epilepsy. (2) Seizure forecasting, arising from predictive algorithms trained on physician-identified seizures, may allow patients to manage their epilepsy better. (3) Modulating stimulation based on electrographic biomarkers of sleep and seizures may enable the physician better to treat a patient's epilepsy with fewer side effects.

Software that is part of or controls a medical device is subject to strict regulation due to its safety-critical nature. Therefore, the EPAD system was developed following work instruction that meets the Food and Drug Administration (FDA) requirements for Investigational Device Exemptions (IDEs) as defined in 21 CFR 812.1 and Design Controls as defined in 21 CFR 820.30. In order to integrate traditional software development standards with the regulatory requirements, the EPAD system was developed with the V-model (20), a well-established software development life cycle model, also known as the Verification and Validation model. By its nature, the V-model is a good fit for many medical devices software development as the requirements is understood and clearly defined, and phases are complete one at a time with a testing phase at each step. That structure allows the detection of issues and inconsistencies in an early stage and is why the V-model is typically implemented within the field.

For the EPAD system, design and development were comprised of two main phases: Planning and Execution. The execution phase was further subdivided into Design, Implementation, and Delivery phases. The planning phase consisted of assessing stakeholder needs, performing a preliminary Safety Risk Analysis, and obtaining proponent review and acceptance of the proposed project plan. The execution phase was initiated with the design phase, where a System Requirements document was developed in consultation with physicians, patients, the Medtronic Summit System staff, and the Mayo design team. The System Requirements document captures the stakeholder needs translation into system requirements that describes the system's required functionality, performance, attributes, boundaries, and constraints. System Validation Test Protocol was developed during the design phase to define the necessary tests to ensure that the research system operates as intended in its operational environment according to the System Requirements document. During the development process's Implementation phase, the software and system requirements were translated into a working system and described in detail by the software design specifications. Finally, during the Delivery phase of the development process, the EPAD software was installed and configured on a tablet computer, and verification testing was performed. Residual system deficiencies were addressed, and final testing reports

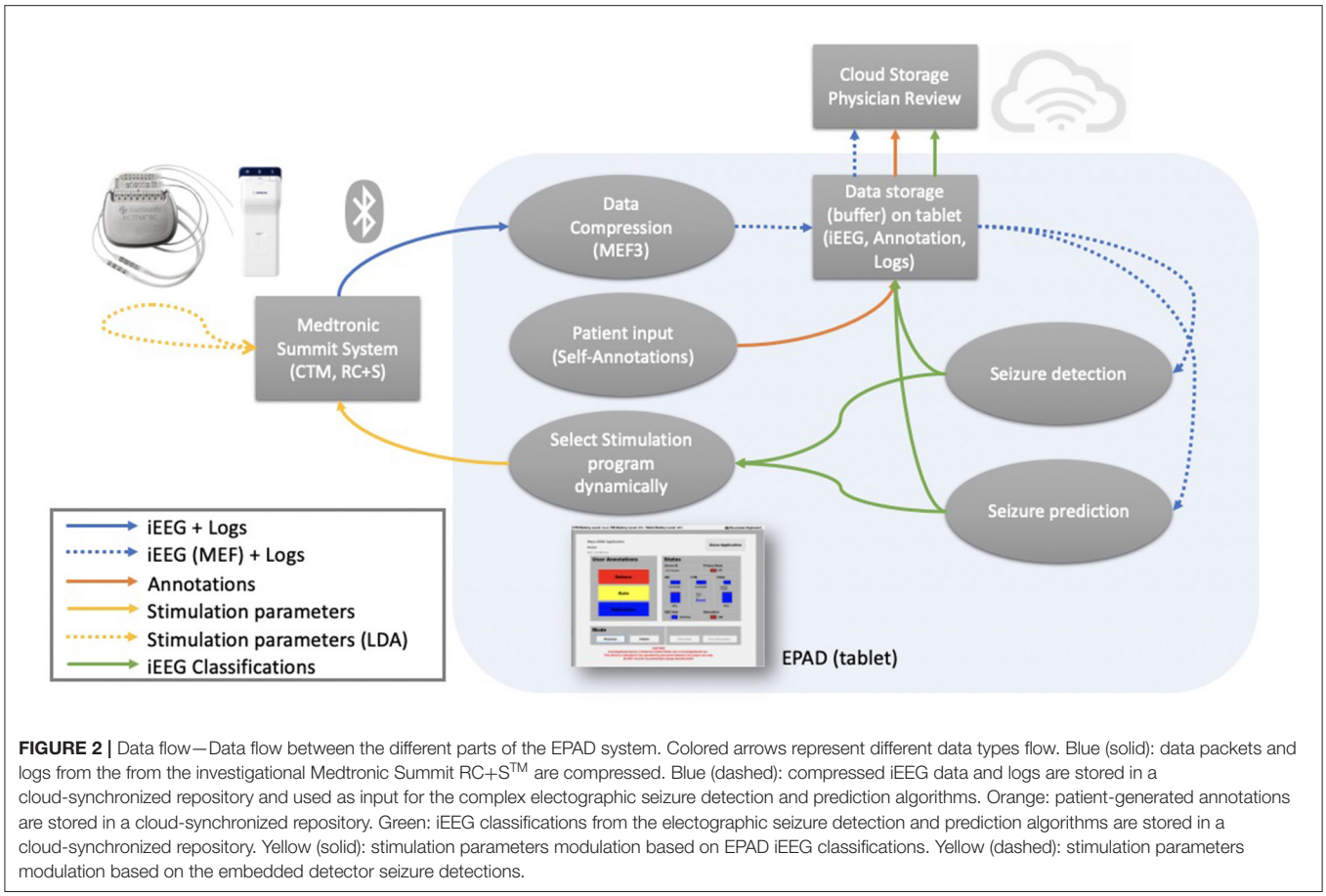

FIGURE 2 | Data flow—Data flow between the different parts of the EPAD system. Colored arrows represent different data types flow. Blue (solid): data packets and logs from the from the investigational Medtronic Summit RC+S™ are compressed. Blue (dashed): compressed iEEG data and logs are stored in a cloud-synchronized repository and used as input for the complex electographic seizure detection and prediction algorithms. Orange: patient-generated annotations are stored in a cloud-synchronized repository. Green: iEEG classifications from the electographic seizure detection and prediction algorithms are stored in a cloud-synchronized repository. Yellow (solid): stimulation parameters modulation based on EPAD iEEG classifications. Yellow (dashed): stimulation parameters modulation based on the embedded detector seizure detections.

were generated, including the verification testing report and unresolved anomalies report.

The majority of the EPAD system's design effort consists of developing the EPAD software application and is detailed below.

Medtronic Summit Research Development Kit

The Medtronic Summit System consists of a Model B35300R Olympus RC+S™ implantable device (INS), commercial leads, and extensions, Model 97755 Charger, Summit Programming Application, Model 4NR010 Summit Research Lab Programmer (RLP), Model 4NR011 Continuous Telemetry Module Gateway (CTM), and Model 4NR009 Summit Patient Programmer. Stanslaski et al. (16) detail the two major parts of the investigational Medtronic Summit RC+S™ system, including (1) an implantable hardware firmware subsystem for neural interaction and running embedded algorithms and (2) a supporting firmware-software system for communicating, recharging, streaming, and analyzing data. The EPAD system interaction with the investigational Medtronic Summit RC+S™ systems enables the iEEG monitoring, processing, and control functions of the overall EPAD system. In addition to analysis on the electrographic signals to trigger changes in physician-defined safe neurostimulation approaches.

The Medtronic Summit Research Development Kit (RDK), a software interface library, was incorporated into the EPAD system and used to access gateway functionality. The RDK Library is a pre-compiled Dynamic-Link Library (DLL) file written in the C# programming language. All control and feedback functions with the investigational Medtronic Summit RC+S™ INS must be handled through the API. Therefore, methods implemented in the RDK are called directly throughout the EPAD system. The Medtronic Summit RDK requires the Application Programming Interface (API) to run under Microsoft Windows. Hence, the EPAD system was developed as a mobile application capable of running on a Microsoft Windows Tablet computer.

The Research Lab Programmer (RLP) is the application/hardware the clinician uses to configure INS therapy safety-related settings and determine system status. Initial stimulation configuration, including contact selection and parameter limits, must be done on the RLP to ensure patient safety. After defining stimulation parameter space available with the RLP, the EPAD system can modulate stimulation within clinician-defined limits and modify other configurations using the Medtronic Summit API. However, it must adhere to the clinician-defined limits, or it will be rejected.

The Medtronic Summit API is used throughout the EPAD system to control and communicate with the entire Summit

system and, specifically, the INS. This allows various actions, including initiating a link to the CTM and INS, device status queries, interactions logging, data streaming, and configuration of the device's sensing, data processing, classifiers, and adaptive control policy. The SummitManager enumerates and manages the telemetry to the implantable device. Using telemetry information, the SummitManager can create a Summit system object. The SummitSystem and SummitManager objects are vital objects within the Medtronic API to maintain the connection between the tablet, CTM and INS.

The EPAD application utilizes a 30-s keepalive timer active while running. The keepalive timer reads the CTM battery status and the INS battery status. These status queries are used to report status on the main screen and write hourly status annotations. Also, by querying the battery levels, we can ensure that a proper connection is maintained between the tablet, the CTM, and the INS. If more than three attempts to communicate with the CTM fail, then API commands can re-establish communication. The Medtronic API offers a callback function that signals the EPAD system when the connection is broken and should be re-established. When a new connection to the INS and CTM is needed, the keepalive timer re-initializes the data collection using a customized helper function. The function uses a Medtronic Summit API function to search over Bluetooth for known CTM devices, as only a CTM device previously paired with the tablet can be connected. Then uses a Medtronic Summit API function to discover and connect to the INS and an abstraction layer to manage all underlying functionality of a single INS.

The INS is queried to its state in terms of streaming data and stimulation. This information is used in additional features of the keepalive timer function, including a warning message that is displayed to the user when EEG data is expected, however, the tablet has received no data in 30 min. Also, the current set of stimulation parameters set on the INS are compared against desired stimulation parameters. If a discrepancy is found, the stimulation parameters are re-sent to the INS. These stimulation parameters, along with other basic setup parameters, are saved when any system parameter is changed, and hourly status updates of the entire system are generated. Furthermore, parameters, such as stimulation and LDA classifier settings, can have a daytime/nighttime mode to allow the patient to sleep better. This is also monitored and adjusted during the 30-s timer.

MEF 3.0

Multiscale Electrophysiology Format (MEF) is an open-source file format designed to store electrophysiology and EEG (21) but is extensible to most time-series data. The format incorporates a header, which contains technical information about the file, stored data, and subject identifiers. The header is followed by a variable length sequence of compressed data blocks, each of varying size. Each compressed data block contains a block header, which contains the uUTC timestamp of the first data sample in the block, the number of samples stored in the block, a cyclic redundancy check value computed on the compressed data block, and a statistical model of the stored data samples. The format incorporates 128-bit encryption, which can be applied optionally to subject identifiers in the file header, technical acquisition details in the file header, and data blocks. Version 3.0 of MEF is designed to be a real-time data format, which means that a viewer/analyzer can read files even as another process is writing them. The MEF 3.0 file format is fully detailed in the Multiscale Electrophysiology File Format Version 3.0[1].

The EPAD system receives data in packets from the Medtronic API callback commands. Packets typically represent either 50 or 100 ms with a corresponding timestamp. Upon receipt, packets are added to a buffer, which collects between 5 and 10 s of data, and sorts the packets into order using the given timestamp. Packets that are severely delayed (due to Bluetooth or other problems) and cannot be ordered correctly are discarded. Statistics of discarded packets are kept and monitored to ensure that data loss is not unreasonably high.

The MEF 3.0 API library ("meflib"[2]) is written in the c language and is a collection of ∼100 functions designed to ease the use of the MEF 3.0 format. In addition, a secondary library ("mefwriter"[3]) is used to simplify the MEF 3.0 encoding process. This allows complete MEF 3.0 data channels to be encoded by using as few as three function calls, and most details of the file format are abstracted from view. In the EPAD system, both the meflib and mefwriter libraries are compiled as c functions and exported as dll files for use by the C# environment. This allows seamless integration with the EPAD system without having to recompile the libraries under C#.

MEF 3.0 supports segments, which allows EEG channels to be divided into arbitrary size files. The EPAD system takes advantage of this by beginning a new segment each time the application runs (typically daily, since EPAD software restarts at midnight each day). During the process of creating a new segment, the previous segment (and only the previous segment) is read and verified for consistency. This is necessary for both technical reasons (some data persists across segments) and guarantees that the on-board analytics algorithms can successfully read the entire channel. If even one segment were to be unreadable, then potentially, the entire channel might be unreadable. Since only the previous segment is read before creating a new segment, this allows much older segments to simply be deleted in the interest of reducing hard drive usage. The meflib library is sufficiently robust to merely ignore non-existent segments.

Analysis shows that using MEF 3.0 in the EPAD system, the EEG data (or time-domain data) is losslessly compressed at a ratio of better than 5 to 1, relative to the original JSON data produced by the Medtronic Summit API. This compressed MEF 3 version of the data is immediately indexed and readable using MEF 3.0 tools as the files continue growing in size. The compressed nature of the data represents less network traffic when uploading to the cloud and greater data storage capacity on the tablet hard drive. The uncompressed JSON version of the data is deleted every 24 h due to being redundant.

In addition to writing MEF 3.0 data, the EPAD system also uses a Python version of the MEF 3.0 library ("pymef"[4]) to read

[1]https://msel.mayo.edu/files/codes/MEF%203%20Specification.pdf
[2]https://github.com/msel-source/meflib
[3]https://github.com/msel-source/mefwriter
[4]https://github.com/msel-source/pymef

MEF 3.0 data that has already been written. This library consists of a Python interface designed around the native MEF c code compiled for Windows. As mentioned above, the EPAD system writes MEF 3.0 data, and data analysis is done in near real-time for seizure detection and prediction purposes in separate spawned processes that use the python MEF 3.0 reader library.

Hardware Settings

The EPAD system can read or write INS settings using the various Medtronic API functions to manage the INS settings. There are write parameters functions to directly modify, change, or set various INS firmware settings and read parameters functions to access the INS state.

Sensing Parameters

The Summit system is sensing signals measured using the INS. The INS can stream up to four channels of local field potentials (LFPs) from the implanted electrodes. The EPAD system presents the physician with a series of configurable options representing the operation of the EPAD system and INS, including iEEG electrode configuration, sampling rates, sampling interval, duration, and accelerometer data telemetry from the INS. Initial selected values reflect options previously configured using the Medtronic Summit RLP.

A Medtronic API function is used to configure the sensing state and then sensing data that can be streamed from the INS to the EPAD system tablet. Individual streams can be enabled or disabled at any time. Each enabled data stream indicates the INS to send data packets, which is then handled on the EPAD system accordingly. The function first parameter is a Boolean, which determines if time-domain (TD) packets are sent from the INS/CTM to the tablet. The rest of the function Boolean inputs correspond to the following individual streams: Fast Fourier Transform (FFT) of the signal, Power (the input to the on-board classifier), Detection Events, Adaptive Stim (active state and stim settings), 3-axis Accelerometer data, Time-Sync (enables packet gen times), and Loop Recorder (LR) status updates and external marker echoing. General practice is not to request more information than is needed since the INS-CTM connection and the CTM-tablet Bluetooth connection have a data throughput limit.

The EPAD system is set by default to continuous real-time streaming but can also operate in periodic streaming. When designing the EPAD system, the design included putting the INS into a periodic streaming mode to save battery life, as it would only be streaming for 1 min out of every 3 (for example). However, it is necessary to close and reconnect the Bluetooth connection repeatedly to save a meaningful amount of battery power, and reconnection could be problematic if the CTM is not maintained in close proximity to the INS.

Stimulation Parameters

The ability to modulate stimulation based on patients' electrophysiological biomarkers, seizure diary and cyclical patterns holds unique potential for responsive and predictive adaptive neuromodulation. Modulating the intensity of stimulation based on electrophysiological biomarkers could allow applying high stimulation when a patient is at high risk of seizure and low stimulation when a patient is at low risk of seizure, by doing so reducing side effects and prolonging battery life. Also, neurostimulation intensity could be increased/decreased during sleep stages which a patient's seizure diary suggests a correlation with an increased/decreased likelihood of seizure occurrence. As well as, seizure diaries coupling to increase stimulation during sleep after seizures to disrupt memory consolidation and prevent the brain from strengthening seizure pathways (22).

To mitigate patient risk, the Medtronic API is limited by design in its ability to adjust therapy for a patient dynamically. Therefore, the EPAD system is limited to turning therapy on/off, switching between stimulation groups, and changing stimulation parameters within clinician-defined limits (configured with the RLP). The INS can be configured with up to four stimulation groups A, B, and C for general open-loop therapy and group D for adaptive stimulation.

A Medtronic API function is used to change the active group to a different one specified by the function argument. The EPAD system uses group A as a "safe mode" state where the baseline settings are used, when adaptive stimulation is turned off. Groups B and C are used for the stimulation trial. Finally, group D is used for adaptive on-board stimulation in combination with the classified state [baseline (wake and sleep), seizure, pre-seizure].

The EPAD system presents the physician a set of configurable options affecting the stimulation modes, including stimulation rates and stimulation current amplitudes for each classified state [baseline (wake and sleep), seizure, pre-seizure]. When configuring an INS group program with the RLP, a clinician can define an upper and lower bound for each parameter. Because of the safety-critical nature of stimulation parameters effect on the patient, these are validated within the EPAD system against desired settings, clinician-defined limits and globally defined limits, every time new parameters are applied and within every EPAD system 30-s keepalive timer. When calling the API function that is used to turn on the stimulation engine and is required for any therapy to be output to the patient, additional validation occurs. The function will be rejected if there is no valid therapy configured or the INS has shutdown unexpectedly. The EPAD system includes a real-time data visualization capability that allows the physician to view the real-time effects of the configured stimulation parameters (**Figure 3**). This is a valuable tool giving the physician a unique view of the data immediately. The data visualization also assists in the Verification and Validation test.

The Summit system supports sensing-based adaptive algorithms, where the algorithm acts autonomously on the INS. Embedded adaptive therapy is only allowed in Group D. The system will be configured to operate with the on-device linear discriminant analysis (LDA) closed-loop classifier active, employing one LD with one threshold. It can have a value above the maximum threshold (High) and below the minimum threshold (Low). The embedded classifier will be configured to detect iEEG characteristics similar to physician-confirmed electrographic seizures and will implement physician-configured stimulation parameters (Amplitude and Stimulation Rate) in

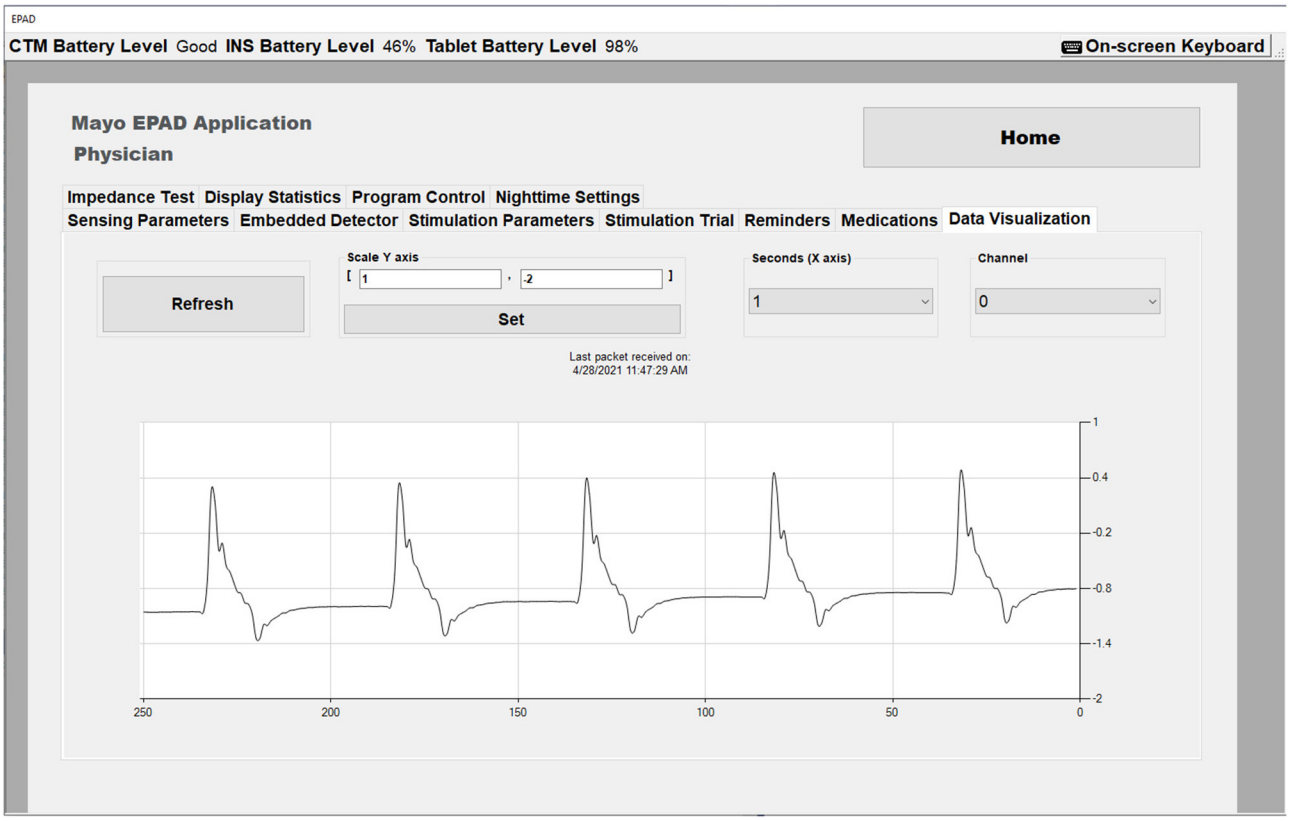

FIGURE 3 | The EPAD Data Visualization tab in Physician mode showing real time data with stimulation artifact (Amplitude = 2 mA, Rate = 5 Hz).

response to these detections. Using the embedded detector to detect known electrographic seizure events provides the fastest possible response to these iEEG changes, while maintaining reasonably high sensitivity and specificity.

Stimulation Trial Parameters

Finding the right set of stimulation parameters for each patient is complicated due to the time-consuming nature and the need to record real-word responses to the parameters. This feature allows the physician to pre-configure up to 24 parameter combinations, including stimulation amplitudes (3), rates (4), and pulse widths (2). Stimulation groups B and C are used for the stimulation parameters trial. Parameter groups are arranged in two sets, each of which can have unique pulse widths and electrode contacts. Within a set the parameter sequences occur in sequential combination so that every stimulation rate is tested with every set of amplitudes. The physician can specify the duration of each stimulation cycle as well as a "rest interval" between stimulation cycles. The stimulation trial can be repeated by selecting the number of test cycles and can be stopped at any point in the process while the tablet is connected. In case the software crashes or the tablet turns off during the trial, upon reconnection, the stimulation trial shall resume from the last set of parameters tested.

Impedance Measurements

The EPAD system can conduct an impedance measurement on up to 16 contact pairs in a test using an API function. The EPAD system warns the user that stimulation and sensing will be temporarily discontinued and waits for any active sensing loops to complete before turning off sensing and stimulation functions. Once these functions are confirmed to have stopped by the INS, the EPAD system conducts the impedance test. Measured impedances for electrode contacts shall be written to the log file and the Annotations file.

User Interaction

Technology is advancing rapidly, and there are more and more digital personal assistants with advanced capabilities. Also, there are many new technologies for better diagnosis of diseases and better-targeted therapy to such conditions. The EPAD system combines these possibilities and provides an interface to allow the epilepsy patient to enter annotations regarding seizures, auras, and medications. The patient can make an annotation, by simply clicking the appropriate button on the main screen of EPAD. Once the patient presses the Seizure or Aura buttons, a video recording is started using both the tablet's front and back cameras, encrypted and saved in Audio Video Interleave (AVI) format. The EPAD system also provides the reminder feature, allowing the physician to pre-schedule reminders for

medication dosages and battery charging. Reminders and alerts for INS, CTM, and Tablet batteries can be sent to the patient's smartphone via SMS text message. The physician medications tab allows the physician to enter the patient's medication dosages then automatically generates reminders for each dose. When the Medication button is pressed, a "medication dose" dialog is presented, which allows the patient to select the appropriate medication and dose taken. In the Patient-only section, an additional option is given for extra medications taken that are not part of the usual regimen specified by the physician.

Epilepsy is associated with sleep, cognitive, and psychiatric comorbidities, which significantly impact the quality of life. The EPAD system offers a unique opportunity for long-term tracking of cognitive performance and psychiatric symptoms using the questioners feature of the reminders that allow the physician to schedule mood survey questionnaires, including the IMS-12 (23) and surveys of premonitory symptoms of seizures (24).

All patient-generated annotations are displayed in the Patient Annotation Diary, and the physician has access to these annotations through synchronization of offline data files.

Annotations

Prior studies have documented significant under-reporting of seizures in many patients (13). Chronic recordings may help physicians identify unreported seizures and adjust treatment accordingly. This could identify patients at significant risk of status epilepticus or SUDEP. Also, it may be possible to identify circadian or ultradian patterns in a patient's seizures and use these patterns to optimize therapy (25). Additionally, chronic monitoring and seizure diaries could provide a clearer view of a patient's seizure patterns and suggest a potential resection target not apparent upon initial monitoring. Many patients with intractable epilepsy also exhibit behavioral, non-epileptic spells. Therefore, objective recordings may help physicians differentiate among conflicting patient reports or evidence and provide an alert for physicians or caregivers in the event of prolonged seizures or status epilepticus.

To investigate the potential benefits of an electronic seizure diary, we incorporated the ability for seizure annotations within the system to be generated by the patient or generated by automated seizure detection algorithms. In addition to user interface interactions, a back-end database is updated with auto-generated events. Events are notated in two different ways to allow greater flexibility upon reading. First, through the use of a simple text file in Comma-Separated Value (CSV) format, and second, in a relational database structure using Structured Query Language (SQL). In the interest of being lightweight and not computationally intensive, the EPAD system makes use of SQLite, which is an embedded, open-source c-language-based SQL management system. The resulting csv and sqlite files are synchronized to the Mayo BNEL lab's servers via Dropbox.

Besides the patient-generated events, numerous system status events are also incorporated into these files. These include embedded (INS) detections of seizure-like electrographic anomalies, on-tablet detections of seizure-like electrographic anomalies, on-tablet computed pre-seizure state warnings, battery levels for INS, CTM, and tablet computer, stimulation pulse rate, amplitudes, channels, and pulse width when configured, and on/off states, timestamps, and settings for detectors, stimulation, accelerometer, and other signals saved. These parameters are updated at least hourly and upon predefined trigger events to give the physician a complete picture of the EPAD system's configuration at any point in time.

Data Analysis

Reliable seizure forecasting holds great benefits to the patient, including permitting patients to take fast-acting medications to prevent seizures and also may improve patient safety by allowing patients to avoid potentially hazardous activities during high seizure likelihood periods. Additionally, seizure forecasting may reduce psychiatric comorbidities of epilepsy by reducing the anxiety and depression associated with seizure unpredictability. Moreover, seizure forecasting could enable increasing the intensity of neurostimulation during seizure-prone periods to prevent seizures.

Beyond the embedded detector used to detect electrographic seizure events that provide the fastest possible response, the EPAD system also runs more complex analytic algorithms to detect iEEG changes preceding physician-confirmed electrographic seizures, and iEEG changes associated with physician-confirmed wake and sleep states. The algorithms for classification of brain state (e.g., seizure, pre-seizure, wake, sleep, epileptiform activity) from acquired iEEG data have been developed in Python and compiled for Windows. The algorithms are trained offline and algorithm parameters are loaded to the tablet after training. The main EPAD program calls the compiled Python executable files through the Windows file system with the necessary parameters. Based on these iEEG classifications, the EPAD System will change the baseline stimulation parameters to physician-defined values designed to optimize neuromodulation therapy for particular brain states.

Electrographic Seizure Detection

The role of EPAD system seizure detection algorithm is to support a seizure diary of physician-confirmed electrographic seizures. The EPAD system implements a modified version of the best performing seizure detection algorithm from the recent machine learning seizure detection contest (26) to accommodate continuous iEEG data. The algorithm was initially developed for the competition, used a Random Forest classifier (3,000 trees) with frequency spectrum, time-domain correlation, and frequency-domain correlation features. Specifically, the algorithm aggregates the logarithm of the Fourier transform from 1 to 47 Hz (in 1 Hz bins), the correlation coefficients, and eigenvalues of the correlation matrix between Fourier transformed iEEG channels from 1 to 47 Hz, and the correlation coefficients and eigenvalues between the raw iEEG channels. This algorithm's EPAD system implementation uses the same feature set described above, with a reduced number of 150-tree Random Forest classifier, operating on 1-s iEEG data segments.

TRACEABILITY MATRIX

Project Name:	**Mayo Epilepsy Personal Assistant Device**
Center:	Mayo Foundation, Rochester MN
Project Manager Name:	Benjamin H. Brinkmann PhD
Project Description:	Off-body Platform for iEEG Streaming, Analytics, and Modulated Stimulation

Document Number: 00274208

Revision: 2

				Verification Test								Validation
Trace ID	*Document ID*	*Requirement ID*	*Requirement*	4.1	4.2	4.3	4.4	4.5	4.6	4.7	4.8	Stakeholder Need ID
TR001	00269473	**2.1.1**	Identification and Model Number	X								
TR002	00269473	**2.1.2**	Version, and Build	X								
TR003	00269473	**2.1.3**	Summit RDK Libraries	X								SH003, SH004
TR004	00269473	**2.1.4**	User Limitation	X								
TR005	00269473	**2.1.5**	Investigational Device	X								
TR006	00269473	**3.1.1**	Bluetooth	X								
TR007	00269473	**3.1.2**	USB Ports	X								SH003
TR008	00269473	**3.1.3**	Touch Screen Interface	X								
TR009	00269473	**3.2.1**	File System		X							SH002, SH0013
TR010	00269473	**3.2.2**	Log File		X					X		
TR011	00269473	**3.2.3**	EEG Data Files		X							SH002, SH0013
TR012	00269473	**3.2.4**	Annotation Files		X					X		
TR013	00269473	**3.3.1**	Main-form (Home screen		X							
TR014	00269473	**4.1.1**	Initialization Mode		X							SH003, SH006
TR015	00269473	**4.1.2**	Home Mode	X								SH003
TR016	00269473	**4.1.3**	Password Validation		X							SH001
TR017	00269473	**4.1.4**	User Role		X							SH001
TR018	00269473	**4.1.5**	User Privileges		X							SH001
TR019	00269473	**4.1.6**	Entry to Patient Mode		X							SH001
TR020	00269473	**4.1.7**	Exit from Patient Mode				X					
TR021	00269473	**4.1.8**	Entry to Physician Mode		X							SH001
TR022	00269473	**4.1.9**	Exit from Physician Mode				X					
TR023	00269473	**4.1.10**	Display Statistics Mode		X							
TR024	00269473	**4.1.11**	Exit Display Statistics Mode				X					
TR025	00269473	**4.1.12**	View Diary Mode		X							

FIGURE 4 | An excerpt from the EPAD Requirements Traceability Matrix.

Electrographic Seizure Prediction

The seizure prediction algorithm's role is to support stimulation parameters modulation in periods preceding physician-confirmed electrographic seizures. It is reported in the literature (13, 14) and supported by our internal testing that these identifiable iEEG signatures occur 60 or more minutes before the onset of a seizure. The EPAD system implements a modified version of the best performing seizure prediction algorithm from a recent machine learning seizure prediction contest (27), to accommodate continuous iEEG data. The algorithm was initially developed for the competition used a cross-validation strategy to select the best performing classifier among Logistic Regression, Linear Regression, and Support Vector Machine classifiers, and used a genetic algorithm (or random index) to select a subset of features from among the following: Time correlation matrix upper right triangle and sorted eigenvalues, frequency correlation matrix upper right triangle and sorted eigenvalues, the logarithm of the FFT magnitude for various frequency ranges, power-in-band spectral entropies, Higuchi fractal dimension with Kmax of 2, Petrosian fractal dimension, and Hurst exponent.

The code developed for the contest was modified to run with iEEG data from the EPAD system and simplified to improve execution time. Preliminary algorithm testing on canine iEEG recordings revealed that the Logistic Regression classifier was the most reliable algorithm, and that a vastly reduced feature set was adequate to achieve good performance. The EPAD implementation of this algorithm uses the Logistic Regression classifier, operating on 10-min iEEG data segments (28). The feature set was reduced to interelectrode correlation and the FFT magnitude between 0.25 and 24 Hz. The prediction algorithm was deployed as a separate executable, so that future advances in prediction algorithms could be incorporated without recoding the core application.

Risk Analysis

The EPAD system was developed with a test-driven evolutionary development strategy. We conducted an analysis of risks associated with the use of the EPAD system and evaluated these risks using an acceptability framework defined by our institution's Division of Engineering. This analysis of risks includes a summary of the overall residual risk and the acceptability of residual risk levels that have been attained through specific risk mitigations. The main residual risks of the EPAD system include loss of therapy due to battery depletion in the implanted neurostimulator, changes in electrode impedances over long time periods decreasing effectiveness of sensing and stimulation, electromagnetic noise triggering high stimulation states when not intended, and unsafe stimulation programs being implemented by the physician.

TABLE 1 | Verification tests used in the EPAD quality system.

Requirement	Test
EPAD shall disconnect when the INS battery reaches 25% to prolong battery life and prevent loss of therapy	Canine subject's INS battery was partially charged, and EPAD disconnection was observed when it reached 25% power
The embedded LDA detector shall identify at least 80% of physician identified electrographic seizures with a false positive rate of <20%	The benchtop device is attached to electrodes immersed in a saline bath. EEG signals previously recorded from canines with epilepsy were electrically conducted into the saline bath using an Arduino. EPAD recorded the EEG and LDA seizure detections, and these detections were compared to the canine EEG signal annotations
The Application shall modulate the amplitude and frequency of stimulation in response to the output of iEEG analytics, with frequencies and amplitudes as configured by the physician. iEEG analytics shall identify iEEG characteristics similar to data preceding physician-identified seizures (pre-ictal)	Phase I: The python executable performing seizure prediction was trained on retrospective canine iEEG data and tested on over 60 days of data on a separate computer to verify performance Phase 2: The same executable running on the tablet computer as part of EPAD was trained to identify delta wave sleep and to initiate very low amplitude (0.5 mA) stimulation on a canine subject. Recorded iEEG data was reviewed to confirm stimulation artifact was visible during delta wave sleep
EPAD shall provide the ability to conduct a stimulation trial, cycling through at least 12 sets of stimulation amplitudes and frequencies on up to 2 sets of electrodes	Stimulation trial was configured with notably different amplitudes and frequencies on different electrodes. The stimulation trial was run first on the benchtop device and then on a canine subject's device with EEG recording enabled. Stimulation artifacts on recording electrodes were used to confirm relative stimulation rate and amplitude changes

TABLE 2 | Validation tests used in the EPAD quality system.

User need	Test
Ensure the EPAD system initializes a connection to the Medtronic Summit System if available	Medtronic INS and CTM initially paired with EPAD system is moved out of range (>2 m) until connection drops. When moved back within range the system initiates a wireless connection within 60 s
Ensure the EPAD system can provide near real-time EEG data display	With a benchtop device paired, the user navigates to the EPAD Data Display tab, which provides near real-time display of captured iEEG data. While watching streaming iEEG data, the user taps the electrodes and confirms that high amplitude artifacts appear in the display within a few seconds
Ensure the EPAD system buffers acquired data locally if no network data connection is available	With a benchtop or canine EPAD system the user disconnects from Wi-Fi networks and enables iEEG streaming for 24 h. The user confirms that iEEG data files from the disconnected day are stored on the tablet and that iEEG files are transferred once Wi-Fi is re-established
Ensure the EPAD can provide reminders, queries, and questionnaires to the patient	The EPAD system was configured to provide notifications via dialog windows and SMS notifications for medications, mood surveys, and battery charging. Notifications of each type were set to occur at 5-min intervals over the course of a few hours with SMS messages directed to the user's phone

A definition of Essential Performance is established, as well as the safety classification of software components used as part of the device system. AAMI/IEC 60601-1 defines Essential Performance to be "Performance necessary to achieve freedom from unacceptable risk." The standard notes that "Essential Performance is most easily understood by considering whether its absence or degradation would result in an unacceptable risk." Risk analysis suggests that the Essential Performance of the EPAD is to notify the user of its operational status. Because it operates via an external connection to the Medtronic Summit System, failure of the EPAD system to operate would not interfere with the Summit System's ability to deliver stimulation. "Safety Classification" is used to establish the classification of the software component and is used to inform software development and verification efforts. Software safety classes include: Class A: No injury or damage to health is possible, Class B: Non-serious injury is possible, and Class C: Death or serious injury is possible. The software components related to iEEG recording are found to be Class A, while the stimulation modulation is found to be Class C; the system as a whole is considered Class C.

Verification and Validation

Verification and validation testing are done to confirm that a device and software meets its design specifications and if it fulfills its intended purpose. An essential component in a quality management system is the Requirement Traceability Matrix which is shown in **Figure 4**. The Requirement Traceability Matrix links verification tests to the individual design requirements they test, and similarly validation tests to user needs. This ensures that all necessary design inputs are addressed by the design and confirmed by testing. Best practices in software verification include embedded and manual build-time testing. With every new build of an EPAD version, we performed manual tests designed to cover broad use cases and reveal deficiencies quickly broadly. Unit testing of individual software elements is also part of best practices in software design and was employed throughout the EPAD code base and performed automatically with each build. Unit testing generates pass/fail reports for each test, and these are logged and reported in the Verification Testing Report. A comprehensive verification testing plan was followed which specified the testing environment, the materials needed, and the pass/fail criteria for the test, in order to verify that requirements defined for the EPAD had been implemented successfully. A vital element of the EPAD system is the integration of several independent software components. For that reason, verification of successful component integration was explicitly tested as part of the verification test plan. Testing integration of modules within

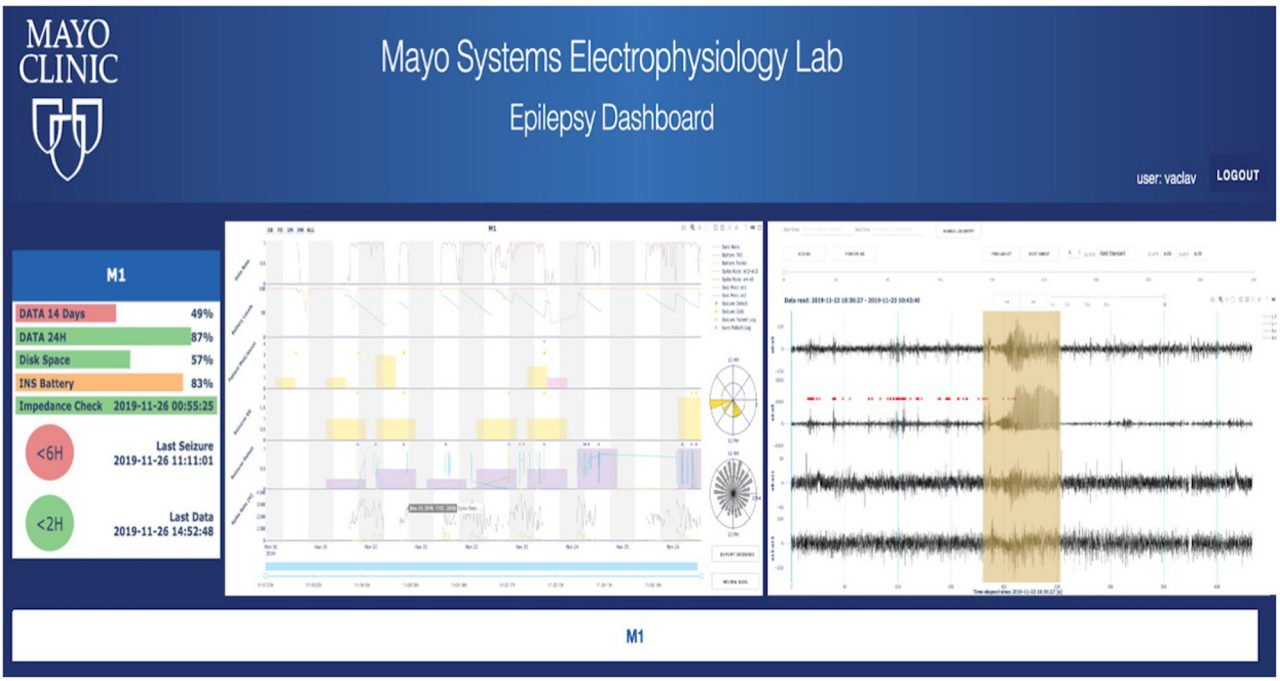

FIGURE 5 | Cloud analytics—First human subject data in the cloud longitudinal analytics system, including automated seizure detections and gold standard (expert reviewed) annotations in raw iEEG data. Other features of the iEEG are displayed, such as spike rates and their circadian timing.

the code was handled using bottom-up automated testing at build time, with integration tests written to confirm the correct cross-module operation. Specifically, the interactions with the main EPAD code and the Medtronic Summit RDK, Seizure Detection Algorithm, Seizure Prediction Algorithm, and MEF Library were confirmed. Finally, validation tests were performed according to a detailed testing protocol to confirm the design and implementation met the input stakeholder needs. All testing results were carefully documented and stored in a document control system (SolidWorks PDM, 3DS Inc., Waltham MA).

Tables 1, **2** summarizes some of the basic verification and validation tests used in the EPAD quality system. Testing was performed on a dedicated benchtop system or in preclinical canine studies in a colony of research dogs with epilepsy (29). A particular challenge in testing this type of application is the requirement to test detection algorithms over a large number of seizures. Doing this sort of testing in real-time in canines would require a prohibitively long time to accomplish, and it was necessary to use some creativity in devising achievable tests that would confirm the system's performance. Availability of both benchtop INS systems and implanted canines was essential for system design and testing. While some tests could be performed in both environments, many required one or the other.

Analytical Platform and Data Visualization

To take advantage of rich data streamed from the EPAD system, the analytical backend and the cloud-based physician Epilepsy Dashboard provide a platform for reviewing electrophysiology data wirelessly telemetered off the implant. The data are automatically processed with a battery of algorithms running on the patient's local handheld for detecting seizures, IES, and classifying sleep/wake behavioral state. Results are stored in a database and accessible via a web-based dashboard. The Epilepsy Dashboard enables swift review of immediate and long-term data trends from the device (e.g., battery, electrode impedances), electrophysiology data, and patient inputs. The physician can quickly review and either confirm or reject automatically detected, and patient reported events. An example of the Epilepsy Dashboard is shown in **Figure 5**.

DISCUSSION

The integration of implanted neuromodulation devices, external wearable sensors, and dense behavioral sampling with cloud data storage and computational capabilities represents a potentially transformative advancement toward fully integrated digital medicine. The EPAD system, in its role of collecting data and interacting with patients, facilitates new scientific investigations which would not otherwise be possible. The EPAD system was tested and validated in preclinical studies in canines with epilepsy (29) including pet dogs living at home with their owners, and has currently been used in three human subjects with drug-resistant epilepsy. In addition, the EPAD system plays a vital role in many of our group's ongoing projects. To investigate circadian and multidian cycles our group characterized these in 16 dogs with naturally occurring focal epilepsy that were continuously monitored with the investigational Medtronic Summit RC+S^{TM} combined with the

EPAD system (10). This study shows that seizure timing in dogs with naturally occurring epilepsy is not random, and that circadian and multiday seizure periodicities, and seizure clusters are common. In addition, circadian, 7-day, and monthly seizure periodicities occur independent of antiseizure medication dosing, and these patterns likely reflect endogenous rhythms of seizure risk. The EPAD system was also used to improve seizure detection algorithm on-board of the investigational Medtronic Summit RC+S^{TM} device as the on-board detector offers the fastest possible response to iEEG changes, while maintaining reasonably high sensitivity and specificity. In this study, our group developed an algorithm using two power-in-band features with the on-board linear discriminant classifier to distinguish between seizure and non-seizure states. This simple algorithm can be implemented on the investigational Medtronic Summit RC+S^{TM} combined with the EPAD system and showed promise for detecting seizures recorded with leads in bilateral hippocampus (HC) and anterior nucleus of the thalamus (ANT). To investigate comorbid psychiatric disorders that are very common in drug-resistant epilepsy our group used the investigational Medtronic Summit RC+S^{TM} combined with the EPAD system to underline connections between epileptiform activity, mood, and therapeutic deep brain stimulation. Finally, in our group recent work we described the first application of a distributed brain co-processor, made possible by the EPAD system, providing an intuitive, bi-directional interface between device and patient, and implement it with human and canine epilepsy patients in their natural environments (30). Different algorithms, including automated behavioral state (wake and sleep) and electrophysiologic biomarker (interictal epileptiform spikes and seizures), were first developed and parameterized using long-term retrospective data from 10 humans and 11 canines with epilepsy and then implemented prospectively in implanted co-processors for two pet canines and one human with drug-resistant epilepsy as they live naturally in society.

The challenges remaining in remote monitoring and dynamic neuromodulation are primarily engineering challenges associated with battery life and reducing the overall burden of the system on patients. The success to date of the EPAD system serves as proof of feasibility, and we anticipate new systems with these capabilities will emerge in coming years. The EPAD and associated cloud infrastructure are applicable to other emerging devices (31–34), and continued development will allow integration of different physiological data streams in near real time from remote subjects.

The need for fully integrated remote monitoring and neuromodulation systems in clinical epilepsy is clear, and these systems have the potential to help address significant problems in epilepsy, including seizure under-reporting (35, 36), seizure forecasting (13, 37), psychiatric and cognitive comorbidities (38–40), and the lengthy duration currently needed to adjust neuromodulation parameters to optimize seizure control (6). Furthermore, this infrastructure facilitates new scientific insights into long-term patterns and trends in human and animal neurophysiology (9, 10, 41).

Important scientific investigation often requires innovative engineering solutions to enable measurement, study, and data gathering in ways not previously possible. The investigational Medtronic Summit RC+S^{TM} and EPAD systems are examples of cutting-edge engineering that enable continuous iEEG data collection for months to years across the full range of normal and pathological brain states, in concert with associated mood and symptom information, along with a full range of stimulation paradigms. The data accessible via this system is unparalleled and has the potential to transform neuromodulation therapy for epilepsy, mood disorders, and other conditions, and to advance our basic understanding of neuronal ensembles and local field potentials.

DATA AVAILABILITY STATEMENT

The data analyzed in this study was subject to the following licenses/restrictions: human data are restricted by patient privacy and HIPAA considerations. Requests to access these datasets should be directed to brinkmann.benjamin@mayo.edu.

ETHICS STATEMENT

The studies involving human participants were reviewed and approved by Mayo Clinic Institutional Review Board. The patients/participants provided their written informed consent to participate in this study. The animal study was reviewed and approved by Mayo Clinic Institutional Animal Care and Use Committee. Written informed consent was obtained from the owners for the participation of their animals in this study.

AUTHOR CONTRIBUTIONS

TPA, DC, and BB drafted the manuscript. All authors contributed to editing, collecting, and analyzing data.

FUNDING

This work was supported by the National Institutes of Health (UH3-NS095495, UH3-NS112826, and R01NS 92882-5), the Epilepsy Foundation of America Epilepsy Innovation Institute My Seizure Gauge, and the Mayo Clinic Bioelectronics Center. VK was partially supported by institutional resources of Czech Technical University in Prague. The funders were not involved in the study design, collection, analysis, interpretation of data, the writing of this article or the decision to submit it for publication.

ACKNOWLEDGMENTS

The authors acknowledge the technical and administrative contributions of Karla Crockett, Cindy Nelson, Sherry Klingerman, Delana Weis, Nathaniel Nelson, Erin Jagodzinski, and Kathleen McDonald.

REFERENCES

1. Hauser WA, Annegers JF, Kurland LT. Incidence of epilepsy and unprovoked seizures in Rochester, Minnesota: 1935-1984. *Epilepsia*. (1993) 34:453–68. doi: 10.1111/j.1528-1157.1993.tb02586.x
2. Christensen J, Vestergaard M, Pedersen MG, Pedersen CB, Olsen J, Sidenius P. Incidence and prevalence of epilepsy in Denmark. *Epilepsy Res*. (2007) 76:60–5. doi: 10.1016/j.eplepsyres.2007.06.012
3. Kwan P, Brodie MJ. Early identification of refractory epilepsy. *N Engl J Med*. (2000) 342:314–9. doi: 10.1056/NEJM200002033420503
4. Camfield P, Camfield C. Idiopathic generalized epilepsy with generalized tonic-clonic seizures (IGE-GTC): a population-based cohort with >20 year follow up for medical and social outcome. *Epilepsy Behav*. (2010) 18:61–3. doi: 10.1016/j.yebeh.2010.02.014
5. Salanova V, Witt T, Worth R, Henry TR, Gross RE, Nazzaro JM, et al. Long-term efficacy and safety of thalamic stimulation for drug-resistant partial epilepsy. *Neurology*. (2015) 84:1017–25. doi: 10.1212/WNL.0000000000001334
6. Nair DR, Laxer KD, Weber PB, Murro AM, Park YD, Barkley GL, et al. Nine-year prospective efficacy and safety of brain-responsive neurostimulation for focal epilepsy. *Neurology*. (2020) 95: e1244–56. doi: 10.1212/WNL.0000000000010154
7. Dumpelmann M. Early seizure detection for closed loop direct neurostimulation devices in epilepsy. *J Neural Eng*. (2019) 16:041001. doi: 10.1088/1741-2552/ab094a
8. Hoppe C, Poepel A, Elger CE. Epilepsy: accuracy of patient seizure counts. *Archiv Neurol*. (2007) 64: 1595–9. doi: 10.1001/archneur.64.11.1595
9. Baud MO, Kleen JK, Mirro EA, Andrechak JC, King-Stephens D, Chang EF, et al. Multi-day rhythms modulate seizure risk in epilepsy. *Nat Commun*. (2018) 9:88. doi: 10.1038/s41467-017-02577-y
10. Gregg NM, Nasseri M, Kremen V, Patterson EE, Sturges BK, Denison TJ, et al. Circadian and multiday seizure periodicities, and seizure clusters in canine epilepsy. *Brain communications*. (2020) 2: fcaa008. doi: 10.1093/braincomms/fcaa008
11. Kuhlmann L, Lehnertz K, Richardson MP, Schelter B, Zaveri HP. Seizure prediction - ready for a new era. *Nat Rev Neurol*. (2018) 14:618–30. doi: 10.1038/s41582-018-0055-2
12. Mormann F, Andrzejak RG, Elger CE, Lehnertz K. Seizure prediction: the long and winding road. *Brain*. (2007) 130(Pt 2):314–33. doi: 10.1093/brain/awl241
13. Cook MJ, O'Brien TJ, Berkovic SF, Murphy M, Morokoff A, Fabinyi G, et al. Prediction of seizure likelihood with a long-term, implanted seizure advisory system in patients with drug-resistant epilepsy: a first-in-man study. *Lancet Neurol*. (2013) 12:563–71. doi: 10.1016/S1474-4422(13)70075-9
14. Brinkmann BH, Patterson EE, Vite C, Vasoli VM, Crepeau D, Stead M, et al. Forecasting seizures using intracranial EEG measures and SVM in naturally occurring canine epilepsy. *PLoS ONE*. (2015) 10: e0133900. doi: 10.1371/journal.pone.0133900
15. Davis SF, Altstadt T, Flores R, Kaye A, Oremus G. Report of seizure following intraoperative monitoring of transcranial motor evoked potentials. *Ochsner J*. (2013) 13:558–60.
16. Stanslaski S, Herron J, Chouinard T, Bourget D, Isaacson B, Kremen V, et al. A chronically implantable neural coprocessor for investigating the treatment of neurological disorders. *IEEE Trans Biomed Circuits Syst*. (2018) 12:1230–45. doi: 10.1109/TBCAS.2018.2880148
17. Carroll N, Richardson I. Software-as-a-medical device: demystifying connected health regulations. *J Syst Inform Technol*. (2016) 18:186–215. doi: 10.1108/JSIT-07-2015-0061
18. Yaeger KA, Martini M, Yaniv G, Oermann EK, Costa AB. United States regulatory approval of medical devices and software applications enhanced by artificial intelligence. *Health Policy Technol*. (2019) 8:192–7. doi: 10.1016/j.hlpt.2019.05.006
19. Butler D. Translational research: crossing the valley of death. *Nat News*. (2008) 453:840–2. doi: 10.1038/453840a
20. Forsberg K, Mooz H. The relationship of system engineering to the project cycle. In: *INCOSE International Symposium*. Chattanooga, TN: Wiley Online Library (1991). doi: 10.1002/j.2334-5837.1991.tb01484.x
21. Brinkmann BH, Bower MR, Stengel KA, Worrell GA, Stead M. Large-scale electrophysiology: acquisition, compression, encryption, and storage of big data. *J Neurosci Methods*. (2009) 180: 185–92. doi: 10.1016/j.jneumeth.2009.03.022
22. Bower MR, Stead M, Bower RS, Kucewicz MT, Sulc V, Cimbalnik J, et al. Evidence for consolidation of neuronal assemblies after seizures in humans. *J Neurosci*. (2015) 35:999–1010. doi: 10.1523/JNEUROSCI.3019-14.2015
23. Nahum M, Van Vleet TM, Sohal VS, Mirzabekov JJ, Rao VR, Wallace DL, et al. Immediate Mood Scaler: tracking symptoms of depression and anxiety using a novel mobile mood scale. *JMIR mHealth uHealth*. (2017) 5:e44. doi: 10.2196/mhealth.6544
24. Haut SR, Hall CB, Borkowski T, Tennen H, Lipton RB. Clinical features of the pre-ictal state: mood changes and premonitory symptoms. *Epilepsy Behav*. (2012) 23:415–21. doi: 10.1016/j.yebeh.2012.02.007
25. Karoly PJ, Freestone DR, Boston R, Grayden DB, Himes D, Leyde K, et al. Interictal spikes and epileptic seizures: their relationship and underlying rhythmicity. *Brain*. (2016) 139: 1066–78. doi: 10.1093/brain/aww019
26. Baldassano SN, Brinkmann BH, Ung H, Blevins T, Conrad EC, Leyde K, et al. Crowdsourcing seizure detection: algorithm development and validation on human implanted device recordings. *Brain*. (2017) 140:1680–91. doi: 10.1093/brain/awx098
27. Brinkmann BH, Wagenaar J, Abbot D, Adkins P, Bosshard SC, Chen M, et al. Crowdsourcing reproducible seizure forecasting in human and canine epilepsy. *Brain*. (2016) 139(Pt 6):1713–22. doi: 10.1093/brain/aww045
28. Nasseri M, Kremen V, Nejedly P, Kim I, Chang SY, Jo HJ, et al. Semi-supervised training data selection improves seizure forecasting in canines with epilepsy. *Biomed Signal Proc Control*. (2020) 57:101743. doi: 10.1016/j.bspc.2019.101743
29. Kremen V, Brinkmann BH, Kim I, Guragain H, Nasseri M, Magee AL, et al. Integrating brain implants with local and distributed computing devices: a next generation epilepsy management system. *IEEE J Transl Eng Health Med*. (2018) 6:2500112. doi: 10.1109/JTEHM.2018.2869398
30. Sladky V, Nejedly P, Mivalt F, Brinkmann BH, Kim I, Louis EKS, et al. Distributed brain co-processor for neurophysiologic tracking and adaptive stimulation: application to drug resistant epilepsy. *bioRxiv [Preprint]*. (2021). doi: 10.1101/2021.03.08.434476
31. Toth R, Zamora M, Ottaway J, Gillbe T, Martin S, Benjaber M, et al. DyNeuMo Mk-2: an investigational circadian-locked neuromodulator with responsive stimulation for applied chronobiology. *Conf Proc IEEE Int Conf Syst Man Cyber*. (2020) 2020:3433–440. doi: 10.1109/SMC42975.2020.9283187
32. Nasseri M, Nurse E, Glasstetter M, Böttcher S, Gregg NM, Laks Nandakumar A, et al. Signal quality and patient experience with wearable devices for epilepsy management. *Epilepsia*. (2020) 61:S25–35. doi: 10.1111/epi.16527
33. Biondi, Laiou P, Bruno E, Viana PF, Schreuder M, Hart W, Nurse E, et al. Remote and long-term self-monitoring of electroencephalographic and noninvasive measurable variables at home in patients with epilepsy (EEG@HOME): protocol for an observational study. *JMIR Res Protocols*. (2021) 10: e25309. doi: 10.2196/25309
34. Viana PF, Duun-Henriksen J, Glasstëter M, Dümpelmann M, Nurse ES, Martins IP, et al. 230 days of ultra long-term subcutaneous EEG: seizure cycle analysis and comparison to patient diary. *Ann Clin Transl Neurol*. (2021) 8:288–93. doi: 10.1002/acn3.51261
35. Elger CE, Hoppe C. Diagnostic challenges in epilepsy: seizure under-reporting and seizure detection. *Lancet Neurol*. (2018) 17:279–88. doi: 10.1016/S1474-4422(18)30038-3
36. Fisher RS, Cross JH, French JA, Higurashi N, Hirsch E, Jansen FE, et al. Operational classification of seizure types by the International League Against Epilepsy: Position Paper of the ILAE Commission for Classification and Terminology. *Epilepsia*. (2017) 58:522–30. doi: 10.1111/epi.13670
37. Nejedly P, Kremen V, Sladky V, Nasseri M, Guragain H, Klimes P, et al. Deep-learning for seizure forecasting in canines with epilepsy. *J Neural Eng*. (2019) 16:036031. doi: 10.1088/1741-2552/ab172d

38. Salpekar JA, Mula M. Common psychiatric comorbidities in epilepsy: how big of a problem is it? *Epilepsy Behav.* (2019) 98:293–7. doi: 10.1016/j.yebeh.2018.07.023
39. Helmstaedter C, Witt JA. Epilepsy and cognition–a bidirectional relationship? *Seizure*. (2017) 49:83–9. doi: 10.1016/j.seizure.2017.02.017
40. Haut SR, Gursky JM, Privitera M. Behavioral interventions in epilepsy. *Curr Opin Neurol.* (2019) 32:227–36. doi: 10.1097/WCO.0000000000000661
41. Karoly PJ, Goldenholz DM, Freestone DR, Moss RE, Grayden DB, Theodore WH, et al. Circadian and circaseptan rhythms in human epilepsy: a retrospective cohort study. *Lancet Neurol.* (2018) 17: 977–85. doi: 10.1016/S1474-4422(18)30274-6

Conflict of Interest: BB and GW declare licensed IP to Cadence Neuroscience Inc. GW has equity in NeuroOne Inc. MS was employed by the company DarkHorse Neuro. Medtronic Inc. supplied devices for this study at no charge and reviewed this manuscript for accuracy related to their device, but did not edit results or conclusions.

The remaining authors declare that the research was conducted in the absence of any commercial or financial relationships that could be construed as a potential conflict of interest.

Publisher's Note: All claims expressed in this article are solely those of the authors and do not necessarily represent those of their affiliated organizations, or those of the publisher, the editors and the reviewers. Any product that may be evaluated in this article, or claim that may be made by its manufacturer, is not guaranteed or endorsed by the publisher.

frontiers in Neurology

OPINION
published: 04 August 2021
doi: 10.3389/fneur.2021.720328

Epileptic Seizure Cycles: Six Common Clinical Misconceptions

Philippa J. Karoly[1,2], Dean R. Freestone[1], Dominique Eden[1], Rachel E. Stirling[1,2], Lyra Li[2], Pedro F. Vianna[3,4], Matias I. Maturana[1,5], Wendyl J. D'Souza[5], Mark J. Cook[2,5], Mark P. Richardson[3], Benjamin H. Brinkmann[6†] and Ewan S. Nurse[1,5*†]*

[1] Seer Medical, Melbourne, VIC, Australia, [2] Department of Biomedical Engineering, The University of Melbourne, Melbourne, VIC, Australia, [3] School of Neuroscience, Institute of Psychiatry, Psychology & Neuroscience, King's College London, London, United Kingdom, [4] Faculty of Medicine, University of Lisbon, Lisbon, Portugal, [5] Department of Medicine, St Vincent's Hospital Melbourne, The University of Melbourne, Melbourne, VIC, Australia, [6] Bioelectronics Neurophysiology and Engineering Lab, Department of Neurology, Mayo Clinic, Rochester, MN, United States

Keywords: seizure cycles, epilepsy, multiday cycles, EEG, wearables

OPEN ACCESS

Edited by:
Sharon Chiang, University of California, San Francisco, United States

Reviewed by:
Marc Grau Leguia, University Hospital Bern, Switzerland

****Correspondence:***
Ewan S. Nurse
ewan@seermedical.com
Benjamin H. Brinkmann
Brinkmann.Benjamin@mayo.edu

† These authors share senior authorship

Specialty section:
This article was submitted to Epilepsy, a section of the journal Frontiers in Neurology

Received: *04 June 2021*
Accepted: *08 July 2021*
Published: *04 August 2021*

Citation:
Karoly PJ, Freestone DR, Eden D, Stirling RE, Li L, Vianna PF, Maturana MI, D'Souza WJ, Cook MJ, Richardson MP, Brinkmann BH and Nurse ES (2021) Epileptic Seizure Cycles: Six Common Clinical Misconceptions. Front. Neurol. 12:720328. doi: 10.3389/fneur.2021.720328

INTRODUCTION

The propensity for seizures to follow circadian and multiday (i.e., weekly, monthly, or seasonal) rhythms has been documented for centuries (1, 2). More recent findings from chronically recorded EEG in both human and animal studies have further elucidated the existence of multiday rhythms governing seizure timing and rates of epileptic activity [see (3) for a recent review]. These multiday epileptic cycles are found to be prevalent in a number of studies, including from implantable devices (4–7), electronic seizure diaries (8, 9), and wearable monitoring (10). It is becoming clear that multiday seizure cycles are important phenomena in epilepsy, with many implications for seizure management and more broadly in interpreting research studies and clinical trials (11–13).

The integration of knowledge of seizure cycles into clinical practise is in an early phase, with some theoretical studies demonstrating the utility of seizure risk forecasts (14–16) or scheduling diagnostic testing (9) based on multiday cycles. However, several barriers remain before seizure cycles can be widely adopted in clinical management. One barrier is the knowledge gap between data scientists and clinicians. Cycles are measured and described using circular statistics and frequency analysis, making the explanation of the presence and strength of cycles technically complex. It is yet to be determined at what strength a cycle can be deemed to be clinically relevant for making treatment or monitoring decisions. Much progress has been made converging the clinical and engineering aspects of epilepsy, however seizure cycles present new concepts in seizures and epilepsy that need to be clearly interpretable by clinicians (13, 17). This review aims to bridge several gaps that commonly arise between data science and clinical practise.

MISCONCEPTION 1: SEIZURE DIARIES ARE TOO NOISY TO INFER CYCLES

It is well-known that self-reported events (i.e., seizure diaries) are unreliable (18), nevertheless diaries remain the primary method of monitoring disease burden in epilepsy. Notably, it was through the meticulous recording of patients' seizures that early neurologists first recognised multiday seizure cycles (1, 2, 19, 20). These centuries-old hand charting of seizure occurrence resulted in critical insights into multiday periodicity in epilepsy that still await explanation. For instance, in J.R. Reynolds' seminal textbook from 1861 he observed:

"it appears, therefore, that although regular periodicity is rarely observed in epilepsy, and is entirely absent in some cases, yet than in the majority of cases there is an approximation to periodicity, and that the recurrence of attacks occupies a somewhat marked relation to the natural divisions of time; such as the day the month, and fractional parts of the month"

In an earlier 1746 treatise, Richard Mead also noted that, "great regard must be had to the times in which the paroxysms most usually return, in order to effect a cure." Evidently, diary records have been of immense value in establishing the existence of multiday seizure cycles.

On the other hand, advances in chronic EEG recording have shown that seizure cycles are more reliably estimated by continuously monitoring biomarkers of excitability (5). For instance average rates of interictal epileptic activity (4), the variance and autocorrelation of EEG (15), and even average heart rate (21) all show multiday cycles that are more robustly predictive of seizure likelihood than looking at past seizure times. Additionally, a recent comparison of seizure diaries and epileptic activity captured from chronic sub-scalp recording systems (22) showed discrepancies between the cyclic distributions of self-reported and electrographic events, even when diaries were relatively accurate (23). This is perhaps not unexpected given many seizures are not recognised by patients, particularly those occurring in sleep.

Nevertheless, for some people, self-reported events can be used to track seizure cycles (see case study). One recent study found the distributions of seizure diary events and electrographic seizures were not significantly different for nine out of 15 subjects, suggesting that although participants vastly underreported the total number of seizures, the underlying multiday cycles can still be determined for some individuals (8). In a retrospective analysis of the same cohort, forecasts based on self-reported seizures were accurate for electrographic events for four out of eight participants (8). It should be noted that this small cohort may not be representative of the broader diary-using population, and may in fact be more accurate in order to have been selected for this study (24). Another retrospective forecasting study found multiday cycles in the rates of interictal epileptic activity corresponded to self-reported seizure risk for most individuals (14). Similarly, a validation study found cycles measured from seizure diaries corresponded to the occurrence of epileptic activity during ambulatory EEG monitoring (9). Machine learning approaches have also been successfully deployed to forecast seizure risk from electronic diaries (25, 26).

On the whole, although advances in tracking continuous cyclic biomarkers can provide more reliable measures of seizure risk (27), seizure diaries should not be discounted as a useful tool to monitor individuals' seizure cycles and seizure risk within clinical settings. Patient diaries are likely to remain a cornerstone of clinical monitoring, and should be incorporated to characterise seizure cycles where possible, in particular for low risk applications such as scheduling EEG monitoring (9). Further work is needed to characterise the relationship between cycles of interictal epileptic activity and self-reported events, as well as to identify the subset of individuals whose self-reported seizure cycles align with their electrographic events.

Case Study: Self-Reported and Electrographic Seizures Correspond to Underlying Cycle of Epileptic Activity

Figure 1 presents a case study of an individual adult female diagnosed with seizures secondary to a periventricular nodular heterotopia, refractory to polytherapy, implanted with a chronic sub-scalp EEG recording system (Epi-Minder "Minder" system) (28). Event labels and cycles of epileptic activity were detected using the method described in Stirling et al. (28). It can be seen that self-reported and electrographic seizures appeared to align to the same underlying cycle of interictal epileptic activity (**Figure 1A**). Cycles were also measured from seizure times alone (rather than the continuous rate of interictal epileptic activity), using the method described in Karoly et al. (8). Using this approach, both self-reported and EEG seizures showed strong alignment to a fixed underlying cycle of 28-days (**Figure 1B**), which agreed with the cycle of interictal epileptic activity. The phase distributions of self-reported and electrographic events with respect to the 28-day cycle of interictal epileptic activity (**Figure 1C**) were not significantly different ($p > 0.05$ using a Kolmogorov-Smirnov test for equality). Therefore, this individual was able to self-report her seizures reliably enough to

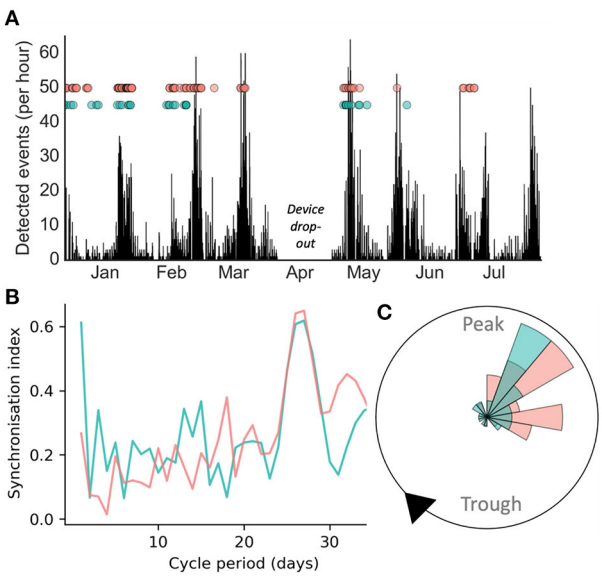

FIGURE 1 | Case study of electrographic seizure detection from sub-scalp EEG (red) and seizure diary self-reported events (green) over >6 months in an individual patient. **(A)**: counts of detected epileptiform events over time, with seizures shown as dots. **(B)** Synchronisation index measured from event times at different fixed cycle periods showed a similar peak around 28-days for both EEG and self-reported seizures **(C)** A polar plot demonstrating that both diary and EEG seizures show similar phase distributions with respect to the underlying 28-day cycle.

estimate the high-risk periods of her underlying multiday cycle, in agreement with validated electrographic seizures.

MISCONCEPTION 2: WEEKLY CYCLES ARE DRIVEN BY WEEKDAY BEHAVIOURS

Multiday seizure cycles are consistently found at about-weekly (5–9 day) and about-monthly (28–32 day) periods (4, 7, 29), which is often attributed to behavioural (weekday) or catamenial effects. For instance, a large cohort study found multiday cycles in 60% of people with epilepsy, with common periods 7, 15, 20, and 30 days (29). Cycles of around 30 days were as common in men as in women, suggesting catamenial influences are probably not explanatory (see subsequent section). Research suggests that behaviours such as diet, alcohol consumption, sleep and wake times and exposure to stress impact seizure risk in an individualised manner (30, 31) and this evidence has led to hypotheses that behavioural triggers underpin multiday seizure cycles. Regular social routines are commonly proposed as the source of weekly seizure cycles however there is no clear evidence linking cyclic behavioural patterns to cycles of seizure susceptibility. Conversely, multiday weekly, and monthly epileptic rhythms are only occasionally modulated by fixed cycles, such as weekdays or day of month (3, 32).

Nevertheless, several studies have noted an effect of weekdays on seizure occurrence, suggesting that the weekly routine leads to some entrainment of naturally occurring rhythms. A large study of seizure diaries found that 7-day seizure cycles were significant in about 20% of people with epilepsy (7). Although, at the population level, there was no clear preference for seizures to occur on a particular day or part of the week. Rao et al. found a weak, significant preference for fewer electrographic seizures on Sunday, similar to the results of Ferastraoaru et al. of seizure diaries (32, 33). On the other hand, alignment of weekly seizure cycles to the 7-day week is often transient (32) (see also case study, **Figure 2**), suggesting there are more prominent endogenous physiological mechanisms that modulate seizure occurrence with approximate weekly rhythms.

It has been hypothesised that endogenous weekly cycles do influence mammalian physiology, with evidence of such cycles affecting the cardio-respiratory, immune, and endocrine systems (34). A recent study found people with epilepsy showed weekly fluctuations in resting heart rate that were related to their seizure occurrence (21). Similar to epileptic activity, heart rate cycles were found at patient-specific periods of between 5 and 9 days and not necessarily linked to weekdays. Overall, the body of evidence suggests that, for some individuals, the 7-day week acts as a synchronizer, rather than a driver, of weekly seizure cycles.

Case Study: Weekly Seizure Cycle Not Aligned to the Day of Week

Figure 2 presents a case study of an individual with focal epilepsy who shows their 8-week seizure diary (**Figure 2A**) to their clinician. After observing the preference for seizures to occur on weekends, the clinician may suspect that this patient's seizures are driven by an after-stress effect, i.e., they occur on the weekend at the end of the stressful working week. The polar plots (**Figures 2C,D**) validate this belief by showing that seizures have a stronger link to the weekly cycle than to an intrinsic 8.5-day heart rate cycle (**Figure 2B**). However, after 15 months have passed (**Figures 2E,F**), seizures are no longer linked to the weekly cycle but remain well-aligned by the 8.5-day heart rate cycle, which is likely to be endogenous in origin. Therefore, based on 2 months of observations (i.e., 7 × 8.5-day cycles) seizures seemed linked to a behavioural driver, although the endogenous long-term pattern of heart rate was more stable over a 15-month observation period.

MISCONCEPTION 3: MONTHLY CYCLES ARE CATAMENIAL EPILEPSY

Despite centuries of data showing that males and females experience about-monthly seizures with similar prevalence (4, 7, 35, 36), there is a persistent view that approximate monthly (i.e., 3–5 weeks) cycles of seizure occurrence in women must be linked to the menstrual cycle. The prevalence of catamenial epilepsy is variously reported to be between 10 and 70% (37). Clinically, catamenial epilepsy is defined as an increase (i.e., 2-fold increase) in seizures during some phase of the menstrual cycle, generally documented by self-report (38). Most studies reporting on the prevalence of catamenial epilepsy are based on short-term analysis of menstrual or hormonal data over just two to three cycles (39). Limited duration studies of several months may not be sufficient to determine whether changes in seizure frequency are significant. Furthermore, monthly seizure cycles can transiently align with the calendar month, despite being more closely linked to underlying cyclic fluctuation in epileptic activity which may not be of exactly one calendar month in duration (32). Therefore, it is possible that monthly cycles of seizure occurrence appear to be linked to menstruation over several months, however the statistical relationship would be abolished after longer term monitoring (see case study).

In contrast, some women with about-monthly seizure cycles may have seizures significantly linked to their menstrual cycle over long-term monitoring. The underlying cause/s of monthly seizure cycles are unknown, and are likely to differ between individuals, with oestrogen or sex hormones playing a role for some individuals. In support of this hypothesis, some studies in animal models have found evidence for the influence of oestrogen on seizure occurrence (40, 41). Furthermore, although a landmark study of hormone treatment for women with suspected catamenial epilepsy did not show a significant effect (42), *post-hoc* analysis revealed a smaller subset of women for whom hormone treatment may have been effective (43). The findings suggest that catamenial effects are just one facet of monthly seizure cycles, rather than being the primary mechanism.

For clinicians, the recognition that about-monthly cycles of seizure activity in women may not relate to underlying menstrual patterns is important in avoiding perhaps futile manipulation of hormonal cycles through medication, as are often proposed by clinicians and patients.

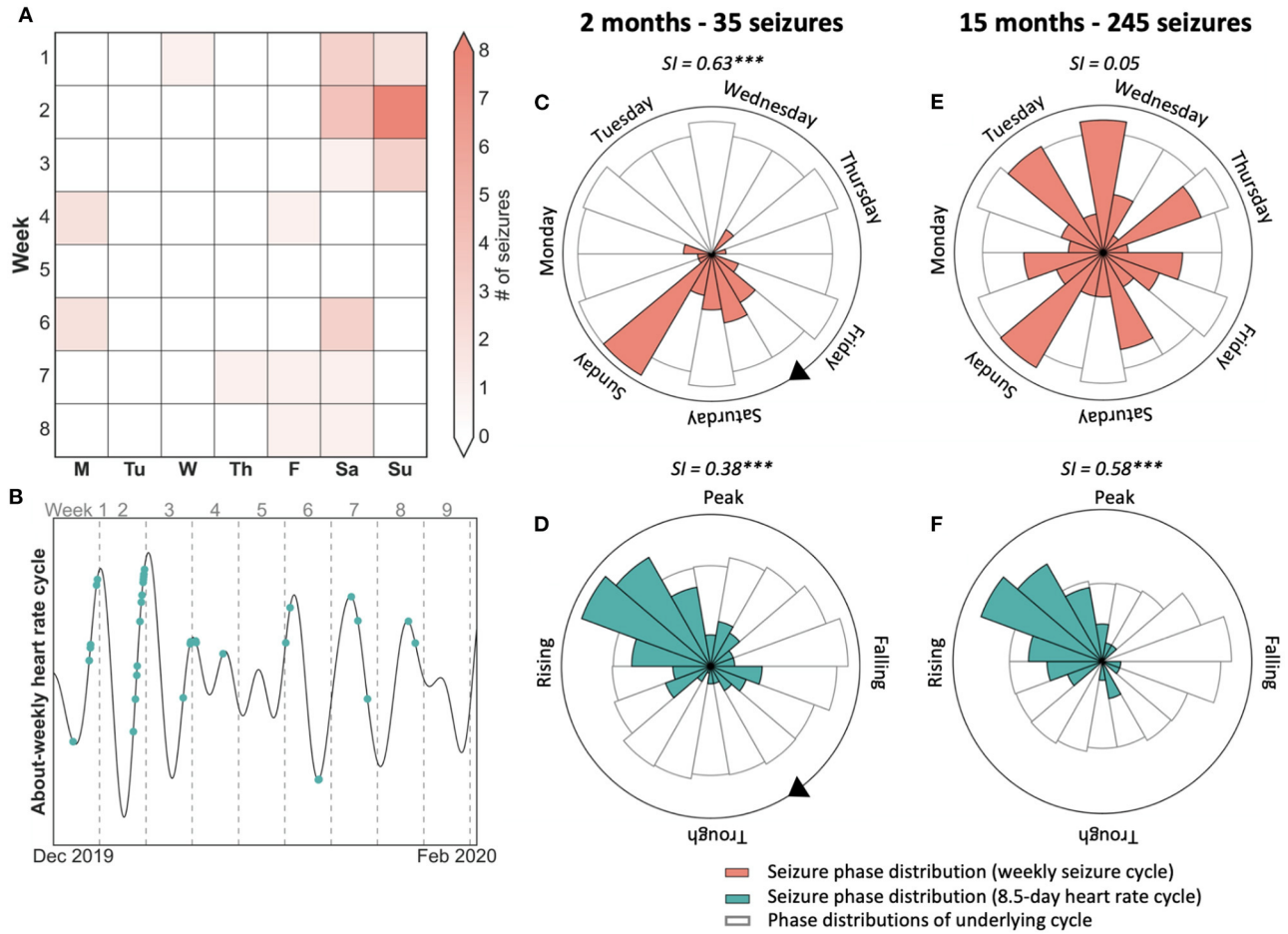

FIGURE 2 | Case study of 7-day weekly seizure cycle and 8.5-day heart rate cycle showing that seizures were not modulated by weekly behaviour. **(A)** 8-week seizure diary showing days that seizures occurred, suggesting a weekly seizure cycle. **(B)** 8.5-day heart rate cycle of the same period as (a), with seizures shown in green. Seizures tend to occur on the rising phase of the cycle, with a few exceptions. **(C,D)** Polar plots demonstrating the location of seizures with respect to the 7-day seizure (red) and 8.5-day heart rate cycle (green) after two months and 35 seizures. Seizures were more strongly locked to the 7-day week. **(E,F)** Polar plots demonstrating seizure timing on the seizure and heart rate cycle after 15 months and 245 seizures. Seizures were no longer locked to the weekly cycle but remained strongly locked to the 8.5-day heart rate cycle. SI, Synchronisation index value with significance according to Omnibus test (***$p <= 0.001$).

Case Study: Monthly Seizure Cycle Not Aligned to Menstruation Times

Figure 3 presents the case of a patient who appeared to have strong phase-locking between seizures and menses when observed over 4 months. However, there was no alignment over an observation period of 19 months. Hence, quantification of cycles using robust statistical techniques over long periods is required to avoid erroneous conclusions.

MISCONCEPTION 4: CYCLES ARE DRIVEN BY MEDICATION

The influence of anti-seizure medications (ASMs) has been suggested as a driver of circadian cycles of epileptic activity and seizures, since the precise time at which medication is taken can shift the peak seizure occurrence within a 24-h period (35, 36). Consequently, medications are sometimes touted as a possible driver for longer, multiday rhythms. Although the circadian rhythm of seizure occurrence may be influenced by ASMs, the short half-life of most ASMs reduces the likelihood that medication is driving longer rhythms (44). It is possible that the interactions between multiple ASMs taken throughout the day can result in periods of high and low therapeutic effect and therefore affect seizure likelihood throughout the day. However, there is no clear explanation for how the timing of daily (or more frequent) medication use could drive fluctuations in seizure likelihood that repeat over weeks to months or even seasonally.

Several animal studies have also established the existence of multiday cycles of epileptic activity in the absence of ASM use. A small study in six dogs with naturally occurring canine epilepsy included one dog where a weekly seizure cycle was maintained in

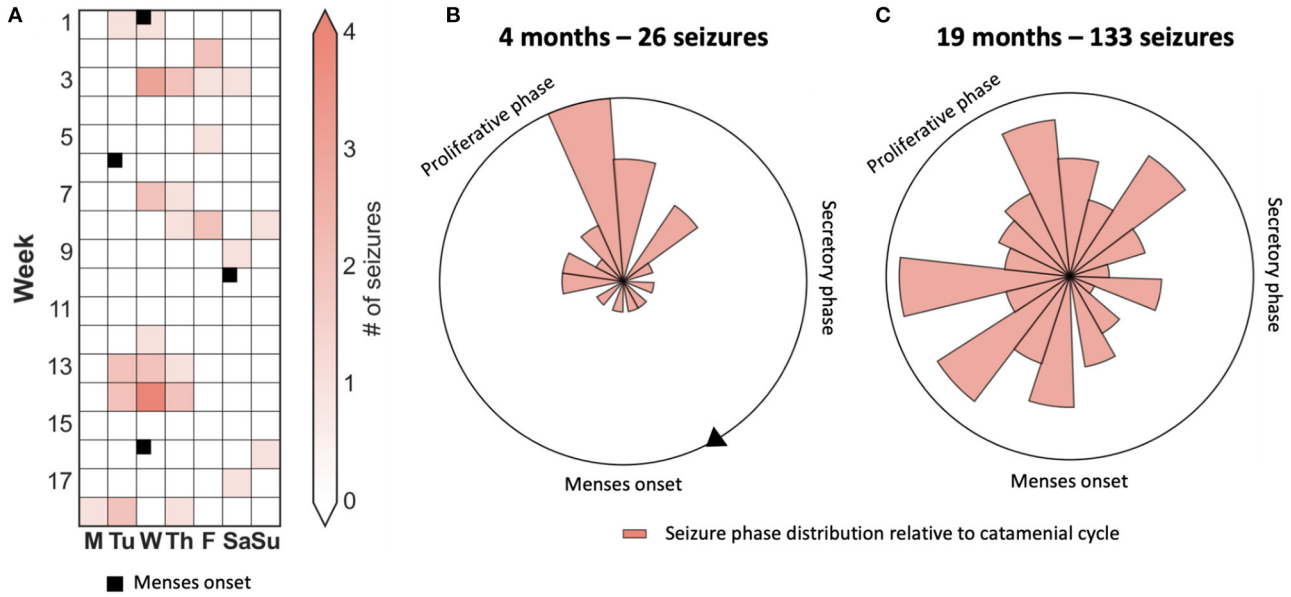

FIGURE 3 | Case study of a catamenial seizure cycle showing that seizures are only transiently aligned to the menstrual phase. **(A)** 4-month seizure diary showing days that seizures occurred, and times of menstruation, suggesting a catamenial seizure cycle. **(B,C)** Polar plots demonstrating the location of seizures with respect to the menstrual cycle after four months and 26 seizures **(B)** and after 19 months and 133 seizures **(C)**.

the absence of ASM usage (45). Another study in a rodent model of epilepsy found multiday weekly cycles in the epileptic activity of rats who were not treated with ASMs (46). Similarly tetanus-toxin models of temporal lobe epilepsy also show cycles where seizures strongly cluster (47).

It is possible that systematic bias affects when people miss their medications (i.e., on weekends, or when each pack runs out), providing a periodic seizure trigger. Missed medication is one of the most common seizure triggers (31, 48), and clinically significant non-adherence has been reported to affect between 29 and 79% of people with epilepsy (with the variance due to different definitions of what constitutes significant non-adherence) (49). For instance, one study found 66% of people reported missing their medications at least once per month (50). However, while the aforementioned studies identify demographic factors that contribute to medication adherence, to our knowledge no studies have investigated the timing of missed medication, such as whether people are more likely to miss medication on certain days or with any regularity. Sustained periods of medication non-adherence could also be particularly relevant, as cyclic fluctuations in seizure risk may build up over slow timescales of days to weeks (3).

There are no studies that systematically analyse the relationship between ASM usage and cycles in epilepsy. Consequently, it is not possible to discount ASMs as a confounding factor in the detection of seizure cycles. However, some evidence suggests that seizure cycles exist despite medications in humans. The ancient Greeks described approximately monthly cycles in seizures that were thought to be associated with lunar cycles (51), a theory that is purported even today (52). A 1,929 investigation into 66 patients with epilepsy reported three types of circadian distributions over 2,524 seizures (53). The authors concluded that while sedatives (bromide or luminal) reduced the rates of seizures, their effects were negligible in driving the cycles. Soon after, a report into seizures in 110 boys at an epileptic colony over a 10 year period discovered circadian, and weekly, monthly, and even yearly cycles in seizures (36). Similarly, the authors concluded that drugs reduced the number of seizures, but the grouping of seizures were resistant to drugs.

Hence, although systematic studies remain to be undertaken, there is a significant body of historical and pre-clinical models suggesting that ASMs do not drive cycles of seizure activity.

MISCONCEPTION 5: CYCLES ARE ONLY RELEVANT FOR FOCAL EPILEPSIES

The prevalence of multiday cycles across different epilepsy types, or whether distinct seizure types adhere to different cycles, are commonly asked questions regarding epileptic cycles. Unfortunately, these questions are difficult to answer since contemporary studies have principally identified cycles of epileptic activity from chronic implanted EEG in patients with focal epilepsies. To our knowledge, there are no studies that report on chronic EEG in individuals with genetic generalised epilepsies (GGE), and long-term electrographic correlates are yet to be reported. Historic records of seizure timing may include individuals with GGE, such as the Griffiths and Fox (36) et al. record of two sisters with early onset epilepsy and "curiously

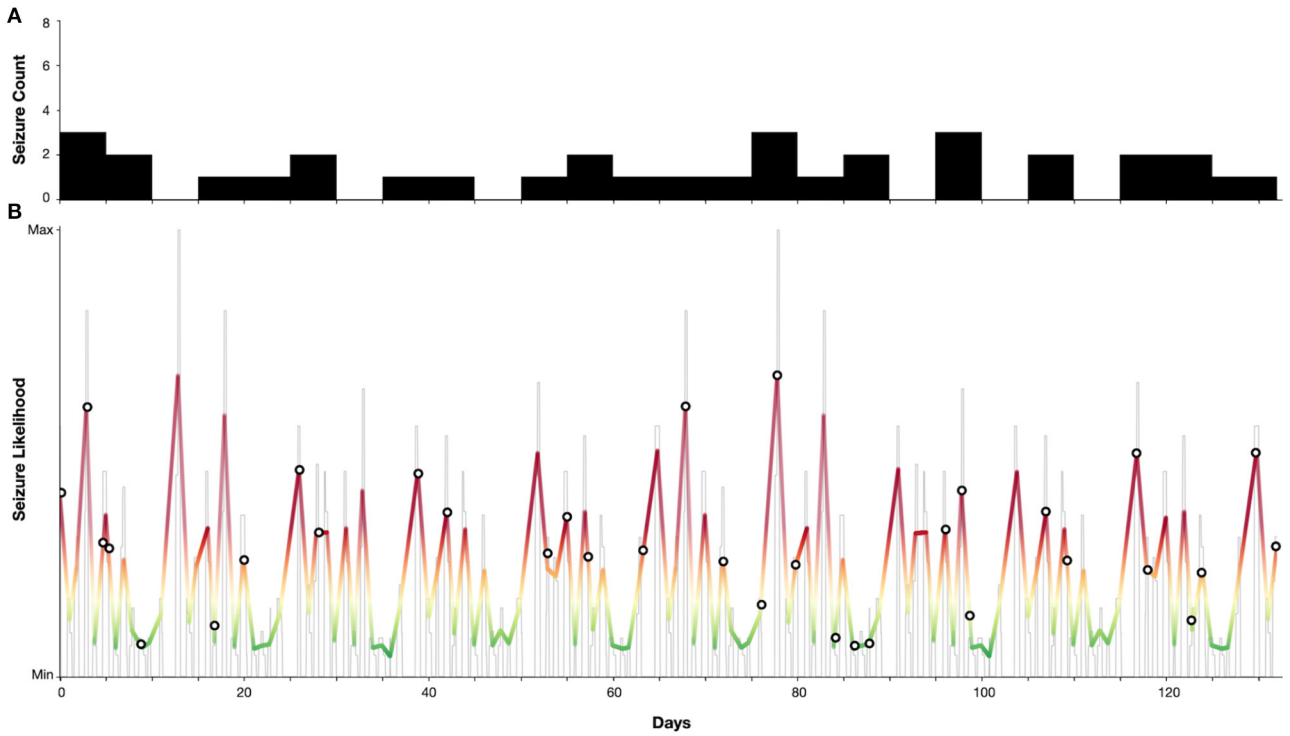

FIGURE 4 | Case study of an individual with juvenile absence epilepsy with 5 and 13-day seizure cycles. **(A)** Self-reported seizure counts (bin-width of 5 days). **(B)** Estimated seizure likelihood (grey—raw likelihood estimate, colour—smoothed likelihood). Markers indicate self-reported seizure occurrences. Note that the majority (79%) of seizures occurred when the seizure likelihood was high.

alike" seizure cycles around 2 years in duration (36). However, such historic diagnoses are highly speculative and cannot be relied upon. Contemporary diary studies have shown multiday seizure cycles can be measured from self-reported event times in people with GGEs (7, 9), and have corresponding cycles of heart rate activity (21).

Particular generalised epilepsy syndromes are well-characterised as having ultradian cycles of interictal and clinical epileptiform activity in both adults and children (54–58), and similar circadian cycles particularly related to sleep-wake transitions (55, 59, 60). The thalamocortical networks associated with slow-wave sleep are also implicated in the generation of generalised spike-wave discharges (56, 61). Hence, despite a lack of longitudinal EEG to validate patient-specific infradian cycles, there are well-studied circadian and ultradian rhythms present in GGE.

From a network perspective, a focal seizure originates from a single region of the brain (and may or may not generalise), while a generalised seizure is a more inherent property of the overall network where no single foci is identifiable (62). Although overlapping symptomatically, this fundamental difference in generalised seizure generation may mean that electrographic multiday cycles are not present in generalised epilepsies due to the difference in the seizure generation process. We anticipate that the next generation of chronic EEG devices (23, 28, 63) will be able to elucidate any such cycles as they have for focal epilepsies.

Case Study: Ultradian Seizure Cycles in an Individual With JAE

Figure 4 demonstrates a case study of multiday cycles derived from an electronic seizure diary (Seer app) from an adult woman with a confirmed diagnosis of juvenile absence epilepsy (JAE), with refractory convulsive and absence seizures. Two distinct cycles were identified at 5 and 13 days from a seizure diary with a total duration of 18 weeks. From these cycles a forecast was generated as per (9), resulting in 24% of time spent in high seizure risk and 79% of seizures occurring in high risk. Hence, although generated from self-reported events, this case presents seizure cycles from an individual with a generalised epilepsy capable of producing an accurate forecast.

MISCONCEPTION 6: CYCLES ARE DRIVEN BY EPILEPSY-SPECIFIC PHENOMENA

To understand the cause/s of multiday seizure cycles, it is necessary to look beyond epilepsy and even beyond neurology. Slow physiological rhythms have been documented across a range of human diseases (64). Episodic psychiatric conditions are

suggestive of multiday modulation, including bipolar disorder (65, 66), depression (67, 68), and other psychopathologies (69). In cardiology, blood pressure and heart rate have been found to show endogenous weekly cycles (70), and 7-day and seasonal patterns have been documented for cardiovascular diseases (71–73). As well, immunologists have long recognised weekly cycles governing inflammatory markers in the blood, including antibody production, circulating lymphocytes, and cellular immunity in animal studies (74), which appear to impact individuals' responses to cancer treatment (75, 76).

Although very limited, some studies have also identified physiological cycles with weekly, monthly, and seasonal patterns for healthy individuals. Seven-day rhythms have been studied, to a small extent, in endocrinology. Circaseptan variations in cortisol were found on 20 healthy subjects after sampling thrice weekly for three months (64). Melatonin has also been observed to vary on a weekly basis (77); however, the study was limited to weeklong recordings on a small cohort. Evidence for monthly rhythms in biological phenomena is limited but includes sleep quality (78) and hormone levels, including testosterone (79). Monthly rhythms can also be found in heart rate, but this is likely to be rare; one study mentioned about 3% of people (80). Within populations, weak seasonal cycles have been observed in some physiological states and biomarkers, including human cognition (81), skin temperature (82), and salivary cortisol (83). However, these seasonal changes were most likely related to environmental drivers, such as ambient temperature and photoperiod.

The collective evidence of multiday cycles in other spheres of human physiology and disease hints that similarly long timescale rhythms in epilepsy do not arise only because of epileptogenesis or ictogenesis. Instead, systemic physiological rhythms may combine into complex, individual-specific oscillations that lead to the periodic emergence of pro-ictal conditions. This hypothetical emergence of seizure cycles from an underlying network of oscillators has been outlined in a recent review of circadian molecular oscillations and rhythmicity of epilepsy (84). Ultimately, to understand cycles in epilepsy, it will be critical to understand how many other physiological cycles interact with rhythms of seizures and epileptic activity.

CONCLUSION

Cycles of epileptic activity have been documented for centuries, however the recent emergence of technologies such as electronic seizure diaries, wearable physiology tracking devices, and chronic EEG recordings have allowed for their thorough investigation. It is increasingly clear that multiday seizure cycles are highly patient specific. Although some seizure types and epilepsy syndromes are known to have population-wide characteristics with respect to circadian seizure timings, analogous features are only just beginning to be characterised at multiday time scales (7, 29). Further work is required to understand whether demographic or clinical factors may be predictive of cycle periods. Most of the work presented here involved retrospective, exploratory data analysis, hence prospective studies with explicit predefined definitions for seizure cycles will be necessary.

Cycles of seizures have been identified both from self-reported and electrographic events. Markers of cyclic activity have been captured from EEG signals and other non-invasive physiological measurements. How these physiological cycles are fundamentally linked to the cycles of seizure activity (such as in **Figure 2**) is still yet to be uncovered. The interaction of cycles and epilepsy therapies, such as ASMs, also remains to be investigated.

Beyond the scientific boundaries of our understanding of seizure cycles, there still exists a communication gap between the clinical and data science worlds with respect to the cyclic nature of seizure timing. We hope these academic communities continue to strive to find a common language and cross-disciplinary definitions to advance the field of seizure cycles in close collaboration.

AUTHOR CONTRIBUTIONS

PK, DF, BB, and EN developed the original concept and design of the manuscript, performed the literature search and analysis of data in the literature, contributed case studies, drafted, reviewed, and edited the manuscript. DE, RS, LL, and MM performed the literature search and analysis of data in the literature, contributed case studies, drafted, reviewed, and edited the manuscript. WD'S, MR, and MC participated in the interpretation of data in the literature, reviewed, and edited the manuscript for important intellectual content. All authors contributed to the article and approved the submitted version.

FUNDING

MR was supported by the National Institute for Health Research Biomedical Research Centre at South London and Maudsley NHS Foundation Trust, and by the Medical Research Council Centre for Neurodevelopmental Disorders (MR/N026063/1).

This project was supported by the My Seizure Gauge grant from the Epilepsy Foundation of America.

REFERENCES

1. Temkin OFS. *A History of Epilepsy From the Greeks to the Beginning of Modern Neurology. 2nd de*. Baltimore: Johns Hopkins Press (1971).
2. Mead R. *A Treatise Concerning the Influence of the Sun and Moon Upon Human Bodies, and the Diseases Thereby Produced*. J. Brindley, (London) (1748).
3. Karoly PJ, Rao VR, Gregg NM, Worrell GA, Bernard C, Cook MJ, et al. Cycles in epilepsy. *Nat Rev Neurol*. (2021) 17:267–84. doi: 10.1038/s41582-021-00464-1
4. Baud MO, Kleen JK, Mirro EA, Andrechak JC, King-Stephens D, Chang EF, et al. Multi-day rhythms modulate seizure risk in epilepsy. *Nat Commun*. (2018) 9:88. doi: 10.1038/s41467-017-02577-y
5. Leguia MG, Rao VR, Kleen JK, Baud MO. Measuring synchrony in bio-medical timeseries. *Chaos*. (2021) 31:013138. doi: 10.1063/5.0026733
6. Cook MJ, Varsavsky A, Himes D, Leyde K, Berkovic SF, O'Brien T, et al. The dynamics of the epileptic brain reveal long-memory processes. *Front Neurol*. (2014) 5:217. doi: 10.3389/fneur.2014.00217

7. Karoly PJ, Goldenholz DM, Freestone DR, Moss RE, Grayden DB, Theodore WH, et al. Circadian and circaseptan rhythms in human epilepsy: a retrospective cohort study. *Lancet Neurol*. (2018) 17:977–85. doi: 10.1016/S1474-4422(18)30274-6
8. Karoly PJ, Cook MJ, Maturana M, Nurse ES, Payne D, Brinkmann BH, et al. Forecasting cycles of seizure likelihood. *Epilepsia*. (2020) p. 776–86. doi: 10.1101/2019.12.19.19015453
9. Karoly PJ, Eden D, Nurse ES, Cook MJ, Taylor J, Dumanis S, et al. Cycles of self-reported seizure likelihood correspond to yield of diagnostic epilepsy monitoring. *Epilepsia*. (2021) 62:416–25. doi: 10.1111/epi.16809
10. Stirling RE, Grayden DB, D'Souza W, Cook MJ, Nurse E, Freestone DR, et al. *Forecasting Seizure Likelihood With Wearable Technology*. Available online at: https://www.medrxiv.org/content/10.1101/2021.05.20.21257495v1.full (accessed, May 28, 2021).
11. Freestone DR, Karoly PJ, Cook MJ. A forward-looking review of seizure prediction. *Curr Opin Neurol*. (2017) 30:167–73. doi: 10.1097/WCO.0000000000000429
12. Baud MO, Rao VR. Gauging seizure risk. *Neurology*. (2018) 91:967–73. doi: 10.1212/WNL.0000000000006548
13. Kuhlmann L, Lehnertz K, Richardson MP, Schelter B, Zaveri HP. Seizure prediction—ready for a new era. *Nat Rev Neurol*. (2018) 14:618–30. doi: 10.1038/s41582-018-0055-2
14. Proix T, Truccolo W, Leguia MG, Tcheng TK, King-Stephens D, Rao VR, et al. Forecasting seizure risk in adults with focal epilepsy: a development and validation study. *Lancet Neurol*. (2021) 20:127–35. doi: 10.1016/S1474-4422(20)30396-3
15. Maturana MI, Meisel C, Dell K, Karoly PJ, D'Souza W, Grayden DB, et al. Critical slowing as a biomarker for seizure susceptibility. *Nat Commun*. (2020) 11:2172. doi: 10.1101/689893
16. Karoly PJ, Ung H, Grayden DB, Kuhlmann L, Leyde K, Cook MJ, et al. The circadian profile of epilepsy improves seizure forecasting. *Brain*. (2017) 140:2169–82. doi: 10.1093/brain/awx173
17. Litt B. Engineering the next generation of brain scientists. *Neuron*. (2015) 86:16–20. doi: 10.1016/j.neuron.2015.03.029
18. Elger CE, Hoppe C. Diagnostic challenges in epilepsy: seizure under-reporting and seizure detection. *Lancet Neurol*. (2018) 17:279–88. doi: 10.1016/S1474-4422(18)30038-3
19. Reynolds JR. Epilepsy: its symptoms, treatment, and relation to other chronic, convulsive diseases. *Am J Psychiatry*. (1862) 19:198–209. doi: 10.1176/ajp.19.2.198
20. Gowers WR. *Epilepsy and Other Chronic Convulsive Diseases: Their Causes, Symptoms & Treatment*. London: William Wood & Company. (1885).
21. Karoly PJ, Stirling RE, Freestone DR, Nurse ES, Doyle B, Halliday A, et al. Multiday cycles of heart rate modulate seizure likelihood at daily, weekly and monthly timescales: an observational cohort study. *medRxiv [Preprint]*. (2020). doi: 10.1101/2020.11.24.20237990
22. Weisdorf S, Duun-Henriksen J, Kjeldsen MJ, Poulsen FR, Gangstad SW, Kjær TW. Ultra-long-term subcutaneous home monitoring of epilepsy−−490 days of EEG from nine patients. *Epilepsia*. (2019) 60:2204–14. doi: 10.1111/epi.16360
23. Viana PF, Duun-Henriksen J, Glasstëter M, Dümpelmann M, Nurse ES, Martins IP, et al. 230 days of ultra long-term subcutaneous EEG: seizure cycle analysis and comparison to patient diary. *Ann Clin Transl Neurol*. (2021) 8:288–93. doi: 10.1002/acn3.51261
24. Cook MJ, O'Brien TJ, Berkovic SF, Murphy M, Morokoff A, Fabinyi G, et al. Prediction of seizure likelihood with a long-term, implanted seizure advisory system in patients with drug-resistant epilepsy: a first-in-man study. *Lancet Neurol*. (2013) 12:563–71. doi: 10.1016/S1474-4422(13)70075-9
25. Goldenholz DM, Goldenholz SR, Romero J, Moss R, Sun H, Westover B. Development and validation of forecasting next reported seizure using e-diaries. *Ann Neurol*. (2020) 88:588–95. doi: 10.1002/ana.25812
26. Chiang S, Goldenholz DM, Moss R, Rao VR, Haneef Z, Theodore WH, et al. Prospective validation study of an epilepsy seizure risk system for outpatient evaluation. *Epilepsia*. (2020) 61:29–38. doi: 10.1111/epi.16397
27. Stirling RE, Cook MJ, Grayden DB, Karoly PJ. Seizure forecasting and cyclic control of seizures. *Epilepsia*. (2020) 62:S2–14. doi: 10.1111/epi.16541
28. Stirling RE, Karoly PJ, Maturana MI, Nurse ES, McCutcheon K, Grayden DB, et al. Seizure forecasting using a novel sub-scalp ultra-long term EEG monitoring system. *medRxiv [Preprint]*. doi: 10.1101/2021.05.09.21256558
29. Leguia MG, Andrzejak RG, Rummel C, Fan JM, Mirro EA, Tcheng TK, et al. Seizure cycles in focal epilepsy. *JAMA Neurol*. (2021) 78:454–63. doi: 10.1001/jamaneurol.2020.5370
30. Haut SR, Hall CB, Borkowski T, Tennen H, Lipton RB. Clinical features of the pre-ictal state: mood changes and premonitory symptoms. *Epilepsy Behav*. (2012) 23:415–21. doi: 10.1016/j.yebeh.2012.02.007
31. Haut S, Hall C, Masur J, Lipton R. Seizure occurrence - precipitants and prediction. *Neurology*. (2007) 69:1905–10. doi: 10.1212/01.wnl.0000278112.48285.84
32. Rao VR, Leguia GM, Tcheng TK, Baud MO. Cues for seizure timing. *Epilepsia*. (2020) 62:S15–31. doi: 10.1111/epi.16611
33. Ferastraoaru V, Goldenholz DM, Chiang S, Moss R, Theodore WH, Haut SR. Characteristics of large patient-reported outcomes: where can one million seizures get us? *Epilepsia Open*. (2018) 3:364–73. doi: 10.1002/epi4.12237
34. Reinberg AE, Dejardin L, Smolensky MH, Touitou Y. Seven-day human biological rhythms: an expedition in search of their origin, synchronization, functional advantage, adaptive value and clinical relevance. *Chronobiol Int*. (2017) 34:162–91. doi: 10.1080/07420528.2016.1236807
35. Bercel NA. The periodic features of some seizure states. *Ann N Y Acad Sci*. (1964) 117:555–62. doi: 10.1111/j.1749-6632.1964.tb48206.x
36. Griffiths G, Fox JT. Rhythm in epilepsy. *Lancet*. (1938) 232:409–16. doi: 10.1016/S0140-6736(00)41614-4
37. Verrotti A, D'Egidio C, Agostinelli S, Verrotti C, Pavone P. Diagnosis and management of catamenial seizures: a review. *Int J Womens Health*. (2012) 4:535–41. doi: 10.2147/IJWH.S28872
38. Herzog AG, Klein P, Rand BJ. Three patterns of catamenial epilepsy. *Epilepsia*. (1997) 38:1082–8. doi: 10.1111/j.1528-1157.1997.tb01197.x
39. Herzog AG. Catamenial epilepsy: definition, prevalence pathophysiology and treatment. *Seizure*. (2008) 17:151–9. doi: 10.1016/j.seizure.2007.11.014
40. Maguire JL, Stell BM, Rafizadeh M, Mody I. Ovarian cycle–linked changes in GABA a receptors mediating tonic inhibition alter seizure susceptibility and anxiety. *Nat Neurosci*. (2005) 8:797–804. doi: 10.1038/nn1469
41. D'Amour J, Magagna-Poveda A, Moretto J, Friedman D, LaFrancois JJ, Pearce P, et al. Interictal spike frequency varies with ovarian cycle stage in a rat model of epilepsy. *Exp Neurol*. (2015) 269:102–19. doi: 10.1016/j.expneurol.2015.04.003
42. Herzog AG, Fowler KM, Smithson SD, Kalayjian LA, Heck CN, Sperling MR, et al. Progesterone vs placebo therapy for women with epilepsy: a randomized clinical trial. *Neurology*. (2012) 78:1959–66. doi: 10.1212/WNL.0b013e318259e1f9
43. Herzog AG. Catamenial epilepsy: update on prevalence, pathophysiology and treatment from the findings of the NIH Progesterone Treatment Trial. *Seizure*. (2015) 28:18–25. doi: 10.1016/j.seizure.2015.02.024
44. Perucca E, Brodie MJ, Kwan P, Tomson T. 30 years of second-generation antiseizure medications: impact and future perspectives. *Lancet Neurol*. (2020) 19:544–56. doi: 10.1016/S1474-4422(20)30035-1
45. Gregg NM, Nasseri M, Kremen V, Patterson EE, Sturges BK, Denison TJ, et al. Circadian and multiday seizure periodicities, and seizure clusters in canine epilepsy. *Brain Commun*. (2020) 2:fcaa008. doi: 10.1093/braincomms/fcaa008
46. Baud MO, Ghestem A, Benoliel J-J, Becker C, Bernard C. Endogenous multidien rhythm of epilepsy in rats. *Exp Neurol*. (2019) 315:82–7. doi: 10.1016/j.expneurol.2019.02.006
47. Kudlacek J, Chvojka J, Kumpost V, Hermanovska B, Posusta A, Jefferys JGR, et al. Long-term seizure dynamics are determined by the nature of seizures and the mutual interactions between them. *Neurobiol Dis*. (2021) 154:105347. doi: 10.1016/j.nbd.2021.105347
48. Cramer JA, Glassman M, Rienzi V. The relationship between poor medication compliance and seizures. *Epilepsy Behav EB*. (2002) 3:338–42. doi: 10.1016/S1525-5050(02)00037-9
49. Malek N, Heath C, Greene J. A review of medication adherence in people with epilepsy. *Acta Neurol Scand*. (2017) 135:507–15. doi: 10.1111/ane.12703
50. Paschal AM, Rush SE, Sadler T. Factors associated with medication adherence in patients with epilepsy and recommendations for improvement. *Epilepsy Behav*. (2014) 31:346–50. doi: 10.1016/j.yebeh.2013.10.002

51. Stahl WH. Moon Madness*Read before the Section of Historical and Cultural Medicine. N. V. Academy of Medicine, Nov. 11, 1936. *Ann Med Hist*. (1937) 9:248–63.
52. Terra-Bustamante VC, Scorza CA, de Albuquerque M, Sakamoto AC, Machado HR, Arida RM, et al. Does the lunar phase have an effect on sudden unexpected death in epilepsy? *Epilepsy Behav*. (2009) 14:404–6. doi: 10.1016/j.yebeh.2008.11.013
53. Langdon-Down M, Russell Brain W. Time of day in relation to convulsions in epilepsy. *Lancet*. (1929) 213:1029–32. doi: 10.1016/S0140-6736(00)79288-9
54. Stevens JR, Kodama H, Lonsbury B, Mills L. Ultradian characteristics of spontaneous seizures discharges recorded by radio telemetry in man. *Electroencephalogr Clin Neurophysiol*. (1971) 31:313–25. doi: 10.1016/0013-4694(71)90227-6
55. Seneviratne U, Boston RC, Cook M, D'Souza W. Temporal patterns of epileptiform discharges in genetic generalized epilepsies. *Epilepsy Behav*. (2016) 64:18–25. doi: 10.1016/j.yebeh.2016.09.018
56. Khan S, Nobili L, Khatami R, Loddenkemper T, Cajochen C, Dijk D-J, et al. Circadian rhythm and epilepsy. *Lancet Neurol*. (2018) 17:1098–108. doi: 10.1016/S1474-4422(18)30335-1
57. Halász P, Filakovszky J, Vargha A, Bagdy G. Effect of sleep deprivation on spike-wave discharges in idiopathic generalised epilepsy: a 4×24 h continuous long term EEG monitoring study. *Epilepsy Res*. (2002) 51:123–32. doi: 10.1016/S0920-1211(02)00123-7
58. Zarowski M, Loddenkemper T, Vendrame M, Alexopoulos AV, Wyllie E, Kothare SV. Circadian distribution and sleep/wake patterns of generalized seizures in children. *Epilepsia*. (2011) 52:1076–83. doi: 10.1111/j.1528-1167.2011.03023.x
59. Seneviratne U, Cook M, D'Souza W. The electroencephalogram of idiopathic generalized epilepsy. *Epilepsia*. (2012) 53:234–48. doi: 10.1111/j.1528-1167.2011.03344.x
60. Seneviratne U, Lai A, Cook M, D'Souza W, Boston RC. "Sleep Surge": the impact of sleep onset and offset on epileptiform discharges in idiopathic generalized epilepsies. *Clin Neurophysiol*. (2020) 131:1044–50. doi: 10.1016/j.clinph.2020.01.021
61. Seneviratne U, Cook MJ, D'Souza WJ. Electroencephalography in the diagnosis of genetic generalized epilepsy syndromes. *Front Neurol*. (2017) 8:499. doi: 10.3389/fneur.2017.00499
62. Kramer MA, Cash SS. Epilepsy as a disorder of cortical network organization. *Neuroscientist*. (2012) 18:360–72. doi: 10.1177/1073858411422754
63. Duun-Henriksen J, Baud M, Richardson MP, Cook M, Kouvas G, Heasman JM, et al. A new era in electroencephalographic monitoring? Subscalp devices for ultra–long-term recordings. *Epilepsia*. (2020) 61:1805–17. doi: 10.1111/epi.16630
64. Haus E, Touitou Y. *Biologic Rhythms in Clinical and Laboratory Medicine*. Berlin; Heidelberg: Springer. (1992). doi: 10.1007/978-3-642-78734-8
65. Bullock B, Murray G, Meyer D. Highs and lows, ups and downs: meteorology and mood in bipolar disorder. *PLoS ONE*. (2017) 12:e0173431. doi: 10.1371/journal.pone.0173431
66. Wehr TA. Bipolar mood cycles and lunar tidal cycles. *Mol Psychiatry*. (2018) 23:923–31. doi: 10.1038/mp.2016.263
67. Ehlers CL, Frank E, Kupfer DJ. Social zeitgebers and biological rhythms: a unified approach to understanding the etiology of depression. *Arch Gen Psychiatry*. (1988) 45:948–52. doi: 10.1001/archpsyc.1988.01800340076012
68. Little JC, McPhail NI. Measures of depressive mood at monthly intervals. *Br J Psychiatry*. (1973) 122:447–52. doi: 10.1192/bjp.122.4.447
69. Luce GG, Health. (U.S.) NI of MH, Branch NI of MH. (U S) PA and E. *Biological Rhythms in Psychiatry and Medicine*. U.S. National Institute of Mental Health (1970).
70. Siegelová J, Fišer B, Brázdová Z, Forejt M, Homolka P, Vank P, et al. Disturbance of circadian rhythm in blood pressure by lack of darkness at night. *Scr Medica Fac Medicae Univ Brun Masaryk*. (2006) 79:147–54.
71. Nicolau GY, Haus E, Popescu M, Sackett-Lundeen L, Petrescu E. Orcadian, weekly, and seasonal variations in cardiac mortality, blood pressure, and catecholamine excretion. *Chronobiol Int*. (1991) 8:149–59. doi: 10.3109/07420529109059165
72. Gallerani M, Pala M, Fedeli U. Circaseptan periodicity of cardiovascular diseases. *Heart Fail Clin*. (2017) 13:703–17. doi: 10.1016/j.hfc.2017.05.007
73. Stewart S, Keates AK, Redfern A, McMurray JJV. Seasonal variations in cardiovascular disease. *Nat Rev Cardiol*. (2017) 14:654–64. doi: 10.1038/nrcardio.2017.76
74. Levi F, Halberg F. Circaseptan (about-7-day) bioperiodicity-spontaneous and reactive-and the search for pacemakers. *Ric Clin Lab*. (1982) 12:323–70. doi: 10.1007/BF02909422
75. Haus E, Smolensky MH. Biologic rhythms in the immune system. *Chronobiol Int*. (1999) 16:581–622. doi: 10.3109/07420529908998730
76. Coventry BJ, Ashdown ML, Quinn MA, Markovic SN, Yatomi-Clarke SL, Robinson AP. CRP identifies homeostatic immune oscillations in cancer patients: a potential treatment targeting tool? *J Transl Med*. (2009) 7:102. doi: 10.1186/1479-5876-7-102
77. Herold M, Cornélissen G, Rawson MJ, Katinas GS, Alinder C, Bratteli C, et al. About-daily (circadian) and about-weekly (circaseptan) patterns of human salivary melatonin. *J Anti-Aging Med*. (2000) 3:263–7. doi: 10.1089/rej.1.2000.3.263
78. Cajochen C, Altanay-Ekici S, Münch M, Frey S, Knoblauch V, Wirz-Justice A. Evidence that the lunar cycle influences human sleep. *Curr Biol*. (2013) 23:1485–8. doi: 10.1016/j.cub.2013.06.029
79. Celec P, Ostatníková D, Putz Z, Hodosy J, Bursk? P, Stárka L, et al. Circatrigintan cycle of salivary testosterone in human male. *Biol Rhythm Res*. (2003) 34:305–15. doi: 10.1076/brhm.34.3.305.18807
80. Goya-Esteban R, Barquero-Pérez O, Alzueta J, Vinolas X, Basterra N, García E, et al. A multicentric study of long-term rhythm patterns in heart rate. In: *2016 Computing in Cardiology Conference (CinC)* (IEEE) (2006). p. 909–12.
81. Meyer C, Muto V, Jaspar M, Kussé C, Lambot E, Chellappa SL, et al. Seasonality in human cognitive brain responses. *Proc Natl Acad Sci USA*. (2016) 113:3066–71. doi: 10.1073/pnas.1518129113
82. Harding C, Pompei F, Bordonaro SF, McGillicuddy DC, Burmistrov D, Sanchez LD. The daily, weekly, and seasonal cycles of body temperature analyzed at large scale. *Chronobiol Int*. (2019) 36:1646–57. doi: 10.1080/07420528.2019.1663863
83. Persson H, Kumlien E, Ericson M, Tomson T. Circadian variation in heart-rate variability in localization-related epilepsy. *Epilepsia*. (2007) 48:917–22. doi: 10.1111/j.1528-1167.2006.00961.x
84. Bernard C. Circadian/multidien Molecular Oscillations and Rhythmicity of Epilepsy (MORE). *Epilepsia*. (2021) 62:S49–68. doi: 10.1111/epi.16716

Conflict of Interest: PK, DE, RS, EN, MM, DF, and MC have employment or financial interest in Seer Medical Pty. Ltd., which provides diagnostic EEG services. WD'S has employment or financial interest in KeyLead Health. WD'S and MC have employment or financial interest in Epi-Minder Pty. Ltd. MR has a research collaboration with UNEEG medical and has been a member of their advisory board. BB has a financial interest in Cadence Neurosciences Inc., and has received nonfinancial research support (devices for a study) from Medtronic Inc.

The remaining authors declare that the research was conducted in the absence of any commercial or financial relationships that could be construed as a potential conflict of interest.

frontiers in Neurology

ORIGINAL RESEARCH
published: 18 August 2021
doi: 10.3389/fneur.2021.724904

Prospective Study of a Multimodal Convulsive Seizure Detection Wearable System on Pediatric and Adult Patients in the Epilepsy Monitoring Unit

Francesco Onorati[1], Giulia Regalia[1]*, Chiara Caborni[1], W. Curt LaFrance Jr.[2], Andrew S. Blum[3], Jonathan Bidwell[4], Paola De Liso[5], Rima El Atrache[6], Tobias Loddenkemper[6], Fatemeh Mohammadpour-Touserkani[7], Rani A. Sarkis[8], Daniel Friedman[9], Jay Jeschke[9] and Rosalind Picard[1,10]*

[1] Empatica, Inc., Boston, MA, United States, [2] Division of Neuropsychiatry and Behavioral Neurology, Rhode Island Hospital, Brown University, Providence, RI, United States, [3] Department of Neurology, Rhode Island Hospital, Brown University, Providence, RI, United States, [4] Harvard Medical School, Boston, MA, United States, [5] Department of Neuroscience, Bambino Gesù Children's Hospital, Istituto di Ricovero e Cura a Carattere Scientifico, Rome, Italy, [6] Department of Neurology, Boston Children's Hospital, Boston, MA, United States, [7] Department of Neurology, Downstate Medical Center, State University of New York, Brooklyn, NY, United States, [8] Department of Neurology, Brigham and Women's Hospital, Boston, MA, United States, [9] Department of Neurology, New York University Langone Medical Center, New York, NY, United States, [10] MIT Media Lab, Massachusetts Institute of Technology, Cambridge, MA, United States

Background: Using machine learning to combine wrist accelerometer (ACM) and electrodermal activity (EDA) has been shown effective to detect primarily and secondarily generalized tonic-clonic seizures, here termed as convulsive seizures (CS). A prospective study was conducted for the FDA clearance of an ACM and EDA-based CS-detection device based on a predefined machine learning algorithm. Here we present its performance on pediatric and adult patients in epilepsy monitoring units (EMUs).

Methods: Patients diagnosed with epilepsy participated in a prospective multi-center clinical study. Three board-certified neurologists independently labeled CS from video-EEG. The Detection Algorithm was evaluated in terms of Sensitivity and false alarm rate per 24 h-worn (FAR) on all the data and on only periods of rest. Performance were analyzed also applying the Detection Algorithm offline, with a less sensitive but more specific parameters configuration ("Active mode").

Results: Data from 152 patients (429 days) were used for performance evaluation (85 pediatric aged 6–20 years, and 67 adult aged 21–63 years). Thirty-six patients (18 pediatric) experienced a total of 66 CS (35 pediatric). The Sensitivity (corrected for clustered data) was 0.92, with a 95% confidence interval (CI) of [0.85-1.00] for the pediatric population, not significantly different ($p > 0.05$) from the adult population's Sensitivity (0.94, CI: [0.89–1.00]). The FAR on the pediatric population was 1.26 (CI: [0.87–1.73]), higher ($p < 0.001$) than in the adult population (0.57, CI: [0.36–0.81]). Using the Active mode, the FAR decreased by 68% while reducing Sensitivity to 0.95 across the population. During rest periods, the FAR's were 0 for all patients, lower than during activity periods ($p < 0.001$).

OPEN ACCESS

Edited by:
Vikram Rao, University of California, San Francisco, United States

Reviewed by:
Robert Scott Fisher, Stanford University, United States
David Spencer, Oregon Health and Science University, United States
Troels Kjær, University of Copenhagen, Denmark

***Correspondence:**
Francesco Onorati
francesco.onorati.bio@gmail.com
Giulia Regalia
gr@empatica.com

Specialty section:
This article was submitted to Epilepsy, a section of the journal Frontiers in Neurology

Received: *14 June 2021*
Accepted: *27 July 2021*
Published: *18 August 2021*

Citation:
Onorati F, Regalia G, Caborni C, LaFrance WC Jr, Blum AS, Bidwell J, De Liso P, El Atrache R, Loddenkemper T, Mohammadpour-Touserkani F, Sarkis RA, Friedman D, Jeschke J and Picard R (2021) Prospective Study of a Multimodal Convulsive Seizure Detection Wearable System on Pediatric and Adult Patients in the Epilepsy Monitoring Unit. Front. Neurol. 12:724904. doi: 10.3389/fneur.2021.724904

Conclusions: Performance complies with FDA's requirements of a lower bound of CI for Sensitivity higher than 0.7 and of a FAR lower than 2, for both age groups. The pediatric FAR was higher than the adult FAR, likely due to higher pediatric activity. The high Sensitivity and precision (having no false alarms) during sleep might help mitigate SUDEP risk by summoning caregiver intervention. The Active mode may be advantageous for some patients, reducing the impact of the FAR on daily life. Future work will examine the performance and usability outside of EMUs.

Keywords: epilepsy, seizure detection, wearable sensors, machine learning, clinical validation

INTRODUCTION

Generalized tonic-clonic seizures and focal-to-bilateral tonic-clonic seizures are the most dangerous types of seizures and represent major risk factors for sudden unexpected death in epilepsy (SUDEP), especially when patients are left unattended, e.g., nighttime (1–4). Beyond the risk of serious or life-threatening injuries (5), the lives of patients and their caregivers are heavily influenced by the unpredictability of seizures, which results in decreased quality of life and contributes to social isolation, especially in adolescents (6, 7).

Over the past decade, wearable devices equipped with automated seizure detection algorithms have been suggested to complement and overcome limitations of the gold standard video-electroencephalography (v-EEG) performed in the Epilepsy Monitoring Unit (EMU) (8–12). Such devices target a continuous, remote, unobtrusive and less expensive monitoring of patients. They are useful mainly for two reasons: (i) to prompt caregivers' intervention during or shortly after a seizure while the patient is unattended, when the risk of injury and SUDEP is the highest (13), consequently relieving both patients and caregivers; (ii) to provide objective and more accurate seizure counts in outpatient settings, overcoming the limitations of seizure diaries (14, 15). Several surveys have demonstrated the need for accurate wearable seizure detection (16–22).

Most of the proposed systems can detect seizures with a clear motor activity component; however, they can have high false alarm rates (FAR) (11, 23). Among the non-EEG seizure-monitoring devices, multimodal systems hold the most promise for attaining both high sensitivity and a low number of false alerts (24, 25). Moreover, these systems have the potential to assess seizure severity by tracking and analyzing multiple bio-signals in the peri-ictal period (13, 26, 27).

Growing efforts have been made by the scientific and clinical community to standardize the studies on wearable seizure detection devices to perform a rigorous validation and to enable their ubiquitous adoption in outpatient settings (24, 28, 29). Published guidelines have tried to adapt the STARD criteria to the specific use case of seizure detection (30). The main recommendation is to test the performance of seizure detection devices during prospective "phase III" multi-center EMU studies and "phase IV" in-field studies, where the detection algorithm is "fixed-and-frozen" on a set of patients' data previously recorded from a dataset completely different from the Test Cohort (28, 29). A few studies have been published that fulfilled phase III or IV criteria, using a dedicated device and fixed algorithm (31–35). Only one of them used multimodal seizure detection (32) and it was tested only during nighttime and only on a group of patients that included some of the same people used to develop the algorithm, two conditions that can inflate the algorithm's performance. There is a need for studies examining the 24-h performance of multimodal devices on independent data sets, which do not include any patients used when developing the algorithm.

In this work, we present an evaluation using a prospective, multi-center study with 24-h data from an independent group of patients wearing multimodal wrist-worn devices combining accelerometers (ACM) and electrodermal activity (EDA) sensors. We evaluate the detection of two seizure types, i.e., "focal onset to bilateral/unilateral tonic-clonic" (FBTC) seizures, previously known as secondary generalized tonic-clonic seizure, and "generalized onset tonic-clonic" (GTC) seizures, previously defined as primary generalized tonic-clonic seizures. For brevity, we will use "convulsive seizures" (CS) to generically refer to the two seizure types included in the study. The ACM with EDA sensor combination has been shown as promising to capture signs of ongoing CS (36–38), leading to the commercialization of a wristband specifically designed to provide real-time alerts of detected CS (Embrace wristband, Empatica Inc). A previous multicenter study reported high sensitivity (52 of 55 CS detected) and low false alarm rate (1 false alarm every 5 days) using a machine learning algorithm (38) that outperformed the pioneering state-of-the-art ACM and EDA system (37) in a direct performance comparison, both using independent 24-h test data. However, the study qualified for phase II, as it reported a cross-validation analysis, meaning that the parameters of the algorithm were not the same for all the analyzed patients (29). Here we report the performance of a "fixed-and-frozen" algorithm on a Test Cohort of participants that are non-overlapping with participants used in the training dataset. Three main sets of analyses are shown in this study:

1. Performance in detecting CS on the whole (24-h a day, all ages) dataset and on pediatric and adult populations, separately, which provides indications on potential implications of age on the CS detection effectiveness.

2. Performance in detecting CS during low-motion conditions, i.e., on periods of sedentary behavior, which tend to be sleep periods associated with greater isolation and SUDEP risk.

3. Performance in detecting CS with two operating points, i.e., the FDA-cleared[1] settings and a less sensitive Active operating point, to provide indications on the potential of the algorithm to be adapted according to different populations or individual needs and expectations.

MATERIALS AND METHODS

Study Design and Endpoints

This is a prospective, non-randomized multi-site EMU clinical trial undertaken to get the clearance by the US Food and Drug Administration (FDA) of an investigational monitoring and alerting system for the identification of specific types of seizures (i.e., CS) using a device worn on the wrist. The device embeds a Detection Algorithm that processes 3-axis ACM and EDA sensor data to detect CS events. As per the requirements by the FDA on medical software, the Detection Algorithm must be "fixed-and-frozen."

The population intended for the usage of the device included children age 6 (included) to 20 (included) and adults age 21 (included) and up.

The performance of the fixed-and-frozen Detection Algorithm on the Test Cohort has been evaluated in terms of sensitivity (or percent positive agreement) as the primary endpoint, and false alarm rate per 24 h-worn (FAR) as the secondary endpoint. The primary endpoint for the clinical validation of the wearable medical device was to reach a lower bound of the 95% confidence interval of the sensitivity higher than 0.7, for pediatric and adult groups, separately. The secondary endpoint required that the Detection Algorithm reached a FAR lower than 2 false alarms per day, for pediatric and adult groups, separately.

Data Development Plan

Clinical Sites

The clinical sites involved in the study are members of the National Association of Epilepsy Centers (NAEC) certified as level IV in the USA, or members of LICE (Italian League against Epilepsy) and advanced epilepsy center[2] in Italy. From 2014 to 2018, a series of IRB approved research studies using ACM and EDA wrist-worn devices were carried on in several Level IV NAEC members in the US, including Boston Children's Hospital (CHB), New York Langone Medical Center (NYU), Emory Healthcare (EMORY), Children's Hospital of Atlanta (CHOA), and Rhode Island Hospital (RIH). The studies were conducted following US government research regulations, and applicable international standards of Good Clinical Practice, and institutional research policies and procedures. Additionally, from 2017 to August 2018, a Pivotal study was conducted in a Level IV center in the US, namely New York Langone Medical Center (NYUP[3]) and in an advanced epilepsy center in Rome, Italy, Ospedale Pediatrico Bambin Gesú (OPBGP)[4]. The collected labeled data have been used to test the Detection Algorithm. The timeline of data collection at each clinical center is reported in the **Supplementary Figure 1**.

Sample Size Estimation

The estimation of a minimum required sample size was based on the Sensitivity requirements of the primary endpoint, i.e., meaning that we computed the minimum required number of patients experiencing at least one convulsive seizure during admission. The sample size was computed taking into account the possible presence of multiple events for the same subject (clustered data) and the need for a high value of sensitivity (39). For an expected sensitivity of 0.95 (37, 38) with a confidence interval width of 0.1, and assuming an intra-cluster correlation based on the Test Cohort of the study for the previous clearance (40), we estimated a minimum sample size of 17 patients having seizures, for both adult and pediatric patients. No requirement was set for the number of epilepsy patients not experiencing seizures, but we included the available data from all patients to provide the most accurate measure of FAR.

Reference Standard

The identification of seizures was performed by three board-certified clinical neurologists, who independently examined v-EEG recordings synchronized with the data recordings of the wearable device under evaluation. A "2 out of 3" majority rule inter-rater agreement has been used to mitigate interrater variability in marking v-EEG data for seizure activity (41). The reviewers were blinded to other sources of data, including raw or processed data from the wearable and the algorithm output. Seizure types were classified according to the most recent International League Against Epilepsy (ILAE) seizure classification (42). Two seizure types were targeted in this study: "focal onset to bilateral/unilateral tonic-clonic" (FBTC) seizures, previously known as secondary generalized tonic-clonic seizures, and "generalized onset tonic-clonic" (GTC) seizures, previously defined as primary generalized tonic-clonic seizures. The video-EEG review process consisted of the following steps:

1. The EMU technicians reviewed the v-EEG recordings and filtered out all non-relevant segments. They did not perform any filtering on the remaining v-EEG data. The result is a pruned v-EEG dataset.
2. The research assistants removed any notes in the pruned dataset added by the EMU technician to prevent any potential bias to the three independent reviewers.
3. The principal investigators conducted a review on the pruned v-EEG dataset.
4. Second and third reviewers independently conducted reviews on the pruned v-EEG dataset.

[1]Note that the FDA does not declare a wearable device to be "approved"; the language they use after validating a wearable medical device and accepting its claims to allow it to be marketed is that the device is "cleared".

[2]Advanced epilepsy center is equivalent to a Level IV center in US.

[3]The abbreviation "NYUP" (i.e., NYU Pivotal) differentiates data recorded for the pivotal study from data previously recorded at the same medical center. Different patients have been enrolled in the new data collection with respect to the previous study. The two studies were performed at different times and using two different wearable devices (Empatica E4 for NYU and Empatica Embrace for NYUP).

[4]"Generalized Seizure Detection And Alerting In The EMU With The Empatica Embrace Watch And Smartphone-Based Alert System" (ClinicalTrials.gov Identifier: NCT03207685).

The review process consisted of confirming the onset and offset times of a seizure and assigning a classification label to the event based on the most recent ILAE seizure classification (42). At each site, the following data were documented per patient:

1) v-EEG-based labeled seizure data with clinical observations, and three independent experts validating the labeled events.
2) Seizure onset and end time (video/clinical read).
3) Seizure onset and end time (EEG read).
4) Post-ictal generalized EEG suppression (PGES) duration (if present).
5) Seizure type according to the most recent ILAE seizure classification (42).
6) Clinical presentation.
7) Demographic information (age at enrollment, gender, height, weight, diagnosis, and autonomic related pathologies or relevant chart information).

Wearable Devices

Two multimodal wrist-worn devices were used in this study, the E4 and the Embrace, both manufactured by Empatica Inc. Both devices received CE medical clearance from the European Union in 2016 (class IIa). Embrace received clearance by the US FDA in January 2018 (Class II) for CS monitoring during periods of rest for adults and in January 2019 for children aged 6 and up.

The E4 wristband embeds a three-axis ACM sensor (sampling frequency: 32 Hz; range; [−2; +2] g), an EDA sensor (sampling frequency: 4 Hz; range; [0.01; 100] μS), a reflective photoplethysmography (PPG) sensor (sampling frequency: 64 Hz), and a temperature sensor (sampling frequency: 4 Hz; range: [−40; +115]°C). The Embrace wristband embeds a three-axis ACM sensor (sampling frequency: 32 Hz; range; [−16; +16] g), a three-axis gyroscope sensor (sampling frequency: 32 Hz; range; [-500; +500] °/s), an EDA sensor (sampling frequency: 4 Hz; range; [0.01; 85] μS) and a temperature sensor (sampling frequency: 1 Hz; range: [−20; +70]°C). The automated detection of CS relies solely on ACM and EDA data. Therefore, only recorded ACM and EDA data acquired by the two devices were used as inputs to the Detection Algorithm. The two devices have been shown to be equivalent in terms of their ACM and EDA sensor data (see details in the **Supplementary Material**) and therefore were used interchangeably in this study.

Experimental Protocol

Patients with a known history of epilepsy were admitted for long-term v-EEG monitoring at the EMU of each clinical site. The recruitment process was conducted by each site. Only patients (or their caregivers) who provided their written informed consent were enrolled. All patients were recorded following the same protocol in order to provide homogeneous wearable device data for inclusion in the clinical study.

In all sites, concomitant electrocardiogram (EKG) data were recorded, which were not used either for the seizure labeling nor for informing the classification model of the wearable medical device.

During their time in the EMU, patients wore the E4 or the Embrace wristband, synchronized with the v-EEG at the start of each monitoring period. If seizure semiology reported an asymmetric involvement of arms, the wristband was placed on the wrist where convulsions appeared earlier and/or were more evident; otherwise, the device was worn on the non-dominant arm. When the wearable device used was an Embrace, the patients were also provided with a paired wireless device to download the sensor data from the wearable device and upload them to a dedicated cloud data storage. Following enrollment, study subjects were seen daily during their inpatient hospital stay, continuously monitored with v-EEG and given the usual standard of care.

Development of the Detection Algorithm

Machine learning algorithms use information embedded in a training dataset, labeled or unlabeled, in order to build a classification model and a decision rule function able to identify and/or distinguish one or more events of interest. The tuning of all the parameters can be performed minimizing a cost function or maximizing one or more performance metrics on validation datasets. The selection of the performance metrics to maximize is usually motivated by the specific application. More specifically, for clinical applications, the performance metrics need to reflect the costs and benefits for patients (43), and thus how to evaluate the performance of a medical device is usually decided at the clinical level (44). The selected performance metrics are described in section Performance Metrics.

Figure 1 represents the workflow of the Detection Algorithm validated in this study. At a very high level, data from the ACM and EDA sensors are processed to compute features from a pre-determined feature set, which are analyzed by a pre-trained classification model to obtain an estimation of the probability that a CS pattern is present in the sensor data. The probability estimates are then evaluated by a decision rule function, to establish whether to issue an alert or not, thus classifying the associated event as a CS.

To identify the features that could represent the pattern of a CS and distinguish it from other types of events, a feature engineering approach was performed. To distinguish CS from all other events, features that characterize both types of events needed to be included in the classification model. A feature set of 160 ACM- and EDA-based features was firstly developed, mostly to better represent the frequency and non-linear characteristics of the sensor data. Due to computational limitations, a subset of 40 features was selected using a sequential floating forward feature selection strategy (45), to maximize the trade-off between performance and computational cost. Features were extracted on consecutive 10-s windows overlapped by 75%.

The process to obtain a classification model for the detection of CS is schematized in **Figure 2** and consisted of two main steps. At first, the training dataset, i.e., a collection of labeled sensor data, was processed to obtain a set of features on windowed sensor data. The same procedure was performed on separate validation datasets. Then, after defining performance metrics to maximize, the labeled features from the training dataset were provided to the machine learning algorithm to obtain a classification model and a decision rule function, whose

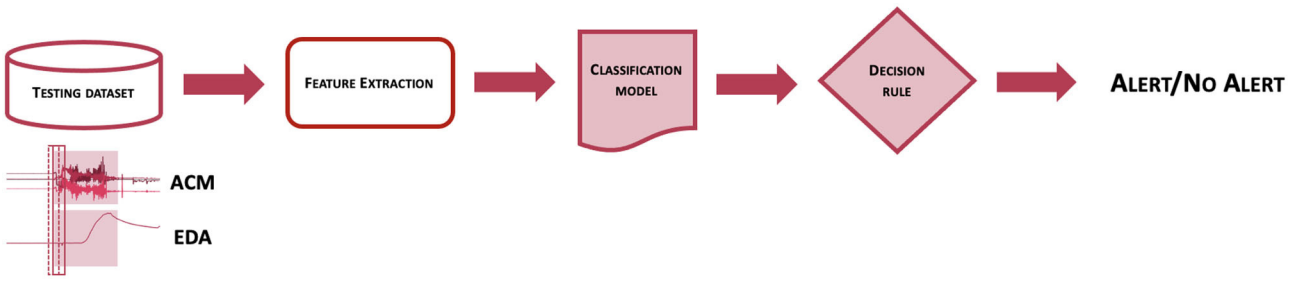

FIGURE 1 | Scheme of the workflow used to classify epochs of EDA and ACM sensor signals into seizure or non-seizure epochs.

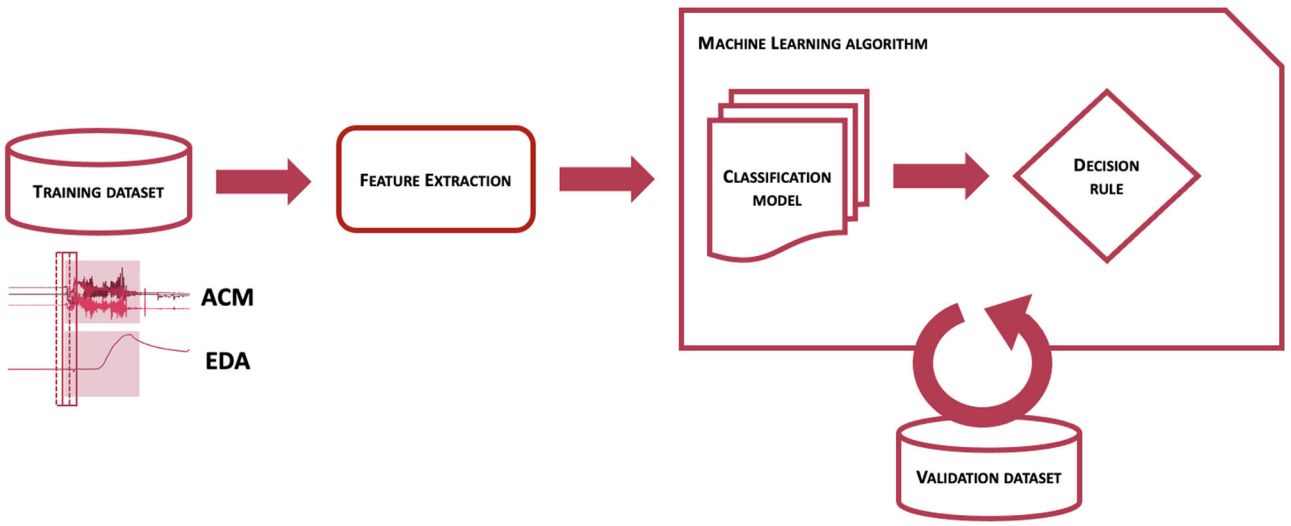

FIGURE 2 | Description of the training phase of the Detection Algorithm.

parameters were tuned by maximizing performance metrics evaluated on the validation dataset. To train a classification model able to distinguish CS from non-CS events, it was crucial to provide labeled samples to the machine learning algorithm responsible to build the classification model. For this reason, not only previously recorded clinical data, but also previously logged data from real-life activities showing patterns potentially similar to CS (e.g., tooth brushing, hands clapping, hands washing, gesturing, driving or biking on an uneven surface) were used to make a training dataset, as this procedure of showing both good and bad examples showed improved performance on previous preliminary analyses (46). This process was strictly controlled and highly selective to preserve the correct representability and distribution of the data in the training dataset, to avoid mislabeling of data, and most importantly to prevent overlap between training, validation, and testing datasets. No patients whose data were used in the test sets contributed data to the training or validation processes.

The Test Cohort described in section Test Cohort Allocation and Demographics represents the testing dataset for the Detection Algorithm.

Rest Detection Algorithm

A proprietary and validated actigraphy-based rest detection algorithm was used to evaluate the performance of the Detection Algorithm during rest conditions (47). Briefly, the magnitude of the 3-axis ACM channels is band-pass filtered. Then, activity counts are obtained as the number of crossings of the ACM magnitude through a specified threshold and accumulated over 30-s epochs. Rest onset and offset are obtained using a rule applied to the moving average of activity counts from a 30-min window. Rest periods <2 h apart were merged assuming a rest interruption between them. The output of the rest detection typically includes sleep periods, and occasionally long quiescent periods of wakefulness.

Performance Evaluation

Performance Metrics

Atrue positive occurred when the Detection Algorithm provided an alarm between the clinical onset and the clinical offset times of an event that was labeled a CS according to the "2 out of 3" majority rule by three independent board-certified clinical

neurologists. Given the count of true positives and the expert-labeled number of CS, sensitivity was estimated as the number of true positives divided by the number of expert-labeled CS ("Sensitivity" in **Table 3**). This value was corrected ("cSensitivity" in **Table 3**) for the presence of clusters in the data, more specifically for multiple CS from the same patient, by estimating the intra-cluster-correlation (48) and thus removing the resulting inflation in the sensitivity (39). Similarly, the 95% confidence interval of the so-obtained corrected sensitivity was estimated with the classic Wilson Score method corrected for the cluster effect (39).

A false positive, or a false alarm, occurred when the algorithm provided an alarm not corresponding to any labeled CS. FAR, defined as the number of false alarms per 24 h-worn, a typically reported performance metric in non-EEG seizure detection systems (11), was computed as the total number of false alarms divided by the total recording hours, and normalized for 24 h. The 95% confidence interval of the FAR was computed with a non-parametric bootstrapping method. Specifically, 100,000 samplings with replacement were performed at the level of the patients to incorporate all the sources of within-patient variability (49–51). The number of iterations was chosen equal to 100,000 since it is considered to be a reasonably large number for bootstrapping confidence intervals (49, 52). Since the FAR distribution did not follow a normal distribution, the 95% confidence interval was computed as the 2.5th and the 97.5th percentile (49) of the 100,000 FAR samples.

Two additional statistics were computed to represent a patient-centric point of view on the performance of the detection system: (1) the precision, which is the ratio between the total number of true positives and the total number of alerts, with its 95% confidence interval, computed using the classical Wilson score method (53). In the case of no false alarms (e.g., during rest), to provide a more realistic and conservative estimation for both the precision and its 95% confidence interval, a correction due to Laplace, namely the "Rule of succession," has been applied, as it has been reported as a good correction for probability equal to 1 with relatively small sample sizes (54); (2) the mean and the standard deviation of the seizure detection latency, defined as the number of seconds between the seizure clinical onset and the algorithm detection time.

To provide a depiction as complete as possible of the relationship between the different performance metrics and the operating points, the receiver operating characteristic (ROC) curve was obtained, which graphs in a two-dimensional space the sensitivity and the false positive rate, or equivalently (1 - specificity), while varying the operating point of the Detection Algorithm (55). For monitoring devices, computing the specificity is not a well-defined task, as while it is easy to count the number of CS events, there are not commensurate "no CS events" that can be easily counted (56). To be able to compute the ROC curve, we assumed that the wearable sensor data periods labeled as non-seizure, could be represented as a sequence of non-overlapping negative events (56), whose duration is equal to the mean duration of the CS events. Additionally, the precision-recall (PR) curve (57) was analyzed, as it is useful when classes are unbalanced, which is the case in epilepsy as most data are from the class "no CS." The PR curve graphs in a two-dimensional space the recall (an alternative name for the sensitivity) and the precision, while varying the operating curve. It thus attempts to estimate the benefit of detecting the event of interest vs. the burden of providing a false alarm to the patient/caregiver. Finally, the variation of the sensitivity and the FAR at each operating point were analyzed, representing the primary and the secondary endpoints, respectively, for the clinical validation of the detection system. Along with the point estimates of sensitivity, specificity, precision, and FAR, the respective 95% confidence intervals were also computed with the Wilson score method for the proportion-like metrics (sensitivity, specificity and precision) (53), and with a simple normal approximation for the FAR.

All of the components and parameters of the validated wearable device, including all parameters of the algorithm, needed to be "fixed-and-frozen" before the clinical validation. In the Result section, we focus on two operating points of the decision rule function: the first one, FDA-cleared, was fixed under the rationale of maximizing the detection of all the events during periods of rest or low activity; the second one, Active mode, was fixed to balance the ability of the Detection algorithm to identify the majority of the events, while reducing the burden of false alarms on the patients and their caregivers during moderate to intense activities. In section Performance Analysis, the performance metrics are presented for the two different operating points, with a particular emphasis on the FDA-cleared mode. The performance analyses are presented over three groupings of the test data: for all the patients, for pediatric (6–20), and for adult patients (21+). Finally, we present the performance of the seizure detection system during rest, as computed by the automated rest detection algorithm, and show the results for all three groupings.

Statistical Tests

Specific statistical tests were performed to establish whether different populations (pediatric vs. adult groups) and behavioral or environmental conditions (rest vs. active groups) showed statistically significant differences. The 95% confidence intervals were computed on each grouping. To test whether there was a statistical difference for "cSensitivity" in each comparison, we computed the 95% confidence interval of the difference between the corrected sensitivities for each group and tested it with a method for independent binomial proportions for clustered data (58). The null hypothesis that there was no difference between the groups can be rejected if the 95% confidence interval does not contain the 0 value. To examine if there were statistically significant differences in the FAR since each group had different exposure times, we performed a normal approximation of a statistical test based on the null hypothesis that the expected number of events experienced by each group were equal (58).

RESULTS

Test Cohort Allocation and Demographics

A total of 304 patients' data was recorded from the 6 clinical centers. Upon completion of the study, the Indications for Use (IFU) of the wearable seizure detection device were reviewed by

TABLE 1 | Summary of reasons for withdrawal of patients from the analysis.

Motivation for exclusion	# Patients excluded	Description
Out of the IFU	112	Wearable device placement at the ankle
	22	Age below 6
	1	Non-epileptic seizures
Lost/corrupted data	10	Issues with the reference device (v-EEG)
	3	Corrupted wearable device data
	1	Wearable device hardware failure
Compliance	1	Wearable device not worn
	2	Early termination upon request from the patient

TABLE 2 | Distribution of patients, wearable device type and CS events across the different clinical sites.

Site	Location	Patients		Device		CS	
		Pediatric	Adult	E4	Embrace	GTC	FBTC
BCH	US	52 (F: 26)	3 (F: 2)	55	0	5	16
CHOA	US	13 (F: 5)	0	13	0	3	2
EMORY	US	1 (F: 0)	13 (F: 10)	14	0	3	0
NYU	US	0	18 (F: 10)	18	0	0	10
NYUP	US	1 (F: 1)	13 (F: 4)	0	14	0	11
OPBGP	IT	13 (F: 3)	1 (F: 0)	0	14	0	10
RIH	US	5 (F: 4)	19 (F: 12)	24	0	1	5
Total		85 (F: 39)	67 (F: 38)	124	28	12	54

F, female.

the FDA, which resulted in the exclusion of some patients from the analysis even if the reasons for withdrawal had not been set as exclusion criteria prior to the start of the study. The FDA requested to use only one location for the device, so we chose the wrist. Accordingly, 135 patients were excluded from the study because they did not wear the sensor on the wrist (112)[5], did not have a prior epilepsy diagnosis (1), or were <6 years old (22), as already explained in Section 2.1. An additional 14 patients were excluded due to hardware, software or data issues of the EEG reference device (10) or the wearable device (4). Only 3 patients were excluded because of lack of compliance (1) or dropping out from the study (2). **Table 1** summarizes all of the cases excluded from the study.

Thus, the analyzed dataset consisted of a total of 152 patients (77 females, age range: 6–63 years, median age: 17 years), of which 85 were pediatric patients (38 females, age range: 6–20 years, median age: 12) and 67 were adults (37 females, age range: 21–63 years, median age: 38 years). The total duration of the recordings was 10,296 h (429 days), including 3,939 h (162 days) from pediatric patients and 6,357 h (265 days) from adult patients. A total of 36 of the 152 patients experienced at least one of the seizures included in the clinical trial during the monitoring period, equally distributed among children (9 females) and adults (6 females). A total of 66 CS events experienced by 36 patients were independently identified by at least 2 out of 3 board-certified clinical neurologists who reviewed the v-EEG recordings: Of these, 35 were experienced by 18 pediatric patients (17 by female pediatric patients), and 31 by 18 adult patients (10 by female adult patients). **Table 2** shows the distribution of patients and CS across the different clinical sites, along with the wearable device used by each patient.

[5]Some patients, especially with sensory disorders, may become distracted or stressed by a wrist-worn device. Some patients had wrists that were too small for the E4 device. To allow both types of patients to contribute data, they could wear an E4 on the lower calf, just above the ankle. However, FDA later asked us to focus only on data from one location, so we chose the wrist.

Performance Analysis

Figure 3 shows the ROC curve, the PR curve and the sensitivity and FAR curves while varying the operating point of the Detection Algorithm. Different portions of the curves are shown to emphasize the two selected operating points and their relationship with the different performance metrics. The specificity spanned a very narrow range of values, very close to 0.99, due to the highly unbalanced class distribution and the high specificity of the Detection Algorithm. The sensitivity at the two operating points was 0.95 and 0.98, respectively, with a higher value for the FDA-cleared operating point (blue circle in **Figure 3**). The overall precision across all conditions, rest and non-rest, was relatively low: for the FDA-cleared operating point the precision was 0.15, which indicates 1 true detection for every 6 false alerts on average, while for the Active operating point the precision was 0.35, resulting in 1 true detection for every 2 false alerts. The FAR of 0.84 implied on average <1 false alarm per full day of recording at the FDA-cleared high-sensitivity operating point, and the FAR of 0.27 implied on average about 1 false alarm every 4 days of continuous wear while operating in the less sensitive Active mode.

Figure 4 shows the detected CS and the FAR for each patient in the Test Cohort, grouped according to the operating point of the Detection Algorithm and the age group. In the Active mode, most patients experienced no false alarms (72 and 63% for pediatric and adult patients, respectively, had FAR = 0). In the FDA-cleared mode, an individual FAR of 0 was experienced by 47 and 46% for pediatric and adult patients, respectively.

Table 3 reports the characteristics of the datasets included in each performance evaluation (rows "Test cohort") and the results for each operating point (rows "FDA-cleared" mode and "Active" mode), for the whole Test Cohort (columns "Overall") and each age group separately (columns "Pediatric" and "Adult," respectively). Also, the performance evaluation was conducted including all the data (columns "All data"), or only the data recognized as rest by the automated rest detection algorithm described in paragraph 2.7 (columns "Automatically-Detected Rest"). Overall, rest periods accounted for ∼38% of the total recording duration. The median duration of rest periods was

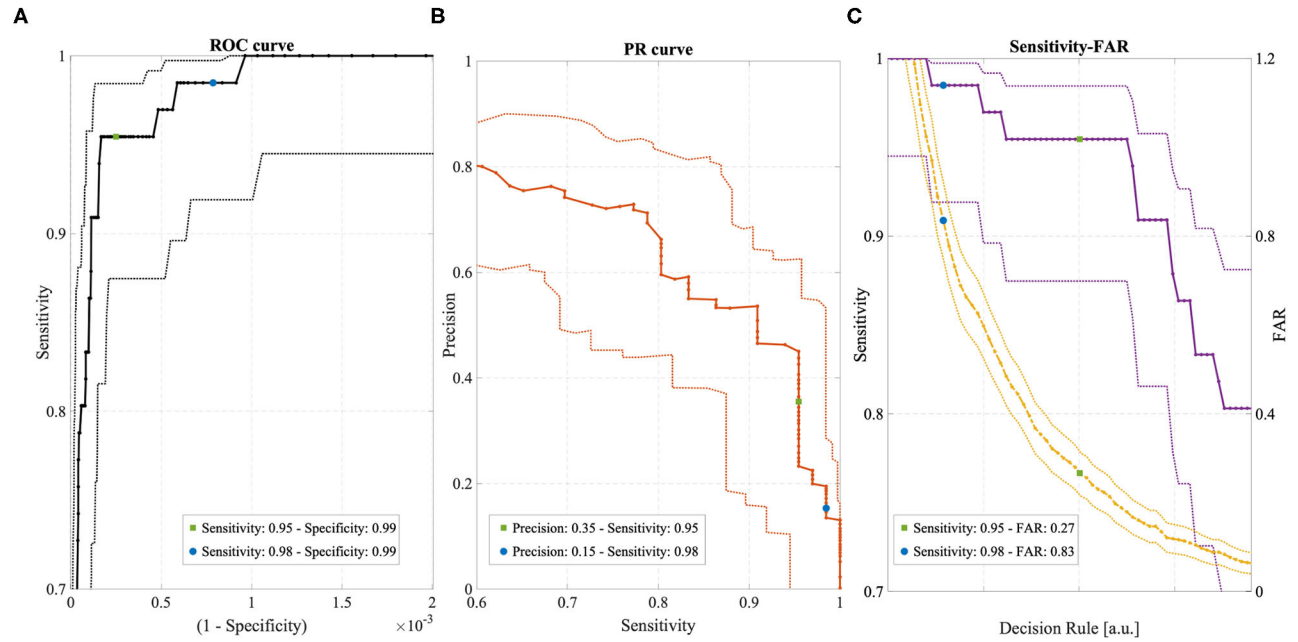

FIGURE 3 | (A) ROC curve with 95% confidence intervals (dotted lines). **(B)** Precision-Recall (PR) curve with 95% confidence intervals (dotted lines). **(C)** Sensitivity (violet) and FAR (yellow) curves with 95% confidence intervals (dotted lines). All curves were obtained by varying the operating point of the Detection Algorithm. Two operating points are highlighted in each curve, corresponding to "FDA-cleared" mode (blue circles) and "Active" mode (green circles).

7.1 h and the median number of rest periods per recording day was 1.2. These statistics lend support to a hypothesis that most of the rest periods were probably sleep periods. More detailed statistics are reported in the **Supplementary Figure 2**.

As expected, the estimated sensitivity was inflated by the presence of clustered data (i.e., multiple CS per patient), and therefore we computed its statistical correction "cSensitivity," which was lower. Nonetheless, the lower bound of the 95% confidence interval for cSensitivity was higher than 0.7 for all age groups and both operating points when considering the whole dataset in the analysis (columns "All data"). Even though only one operating point has been clinically validated and FDA-cleared, the less sensitive operating point ("Active" mode, in **Table 3**) also reached a good overall performance in detecting CS.

The requirement expressed in the secondary endpoint regarding the FAR has been met for all three age groupings and both operating points. When considering only the data recognized as rest by the rest detection algorithm, corresponding to sleep periods and occasional long periods of inactivity, the number of the false alarms dropped to 0 for all the grouped analyses and both operating points, leading ideally to a FAR equal to 0. As a consequence, the precision drastically increased. Even applying a conservative estimate of precision with a 95% confidence interval adjusted by the "rule of succession" correction of Laplace, the corrected precision reached a value of 0.95.

Table 4 shows the results of the statistical analysis of the main performance metrics, i.e., sensitivity and FAR, between the age groups and the activity groups. As expected, there was no difference in the ability of the Detection Algorithm in identifying CS between the two age groups and between the two contexts in which the CS occurred, i.e., during rest or during a moderate to high activity. On the contrary, the difference in the occurrence of the false alarms was statistically significant, as expected when comparing rest vs. moderate to high activity, and between the two age groups.

The detection latency of the system was on the order of 30–40 s (**Table 3**). Seizures occurring during the whole recording period were detected with a median detection latency of 37.46 s and 40.03 s when using the FDA-cleared or the Active mode, respectively. Considering only seizures occurring during rest periods, the latency was 33.05 s and 38.36 s with the two modalities, respectively.

DISCUSSION

Key Findings and Advances Over Prior Research

Wearable technologies designed to accurately and automatically monitor for CS seizures provide advantages of improved detection and alerting to caregivers of potentially life-threatening events, enabling attention to seizures, and potentially lowering the risk of serious injury or death from accidents and SUDEP. A recent study of 255 SUDEP cases (definite and probable) and 1,148 matched controls showed that 69% of SUDEP cases in patients with GTC seizures who live alone may be prevented if patients are attended, or if their GTC seizures are controlled.

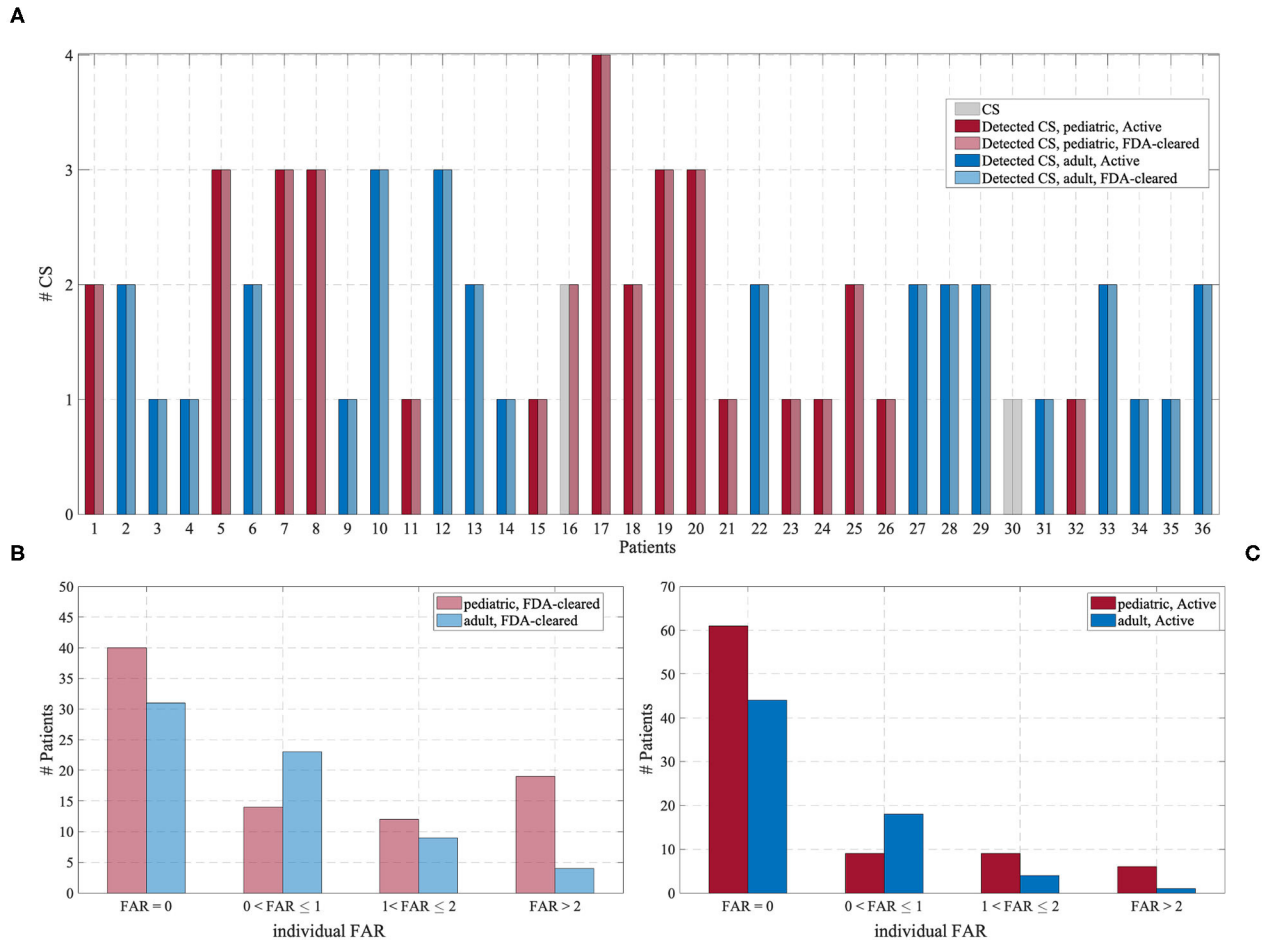

FIGURE 4 | (A) Number of CS (gray) and the number of detected CS for each of the 36 patients experiencing CS, grouped according to the operating point of the Detection Algorithm and the age group. **(B)** Distribution of the individual FAR for the "FDA-cleared" mode. **(C)** Distribution of the individual FAR for the "Active" mode.

Recent practical clinical guidelines recommend using clinically validated devices for automated detection of CS, the seizure types included in this study, especially in unsupervised patients, where alarms can facilitate rapid interventions (28).

To the authors' knowledge, this is the first prospective study on a multimodal wearable CS detection system based on wrist ACM and EDA sensors evaluated on a large patients' pool (152 patients). Prior work has presented prospective analyses of non-EEG seizure detection devices (31–35), but none of them combined ACM and EDA sensors or used multi-modal methods on continuous 24-h patient data, i.e., including activity as well as sleep. While ACM sensors are intuitively fundamental to capture signs of ongoing CS, EDA sensors, which convey information on sympathetic autonomic nervous system activity, improve the specificity of the detection (37) and provide additional information for seizure characterization (59, 60). Apart from the unique combination of sensors to the authors' knowledge, the presented Detection Algorithm is the only machine learning algorithm used in commercialized non-EEG seizure detection systems. Machine learning algorithms are becoming increasingly recognized as effective tools for the detection of seizures (61, 62), despite the challenges they pose for traditional medical regulatory systems (63).

This work further contributes to the field detailed analyses examining performance differences between pediatric and adult patients, between rest and active conditions, and using two different operating modes of the automated algorithm (both defined *a priori* during the previous training phase of the Detection Algorithm and fixed and frozen before applying them to the test data here). To the authors' knowledge, these types of analyses are novel and provide an expanded understanding of the capabilities and potential shortcoming of the wearable multimodal system under investigation.

This study may qualify for the recently proposed label of a phase III validation study (28, 29): Multiple EMU centers were involved; the reference standard was v-EEG recordings interpreted by experts; more than 20 patients ($n = 36$) with seizures were included with more than 30 seizures ($n = 66$); the data and patients analyzed were disjointed from those

TABLE 3 | Characteristics of the Test Cohort and performance of the Detection Algorithm for all the patients and the two age groups, for the two different operating points of the algorithm ("FDA-cleared" mode and "Active" mode, and for all the data ("All data") vs. only periods of rest ("Automatically-Detected Rest").

		All data			Automatically-detected rest		
		Overall	**Pediatric**	**Adult**	**Overall**	**Pediatric**	**Adult**
Test cohort	# Patients (w/ CS)	152 (36)	85 (18)	67 (18)	144 (13)	78 (7)	66 (6)
	Total hours	10,296	3,939	6,357	3,995	1,703	2,292
	Average hours/pat.	68	46	95	26	20	34
	Total CS	66	35	31	20	13	7
	Mean duration [sec] (St. Dev.)	84.56 (34.57)	89.37 (39.09)	79.13 (28.27)	78.65 (26.49)	79.61 (24.25)	76.86 (32.26)
"FDA-cleared" mode	Detected CS	65	34	31	19	12	7
	Mean delay [sec] (St. Dev.)	37.46 (21.09)	37.76 (24.06)	37.13 (17.64)	33.05 (12.09)	32.08 (7.77)	34.71 (17.96)
	Sensitivity	0.98	0.97	1.00	0.90	0.92	1.00
	cSensitivity [95% CI]	0.96 [0.92, 1.00]	0.92 [0.85, 1.00]	0.94 [0.89, 1.00]	0.83 [0.69, 0.97]	0.82 [0.65, 0.99]	0.82 [0.65, 1.00]
	Precision [95% CI]	0.15 [0.12, 0.19]	0.14 [0.10, 0.19]	0.17 [0.12, 0.23]	0.95* [0.76, 0.99]	0.93* [0.66, 0.99]	0.89* [0.52, 0.98]
	Total false alarms	357	207	150	0	0	0
	FAR [95% CI]	0.83 [0.63, 1.07]	1.26 [0.87, 1.73]	0.57 [0.36, 0.81]	0	0	0
"Active" mode	Detected CS	63	32	31	19	12	7
	Mean Delay [sec] (St. Dev.)	40.03 (16.25)	37.44 (12.96)	42.71 (18.91)	38.26 (12.43)	36.75 (7.62)	40.86 (18.57)
	Sensitivity	0.95	0.91	1.00	0.90	0.92	1.00
	cSensitivity [95% CI]	0.91 [0.84, 0.99]	0.85 [0.72, 0.98]	0.94 [0.89, 1.00]	0.83 [0.69, 0.97]	0.82 [0.65, 0.99]	0.82 [0.65, 1.00]
	Precision [95% CI]	0.36 [0.29, 0.43]	0.33 [0.24, 0.43]	0.39 [0.29, 0.50]	0.95* [0.76, 0.99]	0.93* [0.66, 0.99]	0.89* [0.52, 0.98]
	Total false alarms	113	65	48	0	0	0
	FAR [95% CI]	0.27 [0.18, 0.36]	0.40 [0.23, 0.59]	0.18 [0.10, 0.28]	0	0	0

*CI, Confidence Interval. *Laplace correction (i.e., the "rule of succession") was applied to improve the estimation of the precision and its 95% confidence interval.*

TABLE 4 | Statistical comparison of "cSensitivity" and FAR between pediatric and adult patients, and between Rest and Active periods, for the two operating points.

Operating point	**Variable**	**Groups**	***p*-value**
"FDA-cleared"	cSensitivity	Children vs. adults	0.177
		Rest vs. active	0.496
	FAR ratio	Children vs. adults	**$<< 10^{-3}$**
		Rest vs. active	**$<< 10^{-3}$**
"Active"	cSensitivity	Children vs. adults	0.478
		Rest vs. active	0.227
	FAR ratio	Children vs. adults	**$< 10^{-3}$**
		Rest vs. active	**$<< 10^{-3}$**

Values in bold indicate a statistically significant difference (p-value < 0.05).

used to develop the Detection Algorithm, removing the risk of overfitting, and all of the analyses were performed in a real-time manner fully mimicking the functioning of the algorithm on-board. Offline analysis of bio-signals may raise the possibility of overfitting to the recorded data set and can call the generalizability of results into question (28). However, given that the Detection Algorithm was trained on separate data and a fully separate patient group, and that it was "fixed-and-frozen" before being applied to the test set, and still uses the same code that runs on-board the Embrace device, we believe that overfitting is not affecting these results, as also supported by FDA's careful evaluation.

The performance of the FDA-cleared Detection Algorithm complies with and surpasses the performance requirements on non-EEG seizure monitoring devices, which focus on sensitivity and FAR. The Detection Algorithm showed an excellent sensitivity, capturing 65 out of 66 CS occurred in 36 patients, with a lower bound of the 95% confidence interval substantially higher than the study endpoint on sensitivity. The system provided reasonably timely detection of CS, within an average of 37.46 s from the onset of clinical manifestations as annotated by expert v-EEG raters. Rapid detection is of utmost importance, given that timely treatment of seizures can be life-saving, especially after CS, which bear a higher risk of SUDEP (3, 13). Even if the observed delay is slightly higher than systems using arm-worn electromyography patches (33, 35), it is comparable to previous results using wrist-worn ACM-only sensors (31) and combined ACM and EDA sensors (38) which seem to be preferred by

patients (19). A delay of ∼30–40 s seemingly would be sufficient warning to allow caregivers to provide interventions (if they are nearby), e.g., turning patients to minimize postictal respiratory dysfunction, considering that the minimum duration of CS is around 30–40 s (64, 65) and that apnea, bradycardia and oxygen desaturation onset may occur in the postictal phase, ∼50–150 s after the onset of GTCS (66).

The FAR was well-below the endpoint of <2 false alarms per day, with almost half of the patients experiencing no false alarms and only 15% of all the patients experiencing more than 2 false alarms per day. The precision of the Detection Algorithm was relatively low (∼0.15) indicating that around 1 out of 7 alerts was a true seizure; this is an area where continued improvement is needed. There is a very large variance in the prevalence of CS (67), resulting in a very large range of individual precision estimates; thus, the ratio of true alarms to false ones can vary widely (4, 68). This may be a reason why FDA does not include precision, but focuses on sensitivity and FAR for evaluating non-EEG seizures detection systems (29).

The FAR provides a measure of the average frequency of false alarms independently from the frequency of the CS individually experienced by the patients, resulting in an estimate of the potential burden of false alarms in the daily life of the patients and their caregivers.

When comparing the present results with the previous phase II multi-center study using the same sensor set (38), the Sensitivity was slightly higher (0.96 with CI = [0.92, 1.00] in the current study vs. 0.94 with CI = 0.85–0.98). The FAR observed in the previous study when pooling data from the 69 patients was lower (0.2) than the FAR observed in this study (0.83) on all 152 patients. This difference might be ascribed to the much longer duration of the recordings in the present study (429 days vs. 247 days), likely containing more varied motor patterns during longer awake time[6] and a higher absolute and relative number of more active, pediatric patients in the present study (85/152 vs. 24/69 patients). The prior phase III validation of another multimodal seizure detection device based on ACM and PPG (32) reported a Sensitivity of 0.96 (CI = 0.8–1.00) on 22 tonic-clonic seizures and a median FAR of 0.25 per night (CI = 0.04–0.35). However, the system was tested only during nighttime and only on a group of patients that included some of the same people used to develop the algorithm, two conditions that can inflate the algorithm's performance. The present results, both sensitivity and FAR, show improvements over the FDA-pivotal study for a surface-EMG bicep-worn automated seizure detection system (SPEAC; Brain Sentinel), which originally detected 35 of 46 GTC seizures (0.76 with CI = 0.61–0.87) with a FAR of 2.52 per 24 h, and with corrected midline-biceps positioning was improved to detect 29 of 29 GTC seizures (1.00, CI = 0.88–1.00) with a mean FAR of 1.44 per 24 h (35). Another phase III study on a surface-EMG bicep-worn device (EDDI; Ictal Care) reported a sensitivity of 0.938 (30 out of 32 GTC seizures were detected, CI = 0.86–1) with a mean FAR 0.67 per 24 h (33), slightly lower than the FAR observed here but evaluated on much shorter periods (155 days from 71 patients). The present results also showed sensitivity improvements over a previously published phase III study of a wrist-worn ACM-triggered seizure detector (Epi-Care; Danish Care Technology, Sorø, Denmark) evaluated in EMU's that showed a sensitivity of 0.9 (CI = 0.85–1.00) and a FAR of 0.2/day for detecting bilateral tonic-clonic seizures (31). The same device was later evaluated in what was described as a phase IV field study (34), again reporting a median sensitivity of 90% but with a lower average FAR of 0.1/day. Of the patients who completed the latter study (ages 7–72, average = 27), about half were in an institution, 27% used it only at night, and four patients discontinued use because of a high FAR. The use only at night and the removal of participants having a high FAR are adjustments that we did not make in our study, which make the two sets of results less comparable as each of these adjustments generally reduces the FAR. That ambulatory study differs from our study also in that its seizure logs were based on observation, without v-EEG confirmation; these factors raise the possibility that seizures might have been missed both by the device and by human observers. The prospective nature of the present study as well as its longer duration of recordings and validated labels (with both seizure and non-seizure epochs validated separately by three independent experts using only video and EEG while blinded to the wearable data) make it more valuable in terms of providing realistic gold-standard performance estimates.

The comparison between pediatric and adult patients did not show significant differences regarding Sensitivity. The only missed CS, when using the FDA-cleared Detection algorithm, was from a pediatric patient whose convulsions were rather mild (by inspection of the ACM sensors). Our findings are in line with the absence of difference between pediatric and adult seizures reported in the literature. The seizure types used in this work are independent of patient characteristics such as age and gender. In the 11 classifications of epileptic seizures and epilepsy syndromes and revisions by the ILAE, starting in 1964 and ending in 2017 (69), no distinction has been made for tonic-clonic seizures in patients of different gender or age. Very few studies have been published about the differences by age or gender in the EEG or clinical features of CS, and in none of the seizure types we examined has age or gender been identified as a significant factor of differentiation (70–72). Moreover, in the non-EEG-based seizure detection literature, a pivotal trial that was used to clear a motion-based CS detection device for medical use in Europe presented no distinctions in age or gender of patients (31). Differently from the sensitivity, a significant difference for the FAR between the two age groups was observed, even if the performance was in line with the recommended limits (FAR<2) for both subgroups. This may be ascribed to the fact that children are more likely than adults to engage in repetitive, activating motions (like excitedly shaking a dice, dancing, or playing video games, etc.) while in the inpatient EMU, which resulted in a higher number of false alerts. It is worth noticing the high variability of the individual FAR perceived by the patients during their admission in the EMU. Counterintuitively, pediatric

[6]During longer-duration recording periods it is more likely that the patients are not always resting, but are getting up and about, engaging in more diverse activities that trigger more false alarms; thus, the estimation of the FAR when made over longer durations may be higher, even though it is always normalized by the duration.

patients more frequently experienced no false alerts than adults, but at the same time pediatric patients experienced overall more false alerts than adults. Specifically, pediatric patients with FAR higher than 2 outnumbered adult patients. In other words, a few pediatric patients had a very high FAR, which raised the group average FAR.

The comparison between periods of rest and periods of activity showed that the FAR was significantly higher during periods of activity, for both age groups. This was not surprising, as non- seizure motor patterns resembling convulsions (e.g., periodic movements with relatively high frequency) are more likely to happen during periods of activity. During sleep, the number of false alarms was 0, while all seizures except one were correctly recognized. Issuing an alert for real seizures during sleep is fundamental to mitigate the risk of SUDEP (73). Having a precision of 100% during sleep is important to reduce the burden on both caregivers and patients.

To provide a detailed overview on the capability of the Detection Algorithm, results were presented at two different operating points: Active mode, designed to be less sensitive but more specific than FDA-cleared mode, is characterized by a FAR 68% lower than the FDA-cleared one, while keeping the sensitivity slightly lower than the FDA-cleared mode, and most importantly still above the requirement. At a first glance, the advantage of FDA-cleared mode vs. Active mode (i.e., a higher sensitivity) doesn't seem to counterbalance the cost of an increase in the FAR. However, it's worth considering that for applications developed for saving lives, or to prevent serious consequences, as the case of the Detection Algorithm presented here, the cost of type II errors (missed events) is higher than the cost of type I errors (false positives). For the most dangerous context—sleep—the FAR is equivalent (FAR=0 for both operating points), so identifying more CS events becomes the key discriminating factor for the selection of the operating point. Finally, the decrease in the detection time, mostly during sleep, is another important factor that suggests operating the Detection Algorithm at its more sensitive configuration: a timely intervention in the case of a near-SUDEP can dramatically increase the chances to save the patient's life (74). The Embrace system currently allows the user to switch between the FDA-cleared mode and the Active mode, which is suggested during situations in which a lower FAR is desirable. For example, the patient may switch to Active mode when engaging in daytime activities likely to cause false alerts and when they can be sure that their chances of a CS are relatively low, as some patients have certain times of the day or certain phases of a hormonal or other multidien cycles (75) with very low seizure probability.

Limitations

One of the significant strengths of this study is also its most significant limitation: the system has been tested in EMU environments. Its validation for outpatient environments still needs to be fully documented via an appropriately large "phase IV" study, following the recommendations of the scientific community (28, 29). To those recommendations, we have also suggested to add additional criteria that we think are important such as making sure no participants in the test set were used to develop or tune the algorithm, and making sure that there is a high-quality process in place to validate both the presence *and absence* of any seizures in the field, as there is typically no video or EEG when seizures happen in daily-life outpatient settings. Outpatient settings typically involve increased patient movement, which as we saw in the EMU was correlated with higher FAR. In an outpatient setting, if a seizure happens when a patient is alone and a device (with poor sensitivity) does not alert anybody to come, then the seizure may not be noted in a diary and it may not be properly counted as a "missed event." Patients are well-known to underreport CS and thus if the patient is not continuously observed, this can result in a reported sensitivity that is significantly inflated, as the number of undetected CS will be under-reported (14). Preliminary studies, where reliable observers accompanied outpatients continuously to label their data, have shown that the performance of a previous version of the ACM and EDA Detection Algorithm, when evaluated in outpatient settings, has been comparable to the performance in inpatient settings in both short-term and explorative longitudinal analysis (36).

Future Research Directions

Future research goals include further reducing the FAR without reducing the sensitivity of the Detection Algorithm. Future goals also include adding additional modalities to the ACM and EDA to discriminate between epileptic and non-epileptic events (76) and to detect other types of motor epileptic seizures, such as myoclonic seizures [for which a preliminary analysis showed promising results (77)]. The recognition of non-convulsive seizures, e.g., focal seizures, is also a target of growing interest. At present, a clear evidence gap has still to be filled before introducing the automated ambulatory detection of non-convulsive seizures into clinical practice (28, 78, 79). However, promising results using the E4 wristband indicated that this may be possible with a wrist-worn device (80–82). Additionally, advanced post-processing analytics on the peri-ictal periods may provide seizure semiology information, thereby expanding the quality of available patient data. The characterization of the post-ictal phase may also be useful to determine the risk of SUDEP (83); the wearable sensor studied here continuously monitored activity vs. inactivity, sleep/wake, respiration during rest, and sympathetic nervous system function at the time of a recorded "probable SUDEP" where an alert was sent but nobody arrived, and a large surge in EDA occurred (27). Several biomarkers of interest in SUDEP, in seizure-prevention, and other neurological studies can be monitored continuously by a smart watch, particularly if it also measures EDA (59, 60, 84). The development of automated methods for objective risk assessment of the recorded seizures may lead ultimately to a paradigm shift of patient monitoring and outcome assessment in the field of mobile seizure detection (22).

DATA AVAILABILITY STATEMENT

The datasets presented in this article are not readily available because the sensor data recorded on the patients are proprietary of Empatica Inc. The authors can share the data about seizure counts and the output of the Detection Algorithm for each patient upon request to the corresponding

author. Requests to access the datasets should be directed to francesco.onorati.bio@gmail.com.

ETHICS STATEMENT

The studies involving human participants were reviewed and approved by the New England Independent Review Board (WIRB-Copernicus), Needham, MA, US, and the Ethics Committee of Bambino Gesù Children's Hospital, Rome, Italy. Written informed consent to participate in this study was provided by the participants' legal guardian/next of kin.

AUTHOR CONTRIBUTIONS

FO, GR, and RP contributed to the conception and design of the study. WL, AB, JB, PD, RE, TL, FM-T, RS, DF, and JJ contributed to data collection and the labeling of v-EEG data. CC organized the database. FO and GR defined the performance and statistical analysis presented in the paper. FO performed the analysis reported in the Results section. FO and GR wrote the first draft of the manuscript. RP substantially contributed to the revision of the manuscript. All authors contributed to the article and approved the submitted version.

FUNDING

Some of this work was supported by grants from: Epilepsy Foundation, Norman Prince Neurosciences Institute, Brown Institute for Brain Sciences, Epilepsy Research Foundation, American Epilepsy Society, Patient-Centered Outcomes Research Institute (PCORI), Pediatric Epilepsy Research Foundation, Citizens United for Research in Epilepsy (CURE) Foundation, HHV-6 Foundation, Lundbeck, Eisai Ltd, Upsher-Smith Inc., Acorda Therapeutics Inc., and Pfizer Inc. These funders were not involved in the study design, collection, analysis, interpretation of data, the writing of this article or the decision to submit it for publication.

ACKNOWLEDGMENTS

We are grateful to Francesca Coughlin and Sarah Hammond at Boston Childrens Hospital, Sarah Barnard at NYU Langone Medical Center, Kevin Taylor at Emory and Children's Healthcare of Atlanta Hospital (CHOA), Anita Curran at Lifespan and Rhode Island Hospital, for their generous support in helping collect and label v-EEG and wristband data.

SUPPLEMENTARY MATERIAL

The Supplementary Material for this article can be found online at: https://www.frontiersin.org/articles/10.3389/fneur.2021.724904/full#supplementary-material

Supplementary Figure 1 | Timeline of the data collection at each clinical site.

Supplementary Figure 2 | Statistics on rest periods. **(A)** Distribution of the duration of the detected rest periods. **(B)** Distribution of the individual number of rest periods per days of recording.

REFERENCES

1. Cheshire W, Tatum W. *Sudden Unexpected Death in Epilepsy. Epilepsy Board Rev Man Hosp Physician Board Rev Man Epilepsy*. (2016). Available online at: https://pdfs.semanticscholar.org/1cfa/1123568c9c95548dd065f75da0a2e6d9173f.pdf (accessed August 5, 2016).
2. Watkins L, Shankar R. Reducing the risk of sudden unexpected death in epilepsy (SUDEP). *Curr Treat Options Neurol.* (2018) 20:40. doi: 10.1007/s11940-018-0527-0
3. Devinsky O, Hesdorffer DC, Thurman DJ, Lhatoo S, Richerson G. Sudden unexpected death in epilepsy: epidemiology, mechanisms, and prevention. *Lancet Neurol.* (2016) 15:1075–88. doi: 10.1016/S1474-4422(16)30158-2
4. Tomson T, Surges R, Delamont R, Haywood S, Hesdorffer DC. Who to target in sudden unexpected death in epilepsy prevention and how? Risk factors, biomarkers, and intervention study designs. *Epilepsia.* (2016) 57(Suppl. 1):4–16. doi: 10.1111/epi.13234
5. Salas-Puig X, Iniesta M, Abraira L, Puig J. Accidental injuries in patients with generalized tonic-clonic seizures. A multicenter, observational, cross-sectional study (QUIN-GTC study). *Epilepsy Behav EB.* (2019) 92:135-9. doi: 10.1016/j.yebeh.2018.10.043
6. Van Andel J, Zijlmans M, Fischer K, Leijten FS. Quality of life of caregivers of patients with intractable epilepsy. *Epilepsia.* (2009) 50:1294–6. doi: 10.1111/j.1528-1167.2009.02032.x
7. Thompson ME, Langer J, Kinfe M. Seizure detection watch improves quality of life for adolescents and their families. *Epilepsy Behav EB.* (2019) 98:188–94. doi: 10.1016/j.yebeh.2019.07.028
8. Lockman J, Fisher RS, Olson DM. Detection of seizure-like movements using a wrist accelerometer. *Epilepsy Behav.* (2011) 20:638–41. doi: 10.1016/j.yebeh.2011.01.019
9. Kramer U, Kipervasser S, Shlitner A, Kuzniecky R. A novel portable seizure detection alarm system: preliminary results. *J Clin Neurophysiol Off Publ Am Electroencephalogr Soc.* (2011) 28:36–8. doi: 10.1097/WNP.0b013e3182051320
10. Van de Vel A, Cuppens K, Bonroy B, Milosevic M, Jansen K, Van Huffel S, et al. Non-EEG seizure-detection systems and potential SUDEP prevention: state of the art. *Seizure.* (2013) 22:345–55. doi: 10.1016/j.seizure.2013.02.012
11. Beniczky S, Jeppesen J. Non-electroencephalography-based seizure detection. *Curr Opin Neurol.* (2019) 32:198–204. doi: 10.1097/WCO.0000000000000658.aspx
12. Ryvlin P, Beniczky S. Seizure detection and mobile health devices in epilepsy: Update and future developments. *Epilepsia.* (2018) 59:7–8. doi: 10.1111/epi.14088
13. Ryvlin P, Ciumas C, Wisniewski I, Beniczky S. Wearable devices for sudden unexpected death in epilepsy prevention. *Epilepsia.* (2018) 59(Suppl. 1):61–6. doi: 10.1111/epi.14054
14. Karoly P, Goldenholz DM, Cook M. Are the days of counting seizures numbered? *Curr Opin Neurol.* (2018) 31:162–8. doi: 10.1097/WCO.0000000000000533
15. Zhao X, Lhatoo SD. Seizure detection: do current devices work? And when can they be useful? *Curr Neurol Neurosci Rep.* (2018) 18:40. doi: 10.1007/s11910-018-0849-z
16. Simblett SK, Bruno E, Siddi S, Matcham F, Giuliano L, López JH, et al. Patient perspectives on the acceptability of mHealth technology for remote measurement and management of epilepsy: A qualitative analysis. *Epilepsy Behav.* (2019) 97:123–9. doi: 10.1016/j.yebeh.2019.05.035
17. Bruno E, Simblett S, Lang A, Biondi A, Odoi C, Schulze-Bonhage A, et al. Wearable technology in epilepsy: The views of patients, caregivers, and healthcare professionals. *Epilepsy Behav EB.* (2018) 85:141–9. doi: 10.1016/j.yebeh.2018.05.044
18. Van de Vel A, Smets K, Wouters K, Ceulemans B. Automated non-EEG based seizure detection: Do users have a say? *Epilepsy Behav EB.* (2016) 62:121–8. doi: 10.1016/j.yebeh.2016.06.029
19. Hoppe C, Feldmann M, Blachut B, Surges R, Elger CE, Helmstaedter C. Novel techniques for automated seizure registration: Patients' wants and needs. *Epilepsy Behav EB.* (2015) 52:1–7. doi: 10.1016/j.yebeh.2015.08.006

20. Nasseri M, Nurse E, Glasstetter M, Böttcher S, Gregg NM, Nandakumar AL, et al. Signal quality and patient experience with wearable devices for epilepsy management. *Epilepsia.* (2018) [cited (2020). 16:S25–35. doi: 10.1111/epi.16527
21. Chiang S, Moss R, Patel AD, Rao VR. Seizure detection devices and health-related quality of life: A patient- and caregiver-centered evaluation. *Epilepsy Behav.* (2020) 105:106963. doi: 10.1016/j.yebeh.2020.106963
22. Beck M, Simony C, Zibrandtsen I, Kjaer TW. Readiness among people with epilepsy to carry body-worn monitor devices in everyday life: A qualitative study. *Epilepsy Behav.* (2020) 112:107390. doi: 10.1016/j.yebeh.2020.107390
23. Verdru J, Van Paesschen W. Wearable seizure detection devices in refractory epilepsy. *Acta Neurol Belg.* (2020) 120:1271–81. doi: 10.1007/s13760-020-01417-z
24. Leijten FSS. Multimodal seizure detection: A review. *Epilepsia.* (2018) 59(Suppl. 1):42–7. doi: 10.1111/epi.14047
25. van Westrhenen A, De Cooman T, Lazeron RHC, Van Huffel S, Thijs RD. Ictal autonomic changes as a tool for seizure detection: a systematic review. *Clin Auton Res.* (2018) 29:161–81. doi: 10.1007/s10286-018-0568-1
26. Beniczky S, Arbune AA, Jeppesen J, Ryvlin P. Biomarkers of seizure severity derived from wearable devices. *Epilepsia.* (2020) 58:522–30. doi: 10.1111/epi.16492
27. Picard RW, Migliorini M, Caborni C, Onorati F, Regalia G, Friedman D, et al. Wrist sensor reveals sympathetic hyperactivity and hypoventilation before probable SUDEP. *Neurology.* (2017) 89:633–5. doi: 10.1212/WNL.0000000000004208
28. Beniczky S, Wiebe S, Jeppesen J, Tatum WO, Brazdil M, Wang Y, et al. Automated seizure detection using wearable devices: a clinical practice guideline of the international league against epilepsy and the international federation of clinical neurophysiology. *Epilepsia.* (2021) 62:632–46. doi: 10.1111/epi.16818
29. Beniczky S, Ryvlin P. Standards for testing and clinical validation of seizure detection devices. *Epilepsia.* (2018) 59:9–13. doi: 10.1111/epi.14049
30. Bossuyt PM, Reitsma JB, Bruns DE, Gatsonis CA, Glasziou PP, Irwig L, et al. STARD 2015: an updated list of essential items for reporting diagnostic accuracy studies. *BMJ.* (2015) 351:h5527. doi: 10.1136/bmj.h5527
31. Beniczky S, Polster T, Kjaer TW, Hjalgrim H. Detection of generalized tonic-clonic seizures by a wireless wrist accelerometer: A prospective, multicenter study. *Epilepsia.* (2013) 54:e58–61. doi: 10.1111/epi.12120
32. Arends J, Thijs RD, Gutter T, Ungureanu C, Cluitmans P, Van Dijk J, et al. Multimodal nocturnal seizure detection in a residential care setting: A long-term prospective trial. *Neurology.* (2018) 91:e2010–9. doi: 10.1212/WNL.0000000000006545
33. Beniczky S, Conradsen I, Henning O, Fabricius M, Wolf P. Automated real-time detection of tonic-clonic seizures using a wearable EMG device. *Neurology.* (2018) 90:e428–34. doi: 10.1212/WNL.0000000000004893
34. Meritam P, Ryvlin P, Beniczky S. User-based evaluation of applicability and usability of a wearable accelerometer device for detecting bilateral tonic-clonic seizures: A field study. *Epilepsia.* (2018) 59:48–52. doi: 10.1111/epi.14051
35. Halford JJ, Sperling MR, Nair DR, Dlugos DJ, Tatum WO, Harvey J, et al. Detection of generalized tonic-clonic seizures using surface electromyographic monitoring. *Epilepsia.* (2018) 58:1861–9. doi: 10.1111/epi.13897
36. Regalia G, Onorati F, Lai M, Caborni C, Picard RW. Multimodal wrist-worn devices for seizure detection and advancing research: Focus on the Empatica wristbands. *Epilepsy Res.* (2019) 153:79–82. doi: 10.1016/j.eplepsyres.2019.02.007
37. Poh M-Z, Loddenkemper T, Reinsberger C, Swenson NC, Goyal S, Sabtala MC, et al. Convulsive seizure detection using a wrist-worn electrodermal activity and accelerometry biosensor. *Epilepsia.* (2012) 53:e93–7. doi: 10.1111/j.1528-1167.2012.03444.x
38. Onorati F, Regalia G, Caborni C, Migliorini M, Bender D, Poh M-Z, et al. Multicenter clinical assessment of improved wearable multimodal convulsive seizure detectors. *Epilepsia.* (2017) 58:1870–9. doi: 10.1111/epi.13899
39. Saha KK, Miller D, Wang S. A Comparison of Some Approximate Confidence Intervals for a Single Proportion for Clustered Binary Outcome Data. *Int J Biostat.* (2016) 12(2). doi: 10.1515/ijb-2015-0024
40. (k) Premarket Notification [Internet]. Available online at: https://www.accessdata.fda.gov/scripts/cdrh/cfdocs/cfpmn/pmn.cfm?ID=K172935 (accessed June 5, 2021).
41. Haider HA, Esteller R, Hahn CD, Westover MB, Halford JJ, Lee JW, et al. Sensitivity of quantitative EEG for seizure identification in the intensive care unit. *Neurology.* (2016) 87:935–44. doi: 10.1212/WNL.0000000000003034
42. Fisher RS, Cross JH, French JA, Higurashi N, Hirsch E, Jansen FE, et al. Operational classification of seizure types by the International League Against Epilepsy: Position Paper of the ILAE commission for classification and terminology. *Epilepsia.* (2017) 58:522–30. doi: 10.1111/epi.13670
43. Faris O, Shuren J. An FDA viewpoint on unique considerations for medical-device clinical trials. Drazen JM, Harrington DP, McMurray JJV, Ware JH, Woodcock J, editors. *N Engl J Med.* (2017) 376:1350–7. doi: 10.1056/NEJMra1512592
44. *Design Considerations for Pivotal Clinical Investigations for Medical Devices*. (2019). Available online at: https://www.fda.gov/regulatory-information/search-fda-guidance-documents/design-considerations-pivotal-clinical-investigations-medical-devices (accessed November 5, 2019).
45. Pudil P, Novovičová J, Kittler J. Floating search methods in feature selection. *Pattern Recognit Lett.* (1994) 15:1119–25. doi: 10.1016/0167-8655(94)90127-9
46. Onorati F, Regalia G, Caborni C, Migliorini M, Picard R. *Improving Convulsive Seizure Detection by Exploiting Data From Outpatient Settings Using the Embrace Wristband*. New York, NJ (2016).
47. Regalia G, Gerboni G, Migliorini M, Lai M, Pham J, Puri N, et al. Sleep assessment by means of a wrist actigraphy-based algorithm: agreement with polysomnography in an ambulatory study on older adults. *Chronobiol Int.* (2020) 38:400–14. doi: 10.1080/07420528.2020.1835942
48. Fleiss JL, Levin B, Paik MC. *Statistical Methods for Rates and Proportions. 3rd ed*. Hoboken, NJ: J. Wiley (2003).
49. Davison AC, Hinkley DV. *Bootstrap Methods and their Application*. (1997). Available online at: /core/books/bootstrap-methods-and-their-application/ED2FD043579F27952363566DC09CBD6A (accessed December 22, 2017).
50. Rutter CM. Bootstrap estimation of diagnostic accuracy with patient-clustered data. *Acad Radiol.* (2000) 7:413–9. doi: 10.1016/S1076-6332(00)80381-5
51. Ren S, Lai H, Tong W, Aminzadeh M, Hou X, Lai S. Nonparametric bootstrapping for hierarchical data. *J Appl Stat.* (2010) 37:1487–98. doi: 10.1080/02664760903046102
52. Altman DG, Machin D, Bryant T, Garnder MJ. *Statistics With Confidence*. London: Britsh Medical Journal (2000). p. 254.
53. Wilson EB. Probable inference, the law of succession, and statistical inference. *J Am Stat Assoc.* (1927) 22:209–12. doi: 10.1080/01621459.1927.10502953
54. Chew V. Point estimation of the parameter of the binomial distribution. *Am Stat.* (1971) 25:47. doi: 10.2307/2686085
55. Fawcett T. An introduction to ROC analysis. *Pattern Recognit Lett.* (2006) 27:861–74. doi: 10.1016/j.patrec.2005.10.010
56. Biswas B. Study design and analysis issues for diagnostic monitoring devices. In: *Proceedings of Joint Statistical Meeting 2015 Aug*; Seattle, CA, United States. Boston, MA: Cengage Learning p. 261–8.
57. Sofaer HR, Hoeting JA, Jarnevich CS. The area under the precision-recall curve as a performance metric for rare binary events. McPherson J, editor. *Methods Ecol Evol.* (2019) 10:565–77. doi: 10.1111/2041-210X.13140
58. Rosner B. *Fundamentals of Biostatistics*. Boston: Cengage Learning (2016).
59. Poh M-Z, Loddenkemper T, Reinsberger C, Swenson NC, Goyal S, Madsen JR, et al. Autonomic changes with seizures correlate with postictal EEG suppression. *Neurology.* (2012) 78:1868–76. doi: 10.1212/WNL.0b013e318258f7f1
60. Sarkis RA, Thome-Souza S, Poh M-Z, Llewellyn N, Klehm J, Madsen JR, et al. Autonomic changes following generalized tonic clonic seizures: An analysis of adult and pediatric patients with epilepsy. *Epilepsy Res.* (2015) 115:113–8. doi: 10.1016/j.eplepsyres.2015.06.005
61. Beniczky S, Karoly P, Nurse E, Ryvlin P, Cook M. Machine learning and wearable devices of the future. *Epilepsia.* (2020) 62(Suppl. 2):S116–24. doi: 10.1111/epi.16555
62. Abbasi B, Goldenholz DM. Machine learning applications in epilepsy. *Epilepsia.* (2019) 60:2037–47. doi: 10.1111/epi.16333

63. Shah P, Kendall F, Khozin S, Goosen R, Hu J, Laramie J, et al. Artificial intelligence and machine learning in clinical development: a translational perspective. *Npj Digit Med.* (2019) 2:1–5. doi: 10.1038/s41746-019-0148-3
64. Jenssen S, Gracely EJ, Sperling MR. How long do most seizures last? A systematic comparison of seizures recorded in the epilepsy monitoring unit. *Epilepsia.* (2006) 47:1499–503. doi: 10.1111/j.1528-1167.2006.00622.x
65. Pan S, Wang F, Wang J, Li X, Liu X. Factors influencing the duration of generalized tonic-clonic seizure. *Seizure.* (2016) 34:44–7. doi: 10.1016/j.seizure.2015.11.008
66. Ryvlin P, Nashef L, Lhatoo SD, Bateman LM, Bird J, Bleasel A, et al. Incidence and mechanisms of cardiorespiratory arrests in epilepsy monitoring units (MORTEMUS): a retrospective study. *Lancet Neurol.* (2013) 12:966–77. doi: 10.1016/S1474-4422(13)70214-X
67. Chen E, Sajatovic M, Liu H, Bukach A, Tatsuoka C, Welter E, et al. Demographic and clinical correlates of seizure frequency: findings from the managing epilepsy well network database. *J Clin Neurol Seoul Korea.* (2018) 14:206–11. doi: 10.3988/jcn.2018.14.2.206
68. Thomas SV, Koshy S, Nair CRS, Sarma SP. Frequent seizures and polytherapy can impair quality of life in persons with epilepsy. *Neurol India.* (2005) 53:46–50. doi: 10.4103/0028-3886.15054
69. Scheffer IE, Berkovic S, Capovilla G, Connolly MB, French J, Guilhoto L, et al. ILAE classification of the epilepsies: Position paper of the ILAE commission for classification and terminology. *Epilepsia.* (2017) 58:512–21. doi: 10.1111/epi.13709
70. Pavlova M, Singh K, Abdennadher M, Katz ES, Dworetzky BA, White DP, et al. Comparison of cardiorespiratory and EEG abnormalities with seizures in adults and children. *Epilepsy Behav EB.* (2013) 29:537–41. doi: 10.1016/j.yebeh.2013.09.026
71. Asadi-Pooya AA, Emami M, Sperling MR. Age of onset in idiopathic (genetic) generalized epilepsies: clinical and EEG findings in various age groups. *Seizure.* (2012) 21:417–21. doi: 10.1016/j.seizure.2012.04.004
72. Widdess-Walsh P, Dlugos D, Fahlstrom R, Joshi S, Shellhaas R, Boro A, et al. Lennox-Gastaut syndrome of unknown cause: phenotypic characteristics of patients in the Epilepsy Phenome/Genome Project. *Epilepsia.* (2013) 54:1898–904. doi: 10.1111/epi.12395
73. Sveinsson O, Andersson T, Mattsson P, Carlsson S, Tomson T. Clinical risk factors in SUDEP: A nationwide population-based case-control study. *Neurology.* (2020) 94:e419–29. doi: 10.1212/WNL.0000000000008741
74. Seyal M, Bateman LM, Li C-S. Impact of periictal interventions on respiratory dysfunction, postictal EEG suppression, and postictal immobility. *Epilepsia.* (2013) 54:377–82. doi: 10.1111/j.1528-1167.2012.03691.x
75. Baud MO, Kleen JK, Mirro EA, Andrechak JC, King-Stephens D, Chang EF, et al. Multi-day rhythms modulate seizure risk in epilepsy. *Nat Commun.* (2018) 9:88. doi: 10.1038/s41467-017-02577-y
76. Zsom A, LaFrance WC, Blum AS, Li P, Wahed LA, Shaikh MA, et al. Ictal autonomic activity recorded via wearable-sensors plus machine learning can discriminate epileptic and psychogenic nonepileptic seizures. In: *2019 41st Annual International Conference of the IEEE Engineering in Medicine and Biology Society (EMBC)*. (2019). p. 3502-6. doi: 10.1109/EMBC.2019.8857552
77. Onorati F, Babilliot L, Regalia G, El Atrache R, Picard R. *Wrist Accelerometry-Based Detection of Nocturnal Myoclonic Seizures*. Lausanne (2019).
78. Bruno E, Viana PF, Sperling MR, Richardson MP. Seizure detection at home: Do devices on the market match the needs of people living with epilepsy and their caregivers? *Epilepsia.* (2020) 61(Suppl. 1):S11–24. doi: 10.1111/epi.16521
79. Ryvlin P, Cammoun L, Hubbard I, Ravey F, Beniczky S, Atienza D. Noninvasive detection of focal seizures in ambulatory patients. *Epilepsia.* (2020) 61:547–54. doi: 10.1111/epi.16538
80. Atrache RE, Tamilia E, Touserkani FM, Hammond S, Papadelis C, Kapur K, et al. Photoplethysmography: A measure for the function of the autonomic nervous system in focal impaired awareness seizures. *Epilepsia.* (2020) 61:1617–26. doi: 10.1111/epi.16621
81. Böttcher S, Manyakov NV, Epitashvili N, Folarin A, Richardson MP, Dümpelmann M, et al. Using multimodal biosignal data from wearables to detect focal motor seizures in individual epilepsy patients. In: *Proceedings of the 6th international Workshop on Sensor-based Activity Recognition and Interaction [Internet]*. Rostock: ACM (2019).
82. Tang J, El Atrache R, Yu S, Asif U, Jackson M, Roy S, et al. Seizure detection using wearable sensors and machine learning: Setting a benchmark. *Epilepsia.* (2021). doi: 10.1111/epi.16967. [Epub ahead of print].
83. Ryvlin P, Rheims S, Lhatoo SD. Risks and predictive biomarkers of sudden unexpected death in epilepsy patient. *Curr Opin Neurol.* (2019) 32:205–12. doi: 10.1097/WCO.0000000000000668
84. Johnson KT, Picard RW. Advancing neuroscience through wearable devices. *Neuron.* (2020) 108:8–12. doi: 10.1016/j.neuron.2020.09.030

Conflict of Interest: FO, GR, and CC are shareholders of Empatica Inc., which manufactured two of the devices used in this work and developed the two new algorithms tested in this work. GR is also an employee of Empatica and RP is also a consultant and chairs the board of directors for Empatica. TL is part of pending patent applications to detect and predict seizures and to diagnose epilepsy with devices different from the ones used in this work and has received research support from Empatica to conduct this research. TL, WL, and AB have received sensors from Empatica to perform the reported research.

The remaining authors declare that the research was conducted in the absence of any commercial or financial relationships that could be construed as a potential conflict of interest.

Publisher's Note: All claims expressed in this article are solely those of the authors and do not necessarily represent those of their affiliated organizations, or those of the publisher, the editors and the reviewers. Any product that may be evaluated in this article, or claim that may be made by its manufacturer, is not guaranteed or endorsed by the publisher.

frontiers in Neurology

ORIGINAL RESEARCH
published: 23 August 2021
doi: 10.3389/fneur.2021.713794

Seizure Forecasting Using a Novel Sub-Scalp Ultra-Long Term EEG Monitoring System

Rachel E. Stirling[1,2†], Matias I. Maturana[1,3†], Philippa J. Karoly[1,2], Ewan S. Nurse[1,3], Kate McCutcheon[1], David B. Grayden[2,3], Steven G. Ringo[4], John M. Heasman[4,5], Rohan J. Hoare[4], Alan Lai[3,6], Wendyl D'Souza[3,6], Udaya Seneviratne[3,7,8], Linda Seiderer[6], Karen J. McLean[4,6], Kristian J. Bulluss[3,6], Michael Murphy[3,6], Benjamin H. Brinkmann[9], Mark P. Richardson[10], Dean R. Freestone[1] and Mark J. Cook[1,2,3,4]*

[1] Seer Medical Pty Ltd, Melbourne, VIC, Australia, [2] Department of Biomedical Engineering, The University of Melbourne, Melbourne, VIC, Australia, [3] Department of Medicine at St. Vincent's Hospital Melbourne, The University of Melbourne, Fitzroy, VIC, Australia, [4] Epi-Minder Pty. Ltd., Melbourne, VIC, Australia, [5] Cochlear Limited, Sydney, NSW, Australia, [6] Department of Neuroscience, St. Vincent's Hospital Melbourne, Fitzroy, VIC, Australia, [7] Department of Neuroscience, Monash Medical Centre, Melbourne, VIC, Australia, [8] Department of Medicine, School of Clinical Sciences at Monash Health, Monash University, Melbourne, VIC, Australia, [9] Bioelectronics Neurophysiology and Engineering Lab, Department of Neurology, Mayo Clinic, Rochester, MN, United States, [10] School of Neuroscience, Institute of Psychiatry, Psychology and Neuroscience, King's College London, London, United Kingdom

OPEN ACCESS

Edited by:
Vikram Rao, University of California, San Francisco, United States

Reviewed by:
Daniel Friedman, NYU Grossman School of Medicine, United States
Sydney S. Cash, Massachusetts General Hospital and Harvard Medical School, United States

***Correspondence:**
Matias I. Maturana
matiasim@unimelb.edu.au

[†] *These authors share first authorship*

Specialty section:
This article was submitted to Epilepsy, a section of the journal Frontiers in Neurology

Received: *24 May 2021*
Accepted: *27 July 2021*
Published: *23 August 2021*

Citation:
Stirling RE, Maturana MI, Karoly PJ, Nurse ES, McCutcheon K, Grayden DB, Ringo SG, Heasman JM, Hoare RJ, Lai A, D'Souza W, Seneviratne U, Seiderer L, McLean KJ, Bulluss KJ, Murphy M, Brinkmann BH, Richardson MP, Freestone DR and Cook MJ (2021) Seizure Forecasting Using a Novel Sub-Scalp Ultra-Long Term EEG Monitoring System. Front. Neurol. 12:713794. doi: 10.3389/fneur.2021.713794

Accurate identification of seizure activity, both clinical and subclinical, has important implications in the management of epilepsy. Accurate recognition of seizure activity is essential for diagnostic, management and forecasting purposes, but patient-reported seizures have been shown to be unreliable. Earlier work has revealed accurate capture of electrographic seizures and forecasting is possible with an implantable intracranial device, but less invasive electroencephalography (EEG) recording systems would be optimal. Here, we present preliminary results of seizure detection and forecasting with a minimally invasive sub-scalp device that continuously records EEG. Five participants with refractory epilepsy who experience at least two clinically identifiable seizures monthly have been implanted with sub-scalp devices (Minder®), providing two channels of data from both hemispheres of the brain. Data is continuously captured via a behind-the-ear system, which also powers the device, and transferred wirelessly to a mobile phone, from where it is accessible remotely via cloud storage. EEG recordings from the sub-scalp device were compared to data recorded from a conventional system during a 1-week ambulatory video-EEG monitoring session. Suspect epileptiform activity (EA) was detected using machine learning algorithms and reviewed by trained neurophysiologists. Seizure forecasting was demonstrated retrospectively by utilizing cycles in EA and previous seizure times. The procedures and devices were well-tolerated and no significant complications have been reported. Seizures were accurately identified on the sub-scalp system, as visually confirmed by periods of concurrent conventional scalp EEG recordings. The data acquired also allowed seizure forecasting to be successfully undertaken. The area under the receiver operating characteristic curve (AUC score) achieved (0.88), which is comparable to the best score in recent, state-of-the-art forecasting work using intracranial EEG.

Keywords: seizure, seizure cycles, seizure forecasting, epilepsy, implantable device, sub scalp

INTRODUCTION

For people with epilepsy, an estimation of total seizure burden is fundamental to clinical management as well as for the evaluation of new therapies, such as drugs or devices. For over a century, clinicians have relied on their patients' reports of their seizure frequency, "that it may be taken as an index of the severity of the epileptic condition" (1). Although the rate of clinical seizures influences an individual's perception of disease severity, the physiological basis for this remains ambiguous (2, 3). Indeed, the number of clinical seizures is not representative of (nor closely correlated with) the total seizure burden (4). Rates of subclinical epileptiform activity seen on electroencephalography (EEG) are typically orders of magnitude higher than clinical seizures. These subclinical events may impact cognition (5, 6) and quality of life, and are important in epilepsy diagnosis and treatment, particularly for syndromes that are characterized by stereotypical discharges. Interictal epileptiform activity is also relevant for surgical planning (7) and forecasting seizure likelihood (8). Therefore, capturing both clinical and subclinical events, and interictal epileptiform activity, is important for the clinical management of epilepsy. Henceforth, we define Epileptiform Activity (EA) as interictal and ictal epileptic activity, comprising interictal discharges and electrographic events (clinical and subclinical). Often we specify "interictal EA," which refers to interictal epileptiform discharges only.

The easiest and most common method of capturing clinical seizure events is through patient self-reporting. Unfortunately, the accuracy of self-reported events is unreliable (9, 10). In addition to unawareness of subclinical events, patients are often unaware or forgetful of their clinical seizures, and may also report other non-epileptic symptoms as seizures. As there have been no real alternatives, seizure diaries (both paper and electronic) are used almost exclusively to manage patients, and regulatory authorities assess new treatments primarily on evidence from diaries (11). It is possible that the unreliability of self-reporting has impeded progress in the development of anti-seizure medications (12). In addition to inaccurate records of seizure frequency, people with epilepsy and caregivers typically cannot provide an objective assessment of the time of seizure onset, seizure duration or seizure type (11). This detailed information about seizures is important for patient management, particularly with regard to medication titration and safety. For this reason, capturing EEG correlates of seizures remains the reference standard in clinical epilepsy management.

Short-term (up to 10 days) inpatient video-EEG assessment can be used to assess treatment efficacy, for surgical planning, and has been proposed as an objective metric for randomized controlled trials. However, short-term monitoring has major limitations. The spatiotemporal organization of interictal EA, including epileptiform spikes and high frequency oscillations (HFOs), changes over long time scales (months to years), so short-term capture of interictal EA is unreliable (13, 14). In addition, seizure rates show high natural variability and require long-term recording to identify clinically relevant improvements (15, 16). Short-term monitoring is particularly inadequate for people with lower seizure frequencies and cannot detect multiday cycles of interictal EA that occur in most individuals (17, 18).

Ultra-long term monitoring is required for better diagnosis, management and treatment of epilepsy, including seizure forecasting. Currently, scalp EEG is not suitable for ultra-long term monitoring due to limited data quality and the need for external electrode maintenance (19). Invasive intracranial systems, such as the RNS System (NeuroPace) and the Percept PC (Medtronic), are available but are built for neurostimulation, do not store sufficient data and are too invasive for diagnostic applications (19). Alternatively, sub-scalp EEG systems are minimally-invasive tools that may address the need for objective ultra-long term EEG recordings (19, 20), allowing for personalized and accurate epilepsy management.

Our earlier work with an implantable intracranial device (4) demonstrated that continuous EEG permitted characterization of EEG features (21, 22), epileptic activity (18, 23) and sleep (24, 25), and enabled successful seizure forecasting (26–28). As similar data could be acquired from a less invasive (sub-scalp) EEG recording system, we have developed a minimally invasive device that is inserted into a sub-scalp location to continuously record EEG. This work reports on the feasibility of the system to detect interictal EA and seizures in five subjects. Therefore, the primary aim of this manuscript was to report on the preliminary results of interictal EA and seizure detection using the sub-scalp device, and to qualitatively compare these recordings to reference-standard 7-day ambulatory video-EEG monitoring. As a secondary aim, we also present a case study to illustrate the potential for seizure forecasting using sub-scalp EEG. The case study provides a proof-of-concept on how cycles can be derived from event detections in the EEG and how these cycles can be used to forecast epileptic seizures. The presented forecasting method builds on previous work in seizure cycles (20, 29–31) and interictal EA cycles (17, 18, 32).

MATERIALS AND METHODS

Patient Selection and Criteria

Data used in this work were acquired during a registered trial (ACTRN 12619001587190). Subjects participating in the Minder® sub-scalp system (**Table 1**) trial were 18-75 years of age at the time of implantation, had an established clinical diagnosis of epilepsy (33) with a minimum of two clinically identifiable epileptic seizure events per month, and otherwise were medically and neurologically stable as defined by their clinician. All participants had EEG profiles that were consistent with epilepsy diagnosis, and had prior neuroimaging. Subjects were excluded if they had a neurostimulation implant device for epilepsy or another condition, or had any other condition that may impact the study outcome or safety of the device.

All participants wore the sub-scalp system for at least 8 months during both wake and sleep. Subjects were also expected to maintain a seizure diary, if necessary with the assistance of a caregiver, and attend regular study appointments. All participants gave written, informed consent and the study protocol was approved by St Vincent's Hospital Melbourne Human Research Ethics Committee (HREC 063/15).

TABLE 1 | Participant demographics.

Participant	Gender	Age (years)	Epilepsy type	Epilepsy etiology	Seizure onset localization	Seizure types	Antiepileptic medications
1	F	49	Multifocal	Periventricular nodular heterotopia	Multifocal	Focal impaired Aware-ness	Lacosamide sodium Valproate, Pregabalin, Brivaracetam
2	M	60	Focal	Cortical dysplasia	Right temporo-parietal junction	Focal impaired Aware-ness	Carbamazepine, Lacosamide
4	F	44	Focal	Hypothalamic hamartoma	Hypo-thalamus	Focal impaired Aware-ness	Carbamazepine, Brivaracetam, Phenobarbital, Clonazepam
5	F	47	Focal	Non-lesional temporal lobe epilepsy	Right temporal lobe	Focal impaired aware-ness	Lamotrigine
6	M	45	General-ized	Genetic generalized epilepsy	Generalized	Absence, general-ized tonic-clonic	Sodium valproate, levetiracetam, lamotrigine, zonisamide

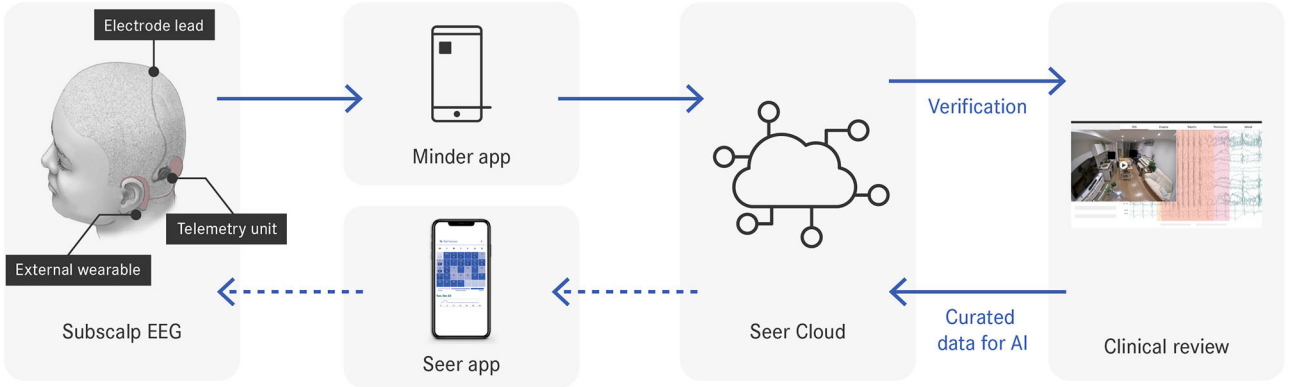

FIGURE 1 | Data flow throughout the system. Dotted arrows indicate system components under development.

Implantable System

The Minder® sub-scalp system (Epi-Minder Pty Ltd) is an investigational device comprising an implanted device, which communicates with an external wearable unit, a mobile phone and a secure cloud (**Figure 1**). The implanted device is positioned under the scalp, with a small burrhole to recess the telemetry device and includes an electrode array that is passed superiorly with two contacts located over each parietal bone. The electrodes record differential EEG signals across two contacts at 250 Hz, which are captured by the telemetry unit. The telemetry unit communicates with an external behind-the-ear (BTE) processor via an inductive radio frequency (RF) link, which allows data and power transfer between the external wearable device and the implant. The BTE processor communicates with a mobile phone via Bluetooth. The mobile phone application (Minder app) facilitates the transfer of EEG data from the implant to the phone, and ultimately to a secure cloud for processing. The Minder app also captures audio and accelerometry data from the phone and stores it together with the EEG data in the Seer Cloud (Seer Medical Pty Ltd). Data captured by the implanted device is reviewed and curated on the Seer Cloud platform. Curated events are used for training a machine learning algorithm that detects EA and whose output is used for seizure forecasting. In future, seizure forecasting will be delivered to patients through the Seer App.

Surgical Procedure and Follow Up Assessments

The device is implanted under general anesthetic in a specific position for the implanted receiver located in the mastoid bone. The electrode array is passed subcutaneously and over the pericranium, posterior to the vertex and over the parietal regions. The location of the sub-scalp electrode was chosen to optimize EA detection rates (modeling from scalp data indicated this produced the highest yield of event capture) and minimize artifact from nearby temporalis muscles. The surgical procedure for implantation of the Minder implant housing and coil was modeled closely on that used for commercial cochlear implants. Regular check-ups (every 2–6 weeks) were conducted in person and participants communicated with

study doctors and coordinators between in-person visits. In addition, 7-day scalp EEG was performed at weeks 4 and 24 after implantation. The scalp EEG recordings consisted of a standard 10–20 electrode placement with an additional four scalp electrodes placed as close as practically feasible to the underlying implanted sub-scalp electrodes. The purpose of the scalp EEG assessment was to compare the sub-scalp EEG signal to the scalp EEG, particularly during seizures and interictal EA, and as well activities including sleep, and potential sources of artifact. Subjects were asked to keep their seizure diaries during monitoring so that the three modalities of seizure detection (sub-scalp implant, scalp EEG and seizure diary) could be compared.

Epileptic Activity Detection

For both sub-scalp EEG and ambulatory EEG, the detection of EA was aided by a machine learning algorithm designed to detect relevant events in the EEG (34, 35). The algorithm was designed to label suspect EA with high sensitivity to ensure that all interictal and ictal events were detected.

EEG recordings and suspect events highlighted by the algorithm were accessed from the cloud through an online portal and reviewed by expert neurophysiologists, who marked interictal EA and seizures. Interictal EA marked by the neurophysiologists consisted of typical epileptiform EEG activity such as spike discharges. EEG seizures consisted of EEG activity substantially larger than background and lasting a minimum of 10 s. Seizure morphologies were first confirmed in each participant by observing correlated seizures in the ambulatory scalp video-EEG, however ambulatory scalp EEG and sub-scalp EEG were reviewed independently when compared qualitatively in this manuscript.

Seizure Forecasting Case Study

In this case study, we demonstrate the potential for forecasting using sub-scalp EEG in participant 1. This participant was chosen because of their comparatively larger amount of reviewed data and high seizure count relative to the other participants.

This retrospective case study was designed using training and testing datasets. To train the forecasting algorithm, we utilized cycles in both machine-detected suspect events and manually confirmed electrographic seizures to forecast seizure likelihood per hour. During testing, the forecaster attempted to predict human confirmed electrographic seizures.

Data Pre-processing and Feature Extraction

Two features were incorporated into the forecaster: significant cycles based on rates of machine-detected events and significant cycles based on seizures. To compute event-based cycles, we used a similar approach to a previously published method for extracting rhythms of EA (17). Briefly, a Morlet wavelet transform was computed on the z-standardized hourly event rates to produce a global wavelet spectrum of power for each scale (cycle period). The cycle periods considered were every 1.2 h between 2.4 and 31.2 h, every 2.4 h between 33.6 and 48 h, every 4.8 h between 52.8 and 4 days and every 12 h between 5 days and up to a maximum period of a quarter of the recording duration. At least four cycle periods had to be present to confirm a cycle. Peaks in the wavelet spectrum were found by comparing neighboring values. Peaks above the global significance (99% confidence) level were determined to be significant EA cycle periods using a time-averaged significance test (36).

Once significant cycle periods were computed, event rates were filtered at each significant cycle period using a zero-order Butterworth bandpass filter. The bandpass filter used cut-off frequencies at ±33% of the cycle frequency [consistent with (17)]. These cut-off frequencies were chosen to account for phase shifts in the cycle over the recording time. To account for bandpass overlap in significant cycle frequencies, we introduced a sparsity criterion whereby only the strongest peak (greatest power in the wavelet spectrum) within any cycle's bandpass filter pass band was considered. The instantaneous phase of the cycle at each timepoint was then estimated using a Hilbert transform. Filtered cycles in event rates were used as features for the forecaster if seizures were significantly phase-locked to the cycle [$p < 0.05$, according to the omnibus/Hodges-Ajne test for circular uniformity (37)].

Cycles in seizure times were detected using a similar approach to our previous work (29, 38). We assessed the phase locking of seizure times to a range of possible cycles using both the Omnibus test ($p < 0.05$) and the synchronization index (SI $\geq$ 0.4) value to quantify phase locking. The SI value–a measure of the magnitude of the resultant vector–ranges from 0 to 1, where 0 represents a perfectly uniform circular distribution and 1 represents perfect alignment with respect to an underlying cycle (30). To account for multiple cycle periods meeting the criteria within close proximity, we used only the strongest cycle period (based on the highest SI value) within ±33% of any other cycle period.

All features were transformed from cyclical to linear features by normalizing the signals from 0 to 2π and computing the sine and cosine of the normalized signal.

TABLE 2 | Clinically relevant EEG events during the two 7-day EEG sessions.

Participant	Interictal EA discharges	Seizures	Patient reported seizures (confirmed events)
1	S1: 1476	S1: 27	S1: 7 (6)
	S2: 5981	S2: 17	S2: 1 (1)
2*	S1: 245	S1: 3	S1: 6 (0)
4	S1: 179	S1: 3	S1: 4 (3)
	S2: 52	S2: 0	S2: 0
5	S1: 519	S1: 0	S1: 3 (0)
	S2: 110	S2: 0	S2: 0
6	S1: 5783	S1: 5	S1: 1 (0)
	S2: 2084	S2: 0	S2: 0

Confirmed events are seizures confirmed through clinical review.
S1 - 7-day monitoring at 4 weeks post-implant.
S2 - 7-day monitoring at 24 weeks post-implant.
**: Note participant 2 did not have monitoring at 24 weeks.*

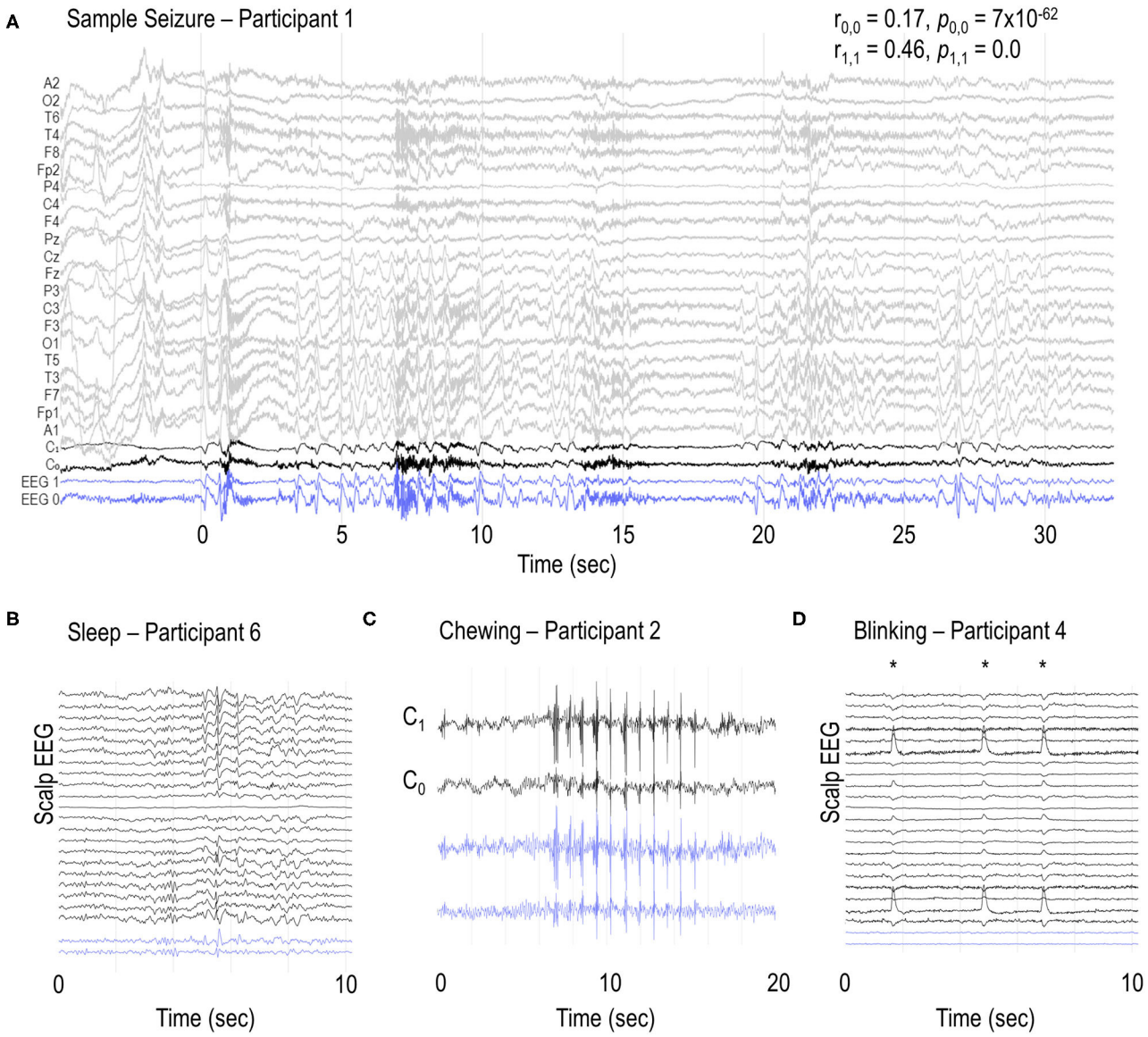

FIGURE 2 | Sample EEG recordings. **(A)** Sample seizure in participant 1 and examples of **(B)** vertex waves and spindles during sleep, **(C)** chewing and **(D)** blinking artifacts (*) in participants 6, 2 and 4, respectively. C_0 and C_1 channels represent the bipolar recordings from the additional scalp electrodes placed over the sub-scalp electrodes. Blue traces (EEG 0 and EEG 1) represent the sub-scalp recordings. $r_{0,0}$ and $r_{1,1}$ represent the Pearson correlation coefficient between C_0 and EEG 0, and C_1 and EEG 1, respectively. $p_{0,0}$ and $p_{1,1}$ represent the respective p values. Ambulatory scalp EEG and sub-scalp EEG recordings were reviewed independently.

Forecasting Algorithm

To forecast the likelihood of a seizure on an hourly basis, we used an ensemble machine learning algorithm that combined a random forest (RF) regressor and a logistic regression (LR) classifier. The output of the model was the final likelihood of a seizure (risk value), which was represented as a continuous value between 0 for no seizure and 1 for a guaranteed seizure within the next hour. Note that a likelihood was given every hour based on "clock hours" (e.g., 12 a.m., 1 a.m., etc) rather than just an arbitrary moving time window.

The RF regressor with the bootstrap aggregating technique was trained on all features. In the model, the number of decision trees was 80 and the minimum number of samples required to be at a leaf node was 15. From observation, these model parameters achieved the highest accuracy on the training dataset. Since seizures typically account for <1% of daily life (4), the dataset is usually imbalanced, with non-seizure hours occurring far more frequently than seizure hours. RF models typically performed better on balanced datasets (39), so oversampling of seizure hours was undertaken before training the RF model. The output of the RF model was used as an input to the LR classifier. The LR

classifier was trained on all features, including the output of the RF model. For simplicity, the default logistic regression model was used from Python's *sklearn* library. The output of the LR model was the final likelihood of a seizure (risk value) within the next hour.

Using the likelihood values, the forecaster classified hours as either low, medium or high risk. The medium and high risk cut-off thresholds were computed by optimizing (26):

(C1) time spent in low risk > time spent in medium risk > time spent in high risk;

(C2) seizures in high risk > seizures in medium risk > seizures in low risk;

If C1 or C2 could not be satisfied, the optimisation algorithm maximized the product of the time in low risk and the number of seizures in high risk (C3 and C4):

(C3) maximize the time spent in a low risk state;

(C4) maximize the number of seizures occurring in the high risk state.

Note that the likelihood is distinct from a traditional probability value where all outcomes sum to 1. This distinction is caused by oversampling the seizure class in the RF model, which generates synthetic seizure-hours such that the number of seizure hours is equal to the number of non-seizure hours. The result is that the likelihood values are higher than the true probability values.

Training and Testing Datasets

After preprocessing and feature extraction, the dataset was split into training and testing datasets. Initial algorithm training occurred using seizures captured over the first 14 days (15 seizures) but using cycles derived from the entire dataset. After the initial training, re-training occurred after each new seizure was observed. Re-training occurred on all past data, which recomputed the algorithm coefficients and risk thresholds for future predictions.

All analyses were executed in Python (version 3.7.9) using pandas (v1.2.0), numpy (v1.19.2), matplotlib (v3.3.2), datetime (v3.7.9), scipy (v1.5.2), pycwt (v0.3.0), sklearn (0.23.1), imblearn (v0.6.2) and pycircstat (v0.0.2) libraries.

RESULTS

The surgical procedure and devices were well tolerated. No significant complications have been reported in the five participants. Overnight use of the system was well tolerated and the BTE processor was worn either on the ear or attached to the clothing during sleep. The 7-day EEG recordings revealed interictal EA in all participants and seizures in four of the five participants (**Table 2**).

Seizures were identified on the sub-scalp system, as confirmed by periods of concurrent conventional scalp EEG recordings (**Figure 2A**). Many other neurological events and artifacts were also present in the sub-scalp recordings. In all participants, clear sleep-related transients were visible in the sub-scalp recordings (**Figure 2B**). Head scratching and muscular artifacts, such as chewing or jaw clenching artifacts, typically appeared very large across the sub-scalp recordings (**Figure 2C**), while other artifacts, such as blinking, were largely invisible (**Figure 2D**).

Seizure Forecasting Case Study

We conducted a proof-of-principle analysis of seizure forecasting for Participant 1. This participant had a total of 134 seizures over a 6 month period. **Figure 3A** shows the hourly rate of detected events from a machine learning algorithm (see Methods: epileptic activity detection) over the 6 month period. Shaded blue regions represent the two 7-day EEG sessions recorded at weeks 4 and 24. The purple region represents an extended period where data was not collected (device was removed). Note that the device was removed during this period to undertake a physical examination of the scalp for any changes to the skin before reapplication of the system, as part of our safety assessment process.

Figure 3A highlights the presence of multi day cycles (approximately monthly). The hourly event counts were used to identify significant periodic cycles ranging from 12 h to 40 days, as shown in the wavelet spectrum in **Figure 3B**. Confirmed seizures were only phased locked to some of these cycles (quantified by significant SI values). Two examples of seizure phase locking to cycles of hourly event count (18 days and 29 days) are shown (**Figures 3C,D**).

A practical forecaster minimizes the amount of time the forecaster displays a high risk warning while maximizing the number of seizures occurring during high risk. Alternatively, an opposite, suboptimal forecaster would always show high risk, achieving perfect predictive performance but of no utility to the end-user. **Figure 3E** demonstrates seizure likelihood over 6 months in participant 1, where risk levels have been optimized to be of highest utility to the user. The likelihood trace peaks in a cyclical manner, with seizures typically occurring close to the peaks (**Figure 3F**). The participant had 134 seizures during this period, 15 of which occurred in the first 14 days (initial training phase) and 119 of which occurred during the testing period.

The time spent in low, medium and high risk warnings and seizures that occured during these periods are given in **Table 3** for the testing phase. The distribution of seizure likelihoods can also be visualized in **Figure 3G**. The forecast resulted in the participant spending 26% of time in a high risk state, 11% of time in a medium risk state and 63% of time in a low risk state. Of 119 testing seizures, 99 (83%) occurred during high risk, 8 (7%) occurred during medium risk and 12 (10%) occurred during low risk. The median time spent in the high risk state before a seizure occurred was 28 h. The Area Under the Receiver Operating Characteristic Curve (AUC score), which demonstrates how good the model is at distinguishing non-seizure hours from seizure hours during testing, was 0.88. These results underscore the feasibility of seizure forecasting using data from the sub-scalp EEG device.

DISCUSSION

Here, we have successfully shown that a sub-scalp system can accurately record ultra-long term EEG (>12 months) and detect focal seizure activity (**Figure 2**). The device was well tolerated in all five participants, with no serious adverse events to date. This

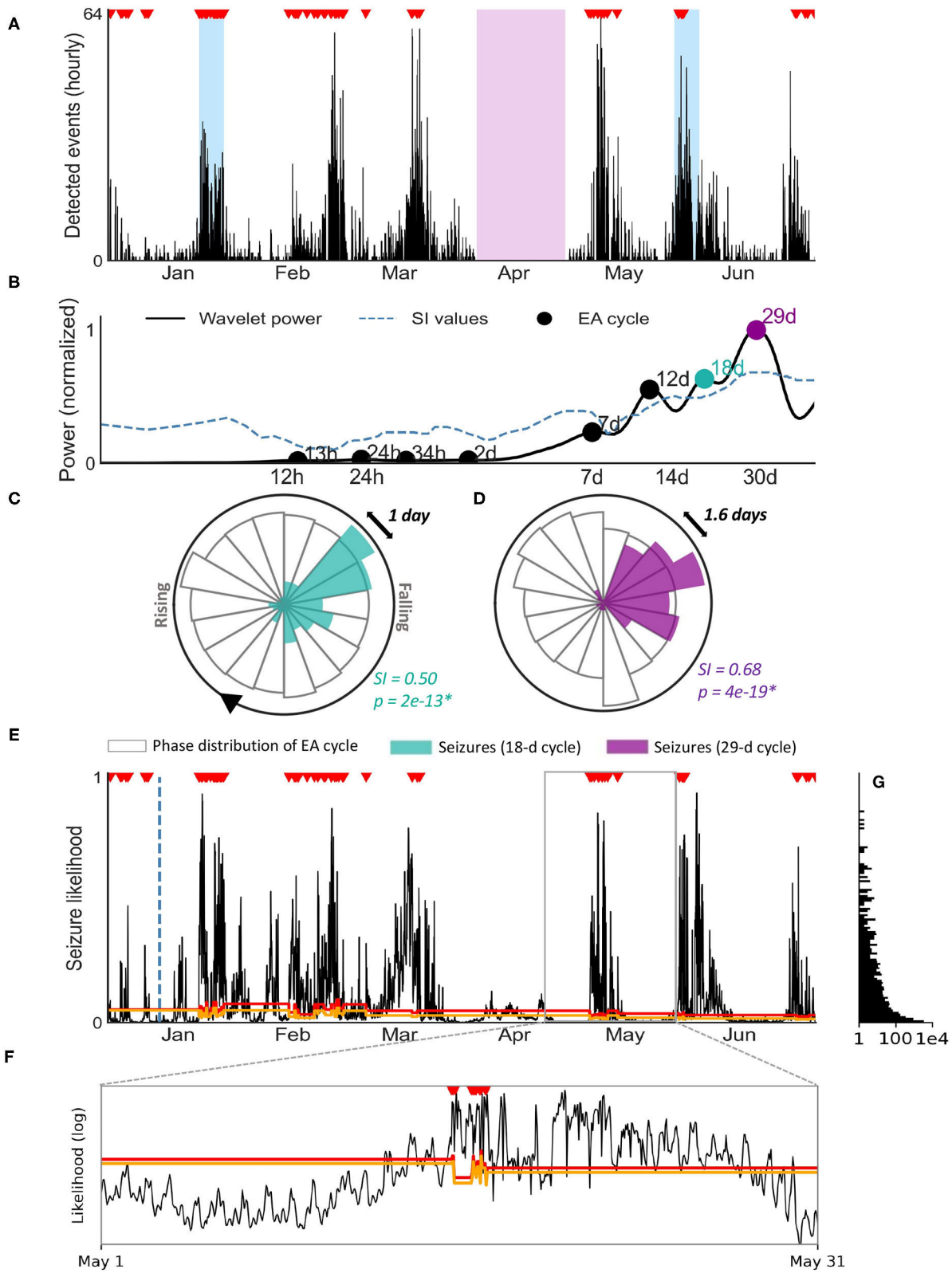

FIGURE 3 | Seizure forecasting case study for patient 1. **(A)** Hourly rate of machine-learning detected events using the sub-scalp EEG device. Verified seizures (red markers) from manual review of sub-scalp EEG device are shown. The blue regions represent scalp video-EEG assessment periods and the purple region represents a period where the device was removed. **(B)** Cycle detection in EA using a Morlet wavelet approach. The wavelet spectrum is shown for a range of time periods

(Continued)

FIGURE 3 | (x-axis), with cycles reaching significance denoted by a black or colored marker. The two colored markers indicate the two cycles shown in the circular histograms **(C,D)**. **(C,D)** Circular histograms showing the phase distribution of event cycles (transparent bars) and seizure occurrence (colored bars). Seizures were strongly locked onto 18 day **(C)** and monthly cycles **(D)** of detected events. Seizures only occur in a narrow phase of the periodic activity suggesting a strong relationship between the cycle and seizures ($p < 0.05$ with Omnibus test and high SI values). **(E)** Hourly likelihood of seizures. The likelihood of seizures occurring within the next hour is given by the black line and seizures are shown by the red markers.The training cut off date (day 14) is indicated by the blue dotted line. The orange and red lines represent the medium and high risk thresholds, respectively. **(F)** Inset of **(E)**: hourly likelihood (x-axis, log scale) of seizures for the month of May, with seizures and threshold lines shown. **(G)** Frequency (x-axis, log scale) of each seizure likelihood value [y-axis, shared with **(E)**].

suggests that continuous monitoring of EA chronically is possible with a minimally invasive and discrete device. The benefits of this are ubiquitous, not only for seizure forecasting, but also for medication management, anti-seizure medication trials and surgical planning. It is highly likely that accurate and objective quantification of seizures and interictal EA will become essential for future drug trials to provide more objective assessments of therapeutic benefit; sub-scalp EEG would be highly suitable for this purpose.

Our results demonstrate that sub-scalp devices record high quality neurological signals that are similar to scalp EEG. Sub-scalp recordings are also sensitive to other small neurological events such as sleep transients (**Figure 2B**). Lack of sleep and deviations from normal sleep patterns are known risk factors for seizures. Conversely, the treatment of seizures and seizures themselves can disrupt normal sleep patterns (40, 41). Sub-scalp devices provide an opportunity to investigate the complex relationship between sleep and seizures and can aid in patient management and seizure forecasting (39). The sub-scalp EEG was less noisy compared to scalp EEG. Sub-scalp EEG contained much less interference from electrical line noise (50 Hz in Australia) and was not affected by movement artifacts typically observed in scalp EEG due to the movement of wires. Sub-scalp devices are, however, susceptible to other noise and artifacts, such as muscle activity recorded by electromyography (EMG). While jaw EMG artifacts may obscure the underlying EEG activity (**Figure 2C**), it can also identify jaw activity that is a feature of the seizures. In contrast, blinking artifacts could not be seen in the sub-scalp recordings, most probably because of the parietal positioning of electrodes (**Figure 2D**).

The sub-scalp device can be used to continuously monitor interictal and ictal events, which may provide better understanding of the burden of disease. This information is also of importance for clinical trials of novel therapies and for routine patient management. Currently, clinical trials of novel therapies rely on patient seizure diaries, which are known to be unreliable in most people (11). The inconsistency of patient seizure diaries impacts the estimate of disease burden and distorts the estimated benefit of new therapies. Our case study demonstrates long-term fluctuations in detected events which were linked to seizures (**Figure 3A**).The detected events are likely to represent similar fluctuations in EA, which have been implicated in cognition and memory performance (5, 6). Understanding how EA changes over time is important for tailoring treatments that not only reduce seizures but ultimately improve quality of life.

The Minder® sub-scalp system demonstrated utility in capturing seizure cycles. In the current work, there was clear rhythmicity in the detected events (**Figure 3A**), which is concordant with previous work with invasive EEG showing the prevalence of circadian and multiday cycles in interictal EA (17, 18) and seizures (20, 29, 31). Using a similar approach to previous work (20, 40), cycles were detected at circadian and multiday periodicities for one individual (**Figure 3B**), with 18-day and 29-day cycles in the detected events showing the strongest relationships with seizure timing (**Figures 3C,D**). Interestingly, multiday cyclesin this subject were stronger than the circadian rhythm. Capturing multiday cycles requires long term monitoring and, in addition to demonstrated utility for forecasting, an understanding of seizure cycles may be critical for the development of new therapies.

TABLE 3 | Forecast results based on electrographic seizures.

	In high risk state	In medium risk state	In low risk state
Seizures	99 (83%)	8 (7%)	12 (10%)
Time	26%	11%	63%

Number of electrographic seizures occurring in and time spent in high, medium and low risk states during testing. Training was performed on electrographic seizures. AUC = 0.88.

We have also demonstrated the potential for seizure forecasting with sub-scalp systems. In this example, a forecaster achieved high accuracy (83%) and spent 26% of time in a high risk state, despite the high probability of seizures (2.2%) in this participant. These results are comparable to the only prospective seizure forecasting trial to-date, where patients spent 23% of their time in the warning state on average, but had a lower sensitivity of 66% (4). The AUC score (0.88) was also comparable to recent, state-of-the-art forecasting using interictal EA cycles derived from intracranial EEG (26, 32).

The case study demonstrates the high performance that can be achieved through an event-based seizure forecaster. This forecaster may be used to generate powerful prior probabilities for a more advanced seizure forecaster that combines other features, such as non-invasive information (e.g., medication adherence, heart rate etc.) and continuous features derived from the EEG (e.g., spectral power, autocorrelation etc.). Additionally, the forecast was able to continue making predictions despite the missing data during the period the device was not connected. Whilst cycles were attenuated during this period, seizure cycles were still utilized, as they rely on a fitted sinusoid of fixed period-length. The relative low likelihood of seizures during April compared to other months suggests that cycles in the detected events were stronger predictors

of seizures than seizure cycles. This is in line with previous work, which suggests seizures are more robustly synchronized to cycles of a continuous biomarker than fitted sinusoids of fixed period-length (41).

Cyclic features in the EEG were stable and no adaptation period was required to start forecasting in this participant. The lack of implantation effect of sub-scalp systems (42) is in contrast to intracranial devices, which require a craniotomy and often a substantial time period before the signal stabilizes (21). This may require months of data to be discarded prior to training forecasting algorithms (28, 32). In this case, forecaster training was undertaken immediately, and only 14 days of training data were required to generate forecasts (although this will depend on seizure frequency). Further work will investigate the utility of forecasting using sub-scalp recordings in a prospective study.

There are limitations with sub-scalp EEG systems. First, despite the limited invasiveness of subcutaneous electrodes, this surgical procedure may not be acceptable to all people with epilepsy (43). Hence, patient seizure diaries will remain a useful tool in clinical settings, and non-invasive forecasting systems based on mobile and wearable devices are desired by the epilepsy community (43, 44). Wearable sensors and non-invasive features may be useful to forecast seizure likelihood (25, 45, 46), and self-reported events and biomarkers derived from wearables also demonstrate cycles that are co-modulated with seizure likelihood (30, 38, 40). However, the correlation between self-reported events and electrographic events is patient-specific. In cases where the accuracy is less than perfect, it is unlikely that forecasts using self-reported events will perform as well as forecasts using chronic EEG. Despite advances in wearable technology for seizure detection, there remain significant false positives and many seizure types are missed (47). It is likely that chronic sub-scalp EEG recordings will prove to be a critical "ground-truth" to develop wearable seizure detection and forecasting.

Second, validating electrographic seizures also remains a significant challenge, even with the aid of an algorithm detecting suspect events. A short 24-h segment of continuous EEG alone can take hours for a trained neurophysiologist to review, which is not viable for large scale use of sub-scalp devices, and so optimizing seizure detection algorithms will be critical. The time taken for clinical review placed several limitations on the validation of the signal quality and the algorithms used in this preliminary study. Qualitatively, EEG signals between scalp and sub-scalp were found to be similar (**Figure 2**). Furthermore, the algorithm presented in this work highlighted strong cycles in detected activity, which are similar to cycles of epileptiform activity observed in previous studies (8, 17, 18). However, a more comprehensive assessment of signal equivalence and algorithm performance is required and will be addressed in future work.

Third, the retrospective forecasting case study was only presented in one participant. We acknowledge that a larger cohort study is necessary to demonstrate the generalisability of our forecasting results. Finally, it should be noted that the highly clustered nature of the electrographic seizures in participant 1 may have aided the algorithm in achieving a high AUC score. On the other hand, clusters tend to result in short cycles, but the long 18d and 29d event cycles were the strongest predictors in this algorithm, and these are present irrespective of clusters. To understand this further, future work may investigate the forecasting performance on lead seizures only.

This study has demonstrated the feasibility of using a continuous sub-scalp EEG device to record data of sufficient resolution to capture relevant events, detect the events algorithmically, and use the events in a seizure forecasting algorithm. This data is extremely valuable for the assessment of epilepsy, and could be linked to systems to improve safety and independence, potentially changing fundamentally our approach to the management of the condition.

DATA AVAILABILITY STATEMENT

The datasets presented in this article are not readily available because data is commercially sensitive. Applications for reasonable use will be considered. Requests to access the datasets should be directed to Mark J. Cook, mark@seermedical.com.

ETHICS STATEMENT

The studies involving human participants were reviewed and approved by St. Vincent's Hospital Melbourne Human Research Ethics Committee. The patients/participants provided their written informed consent to participate in this study.

DISCLOSURE

RS, MMa, PK, EN, KM, DF, and MC had employment or a financial interest in Seer Medical Pty. Ltd. MC, SR, JH, and RH have employment or a financial interest in Epi-Minder Pty. Ltd.

AUTHOR CONTRIBUTIONS

JH, SR, RH, AL, WD'S, US, LS, KM, KB, MMu, and MC contributed to the data collection. WD'S, US, LS, and KM contributed to the results analysis. SR, JH, RH, and AL, contributed to the manuscript writing. PK, EN, DG, BB, MR, DF, and MC contributed to the study and concept design and manuscript writing. RS and MMa contributed to the study and concept design, results analysis and manuscript writing. All authors contributed to the article and approved the submitted version.

FUNDING

MR had a research collaboration with UNEEG medical and has been a member of their advisory board. MR was supported by the National Institute for Health Research Biomedical Research Centre at South London and Maudsley NHS Foundation Trust, and by the Medical Research Centre for Neurodevelopmental Disorders (MR/N026063/1). BB had a financial interest in Cadence Neurosciences Inc., and has received non-financial research support (devices for a study) from Medtronic Inc. AL acknowledges support from the Victorian Medical Research Acceleration Fund. This project was supported by the My Seizure Gauge grant from the Epilepsy Foundation of America.

REFERENCES

1. Reynolds JR. Epilepsy: its symptoms, treatment, and relation to other chronic, convulsive diseases. *Am J Psychiatry.* (1862) 19:198–209. doi: 10.1176/ajp.19.2.198
2. Karoly P, Goldenholz DM, Cook M. Are the days of counting seizures numbered? *Curr Opin Neurol.* (2018) 31:162–8. doi: 10.1097/WCO.0000000000000533
3. Luoni C, Bisulli F, Canevini MP, Sarro GD, Fattore C, Galimberti CA, et al. Determinants of health-related quality of life in pharmacoresistant epilepsy: results from a large multicenter study of consecutively enrolled patients using validated quantitative assessments. *Epilepsia.* (2011) 52:2181–91. doi: 10.1111/j.1528-1167.2011.03325.x
4. Cook MJ, O'Brien TJ, Berkovic SF, Murphy M, Morokoff A, Fabinyi G, et al. Prediction of seizure likelihood with a long-term, implanted seizure advisory system in patients with drug-resistant epilepsy: a first-in-man study. *Lancet Neurol.* (2013) 12:563–71. doi: 10.1016/S1474-4422(13)70075-9
5. Loughman A, Seneviratne U, Bowden SC, D'Souza WJ. Epilepsy beyond seizures: predicting enduring cognitive dysfunction in genetic generalized epilepsies. *Epilepsy Behav.* (2016) 62:297–303. doi: 10.1016/j.yebeh.2016.07.010
6. Ung H, Cazares C, Nanivadekar A, Kini L, Wagenaar J, Becker D, et al. Interictal epileptiform activity outside the seizure onset zone impacts cognition. *Brain J Neurol.* (2017) 140:2157–68. doi: 10.1093/brain/awx143
7. Plummer C, Vogrin SJ, Woods WP, Murphy MA, Cook MJ, Liley DTJ. Interictal and ictal source localization for epilepsy surgery using high-density EEG with MEG: a prospective long-term study. *Brain.* (2019) 142:932–51. doi: 10.1093/brain/awz015
8. Karoly PJ, Rao VR, Gregg NM, Worrell GA, Bernard C, Cook MJ, et al. Cycles in epilepsy. *Nat Rev Neurol.* (2021) 17:267–84. doi: 10.1038/s41582-021-00464-1
9. Tatum WOI, Winters L, Gieron M, Passaro EA, Benbadis S, Ferreira J, et al. Outpatient seizure identification: results of 502 patients using computer-assisted ambulatory EEG. *J Clin Neurophysiol.* (2001) 18:14–9. doi: 10.1097/00004691-200101000-00004
10. Blum DE, Eskola J, Bortz JJ, Fisher RS. Patient awareness of seizures. *Neurology.* (1996) 47:260–4. doi: 10.1212/WNL.47.1.260
11. Elger CE, Hoppe C. Diagnostic challenges in epilepsy: seizure under-reporting and seizure detection. *Lancet Neurol.* (2018) 17:279–88. doi: 10.1016/S1474-4422(18)30038-3
12. Chen Z, Brodie MJ, Liew D, Kwan P. Treatment outcomes in patients with newly diagnosed epilepsy treated with established and new antiepileptic drugs: a 30-year longitudinal cohort study. *JAMA Neurol.* (2018) 75:279–86. doi: 10.1001/jamaneurol.2017.3949
13. Gliske SV, Irwin ZT, Chestek C, Hegeman GL, Brinkmann B, Sagher O, et al. Variability in the location of high frequency oscillations during prolonged intracranial EEG recordings. *Nat Commun.* (2018) 9:1–14. doi: 10.1038/s41467-018-04549-2
14. Chen Z, Grayden DB, Burkitt AN, Seneviratne U, D'Souza WJ, French C, et al. Spatiotemporal patterns of high-frequency activity (80-170 hz) in long-term intracranial eEG. *Neurology.* (2020) 96. doi: 10.1101/2020.03.26.999425
15. Goldenholz DM, Moss R, Scott J, Auh S, Theodore WH. Confusing placebo effect with natural history in epilepsy: a big data approach. *Ann Neurol.* (2015) 78:329–36. doi: 10.1002/ana.24470
16. Karoly PJ, Romero J, Cook MJ, Freestone DR, Goldenholz DM. When can we trust responders? Serious concerns when using 50% response rate to assess clinical trials. *Epilepsia.* (2019) 60:e99–103. doi: 10.1111/epi.16321
17. Baud MO, Kleen JK, Mirro EA, Andrechak JC, King-Stephens D, Chang EF, et al. Multi-day rhythms modulate seizure risk in epilepsy. *Nat Commun.* (2018) 9:88. doi: 10.1038/s41467-017-02577-y
18. Karoly PJ, Freestone DR, Boston R, Grayden DB, Himes D, Leyde K, et al. Interictal spikes and epileptic seizures: their relationship and underlying rhythmicity. *Brain.* (2016) 139:1066–78. doi: 10.1093/brain/aww019
19. Duun-Henriksen J, Baud M, Richardson MP, Cook M, Kouvas G, Heasman JM, et al. A new era in electroencephalographic monitoring? Subscalp devices for ultra–long-term recordings. *Epilepsia.* (2020) 61:1805–17. doi: 10.1111/epi.16630
20. Viana PF, Duun-Henriksen J, Glasstëter M, Dümpelmann M, Nurse ES, Martins IP, et al. 230 days of ultra long-term subcutaneous EEG: seizure cycle analysis and comparison to patient diary. *Ann Clin Transl Neurol.* (2021) 8:288–93. doi: 10.1002/acn3.51261
21. Ung H, Baldassano SN, Bink H, Krieger AM, Williams S, Vitale F, et al. Intracranial eEG fluctuates over months after implanting electrodes in human brain. *J Neural Eng.* (2017) 14:056011. doi: 10.1088/1741-2552/aa7f40
22. Nurse ES, John SE, Freestone DR, Oxley TJ, Ung H, Berkovic SF, et al. Consistency of long-term subdural electrocorticography in humans. *IEEE Trans Biomed Eng.* (2018) 65:344–52. doi: 10.1109/TBME.2017.2768442
23. *Spatiotemporal Patterns of High-Frequency Activity (80–170 Hz) in Long-Term Intracranial EEG | Neurology*. Available online at: https://n.neurology.org/content/96/7/e1070.long (accessed April 22, 2021).
24. Dell KL, Cook MJ, Maturana MI. Deep brain stimulation for epilepsy: biomarkers for optimization. *Curr Treat Options Neurol.* (2019) 21:47. doi: 10.1007/s11940-019-0590-1
25. Payne DE, Dell KL, Karoly PJ, Kremen V, Gerla V, Kuhlmann L, et al. Identifying seizure risk factors: a comparison of sleep, weather, and temporal features using a bayesian forecast. *Epilepsia.* (2021) 62:371–382. doi: 10.1111/epi.16785
26. Maturana MI, Meisel C, Dell K, Karoly PJ, D'Souza W, Grayden DB, et al. Critical slowing down as a biomarker for seizure susceptibility. *Nat Commun.* (2020) 11:2172. doi: 10.1038/s41467-020-15908-3
27. Kuhlmann L, Lehnertz K, Richardson MP, Schelter B, Zaveri HP. Seizure prediction — ready for a new era. *Nat Rev Neurol.* (2018) 14:618–630. doi: 10.1038/s41582-018-0055-2
28. Karoly PJ, Ung H, Grayden DB, Kuhlmann L, Leyde K, Cook MJ, et al. The circadian profile of epilepsy improves seizure forecasting. *Brain.* (2017) 140:2169–82. doi: 10.1093/brain/awx173
29. Karoly PJ, Goldenholz DM, Freestone DR, Moss RE, Grayden DB, Theodore WH, et al. Circadian and circaseptan rhythms in human epilepsy: a retrospective cohort study. *Lancet Neurol.* (2018) 17:977–85. doi: 10.1016/S1474-4422(18)30274-6
30. Karoly PJ, Cook MJ, Maturana M, Nurse ES, Payne D, Brinkmann BH, et al. Forecasting cycles of seizure likelihood. *Epilepsia.* (2020) 61:776–86. doi: 10.1101/2019.12.19.19015453
31. Leguia MG, Andrzejak RG, Rummel C, Fan JM, Mirro EA, Tcheng TK, et al. Seizure cycles in focal epilepsy. *JAMA Neurol.* (2021) 78:454–63. doi: 10.1001/jamaneurol.2020.5370
32. Proix T, Truccolo W, Leguia MG, Tcheng TK, King-Stephens D, Rao VR, et al. Forecasting seizure risk in adults with focal epilepsy: a development and validation study. *Lancet Neurol.* (2021) 20:127–35. doi: 10.1016/S1474-4422(20)30396-3
33. Scheffer IE, Berkovic S, Capovilla G, Connolly MB, French J, Guilhoto L, et al. ILAE classification of the epilepsies: position paper of the ILAE commission for classification and terminology. *Epilepsia.* (2017) 58:512–21. doi: 10.1111/epi.13709
34. Clarke S, Karoly PJ, Nurse E, Seneviratne U, Taylor J, Knight-Sadler R, et al. Computer-assisted EEG diagnostic review for idiopathic generalized epilepsy. *Epilepsy Behav.* (2019) 106556. doi: 10.1101/682112
35. Eden D, Nurse ES, Clarke S, Karoly PJ, Seneviratne U, Cook M, et al. Computer-assisted estimation of interictal discharge burden in idiopathic generalized epilepsy. *Epilepsy Behav EB.* (2020) 105:106970. doi: 10.1016/j.yebeh.2020.106970
36. Torrence C, Compo GP. A practical guide to wavelet analysis. *Bull Am Meteorol Soc.* (1998) 79:61–78. doi: 10.1175/1520-0477(1998)079<0061:APGTWA>2.0.CO;2
37. Berens P. CircStat: a MATLAB toolbox for circular statistics. *J Stat Softw.* (2009) 37:1–21. doi: 10.18637/jss.v031.i10
38. Karoly PJ, Eden D, Nurse ES, Cook MJ, Taylor J, Dumanis S, et al. Cycles of self-reported seizure likelihood correspond to yield of diagnostic epilepsy monitoring. *Epilepsia.* (2021) 62:416–25. doi: 10.1111/epi.16809

39. Dell KL, Payne DE, Kremen V, Maturana MI, Gerla V, Nejedly P, et al. Seizure likelihood varies with day-to-day variations in sleep duration in patients with refractory focal epilepsy: a longitudinal electroencephalography investigation. *EClin Med.* (2021). 37:100934. doi: 10.1016/j.eclinm.2021.100934
40. Karoly PJ, Stirling RE, Freestone DR, Nurse ES, Doyle B, Halliday A, et al. Multiday cycles of heart rate modulate seizure likelihood at daily, weekly and monthly timescales: an observational cohort study. *medRxiv*. (2020). doi: 10.1101/2020.11.24.20237990
41. Leguia MG, Rao VR, Kleen JK, Baud MO. Measuring synchrony in biomedical timeseries. *Chaos Interdiscip J Nonlinear Sci.* (2021) 31:013138. doi: 10.1063/5.0026733
42. Viana PF, Remvig LS, Duun-Henriksen J, Glasstetter M, Dümpelmann M, Nurse ES, et al. Signal quality and power spectrum analysis of remote ultra long-term subcutaneous EEG. *Epilepsia*. (2021) 1–9. doi: 10.1111/epi.16969
43. Janse SA, Dumanis SB, Huwig T, Hyman S, Fureman BE, Bridges JFP. Patient and caregiver preferences for the potential benefits and risks of a seizure forecasting device: a best–worst scaling. *Epilepsy Behav.* (2019) 96:183–91. doi: 10.1016/j.yebeh.2019.04.018
44. Dumanis SB, French JA, Bernard C, Worrell GA, Fureman BE. Seizure forecasting from idea to reality. Outcomes of the My Seizure Gauge Epilepsy Innovation Institute Workshop. *Eneuro.* (2017) 4:ENEURO.0349-17.2017. doi: 10.1523/ENEURO.0349-17.2017
45. Meisel C, El Atrache R, Jackson M, Schubach S, Ufongene C, Loddenkemper T. Machine learning from wristband sensor data for wearable, noninvasive seizure forecasting. *Epilepsia.* (2020) 61:2653–66. doi: 10.1111/epi.16719
46. Stirling RE, Grayden DB, D'Souza W, Cook MJ, Nurse E, Freestone DR, et al. Forecasting seizure likelihood with wearable technology. *Front Neurol.* (2021) 12:704060. doi: 10.3389/fneur.2021.704060
47. Beniczky S, Karoly P, Nurse E, Ryvlin P, Cook M. Machine learning and wearable devices of the future. *Epilepsia*. (2020) 62:116–24. doi: 10.1111/epi.16555

Conflict of Interest: RS, MMa, PK, EN, KM, DF, and MC were employed or have a financial interest in Seer Medical Pty. Ltd. MC, SR, JH, and RH were employed or have a financial interest in Epi-Minder Pty. Ltd. MR had a research collaboration with UNEEG medical and has been a member of their advisory board. BB had a financial interest in Cadence Neurosciences Inc., and had received nonfinancial research support (devices for a study) from Medtronic Inc. JH was employed by company Cochlear Limited.

The remaining authors declare that the research was conducted in the absence of any commercial or financial relationships that could be construed as a potential conflict of interest.

The handling editor VR declared a past co-authorship/collaboration with one or more authors PK and MC.

Publisher's Note: All claims expressed in this article are solely those of the authors and do not necessarily represent those of their affiliated organizations, or those of the publisher, the editors and the reviewers. Any product that may be evaluated in this article, or claim that may be made by its manufacturer, is not guaranteed or endorsed by the publisher.

frontiers in Neurology

METHODS
published: 13 September 2021
doi: 10.3389/fneur.2021.721491

Seizure Susceptibility Prediction in Uncontrolled Epilepsy

Nhan Duy Truong[1,2], *Yikai Yang*[1], *Christina Maher*[1], *Levin Kuhlmann*[3,4], *Alistair McEwan*[1], *Armin Nikpour*[5,6] *and Omid Kavehei*[1,2]*

[1] Australian Research Council Training Centre for Innovative BioEngineering, School of Biomedical Engineering, Faculty of Engineering, The University of Sydney, Sydney, NSW, Australia, [2] The University of Sydney Nano Institute, Sydney, NSW, Australia, [3] Faculty of Information Technology, Monash University, Melbourne, VIC, Australia, [4] Department of Medicine - St. Vincent's Hospital Melbourne, The University of Melbourne, Fitzroy, VIC, Australia, [5] Comprehensive Epilepsy Service and Department of Neurology at the Royal Prince Alfred Hospital, Sydney, NSW, Australia, [6] Faculty of Medicine and Health, Central Clinical School, The University of Sydney, Sydney, NSW, Australia

Epileptic seizure forecasting, combined with the delivery of preventative therapies, holds the potential to greatly improve the quality of life for epilepsy patients and their caregivers. Forecasting seizures could prevent some potentially catastrophic consequences such as injury and death in addition to several potential clinical benefits it may provide for patient care in hospitals. The challenge of seizure forecasting lies within the seemingly unpredictable transitions of brain dynamics into the ictal state. The main body of computational research on determining seizure risk has been focused solely on prediction algorithms, which involves a challenging issue of balancing sensitivity and false alarms. There have been some studies on identifying potential biomarkers for seizure forecasting; however, the questions of "What are the true biomarkers for seizure prediction" or even "Is there a valid biomarker for seizure prediction?" are yet to be fully answered. In this paper, we introduce a tool to facilitate the exploration of the potential biomarkers. We confirm using our tool that interictal slowing activities are a promising biomarker for epileptic seizure susceptibility prediction.

Keywords: epileptic seizure forecasting, probabilistic programming, Bayesian, variational inference, uncertainty level

OPEN ACCESS

Edited by:
Sharon Chiang, University of California, San Francisco, United States

Reviewed by:
Alberto Cassese, Maastricht University, Netherlands
Qiwei Li, The University of Texas at Dallas, United States

***Correspondence:**
Omid Kavehei
omid.kavehei@sydney.edu.au

Specialty section:
This article was submitted to Epilepsy, a section of the journal Frontiers in Neurology

Received: *07 June 2021*
Accepted: *28 July 2021*
Published: *13 September 2021*

Citation:
Truong ND, Yang Y, Maher C, Kuhlmann L, McEwan A, Nikpour A and Kavehei O (2021) Seizure Susceptibility Prediction in Uncontrolled Epilepsy. Front. Neurol. 12:721491. doi: 10.3389/fneur.2021.721491

1. INTRODUCTION

There has been great interest recently in identifying biomarkers for seizure susceptibility by looking into critical transitions in brain dynamics in order to enhance the precision of seizure forecasting in a cohort of patients with focal epilepsy (1–3). These studies often require a very long recording that is not available and, in fact, are critically lacking. Chronic and often intracranial electroencephalogram (EEG) recordings demonstrated some limited evidence of circadian, multidien, and circannual cycles in epileptic brain dynamics (4–6). In determining seizure-risk, we believe that understanding what features or biomarkers in the EEG signals lead to such seizure-risk level.

The availability of a seizure forecasting system that can notify patients or their carers about forthcoming seizure-risk can drastically improve patients' quality of life and the chance to develop innovative interventions and preventative therapies. Many studies have been on forecasting seizures; most of them used the signal-modal approach based on electroencephalogram (EEG) signals. These studies can be grouped into two categories: (1) finding discriminative features with various signal processing and transformation techniques and (2) leveraging deep learning's

capability of extracting high-level features. In the first group, the most common approach is to use spatio-temporal correlation features, auto-regressive modeling predictive error, Hjorth parameters, spectral power, energy wavelet coefficients, and other statistics (7, 8). Other discriminative features include phase and amplitude lock values (9), common spatial pattern (10), permutation entropy (11), bispectrum features (12). In the second group, the convolutional neural network (CNN) and recurrent neural network (RNN) have shown their capability to extract high-level features that can be used for forecasting seizures. Particularly, CNN was used on the EEG signal spectrogram (13), raw EEG, and fast Fourier transform (FFT) of raw EEG (14), local mean decomposition of raw EEG (15), and the common spatial pattern of multi-channel EEG signals (16). CNN was also used in unsupervised learning as effective feature extraction for seizure prediction (17). To further extract the temporal characteristics over time-series data, Wei et al. (18) applied CNN with long short-term memory recurrent network on the spectrogram of EEG signals. The combination of convolutional and recurrent neural networks is also effective when using multi-timescale of raw time-series EEG signals (19).

In this work, we propose a framework (see **Figure 1**) to minimize the risk of sudden unexpected death in epilepsy (SUDEP), especially for patients with uncontrolled epilepsy. We also introduce a tool to facilitate the exploration of biomarkers for epileptic seizure forecasting. Specifically, we use probabilistic programming and propose a framework to incorporate other relevant information into an EEG-based seizure forecasting system. As an advantage of using probabilistic programming, our system not only can forecast impending seizures but also quantify the uncertainty level of its decision-making.

2. DATASET

EPILEPSIAE is the largest epilepsy database that contains EEG data from 275 patients (22). However, up to the time of this writing, only 30 surface EEG and 30 invasive EEG datasets are made available (23). We believe the use of surface EEG is more beneficial because it is non-invasive so it can be applied to a broader group of patients. In this study, we analyze scalp-EEG of 30 patients with 261 leading seizures and 2881.4 interictal hours in total in this work. The time-series EEG signals were recorded at a sampling rate of 256 Hz and from 19 electrodes. Seizure onset information obtained by two methods, namely EEG based and video analysis, is provided. In our study, we use seizure onset information using an EEG based technique, where the onsets were determined by visual inspection of EEG signals performed

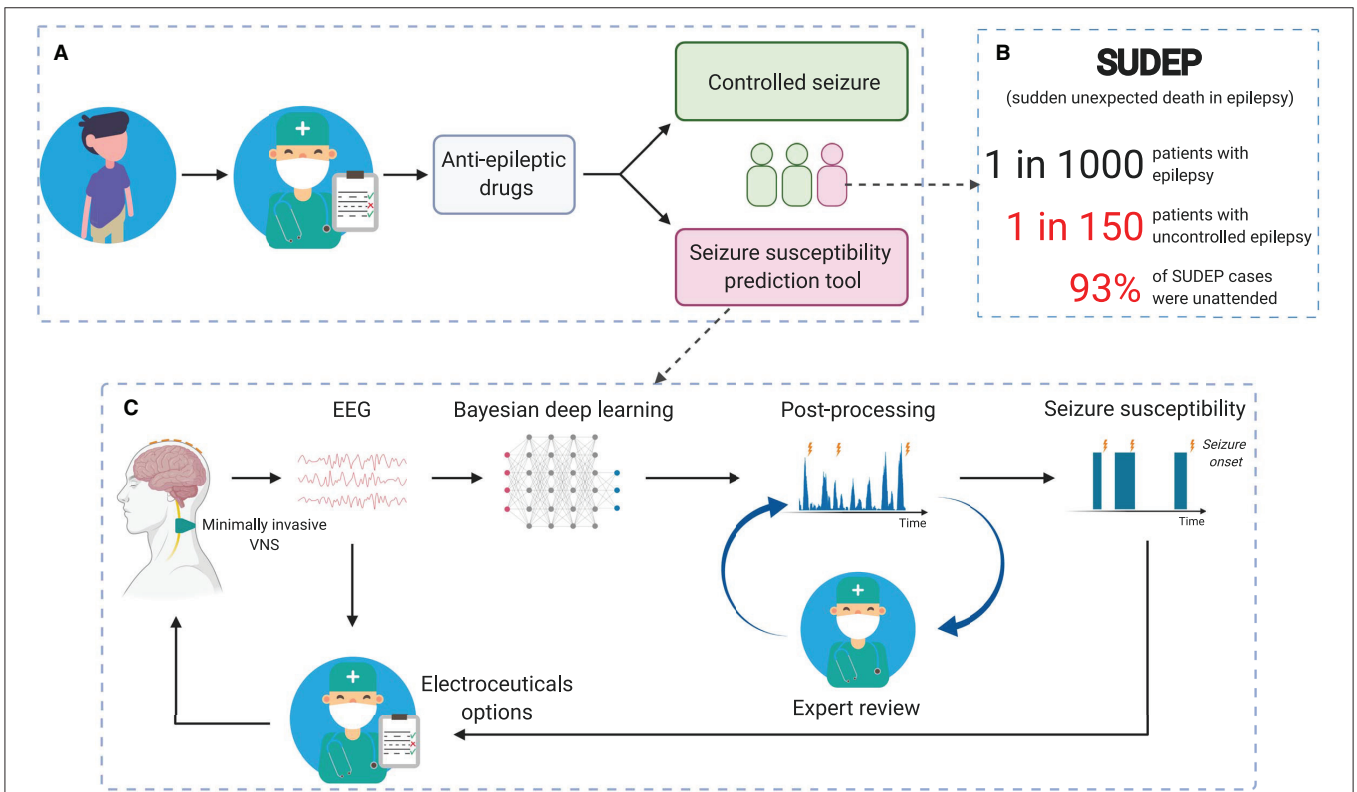

FIGURE 1 | Reducing SUDEP (sudden unexpected death in epilepsy) risk with seizure forecasting based on reliable long-term EEG monitoring. **(A)** Simplified pathway for patients with epilepsy. **(B)** The fact that most SUDEP cases were unattended (20, 21) emerges the need for reliable 24/7 and long-term EEG monitoring. **(C)** Seizure susceptibility prediction tool to suggest alternative treatments [e.g., vagus nerve stimulation (VNS)] for patients with uncontrolled epilepsy.

by an experienced clinician (22). **Table 1** provides a summary of the dataset being studied in this work.

3. METHOD

3.1. Pre-processing

We split EEG signals into 30-s segments with 50% overlap. We perform a short-time Fourier transform (STFT) with a cosine window of 1-s length and 50% overlap on each 30-s segment and get data with a dimension of ($n \times 59 \times 129$), where n is the number of EEG channels. We remove the first and last two elements along the second axis, which corresponds to time, to eliminate any potential disruption of signal near the signal window's edges. We also remove the dc component of the STFT, which is the first element along the last axis. The final dimension of pre-processed data is ($n \times 56 \times 128$).

TABLE 1 | The EPILEPSIAE scalp-EEG dataset.

Patient	Gender	Age	No. of seizures	No. of leading seizures*	Interictal hours
Pat1	Male	36	11	11	68.9
Pat2	Female	46	8	8	114.9
Pat3	Male	41	8	8	96.3
Pat4	Female	67	5	5	126
Pat5	Female	52	8	8	204.1
Pat6	Male	65	8	7	92.2
Pat7	Male	36	5	5	75.7
Pat8	Male	26	22	11	65.6
Pat9	Male	47	6	6	51.1
Pat10	Male	44	11	11	60.7
Pat11	Male	48	14	14	57.8
Pat12	Male	28	9	9	94.1
Pat13	Male	46	8	8	101.3
Pat14	Female	62	6	6	115.7
Pat15	Female	41	5	5	82.8
Pat16	Female	15	6	6	51.1
Pat17	Female	17	9	9	82.4
Pat18	Male	47	7	6	133
Pat19	Male	32	22	21	75.4
Pat20	Male	47	7	7	115.3
Pat21	Female	31	8	8	106.6
Pat22	Male	38	7	7	88.2
Pat23	Male	50	9	9	179.6
Pat24	Female	54	10	10	36.2
Pat25	Male	42	8	8	109.8
Pat26	Male	13	9	9	97.1
Pat27	Male	58	9	8	99.9
Pat28	Female	35	9	9	95.2
Pat29	Male	50	10	10	111.9
Pat30	Female	16	12	12	92.5

**We are considering leading seizures only. Seizures that are <30 min away from the previous one are considered as one seizure only, and the onset of a leading seizure is used as the onset of the combined seizure.*

3.2. Bayesian Convolutional Neural Network

In this paper, we will use variational inference to approximate posterior densities for Bayesian models (24). Consider $x = x_{1:n}$ as a set of observed variables and $z = z_{1:m}$ as a set of hidden variables, with joint density $p(z, x)$. The inference problem calculates the conditional density of the hidden variables given the observed variables, $p(z|x)$.

$$p(z|x) = \frac{p(z,x)}{p(x)}, \tag{1}$$

where $p(x)$ is intractable in many models (24).

Variational inference overcomes this by specifying a variational family $\mathcal{Q}$ over the hidden variables (24). The inference problem becomes finding the best candidate $q(z) \in \mathcal{Q}$ that is closest in Kullback-Leibler (KL) divergence to $p(z|x)$. The optimization subsequently can be achieved by maximizing a function called the evidence lower bound (ELBO) which is equivalent to minimizing the KL divergence between $q(z)$ and $p(z|x)$. ELBO is expressed as follows (24):

$$\begin{aligned} ELBO(q) &= \mathbb{E}\big[\log p(z,x)\big] - \mathbb{E}\big[\log q(z)\big] \\ &= \mathbb{E}\big[\log p(x|z)\big] + \mathbb{E}\big[\log p(z)\big] - \mathbb{E}\big[\log q(z)\big] \\ &= \mathbb{E}\big[\log p(x|z)\big] - \mathrm{KL}\big(q(z)\|p(z)\big) \end{aligned} \tag{2}$$

The stochastic variational inference was proposed by Hoffman et al. (25) to help Bayesian neural networks scale efficiently to large datasets. Particularly, this method generates noisy estimates of the natural gradient of the ELBO by repeatedly sub-sampling (mini-batch) the dataset. The loss function can be defined as the negative of ELBO, i.e., minimizing the loss is equivalent to maximizing the ELBO.

$$\text{loss} = -ELBO(q) = -\mathbb{E}\big[\log p(x|z)\big] + \mathrm{KL}\big(q(z)\|p(z)\big) \tag{3}$$

In an EEG-based seizure prediction system, x is the EEG signals, and z is a variable indicating a seizure to occur in the time window $\mathcal{T} = [SPH : SPH + SOP]$. *SPH* stands for seizure prediction horizon that is defined as the period where seizure should not occur after an alarm rises. *SOP* stands for seizure occurrence period that is defined as the interval where seizure onset is expected to occur (26).

3.3. Probabilistic Convolutional Neural Network With Data Fusion

In this section, we will incorporate signals other than EEG signals into the Bayesian CNN. We want to estimate the probability of having a seizure given EEG signals, $p(z|x)$, which is the Bayesian CNN's output. Besides EEG signals, we have other relevant data and want to combine all the seizure forecasting information. Circadian information or time of the day has been used to improve the performance of a seizure prediction system (27). For another instance, electrocardiogram that could change around and even before seizure onsets has been shown helpful in predicting epileptic seizures (28, 29). Other physiological signals

that have been observed to change prior to seizure onset, such as blood oxygenation, metabolism, can be used as auxiliary data for seizure prediction (30, 31).

Let us start with EEG signals and one extra signal called d. Using Bayes theorem, the posterior probability of having a seizure in the time-window $\mathcal{T}$ can be expressed as:

$$p(z|x,d) = \frac{p(d|z,x)p(z|x)}{p(d|x)} \tag{4}$$

Assume x and d are independent, (e.g., EEG signals are independent with the time of the day and can be considered independent with blood oxygenation), we can rewrite (4) as follows.

$$p(z|x,d) = \frac{p(d|z)p(z|x)}{p(d)} \tag{5}$$

Similarly, for two extra signals, d_1 and d_2 with an assumption that x, d_1, and d_2 are independent of each other (e.g., time of the day and blood oxygenation), the posterior probability of having seizure in the time window $\mathcal{T}$ can be expressed as:

$$\begin{aligned} p(z|x,d_1,d_2) &= \frac{p(d_1|z,d_2)p(z|x,d_2)}{p(d_1|d_2)} \\ &= \frac{p(d_1|z)p(z|x,d_2)}{p(d_1)} \end{aligned} \tag{6}$$

By substituting Equation (5) (with d replaced by d_2) to Equation (6), we have:

$$p(z|x,d_1,d_2) = \frac{p(d_1|z)p(d_2|z)p(z|x)}{p(d_1)p(d_2)} \tag{7}$$

To estimate $p(d_1|z)$ and $p(d_2|z)$, we applied a kernel density estimation using Gaussian kernels on a histogram containing time of the day (ToD) of seizure occurrences (see **Figure 2**) (32). Regarding the kernel density estimation parameters, we used Scott's rule for bandwidth selection and assumed all data points are equally weighted. Note that here we approximate $p(d_1|z) \approx p(d_1|z')$ and $p(d_2|z) \approx p(d_2|z')$, where z' is the variable indicating an occurrence of seizure. The approximation is reasonable because we choose the time window $\mathcal{T} = [5:35\ \text{min}]$ which is <1 h.

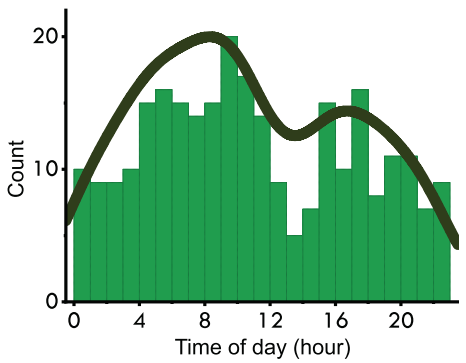

FIGURE 2 | Distribution of time-of-day of seizure occurrences in the EPILEPSIAE scalp-EEG dataset.

To incorporate Equation (7) into the training of the Bayesian CNN, we modify the output of the last fully-connected layer (see Fig. 3), before softmax activation (33) as follows.

$$\text{new-output}_l = \frac{p(d_1|z')p(d_2|z') \times \text{output}_l}{p(d_1)p(d_2)}, \tag{8}$$

where $p(d_1|z')$ and $p(d_2|z')$ can be derived from the kernel density estimation. For example of time of the day, $p(d_1) = 1/24$ because the probability of having the auxiliary signal at a given hour is 1/24); $p(d_1|z')$ can be inferred from **Figure 2**. Note that Equations (7) and (8) can be extended with more extra signals d given that they are independent on each other.

The Bayesian convolutional neural network (BCNN) with Bayesian modulator as data fusion is depicted in **Figure 3**. Unlike a conventional CNN, where each weight is a single value, each weight of a BCNN is a distribution estimated during the training phase. In this work, we model each weight as a Gaussian distribution with mean and standard deviation values are trainable parameters. Input to the BCNN is the STFT of 30-second windows with size of ($n \times 56 \times 128$) (see Session 3.1 for details). The network starts with a convolutional layer consisted of 16 3-dimensional kernels of size ($n \times 5 \times 5$), valid padding, and a stride of ($1 \times 2 \times 2$). A max-pooling layer follows the first convolutional layer with a pooling size of ($1 \times 2 \times 2$). The network continues with two blocks of convolutional-pooling combinations, each consists of one convolutional layer with a kernel size of (3×3), valid padding and stride of (1×1), and one max-pooling layer with a pooling size of (2×2). The number of convolutional kernels in the two blocks is 64 and 128. The next two layers are fully-connected layers with output sizes of 256 and 2, respectively. The output of the last fully-connected layer is fed to the Bayesian modulator where we apply Equation 8 for data fusion, then is applied softmax activation to get the final output of the network.

4. RESULTS

This section tests the Bayesian convolutional neural network (BCNN) with the EPILEPSIAE scalp EEG dataset with and without auxiliary signal: time-of-day (ToD). Following Truong et al. (13), we use SPH of 5 min and SOP of 30 for calculating the performance. We also compare a seizure prediction system using a convolutional neural network (CNN) proposed by Truong et al. (13) as a baseline. **Figure 4A** shows the overall performance of the BCNN with and without auxiliary signal and the baseline CNN. Compared to the CNN that has an average AUC of 71.65%, BCNN achieves an AUC of 68.69% that is around 3% lower than that of CNN. By using the time-of-day information, the overall performance of BCNN-ToD is slightly improved by 0.3–69.03%. There is strong agreement between the methods that

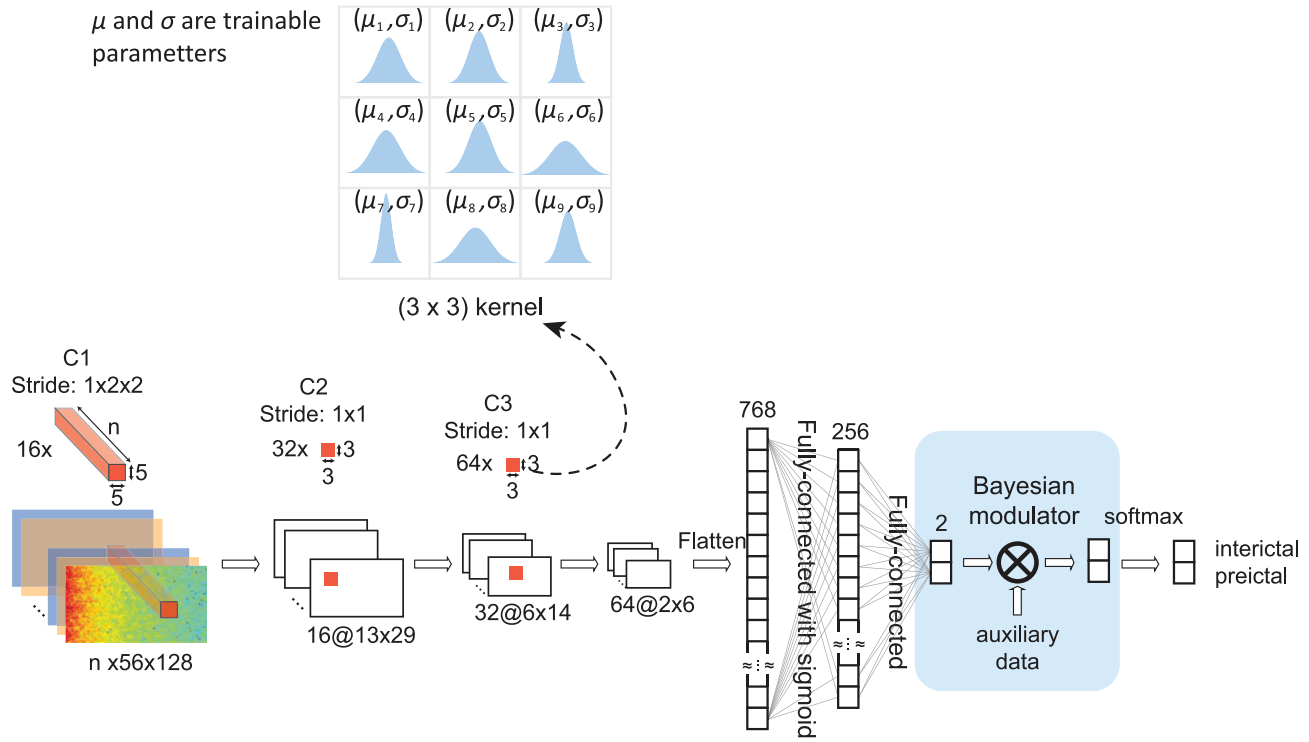

FIGURE 3 | Architecture of Bayesian convolutional neural network (BCNN) with embedded Bayesian modulator. *n* is the number of EEG channels, which is 19 for all 30 patients in this study. Unlike a conventional convolutional neural network where each weight is a single value, each weight of a BCNN is a distribution. In our work, we model each weight as a normal distribution with mean value (μ) and standard deviation (σ) are trainable parameters. The BCNN network has three convolutional layers, each is followed by a max-pooling layer (not shown). Extracted features by the convolutional layers are fed to two fully-connected layers. The Bayesian modulator incorporates other relevant data for seizure forecasting into the last fully-connected layer of the network by using Equation (8).

is reflected via scatter plots of AUC between each pair of them (see **Figure 4B**). We did a one-tailed Wilcoxon signed-rank test and a one-tailed *t*-test between BCNN-ToD and CNN and found that the two methods' performance is not significantly different at the confidence level of 0.05 with *p*-values of 0.063 and 0.243, respectively. However, the BCNN-ToD provides more insights into how the prediction works. Particularly, because each weight of the BCNN or BCNN-ToD is a distribution, we sample those distributions to calculate the output for each forward pass of an input. By running multiple forward passes of the same input, we can estimate the distribution of the corresponding output. The output's distribution can then be used to quantify the uncertainty of the model's decision-making that will be explored in section 5.

5. DISCUSSION

Bayes convolutional neural network (BCNN) can generate the distribution of its output for each input. We sampled the output of the BCNN by feeding forward the same input through the BCNN 500 times. We quantify the uncertainty level of the BCNN's decision making with Equation (9) below. The numerator takes into account the variability of the output with the standard deviation (std). The denominator considers the case where the output has a uniform-like distribution. Uncertainty levels of different types of prediction distributions are illustrated in **Figure 5**.

$$\text{Uncertainty level} = \frac{\text{std}_{\text{inference values}}}{\left|\text{mean}_{\text{inference values}} - 0.5\right|} \quad (9)$$

We trained the BCNN with two types of EEG signals: preictal—35 to 5 min before seizure onset, and interictal—at least 4 h away from any seizures, we are interested in how the BCNN performs with continuous EEG recording. We ran inference over 13 h of continuous EEG recording for one of the best performers, Patient 4, consisting of two seizures. In **Figure 6**, we plot both the prediction scores (from 0 to 1, where higher values indicate a higher probability of having a seizure) and the corresponding uncertainty levels of the BCNN. In general, the prediction scores get higher values when it is closer to the first seizure onset. Interestingly, at around time 40 and 80 min (around 200 and 160 min before the first seizure onset), there are two predictions with high scores. However, the uncertainty levels were also high, which means that the BCNN "thinks" that there might be a seizure incoming, but it has very low confidence about its decision. From about 1 h before seizure to seizure onset, we can see prediction scores were mostly high, but there were also many low prediction scores with high uncertainty levels. We suggest that the "patterns" or bio-markers related to seizure prediction only

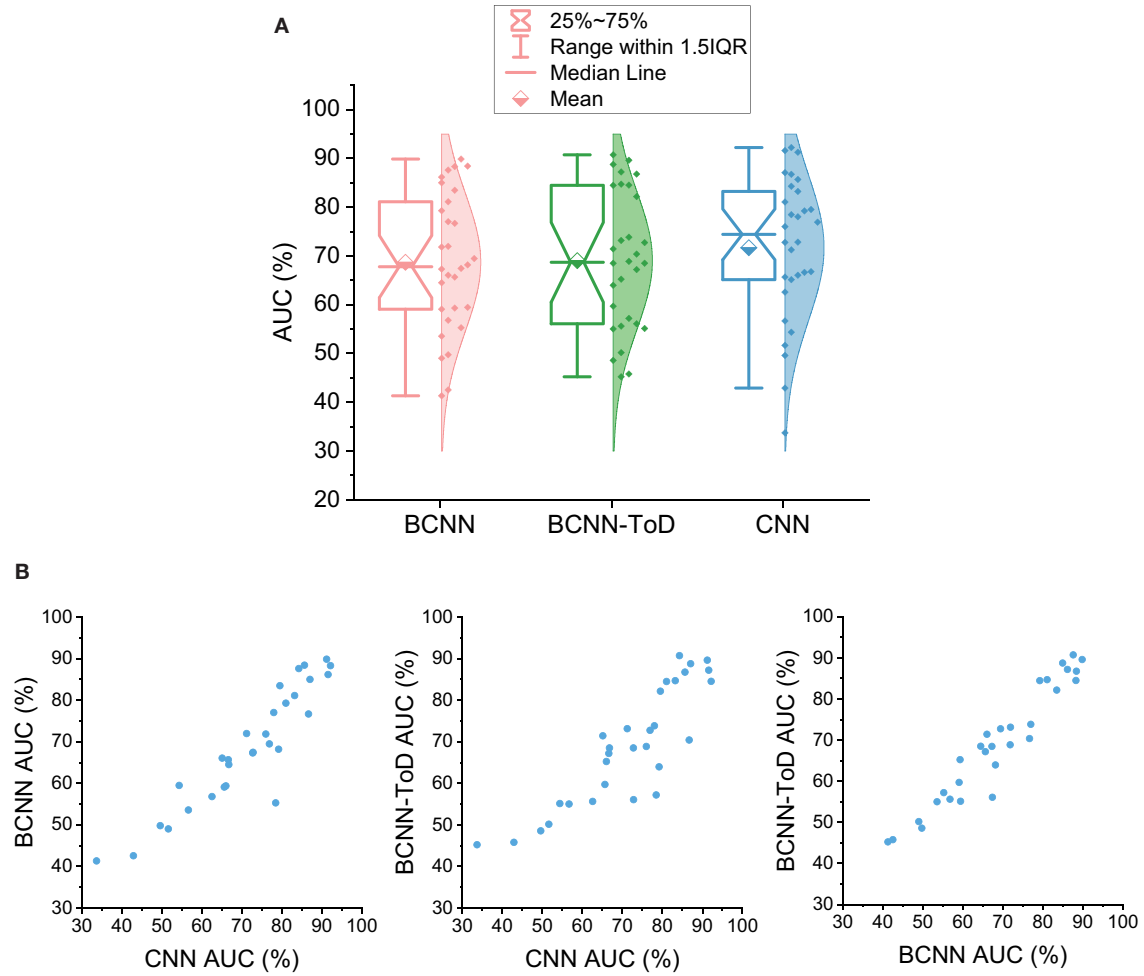

FIGURE 4 | (A) Seizure prediction performance using Bayesian convolutional neural network (BCNN). CNN, Convolutional neural network, average AUC is 71.64%; BCNN, BCNN using EEG signals only, average AUC is 68.69%; BCNN-ToD, BCNN using EEG signals and time-of-day (ToD), average AUC is 69.03%. **(B)** Scatter plots between each pair of the three methods showing concordance between them.

occur at certain particular points in time rather than consistently throughout the whole preictal duration.

Furthermore, we were able to use the trained BCNN as a tool to extract potential bio-markers from EEG signals. We fed 30-s EEG segments to the trained BCNN to sample the output, i.e., run multiple inferences with the same input; in this work, we ran 100 times. Uncertainty level and mean prediction score were extracted from the output samples. For every 30-s segment that has an uncertainty level below 0.1 and means prediction score above 0.9, we extract the attention map over time by accumulating over time the positive values of the feature map of the first convolutional layer. An example is illustrated in **Figure 7**. We observed that, from patients with high performance and with focal seizures, the BCNN focuses on slow EEG activity when performing seizure forecasting. Slow EEG activity has been shown as an important biomarker for studying epilepsy (34).

To verify the possibility of seizure forecasting, we ran the inference over the three patients' EEG recordings with the best seizure prediction performance in the EPILEPSIAE dataset, namely Pat-3, Pat-4, and Pat-12. We used different trained BCNN models at different periods separated by ictal segments to ensure that the trained BCNN being used did not see the current period's preictal segment during training. By doing that, we can have a retrospective risk of having a seizure over time, as shown in **Figure 8**. Generally, the risks are higher when it is closer to the seizure onset, indicating successful seizure forecasting. However, there are cases that we consider as false positive alarms if the risk is assessed as high, but it is too far from the seizure onset, e.g., the day before. For instance, Pat-3 receives a high-risk alarm almost 16 h before the first seizure onset.

Finally, we introduced the Bayesian modulator as a data fusion technique to incorporate relevant auxiliary signals for improving seizure prediction performance. In this work, we

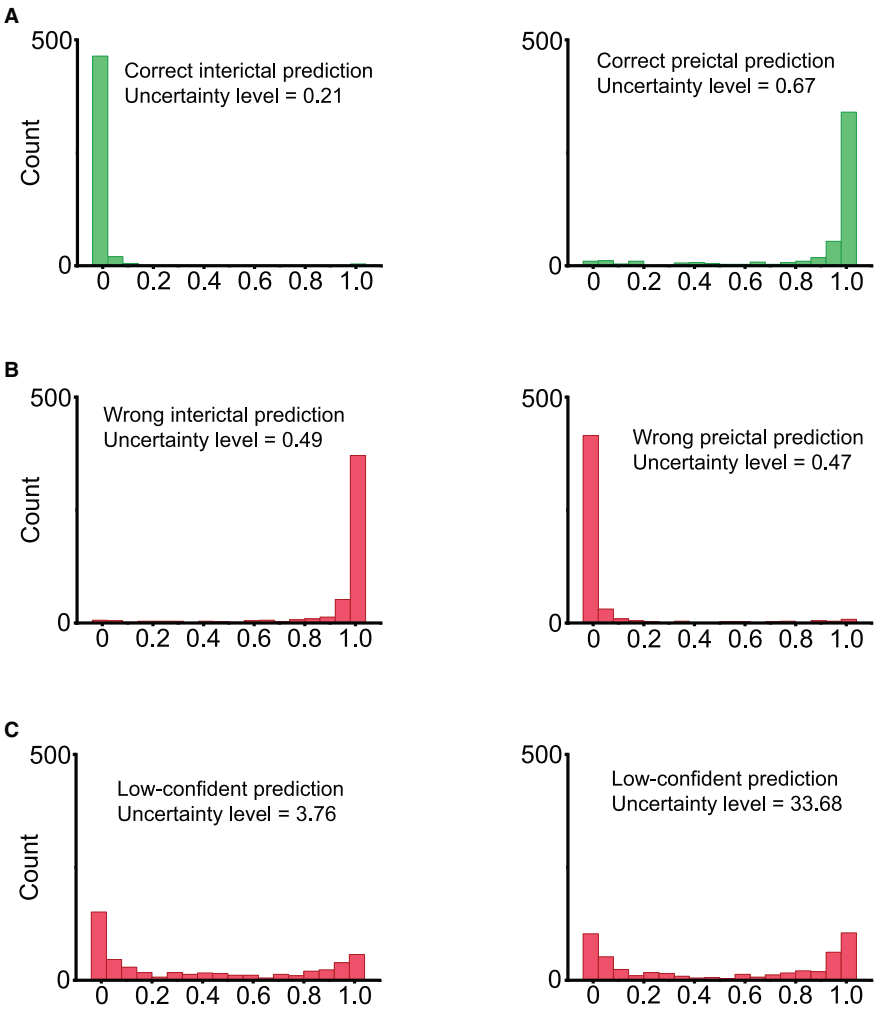

FIGURE 5 | Inference values by sampling the output of Bayesian convolutional neural network 500 times. **(A)** Correct predictions. Left: ground truth is 0 (interictal), most of the model's output samples are close to 0, indicating a correct prediction with high confidence. Right: ground truth is 1 (preictal), most of the model's output samples are close to 1, indicating a correct prediction with high confidence. **(B)** Wrong predictions. Most of the model's output samples are close to the wrong value with high confidence. This is an undesirable case. **(C)** Low-confident predictions with high uncertainty levels. The model's output samples spread randomly between 0 and 1, indicating the high uncertainty of the model.

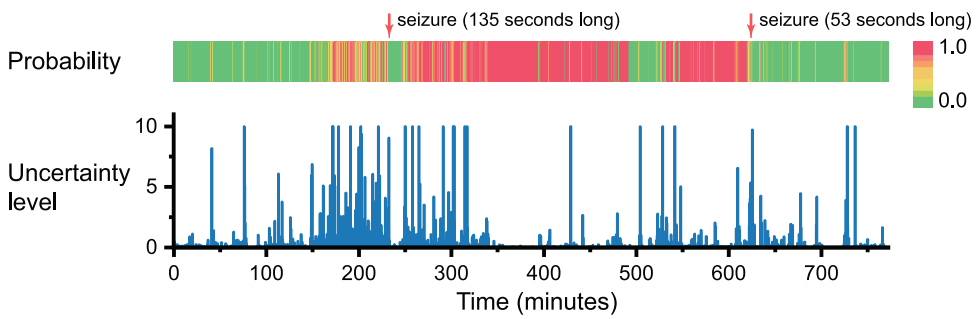

FIGURE 6 | Prediction score and uncertainty level produced by Bayesian convolution neural network in seizure forecasting task over 13 h of continuous EEG recording. For the sake of visualization, for all uncertainty levels higher than 10, we set them to 10.

have only used one extra signal, which is the time of the day, and the performance was not increased significantly. However, we argue that with the Bayesian modulator's capability to embed multiple auxiliary signals, we can achieve a boost in performance which is our aim in future works. Other relevant signals that can be used for data fusion include heart rate variability, blood oxygenation, metabolism. Some signals that have been shown related to seizure onsets, such as electrodermal activity, near-infrared spectroscopy, skin temperature, and respiratory monitor (35), can be used for data fusion as experimental exploration. For example, to use heart rate variability (HRV) for data fusion, one can plot a distribution of HRV during preictal periods (i.e., 35 to 5 min prior to seizure onset), and then apply the kernel density estimation. Lastly, we relied on the assumption that the auxiliary signals are independent of each other and independent of the main signal, i.e., EEG, to derive Equation 7. We are aware that this assumption may not always be entirely met. However, we argue that machine learning models may still work even if the assumptions are weakly met or violated; e.g., in the field of reinforcement learning, Markov property usually is not satisfied, but many models have shown working effectively in practice (36).

6. CONCLUSION

Epileptic seizure forecasting is still a substantially challenging task, but it has a consequential impact on patients' quality of life and their caregivers. While some patient-specific demonstrated excellent performance in a subset of patients, generalized predictions on non-invasive EEG recordings can work well on most patients, which has been a great challenge. This work presented an innovative approach to incorporate uncertainty and auxiliary signals information in seizure-risk forecasting. These informative warning signals will be invaluable for decision-making in employing any risk-mitigation intervention or therapies. We built our method based on the Bayesian convolutional neural network to provide an insight into the uncertainty level of seizure-risk prediction.

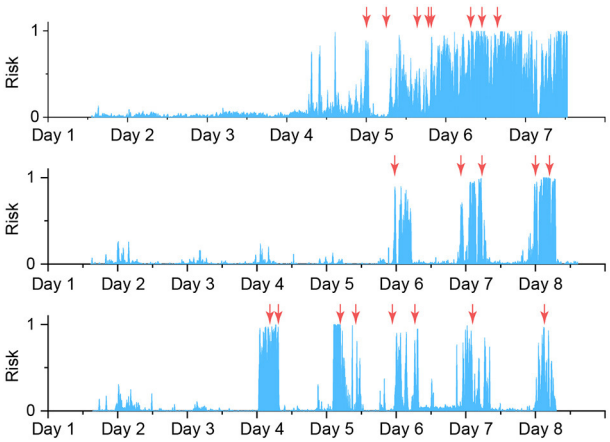

FIGURE 8 | Risk level of having seizures for top three good performance patients, from top to bottom: Pat-3, Pat-4, Pat-12. All decisions with an uncertainty level higher than 1 are discarded and not shown. Moving average of 50 steps backwards is applied to the probability score (risk level). Orange arrows indicate the seizure onsets.

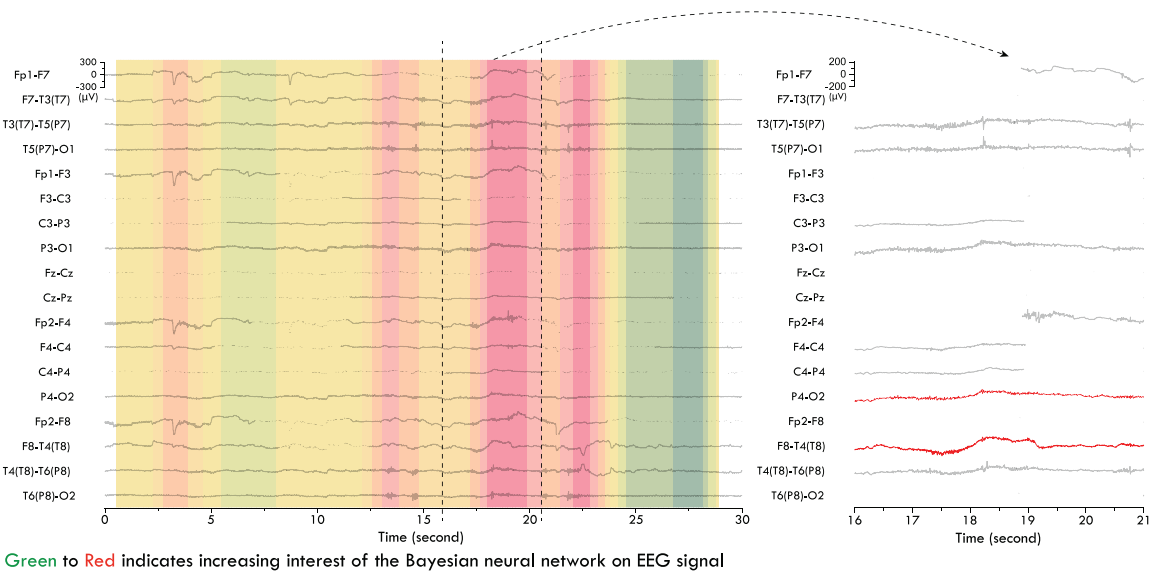

FIGURE 7 | Slow EEG activity as potential bio-marker detected by Bayesian convolutional neural network (BCNN) for epileptic seizure forecasting. Red channels (on the right) were labeled as origin of seizure in the EPILEPSIAE dataset.

CODE AVAILABILITY

The code used to generate all results in this manuscript can be made available upon request.

DATA AVAILABILITY STATEMENT

Publicly available datasets were analyzed in this study. This data can be found at: European database on epilepsy (http://www.epilepsy-database.eu/).

AUTHOR CONTRIBUTIONS

NT carried out data analysis and wrote the manuscript. OK suggested the project and supervised the work. AN provided clinical and diagnostic information. YY, CM, LK, AM, and OK revised the manuscript. All authors contributed to the article and approved the submitted version.

FUNDING

OK acknowledges the support provided by The University of Sydney through a SOAR Fellowship and Microsoft's support through a Microsoft AI for Accessibility grant.

REFERENCES

1. Litt B, Esteller R, Echauz J, D'Alessandro M, Shor R, Henry T, et al. Epileptic seizures may begin hours in advance of clinical onset: a report of five patients. *Neuron*. (2001) 30:51–64. doi: 10.1016/S0896-6273(01)00262-8
2. Maturana MI, Meisel C, Dell K, Karoly PJ, D'Souza W, Grayden DB, et al. Critical slowing down as a biomarker for seizure susceptibility. *Nat Commun*. (2020) 11:2172. doi: 10.1038/s41467-020-15908-3
3. Bosl WJ, Leviton A, Loddenkemper T. Prediction of seizure recurrence. A note of caution. *Front Neurol*. (2021) 12:773. doi: 10.3389/fneur.2021.675728
4. Re CJ, Batterman AI, Gerstner JR, Buono RJ, Ferraro TN. The molecular genetic interaction between circadian rhythms and susceptibility to seizures and epilepsy. *Front Neurol*. (2020) 11:520. doi: 10.3389/fneur.2020.00520
5. Zhong D, Luo S, Zheng L, Zhang Y, Jin R. Epilepsy occurrence and circadian rhythm: a bibliometrics study and visualization analysis via CiteSpace. *Front Neurol*. (2020) 11:984. doi: 10.3389/fneur.2020.00984
6. Baud MO, Proix T, Rao VR, Schindler K. Chance and risk in epilepsy. *Curr Opin Neurol*. (2020) 33:163–72. doi: 10.1097/WCO.0000000000000798
7. Williamson JR, Bliss DW, Browne DW, Narayanan JT. Seizure prediction using EEG spatiotemporal correlation structure. *Epilepsy Behav*. (2012) 25:230–8. doi: 10.1016/j.yebeh.2012.07.007
8. Direito B, Teixeira CA, Sales F, Castelo-Branco M, Dourado A. A realistic seizure prediction study based on multiclass SVM. *Int J Neural Syst*. (2017) 27:1750006. doi: 10.1142/S012906571750006X
9. Myers MH, Padmanabha A, Hossain G, de Jongh Curry AL, Blaha CD. Seizure prediction and detection via phase and amplitude lock values. *Front Hum Neurosci*. (2016) 10:80. doi: 10.3389/fnhum.2016.00080
10. Alotaiby TN, Alshebeili SA, Alotaibi FM, Alrshoud SR. Epileptic seizure prediction using CSP and LDA for scalp EEG signals. *Comput Intell Neurosci*. (2017) 2017:1240323. doi: 10.1155/2017/1240323
11. Yang Y, Zhou M, Niu Y, Li C, Cao R, Wang B, et al. Epileptic seizure prediction based on permutation entropy. *Front Comput Neurosci*. (2018) 12:55. doi: 10.3389/fncom.2018.00055
12. Bou Assi E, Gagliano L, Rihana S, Nguyen DK, Sawan M. Bispectrum features and multilayer perceptron classifier to enhance seizure prediction. *Sci Rep*. (2018) 8:15491. doi: 10.1038/s41598-018-33969-9
13. Truong ND, Nguyen AD, Kuhlmann L, Bonyadi MR, Yang J, Ippolito S, et al. Convolutional neural networks for seizure prediction using intracranial and scalp electroencephalogram. *Neural Netw*. (2018) 105:104–11. doi: 10.1016/j.neunet.2018.04.018
14. Liu C, Xiao B, Hsaio W, Tseng VS. Epileptic seizure prediction with multi-view convolutional neural networks. *IEEE Access*. (2019) 7:170352–61. doi: 10.1109/ACCESS.2019.2955285
15. Yu Z, Nie W, Zhou W, Xu F, Yuan S, Leng Y, et al. Epileptic seizure prediction based on local mean decomposition and deep convolutional neural network. *J Supercomput*. (2020) 76:3462–76. doi: 10.1007/s11227-018-2600-6
16. Zhang Y, Guo Y, Yang P, Chen W, Lo B. Epilepsy seizure prediction on EEG using common spatial pattern and convolutional neural network. *IEEE J Biomed Health Inform*. (2020) 24:465–74. doi: 10.1109/JBHI.2019.2933046
17. Truong ND, Kuhlmann L, Bonyadi MR, Querlioz D, Zhou L, Kavehei O. Epileptic seizure forecasting with generative adversarial networks. *IEEE Access*. (2019) 7:143999–4009. doi: 10.1109/ACCESS.2019.2944691
18. Wei X, Zhou L, Zhang Z, Chen Z, Zhou Y. Early prediction of epileptic seizures using a long-term recurrent convolutional network. *J Neurosci Methods*. (2019) 327:108395. doi: 10.1016/j.jneumeth.2019.108395
19. Duan L, Hou J, Qiao Y, Miao J. Epileptic seizure prediction based on convolutional recurrent neural network with multi-timescale. In: *Proceedings of Intelligence Science and Big Data Engineering* (2019) p. 139–50. doi: 10.1007/978-3-030-36204-1_11
20. Shorvon S, Tomson T. Sudden unexpected death in epilepsy. *Lancet*. (2011) 378:2028–38. doi: 10.1016/S0140-6736(11)60176-1
21. Verducci C, Hussain F, Donner E, Moseley BD, Buchhalter J, Hesdorffer D, et al. SUDEP in the North American SUDEP registry: the full spectrum of epilepsies. *Neurology*. (2019) 93:e227–36. doi: 10.1212/WNL.0000000000007778
22. Klatt J, Feldwisch-Drentrup H, Ihle M, Navarro V, Neufang M, Teixeira C, et al. The EPILEPSIAE database: an extensive electroencephalography database of epilepsy patients. *Epilepsia*. (2012) 53:1669–76. doi: 10.1111/j.1528-1167.2012.03564.x
23. EPILEPSIAE. *The European Epilepsy Database* (2012). Available online at: http://www.epilepsy-database.eu/ (accessed July 13, 2021).
24. Blei DM, Kucukelbir A, McAuliffe JD. Variational inference: a review for statisticians. *J Am Stat Assoc*. (2017) 112:859–77. doi: 10.1080/01621459.2017.1285773
25. Hoffman MD, Blei DM, Wang C, Paisley J. Stochastic variational inference. *J Mach Learn Res*. (2013) 14:1303–47.
26. Maiwald T, Winterhalder M, Aschenbrenner-Scheibe R, Voss HU, Schulze-Bonhage A, Timmer J. Comparison of three nonlinear seizure prediction methods by means of the seizure prediction characteristic. *Phys D Nonlinear Phenomena*. (2004) 194:357–68. doi: 10.1016/j.physd.2004.02.013
27. Karoly PJ, Ung H, Grayden DB, Kuhlmann L, Leyde K, Cook MJ, et al. The circadian profile of epilepsy improves seizure forecasting. *Brain*. (2017) 140:2169–82. doi: 10.1093/brain/awx173
28. Zijlmans M, Flanagan D, Gotman J. Heart rate changes and ECG abnormalities during epileptic seizures: prevalence and definition of an objective clinical sign. *Epilepsia*. (2002) 43:847–54. doi: 10.1046/j.1528-1157.2002.37801.x
29. Pavei J, Heinzen RG, Novakova B, Walz R, Serra AJ, Reuber M, et al. Early seizure detection based on cardiac autonomic regulation dynamics. *Front Physiol*. (2017) 8:765. doi: 10.3389/fphys.2017.00765
30. Schwartz TH. Neurovascular coupling and epilepsy: hemodynamic markers for localizing and predicting seizure onset. *Epilepsy Curr*. (2007) 7:91–4. doi: 10.1111/j.1535-7511.2007.00183.x

31. Zhao M, Nguyen J, Ma H, Nishimura N, Schaffer CB, Schwartz TH. Preictal and ictal neurovascular and metabolic coupling surrounding a seizure focus. *J Neurosci*. (2011) 31:13292–300. doi: 10.1523/JNEUROSCI.2597-11.2011
32. Scipy. *Kernel Density Estimation* (2019). Available online at: https://docs.scipy.org.
33. Dunne RA, Campbell NA. On the pairing of the softmax activation and cross-entropy penalty functions and the derivation of the softmax activation function. *Proc Conf Neural Netw*. (1997) 181:185.
34. Tao JX, Chen XJ, Baldwin M, Yung I, Rose S, Frim D, et al. Interictal regional delta slowing is an EEG marker of epileptic network in temporal lobe epilepsy. *Epilepsia*. (2011) 52:467–76. doi: 10.1111/j.1528-1167.2010.02918.x
35. Ulate-Campos A, Coughlin F, Gaínza-Lein M, Fernández IS, Pearl PL, Loddenkemper T. Automated seizure detection systems and their effectiveness for each type of seizure. *Seizure*. (2016) 40:88–101. doi: 10.1016/j.seizure.2016.06.008
36. Sutton RS, Barto AG. *Reinforcement Learning: An Introduction*. 2nd ed. The MIT Press (2014).

Conflict of Interest: The authors declare that the research was conducted in the absence of any commercial or financial relationships that could be construed as a potential conflict of interest.

frontiers in Neurology

ORIGINAL RESEARCH
published: 20 September 2021
doi: 10.3389/fneur.2021.717428

Seizure Forecasting: Patient and Caregiver Perspectives

Caitlin L. Grzeskowiak[1]* *and Sonya B. Dumanis*[1,2]

[1] *Epilepsy Foundation of America, Greater Landover, MD, United States,* [2] *Coalition for Aligning Science, Chevy Chase, MD, United States*

Accurate seizure forecasting is emerging as a near-term possibility due to recent advancements in machine learning and EEG technology improvements. Large-scale data curation and new data element collection through consumer wearables and digital health tools such as longitudinal seizure diary data has uncovered new possibilities for personalized algorithm development that may be used to predict the likelihood of future seizures. The Epilepsy Foundation recognized the unmet need for development in seizure forecasting following a 2016 survey where an overwhelming majority of respondents across all seizure types and frequencies reported that unpredictability of seizures had the strongest impact on their life while living with or caring for someone living with epilepsy. In early 2021, the Epilepsy Foundation conducted an updated survey among those living with epilepsies and/or their caregivers to better understand the use-cases that best suit the needs of our community as seizure forecast research advances. These results will provide researchers with insight into user-acceptance of using a forecasting tool and incorporation into their daily life. Ultimately, this input from people living with epilepsy and caregivers will provide timely feedback on what the community needs are and ensure researchers and companies first and foremost consider these needs in seizure forecasting tools/product development.

Keywords: seizure forecasting, community survey, patient perception, wearable sensors, epilepsy, seizure forecasting devices

OPEN ACCESS

Edited by:
Sharon Chiang, University of California, San Francisco, United States

Reviewed by:
Robert Scott Fisher, Stanford University, United States
Kais Gadhoumi, Duke University, United States

***Correspondence:**
Caitlin L. Grzeskowiak
cgrzeskowiak@efa.org

Specialty section:
This article was submitted to Epilepsy, a section of the journal Frontiers in Neurology

Received: *30 May 2021*
Accepted: *09 August 2021*
Published: *20 September 2021*

Citation:
Grzeskowiak CL and Dumanis SB (2021) Seizure Forecasting: Patient and Caregiver Perspectives. Front. Neurol. 12:717428. doi: 10.3389/fneur.2021.717428

INTRODUCTION

The epilepsies are a set of conditions characterized by recurring and spontaneous seizures. The seemingly unpredictable nature of epilepsy, for example not knowing when and where an event will occur, has a huge impact on an individual's quality of life (1). A reliable seizure forecasting system could facilitate better management of epilepsy and allow those living with epilepsies more control over their lives.

The first human clinical trial using intracranial electroencephalography (EEG) for developing seizure warning systems (Neurovista) demonstrated the viability of personalized prospective seizure forecasting tailored to the user (2). Subsequent machine learning competitions leveraging the rich Neurovista datasets (3, 4) demonstrated that these seizure forecasting algorithms can be improved. These algorithms were further optimized when variables in addition to EEG data such as circadian rhythms, sleep, weather, and temporal features were incorporated into Bayesian forecasts (5, 6). With the advent of neural engineering, less invasive systems like UNEEG, which uses subcutaneous EEG, have also demonstrated the feasibility to forecast seizure cycles in patients (7). More recent studies have also suggested forecasting from seizure self-reported diaries (despite the known inaccuracies of self-reported seizure events) can still be utilized for above-chance forecasting even when there was no accompanying EEG data (8, 9).

The Epilepsy Foundation created the My Seizure Gauge Initiative with a mission to create a minimally invasive personalized seizure advisory system to assess the likelihood of seizure on a timescale of hours before possible occurrence. Rather than focusing on early warning detection systems that could categorically predict an imminent seizure, the emphasis of the initiative was on developing probabilistic algorithms that would calculate an individuals likely risk of having a seizure during specified time ranges. The desire was to leverage biosensors, EEG, and deep machine learning to improve upon current concepts and create personalized forecasting algorithms for people living with epilepsy (10). Part of the initiative is also to engage the epilepsy community earlier in the research and development process in order to ensure the voice of the patient is incorporated into user-design considerations.

In 2018, the Foundation launched a patient preference survey to quantify patient and caregiver preferences for the potential benefits and risks of a future hypothetical seizure forecasting device (11). Results from the survey highlighted key attributes to consider with a forecasting device such as form factor, cost, and the accuracy of the algorithm. Moreover, the study highlighted that the notions of meaningful benefits and acceptable risks differ between people living with epilepsy and their caregivers. For example, patients were more willing to accept "inaccurate" forecasts of the device compared with a care-partner (11).

As seizure forecasting tools are moving from hypothetical to a likely reality, it is essential to understand the acceptance of the epilepsy community for such tools and how they would incorporate these tools into daily life. In 2021, the Epilepsy Foundation launched a new community survey to evaluate the readiness of the epilepsy community for a forecasting tool and better understand how such a device would be incorporated into daily living.

MATERIALS AND METHODS

A seizure forecasting survey targeted to those living with epilepsy and their caregivers was generated using Qualtrics (Provo, Utah) and distributed online (see **Supplementary Table 1** for survey questions). Demographic survey wording was developed by the Epilepsy Foundation targeting an 8th grade reading level in accordance with previous Epilepsy Foundation surveys. The participants for the survey were not recruited through random selection and therefore any results should not be generalized to a broader population. Participants were recruited through convenience sampling; multiple Epilepsy Foundation media channels were used to ensure widespread distribution including Epilepsy Foundation Facebook and Twitter pages. The study was also distributed via the Epilepsy Foundation newsletter twice via email. The survey collected responses between January 29, 2021, and March 8, 2021. The study only involves survey procedures and observations of public behavior and is therefore exempt from IRB review under 45 CFR § 46.104(d)(2). Provisions were taken to protect the privacy of subjects and to maintain the confidentiality of data. All responses were aggregated and anonymized prior to analysis. The survey did not require input for specific epilepsy diagnosis, age of onset, medications taken, or intellectual disabilities in order to simplify patient experience during survey administration and allow respondents to consider all their seizure types throughout the survey questionnaire.

Inclusion Criteria

Participants were required to be at least 18 years of age and identify as a person with epilepsy (PWE) or a primary caregiver of someone with epilepsy.

Exclusion Criteria

Participants who are not older than 18 years of age at the time of the survey, participants who do not identify as a PWE or caregiver, or participants who did not fully complete the survey.

Statistical Analysis

To assess any potential differences in survey responses between those who identified as a person living with epilepsy or care partners, a non-parametric test—the Mann-Whitney *U*-Test—with a two-tailed hypothesis was calculated, with the significance level set to 0.05.

RESULTS

Survey Demographics

A total of 942 participants started the survey, with 652 progressing until the end (69% completion rate). Only completed surveys are analyzed in the results, and of the 652 respondents analyzed, 64% identified as a person with epilepsy and 36% as a primary caregiver for someone with epilepsy. **Table 1** includes additional demographic information on survey participants subcategorized for a PWE or caregiver. The majority of participants were white (82 and 81% PWE and caregiver, respectively), and were women (70 and 81% PWE and caregiver, respectively). Respondents also reported their highest level of education attained (**Table 1**) in which the majority of respondents indicated they had completed an Associates' degree or higher (68% PWE and 74% caregivers). This demographics assessment is consistent with metrics collected for unique visitors to epilepsy.com. Although caregivers were answering for those with more frequent seizures (**Supplementary Figure 1**), no significant differences were found among their responses regarding user acceptance of the device between the groups (**Supplementary Figures 2–4**).

We also asked respondents how often the individual's seizures occurred, summarized in **Figure 1**. While there was representation from a broad range of seizure frequencies, the majority of responders were reporting seizure frequency as once a month (20%), followed by 1 seizure per week (15%) and 3–4 seizures per year (15%).

Epilepsies Community's Openness to Seizure Forecasting Research

To assess community acceptance of seizure forecasting tools, survey participants were asked to indicate whether they thought it was possible for a device to predict their seizures (**Figure 2A**, **Supplementary Figure 2**). The majority of respondents (79%)

TABLE 1 | Demographics on seizure forecasting survey responses.

Number of respondents	418 (64%) person with epilepsy	234 (36%) caregiver
Age	43+/−16 yrs	45+/−14 yrs
Ethnicity	• Hispanic | 26 (6%) • Not hispanic | 333 (80%) • Prefer not to say | 59 (14%)	• Hispanic | 22 (9%) • Not hispanic | 180 (77%) • Prefer not to say | 32 (14%)
Race	• Asian | 19 (5%) • American Indian or Alaska native | 5 (1%) • Black or African American | 17 (4%) • Native Hawaiian | 6 (1%) • Other Pacific Islander | 1 (0%) • White | 345 (82%) • Prefer not to answer | 41 (10%)	• Asian | 12 (5%) • American Indian or Alaska native | 2 (1%) • Black or African American | 10 (4%) • Native Hawaiian | 2 (1%) • Other Pacific Islander | 0 (0%) • White | 189 (81%) • Prefer not to answer | 26 (11%)
Gender	• Female | 292 (70%) • Male | 105 (25%) • Non-binary/third gender | 2 (0%) • Prefer not to say | 19 (5%)	• Female | 190 (81%) • Male | 33 (14%) • Non-binary/third gender | 0 (0%) • Prefer not to say | 11 (5%)
Education	• Did not complete high school | 8 (2%) • High school diploma/GED | 100 (24%) • Associates or 2-year degree | 65 (15%) • Bachelors or 4-year degree | 150 (36%) • Master's degree | 58 (14%) • Doctorate degree | 13 (3%) • Prefer not to say | 24 (6%)	• Did not complete high school | 7 (3%) • High school diploma/GED | 39 (17%) • Associates or 2-year degree | 39 (17%) • Bachelors or 4-year degree | 72 (31%) • Master's degree | 44 (19%) • Doctorate degree | 17 (7%) • Prefer not to say | 16 (7%)

Percentage of each group in parenthesis.

indicated they believe it is possible or may be possible for a device to predict their seizures. Of those who responded "yes", 80% also explained why they answered that way by entering a descriptive response. Of those free text responses for why a PWE or caregiver believed a device could forecast their seizures, most could be grouped into five broad categories:

1. **Optimism and belief in technology.** A total of 42% of respondents expressed their hope for the future due to innovative advances in technology and belief that anything is possible. For example, one respondent wrote "absolutely, technology is always improving".
2. **Belief that identifiable seizure triggers or physiological changes could be used, measured, and incorporated for a forecasting tool**. In total, 26% of respondents discussed measurable, known seizure triggers such as menstrual cycle patterns and lack of sleep or food intake which could be inputs for a forecasting seizure risk assessment. For example, one respondent wrote "My seizure risk increases based on sleep, stress, activity, and food intake, so forecasting is possible", while another wrote "I imagine that there may be physiological signs or a combination of signs that could be precursors for seizure activity".
3. **Preliminary observation of time patterns in their current seizures that could be incorporated into a device**. Overall, 13% of respondents fell into this category. For example, a respondent wrote "It [seizure forecasting device] could determine seizure times if there are any patterns regarding time of day, day of the week, day of the month, or catamenial seizure".
4. **A belief that brain activity measurements could forecast seizures.** A total of 8% of respondents described an observation relating to how brain activity may be a key to the forecasting component. As an example, a free text entry from a respondent stated: "Yes, a device could predict my seizures because my EEGs show irregular brain activity before a seizure occurs. I believe that data could be used to help the device forecast when a seizure may occur depending on how I'm feeling that day or how far my brain is being "pushed".
5. **Existing seizure premonitions.** Overall, 8% of respondents wrote about auras or a feeling they felt prior to seizure onset that could be incorporated into a forecasting tool. For example, a respondent wrote "I experience times where I can "feel' that it would be a day where seizures might be more likely, so I know there must be some way we could capture that with a device as long as it focuses on specific things". While another respondent wrote, "Sometimes I will feel strange several hours before having one and then after the seizure I realize that was probably a foreboding feeling".

Of the 10% of participants who responded "no", they did not believe it was possible to forecast their seizures based on their experiences, 62% of these respondents also wrote in why they did not believe it would be possible. Most of their free text responses could be grouped into two categories as a belief that:

1. **Their seizures were seemingly random with no obvious warning signs.** Respondents wrote that the unpredictability of their seizures made it unclear what a device could possibly measure. Fifty percent of respondents answered in this way. For example, respondents wrote, "My seizures are random. Nothing in the past has been able to predict my seizures" or "The times of seizures aren't consistent".
2. **It might be possible for others but not for their seizure type.** A total of 19% of respondents were included in this category, writing that their specific seizures were too complicated. For example, one respondent wrote "I have simple partial seizures. Most devices currently only detect tonic clonic seizures" while another wrote "The way my epilepsy manifests has changed too many times, so I don't think any device could take into consideration that many variables".

Regardless of whether a respondent thought it was possible for such a device to exist, when respondents were asked whether a user would use the device if it existed, 76% said they would use the device, 20% said they might use the device and only 2% of respondents said they would not use the device (**Figure 2B**). Similarly, when asked whether it was important

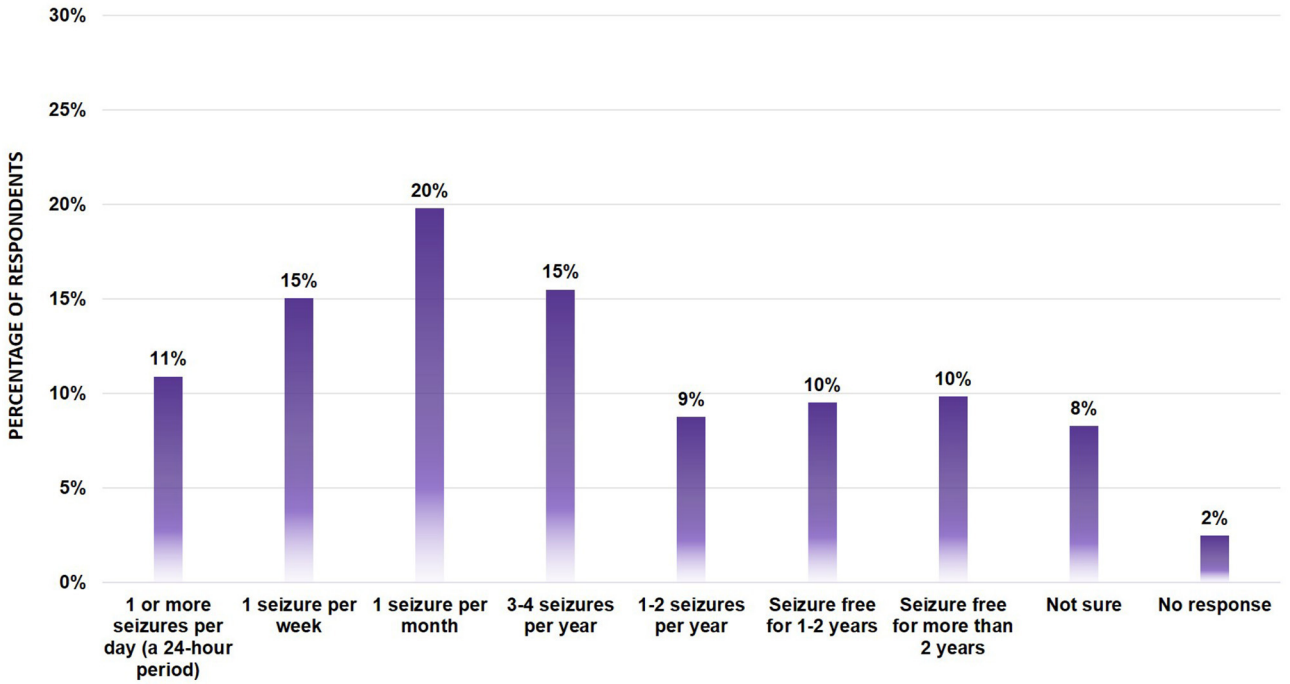

FIGURE 1 | Seizure Frequency of survey participants ($n = 652$). Bar graph showing the percentage of respondents across the various seizure types. No significant differences were found between segments using the Mann-Whitney *U*-Test.

for the epilepsy community to have such a device, a majority (95%) of respondents said it was either extremely (74%) or very important (19%) (**Figure 2C**). Of the individuals who did not believe the device would be useful to them (10%, **Figure 2A**), the majority still thought such a device would be extremely (69%) or very important (18%) for the community to have (88% total) (**Figure 2D**) indicating a true, recognized need within the community, even if no benefit comes to the individual.

The Epilepsies Community Feedback on Considerations for a Forecasting Device

While there are several critical parameters to consider in developing a forecasting device, our survey focused on the timing necessary to make actionable changes to an individual's day based on how the individual would envision using a forecasting device. When asked how far in advance the respondent would need to be alerted to inform plans or activities for their day, there were slightly more (28%) respondents who wished to be alerted within 24 h, however similar preferences were observed at hourly and more than 24 h (20% each) and within 12 h (23%) (**Figure 3A**, **Supplementary Figure 3**). These results indicate that alert preferences vary for individuals, likely depending on what they plan to do with the information of when a seizure will occur. When analyzed by seizure frequency, the most common alert window was still 24 h across most seizure frequencies, with the exception of those with 3–4 seizures per year, who cited they would like more than 24 h of notice, and those with 1 or more seizures per day, who cited a preference for hourly seizure warnings (**Supplementary Figure 5**). Planning may also depend on seizure type, which was not included in this study but should be further evaluated. Further user preference studies will determine the most valuable uses of a device for individual use cases.

Similar to weather forecasting, where people may use information from the forecast (i.e., sunny day vs. rainy day) to determine whether they will go outside for a walk, stay inside, or prepare in advance, users may prefer to know when they are both likely and unlikely to have seizures. Indeed, our results indicate most respondents prefer predictions for both times they are prone to seizures and times they are unlikely to have seizures (60%) (**Figure 3B**), while 38% preferred to only be alerted during times they are more likely to have a seizure. When asked whether a device that could predict a low chance of seizure would impact them, 69% of all respondents indicated this would help them plan their day. Similarly, 89% of respondents indicated a forecasting tool that indicated a high likelihood of seizure would help them plan their day (**Figures 3C,D**). Taken together, these results indicate that users would want to be informed of both the high likelihood and low likelihood of a seizure, but knowing there is a higher chance of a seizure would be more helpful in day-to-day planning.

Those who selected that they would use a forecast tool that indicated a low chance of seizure (**Figure 3C**), when asked how this could change their plans, cited examples such as regaining the ability to drive and participating in sports or physical activities. For those who indicated they would use a forecast tool to determine the high chance of seizure (**Figure 3D**), when asked how this would change their plans, representative responses

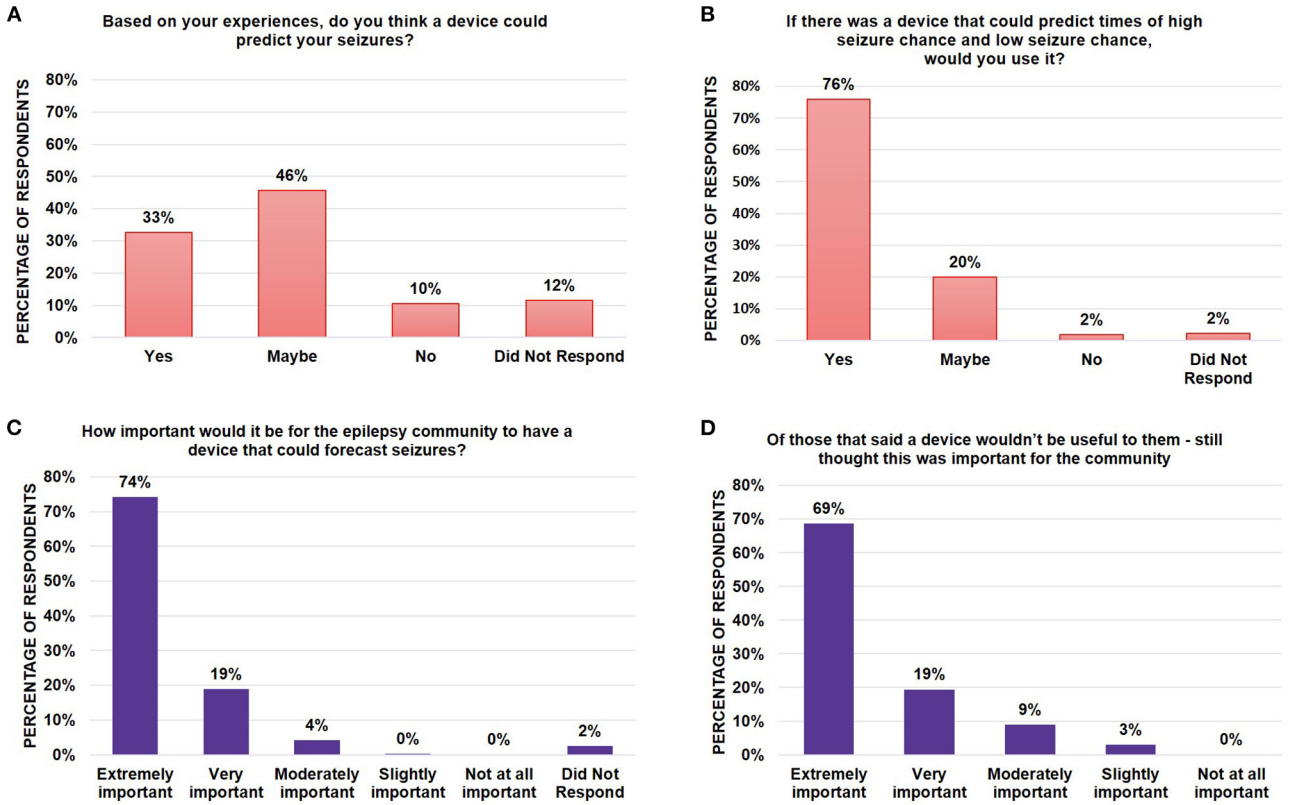

FIGURE 2 | Assessment of epilepsy community perspectives and need for forecasting tools. Bar graphs showing the percentage of survey respondents who indicated **(A)** whether they believed whether it was possible for a device to predict their chance of seizures; **(B)** whether they would use such a device if it existed; and **(C)** whether they believed it was important for the epilepsy community to have the device. Of those who did not believe that a device would be useful to them, **(D)** a bar graph indicated the breakdown of whether those respondents thought this was still an important device for the epilepsy community to have. Note that all numbers have been rounded to two significant figures. No significant differences were found between segments using the Mann-Whitney *U*-Test.

included: staying home (from work or other activities), avoiding public transportation, and plans for rescue medication. For those who stated it would not impact their day, many responded they are used to expecting seizures, do not have seizures often enough, or seizures did not stop them from completing daily tasks.

Risk of Forecasting Tools

To determine an individual's tolerance to having the opposite occurrence given by the forecast, we asked survey respondents whether they would continue using a forecasting tool if the device inaccurately predicted they would have a seizure, but no seizure occurred. In this case, 65% of respondents indicated they were still likely or very likely to continue using the device (**Figure 4A**, **Supplementary Figure 4**). Among those that responded "it depends", there was an indication they would be willing to try the device a few times, but that consistent inaccuracies would result in termination of use of the device. In the event of a seizure occurring during a time when the forecasting tool predicted a low chance of seizure, only 52% of respondents indicated they were likely or very likely to continue using the device (**Figure 4B**), with an increase in those responding they would be unlikely (8%) to use the device compared to **Figure 4A** (3%). These results indicate that users prefer the device to be more likely to warn them of a seizure even if it does not occur, than to have a seizure that was not forecasted by the device. Similar responses were observed when scenario testing was evaluated by seizure frequency (**Supplementary Figure 6**). These results also indicate users within the epilepsy community understand and accept some inaccuracies in a forecasting device.

DISCUSSION

Seizure unpredictability remains a chronic, critical problem for people living with epilepsies or those caring for someone with epilepsy (10). Advances in forecasting algorithms suggest that a personalized seizure forecasting tool may be available in the foreseeable future (8, 9, 12). Respondents to this survey were unanimous in assessing that there was importance in developing this tool for the epilepsy community regardless of whether they themselves would use it (**Figure 2**, **Supplementary Figure 2**). An oft cited rationale for why a person believed that seizure forecasting would not apply to their use-case was because the individual had non-motor seizures that they did not think could be detected with a device. In contrast, those who believed seizure

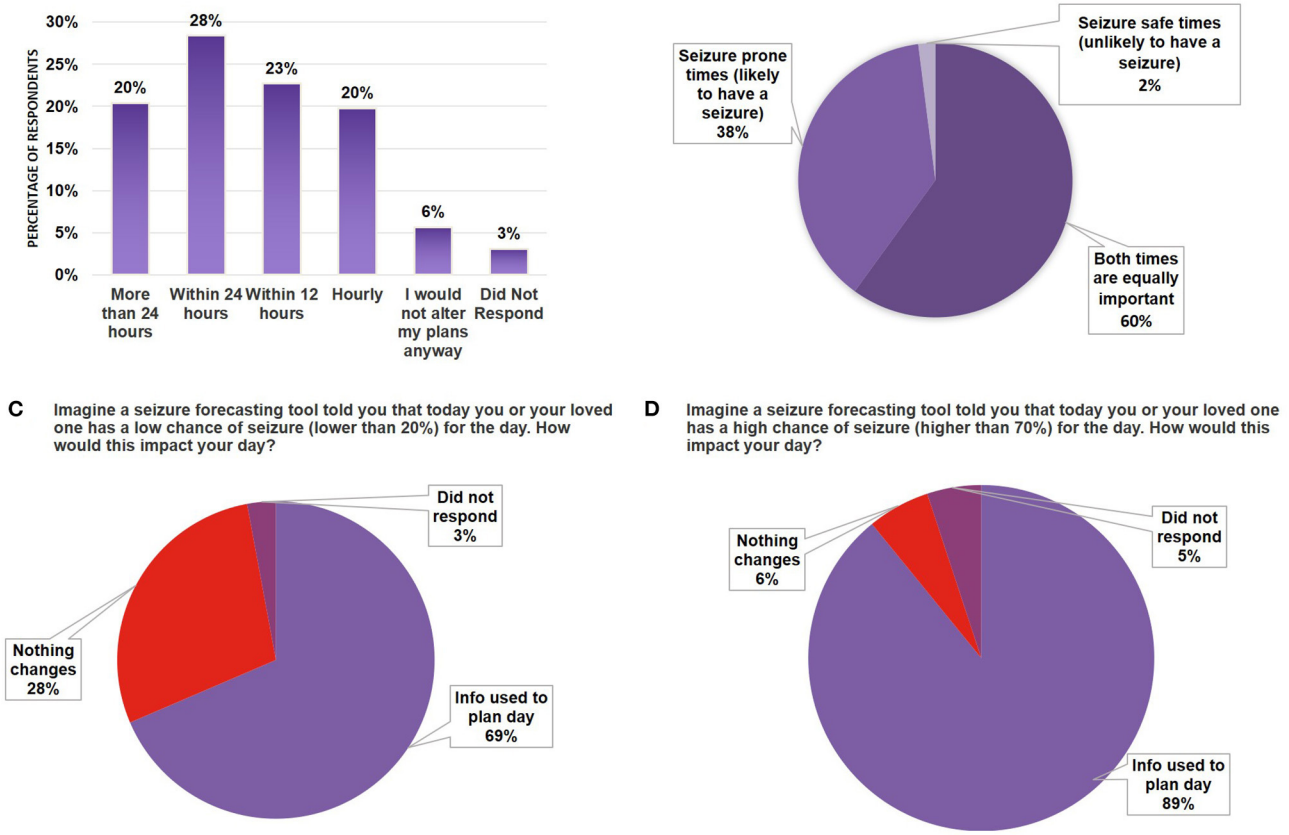

FIGURE 3 | Seizure forecasting device scenario testing. **(A)** Bar graph indicating the breakdown by percentage of survey respondents who wanted to be alerted at different time scales for their likelihood of seizure (time ranges indicated on X-axis). **(B)** Pie chart breaking down the percentage of respondents who indicated whether they had a preference to use a device that would forecast seizure-prone vs. seizure-safe states. **(C,D)** Bar graph indicating the percentage of survey respondents that would use the device in daily planning when the device forecasted a 20% chance of seizure **(C)** or 70% chance of seizure **(D)**. Note that all numbers have been rounded to two significant figures. No significant differences were found between segments using the Mann-Whitney *U*-Test.

forecasting is possible often cite self-observed premonitions, which have been observed to be detectable at an above chance level in a prospective self-prediction study using seizure diaries in a subset of individuals (13, 14). As the research community moves forward with bringing forecasting algorithms to the marketplace, it will be important to educate the community on who the target audiences for seizure forecasting will be and whether these algorithms are inclusive of all seizure types. Indeed, for seizure detection systems, there is a high degree of variability in the effectiveness of detection systems when classified by seizure type (15).

Interestingly, many of the symptoms and stimuli a respondent referenced as a seizure gauge may possibly correlate neatly to parameters already being considered as variables for seizure forecasting algorithm development, from leveraging triggers and the environment (6) to temporal patterns (5, 16–18). While it is possible that the respondents to the online survey collected via epilepsy.com may already be familiar with seizure forecasting, these results indicate that users may intuitively grasp components contributing to how a seizure forecasting algorithm works and have more confidence in using the tool. However, while our data indicate user respondents may accept some degree of "inaccuracy" in a forecasting device, more work will need to be done to educate the community on the distinction between the prediction of a seizure; a determinant, future event that will happen at a precise time (categorical statement); in contrast to forecasting, which indicates likelihood (a probabilistic statement). The 2021 survey questions emphasized language around "prediction of chance" to represent a forecast, although we did not further examine respondents understanding of the difference.

There are a variety of use-cases discussed in the research community for how a seizure forecasting device could be applied: from guiding treatment plans or clinical trial design, to improving quality of life (19). When the epilepsy community was asked about how the device would be used in daily life, a majority said this information would be used to plan their day (**Figure 3**). Specifically, many wrote about using it as a tool for modifying their behavior to reduce their seizure likelihood. For example, one respondent wrote, "(If there was a 70% chance

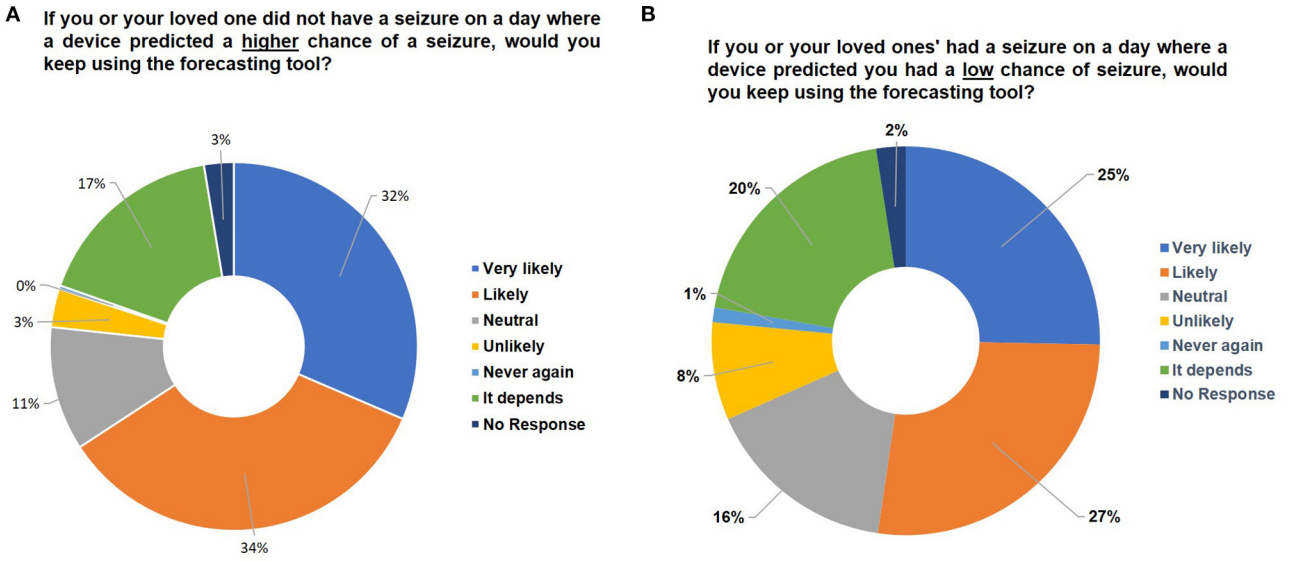

FIGURE 4 | Assessing user tolerance for error. Pie charts indicating the percentage breakdown of survey respondents that would keep using the forecasting tool if **(A)** there was no seizure on a day that forecasted high seizure risk or **(B)** there was a seizure on a day that forecasted low seizure risk. Note that all numbers have been rounded to two significant figures. No significant differences were found between segments using the Mann-Whitney *U*-Test.

of seizure), I would decrease other seizure inducing things (i.e., drinking one cup of coffee instead of three, taking naps) as well as taking my meds exactly 12 h apart. Just like I do during seizure season-when the weather is hot and changing to winter".

As the field of digital therapeutics begins to gain traction within our community, it is possible that seizure forecasting will become a part of managed behavioral intervention strategies. Respondents wrote about how this would help their activity planning for the week. For example, one respondent wrote "If the forecast was that high [70%], I'd work from home that day or maybe consider taking the day off. I could also prepare myself mentally for how rough my week was about to get and maybe make sure other life tasks were in order [like having meals prepped for the week. My recovery period for a (Tonic Clonic) is long]. With that, if the device was able to predict the type of seizure, that would also make a difference. If I knew I was likely to experience a small focal (like Deja vu), that's way less detrimental to my week than a [Tonic Clonic]".

Several survey respondents wrote that an accurate seizure forecasting device may help them complete activities such as swimming or driving. While the notion of independence was repeatedly observed in our survey, device manufacturers must properly consider all potential use-cases from the community and thoroughly warn users of risks associated with inaccurate seizure prediction. For example, if used to make decisions like whether or not to drive, additional clear warning labels will be needed to address limitations of the tool. More research is needed to explore seizure forecasting use-cases in greater detail. However, from the survey text responses, many wrote about how having some indication of seizure chance would still be an improvement over their current seemingly unpredictable seizure patterns.

Moreover, there were a small fraction of survey participants who shared downsides to seizure forecasting, noting their anxiety levels might increase if they were constantly checking the forecast to see if their behavior increased their chance of seizure. It was clear from the responses that different users would want different thresholds for notifications when a forecasting level changed depending on their seizure frequency and their baseline anxiety levels. Although some advances have been made toward this flexibility (20), further technical and design exploration is required to understand the user design aspect of setting personal alerting thresholds.

Seizure forecasting, because of its inherent probabilistic nature, does not have traditional false negative/false positive deterministic evaluations. If a seizure does not occur when a device indicates a high chance of seizure, this does not mean the forecast was incorrect. Some respondents to the survey indicated an understanding of this concept and accepted with the notion of a high chance of seizure not meaning categorically that a seizure would occur. Many referenced the weather not always being 100% accurate in their rationale. If an action could be taken based on the information, they would find it useful (similar to taking an umbrella in case of rain). Others discussed how seizures in themselves were probabilistic in nature and the environment or behavior could impact their chance from moment to moment, and thus influence the forecast. For example, a respondent wrote "If the device predicted a high chance of seizure, and I changed my behavior to reduce stress and emotional triggers, [and I ended up with no seizure] then it doesn't mean the device necessarily is faulty. It's what you do with the information". Another wrote, "Was the device wrong or did the [medication] administered prevent it? I think that is important info that will be hard to measure". It was clear from the responses the community did not anticipate a 100 percent accurate device, but rather an

assessment tool to help them make decisions on what to do based on the information. The claims and labeling that a forecasting tool displays will need to be considered carefully. Understanding these limitations, encouraging conversations with doctors, and educating consumers will be essential for informed decision making. At the same time, it is also imperative for the forecasting tool to provide useful information to the user that is above and beyond what the user already knows. For example, if someone has daily seizures, having a forecasting tool that predicts high daily risk would not be of value to that individual.

A limitation to this study was the convenience sampling of the survey selection. The majority of respondents to this survey were Caucasian, women, and had attained at least an Associates' degree (**Table 1**). It is likely that our survey pool taken from the Epilepsy Foundation digital channels is more aware of seizure forecasting initiatives due to the Foundation's sponsorship and promotion of My Seizure Gauge activities, and their reflections are not representative of the general population. Device manufacturers should consider the health literacy of their target population to ensure they are aware of device limitations and best practices for using a device, as relates to understanding what probability means compared to categorical prediction of a seizure event. A recent study by Chiang et al. examined different ways seizure forecasting could be visually represented, and found noticeable differences in health literacy depending on the understanding of the visual representations, highlighting the importance of incorporating standardized methods for how such information on forecasting should be conveyed (21).

This survey did not include questions around form factor or user design considerations, such as wearability, usability, or user tolerance of the device's invasiveness. We and others have previously examined user preferences when considering how the tool would collect information on the individual (11), and others have examined how it would be visualized (21). Others who have investigated form factor preferences have shown users' willingness to charge a device and a preference toward removable, wearable devices; finding only 5% of patients would accept an implantable device (22). Through the My Seizure Gauge Initiative, we have examined additional design considerations such as charging times and device design compared to user preferences in the determination of wearables used for biosensor data collection, which has also been examined by many other groups (23–28). There is a confirmed need for a joint effort of clinical and non-clinical experts to optimize usability (20). Further work will also need to assess patient preferences for surgical vs. non-invasive devices.

Taken together, the survey highlighted that the community has many early adopters willing to use forecasting tools. A vast majority believe forecasting is possible and see utility in using these tools for their daily living. One note of caution is to ensure these tools are evaluated not just in the accuracy of their algorithms, but also in how the information is conveyed to the user both in language, visualizations, and intended use-cases. Understanding the communities' readiness, preferences, and understanding of seizure forecasting must include multi-faceted research into considerations around device design, and to what degree patients will tolerate invasive methodologies.

DATA AVAILABILITY STATEMENT

The anonymized raw data supporting the conclusions of this article will be made available by the authors, upon request.

AUTHOR CONTRIBUTIONS

CG and SD designed, analyzed experiments, and wrote manuscript. Both authors contributed to the article and approved the submitted version.

FUNDING

This research was funded by the Epilepsy Foundation of America. Through the Epilepsy Foundation Innovation Institute, the Epilepsy Foundation is funding an ongoing grant for the Foundation's My Seizure Gauge initiative.

ACKNOWLEDGMENTS

The authors acknowledge Michelle Bering, Alison Kukla, Laura Weidner, Ewan Nurse, Sarah Kaider, and all survey participants for their inputs into this manuscript.

SUPPLEMENTARY MATERIAL

The Supplementary Material for this article can be found online at: https://www.frontiersin.org/articles/10.3389/fneur.2021.717428/full#supplementary-material

Supplementary Figure 1 | Assessment of epilepsies community perspectives and need for forecasting tools responses segmented by PWE or caregiver. Bar graphs showing the percentage of survey respondents who indicated **(A)** whether they believed whether it was possible for a device to predict their chance of seizures; **(B)** whether they would use such a device if it existed; and **(C)** whether they believed it was important for the epilepsy community to have the device. Note that all numbers have been rounded to two significant figures. No significant differences were found between segments using the Mann-Whitney *U*-Test.

Supplementary Figure 2 | Seizure forecasting device scenario testing responses segmented by PWE or caregiver. **(A)** Bar graph indicating the breakdown by percentage of survey respondents who wanted to be alerted at different time scales for their likelihood of seizure (time ranges indicated on X-axis). **(B)** Bar graph breaking down the percentage of respondents who indicated whether they had a preference to use a device that would forecast seizure prone vs. seizure safe states. **(C,D)** Bar graph indicating the percentage of survey respondents that would use the device in daily planning when the device forecasted 20% chance of seizure **(C)** or 70% chance of seizure **(D)**. Note that all numbers have been rounded to two significant figures. No significant differences were found between segments using the Mann-Whitney *U*-Test.

Supplementary Figure 3 | Assessing user tolerance for error responses segmented by PWE or caregiver. Bar graphs indicating the percentage breakdown of survey respondents that would keep using the forecasting tool if **(A)** there was no seizure on a day that forecasted high seizure risk or **(B)** there was a seizure on a day that forecasted low seizure risk. Note that all numbers have been rounded to two significant figures. No significant differences were found between segments using the Mann-Whitney *U*-Test.

Supplementary Figure 4 | Assessment of time window preference segmented by seizure frequency. Bar graph indicating the percentage breakdown by self-identified seizure frequency of when respondents would want to be alerted at

different time scales for their likelihood of seizure (time ranges indicated on X-axis).

Supplementary Figure 5 | Seizure forecasting device scenario testing segmented by seizure frequency Bar graphs indicating the percentage breakdown of survey respondents by their self-identified seizure frequencies indicating whether **(A)** a forecasting tool indicating lower than a 20% chance of seizure would impact their day or **(B)** a forecasting tool indicating higher than 70% chance of seizure would impact their day. Note that all numbers have been rounded to two significant figures.

Supplementary Table 1 | Survey Questionnaire. List of questions and logic flow of the survey questionnaire.

REFERENCES

1. Foundation E. *2016 Community Survey* Landover, MD: Epilepsy Foundation (2016).
2. Cook MJ, O'Brien TJ, Berkovic SF, Murphy M, Morokoff A, Fabinyi G, et al. Prediction of seizure likelihood with a long-term, implanted seizure advisory system in patients with drug-resistant epilepsy: a first-in-man study. *Lancet Neurol.* (2013) 12:563–71. doi: 10.1016/S1474-4422(13)70075-9
3. Brinkmann BH, Wagenaar J, Abbot D, Adkins P, Bosshard SC, Chen M, et al. Crowdsourcing reproducible seizure forecasting in human and canine epilepsy. *Brain.* (2016) 139 (Pt. 6):1713–22. doi: 10.1093/brain/aww045
4. Kuhlmann L, Karoly P, Freestone DR, Brinkmann BH, Temko A, Barachant A, et al. Epilepsyecosystem.org: crowd-sourcing reproducible seizure prediction with long-term human intracranial EEG. *Brain.* (2018) 141:2619–30. doi: 10.1093/brain/awy210
5. Karoly PJ, Ung H, Grayden DB, Kuhlmann L, Leyde K, Cook MJ, et al. The circadian profile of epilepsy improves seizure forecasting. *Brain.* (2017) 140:2169–82. doi: 10.1093/brain/awx173
6. Payne DE, Dell KL, Karoly PJ, Kremen V, Gerla V, Kuhlmann L, et al. Identifying seizure risk factors: a comparison of sleep, weather, and temporal features using a Bayesian forecast. *Epilepsia.* (2021) 62:371–82. doi: 10.1111/epi.16785
7. Viana PF, Duun-Henriksen J, Glassteter M, Dumpelmann M, Nurse ES, Martins IP, et al. 230 days of ultra long-term subcutaneous EEG: seizure cycle analysis and comparison to patient diary. *Ann Clin Transl Neurol.* (2021) 8:288–93. doi: 10.1002/acn3.51261
8. Goldenholz DM, Goldenholz SR, Romero J, Moss R, Sun H, Westover B. Development and validation of forecasting next reported seizure using e-diaries. *Ann Neurol.* (2020) 88:588–95. doi: 10.1002/ana.25812
9. Karoly PJ, Cook MJ, Maturana M, Nurse ES, Payne D, Brinkmann BH, et al. Forecasting cycles of seizure likelihood. *Epilepsia.* (2020) 61:776–86. doi: 10.1111/epi.16485
10. Dumanis SB, French JA, Bernard C, Worrell GA, Fureman BE. Seizure forecasting from idea to reality. Outcomes of the my seizure gauge epilepsy innovation institute workshop. *eNeuro.* (2017) 6. doi: 10.1523/ENEURO.0349-17.2017 Available online at: https://www.eneuro.org/content/4/6/ENEURO.0349-17.2017
11. Janse SA, Dumanis SB, Huwig T, Hyman S, Fureman BE, Bridges JFP. Patient and caregiver preferences for the potential benefits and risks of a seizure forecasting device: a best-worst scaling. *Epilepsy Behav.* (2019) 96:183–91. doi: 10.1016/j.yebeh.2019.04.018
12. Proix T, Truccolo W, Leguia MG, Tcheng TK, King-Stephens D, Rao VR, et al. Forecasting seizure risk in adults with focal epilepsy: a development and validation study. *Lancet Neurol.* (2021) 20:127–35. doi: 10.1016/S1474-4422(20)30396-3
13. Privitera M, Haut SR, Lipton RB, McGinley JS, Cornes S. Seizure self-prediction in a randomized controlled trial of stress management. *Neurology.* (2019) 93:e2021–31. doi: 10.1212/WNL.0000000000008539
14. Schulze-Bonhage A, Haut S. Premonitory features and seizure self-prediction: artifact or real? *Epilepsy Res.* (2011) 97:231–5. doi: 10.1016/j.eplepsyres.2011.09.026
15. Ulate-Campos A, Coughlin F, Gainza-Lein M, Fernandez IS, Pearl PL, Loddenkemper T. Automated seizure detection systems and their effectiveness for each type of seizure. *Seizure.* (2016) 40:88–101. doi: 10.1016/j.seizure.2016.06.008
16. Baud MO, Kleen JK, Mirro EA, Andrechak JC, King-Stephens D, Chang EF, et al. Multi-day rhythms modulate seizure risk in epilepsy. *Nat Commun.* (2018) 9:88. doi: 10.1038/s41467-017-02577-y
17. Leguia MG, Andrzejak RG, Rummel C, Fan JM, Mirro EA, Tcheng TK, et al. Seizure cycles in focal epilepsy. *JAMA Neurol.* (2021) 78:454–63. doi: 10.1001/jamaneurol.2020.5370
18. Rao VR, M GL, Tcheng TK, Baud MO. Cues for seizure timing. *Epilepsia.* (2021) 62 (Suppl. 1):S15–31. doi: 10.1111/epi.16611
19. Baud MO, Rao VR. Gauging seizure risk. *Neurology.* (2018) 91:967–73. doi: 10.1212/WNL.0000000000006548
20. Kiral-Kornek I, Roy S, Nurse E, Mashford B, Karoly P, Carroll T, et al. Epileptic seizure prediction using big data and deep learning: toward a mobile system. *EBioMedicine.* (2018) 27:103–11. doi: 10.1016/j.ebiom.2017.11.032
21. Chiang S, Moss R, Black AP, Jackson M, Moss C, Bidwell J, et al. Evaluation and recommendations for effective data visualization for seizure forecasting algorithms. *JAMIA Open.* (2021) 4:ooab009. doi: 10.1093/jamiaopen/ooab009
22. Hoppe C, Feldmann M, Blachut B, Surges R, Elger CE, Helmstaedter C. Novel techniques for automated seizure registration: patients' wants and needs. *Epilepsy Behav.* (2015) 52 (Pt. A):1–7. doi: 10.1016/j.yebeh.2015.08.006
23. Bruno E, Simblett S, Lang A, Biondi A, Odoi C, Schulze-Bonhage A, et al. Wearable technology in epilepsy: the views of patients, caregivers, healthcare professionals. *Epilepsy Behav.* (2018) 85:141–9. doi: 10.1016/j.yebeh.2018.05.044
24. Meisel C, El Atrache R, Jackson M, Schubach S, Ufongene C, Loddenkemper T. Machine learning from wristband sensor data for wearable, noninvasive seizure forecasting. *Epilepsia.* (2020) 61:2653–66. doi: 10.1111/epi.16719
25. Onorati F, Regalia G, Caborni C, Migliorini M, Bender D, Poh MZ, et al. Multicenter clinical assessment of improved wearable multimodal convulsive seizure detectors. *Epilepsia.* (2017) 58:1870–9. doi: 10.1111/epi.13899
26. Patel AD, Moss R, Rust SW, Patterson J, Strouse R, Gedela S, et al. Patient-centered design criteria for wearable seizure detection devices. *Epilepsy Behav.* (2016) 64 (Pt. A):116–21. doi: 10.1016/j.yebeh.2016.09.012
27. Regalia G, Onorati F, Lai M, Caborni C, Picard RW. Multimodal wrist-worn devices for seizure detection and advancing research: focus on the empatica wristbands. *Epilepsy Res.* (2019) 153:79–82. doi: 10.1016/j.eplepsyres.2019.02.007
28. Simblett SK, Biondi A, Bruno E, Ballard D, Stoneman A, Lees S, et al. Patients' experience of wearing multimodal sensor devices intended to detect epileptic seizures: a qualitative analysis. *Epilepsy Behav.* (2020) 102:106717. doi: 10.1016/j.yebeh.2019.106717

Conflict of Interest: The authors declare that the research was conducted in the absence of any commercial or financial relationships that could be construed as a potential conflict of interest.

frontiers in Neurology

MINI REVIEW
published: 01 October 2021
doi: 10.3389/fneur.2021.740743

The Challenging Path to Developing a Mobile Health Device for Epilepsy: The Current Landscape and Where We Go From Here

Ilona Hubbard[1]*, *Sandor Beniczky*[2,3] and *Philippe Ryvlin*[1]

[1] Department of Clinical Neurosciences, Vaud University Hospital, Lausanne, Switzerland, [2] Department of Clinical Neurophysiology, Danish Epilepsy Center, Dianalund, Denmark, [3] Department of Clinical Neurophysiology, Aarhus University Hospital, Aarhus, Denmark

Seizure detection, and more recently seizure forecasting, represent important avenues of clinical development in epilepsy, promoted by progress in wearable devices and mobile health (mHealth), which might help optimizing seizure control and prevention of seizure-related mortality and morbidity in persons with epilepsy. Yet, very long-term continuous monitoring of seizure-sensitive biosignals in the ambulatory setting presents a number of challenges. We herein provide an overview of these challenges and current technological landscape of mHealth devices for seizure detection. Specifically, we display, which types of sensor modalities and analytical methods are available, and give insight into current clinical practice guidelines, main outcomes of clinical validation studies, and discuss how to evaluate device performance at point-of-care facilities. We then address pitfalls which may arise in patient compliance and the need to design solutions adapted to user experience.

Keywords: epilepsy, seizure detection, seizure forecasting, mobile health devices, extracerebral biosensors, wearables, EEG signals, usability and user experience

OPEN ACCESS

Edited by:
Maxime O. Baud,
University Hospital Bern, Switzerland

Reviewed by:
Ewan Nurse,
Seer Medical, Australia
Benjamin H. Brinkmann,
Mayo Clinic, United States

***Correspondence:**
Ilona Hubbard
ilona.hubbard@chuv.ch

Specialty section:
This article was submitted to Epilepsy, a section of the journal Frontiers in Neurology

Received: *13 July 2021*
Accepted: *03 September 2021*
Published: *01 October 2021*

Citation:
Hubbard I, Beniczky S and Ryvlin P (2021) The Challenging Path to Developing a Mobile Health Device for Epilepsy: The Current Landscape and Where We Go From Here. Front. Neurol. 12:740743. doi: 10.3389/fneur.2021.740743

INTRODUCTION

We live in the Internet of Things (IoT) era where wearables have become an integral part of day-to-day life. Health and sleep trackers, fitness wristbands, smartwatches, and other technologies attached to the human body offer users continuous biometric measurements (i.e., movement, heart rate, sweating) over time, providing analytics via Bluetooth (or similar wireless transmission protocols, e.g., wi-fi), and sending feedback to applications integrated into generic devices (e.g., smartwatches). These wearable devices offer considerable potential in regards to delivering novel options to shape personalized medical solutions (1). In the field of epilepsy, specific types of wearable solutions have been developed with the aim of detecting individual seizures, several of which have penetrated the consumer market. The overarching goal of these devices is to provide continuous long-term monitoring of non-EEG seizure related signals in order to detect or forecast seizures (2–9). Currently, however, seizure detection with appropriate sensitivity and false-alarm rates has only been possible for generalized tonic-clonic seizures (GTCS) (10, 11), while clinically-relevant accuracy is still lacking for most other seizures types (12). Solutions to this limitation are likely to emerge from the rapid advances in machine-learning seizure detection and algorithms forecasting

the cyclic nature of seizures (13, 14). In parallel, progress has been made in the field of long-term ambulatory EEG (15). Subcutaneous electrode implants, embedded with a wearable data receiver have allowed for the first-time real-world EEG data collections over very long periods (16).

This short review gives an insight into the ambitious and challenging field of wearable health devices for seizure detection and forecasting applications and provides context for progress to date, as well as possible pitfalls and how they might be resolved.

CLINICAL APPLICATIONS

With those suffering from chronic epilepsy, IoT technologies have the potential to advance personalized epilepsy management strategies, with the end result of increasing the positive disease outcome for patients. To date, the epilepsy community has demonstrated significant interest in wearable seizure detection (17–21) and forecasting (22) companions. In the following section, we have highlighted several avenues for their clinical application, which could prove clinically relevant and useful to patients.

In patients with high seizure frequency (20) and GTCS, alarm-triggering to a caregiver's smartphone might prompt life-saving procedures and prevent Sudden Unexpected Death from Epilepsy (SUDEP). It might also help decreasing the risks of SUDEP and of other causes of GTCS-related mortality (23–25) and morbidity, by providing predictive biomarkers of such outcomes (12, 26) and of GTCS severity (26). However, no study has yet demonstrated that the use of mobile health solutions, including seizure detection devices coupled with alarms has an impact on the risk of SUDEP.

A reliable seizure detection device could also provide physicians with more accurate information on seizure frequency than patients' diary entries or recollection, which in turn can help adjust both the type and dosage of medication and subsequent treatment outcome, [e.g., (27–31)]. However, despite long-term ambulatory EEG (32) and/or ambulatory implanted intracranial EEG (15) studies demonstrating that patients tend to under-report seizures, there is still need for more evidence to show that optimized seizure tracking for patients who use connected devices, is more reliable than diaries or direct communication with the patient. For instance, a phase-4 study has shown that a wearable accelerometer based system helped patients and caregiver to log GTCS into the seizure diary in 44% of the cases (32).

Major disruptions to quality of life can be attributed to the uncertainty of when seizures will occur (33). When responding to questions concerning their medical history, patients commonly report a periodicity in seizure occurrence and familiarize themselves with individual risk factors and triggers that they observe preceding seizure events. These then serve as reference points for certain individuals to keep an overview of their disease progression (34–39). The capacity to foresee a seizure event would transform epilepsy care and ultimately allow patients to counteract impending seizures by proactively adapting their behavior. For example, a patient could potentially self-target neurostimulation to abort the seizure (40), or rely on a closed-loop apparatus that offered immediate seizure-triggered therapy (41).

SENSORS

EEG and non-EEG sensors can be embedded in a wearable tool, and are directly in contact with the body in order to acquire physiological signals. The set-up should be appropriate to measure epilepsy-related activity over long periods of time during the day and night and has specific constraints in terms of comfort and stigma (42). Especially for EEG systems, usability comes as a challenge, as full-array scalp electrodes can only be used in hospitals, or in controlled home-monitoring settings (43), over time periods of up to several days maximum. Non-obtrusive solutions have been developed, using only few electrodes positioned either around (44) or in the ear (45, 46), but signal quality often remains inadequate, characterized by artifacts and sub-optimal electrode impedance. In order to facilitate continuous EEG recordings, subcutaneous (a.k.a. subscalp or subdermal) electrodes, placed by means of a minimally invasive surgical procedure under the scalp, have been proposed (37, 47). Subcutaneous electrodes set-up showed similar SNR levels, and even better signal quality than standard scalp EEG montages (48). After the development of first prototypes (49–51), a few products have started their incubation process, but so far, only one device has undergone clinical trials to be approved for commercial use by regulatory bodies (52). First studies in epilepsy patients showed that surgeries (37, 47) and ultra-long-term use for real life monitoring for up to 3 months at home (37) were technically feasible, well-tolerated, and for in a first use-case with eight epilepsy patients, successfully detected seizures (37, 47). Recently, a larger multicenter trial involving the implantation of subcutaneous EEG devices in 14 patients with epilepsy and 12 healthy subjects, demonstrated the technological viability of stable long-term EEG recordings (52).

Currently, four additional diagnostic solutions are progressing in their development (16). Different electrode designs (i.e., bipolar electrodes, multichannel strips), and placement underneath the scalp (i.e., from focal to covering both hemispheres) determine the type of seizures that can be recorded (37, 47). Subcutaneous solutions are quasi invisible and existing studies show that patients are willing to undergo the operation and insertion of the material for long periods of time (37, 47, 53). However, additional data involving larger patient samples are required to confirm overall acceptance of these devices. Non-EEG based sensors, are primarily based on accelerometers, surface electromyography (EMG), electrocardiography (ECG), photoplethysmography (PPG) and electrodermal activity (EDA). They are easily integrated in fashionable wearables, such as bracelets, without displaying the disease and stigmatizing patients. Accelerometers strapped to a limb appropriately identify GTCS, and other seizures with strong motor components (54–56). Surface EMG on the biceps muscle is particularly useful for the detection of tonic seizures early on in the course of GTCS (57–60). The prerequisite for performance

of movement sensors is to fasten them to a body part that participates in the seizure semiology. Heart rate parameters are known to vary during and even shortly before seizures (61, 62). They can be recorded using self-adhesive ECG electrode patches (63, 64) or via measures of heart rate (HR) by means of an optical sensor that captures a PPG signal at the wrist (65, 66). Finally, a clear-cut surge in EDA is observed at onset of GTCS (67–69), while imbalance in this autonomic biomarker can also be observed in the pre-ictal state (70). A combination of signals can be used for seizure monitoring in the real-world setting, yet the pitfall of this approach is that signal quality, and thus reliability of the approach, is influenced by daily activities and

FIGURE 1 | (A,B) A wrist worn commercially available seizure detector with integrated ACC and EDA sensor, **(B)** displays three electrodes for EDA measure that are in contact with the skin. **(C,D)** A wrist worn commercially available sensing device with integrated ACC, EDA, and PPG sensor. **(D)** Displays the PPG sensor that is in contact with the skin. **(E)** A wired galvanic skin response (EDA) sensing solution, with velcro fabric finger cuffs and a small receiver unit that attaches to the wrist.

psychological arousal (70, 71). Please view **Figures 1A–E** for an illustration of different form factors of sensing solutions.

POSSIBLE ANALYTICAL APPROACHES

In validation studies, the accuracy of seizure detection algorithms must be compared to the gold standard for seizure-diagnosis: video-EEG recording or (for motor seizures) video recordings. The presence or absence of an epileptic event will then be mathematically treated as a binary variable. To increase the accuracy of seizure detection algorithms, various machine learning methods are available (72). Their performance is typically evaluated by determining the area under a receiver-operating characteristic curve (ROC) (2–9). Seizure prediction algorithms aim at identifying pre-ictal changes immediately before the seizure in order to anticipate the precise onset of a given seizure (73–77). Meanwhile, data from a clinical trial (15, 36), animal studies (34, 78–81), crowdsourcing analysis efforts of EEG databases (82, 83), and cohort studies of mobile seizure diaries (39, 84, 85), have identified that epileptic activity in some patients followed circadian, ultradian, and infradian (multidian) cycles, and was highly correlated with self-forecasting techniques (86). Thus, an alternative conceptual approach (87) to single seizure event prediction, is the ability to algorithmically forecast them. A successful seizure forecast would provide the patient with a seizure cluster likelihood measure within a given time-window, based on intraindividual cyclic distribution of events. Companions using this approach might require more complex designs than their seizure detection analogs. For instance, the varying scales of forecasting windows (22) and data visualization features (88) would be attuned according to frequency and characteristics of the seizure cycles. Forecasting will also benefit from the development of new EEG methods for very-long-term data collection. Currently, clinical trials have been advised (89) and are urgently needed to further existing knowledge about seizure networks, the characteristics of interictal changes, ictogenesis, as well as their cyclicity and predictive value over prolonged time periods (13, 90, 91). Research on seizure periodicity function will constitute the basis for addressing this bottleneck in the advance of algorithmic approaches.

RESEARCH AND DEVELOPMENT

In Europe, clinical trials of wearable devices are steadily increasing and are required to follow the regulatory framework of *Council Directive 93/42/EEC* concerning medical devices. In order to optimize study quality in the epilepsy domain, recommendations for standardized testing and clinical validation of seizure detection devices have been recently proposed (92). This new standard classifies studies into 5 phases (0–4), with key trial design features concerning the number of subjects, types of recordings, data analysis, and alarm criteria. For example, whereas a phase 0 study can still be performed on retrospective datasets and serve as a proof of concept for algorithm development, subsequent phases will require technical feasibility testing and signal validation against standard hospital Video-EEG. The final phase (4), will have to include a large patient sample and be performed in a prospective manner at multiple sites under real world-settings. As previously proposed (76), seizure detection criteria for all devices will represent the first qualitative control with the aim of complementing aspects specifically relevant for digital forecasting companions. Overall, device developers must consider that high quality product R&D will require several years. Furthermore, trials will have to contain a clear set of outcome measures and criteria to be reported to and evaluated by regulatory bodies. Result summaries containing transparent research data should also be made available to the medical community at large.

DEVICE VALIDITY

The working group of the International League Against Epilepsy (ILAE) and the International Federation of Clinical Neurophysiology (IFCN) recently performed a literature search and published evidence from 28 papers (10, 11), leading to consensus in the endorsement of "*clinically validated wearable devices for automated detection of GTCS including the focal-to-bilateral tonic-clonic seizures (FBTCS) when significant safety concerns exist, especially in unsupervised patients (…).*" Only a handful of validation studies have focused on the detection of focal, non-convulsive seizures (10–12). As a consequence, no commercially available wearable devices have received regulatory authorization for the detection of focal epileptic seizures, and "*the ILAE-IFCN Working Group, does not recommend clinical use of the currently available wearable devices for seizure types other than GTCS and FBTCS, as more research and development are needed for this application (…).*"

For the purposes of this short review, we have summarized and updated the efforts of the ILAE-IFCN workforce below (10, 11). **Table 1** included the outcomes of nineteen phase 2–4 prospective studies that span the development of novel analytical methods, confirm their safety and accuracy with respect to regulatory bodies, and their ability to assess seizure detection performances in the patient's homes, as opposed to the laboratory environment.

There is ample evidence regarding the detection rates for convulsive seizures using a self-adhesive EMG patch placed on the bicep muscle. In this case, a reasonable true positive/false positive ratio was achieved using the algorithm, with a GTCS detection sensitivity of 94% and a false alarm rate of 0.7/24-h (94). Interestingly, when different detection-thresholds were used, 100% sensitivity could be attained, however the false positive rate was consequently increased to 1.44/24-h (93).

An alternative GTCS detection method using wrist accelerometers has approached a relatively high sensitivity of >89.7% in several phase 2 studies, with the rate of false alarms significantly reduced <0.24 per day (32, 55, 95–98). ACCs are most effective when attached to several areas of a patient's body known to be implicated in the seizure semiology. Using multiple ACCs, several phase 1 studies, identified myoclonic-, clonic-, tonic- (108, 109), and hypermotor seizures (110, 111) with a sensitivity rate of at least 95%. However, a different phase 2 study

TABLE 1 | Outcomes of phase 2–4 prospective seizure detection algorithm reliability studies.

Modality	Study	Phase	Study site/design	Seizure type	Device	Performance	Time to positive detection after seizure onset
Surface EMG	Szabo et al. (59)	2	EMU/Offline	GTCS	Brain Sentinel	Sensitivity = 95% FP = 0.017/24 h	μ = 15.2 s
Surface EMG	Halford et al. (93)	2	EMU/Offline	GTCS	Brain Sentinel	Sensitivity depending on cohort = 100%, 76% FP = 1.4/24 h, 2.5/24 h	μ = 7.45 s
Surface EMG	Beniczky et al. (94)	3	EMU/Real-time	GTCS	Seizure detector by Ictal Care	Sensitivity = 93.8% FP = 0.67/24 h	μ = 9 s
Wrist 3D-ACC	Kramer et al. (95)	2	EMU/Real-time	Motor seizures, GTCS	Not specified	Sensitivity = 90.9% FP = 0.11/24	μ = 17 s
Wrist 3D-ACC	Beniczky et al. (96)	3	EMU/Real-time	GTCS	Epi-care	Sensitivity = 89.7% FP = 0.2/24 h	μ = 33 s from GTCS, μ = 55 s from FS
Wrist 3D-ACC	Meritam et al. (32)	4	In-field/Real-time	GTCS	Epi-care	Sensitivity = 90% FP = 0.1/24 h	n.a (infield)
Wrist ACC	Patterson et al. (97)	2	EMU/Real-time	GTCS, tonic, myoclonic, hypermotor, complex partial	Smartwatch by Smartmonitor	GTCS: Sensitivity = 31% FS: Sensitivity = 16% FP = n.r	Not reported
Wrist ACC	Velez at al. (98)	2	EMU/Real-time	GTCS	Smartwatch by Smartmonitor	GTCS: Sensitivity = 92.3% FP = n.r FS = Not detected	Not reported
Wrist 3D- ACC	Johansson et al. (55)	2	EMU/Offline	GTCS	Shimmer	Sensitivity = 90–100% FP = 0.24–1.2/24 h	Not reported
Wrist ACC + EDA	Onorati et al. (99)	2	EMU/Offline	GTCS	Embrace	Sensitivity = 94.55% FP = 0.2/24 h	Median = 29.3%
ACC +ECG	Van Andel et al. (100)	2	EMU/Offline	GTCS, tonic, clonic, hypermotor	Shimmer	Clinically urgent GTCS: Sensitivity = 87% FS: Sensitivity = 56–71% FP = 2.3–5.7/24 h for all seizures per night	μ = 13 s
Wrist 3D-ACC + PPG	Arends et al. (101)	3+4	EMU + In-field/Real-time	GTCS, myoclonic/ tonic, hyperkinetic	Nightwatch	GTCS: Sensitivity = 81% Other motor seizures: Sensitivity = 77% FP = 0.3 per night	Not reported
ECG	Boon et al. (102)	2	EMU/Offline	GTCS, FS	Hospital ECG& VNS Aspire SR	For HR increase >20%: Sensitivity = 52.3% FP = 7.2/h	Not reported
ECG	Fisher et al. (103)	2	EMU/Offline	GTCS, FS	Hospital ECG&VNS Aspire SR	For HR increase >20%: Sensitivity = 91% FP = 0.7/24 h	μ = 8 s
ECG, PPG	Vandecasteele et al. (104)	2	EMU/Offline	FS	Hospital ECG, 180° eMotion, E4	ECG: Sensitivity = 57% FP = 1.92/24 h 180°: Sensitivity = 70% FP = 2.11/24 h E4: Sensitivity = 32% FP = 1.8/24 h	Not reported
ECG	Jeppesen et al. (63)	2	EMU/Offline	GTCS, FS	ePatch ECG	GTCS: Sensitivity = 100% FS: Sensitivity = 90.5% FP = 1/24 h	μ = 30 s
In-the-ear NIRS	Jeppesen et al. (105)	2	EMU/Offline	FS	PortaLite	Sensitivity = 6–24%	Not reported
Behind-the-Ear-EEG	Gu et al. (106)	2	EMU/Offline	FS	Ambu Neuroline Cup	Sensitivity = 94.5% FP = 0.52/24 h	Not reported
PPG + Oxygen saturation	Brotherstone et al. (107)	3	EMU/Real-time	Clinically significant seizures	Nonin finger sensor	For HR change > 25% + Oxygen desaturation <85%: Sensitivity = 87% FP = 4.5/24 h	μ = 69.6 s for HR μ = 83 s for oxygen desaturation

EMG, Electromyogramm; EMU, Epilepsy monitoring unit; FP, False positive; GTCS, Generalized tonic-clonic seizures; HR, heart rate; h, hour; μ, mean; n.a, not applicable; NIRS, near-infrared spectroscopy; s, second.

found that ACC-based wristwatches were less sensitive for the detection of different types of focal motor seizures (0–24%) (97).

Conversely, heart rate parameters from ECG systems were able to detect arrhythmias associated with focal seizures and were showed sensitivity as high as (<91%). Nonetheless, many algorithms still produced false positives from 0.5 to 5.4 per hour (112–114). PPG signals measured from the wrist, may also be appropriate detectors, however, they have so far not been shown to have lower false positives rates than hospital ECGs (2.11 vs. 1.92) (104).

Combining the outputs from several sensors into a single algorithm, has been considered in order to raise the detection rate of GTCS (21, 115, 116). For instance, a clinical trial combining phase-3 and 4, evaluated a band placed on the upper arm, recording accelerometry and heart rate, and succeeded to isolate nocturnal GTCS with a sensitivity of 81% (and 77% of motor seizures), and a reduced false alarm rate of 0.03 per night (101). A phase 2 EMU study, using a retrospective cross-validation approach, demonstrated that fusing accelerometry signals with electrodermal activity (EDA) recorded from a wrist-worn device, resulted in a sensitivity of 95% for GTCS and a false positive rate of 0.2 per day (99). Most recently, a phase 3 EMU study applied pre-defined cut-off points to data obtained in real-time, and showed that when heart rate changes and oximetry endpoints are combined, the sensitivity is highest, and lowest when the parameters are used alone (117).

Wearable EEG devices are potentially well-suited to reflect the focal seizure onset when placed above the area of seizure onset. A phase two study performed in the EMU showed the aptitude of a behind the-ear-EEG set-up with a sensitivity of 94.5%. In order to allow for ultra-long term monitoring, with the goal to create personalized seizure forecasting (34, 37–39), subcutaneous wearable EEG devices are currently being developed (16). To date, only one device has received approval for sale by the regulatory authorities (52). For this purpose, Duun-Herniksen et al. performed EMU-based clinical trials for safety and signal quality in patients with epilepsy originating from the temporal lobe (47, 48) and performed the first ultra-long-term home study in a sample of eight patients. This real-life monitoring, for up to 3 months, was shown to be safe, well-tolerated by participants, and technically feasible (37).

CLINICAL EVIDENCE

While there is strong evidence to prove the accuracy of non-EEG wearables, the average time to detect a seizure has been situated between 7.45 (90) and 83 s (91) from onset. Therefore, until now the purpose of seizure companions has mostly found applications such as alarm systems for SUDEP prevention, and the optimization of seizure diaries. However, first studies have been published that report having successfully developed seizure forecasts based on extracerebral biosignals (76, 118). Phase 4 trials for subcutaneous EEG seizure prediction/forecasting devices have yet to be performed (93). Consequently, clinical evidence on the impact of wearable solutions is sparse, and has so far, only been indirectly deduced from epidemiological data reflecting mortality rates in unsupervised patients who do not share a bedroom with another person and are found in prone position following a GTCS (100).

USER EXPECTATIONS AND FIRST EXPERIENCES WITH DEVICE IMPLEMENTATION

Surveys have demonstrated the clinical relevance of seizure detection, giving patients (22, 119, 120), as well as caregivers and healthcare professionals (17–20, 22), the opportunity to express their needs and wishes for wearable health companions. Several studies have specifically addressed user feedback about acceptable rates in both sensitivity and false alarms (19, 20, 120), finding that at minimum, patients desire both an accurate detection/prediction rate > 90% and incorrect seizure triggering of less than once per day. However, at present only the ACC wristband and EMG patch have achieved this reliability ratio for the detection of GTCS, whereas other available consumer devices have not (121). One way to increase seizure recognition has been to lower the threshold, although consequent higher false positive rates exist, creating a challenge for software developers who must then determine how best to tune their devices. For example if a seizure is missed (false negative), this is considered more harmful than incorrectly identifying it (false positive) (120). Furthermore, in patients where seizure frequency is lower, false alarms were more tolerable, as statistically they would occur only under certain conditions. Nonetheless, interest in continuous real-time monitoring and alarms has increased, especially in patients with a high seizure frequency and concomitant risk of SUDEP (20), where high rates of daily false alarms would become unbearable for those most affected. Nonetheless, it was shown that a system could possibly permit users to tune their sensitivity and false positive rates (122), allowing to adjust for the patients' individual preferences of control, which might be quite different (123).

Regarding seizure forecasting, to date only one survey has directly questioned patient and caretaker preferences, finding that high accuracy and short forecasting windows were favored over long-term, less precise ones (22). Broadly speaking, forecasting has significant potential, as it covers physiological parameters and time-frames of various length, with the ability to provide predictive information of higher complexity than a binary seizure detector (76). To outline future applications of this methodology, further studying of end-user requirements and focusing on user-centric development, are of the utmost importance.

At present, several wearable companions have reached the market. Preliminary studies have aimed to evaluate how patients have implemented wearables in daily life, moving away from assessing hypothetical tolerability and toward the evaluation of hands-on device experiences. Major complaints have arisen such as the disapproval of bulky designs, the presence of wires and/or electrodes, and the necessity for adhesive material on the skin (124), whereas those devices deemed comfortable had secure fittings and discrete form factors (122). In general, patients are "device-naïve" insomuch as they have not previously used

wearables. Thus, an uncertainty exists as to whether user-error could impact the implementation of a seizure detection strategy, and consequently hinder further development efforts. Depending on a device's user interaction, its manipulation may require sufficiently preserved executive function in order to learn a sequence of procedures, such as pairing a sensor bracelet to a mobile application. Furthermore, rapidly adapting to the device when prompted, such as charging or even changing the battery, could create obstacles for efficient use. Recently, a study examining a wrist-worn device demonstrated that only 50% of patients were able to fully and independently control it, whilst others needed both appropriate support and training, and a subgroup of patients (13.3%) required constant supervision (123). In several devices, users have identified constraints early on. For example, a phase 2 study showed that 14% of patients consistently misplaced the EMG patch (93), whereas another lost 54% of the patient samples due to mishandling and data connection failures (100). Still others found possible handling issues in real-world conditions, leading to a 10% loss in device users during a phase 4 study (32).

Roadblocks such as these will specifically deter patients with high seizure frequency rates, as cognitive impairment is increased in the majority of these cases (125). In essence, difficulties in usability risk hinder the effectiveness of these detection and forecasting devices in patients with very active epilepsy, a population subset which should be the ones who benefit most from wearables with alarms.

CONCLUSION

Mobile health devices show promise for patients suffering from epileptic seizures. However, before they can be widely proposed, and/or medical insurance coverage can be assured, several key efforts need to be solidified. When following state-of-the-art research (92) and clinical practice guidelines (10, 11), the overall recommendation is to perform robustly designed clinical validation studies in EMUs, in addition to real-life environment situations, to concretely demonstrate the reliability of GTCS detection and quantification algorithms, as well as other seizures types. Especially, since currently, mobile health devices have only shown validity for the detection of GTCS, and not for other seizure types. Furthermore, clinical outcomes need to be assessed, including the decreased morbidity and mortality associated with seizures and improvements in quality of life. The future of wearable mobile health devices related to epileptic seizure detection or forecasting must continue to focus on the advancement of adequate sensors, and their development should emphasize user-centric methods prior to products entering beta testing. At present, there is still a gap between what seizure detection devices are capable of measuring and the needs of patients. Specifically, prior to the implementation of mobile health companions into real-world situations, device developers should consider the clinical characteristics of the patients themselves and directly assess how digital health tools can directly benefit the management of epilepsy.

AUTHOR CONTRIBUTIONS

All authors listed have made a substantial, direct and intellectual contribution to the work, and approved it for publication.

FUNDING

The review work and the publishing fees were funded by a grant from the Swiss National Science Foundation (SNF). Number: 320030_179240 Quantifying the severity of generalized tonic-clonic seizures (GTCS) with ambulatory connected devices (SEVERITY).

REFERENCES

1. Beniczky S, Karoly P, Nurse E, Ryvlin P, Cook M. Machine learning and wearable devices of the future. *Epilepsia.* (2020) 116–24. doi: 10.1111/epi.16555
2. Bidwell J, Khuwatsamrit T, Askew B, Ehrenberg JA, Helmers S. Seizure reporting technologies for epilepsy treatment: a review of clinical information needs and supporting technologies. *Seizure.* (2015) 32:109–17. doi: 10.1016/j.seizure.2015.09.006
3. van Andel J, Thijs RD, de Weerd A, Arends J, Leijten F. Non-EEG based ambulatory seizure detection designed for home use: what is available and how will it influence epilepsy care? *Epilepsy Behav.* (2016) 57:82–9. doi: 10.1016/j.yebeh.2016.01.003
4. Van de Vel A, Cuppens K, Bonroy B, Milosevic M, Jansen K, Van Huffel S, et al. Non-EEG seizure-detection systems and potential SUDEP prevention: state of the art. *Seizure.* (2013) 22:345–55. doi: 10.1016/j.seizure.2013.02.012
5. Jory C, Shankar R, Coker D, McLean B, Hanna J, Newman C. Safe and sound? A systematic literature review of seizure detection methods for personal use. *Seizure.* (2016) 36:4–15. doi: 10.1016/j.seizure.2016.01.013
6. Aghaei-Lasboo A, Fisher RS. Methods for measuring seizure frequency and severity. *Neurol Clin.* (2016) 34:383–94. doi: 10.1016/j.ncl.2015.11.001
7. Kearney H, Byrne S, Cavalleri GL, Delanty N. Tackling epilepsy with high-definition precision medicine: a review. *JAMA Neurol.* (2019) 76:1109–16. doi: 10.1001/jamaneurol.2019.2384
8. Kurada AV, Srinivasan T, Hammond S, Ulate-Campos A, Bidwell J. Seizure detection devices for use in antiseizure medication clinical trials: a systematic review. *Seizure.* (2019) 66:61–9. doi: 10.1016/j.seizure.2019.02.007
9. Osorio I, Schachter S. Extracerebral detection of seizures: a new era in epileptology? *Epilepsy Behav.* (2011) 22:S82–7. doi: 10.1016/j.yebeh.2011.09.012
10. Beniczky S, Wiebe S, Jeppesen J, Tatum WO, Brazdil M, Wang Y, et al. Automated seizure detection using wearable devices: a clinical practice guideline of the international league against epilepsy and the international federation of clinical neurophysiology. *Clin Neurophysiol.* (2021) 132:1173–84. doi: 10.1016/j.clinph.2020.12.009
11. Beniczky S, Wiebe S, Jeppesen J, Tatum WO, Brazdil M, Wang Y, et al. Automated seizure detection using wearable devices: a clinical practice guideline of the international league against epilepsy and the international federation of clinical neurophysiology. *Epilepsia.* (2021) 62:632–46. doi: 10.1111/epi.16818
12. Ryvlin P, Cammoun L, Hubbard I, Ravey F, Beniczky S, Atienza D. Noninvasive detection of focal seizures in ambulatory patients. *Epilepsia.* (2020) 61:S47–54. doi: 10.1111/epi.16538

13. Maturana MI, Meisel C, Dell K, Karoly PJ, D'Souza W, Grayden DB, et al. Critical slowing down as a biomarker for seizure susceptibility. *Nat Commun.* (2020) 11:2172. doi: 10.1038/s41467-020-15908-3
14. Proix T, Truccolo W, Leguia MG, Tcheng TK, King-Stephens D, Rao VR, et al. Forecasting seizure risk in adults with focal epilepsy: a development and validation study. *Lancet Neurol.* (2021) 20:127–35. doi: 10.1016/S1474-4422(20)30396-3
15. Cook MJ, O'Brien TJ, Berkovic SF, Murphy M, Morokoff A, Fabinyi G, et al. Prediction of seizure likelihood with a long-term, implanted seizure advisory system in patients with drug-resistant epilepsy: a first-in-man study. *Lancet Neurol.* (2013) 12:563–71. doi: 10.1016/S1474-4422(13)70075-9
16. Duun-Henriksen J, Baud M, Richardson MP, Cook M, Kouvas G, Heasman JM, et al. A new era in electroencephalographic monitoring? Subscalp devices for ultra-long-term recordings. *Epilepsia.* (2020) 61:1805–17. doi: 10.1111/epi.16630
17. Bruno E, Simblett S, Lang A, Biondi A, Odoi C, Schulze-Bonhage A, et al. Wearable technology in epilepsy: The views of patients, caregivers, and healthcare professionals. *Epilepsy Behav.* (2018) 85:141–9. doi: 10.1016/j.yebeh.2018.05.044
18. Davis MM, Freeman M, Kaye J, Vuckovic N, Buckley DI. A systematic review of clinician and staff views on the acceptability of incorporating remote monitoring technology into primary care. *Telemed J e-health.* (2014) 20:428–38. doi: 10.1089/tmj.2013.0166
19. Tovar Quiroga DF, Britton JW, Wirrell EC. Patient and caregiver view on seizure detection devices: a survey study. *Seizure.* (2016) 41:179–81. doi: 10.1016/j.seizure.2016.08.004
20. Van de Vel A, Smets K, Wouters K, Ceulemans B. Automated non-EEG based seizure detection: do users have a say? *Epilepsy Behav.* (2016) 62:121–8. doi: 10.1016/j.yebeh.2016.06.029
21. Nasseri M, Nurse E, Glasstetter M, Böttcher S, Gregg NM, Laks Nandakumar A, et al. Signal quality and patient experience with wearable devices for epilepsy management. *Epilepsia.* (2020) 61:S25–35. doi: 10.1111/epi.16527
22. Janse SA, Dumanis SB, Huwig T, Hyman S, Fureman BE, Bridges JFP. Patient and caregiver preferences for the potential benefits and risks of a seizure forecasting device: a best-worst scaling. *Epilepsy Behav.* (2019) 96:183–91. doi: 10.1016/j.yebeh.2019.04.018
23. Ryvlin P, Ciumas C, Wisniewski I, Beniczky S. Wearable devices for sudden unexpected death in epilepsy prevention. *Epilepsia.* (2018) 59:61–6. doi: 10.1111/epi.14054
24. Tomson T, Surges R, Delamont R, Haywood S, Hesdorffer DC. Who to target in sudden unexpected death in epilepsy prevention and how? Risk factors, biomarkers, and intervention study designs. *Epilepsia.* (2016) 57:4–16. doi: 10.1111/epi.13234
25. Devinsky O, Hesdorffer DC, Thurman DJ, Lhatoo S, Richerson G. Sudden unexpected death in epilepsy: epidemiology, mechanisms, and prevention. *Lancet Neurol.* (2016) 15:1075–88. doi: 10.1016/S1474-4422(16)30158-2
26. Beniczky S, Arbune AA, Jeppesen J, Ryvlin P. Biomarkers of seizure severity derived from wearable devices. *Epilepsia.* (2020) 61:S61–6. doi: 10.1111/epi.16492
27. Riviello JJ. Classification of seizures and epilepsy. *Curr Neurol Neurosci Rep.* (2003) 3:325–31. doi: 10.1007/s11910-003-0010-4
28. Blachut B, Hoppe C, Surges R, Elger C, Helmstaedter C. Subjective seizure counts by epilepsy clinical drug trial participants are not reliable. *Epilepsy Behav.* (2017) 67:122–7. doi: 10.1016/j.yebeh.2016.10.036
29. Fattouch J, Di Bonaventura C, Lapenta L, Casciato S, Fanella M, Morano A, et al. Epilepsy, unawareness of seizures and driving license: the potential role of 24-hour ambulatory EEG in defining seizure freedom. *Epilepsy Behav.* (2012) 25:32–5. doi: 10.1016/j.yebeh.2012.07.001
30. Blum DE, Eskola J, Bortz JJ, Fisher RS. Patient awareness of seizures. *Neurology.* (1996) 47:260–64. doi: 10.1212/WNL.47.1.260
31. Hoppe C, Poepel A, Elger CE. Epilepsy: accuracy of patient seizure counts. *Arch Neurol.* (2007) 64:1595–9. doi: 10.1001/archneur.64.11.1595
32. Meritam P, Ryvlin P, Beniczky S. User-based evaluation of applicability and usability of a wearable accelerometer device for detecting bilateral tonic-clonic seizures: a field study. *Epilepsia.* (2018) 59:48–52. doi: 10.1111/epi.14051
33. Schulze-Bonhage A, Kuhn A. Unpredictability of seizures and the burden of epilepsy. In: Schelter B, Timmer J, Schulze-Bonhage A, editors. *Seizure Prediction in Epilepsy*. Weinheim: WILEY-VCH Verlag GmbH & Co. KGaA (2008).
34. Baud MO, Kleen JK, Mirro EA, Andrechak JC, King-Stephens D, Chang EF, et al. Multi-day rhythms modulate seizure risk in epilepsy. *Nat Commun.* (2018) 9:88. doi: 10.1038/s41467-017-02577-y
35. Cook MJ, Karoly PJ, Freestone DR, Himes D, Leyde K, Berkovic S, et al. Human focal seizures are characterized by populations of fixed duration and interval. *Epilepsia.* (2016) 57:359–68. doi: 10.1111/epi.13291
36. Cook MJ, Varsavsky A, Himes D, Leyde K, Berkovic SF, O'Brien T, et al. The dynamics of the epileptic brain reveal long-memory processes. *Front Neurol.* (2014) 5:217. doi: 10.3389/fneur.2014.00217
37. Weisdorf S, Duun-Henriksen J, Kjeldsen MJ, Poulsen FR, Gangstad SW, Kjaer TW. Ultra-long-term subcutaneous home monitoring of epilepsy-490 days of EEG from nine patients. *Epilepsia.* (2019) 60:2204–14. doi: 10.1111/epi.16360
38. Karoly PJ, Freestone DR, Boston R, Grayden DB, Himes D, Leyde K, et al. Interictal spikes and epileptic seizures: their relationship and underlying rhythmicity. *Brain.* (2016) 139:1066–78. doi: 10.1093/brain/aww019
39. Karoly PJ, Goldenholz DM, Freestone DR, Moss RE, Grayden DB, Theodore WH, et al. Circadian and circaseptan rhythms in human epilepsy: a retrospective cohort study. *Lancet Neurol.* (2018) 17:977–85. doi: 10.1016/S1474-4422(18)30274-6
40. Kravalis K, Schulze-Bonhage A. PIMIDES I: a pilot study to assess the feasibility of patient-controlled neurostimulation with the EASEE® system to treat medically refractory focal epilepsy. *Neurol Res Pract.* (2020) 2:15. doi: 10.1186/s42466-020-00061-5
41. Ramgopal S, Thome-Souza S, Jackson M, Kadish NE, Sánchez Fernández I, Klehm J, et al. Seizure detection, seizure prediction, and closed-loop warning systems in epilepsy. *Epilepsy Behav.* (2014) 37:291–307. doi: 10.1016/j.yebeh.2014.06.023
42. Casson AJ, Smith S, Duncan JS, Rodriguez-Villegas E. Wearable EEG: what is it, why is it needed and what does it entail? *Annu Int Conf IEEE Eng Med Biol Soc.* (2008) 2008:5867–70. doi: 10.1109/IEMBS.2008.4650549
43. Biswas S, Luz R, Brunnhuber F. Home video telemetry vs inpatient telemetry: a comparative study looking at video quality. *Clin Neurophysiol Pract.* (2016) 1:38–40. doi: 10.1016/j.cnp.2016.05.001
44. Debener S, Emkes R, De Vos M, Bleichner M. Unobtrusive ambulatory EEG using a smartphone and flexible printed electrodes around the ear. *Sci Rep.* (2015) 5:16743. doi: 10.1038/srep16743
45. Bleichner MG, Lundbeck M, Selisky M, Minow F, Jager M, Emkes R, et al. Exploring miniaturized EEG electrodes for brain-computer interfaces. An EEG you do not see? *Physiol Rep.* (2015) 3:e12362. doi: 10.14814/phy2.12362
46. Zibrandtsen IC, Kidmose P, Christensen CB, Kjaer TW. Ear-EEG detects ictal and interictal abnormalities in focal and generalized epilepsy - a comparison with scalp EEG monitoring. *Clin Neurophysiol.* (2017) 128:2454–61. doi: 10.1016/j.clinph.2017.09.115
47. Weisdorf S, Gangstad SW, Duun-Henriksen J, Mosholt KSS, Kjaer TW. High similarity between EEG from subcutaneous and proximate scalp electrodes in patients with temporal lobe epilepsy. *J Neurophysiol.* (2018) 120:1451–60. doi: 10.1152/jn.00320.2018
48. Duun-Henriksen J, Kjaer TW, Looney D, Atkins MD, Sørensen JA, Rose M, et al. EEG signal quality of a subcutaneous recording system compared to standard surface electrodes. *J Sens.* (2015) 2015:341208. doi: 10.1155/2015/341208
49. Xu J, Wang B, Mclaughlin B, Schachther S, Yang Z. An integrated sub-scalp EEG sensor for diagnosis in epilepsy. In: *IEEE Biomedical Circuits and Systems Conference (BioCAS), Atlanta, GA.* (2015). p. 1–4.
50. Young GB, Ives JR, Chapman MG, Mirsattari SM. A comparison of subdermal wire electrodes with collodion-applied disk electrodes in long-term EEG recordings in ICU. *Clin Neurophysiol.* (2006) 117:1376–9. doi: 10.1016/j.clinph.2006.02.006
51. Do Valle BG, Cash SS, Sodini CG. Low-power, 8-channel EEG recorder and seizure detector ASIC for a subdermal implantable system. *IEEE Trans Biomed Circ Syst.* (2016) 10:1058–67. doi: 10.1109/TBCAS.2016.2517039
52. 24/7 EEG^{TM} SubQ. Available online at: www.uneeg.com (accessed July 13, 2021).
53. Viana PF, Remvig LS, Duun-Henriksen J, Glasstetter M, Dumpelmann M, Nurse ES, et al. Signal quality and power spectrum analysis of

remote ultra long-term subcutaneous EEG. *Epilepsia.* (2021) 62:1820–8. doi: 10.1111/epi.16969
54. Becq G, Bonnet S, Minotti L, Antonakios M, Guillemaud R, Kahane P. Classification of epileptic motor manifestations using inertial and magnetic sensors. *Comput Biol Med.* (2011) 41:46–55. doi: 10.1016/j.compbiomed.2010.11.005
55. Johansson D, Ohlsson F, Krýsl D, Rydenhag B, Czarnecki M, Gustafsson N, et al. Tonic-clonic seizure detection using accelerometry-based wearable sensors: a prospective, video-EEG controlled study. *Seizure.* (2019) 65:48–54. doi: 10.1016/j.seizure.2018.12.024
56. Lockman J, Fisher RS, Olson DM. Detection of seizure-like movements using a wrist accelerometer. *Epilepsy Behav.* (2011) 20:638–41. doi: 10.1016/j.yebeh.2011.01.019
57. Conradsen I, Beniczky S, Wolf P, Kjaer TW, Sams T, Sorensen HB. Automatic multi-modal intelligent seizure acquisition (MISA) system for detection of motor seizures from electromyographic data and motion data. *Comput Methods Programs Biomed.* (2012) 107:97–110. doi: 10.1016/j.cmpb.2011.06.005
58. Conradsen I, Beniczky S, Wolf P, Jennum P, Sorensen HB. Evaluation of novel algorithm embedded in a wearable sEMG device for seizure detection. *Annu Int Conf IEEE Eng Med Biol Soc.* (2012) 2012:2048–51. doi: 10.1109/EMBC.2012.6346361
59. Szabó C, Morgan LC, Karkar KM, Leary LD, Lie OV, Girouard M, et al. Electromyography-based seizure detector: preliminary results comparing a generalized tonic-clonic seizure detection algorithm to video-EEG recordings. *Epilepsia.* (2015) 56:1432–7. doi: 10.1111/epi.13083
60. Beniczky S, Conradsen I, Wolf P. Detection of convulsive seizures using surface electromyography. *Epilepsia.* (2018) 59:23–9. doi: 10.1111/epi.14048
61. Billeci L, Marino D, Insana L, Vatti G, Varanini M. Patient-specific seizure prediction based on heart rate variability and recurrence quantification analysis. *PLoS ONE.* (2018) 13:e0204339. doi: 10.1371/journal.pone.0204339
62. Leal A, Pinto MF, Lopes F, Bianchi AM, Henriques J, Ruano MG, et al. Heart rate variability analysis for the identification of the preictal interval in patients with drug-resistant epilepsy. *Sci Rep.* (2021) 11:5987. doi: 10.1038/s41598-021-85350-y
63. Jeppesen J, Fuglsang-Frederiksen A, Johansen P, Christensen J, Wüstenhagen S, Tankisi H, et al. Seizure detection based on heart rate variability using a wearable electrocardiography device. *Epilepsia.* (2019) 60:2105–13. doi: 10.1111/epi.16343
64. Jeppesen J, Fuglsang-Frederiksen A, Johansen P, Christensen J, Wüstenhagen S, Tankisi H, et al. Seizure detection using heart rate variability: a prospective validation study. *Epilepsia.* (2020) 61:S41–6. doi: 10.1111/epi.16511
65. Jansen K, Varon C, Van Huffel S, Lagae L. Peri-ictal ECG changes in childhood epilepsy: implications for detection systems. *Epilepsy Behav.* (2013) 29:72–6. doi: 10.1016/j.yebeh.2013.06.030
66. Zijlmans M, Flanagan D, Gotman J. Heart rate changes and ECG abnormalities during epileptic seizures: prevalence and definition of an objective clinical sign. *Epilepsia.* (2002) 43:847–54. doi: 10.1046/j.1528-1157.2002.37801.x
67. Cogan D, Birjandtalab J, Nourani M, Harvey J, Nagaraddi V. Multi-biosignal analysis for epileptic seizure monitoring. *Int J Neural Syst.* (2017) 27:1650031. doi: 10.1142/S0129065716500313
68. Regalia G, Onorati F, Lai M, Caborni C, Picard RW. Multimodal wrist-worn devices for seizure detection and advancing research: focus on the Empatica wristbands. *Epilepsy Res.* (2019) 153:79–82. doi: 10.1016/j.eplepsyres.2019.02.007
69. Poh MZ, Loddenkemper T, Reinsberger C, Swenson NC, Goyal S, Sabtala MC, et al. Convulsive seizure detection using a wrist-worn electrodermal activity and accelerometry biosensor. *Epilepsia.* (2012) 53:e93–7. doi: 10.1111/j.1528-1167.2012.03444.x
70. Vieluf S, Amengual-Gual M, Zhang B, El Atrache R, Ufongene C, Jackson MC, et al. Twenty-four-hour patterns in electrodermal activity recordings of patients with and without epileptic seizures. *Epilepsia.* (2021) 62:960–72. doi: 10.1111/epi.16843
71. Cogan D, Nourani M, Harvey J, Nagaraddi V. Epileptic seizure detection using wristworn biosensors. *Annu Int Conf IEEE Eng Med Biol Soc.* (2015) 2015:5086–9. doi: 10.1109/EMBC.2015.7319535
72. Paul Y. Various epileptic seizure detection techniques using biomedical signals: a review. *Brain Inform.* (2018) 5:6. doi: 10.1186/s40708-018-0084-z
73. Milanowski P, Suffczynski P. Seizures start without common signatures of critical transition. *Int J Neural Syst.* (2016) 26:1650053. doi: 10.1142/S0129065716500532
74. Wilkat T, Rings T, Lehnertz K. No evidence for critical slowing down prior to human epileptic seizures. *Chaos.* (2019) 29:091104. doi: 10.1063/1.5122759
75. Kuhlmann L, Lehnertz K, Richardson MP, Schelter B, Zaveri HP. Seizure prediction - ready for a new era. *Nat Rev Neurol.* (2018) 14:618–30. doi: 10.1038/s41582-018-0055-2
76. Stirling RE, Cook MJ, Grayden DB, Karoly PJ. Seizure forecasting and cyclic control of seizures. *Epilepsia.* (2021) 62:S2–14. doi: 10.1111/epi.16541
77. Mormann F, Andrzejak RG, Elger CE, Lehnertz K. Seizure prediction: the long and winding road. *Brain J Neurol.* (2007) 130:314–33. doi: 10.1093/brain/awl241
78. Brinkmann BH, Wagenaar J, Abbot D, Adkins P, Bosshard SC, Chen M, et al. Crowdsourcing reproducible seizure forecasting in human and canine epilepsy. *Brain J Neurol.* (2016) 139:1713–22. doi: 10.1093/brain/aww045
79. Howbert JJ, Patterson EE, Stead SM, Brinkmann B, Vasoli V, Crepeau D, et al. Forecasting seizures in dogs with naturally occurring epilepsy. *PLoS ONE.* (2014) 9:e81920. doi: 10.1371/journal.pone.0081920
80. Nejedly P, Kremen V, Sladky V, Nasseri M, Guragain H, Klimes P, et al. Deep-learning for seizure forecasting in canines with epilepsy. *J Neural Eng.* (2019) 16:036031. doi: 10.1088/1741-2552/ab172d
81. Gregg NM, Nasseri M, Kremen V, Patterson EE, Sturges BK, Denison TJ, et al. Circadian and multiday seizure periodicities, and seizure clusters in canine epilepsy. *Brain Commun.* (2020) 2:fcaa008. doi: 10.1093/braincomms/fcaa008
82. Schelter B, Feldwisch-Drentrup H, Timmer J, Gotman J, Schulze-Bonhage A. A common strategy and database to compare the performance of seizure prediction algorithms. *Epilepsy Behav.* (2010) 17:154–6. doi: 10.1016/j.yebeh.2009.11.017
83. Kuhlmann L, Karoly P, Freestone DR, Brinkmann BH, Temko A, Barachant A, et al. Epilepsyecosystem.org: crowd-sourcing reproducible seizure prediction with long-term human intracranial EEG. *Brain J Neurol.* (2018) 141:2619–30. doi: 10.1093/brain/awy210
84. Ferastraoaru V, Goldenholz DM, Chiang S, Moss R, Theodore WH, Haut SR. Characteristics of large patient-reported outcomes: where can one million seizures get us? *Epilepsia Open.* (2018) 3:364–73. doi: 10.1002/epi4.12237
85. Karoly PJ, Cook MJ, Maturana M, Nurse ES, Payne D, Brinkmann BH, et al. Forecasting cycles of seizure likelihood. *Epilepsia.* (2020) 61:776–86. doi: 10.1111/epi.16485
86. Privitera M, Haut SR, Lipton RB, McGinley JS, Cornes S. Seizure self-prediction in a randomized controlled trial of stress management. *Neurology.* (2019) 93:e2021–31. doi: 10.1212/WNL.0000000000008539
87. Karoly PJ, Ung H, Grayden DB, Kuhlmann L, Leyde K, Cook MJ, et al. The circadian profile of epilepsy improves seizure forecasting. *Brain J Neurol.* (2017) 140:2169–82. doi: 10.1093/brain/awx173
88. Chiang S, Moss R, Black AP, Jackson M, Moss C, Bidwell J, et al. Evaluation and recommendations for effective data visualization for seizure forecasting algorithms. *JAMIA Open.* (2021) 4:ooab009. doi: 10.1093/jamiaopen/ooab009
89. Cook MJ. Advancing seizure forecasting from cyclical activity data. *Lancet Neurol.* (2021) 20:86–7. doi: 10.1016/S1474-4422(20)30414-2
90. Baud MO, Proix T, Rao VR, Schindler K. Chance and risk in epilepsy. *Curr Opin Neurol.* (2020) 33:163–72. doi: 10.1097/WCO.0000000000000798
91. Chang WC, Kudlacek J, Hlinka J, Chvojka J, Hadrava M, Kumpost V, et al. Loss of neuronal network resilience precedes seizures and determines the ictogenic nature of interictal synaptic perturbations. *Nat Neurosci.* (2018) 21:1742–52. doi: 10.1038/s41593-018-0278-y
92. Beniczky S, Ryvlin P. Standards for testing and clinical validation of seizure detection devices. *Epilepsia.* (2018) 59:9–13. doi: 10.1111/epi.14049
93. Halford JJ, Sperling MR, Nair DR, Dlugos DJ, Tatum WO, Harvey J, et al. Detection of generalized tonic-clonic seizures using surface electromyographic monitoring. *Epilepsia.* (2017) 58:1861–9. doi: 10.1111/epi.13897

94. Beniczky S, Conradsen I, Henning O, Fabricius M, Wolf P. Automated real-time detection of tonic-clonic seizures using a wearable EMG device. *Neurology.* (2018) 90:e428–34. doi: 10.1212/WNL.0000000000004893
95. Kramer U, Kipervasser S, Shlitner A, Kuzniecky R. A novel portable seizure detection alarm system: preliminary results. *J Clin Neurophysiol.* (2011) 28:36–8. doi: 10.1097/WNP.0b013e3182051320
96. Beniczky S, Polster T, Kjaer TW, Hjalgrim H. Detection of generalized tonic-clonic seizures by a wireless wrist accelerometer: a prospective, multicenter study. *Epilepsia.* (2013) 54:e58–61. doi: 10.1111/epi.12120
97. Patterson AL, Mudigoudar B, Fulton S, McGregor A, Poppel KV, Wheless MC, et al. SmartWatch by SmartMonitor: assessment of seizure detection efficacy for various seizure types in children, a large prospective single-center study. *Pediatr Neurol.* (2015) 53:309–11. doi: 10.1016/j.pediatrneurol.2015.07.002
98. Velez M, Fisher RS, Bartlett V, Le S. Tracking generalized tonic-clonic seizures with a wrist accelerometer linked to an online database. *Seizure.* (2016) 39:13–8. doi: 10.1016/j.seizure.2016.04.009
99. Onorati F, Regalia G, Caborni C, Migliorini M, Bender D, Poh MZ, et al. Multicenter clinical assessment of improved wearable multimodal convulsive seizure detectors. *Epilepsia.* (2017) 58:1870–9. doi: 10.1111/epi.13899
100. van Andel J, Ungureanu C, Arends J, Tan F, Van Dijk J, Petkov G, et al. Multimodal, automated detection of nocturnal motor seizures at home: is a reliable seizure detector feasible? *Epilepsia Open.* (2017) 2:424–31. doi: 10.1002/epi4.12076
101. Arends J, Thijs RD, Gutter T, Ungureanu C, Cluitmans P, Van Dijk J, et al. Multimodal nocturnal seizure detection in a residential care setting: a long-term prospective trial. *Neurology.* (2018) 91:e2010–9. doi: 10.1212/WNL.0000000000006545
102. Boon P, Vonck K, van Rijckevorsel K, El Tahry R, Elger CE, Mullatti N, et al. A prospective, multicenter study of cardiac-based seizure detection to activate vagus nerve stimulation. *Seizure.* (2015) 32:52–61. doi: 10.1016/j.seizure.2015.08.011
103. Fisher RS, Afra P, Macken M, Minecan DN, Bagić A, Benbadis SR, et al. Automatic vagus nerve stimulation triggered by ictal tachycardia: clinical outcomes and device performance–the U.S. E-37 trial. *Neuromodul J Int Neuromodul Soc.* (2016) 19:188–95. doi: 10.1111/ner.12376
104. Vandecasteele K, De Cooman T, Gu Y, Cleeren E, Claes K, Paesschen WV, et al. Automated epileptic seizure detection based on wearable ECG and PPG in a hospital environment. *Sensors.* (2017) 17:2338. doi: 10.3390/s17102338
105. Jeppesen J, Beniczky S, Johansen P, Sidenius P, Fuglsang-Frederiksen A. Exploring the capability of wireless near infrared spectroscopy as a portable seizure detection device for epilepsy patients. *Seizure.* (2015) 26:43–8. doi: 10.1016/j.seizure.2015.01.015
106. Gu Y, Cleeren E, Dan J, Claes K, Van Paesschen W, Van Huffel S, et al. Comparison between scalp EEG and behind-the-ear EEG for development of a wearable seizure detection system for patients with focal epilepsy. *Sensors.* (2017) 18:29. doi: 10.3390/s18010029
107. Brotherstone R, McLellan A, Graham C, Fisher K. A clinical evaluation of a novel algorithm in the reliable detection of epileptic seizures. *Seizure.* (2020) 82:109–17. doi: 10.1016/j.seizure.2020.09.017
108. Nijsen TM, Arends JB, Griep PA, Cluitmans PJ. The potential value of three-dimensional accelerometry for detection of motor seizures in severe epilepsy. *Epilepsy Behav.* (2005) 7:74–84. doi: 10.1016/j.yebeh.2005.04.011
109. Nijsen TM, Aarts RM, Cluitmans PJ, Griep PA. Time-frequency analysis of accelerometry data for detection of myoclonic seizures. *IEEE Trans Inform Technol Biomed.* (2010) 14:1197–203. doi: 10.1109/TITB.2010.2058123
110. Van de Vel A, Cuppens K, Bonroy B, Milosevic M, Van Huffel S, Vanrumste B, et al. Long-term home monitoring of hypermotor seizures by patient-worn accelerometers. *Epilepsy Behav.* (2013) 26:118–25. doi: 10.1016/j.yebeh.2012.10.006
111. Cuppens K, Karsmakers P, Van de Vel A, Bonroy B, Milosevic M, Luca S, et al. Accelerometry-based home monitoring for detection of nocturnal hypermotor seizures based on novelty detection. *IEEE J Biomed Health Inform.* (2014) 18:1026–33. doi: 10.1109/JBHI.2013.2285015
112. Fujiwara K, Miyajima M, Yamakawa T, Abe E, Suzuki Y, Sawada Y, et al. Epileptic seizure prediction based on multivariate statistical process control of heart rate variability features. *IEEE Trans Biomed Eng.* (2016) 63:1321–32. doi: 10.1109/TBME.2015.2512276
113. Pavei J, Heinzen RG, Novakova B, Walz R, Serra AJ, Reuber M, et al. Early seizure detection based on cardiac autonomic regulation dynamics. *Front Physiol.* (2017) 8:765. doi: 10.3389/fphys.2017.00765
114. Qaraqe M, Ismail M, Serpedin E, Zulfi H. Epileptic seizure onset detection based on EEG and ECG data fusion. *Epilepsy Behav.* (2016) 58:48–60. doi: 10.1016/j.yebeh.2016.02.039
115. Leijten FSS. Multimodal seizure detection: a review. *Epilepsia.* (2018) 59:42–7. doi: 10.1111/epi.14047
116. van Westrhenen A, De Cooman T, Lazeron RHC, Van Huffel S, Thijs RD. Ictal autonomic changes as a tool for seizure detection: a systematic review. *Clin Autonom Res.* (2019) 29:161–81. doi: 10.1007/s10286-018-0568-1
117. Luo H, Lee PA, Clay I, Jaggi M, De Luca V. Assessment of fatigue using wearable sensors: a pilot study. *Dig Biomark.* (2020) 4:59–72. doi: 10.1159/000512166
118. Meisel C, El Atrache R, Jackson M, Schubach S, Ufongene C, Loddenkemper T. Machine learning from wristband sensor data for wearable, noninvasive seizure forecasting. *Epilepsia.* (2020) 61:2653–66. doi: 10.1111/epi.16719
119. Hoppe C, Feldmann M, Blachut B, Surges R, Elger CE, Helmstaedter C. Novel techniques for automated seizure registration: patients' wants and needs. *Epilepsy Behav.* (2015) 52:1–7. doi: 10.1016/j.yebeh.2015.08.006
120. Schulze-Bonhage A, Sales F, Wagner K, Teotonio R, Carius A, Schelle A, et al. Views of patients with epilepsy on seizure prediction devices. *Epilepsy Behav.* (2010) 18:388–96. doi: 10.1016/j.yebeh.2010.05.008
121. Bruno E, Viana PF, Sperling MR, Richardson MP. Seizure detection at home: do devices on the market match the needs of people living with epilepsy and their caregivers? *Epilepsia.* (2020) 61:S11–24. doi: 10.1111/epi.16521
122. Simblett SK, Biondi A, Bruno E, Ballard D, Stoneman A, Lees S, et al. Patients' experience of wearing multimodal sensor devices intended to detect epileptic seizures: a qualitative analysis. *Epilepsy Behav.* (2020) 102:106717. doi: 10.1016/j.yebeh.2019.106717
123. Bruno E, Biondi A, Thorpe S, Richardson MP. Patients self-mastery of wearable devices for seizure detection: a direct user-experience. *Seizure.* (2020) 81:236–40. doi: 10.1016/j.seizure.2020.08.023
124. Bruno E, Biondi A, Bottcher S, Lees S, Schulze-Bonhage A, Richardson MP, et al. Day and night comfort and stability on the body of four wearable devices for seizure detection: a direct user-experience. *Epilepsy Behav.* (2020) 112:107478. doi: 10.1016/j.yebeh.2020.107478
125. Elger CE, Helmstaedter C, Kurthen M. Chronic epilepsy and cognition. *Lancet Neurol.* (2004) 3:663–72. doi: 10.1016/S1474-4422(04)00906-8

Conflict of Interest: The authors declare that the research was conducted in the absence of any commercial or financial relationships that could be construed as a potential conflict of interest.

frontiers in Neurology

ORIGINAL RESEARCH
published: 18 October 2021
doi: 10.3389/fneur.2021.728484

Wearable Reduced-Channel EEG System for Remote Seizure Monitoring

Mitchell A. Frankel[1], Mark J. Lehmkuhle[1], Mark C. Spitz[2], Blake J. Newman[3], Sindhu V. Richards[3] and Amir M. Arain[3]*

[1] Epitel, Inc., Salt Lake City, UT, United States, [2] Neurology, University of Colorado Anschutz Medical Center, Aurora, CO, United States, [3] Department of Neurology, University of Utah School of Medicine, Salt Lake City, UT, United States

Epitel has developed Epilog, a miniature, wireless, wearable electroencephalography (EEG) sensor. Four Epilog sensors are combined as part of Epitel's Remote EEG Monitoring platform (REMI) to create 10 channels of EEG for remote patient monitoring. REMI is designed to provide comprehensive spatial EEG recordings that can be administered by non-specialized medical personnel in any medical center. The purpose of this study was to determine how accurate epileptologists are at remotely reviewing Epilog sensor EEG in the 10-channel "REMI montage," with and without seizure detection support software. Three board certified epileptologists reviewed the REMI montage from 20 subjects who wore four Epilog sensors for up to 5 days alongside traditional video-EEG in the EMU, 10 of whom experienced a total of 24 focal-onset electrographic seizures and 10 of whom experienced no seizures or epileptiform activity. Epileptologists randomly reviewed the same datasets with and without clinical decision support annotations from an automated seizure detection algorithm tuned to be highly sensitive. Blinded consensus review of unannotated Epilog EEG in the REMI montage detected people who were experiencing electrographic seizure activity with 90% sensitivity and 90% specificity. Consensus detection of individual focal onset seizures resulted in a mean sensitivity of 61%, precision of 80%, and false detection rate (FDR) of 0.002 false positives per hour (FP/h) of data. With algorithm seizure detection annotations, the consensus review mean sensitivity improved to 68% with a slight increase in FDR (0.005 FP/h). As seizure detection software, the automated algorithm detected people who were experiencing electrographic seizure activity with 100% sensitivity and 70% specificity, and detected individual focal onset seizures with a mean sensitivity of 90% and mean false alarm rate of 0.087 FP/h. This is the first study showing epileptologists' ability to blindly review EEG from four Epilog sensors in the REMI montage, and the results demonstrate the clinical potential to accurately identify patients experiencing electrographic seizures. Additionally, the automated algorithm shows promise as clinical decision support software to detect discrete electrographic seizures in individual records as accurately as FDA-cleared predicates.

Keywords: seizure detection, wearables, remote monitoring, machine learning, EEG

OPEN ACCESS

Edited by:
Gregory Worrell, Mayo Clinic, United States

Reviewed by:
Kais Gadhoumi, Duke University, United States
Johannes Koren, Clinic Hietzing, Austria

***Correspondence:**
Mark J. Lehmkuhle
lehmkuhle@epitel.com

Specialty section:
This article was submitted to Epilepsy, a section of the journal Frontiers in Neurology

Received: *21 June 2021*
Accepted: *20 September 2021*
Published: *18 October 2021*

Citation:
Frankel MA, Lehmkuhle MJ, Spitz MC, Newman BJ, Richards SV and Arain AM (2021) Wearable Reduced-Channel EEG System for Remote Seizure Monitoring. Front. Neurol. 12:728484. doi: 10.3389/fneur.2021.728484

INTRODUCTION

Epilepsy affects 1% of the population or ∼70 million people worldwide (1). For people who are experiencing seizure-like activity in their daily lives, the current acceptable method for differential diagnosis requires a visit to an epilepsy monitoring unit (EMU), for which there only exists ∼245 Level III/IV centers out of ∼6,200 hospitals across the U.S (2). Most commonly, this requires a limited multi-day stay in the EMU where video and high-channel-count wired electroencephalography (EEG) are recorded (19+ EEG channels). A diagnosis of epilepsy is determined only after epileptologist review of the video-EEG record for electrographic epileptiform events and clinical seizure activity. EMU visits require time away from home, potentially large travel distances, can be very costly even with insurance, require restricted movements due to the wired and tethered EEG systems, and can be traumatizing (3, 4). During these limited EMU stays, adults are commonly taken off their medications with the intent to record seizures. It is common for some people to feel overwhelmed by the entire process and leave early without any recording of seizures or concrete diagnosis of a seizure disorder (4). Additionally, many people do not have any electrographic seizure activity during their EMU stay for various reasons including the rarity of events that do not occur during a limited EMU stay (3, 5).

Better electrographic seizure recordings and clinical decisions could be made if the EEG was recorded at home in a person's normal daily environment (6). Ambulatory EEG systems (AEEG) have been used by epileptologists for diagnostic purposes when an in-EMU visit is not possible. The AEEG systems allow people to wear the wired AEEG in their home environment, but have substantial limitations including: the EEG electrodes must be positioned and glued to the person's scalp by a trained EEG technician, the long wired tethers create obfuscating motion artifacts in the EEG record especially during convulsive seizures and other movements, the bulky system is restrictive which prevents the person from many normal daily activities like exercise or bathing, and the cumbersome system can be socially stigmatizing if worn out in public (**Figure 1**) (7, 8). Sub-scalp EEG systems, such as UNEEG's SubQ (9) and EpiMinder's Minder™ (10) offer potential solutions for long-term, at-home EEG recording, though they are invasive. A discreet, wireless, easily applied, wearable EEG system would have the potential to make home EEG recording more widely available, less restrictive, and provide EEG with no wired tether artifacts that can obscure the electrographic seizure activity.

To fill this need, Epitel has developed Epilog (**Figure 2**), a miniature, wireless, wearable EEG sensor capable of recording high-fidelity EEG throughout a person's daily life. Epilog is smaller than a cochlear implant, is designed to be aesthetically-pleasing while worn on the scalp below the hairline, and allows unrestricted mobility. The Epilog sensor records a single channel of EEG through a differential electrode pair spaced 18 mm center-to-center, similar to high-density EEG (11). Because all components are self-contained, Epilog data is less susceptible to wired movement artifacts or antenna noise that plague wired EEG systems. Epilog sensors are robust, water-resistant, and designed to meet the rigorous needs of everyday use while providing consistent recording performance.

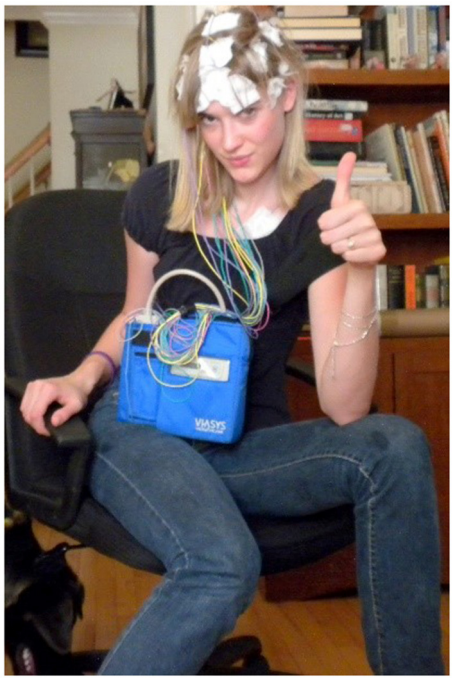

FIGURE 1 | Typical wired ambulatory EEG (with permission from Kelly Falk).

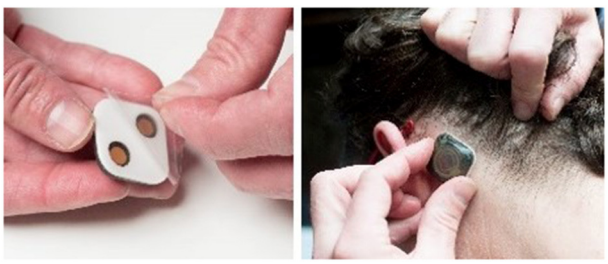

FIGURE 2 | Epilog uses one-piece disposable "stickers," that are both the adhesive and conductive hydrogel that serve as the interface between Epilog and the scalp when used below hairline.

Epitel has developed REMI®, a Remote EEG Monitoring platform. REMI is intended to be used in any clinical situation where near real-time and/or remote EEG is warranted, using four Epilog sensors placed bilaterally below the hairline on the forehead and behind the ear, at the approximate F7/F8 and T5/T6 locations based on the standard International 10–20 system (12). Epitel intends to extend the use of REMI for ambulatory, outpatient EEG recordings, where any physician can prescribe the system for a person suspected of seizures. Their patient would wear the sensors for a specific prescribed duration with no mobility restrictions in their normal daily lives. The EEG data from the four Epilog sensors are directly uploaded to an HIPAA-compliant database, converted into a 10-channel REMI

montage that includes the four individual sensor recordings and six sensor-to-sensor differential channels (herein referred to as "REMI montage"). The REMI montage is accessible for review by a remote epileptologist through REMI's Persyst® Mobile interface. An example of a 30-s focal onset seizure evolving to bilateral tonic-clonic recorded and presented in the REMI montage can be seen in **Figure 3**.

Reviewing long duration EEG recordings can be a very time-consuming processes for epileptologists and having more at-home EEG recordings via wearable systems, such as REMI, would likely become overly burdensome. Automated seizure detection algorithms may be used as Clinical Decision Support Software (CDSS), where the algorithm highlights specific time periods in an EEG record when seizure activity is likely. Epileptologists could use the markers to guide and speed up their EEG review. A wide variety of signal processing and machine learning algorithms have been studied for seizure detection purposes (13–16). There are clinically cleared CDSS that reduce the time required to review EEG in the hospital with high sensitivity and low false detection rates (FDR) (17–23). The most commonly used clinically-cleared software for all types of seizure detection is Persyst®. The Persyst 12 software is the most commonly cited predicate for scalp EEG seizure detection software with a mean sensitivity of 81% and FDR of 0.21 false detections per hour. However effective, automated scalp EEG seizure detection software is currently only clinically available for use on in-hospital, high-channel-count, wired-EEG recordings.

To demonstrate feasibility for long-term ambulatory use of REMI, it is necessary to first determine how accurate remote epileptologist reviewers are at identifying spontaneous, recurrent, electrographic seizures in the REMI montage, and if automated algorithms can be used as CDSS to support expert review. With this study, we hypothesize that (a) Epileptologists can accurately detect focal-onset electrographic seizures in REMI montage data, (b) Automated seizure detection algorithms can be used to detect focal-onset electrographic seizures in REMI montage data with sensitivity and false detection rate similar to FDA-cleared predicates, and (c) Automated seizure detection algorithms can be used as CDSS to guide epileptologist review without a loss in performance.

METHODS

Electroencephalography was recorded by Epilog sensors alongside standard-of-care 19-channel, full-montage, video-EEG (herein referred to as "wired-EEG") in adults during EMU stays at the University of Colorado Anschutz Medical Center. The subjects' wired-EEG included a full array of 19 wired electrodes in the standard International 10–20 system, including T1, T2, and eye leads.

General Methods

All protocols were approved by the Institutional Review Board of the University of Colorado. Adults entering the EMU for long-term EEG evaluation were called prior to their appointment

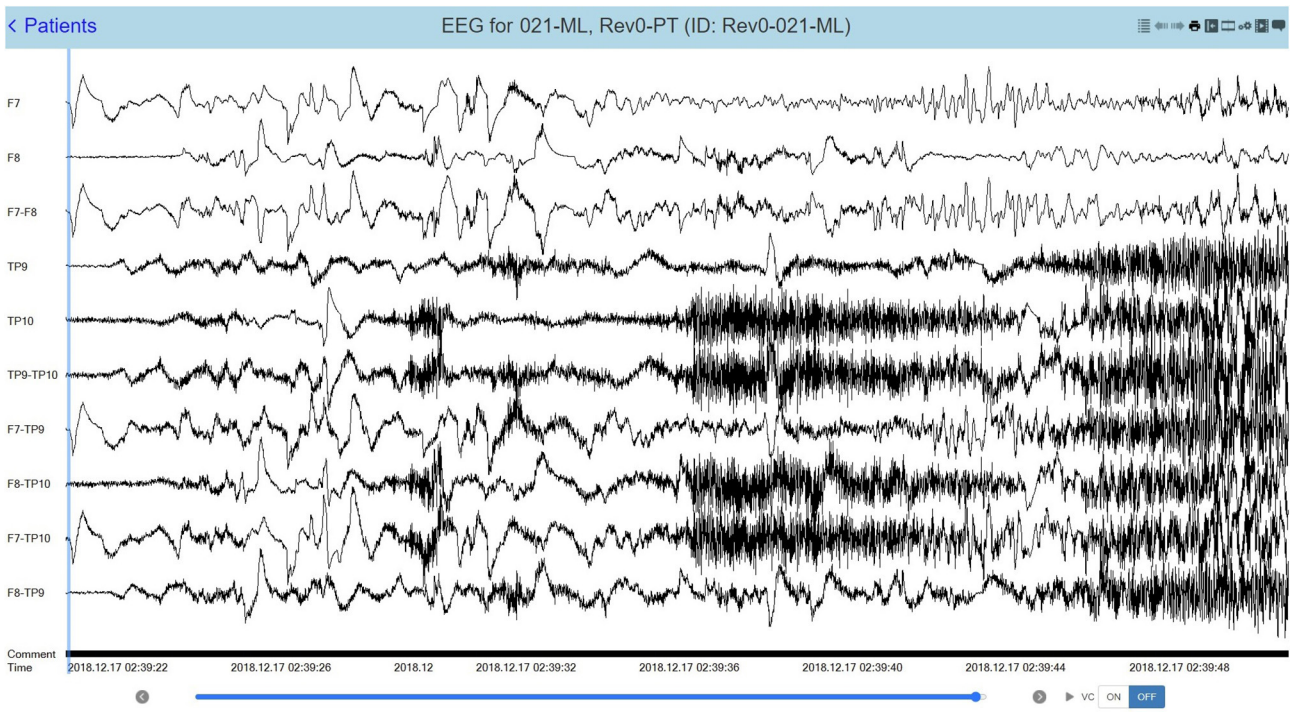

FIGURE 3 | A 30-s recording from four Epilog sensors during a focal-onset seizure evolving to bilateral tonic-clonic (TP10 focal onset), displayed in the 10-channel REMI montage.

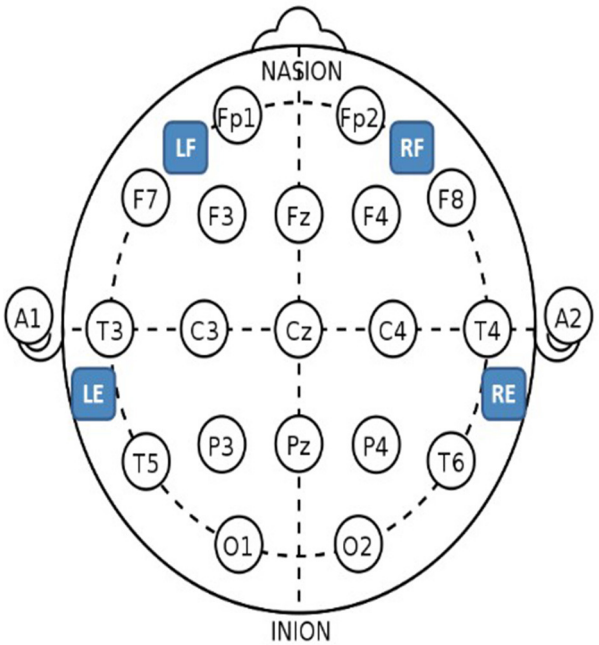

FIGURE 4 | Epilog sensor placement locations with the standard International 10–20 system as reference. For the forehead locations, LF is left-forehead closest to F7, RF is right-forehead closest to F8, and the Epilog sensors were placed as far from forehead/eye muscles as possible. For the behind-the-ear locations, LE is behind left ear closest to T5, and RE is behind right ear closest to T6, and the Epilog sensors were placed as high up as possible over the mastoid while still being below the hairline, making sure placement was not directly over the neck muscles.

to discuss the study objectives. Each subject was consented in the EMU. Epilog sensors were placed by the trained study coordinator after the full-montage wired-EEG electrodes were affixed by an EEG technician. Each subject wore four Epilog sensors, placed at scalp locations below the hairline on the forehead and behind each ear, using an adhesive sticker with embedded conductive hydrogel (see **Figure 2** for hydrogel sticker and see **Figure 4** for sensor proximity to 10–20 locations). The IRB approval allowed for up to 7 days of continuous EEG recording. The Epilog sensor can be worn continuously for up to 7 days in a normal EMU environment and required no daily maintenance from the subject or medical staff. Routine video-EEG review and associated seizure identification was part of the standard patient care.

EEG Recordings

Epilog records a single channel of EEG through two gold electrodes Ø6 mm, spaced 18 mm center-to-center, and data is extracted from the sensor's onboard memory into the European Data Format Plus file type (EDF+). Epilog data were recorded at 10-bit, 512 Hz with an amplifier passband of 0.8–92 Hz. The full-scale signal amplitude was ± 175 μV. The Epilog sensor uses a primary battery that supports continuous EEG recording for 7 days without replacement or recharging. Video-EEG in the EMU was recorded with standard clinical equipment and settings (Nihon Khoden Neurofax EEG-1200, 200 Hz sampling).

Workflow

The study coordinator working with the on-service epileptologist pre-contacted all subjects, consented all subjects upon arrival, placed each Epilog sensor after the EEG Technician had placed wired-EEG electrodes (using training material provided by Epitel), and managed the reporting and data retrieval. The Epilog EEG and wired-EEG were time-synced using a sequence of "taps" on both the Epilog sensor and the Fp1 wired-EEG electrode. During standard-of-care video-EEG review, the epileptologist determined the electrographic start and stop time for each seizure event. The clinical data management specialist then uploaded de-identified subject data and Epilog EEG records to a HIPAA-compliant database. The EEG data from the four Epilog sensors was converted into the 10-channel REMI montage (**Figure 3**) and uploaded into a Persyst 14b server with Persyst Mobile access.

Automated Seizure Detection Algorithm

Prior to designing the algorithm for this study, Epitel began developing a seizure detection algorithm for single-channel EEG recorded with Epilog sensors. Epilog EEG data from patients at clinical partner epilepsy centers were used to determine which specific features, machine learning model types, and machine learning model hyperparameters are most likely to yield the best results for focal seizure detection in Epilog sensor EEG. This was done using common grid search, feature importance, and stratified k-folds cross-validation methods. This early analysis can be considered the train-test data for feature and model determination. The single-channel Epilog EEG data used in the train-test design of the algorithm was from patients who did not wear Epilog sensors at all four scalp locations as in this present study. While the design of the single-channel algorithm is ongoing, the preliminary knowledge supported the use of the specific features and machine learning model and parameters used in the present study.

EEG data is commonly separated into short, seconds-long segments for seizure detection algorithms that use machine learning (15, 16). The 10-channel REMI-montage data was segmented into 2-s windows for scoring and feature extraction. Data segments that occurred during known electrographic seizure times were scored as "ictal" segments; segments that occurred within 15 min before and after known seizure times were scored "near-ictal"; and all other segments were scored "non-ictal." The reasoning behind the "near-ictal" scoring is that there was some pre-ictal evolution in the EEG prior to the noted electrographic onset as well as some post-ictal EEG activity that might confound a machine learning classifier. The 15-min "near-ictal" timing was chosen based on internal review of the Epilog EEG data and knowledge that no known seizure event timings were within <15 min of each other. For each 2-s segment, features were extracted in the time domain (e.g., variance), frequency domain (e.g., power in delta band), time-frequency domain (e.g., wavelet convolutions), and complexity domain (e.g., entropy). Because seizures are known to evolve over time, historical information about each feature was determined as

a weighted average of prior segments' feature values and added to the overall feature set. Cross-channel correlations for all features were determined and added to the overall feature set for each 2-s segment.

For each of the 20 subjects, a training feature set was created by combining the segmented and scored features from all other 19 subjects, essentially a leave-one-out method that occurs 20 independent times. The ratio of non-ictal to ictal data was quite high, even for those who experienced seizures, which would bias any machine learning classifier. Thus, the training set was reduced to keep all of the ictal segments and randomly chosen non-ictal segments in a 3:1 non-ictal:ictal ratio. No "near-ictal" segments were included in the training set. A random forest machine learning classifier was trained using an ensemble of 500 trees, where bootstrapping (sample with replacement) was allowed, and trees were extended to full splits. The trained classifier was then applied to the held-out subject's complete feature set including "near-ictal" segments, and an ictal class likelihood was determined for each 2-s segment.

In most literature, this is when a threshold is applied to classify each segment as ictal or not, and metrics such as receiver operating characteristic curve area-under-the-curve or F1-score can be determined to see how well the classifier performed in out-of-sample segmented data. For seizure detection, this is not enough, as what is necessary is whole seizure start and stop times, where a complete seizure can be between 10 s and 15 min in duration. This has been demonstrated in some recent literature using the classifier likelihood output and an integrate-and-fire neuron (24). For our algorithm, a leaky, weighted integrator was applied to the classifier likelihood output. Using a fixed threshold for all subjects, when the integrated ictal likelihood went above the threshold for five continuous segments (10 s), a seizure start marker was set. The exact time point of the start marker was set based on the start time of the first segment above threshold and accounted for the duration of the integrator. Similarly, when the integrated ictal likelihood went below the threshold for five continuous segments, a seizure stop marker was set. This threshold was set low so that the sensitivity of the machine learning algorithm would be high ($\geq$90% on the training data) at the expense of a possibly high FDR. Some additional processing was done on these whole-seizure detection events: (1) Any events that occurred within 2 min of each other were concatenated into a single event, and (2) After the concatenation, any event that lasted longer than 15 min was discarded. The sensitivity, precision, and FDR of the automated algorithm were determined for each of the 20 subjects, where a true positive (TP) event occurs if there is any overlap between the known the seizure electrographic onset/offset time and the algorithm determined one (25). For TP events, the percent of overlap was determined as the amount of time of the known seizure event that the detection event encompassed.

Blinded Expert Review With Persyst Mobile

Three independent, board certified epileptologists not affiliated with University of Colorado Anschutz Medical Center, and who have never reviewed Epilog EEG in the REMI montage before, were recruited for this study. Each epileptologist was provided the REMI montage from 40 subjects who wore four Epilog sensors, to remotely review through Persyst Mobile. The 40 records consisted of randomized data from: (a) unannotated EEG from 10 subjects who had focal-onset electrographic seizures during their EMU stay, (b) unannotated EEG from 10 subjects who had no electrographic seizures or epileptiform activity during their EMU stay, (c) algorithm-determined seizure-detection start/stop annotated EEG from the same 10 subjects who had focal-onset electrographic seizures during their EMU stay, and (d) algorithm-determined seizure-detection start/stop annotated EEG from the same 10 subjects who had no electrographic epileptiform activity during their EMU stay. The epileptologists were blinded to (a) how many of the 40 subjects were known to have seizures, (b) that the same 20 subjects' EEG was the data that was processed to create the algorithm-determined annotated EEG, and (c) the randomized order that the data was presented in. There were no algorithm-determined seizure events for some of the 10 subjects who did not have electrographic activity, and thus no annotations in the EEG record. Because of this, the 20 EEG records where automated seizure detection was applied were noted in their subject ID with "ML," visible in Persyst Mobile. As far as the epileptologists knew, there were 40 independent data sets, some of which contained focal-onset seizures, and 20 of which had CDSS algorithm-determined events annotated.

The epileptologists were asked to review the non-ML records in their entirety and annotate any sections of the EEG data that they believed to be indicative of electrographic seizure activity. The epileptologists were also asked to review the algorithm-annotated records and annotate electrographic seizure activity, using the algorithm-determined events as CDSS. The reviewers were told that these records were processed with an automated seizure-detection algorithm that was tuned so that the sensitivity would be high across all subjects with possibly high FDR. The reviewers were told to use their judgement as to how much they relied on the algorithm annotations or lack thereof. A majority consensus (best 2 out of 3) was used due to the well-known inter-rater variability in blinded EEG review, even among expert neurologists (26). Sensitivity, precision, and FDR [false positives per hour (FP/h)] were determined for each subject for both algorithm-annotated and unannotated records, using the "any-overlap" method discussed earlier. For TP events, the percent of overlap was determined using the method previously discussed. For all known seizure times, the inter-rater reliability was measured with Cohen's Kappa for pair-wise reviewers and Fleiss' Kappa for group reliability.

RESULTS

As part of a larger study, a total of 40 adult subjects (ages 18–64) were enrolled, and 22 (55%) had at least one seizure in the EMU. For this specific piece of the study, data from 20 subjects (ages 18–64) were used: 10 subjects who had focal-onset seizures as classified according to ILAE (27) and 10 subjects who were determined to have no seizure events or epileptiform activity in their wired-EEG (**Figure 5**). A total of 24 focal onset seizures were

						Naïve Review				Review with CDSS				Algorithm				
ID	Gender	Age	Duration of Stay (hrs)	Number of Clinical Seizures	Seizure Type	TP	FN	FP	FDR (FP/hr)	TP	FN	FP	FDR (FP/hr)	Number of Algorithm Events	TP	FN	FP	FDR (FP/hr)
1	M	60	14	1	IC - Focal Evolving to BL TC	1			0	1			0	2	1		1	0.07
2	F	21	72	0					0				0	0				0
3	F	38	48	0					0				0	1			1	0.02
4	F	53	93	4	IB - Focal Impaired Awareness	1	3		0	2	2		0	20	4		16	0.17
5	F	34	25	0					0			1	0.04	0				0
6	M	23	93	6	IB - Focal Impaired Awareness	1	5		0		6		0	105	6		99	1.07
7	F	30	84	1	IC - Focal Evolving to BL TC	1			0	1			0	1	1			0
8	F	18	53	1	IA1 - Focal Aware w/Motor	1			0	1			0	4	1		3	0.06
9	F	41	93	0					0				0	16			16	0.17
10	F	55	38	1	IC - Focal Evolving to BL TC	1		1	0.03	1			0	1	1			0
11	F	31	28	3	IB - Focal Impaired Awareness		3		0		3		0	3	2	1	1	0.04
12	M	37	91	0					0				0	0				0
13	F	32	20	0					0				0	0				0
14	F	61	74	0				1	0.01				0	0				0
15	M	44	30	0					0				0	0				0
16	F	23	16	3	IA1 - Focal Aware w/Motor	1	2		0	3			0	3	3			0
17	M	47	26	0					0			1	0.04	3			3	0.11
18	F	20	16	1	IC - Focal Evolving to BL TC	1			0	1			0	1	1			0
19	M	64	24	0					0				0	0				0
20	F	36	113	3	IB - Focal Impaired Awareness	1	2	1	0.01	1	2	2	0.02	3	1	2	2	0.02
		Total	1050	24		9	15	3	0.003	11	13	4	0.004	163	21	3	142	0.14

FIGURE 5 | Complete subject demographics and results. Subjects in light green are those that had focal-onset seizures during their EMU stay. "Naive Review" results are consensus epileptologist review of the REMI montage without algorithm-detection annotations. "Review with CDSS" results are consensus epileptologist review with algorithm-detection annotations. "Algorithm" results are for the REMI automated seizure detection algorithm. TP, true positive; FN, false negative; FP, false positive; FDR, false detection rate; BL TC, bilateral tonic-clonic.

recorded in the 10 subjects (min 1, mean 2.4, median 2, max 6). The 20 subjects had EMU stays between 0.5 and 5 days (mean of 2.2 days). **Figure 5** details the demographics and results for all subjects. **Table 1** is a summary of sensitivity, precision, and FDR. **Table 2** is a summary of the inter-rater reliability. **Table 3** is a summary of the results based on seizure type. **Table 4** is a summary of the overlap between known seizures and reviewer- and algorithm-detected TP seizures.

Blinded Consensus Epileptologist Review of Unannotated Data

The consensus review identified at least one electrographic seizure for 9 out of the 10 subjects who had known electrographic seizures during their EMU stay (90% Sensitivity) and identified no false events for 9 out of the 10 subjects who had no electrographic seizures during their EMU stay (90% Specificity). Consensus detection of individual electrographic seizures resulted in a mean sensitivity of 61% across the 10 subjects (100% for 5 out of 10 subjects, **Figure 5**—Naive Review, **Figure 6**—unfilled blue star, **Table 1**). The range of the per-reviewer mean sensitivity was 57–73% (**Table 1**; **Figure 6**—unfilled green markers). The consensus mean precision, or positive predictive value (PPV), was 80% across all subjects, with a per-reviewer mean PPV range of 58–78%. The consensus mean FDR was 0.002 FP/h of data, with a per-reviewer mean FDR range of 0.006–0.031 FP/h. The inter-rater reliability (**Table 2**) ranged from 0.52 (moderate) to 0.71 (good) for the pair-wise comparison as measured with Cohen's Kappa statistic and 0.59 (moderate) for the group as measured with Fleiss' Kappa statistic.

TABLE 1 | Summary of sensitivity, precision, and false detection rate results.

Reader	Sensitivity % ± SD [range]	Precision % ± SD [range]	False detection rate FP/h ± SD [range]
R1—Naive	58 ± 46 [0–100]	75 ± 42 [0–100]	0.006 ± 0.016 [0.0–0.062]
R2—Naive	57 ± 47 [0–100]	58 ± 47 [0–100]	0.031 ± 0.044 [0.0–0.109]
R3—Naive	73 ± 40 [0–100]	78 ± 37 [0–100]	0.006 ± 0.013 [0.0–0.038]
Consensus—Naive	**61 ± 42 [0–100]**	**80 ± 35 [0–100]**	**0.002 ± 0.007 [0.0–0.026]**
R1—CDSS	58 ± 47 [0–100]	70 ± 48 [0–100]	0.007 ± 0.019 [0.0–0.076]
R2—CDSS	53 ± 50 [0–100]	42 ± 44 [0–100]	0.020 ± 0.054 [0.0–0.244]
R3—CDSS	75 ± 41 [0–100]	73 ± 37 [0–100]	0.010 ± 0.020 [0.0–0.072]
Consensus—CDSS	**68 ± 43 [0–100]**	**73 ± 44 [0–100]**	**0.005 ± 0.012 [0.0–0.040]**
Algorithm	**90 ± 22 [33–100]**	**60 ± 38 [6–100]**	**0.087 ± 0.238 [0.0–1.069]**

Naïve results are for epileptologist review without algorithm detection support. CDSS results are for epileptologist review with algorithm detection support. Algorithm results are for the REMI automated seizure detection algorithm (SD, standard deviation; FP, false positive).

TABLE 2 | Inter-rater reliability for known seizure events.

	Naive	CDSS
R1 vs. R2	0.71	0.44
R1 vs. R3	0.59	0.53
R2 vs. R3	0.52	0.53
Group	0.59	0.49

The values shown are Cohen's Kappa statistic for pair-wise (e.g., Reviewer R1 vs. Reviewer R2) and Fleiss' Kappa statistic for the group.

TABLE 3 | Electrographic seizures ending in a convulsion (convulsive) vs. seizures that did not end in a clinical convulsion (non-convulsive).

	Naive review				Review with CDSS				Algorithm	
	Consensus		All 3		Consensus		All 3			
	TP	FN	TP	FN	TP	FN	TP	FN	TP	FN
Conv.	8		5		6	2	6		8	
Non-conv.	3	13		10	3	13		11	13	3

The Consensus review is best 2 out of 3 and the "All 3" is when all three reviewers agree. The consensus, all three reviewers, and the algorithm all performed better for detecting seizures that ended in a convulsion. TP, true positive; FN, false negative.

TABLE 4 | Percent of overlap between known seizures and true positive events marked by reviewers and the automated algorithm.

	Min	Max	Mean	SD
R1—Naive	43	96	80.8	17.3
R2—Naive	54	100	83.5	18.2
R3—Naive	48	100	86.1	15.6
R1—CDSS	64	100	87.2	11.9
R2—CDSS	63	100	90.6	12.5
R3—CDSS	49	100	85.1	15.4
Algorithm	44	100	92.1	13.8

SD, standard deviation.

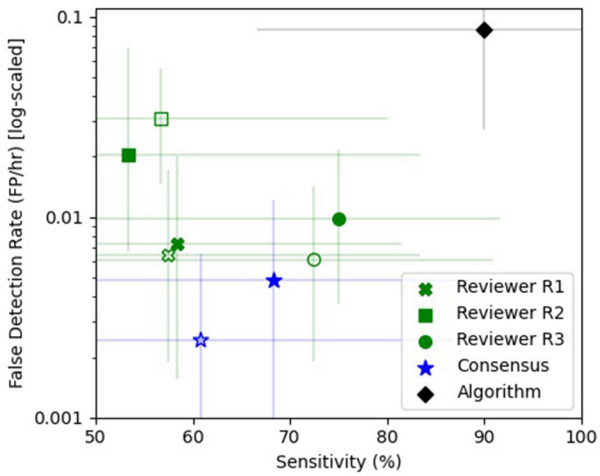

FIGURE 6 | Sensitivity vs. false detection rate. The sensitivity (%) and false detection rate (FDR—FP/h) are shown for the individual reviewers [green x (R1), square (R2), and circle (R3)], the consensus review (blue star), and the automated algorithm (black diamond). The unfilled markers denote the naive epileptologist review and the filled markers denote review with automated algorithm annotations as clinical decision support software (CDSS). Reviewers R1 (green x), R3 (green circle), and the consensus (blue star) showed improved sensitivity with CDSS at the expense of a higher FDR, while reviewer R2 (green square) had a reduced sensitivity and FDR with CDSS. The REMI automated seizure detection algorithm (black diamond) had a higher sensitivity than any one reviewer or consensus, with a higher false detection rate. The error bars are 95% confidence intervals using a bias-corrected and accelerated method (BCa, $N = 1{,}000$).

The consensus review was able to accurately mark 8 out of 8 focal onset seizures that ended in a clinical convulsion (Type IA1—Focal Aware w/Motor and Type IC—Focal Evolving to Bilateral Tonic Clonic) with all three reviewers marking 5 of 8 (**Table 3**). The minimum overlap between known seizures and TP reviewer determined events ranged from 43 to 54%, with means ranging 80.8–86.1% (**Table 4**).

Blinded Consensus Epileptologist Review With Algorithm-Detection as CDSS

When the reviewers were provided algorithm seizure-detection annotations in the EEG record as CDSS, the consensus review identified at least one electrographic seizure for 8 out of the 10 subjects who had known electrographic seizures during their EMU stay (80% Sensitivity) and identified no false events for 8 out of the 10 subjects who had no electrographic seizures during their EMU stay (80% Specificity). The mean sensitivity for consensus detection of individual electrographic seizures improved to 68% across the 10 subjects (100% for 6 out of 10 subjects, **Figure 5**—Review with CDSS, **Figure 6**—filled blue star; **Table 1**). The range of the per-reviewer mean sensitivity was 53–75% (**Table 1**; **Figure 6**—filled green markers). The consensus mean precision (PPV) was reduced to 73% across all 20 subjects, with a per-reviewer mean PPV range of 42–73%. The consensus mean FDR increased to 0.005 FP/h, with a per-reviewer mean FDR range of 0.007–0.020 FP/h. The inter-rater reliability was reduced (**Table 2**) and ranged from 0.44 (moderate) to 0.53 (moderate) for the pair-wise comparison as measured with Cohen's Kappa statistic and 0.49 (moderate) for the group as measured with Fleiss' Kappa statistic. The consensus review accurately marked 6 out of 8 focal onset seizures that ended in a clinical convulsion (Type IA1—Focal Aware with Motor and Type IC—Focal Evolving to Bilateral Tonic Clonic) with all three reviewers marking 6 of 8 (**Table 3**). The minimum overlap between known seizures and TP reviewer determined events ranged from 49 to 64%, with means ranging 85.1–90.6% (**Table 4**).

Automated Seizure Detection

Epitel's automated seizure detection algorithm was able to detect 21 of 24 known focal-onset seizures (out-of-sample), providing a mean sensitivity of 90% across all subjects (100% for 8 out of 10 subjects, **Figure 5**—Algorithm, **Figure 6**—filled black diamond;

Table 1). The three missed events were all Type IB—Focal Onset with Impaired Awareness (**Table 3**). The mean precision (PPV) of the algorithm was 60% and the mean FDR was 0.087 FP/h across all subjects. The FDR was 0.22 FP/h for subjects who had electrographic seizures during their EMU stay and 0.04 FP/h for subjects who did not have seizures. Subject #6 had an outlier FDR of 1.07 FP/h (99 false detections during the 93-h EMU stay), while the maximum FDR for all others was 0.17 FP/h. The algorithm mean sensitivity was higher than any individual reviewer or consensus review, with or without CDSS, but with a higher FDR (**Figure 6**). The algorithm detected at least one TP seizure event for all 10 subjects who had electrographic seizures (100% sensitivity) and detected no false positives (FP) for 7 of the 10 subjects who had no seizures (70% specificity). The number of FP and FDR for the other three non-seizure subjects was one event, 0.02 FP/h (ID #3), 16 events, 0.17 FP/h (ID #9), and three events, 0.11 FP/h (ID #17). The minimum overlap between known seizures and TP algorithm-determined events was 44% with a mean of 92.1% (**Table 4**).

DISCUSSION

This study sought to answer if epileptologists could accurately detect focal-onset electrographic seizures with a remote, wireless, reduced-channel EEG system, and whether automated algorithms could assist with that task.

Blinded Epileptologist Review of Unannotated Data

This is the first study to analyze epileptologists ability to blindly review remote EEG data from four Epilog sensors in the 10-channel REMI montage. There are only a few studies assessing the performance of individual reviewers and consensus review for blind seizure identification in EEG. In a large ICU study using standard clinical wired-EEG, Tu et al. reported a consensus sensitivity of 75% and individual reviewer FDR of 0.085 FP/h (26). Other studies have shown individual reviewer sensitivities between 70 and 85% with FDR between 0.016 and 0.043 FP/h (20). Epileptologists are trained on, and are most commonly experienced with, reviewing 19+ channels of video-EEG in multi-channel montages. Therefore, it is not surprising that they might have some difficulty with the 10-channel REMI montage, especially on their first experience. With no prior training or experience with Epilog EEG in the REMI montage, the reviewer consensus successfully achieved a sensitivity of 61%, precision (PPV) of 80%, and FDR of 0.002 FP/h for identifying spontaneous recurrent electrographic focal-onset seizures (**Figure 6**; **Table 1**). As might be expected, the reviewers were very conservative in marking seizures, including a very low FDR when compared to prior studies. While the reviewers had difficulty determining focal-onset seizures that did not result in a clinical convulsion, they were very good at detecting events that did end in a clinical convulsion where the consensus review found all eight events with all three reviewers finding 5 of the 8 (**Table 3**). The overlap between known seizure timings and reviewer-determined events was generally high, with means above 80% (**Table 4**).

Blinded Epileptologist Review With CDSS Annotations

The reviewers were also provided with randomized copies of the REMI montage records with annotations of seizure event markers determined by an automated algorithm with high sensitivity. The consensus review improved from 61 to 68% on these records, with a slight increase in FDR (0.005 FP/h up from 0.002 FP/h) (**Table 1**). While the results are an improvement, they are not statistically different (**Figure 6**). The reviewers were only told that the algorithm had a high sensitivity with a possible high FDR, but not what the exact values would be, and no training was provided on how to use the algorithm event annotations as CDSS. During a post-analysis debrief, the reviewers mentioned they evaluated the EEG in its entirety and then checked their review against the algorithm-detected events for overlap. The reviewers felt the algorithm "overcalled" events. There were a high number of algorithm-detected FPs for three subjects (4, 6, and 9). Two of the four TP markers and none of the 16 FP markers for Subject 4 were noted by the consensus review, an improvement of 1 TP over blind review without algorithm-annotations (**Figure 5**). None of the 16 FP markers for Subject 9 were noted by the consensus review. None of the 6 TP or 99 FP markers for Subject 6 were noted by the consensus review, though one of the true events was found by consensus in the EEG record without algorithm-determined markers. Only one of the 131 FP markers for these subjects was noted as an electrographic seizure by just one of the reviewers overall. It's possible that the large number of algorithm-annotation markers for these subjects led to a disbelief by the reviewers that any of these markers were valid. It is well-known since Aesop that credibility of a detection system is intricately intertwined with sensitivity and false alarms. Effectiveness of the system depends on this credibility. Yet, each false alarm reduces credibility that in turn affects response to future alarms, known as the false alarm effect (28), or the "cry wolf effect." Paradoxically, the more sensitive a system, the greater the credibility of the system is affected by the false alarm effect due to the false alarm rate. Furthermore, as the credibility of the system is reduced by the false alarm effect, the credibility of the danger simultaneously increases. This is especially the case for sparse events, such as low seizure rates.

The intended benefit of automated algorithm detections as CDSS is to reduce the time it takes an epileptologist to review long-duration recordings while improving the sensitivity for finding relevant electrographic seizures. It is possible and likely that, with epileptologist experience and trust in the algorithm, CDSS could reduce the time it takes to review the REMI montage, as well as improve the sensitivity for detecting electrographic seizure events.

Automated Seizure Detection Software

The results show that the automated algorithm can detect discrete focal-onset seizures in the REMI montage with a mean sensitivity of 90% and mean FDR of 0.087 FP/h across all subjects, on par with the Persyst P12 predicate of 81% sensitivity and FDR

of 0.21 FP/h. There are a wide variety of commercially- and clinically-available software for EEG seizure detection. The most widely used software is Persyst and their P12 software is the most common benchmark for predicate comparison. Persyst has FDA-clearance for their most recent P13 and P14 seizure detection software, where the most notable difference is in the FDR. Recent studies have shown the P13 algorithm to have similar sensitivity to the P12 clearance, but higher FDR [0.5 FP/h in Scheuer et al. (20) and 0.9 FP/h in Koren et al. (18)]. The very recently released P14 seizure detection software has been shown to again have similar sensitivity to both P12 and P13, but with a much reduced FDR [0.04 FP/h, Scheuer et al. (20)]. Other FDA-cleared EEG seizure detection software show similar performance characteristics to the predicate P12 software, including the Nihon Kohden QP-160AK with 77% sensitivity and 0.45 FP/h (22) and Encevis [75% sensitivity and 0.29 FP/h in USFDA (23) and 78% sensitivity and 0.2 FP/h in Koren et al. (18)]. The sensitivity and FDR of the REMI automated algorithm outperforms the P12 predicate characteristics and remains on par with the best results of the other clinical EEG seizure detectors. The overlap between known seizure timings and algorithm-determined events was generally very high, with 92.1% mean overlap (**Table 4**).

The automated algorithm missed three known seizure events, all Type IB—Focal with Impaired Awareness (one for Subject #11 and two for Subject #20). For Subject #11, the one missed event occurred because the integrated ictal likelihood never crossed the seizure event threshold during the known seizure event timing. While there was a spike in the integrated ictal likelihood at this time, the threshold would have to be lowered by ∼3% for an event to be detected at the known event time, though this would lead to a much higher FDR across all subjects. For Subject #20 it is more difficult to speculate why the two events were missed. A few possible reasons exist in that both events were short in duration (<30 s) and both events were noted in the clinician notes and wired-EEG to have strong motor content and some of this was picked up in the Epilog sensor EEG, especially in the sensor located at the right forehead. Thus, the duration of electrographic signal in the REMI montage may have been very short compared to movement-related artifact. None of the individual blinded reviewers noted seizures at the time of these three events.

Subjects 4, 6, and 9 can be considered outliers based on their much higher rate of FP when compared to the other 17 subjects. This is especially evident for the 99 FP found by the automated algorithm for Subject #6. Subjects 4 and 6 were known to have focal-onset seizures with impaired awareness, both with right hemisphere and mainly temporal localization. While not shown here, some of the algorithm-detected FP events for these subjects look very similar to known true events in evolution and localization. In the clinical notes, subject 6 was noted to have "several seizures many of which were subclinical and short in duration." Six of these events occurred while the subject was wearing Epilog sensors and the subject had an additional five events outside the timeframe when the Epilog sensors were worn. It is possible that some or many of the FP events were short duration subclinical events that did not reach the initial expert reviewer's definition of a seizure and were not included in the seizure report. For Subject 9, whose wired-EEG "did not show any abnormalities," there were a couple of FP events that look similar to known seizure events in other subjects, but most of the 16 FP events appear to be because one or more of the Epilog sensors were recording data with poor signal quality for unknown reasons (see channels TP9 and TP10 in **Figure 7**).

There are a number of ways that the REMI automated algorithm can be improved. A larger training data set will improve any bias or variance that the small data set used here contained. Larger training data sets can be created by enrolling more subjects in future studies as well as using data augmentation methods on current training data. Artifact rejection (e.g., muscular EMG contamination) and poor signal quality rejection can be added to the detection algorithm to improve the training data ground truths and seizure detection FDR.

Ruling-In Electrographic Seizures

It is very common for someone to have no epileptic events during their EMU stay, simply because their epileptiform activity is rare and may not occur during a brief EMU stay. Of note are people who experience psychogenic non-epileptic seizures (PNES) that account for ∼25% of all patients who enter the EMU (29). One potential application of REMI would be home monitoring for people experiencing seizures before an EMU visit and diagnosis. In this system, a person could wear Epilog sensors as part of REMI for long durations during their normal daily lives where the data could be remotely analyzed for electrographic seizures. This could help as an early mechanism to provide a better understanding of a patient's EEG before a costly, time-consuming, and possibly unnecessary visit to an EMU. If an EMU stay is warranted, REMI could be used to establish chronicity to an individual patient's electrographic events such that scheduling of the EMU stay could coincide with a higher probability of having a seizure (30, 31). When looking at their ability to rule-in subjects who experience electrographic seizures, the consensus review noted at least one TP seizure event for 9 out of the 10 subjects who had a known seizure event in their record (90% sensitivity). Similarly, the consensus review noted no events for 9 out of the 10 subjects who did not have any noted events in their record (90% specificity). The automated algorithm was tuned for high sensitivity and detected at least one true seizure event for all 10 known seizure subjects (100% sensitivity) and did not detect any false events for 7 of the 10 subjects that did not experience any seizures (70% specificity). For those who are experiencing very sparse epileptiform events, having an at-home, longer-duration EEG recording (as may be provided by REMI), would allow for more efficient and cost-effective electrographic diagnostics to rule them in for electrographic seizures.

LIMITATIONS

This study was limited to EEG seizure data only from subjects who had focal-onset seizures. Focal-onset seizures (ILAE Type I) account for ∼56% of all seizure types (32). Because focal-onset seizures may only show electrographic seizure activity in a very small region of the brain, their EEG correlates may not be captured by reduced-channel EEG systems, though some of these seizures evolve into bilateral tonic-clonic events

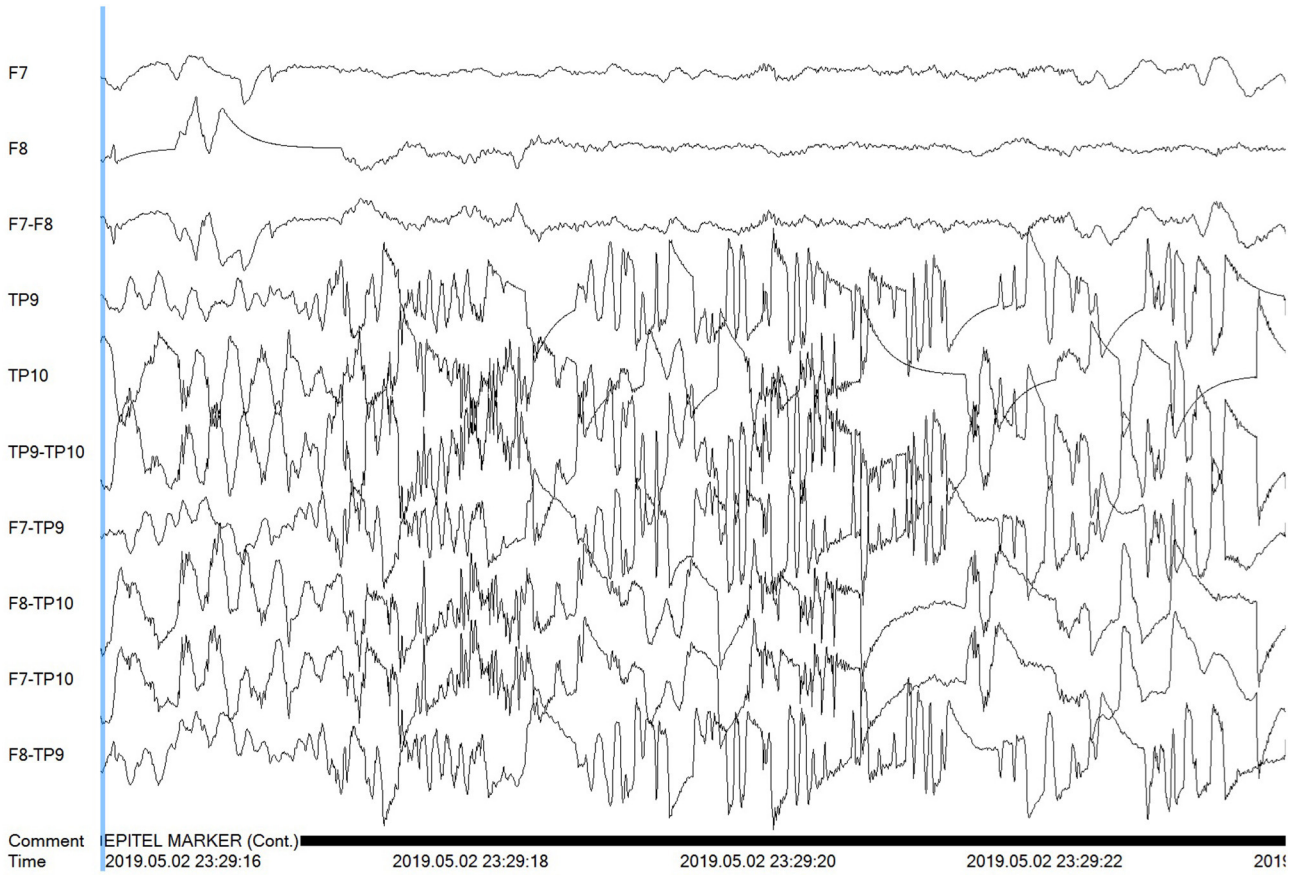

FIGURE 7 | Poor signal quality is shown for the Tp9 and Tp10 Epilog sensors on Subject #9 during a false positive algorithm detection event.

where the electrographic activity becomes generalized across most regions of the brain (17% in this study). REMI is limited to four Epilog sensor placements (eight electrodes) on the scalp below the hairline, bilaterally on the forehead and behind each ear. The current clinical practice of high-channel-count wired electrodes is done to ensure complete spatial coverage of all brain regions and increase the likelihood of being able to differentiate very focalized epileptiform activity. The International Federation of Clinical Neurophysiology has recently recommended a minimum of 25 electrodes and up to 256 if necessary, in both adults and children (33), whereas the American Clinical Neurophysiology Society recommends a minimum of 16 channels (34). REMI does not have the spatial coverage of high-channel count systems and therefore may not be appropriate for seizure onset zone localization. However, EEG recorded from these four locations have been shown to detect 100% of electrographic seizures of both focal and generalized onset (35) due to volume conduction. The REMI montage may be useful for long-term seizure detection and chronicity. It will be important to show that both expert review of the REMI montage and use of detection algorithms can provide electrographic seizure detection in a broader range of seizure types, including those that have a generalized-onset.

Perhaps the greatest limitation of this study was that none of these reviewers had ever seen or reviewed Epilog EEG in the 10-channel REMI montage in the past, and longer-term experience and/or training may improve results. There were a few FP found and false negatives missed by all three reviewers and the automated algorithm. Epileptologists are trained to review video-EEG from EMU patients for the purpose of diagnosing seizure disorders. While these experts are well-trained at reviewing EEG, they can miss some seizures during standard waveform review (26, 36). In most studies on seizure detection, three or more expert reviewers are often relied upon to determine a consensus "ground truth" set of seizure events in the EEG record, and this was not done for the wired-EEG in this study. It may have been advantageous to review the wired-EEG for the FP found and false negatives missed here by the detection algorithm and blinded reviewers. However, EMUs do not typically keep complete wired-EEG records for more than a few months due to their large file size and storage limitations, and the complete wired-EEG records for these subjects were no longer available during this analysis.

There were only a limited number of subjects (20) and seizure events (24) used in this study. Better statistical power would be achieved through a much larger dataset. The long-term intent for the REMI system is for use in a person's everyday environment,

yet the data studied here was collected only in the EMU, where subjects and the environment are very controlled. It will be necessary to show that the accuracy of review and software remains consistent in EEG recorded with REMI during a person's normal daily life.

The preferred method for this type of study would be to have a single, locked algorithm that was previously trained on a large independent data set, and then validated on all 20 of the patient's data included here. The EEG used in this study are the only data sets currently available where patients wore four Epilog sensors concurrently. Thus, the only way to train the automated algorithm was to use the largest data set available, which for each of the 20 patients was the independent data from all other 19 patients. A four-fold validation scheme was initially considered, instead of the 20-fold validation done here, where randomized data from five patients is held out of training, the training data would come from the remaining 15 patients, and then a single algorithm would be validated on five independent patient's data. The decision was made to not do this because it is possible and likely that a large number of seizure events would be held-out from one or more of the four-folds, likely making that fold's algorithm ineffective. Future work will include a single, locked algorithm trained on a large data set, and then validated on a separate set of multiple independent patients. It can be expected that those results would fall somewhere in the range of results described herein.

FUTURE WORK

There are multiple ongoing and planned studies to continue the work described herein. Most importantly, a broader set of data encompassing all seizure types is currently being collected through collaboration with multiple clinical centers. This will allow a more rigorous analysis of which seizure types can be accurately reviewed from Epilog sensor EEG in the REMI montage. Collection and storage of the complete wired-EEG is a key part of these ongoing studies, so that any FP can be re-reviewed later from the wired record. The automated seizure-detection algorithm development is ongoing and future work involves expansion for all seizure types and any intricacies that their differences entail (e.g., absence seizures are very different in evolution and duration and how the algorithm handles these requires more complexity). Because Epilog sensor data can be captured over long durations, it will be critical to determine how long it takes for an epileptologist to blindly review the data, and if automated algorithm-detection annotations can reduce that time without affecting performance. Future studies will compare the automated algorithm performance on the REMI montage with FDA-cleared detection software that will be run on the simultaneously acquired wired-EEG. The Epilog sensors used in this study are intended as single-use, and the current study allowed for up to 7 days of Epilog sensor wear in the EMU. The ambulatory version of the Epilog sensor uses a rechargeable battery that is designed to be recharged once daily. A person would have multiple Epilog sensors, allowing them continuous EEG recording throughout their daily life. There are upcoming studies where Epilog sensors will be worn alongside AEEG systems in home environments to demonstrate the intended effectiveness of REMI for use in a person's normal daily life. Additionally, there are upcoming studies were Epilog sensors will be worn for months in the home environment to demonstrate the intended long-term effectiveness with a rechargeable version of the sensors.

CONCLUSION

Epileptologists, without any REMI training or prior experience, reviewed EEG from just four Epilog sensors in the 10-channel REMI montage and accurately ruled-in subjects experiencing focal onset electrographic seizures with 90% sensitivity and 90% specificity. Consensus detection of individual spontaneous recurrent focal-onset seizures resulted in a mean sensitivity of 61% and mean FDR of 0.002 FP/h. Automated seizure detection algorithms used as Clinical Decision Support Software improved this sensitivity to 68% with little change to FDR (0.005 FP/h). The automated algorithm accurately ruled-in subjects experiencing electrographic seizures with 100% sensitivity and 70% specificity, and detected individual seizures with a very high mean sensitivity of 90% and low mean FDR of 0.087 FP/h, on par with current FDA-cleared software. Blinded epileptologist and automated algorithm review of the REMI montage showed strong potential to delineate patients who experience electrographic seizures. Such a system, when used in a person's everyday environment, could reduce the burden on EMUs to only those who truly need a differential diagnosis of a seizure disorder. Remote EEG systems and support software, as demonstrated here, will be critical to providing seizure diagnostic services to people in their normal daily lives, no matter where they live.

DATA AVAILABILITY STATEMENT

The raw data supporting the conclusions of this article will be made available by the authors, without undue reservation.

ETHICS STATEMENT

The studies involving human participants were reviewed and approved by the University of Colorado, Colorado Multiple Institutional Review Board (COMIRB). The patients/participants provided their written informed consent to participate in this study. Written informed consent was obtained from the individual(s) for the publication of any potentially identifiable images or data included in this article.

AUTHOR CONTRIBUTIONS

MF created the automated algorithm, performed the statistical analysis, and is the main author of this manuscript. ML contributed to the experimental design, supported the algorithm development, and assisted in creation of this manuscript. MS coordinated the collection of all data from Epilog sensors

alongside standard-of-care wired EEG recordings in the EMU. SR, BN, and AA were the reviewing epileptologists and assisted in creation of this manuscript. All authors contributed to the article and approved the submitted version.

FUNDING

This work was supported in part by a grant from the National Institute of Neurological Disorders and Stroke NS100235.

REFERENCES

1. Luoni C, Bisulli F, Canevini MP, De Sarro G, Fattore C, Galimberti CA, et al. Determinants of health-related quality of life in pharmacoresistant epilepsy: results from a large multicenter study of consecutively enrolled patients using validated quantitative assessments. *Epilepsia.* (2011) 52:2181–91. doi: 10.1111/j.1528-1167.2011.03325.x
2. Ward MJ, Shutter LA, Branas CC, Adeoye O, Albright KC, Carr BG. Geographic access to US neurocritical care units registered with the neurocritical care society. *Neurocrit Care.* (2012) 16:232–40. doi: 10.1007/s12028-011-9644-2
3. Agrawal S, Turco L, Goswami S, Faulkner M, Singh S. Yield of monitoring in an adult epilepsy monitoring unit. *Neurology*. (2015) 84(14 Suppl):P2.097. Available online at: https://n.neurology.org/content/84/14_Supplement/P2.097
4. Fahoum F, Omer N, Kipervasser S, Bar-Adon T, Neufeld M. Safety in the epilepsy monitoring unit: a retrospective study of 524 consecutive admissions. *Epilepsy Behav.* (2016) 61:162–7. doi: 10.1016/j.yebeh.2016.06.002
5. Friedman DE, Hirsch LJ. How long does it take to make an accurate diagnosis in an epilepsy monitoring unit? *J Clin Neurophysiol.* (2009) 26:213–7. doi: 10.1097/WNP.0b013e3181b2f2da
6. Casson AJ, Yates DC, Smith SJ, Duncan JS, Rodriguez-Villegas E. Wearable electroencephalography. *IEEE Eng Med Biol Magaz.* (2010) 29:44–56. doi: 10.1109/MEMB.2010.936545
7. Bruno E, Simblett S, Lang A, Biondi A, Odoi C, Schulze-Bonhage A, et al. Wearable technology in epilepsy: the views of patients, caregivers, and healthcare professionals. *Epilepsy Behav.* (2018) 85:141–9. doi: 10.1016/j.yebeh.2018.05.044
8. Patel AD, Moss R, Rust SW, Patterson J, Strouse R, Gedela S, et al. Patient-centered design criteria for wearable seizure detection devices. *Epilepsy Behav.* (2016) 64:116–21. doi: 10.1016/j.yebeh.2016.09.012
9. *UNEEG SubQ*. (2021). Available online at: https://www.uneeg.com/en/products (accessed September 7, 2021).
10. EpiMinder. *Minder*. (2021). Available online at: https://epiminder.com/#system (accessed September 7, 2021).
11. Freeman WJ, Holmes MD, Burke BC, Vanhatalo S. Spatial spectra of scalp EEG and EMG from awake humans. *Clin Neurophysiol.* (2003) 114:1053–68. doi: 10.1016/S1388-2457(03)00045-2
12. Jasper HH. The ten-twenty electrode system of the international federation. *Electroencephalogr Clin Neurophysiol.* (1958) 10:371–5.
13. Acharya UR, Sree SV, Swapna G, Martis RJ, Suri JS. Automated EEG analysis of epilepsy: a review. *Knowl Based Syst.* (2013) 45:147–65. doi: 10.1016/j.knosys.2013.02.014
14. Alotaiby TN, Alshebeili SA, Alshawi T, Ahmad I, Abd El-Samie FE. EEG seizure detection and prediction algorithms: a survey. *EURASIP J Adv Signal Process.* (2014) 2014:183. doi: 10.1186/1687-6180-2014-183
15. Baldassano SN, Brinkmann BH, Ung H, Blevins T, Conrad EC, Leyde K, et al. Crowdsourcing seizure detection: algorithm development and validation on human implanted device recordings. *Brain.* (2017) 140:1680–91. doi: 10.1093/brain/awx098
16. Tzallas AT, Tsipouras MG, Tsalikakis DG, Karvounis EC, Astrakas L, Konitsiotis S, et al. Automated epileptic seizure detection methods: a review study. In: Stevanovic D, editor. *Epilepsy-Histological, Electroencephalographic and Psychological Aspects.* London: IntechOpen (2012) 75–98.
17. Kelly KM, Shiau DS, Kern RT, Chien JH, Yang MCK, Yandora KA, et al. Assessment of a scalp EEG-based automated seizure detection system. *Clin Neurophysiol.* (2010) 121:1832–43. doi: 10.1016/j.clinph.2010.04.016
18. Koren J, Hafner S, Feigl M, Baumgartner C. Systematic analysis and comparison of commercial seizure-detection software. *Epilepsia.* (2021) 62:426–38. doi: 10.1111/epi.16812
19. Scheuer ML, Wilson SB. Data analysis for continuous EEG monitoring in the ICU: seeing the forest and the trees. *J Clin Neurophysiol.* (2004) 21:353–78.
20. Scheuer ML, Wilson SB, Antony A, Ghearing G, Urban A, Bagić AI. Seizure detection: interreader agreement and detection algorithm assessments using a large dataset. *J Clin Neurophysiol.* (2020) 38:439–47. doi: 10.1097/WNP.0000000000000709
21. Wilson SB, Scheuer ML, Emerson RG, Gabor AJ. Seizure detection: evaluation of the Reveal algorithm. *Clin Neurophysiol.* (2004) 115:2280–91. doi: 10.1016/j.clinph.2004.05.018
22. USFDA. *U.S. Food and Drug Administration, Center for Drug Evaluation and Research. Nihon Kohden QP-160AK EEG Trend Program K163644 approval letter, May 19, 2017*. (2017). Available online at: https://www.accessdata.fda.gov/cdrh_docs/pdf16/K163644.pdf (accessed September, 7, 2021).
23. USFDA. *U.S. Food and Drug Administration, Center for Drug Evaluation and Research. Encevis K171720 approval letter, April 1, 2018*. (2018). Available online at: https://www.accessdata.fda.gov/cdrh_docs/pdf17/K171720.pdf (accessed September 7, 2021).
24. Kiral-Kornek I, Roy S, Nurse E, Mashford B, Karoly P, Carroll T, et al. Epileptic seizure prediction using big data and deep learning: toward a mobile system. *EBioMed.* (2018) 27:103–11. doi: 10.1016/j.ebiom.2017.11.032
25. Wilson SB, Scheuer ML, Plummer C, Young B, Pacia S. Seizure detection: correlation of human experts. *Clin Neurophysiol.* (2003) 114:2156–64. doi: 10.1016/S1388-2457(03)00212-8
26. Tu B, Young GB, Kokoszka A, Rodriguez-Ruiz A, Varma J, Eerikäinen LM, et al. Diagnostic accuracy between readers for identifying electrographic seizures in critically ill adults. *Epilepsia Open.* (2017) 2:67–75. doi: 10.1002/epi4.12034
27. Fisher RS, Cross JH, French JA, Higurashi N, Hirsch E, Jansen FE, et al. Operational classification of seizure types by the International League Against Epilepsy: position paper of the ILAE Commission for Classification and Terminology. *Epilepsia.* (2017) 58:522–30. doi: 10.1111/epi.13670
28. Breznitz, S. Cry *Wolf: They Psychology of False Alarms*. Hillsdale, NJ: Lawrence Erlbaum Associates (1984).
29. Salinsky M, Spencer D, Boudreau E, Ferguson F. Psychogenic nonepileptic seizures in US veterans. *Neurology.* (2011) 77:945–50. doi: 10.1212/WNL.0b013e31822cfc46
30. Baud MO, Kleen JK, Mirro EA, Andrechak JC, King-Stephens D, Chang EF, et al. Multi-day rhythms modulate seizure risk in epilepsy. *Nat Commun.* (2018) 9:1–10. doi: 10.1038/s41467-017-02577-y
31. Karoly PJ, Goldenholz DM, Freestone DR, Moss RE, Grayden DB, Theodore WH, et al. Circadian and circaseptan rhythms in human epilepsy: a retrospective cohort study. *Lancet Neurol.* (2018) 17:977–85. doi: 10.1016/S1474-4422(18)30274-6
32. Keränen T, Sillanpää M, Riekkinen PJ. Distribution of seizure types in an epileptic population. *Epilepsia*. (1988) 29:1–7. doi: 10.1111/j.1528-1157.1988.tb05089.x
33. Seeck M, Koessler L, Bast T, Leijten F, Michel C, Baumgartner C, et al. The standardized EEG electrode array of the IFCN. *Clin Neurophysiol.* (2017) 128:2070–7. doi: 10.1016/j.clinph.2017.06.254
34. Sinha SR, Sullivan LR, Sabau D, Orta DSJ, Dombrowski KE, Halford JJ, et al. American clinical neurophysiology society guideline 1: minimum technical requirements for performing clinical electroencephalography. *Neurodiagn J.* (2016) 56:235–44. doi: 10.1080/21646821.2016.1245527

35. Frankel MA, Lehmkuhle MJ, Watson M, Fetrow K, Frey L, Drees C, et al. Electrographic seizure monitoring with a novel, wireless, single-channel EEG sensor. *Clin Neurophysiol Pract.* (2021) 6:172–8. doi: 10.1016/j.cnp.2021.04.003
36. Stevenson NJ, Clancy RR, Vanhatalo S, Rosén I, Rennie JM, Boylan GB. Interobserver agreement for neonatal seizure detection using multichannel EEG. *Ann Clin Transl Neurol.* (2015) 2:1002–11. doi: 10.1002/acn3.249

Conflict of Interest: MF and ML have financial interest in Epitel, Inc.

The remaining authors declare that the research was conducted in the absence of any commercial or financial relationships that could be construed as a potential conflict of interest.

Publisher's Note: All claims expressed in this article are solely those of the authors and do not necessarily represent those of their affiliated organizations, or those of the publisher, the editors and the reviewers. Any product that may be evaluated in this article, or claim that may be made by its manufacturer, is not guaranteed or endorsed by the publisher.

frontiers in Neurology

ORIGINAL RESEARCH
published: 03 November 2021
doi: 10.3389/fneur.2021.738111

Quantification of Epileptogenic Network From Stereo EEG Recordings Using Epileptogenicity Ranking Method

Harilal Parasuram[1,2,3]*, *Siby Gopinath*[1,2,3], *Ashok Pillai*[1,4], *Shyam Diwakar*[3] and *Anand Kumar*[2,3]

[1] Amrita Advanced Centre for Epilepsy (AACE), Amrita Institute of Medical Sciences, Amrita Vishwa Vidyapeetham, Kochi, India, [2] Department of Neurology, Amrita Institute of Medical Sciences, Amrita Vishwa Vidyapeetham, Kochi, India, [3] Amrita Mind Brain Center, Amrita Vishwa Vidyapeetham, Kollam, India, [4] Department of Neurosurgery, Amrita Institute of Medical Sciences, Amrita Vishwa Vidyapeetham, Kochi, India

Introduction: Precise localization of the epileptogenic zone is very essential for the success of epilepsy surgery. Epileptogenicity index (EI) computationally estimates epileptogenicity of brain structures based on the temporal domain parameters and magnitude of ictal discharges. This method works well in cases of mesial temporal lobe epilepsy but it showed reduced accuracy in neocortical epilepsy. To overcome this scenario, in this study, we propose Epileptogenicity Rank (ER), a modified method of EI for quantifying epileptogenicity, that is based on spatio-temporal properties of Stereo EEG (SEEG).

Methods: Energy ratio during ictal discharges, the time of involvement and Euclidean distance between brain structures were used to compute the ER. Retrospectively, we localized the EZ for 33 patients (9 for mesial-temporal lobe epilepsy and 24 for neocortical epilepsy) using post op MRI and Engel 1 surgical outcome at a mean of 40.9 months and then optimized the ER in this group.

Results: Epileptic network estimation based on ER successfully differentiated brain regions involved in the seizure onset from the propagation network. ER was calculated at multiple thresholds leading to an optimum value that differentiated the seizure onset from the propagation network. We observed that ER < 7.1 could localize the EZ in neocortical epilepsy with a sensitivity of 94.6% and specificity of 98.3% and ER < 7.3 in mesial temporal lobe epilepsy with a sensitivity of 95% and specificity of 98%. In non-seizure-free patients, the EZ localization based on ER pointed to brain area beyond the cortical resections.

Significance: Methods like ER can improve the accuracy of EZ localization for brain resection and increase the precision of minimally invasive surgery techniques (radio-frequency or laser ablation) by identifying the epileptic hubs where the lesion is extensive or in nonlesional cases. For inclusivity with other clinical applications, this ER method has to be studied in more patients.

Keywords: epileptogenicity, SEEG, epileptogenicity rank, intracranial EEG (iEEG), stereo EEG

OPEN ACCESS

Edited by:
Gregory Worrell,
Mayo Clinic, United States

Reviewed by:
Sandipan Pati,
University of Texas Health Science Center at Houston, United States
Yang Zheng,
Zhejiang University, China

***Correspondence:**
Harilal Parasuram
harilal.navami@gmail.com

Specialty section:
This article was submitted to Epilepsy, a section of the journal Frontiers in Neurology

Received: *08 July 2021*
Accepted: *31 August 2021*
Published: *03 November 2021*

Citation:
Parasuram H, Gopinath S, Pillai A, Diwakar S and Kumar A (2021) Quantification of Epileptogenic Network From Stereo EEG Recordings Using Epileptogenicity Ranking Method. Front. Neurol. 12:738111. doi: 10.3389/fneur.2021.738111

HIGHLIGHTS

- Epileptogenicity Rank (ER) is a modified method of Epileptogenicity Index (EI) for quantifying epileptogenicity of brain structures in epilepsy patients.
- The ER method employs temporal and spatial properties of intracranial Stereo EEG (SEEG) to localize the epileptogenic zone.
- In neocortical epilepsy, the ER method has higher EZ localization accuracy than the epileptogenicity index method.

INTRODUCTION

According to Lüders, the epileptogenic zone (EZ) is the minimum amount of brain area that requires to be resected to render the patient seizure-free (1). It is approximated by the various zones, with the irritative zone almost always significantly larger than the EZ (2). Precise localization of the EZ is always the major challenge in epilepsy surgery (3). The presurgical workup involves various evaluations including EEG, MRI, PET, SPECT, ESI and MEG that study the electrical, structural and functional abnormalities in the patient brain (4). The recommendation from presurgical evaluation brings a possible hypothesis about the seizure onset and propagation zone. To prove this hypothesis of epileptogenic zone, especially in non-lesional, multilesional or other difficult cases, intracranial stereo EEG (SEEG) electrodes are guided to the suspected brain areas to record the local brain activity during interictal to ictal transition (5–7). SEEGs are reviewed at various intervals, including interictal, preictal, and interictal to ictal transition states to localize the EZ. The visual analysis of SEEG during interictal to ictal transition mainly depends on the spatio-temporal domain-based localization of ictal onset. However, the visual analysis of SEEG in neocortical seizures is extremely difficult due to rapid propagation of ictal discharges facilitated by dense intralobar and interlobar connectivity (8).

The major challenge in localizing the EZ from SEEG recording is the precise detection of ictal onset patterns (frequency change) and spatio-temporal separation of seizure onset zone from the propagation. Seizure onset in SEEG recordings is characterized by any of the following patterns (1) low-voltage fast activity (LVFA), (2) preictal spiking with rhythmic spikes of low frequency followed by LVFA, (3) burst of polyspikes of high frequency and amplitude followed by LVFA, (4) slow wave or baseline shift followed by LVFA, (5) rhythmic spikes or spike-waves, at low frequency and with high amplitude, and (6) theta/alpha sharp activity with progressive increasing amplitude (9, 10). Among these patterns, SEEG signature of LVFA was found to be largely observed (9) and the other onset patterns like burst-suppression and delta brush patterns were very rare and frequency adjustments in detector was required to detect such seizure onset from SEEG (9–11). Seizure onset from SEEG can be detected when there was abrupt change in energy ratio (ratio of emergence of fast oscillation replacing the slow oscillations) of the signal. A cumulative sum algorithm' or 'CUSUM' can be used to detect seizure onset zone by performing a test on the mean of baseline energy calculated from about few minutes of SEEG prior to ictal onset provided EEG seizures are absent (11–13).

Computational tools including Epileptogenicity Index (EI) (11), Epileptogenicity map (14, 15), Labview tool (16), Connectivity Epileptogenicity Index (cEI) (17), and Graph theoretical and machine learning-based approaches (18, 19) were developed to localize the EZ. Among these methods, EI quantifies the epileptogenicity in patient brain using spectral (appearance of abrupt frequency change) and temporal (delay of involvement of brain structure in seizure with respect to seizure onset) properties of SEEG. EI indexes the brain circuit between values "1" (more epileptic) and "0" (less epileptic). The brain area with EI value above 0.3 is recommended as an epileptic brain circuit (20). Though the EI has been defined and invented for mapping fast activities from different sources of seizure onset, this method worked well in mesial temporal seizures where the signal propagation was slow whereas it showed low accuracy (for localizing EZ) in neocortical seizures where the seizure propagation was rapid.

Epilepsy is a network disease, identifying the potential network hubs that initiates epileptic activity is the primary aim of presurgical evaluation (20). Unlike mesial temporal epilepsy, in neocortical epilepsy, the seizures propagate rapidly to the adjacent and anatomically connected areas of the brain that may be facilitated by the cytoarchitecture and short intralobar, interlobar, and interhemispheric connections in the cortex (8). In the literature, EI has been applied in studies of frontal lobe epilepsies (21), focal epilepsy with involvement of ictal discharges in thalamus and basal ganglia (22), heterotopic cortex (23), insular epilepsies (24), and posterior cortex epilepsies (25) with varying thresholds (EI $>$ or $=$ 0.6 or 0.3) as estimated values for localizing the EZ. However, these studies were not suggesting a definite threshold (index) for precise localization of EZ, especially in neocortical epilepsy. This could be due to rapid propagation of ictal discharges in the anatomically connected cortical areas. In these cases, the temporal based epileptogenicity quantification alone may not be enough to localize the EZ. In this study, we postulate that adding spatial parameters along with the EI equation can help to overcome such scenarios.

In the current study, we utilized the time of involvement of brain structures and Euclidean distance between brain structures, along with the energy ratio to localize the epileptogenic zone. Also, we proposed a modified method of EI called Epileptogenicity Rank (ER) to quantify epileptogenicity, especially in neocortical epilepsy. Two important questions we attempted to address in this study were (1) how to quantify epileptogenicity in neocortical epilepsy and derive a parameter to differentiate seizure onset from seizure propagation network, and (2) To find the optimum ER threshold value that accurately localized the EZ in mesial temporal and neocortical epilepsy. This modified method was implemented in MATLAB.

METHODS

Patient Selection and Data Collection

In our study, SEEG recordings from 33 patients (including 23 males and 10 females with a mean age of 24.9 years) evaluated during 2015–2018 were included. Out of 33 patients, 27 of

them were seizure-free (Engel 1 a-d) and 6 were non-seizure-free. For ER threshold estimation, our inclusion criteria were (1) the patients who underwent intracranial EEG evaluation with depth electrodes (Stereo EEG), (2) availability of post-op MRI, and (3) seizure-free/free of disabling seizures (Engel 1 a-d) till the last follow-up (26). The average outcome follow-up was 40.9 months. 6 non-seizure-free patients were analyzed to study how ER localizes EZ in epilepsy surgery failure patients with Engel 2 or 3 outcome. The epilepsy surgery outcome was collected from medical records of the post-OP clinic. The pre-surgical evaluation findings for all patients are given in **Supplementary Table 1**. The study was approved by the institutional review board.

SEEG electrodes were implanted in these patients using ROSA (Robotized Stereotactic Assistant) method (27). Patients were implanted with PMT (PMT Corp. USA) intracranial SEEG electrodes and the acquisition was done at 256 or 1,024 Hz using Nicolate/Natus 128 channel amplifier. After intracranial evaluation, patients underwent tailored resections of the identified epileptogenic zone. Within 12 months duration, a postoperative volumetric 3T MRI of the brain was acquired (using Siemens Magnetom Verio or GE Discovery MR 750 W) for each patient and these images were co-registered to volumetric CT images of the brain with intracranial electrodes to visualize the cortex recorded by the SEEG contacts and locate the electrode contacts within the resection cavity (28, 29). Image acquisition parameters were described in (30).

Localizing Electrode Location From Post Implantation CT Images

Advanced image processing techniques were required to localize SEEG electrodes from CT images, thanks to GARDEL, a computational tool for automatic segmentation and labeling of SEEG electrode contacts (29). In our study, we used GARDEL for (1) to coregister and localize SEEG electrodes in post-op MRI and (2) to export 3D coordinates of SEEG electrode contacts. Each electrode was manually assessed to identify SEEG contacts within the brain resection cavity (**Figure 1**).

Implementation of Epileptogenicity Rank

ER calculates epileptogenicity as a function of energy ratio, time of involvement of brain structures, and the Euclidean distance from the initial seizure onset. ER requires two parameters to localize the EZ: (1) SEEG and (2) the 3D coordinates of SEEG electrode contacts. The EZ localization was partially automated by converting the time-series data to the frequency spectrum and applied a threshold over the mean activity to detect the seizure onset. Page and Hinkely's algorithm was implemented for seizure onset detection (12, 13). The proposed new method was implemented in a graphical interface for easy usability and made available at https://github.com/Brain-Mapping/EPI-rank.

Calculation of Energy Spectral Density (es) and Energy Ratio (er) From the SEEG

Epileptogenic zone localization was implemented in three steps: (1) calculation of energy spectral density from SEEG, (2) the optimal detection of seizure onset, and (3) calculation of epileptogenicity rank (ER). *S(t)* was a mono channel SEEG recorded during a seizure which consisted of interictal, pre-ictal, ictal, and post-ictal states. The computation of spectral density *(E)* of *S(t)* was described in (11). SEEG analysis was performed on a bipolar derivative montage (subtraction of consecutive channels).

Calculation of Epileptogenicity Rank (ER)

ER was calculated as the normalized values of the product of spatio-temporal parameter and energy of the signal. The spatial parameter was added along with the existing temporal domain based index calculation (EI) to bring the new epileptogenicity rank (ER). We set the range of ER from 1 to 10, "ER = 1" being highly epileptogenic and normal brain region ranked as "ER = 10." ER of an SEEG was given by,

$$ER_i = \left[\frac{1}{(t_i - t_0) \ + \ \alpha}\left(\frac{E_\beta + E_\gamma}{E_\theta + E_\alpha}\right)\right] + \left[\frac{1}{d_i \ + \ \alpha}\left(\frac{E_\beta + E_\gamma}{E_\theta + E_\alpha}\right)\right] \quad (1)$$

$$d_i = \sqrt{(x - x_i)^2 + \left(y - y_i\right)^2 + (z - z_i)^2} \quad (2)$$

where S_i denotes the SEEG recorded from electrode contact *i* and 3D coordinate of *i* was given by x_i,y_i,z_i. t_i denotes the time at which the frequency change was detected for electrode contact *i*. "t_o" denotes the very first detection of frequency changes in "t_i." E_θ, E_α, E_β, and E_γ denotes frequency bands theta, alpha, beta, and gamma, respectively (31); d_i denotes the Euclidean distance between the electrode contact *'i'* (x_i,y_i,z_i) and the onset electrode contact (x,y,z); α denotes the constant value to avoid division by zero for the first frequency change detection.

Estimating Optimum Epileptogenicity Rank for Mesial-Temporal and Neocortical Epilepsy

To estimate optimum ER, for each patient, we identified the SEEG electrode contacts within the brain resection cavity from their post-op MRIs (**Figure 1**). For each seizure, the maximum value of ER to localize the EZ (ER_{max}) was estimated by increasing the value of ER from ER = 1 to "n;" the value of "n" was considered as maximum (ER_{max}) when further increasing of ER resulted in localization of EZ outside the resection cavity. The optimum value for the ER was estimated in this study by including the data only from seizure-free patients. The variability in ER_{max} was calculated as mean ± standard deviation with a 95% confidence interval, and the optimum threshold for ER was estimated separately for mesial temporal and neocortical epilepsy by computing the ROC. For each patient, all stereotyped electro clinical seizures were included in the analysis. Patients with slow onset patterns were excluded from the analysis (P 4, 7, and 25 in **Supplementary Table 1**).

The surgical resection cavity in Engel I patients does include the epileptogenic zone, but also other brain tissue that needed to be resected to path the way to the "true" epileptogenic zone. This

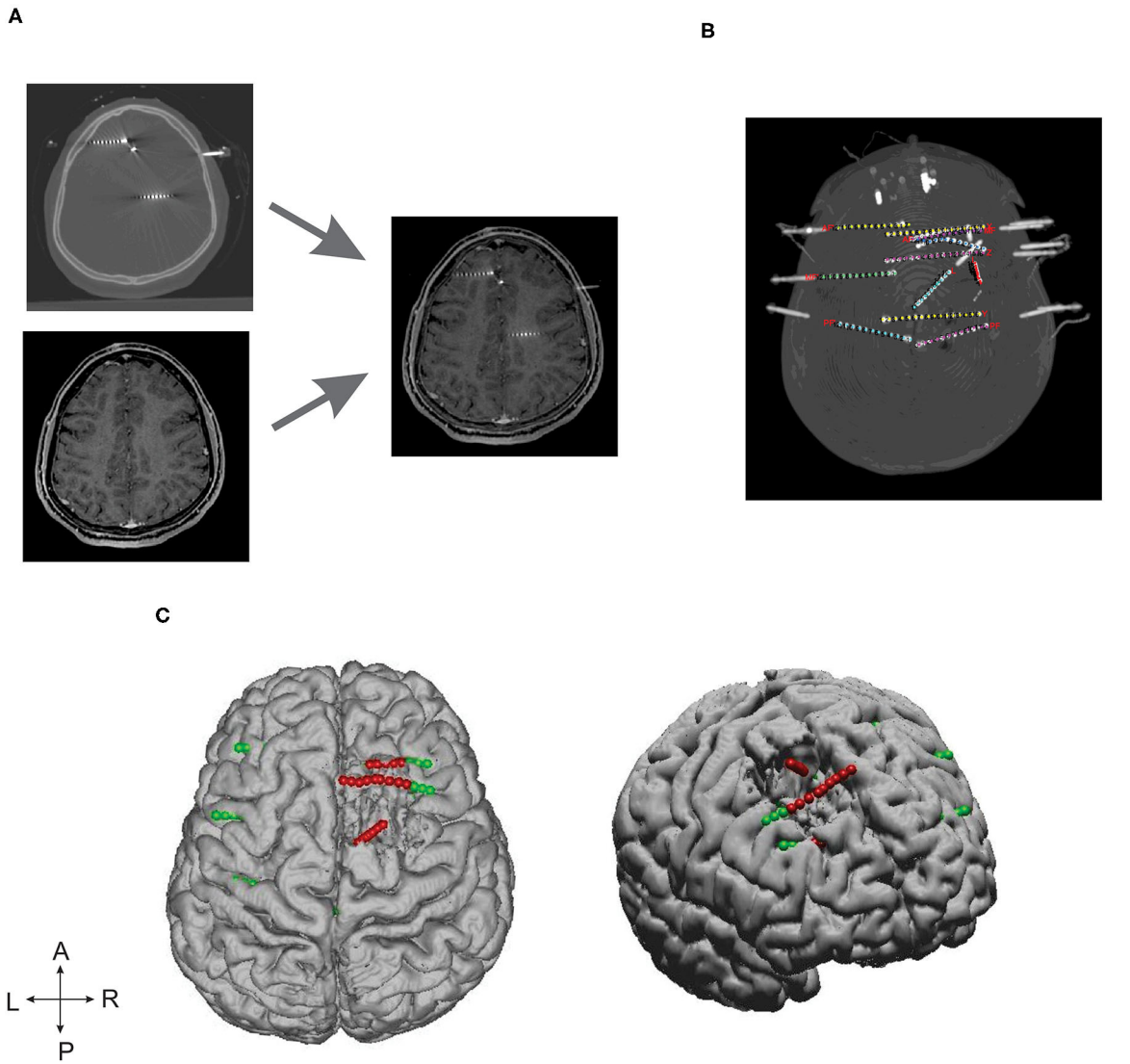

FIGURE 1 | SEEG electrode implantation and post-processing of images. **(A)** Depicts the post-SEEG electrode implantation CT coregistered on post resection MRI. **(B)** Segmented and labeled SEEG electrodes. **(C)** Coregistered SEEG electrode contacts and the brain resection cavity. Axial (left) and lateral (right) patient brain model reconstructed from post-op MRI. Green dots represent the implanted SEEG electrodes, and red dots represent the electrode contacts identified within the resection cavity.

scenario is more obvious in mesial temporal lobe epilepsy where the standard epilepsy surgery (ATLAH: Anterior Temporal Lobectomy + Amygdalo-Hippocampectomy) was offered. In order to accommodate this exception, in our analysis, the seizure onset zone identified by epileptologist was considered as the gold standard for all patients with mesial temporal lobe epilepsy.

Statistical Analysis

To estimate a threshold for EZ localization using ER, a receiver operating characteristic (ROC) curve was computed. ROC was plotted by estimating the sensitivity and specificity at different threshold ranges from ER = 1 to 10. McNemar's chi-square test was performed to assess the difference in EZ localization by EI and ER methods (32). The SEEG contacts were assigned to binary values (EZ localizations = 1 and others = 0) to compute the chi-square. To assess the quality of the methods, the percentage agreement between the EZ localization and the SEEG contacts identified within the resection cavity was also calculated. The percentage agreement was calculated as (no. of correct localization) / (no. of correct localization + no. of incorrect localization).

RESULTS

Of 27 patients included in our study, nine were diagnosed and treated for mesial temporal and 18 were diagnosed and treated for neocortical epilepsy and all were seizure-free till the last follow-up with a mean period of 40.9 months. An additional

six non-seizure-free patients were also analyzed to study how ER localizes EZ in epilepsy surgery failure patients. Presurgical findings and patient details for all 33 patients were given in **Supplementary Table 1**.

ER and EI Methods Localized the EZ Identically for Temporal Lobe Epilepsy and Differently in Neocortical Epilepsy Patients

In this study, we compared the EZ localization of ER and EI based methods in mesial temporal and neocortical epilepsy. The seizure onset and the propagation network were computed by setting the threshold, EI $>$ 0.3 and EI $>$ 0.6 for both the group of patients, and in ER based method, the computed optimum ER values were used, ER $<$ 7.1 for neocortical epilepsy and ER $<$ 7.3 for the temporal lobe epilepsy group (see section Spatiotemporal Quantification of Epileptogenicity Has Helped to Map the Spatial Extent of EZ in Mesial Temporal and Neocortical Epilepsy). We observed that ER and EI methods localized the EZ identically in mesial temporal epilepsy with the p-value $= 0.39$. In neocortical epilepsy patients, EZ detection by the two methods significantly differed with p-value $= 0.01$ using McNemar's chi-square test (see **Figures 2**–**4** and **Supplementary Tables 2, 3**).

In temporal lobe epilepsy, the percentage agreement between the EZ localized and SEEG contacts identified within the resection cavity was found to be 93.06% in ER method and the percentage agreement reduced to 65.60% in EI method. The percentage agreement in neocortical epilepsy was found to be 95.7% in ER, and the percentage agreement reduced to 51.3% in the EI method. From our analysis, we found that the ER (spatio-temporal) based localization could better differentiate seizure onset zone from propagation when compared to temporal domain based EI method (see **Figures 3**, **4** and **Supplementary Tables 2, 3**).

The Spatial Extent of Epileptogenic Network and Underlying Etiologies

The spatial extent of the epileptogenic network was studied in mesial temporal lobe and neocortical epilepsy patients. In the mesial temporal lobe epilepsy group, the ictal involvement was studied in mesial and lateral temporal structures and in neocortical epilepsy ictal involvement in EZ and non-EZ regions were considered. The mean and standard deviation of ER_{max} was estimated, in Hippocampus (5.61 $\pm$ 1.1), Amygdale (5.14 $\pm$ 0.62), Internal Temporal Pole (8.24 $\pm$ 0.06), external Temporal Pole (8.63$\pm$ 0.04), posterior part of the Middle Temporal Gyrus (8.42 $\pm$ 0.2), Superior Temporal Gyrus (8.69 $\pm$ 0.06), and Insular cortex (8.61 $\pm$ 0.14). The mesial structures showed a significantly reduced ER_{max} when compared to lateral structures, indicating a high epileptogenicity for the mesial structures. In neocortical epilepsy, the brain structures that come within EZ showed significantly decreased ER_{max} of 5.05 $\pm$ 2.33, again suggesting high epileptogenicity when compared to the non-EZ regions (8.09 $\pm$ 0.22) (see **Figures 5A,B**).

Localization utility of ER between different etiologies, including Hippocampal Sclerosis (HS) and Focal Cortical Dysplasia (FCD), was also analyzed. The optimal ER (ER_{max}) for HS was found to be 7.72 $\pm$ 0.33 and for FCD 7.41 $\pm$ 0.25. The mean ER_{max} for HS and FCD showed a difference of 0.31 in ER value (see **Figure 5C**). This difference may point to the underlying neuronal connectivity in different etiologies.

Spatiotemporal Quantification of Epileptogenicity Has Helped to Map the Spatial Extent of EZ in Mesial Temporal and Neocortical Epilepsy

ER and EI based method localized EZ in patients with mesial-temporal lobe and neocortical epilepsy. The optimum threshold for detecting EZ in EI based method was set to 0.3 for both groups of patients for localizing EZ. The optimum threshold for localizing EZ based on the newly proposed method (ER) was estimated in this study using ER_{max} of all seizure free-patients (see **Supplementary Tables 2, 3**). We observed that ER $<$ 7.1 was the optimum threshold to localize the EZ in neocortical epilepsy with a sensitivity of 94.6% and specificity of 98.3% and for mesial temporal lobe epilepsy the optimum ER threshold was estimated as ER $<$ 7.3 with a sensitivity of 95% and specificity of 98% (**Figure 6**). These thresholds for ER gave top-left corner curves for both the ROC with the AUC (test accuracy) value of 0.996 (see **Figure 6**).

ER Estimation in Non-Seizure-Free Patients Revealed the Spatial Organization of the Ictal Onset Zone Beyond Brain Resections

With the availability of post-OP MRI, six post-SEEG epilepsy surgery failure patients were analyzed to study the spatial extent of EZ in non-seizure-free patients. In five out of six non-seizure-free patients, the ER method localized the EZ not only within the resection area but also to the areas adjacent to the borders of the resection cavity (see **Figure 7** and **Supplementary Table 4**). The percentage agreement between localized EZ and the SEEG contacts within the resection cavity was found to be significantly less in non-seizure-free patients when compared to seizure-free patients (95.7% in seizure-free and 51.99% in non-seizure-free). The comparison between EI and ER methods in non-seizure-free patients showed less percentage agreement in EI (27.67%) compared to ER method (51.99%). The detailed statistical analysis on this comparison was limited by the low number of non-seizure-free patients in our study.

DISCUSSION

The main objective of this study was to formulate a scale (ER) to quantify epileptogenicity of brain structures in mesial temporal and neocortical epilepsy. We found that quantification of epileptogenicity by spatio-temporal method was more useful to differentiate ictal onset zone from the propagation when compared to temporal domain based EI method.

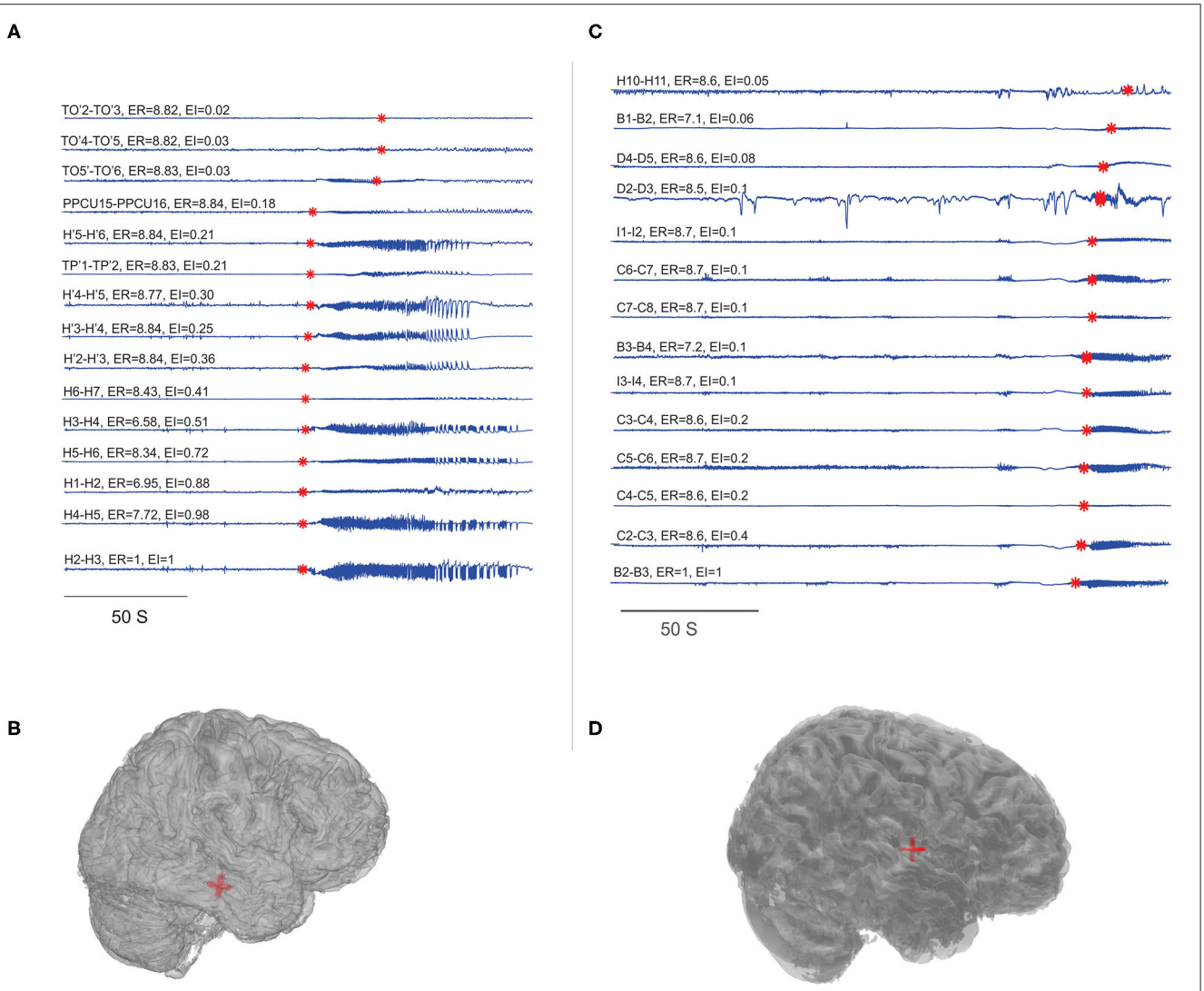

FIGURE 2 | Localization of EZ in mesial temporal and neocortical epilepsy. EI and ER estimated for the patients P23 and P8. **(A,C)** SEEG during preictal to ictal transition, the red mark on each signal indicates the SEEG onset detection by the algorithm and the calculated ER and EI values were mentioned above the respective channels. **(B,D)** Were the patient brain model and the red shaded area indicated the electrode contacts with ER < 7.3. From bottom to top (in **A**), very first ictal discharge was detected in H 1-4 right anterior Hippocampus then spread to left anterior Hippocampus H' 1-4 then to TP' 1-2left amygdala and then to TO'2-TO'6 left temporo-occipital regions. From bottom to top (in **C**), very first ictal discharge was detected in B 2-3 and C 2-3 mid insula then immediately spread to rest of the contacts implanted in the insula. See **Supplementary Table 5** for SEEG electrode names and abbreviations.

Spatio-Temporal Based EZ Localization Method Better Differentiated the Seizure Onset Zone From Propagation Than the Temporal Domain Based Method

To differentiate sequence of events based on the temporal properties of signal (SEEG) alone is significantly complicated during the ictal period. The rapid propagation of ictal discharges was particularly evident in neocortical epilepsy, mainly facilitated by the cytoarchitecture and short intralobar, interlobar, and interhemispheric connections in the cortex (8, 18, 33–35). These fiber connections can be estimated using the tractography based on diffusion tensor imaging (36, 37). On the other hand, in the absence of fiber tractography distances, Euclidian distance between brain structures can be used to estimate the magnitude of cortico-cortical evoked responses (37–40). In our study, we used Euclidian distance between brain areas, time of involvement, and energy ratio to compute the ER.

We found a high percentage agreement in localizing EZ when anatomical distance parameters were introduced, along with temporal parameters in the calculation of epileptogenicity. In the comparative analysis of EI and ER method, we also observed that the temporal domain based estimations and localization often showed reduced EZ percentage agreement of 51.3% in neocortical epilepsy due to the fast propagation

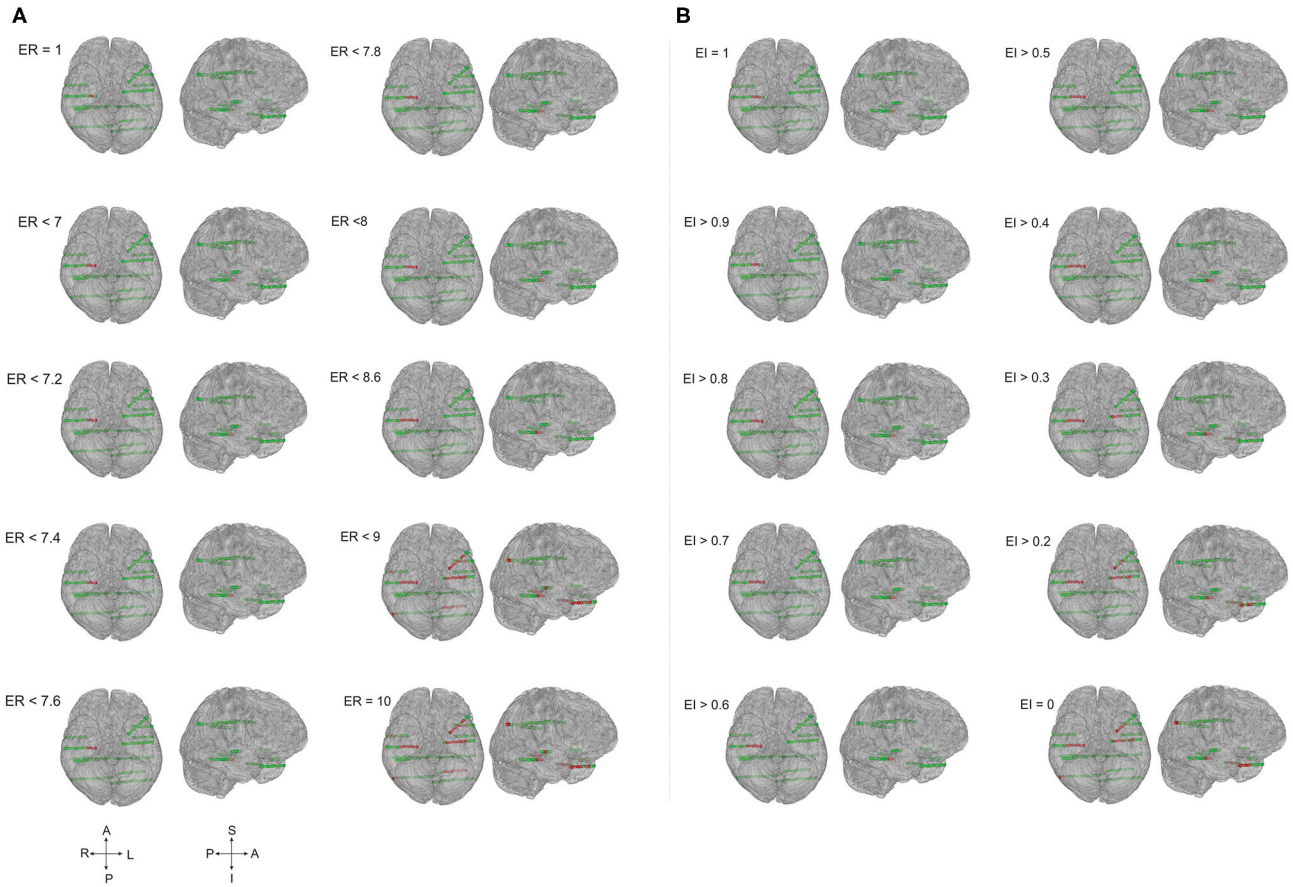

FIGURE 3 | The ER and EI methods localized the EZ identically in temporal lobe epilepsy. Schematic of the patient brain (P23 in **Supplementary Tables 1, 3**) and the SEEG electrode contacts with color indicates, green = normal and red = localized as epileptic. **(A)** EZ localized by computing epileptogenicity using ER method and **(B)**. Epileptogenicity calculated using EI method. ER and EI were calculated for multiple thresholds to analyze the seizure onset zone and propagation. Comparing the localization of EZ by ER and EI; the value of ER varied from 1 to 10 whereas the EI varied from 1 to 0. The ER and EI methods localized the EZ identically in **(A,B)** (temporal lobe epilepsy) with the p-value = 0.39 in McNemar's chi-square test.

of signals in the ictal period. We also found a moderately high percentage agreement between localized EZ and SEEG electrode contacts within the brain resection cavity in ER when compared to EI. These findings suggest that temporal domain based calculation (EI) of epileptogenicity alone may not differentiate ictal onset from the propagation network, especially in neocortical epilepsy. With the spatio-temporal estimation of epileptogenicity as key strengths, this newly proposed "ER" method was helpful to localize EZ in neocortical epilepsy.

Estimating epileptogenicity threshold for localizing EZ is essential for different types of epilepsy. The optimum ER threshold for localizing EZ in mesial temporal and neocortical epilepsy was estimated and found to be ER $<$ 7.1 for neocortical epilepsy and ER $<$ 7.3 for mesial temporal epilepsy. This difference in the optimum threshold for localizing EZ may directly connect to the underlying differences in neuronal circuit and connectivity property that facilitates the seizure initiation and propagation in mesial temporal and neocortical epilepsy (41). Further, theoretical modeling and simulation of various SEEG onset patterns on the biophysical model of neuronal micro-circuit and computation of epileptogenicity can help to better understand the spatial organization of EZ (42–45).

Studying the Spatial Organization of EZ in Different Etiologies

Drawing border for brain resection is still an open question in epilepsy surgery. The patients with large resections may have higher chance of more EZ area being resected. The standard for the spatial extent of EZ based on anatomical landmarks is also not always scientifically definable (18). The ER_{max} is different in different substrates/ brain regions as shown in our study, generalizing a threshold for localizing EZ and

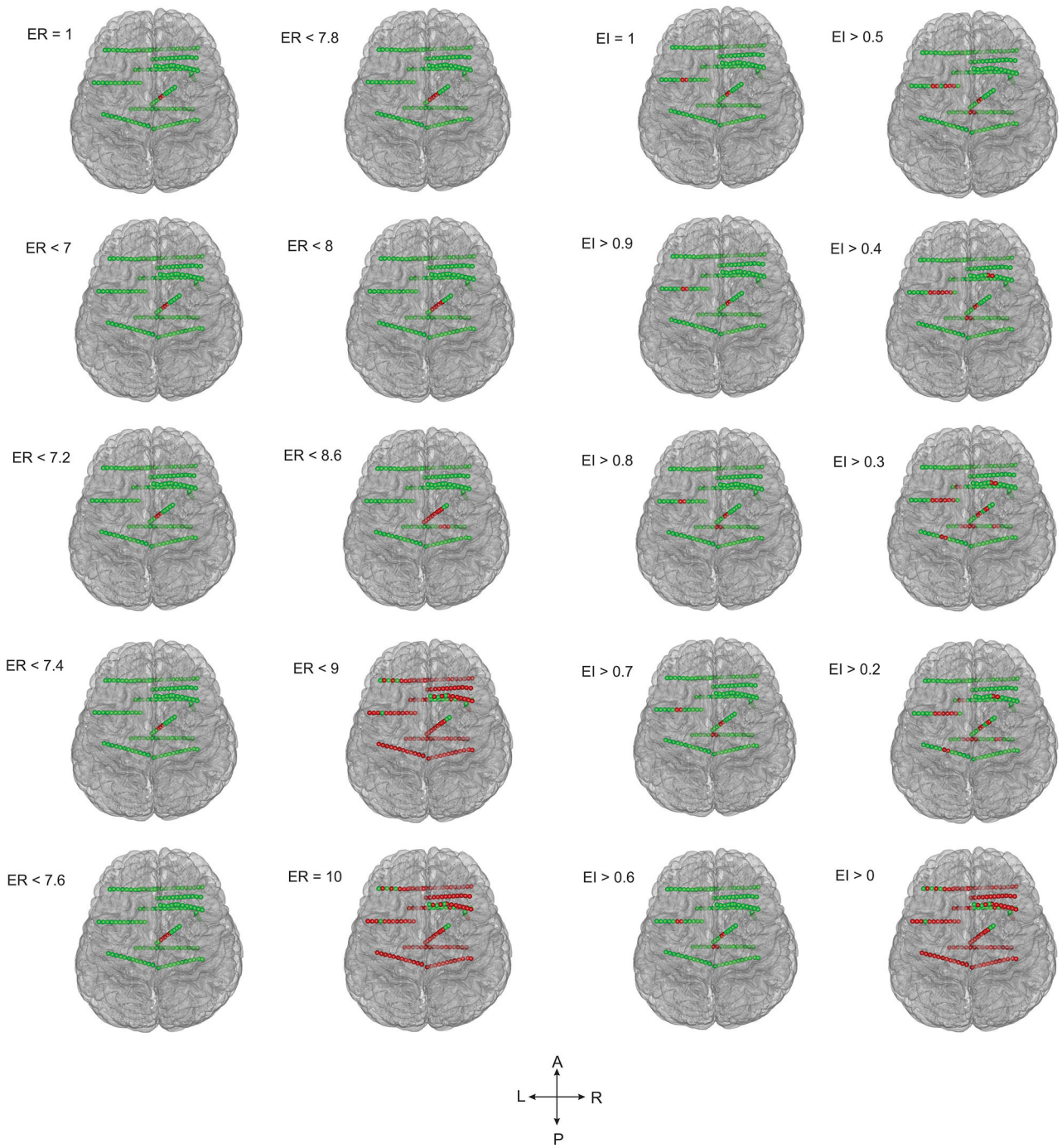

FIGURE 4 | EZ localization by ER and EI methods contrasted significantly in frontal lobe epilepsy. The patient brain model (P1 of **Supplementary Table 1**) and the SEEG electrode contacts were showed (green = normal; red = localized within EZ). Epileptogenicity calculated by ER **(A)** and EI **(B)** methods. ER and EI were calculated for various thresholds (ER varied from 1 to 10 whereas the EI varied from 1 to 0) to localize the seizure onset from the propagation network. The EZ localization using ER and EI differed significantly **(A,B)** in neocortical epilepsy with the p-value = 0.01 in McNemar's chi-square test.

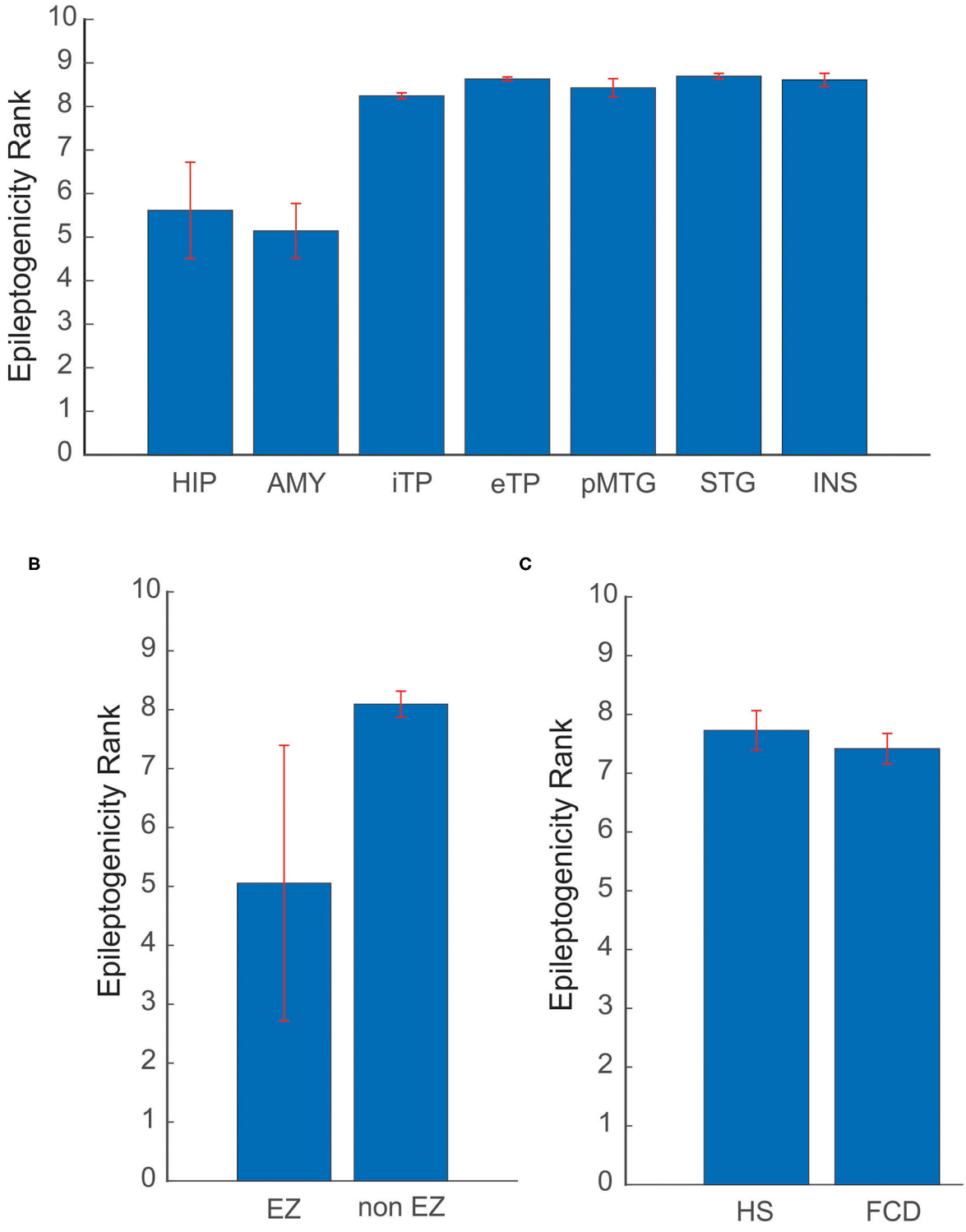

FIGURE 5 | Variability of ER in different etiologies and brain structures. **(A)** Comparison of mean ER max between mesial and lateral structures in mesial temporal lobe epilepsy. **(B)** In neocortical epilepsy, ER max was compared for brain structures that come within EZ and non-EZ regions. **(C)** Localization utility of ER between Hippocampal Sclerosis (HS) and Focal Cortical Dysplasia (FCD). In **(A)** HIP, Hippocampus; AMY, Amygdale; iTP, Internal Temporal Pole; eTP, external Temporal Pole; pMTG, posterior part of the Middle Temporal Gyrus; STG, Superior Temporal Gyrus; INS, Insular cortex. The mean and standard deviation of ER max represents the spatial network of EZ in patients analyzed in this study.

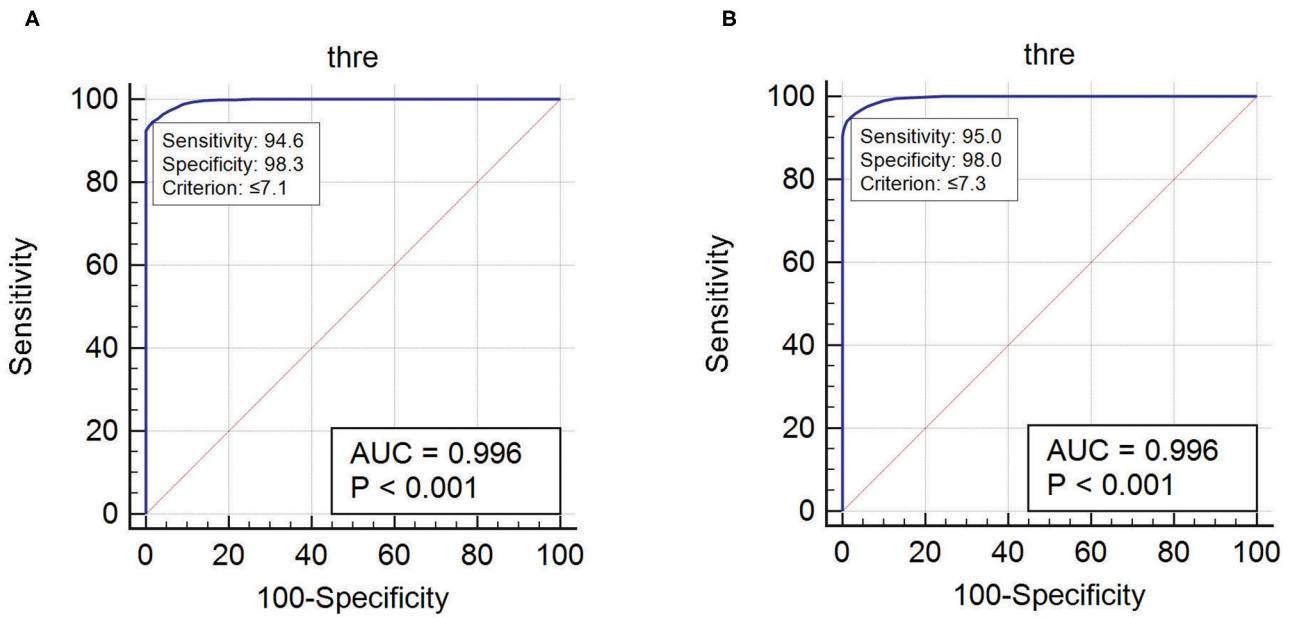

FIGURE 6 | The optimum threshold for localizing EZ in ER method was calculated using ROC curve. **(A)** Optimum ER calculated for neocortical epilepsy. **(B)** Optimum ER calculated for mesial temporal epilepsy.

defining the borders of resection is difficult (18). To better understand these issues, we studied variation in epileptogenicity for localizing EZ in different etiologies like HS and FCD. The variation in ER value in these two groups of patients suggests that seizure initiation and propagation was considerably rapid in FCD (mainly neocortical epilepsy) with ER_{max}7.41 ± 0.25 than in HS (mesial temporal lobe epilepsy) with ER_{max} 7.72 ± 0.33. This difference points to the underlying variation in neuronal connectivity across various etiologies and variation in mechanism of generation and propagation of ictal discharges. Many other factors, including the age of epilepsy onset, can also influence the variation in the spatial extent of epileptic brain circuits (11).

EZ Localization in Non-Seizure-Free Patients Suggests That Spatial Organization of EZ Is Beyond Brain Resection

The post-SEEG epilepsy surgery outcome may be poor mainly because of three reasons: (1) the implantation hypothesis would have missed sampling the primary epileptic hub; (2) the resection of seizure onset zone in those patients was not adequate; and (3) generation of the secondary epileptogenic zone over time (46, 47). To understand some of these aspects, we studied EZ localization in a small population of non-seizure-free patients with the availability of post-OP MRI. The ER analysis of epilepsy surgery failure patients revealed interesting results on the spatial extent of the EZ. In five out of six post SEEG epilepsy surgery failure patients we analyzed, the EZ was localized to the brain structures not only within the resection zone but also to the resection borders. From our limited analysis, we suspect inadequate resection of the cortex to be one of the reasons for poor outcome. Further clinical validation and computational analysis is required on patients undergoing second SEEG evaluation after the first epilepsy surgery failure to prove these assumptions/hypotheses. Modeling and simulation of dynamics of seizure initiation and propagation in patient brain model can contribute to the current understanding of the spatial organization of EZ (48). The development of such detailed patient-specific epilepsy brain models should help better define brain resection border for epilepsy surgery.

Limitations of the Study

The main assumption of quantification of EZ using ER was that the implanted SEEG electrodes always sample the seizure onset zone. Therefore, the current computational methods can fail when the SEEG electrode misses sampling the seizure onset zone. Other limitations of the studies are listed: (1) the optimal detection of frequency change in the ER method still relies on thresholding the detection parameter and (2) the inability to include all ictal onset patterns (especially the slow onset patterns) in the default detection method. Hence, more efficient algorithms need to be developed for the optimal detection of all ictal onset patterns in these non-stationary signals. The limitation with slow SEEG onset was recently studied with the graph theory and incorporated into a quantity, connectivity Epileptogenicity Index

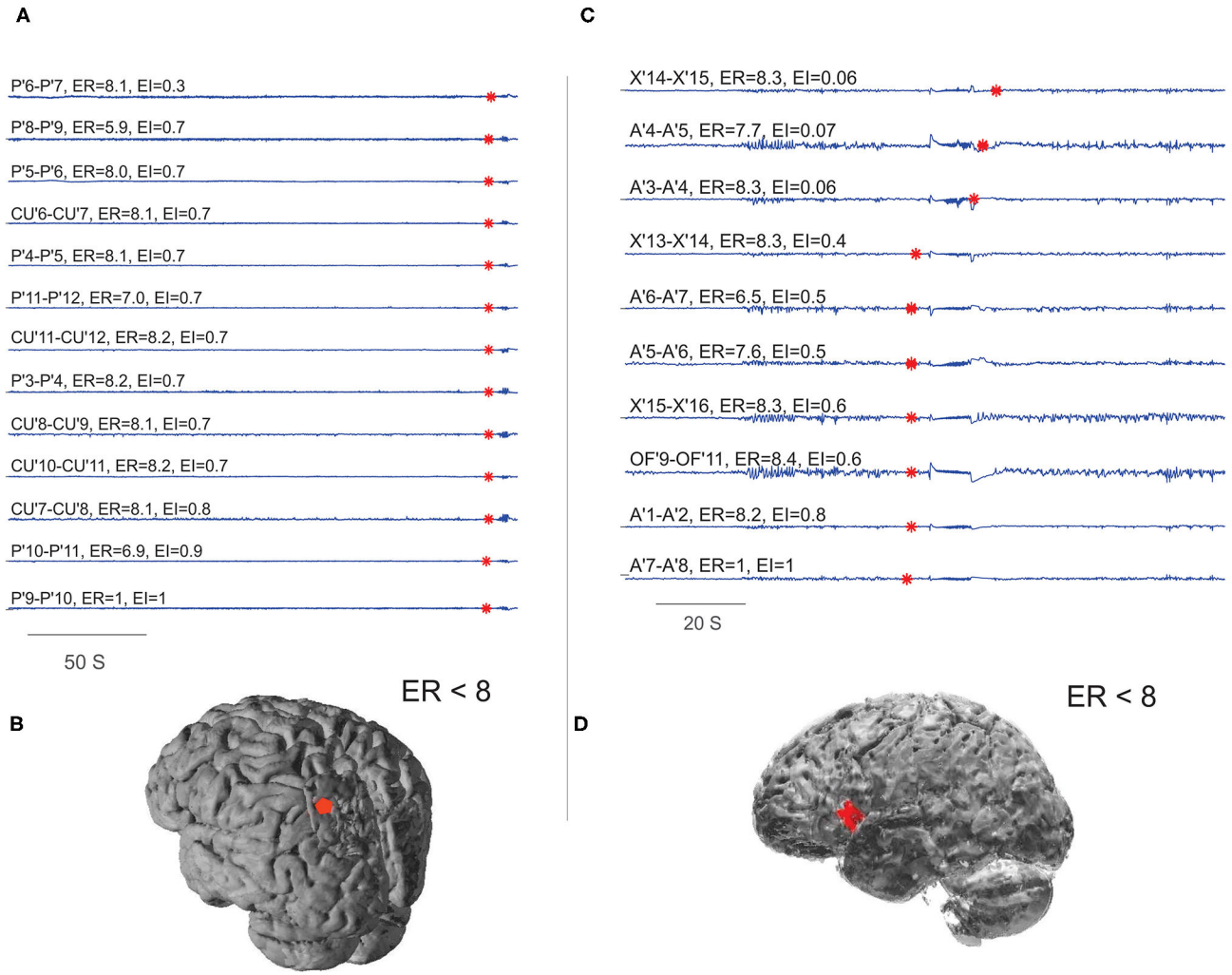

FIGURE 7 | Localizing EZ in non-seizure-free patients. **(A,B)** Were the EZ localized for patient P28 and **(C,D)** for P29 in **Supplementary Table 1**. **(A,C)** Were the SEEG traces plotted during preictal to ictal transition; the red mark on each signal showed the detected frequency change. The estimated ER and EI values corresponding to brain areas were given above the respective traces. **(B,D)** Were schematic of the patient brain, and the red shaded area indicates the SEEG contacts within ER < 8. From bottom to top **(A)**, very first ictal discharge was detected in P' 9–11 left parietal cortex then immediately spread to CU' 7–11 cuneus. From bottom to top **(C)**, very first ictal discharge was detected in A'7–8 frontal operculum then it spread to OF'9–11 orbito frontal and X' 13–16 prefrontal cortex. See **Supplementary Table 5** for SEEG electrode names and abbreviations.

(cEI) (17). The comparison of ER and cEI was not performed in this study, since the current study involves patients with faster SEEG onsets. (3) ER thresholds estimated in this study were optimized for the current dataset, an independent test need to be conducted with other datasets. Also, a study with a larger number of patients is very essential to generalize the current results. "Fingerprint of the epileptogenic zone" is another interesting article which studied the fast gamma activity of SEEG contacts within the resection cavity for localization of EZ (18). They used machine learning algorithms to train the features extracted from the SEEG. Direct comparison between EZ fingerprint and ER may not be possible since we did not use advanced feature extraction and machine learning algorithms for the localization of EZ.

The spatial extent of brain resection for epilepsy surgery is still an open question. However, in clinical practice, the spatial extent of the brain resection is decided by integrating multiple modalities of presurgical evaluation. Computational localization of seizure onset will always complement visual analysis. The computational EZ localization has to be analyzed alongside with the semiology and the visual analysis of SEEG by expert epileptologist before finalizing the seizure onset zone for clinical applications.

ER and Epileptic Hubs—A Future Study

Epilepsy is a network disease, identifying the potential network hub that initiates epileptic activity is the primary aim of presurgical evaluation. Our current study suggested that the

spatio-temporal quantification of epileptogenicity can localize EZ from the local neuronal circuit activity recorded by the SEEG. Inclusion of these brain areas (EZ) involving primary epileptic hubs/ictal onset zone in the resection zone is the cornerstone for seizure freedom. Identification of primary epileptic hub in multilesional and non-lesional epilepsy cases can definitely improve the epilepsy surgery outcome. Targeting of epileptic hubs in these patients will open up an opportunity to use minimally invasive surgery like radiofrequency or laser ablation. Another important aspect of this study is on the generalizability of the findings of this new method. How does this threshold localize EZ in non-lesional vs large lesional patients? The research also needs to be extended to study the utility of ER with different underlying etiologies in larger number of patients.

CONCLUSION

Quantifying epileptogenicity rank can help in localizing epileptic brain circuits for patient-specific surgical planning. Analyzing frequency components in SEEG with spatiotemporal information of rapid discharges between two brain structures was found to be a useful method to differentiate seizure onset from the propagation network. An important key to success for resective or minimally invasive epilepsy surgery depends on an optimal identification of the seizure onset zone and its propagation. We believe computational tools like ER can help to map EZ to a great extent and promise better seizure freedom. A detailed prospective study of ER based EZ localization on multilesional and non-lesional cases has to be conducted with a larger number of patients.

DATA AVAILABILITY STATEMENT

The original contributions generated for the study are included in the article/**Supplementary Material**, further inquiries can be directed to the corresponding author/s.

ETHICS STATEMENT

This retrospective study involving human participants was reviewed and approved by Institutional review board, Amrita Institute of Medical Sciences, Kochi (IRB-AIMS-2020-195).

AUTHOR CONTRIBUTIONS

HP implemented the method and performed all the analysis in this manuscript. HP, SG, AP, and AK contributed to the design of the work, patient selection, and developing the manuscript. HP, SG, AP, SD, and AK contributed to the interpretation of the analysis. All authors contributed to the article and approved the submitted version.

FUNDING

This study was supported by post-doctoral fellowship to HP from Amrita Institute of Medical Sciences, Kochi.

ACKNOWLEDGMENTS

We thank Drs. Sumana Pallegar, Amit Agarwal, Muthukani, Harish Jayakumar, Pushkaran Jayapaul, Rajesh Kannan, Sandya, Shameer Aslam, and EMU technologists for their input in the pre-surgical assessment of patients and help in data collection, and Anjaly Nair for help in statistics interpretation. We also thank Profs. Fabrice Bartolomei and Christian-G. Bénar for their help in understanding the EI analysis.

SUPPLEMENTARY MATERIAL

The Supplementary Material for this article can be found online at: https://www.frontiersin.org/articles/10.3389/fneur.2021.738111/full#supplementary-material

REFERENCES

1. Rosenow F, Lüders H. Presurgical evaluation of epilepsy. *Brain.* (2001) 124:1683–700. doi: 10.1093/brain/124.9.1683
2. Bartolomei F, Trébuchon A, Bonini F, Lambert I, Gavaret M, Woodman M, et al. What is the concordance between the seizure onset zone and the irritative zone? A SEEG quantified study. *Clin Neurophysiol.* (2016) 127:1157–62. doi: 10.1016/j.clinph.2015.10.029
3. Lüders HO, Engel J, Munari C. General principles. In: Engel Jr. J, editor. *Surgical Treatment of the Epilepsies*. 2nd ed. New York, NY: Raven Press (1993). p. 137–53.
4. Zijlmans M, Zweiphenning W, van Klink N. Changing concepts in presurgical assessment for epilepsy surgery. *Nat Rev Neurol.* (2019) 15:594–606. doi: 10.1038/s41582-019-0224-y
5. Bartolomei F, Nica A, Valenti-Hirsch MP, Adam C, Denuelle M. Interpretation of SEEG recordings. *Neurophysiol Clin.* (2018) 48:53–7. doi: 10.1016/j.neucli.2017.11.010
6. Chauvel P, Gonzalez-Martinez J, Bulacio J. Presurgical intracranial investigations in epilepsy surgery. In: *Handbook of Clinical Neurology*. Amsterdam: Elsevier B.V. (2019). p. 45–71. doi: 10.1016/B978-0-444-64142-7.00040-0
7. Jayakar P, Gotman J, Harvey AS, Palmini A, Tassi L, Schomer D, et al. Diagnostic utility of invasive EEG for epilepsy surgery: indications, modalities, and techniques. *Epilepsia.* (2016) 57:1735–47. doi: 10.1111/epi.13515
8. Catani M, Dell'acqua F, Vergani F, Malik F, Hodge H, Roy P, et al. Short frontal lobe connections of the human brain. *Cortex.* (2012) 48:273–91. doi: 10.1016/j.cortex.2011.12.001
9. Lagarde S, Bonini F, McGonigal A, Chauvel P, Gavaret M, Scavarda D, et al. Seizure-onset patterns in focal cortical dysplasia and neurodevelopmental tumors: relationship with surgical prognosis and neuropathologic subtypes. *Epilepsia.* (2016) 57:1426–35. doi: 10.1111/epi.13464
10. Perucca P, Dubeau F, Gotman J. Intracranial electroencephalographic seizure-onset patterns: effect of underlying pathology. *Brain.* (2014) 137:183–96. doi: 10.1093/brain/awt299
11. Bartolomei F, Chauvel P, Wendling F. Epileptogenicity of brain structures in human temporal lobe epilepsy: a quantified study from intracerebral EEG. *Brain.* (2008) 131:1818–30. doi: 10.1093/brain/awn111
12. Hinkley DV. Inference about the change-point from cumulative sum tests. *Biometrika.* (1971) 58:509. doi: 10.1093/biomet/58.3.509
13. Page ES. Continuous inspection schemes. *Biometrika.* (1954) 41:100–15. doi: 10.1093/biomet/41.1-2.100

14. Job A-S, David O, Minotti L, Bartolomei F, Chabardès S, Kahane P. Epileptogenicity maps of intracerebral fast activities (60–100 Hz) at seizure onset in epilepsy surgery candidates. *Front Neurol.* (2019) 10:1263. doi: 10.3389/fneur.2019.01263
15. David O, Blauwblomme T, Job A-S, Chabardès S, Hoffmann D, Minotti L, Kahane P. Imaging the seizure onset zone with stereo-electroencephalography. *Brain.* (2011) 134:2898-911. doi: 10.1093/brain/awr238
16. Gnatkovsky V, Francione S, Cardinale F, Mai R, Tassi L, Lo Russo G, et al. Identification of reproducible ictal patterns based on quantified frequency analysis of intracranial EEG signals. *Epilepsia.* (2011) 52:477–88. doi: 10.1111/j.1528-1167.2010.02931.x
17. Balatskaya A, Roehri N, Lagarde S, Pizzo F, Medina S, Wendling F, et al. The "Connectivity Epileptogenicity Index" (cEI), a method for mapping the different seizure onset patterns in StereoElectroEncephalography recorded seizures. *Clin Neurophysiol.* (2020) 131:1947–55. doi: 10.1016/j.clinph.2020.05.029
18. Grinenko O, Li J, Mosher JC, Wang IZ, Bulacio JC, Gonzalez-Martinez J, et al. A fingerprint of the epileptogenic zone in human epilepsies. *Brain.* (2018) 141:117–31. doi: 10.1093/brain/awx306
19. Wang M-y, Wang J, Zhou J, Guan Y-g, Zhai F, Liu C, et al. Identification of the epileptogenic zone of temporal lobe epilepsy from stereo-electroencephalography signals: a phase transfer entropy and graph theory approach. *NeuroImage Clin.* (2017) 16:184–95. doi: 10.1016/j.nicl.2017.07.022
20. Bartolomei F, Lagarde S, Wendling F, McGonigal A, Jirsa V, Guye M, et al. Defining epileptogenic networks: contribution of SEEG and signal analysis. *Epilepsia.* (2017) 58:1131–47. doi: 10.1111/epi.13791
21. Machado S, Bonini F, McGonigal A, Singh R, Carron R, Scavarda D, et al. Prefrontal seizure classification based on stereo-EEG quantification and automatic clustering. *Epilepsy Behav.* (2020) 112:107436. doi: 10.1016/j.yebeh.2020.107436
22. Pizzo F, Roehri N, Giusiano B, Lagarde S, Carron R, Scavarda D, et al. The ictal signature of thalamus and basal ganglia in focal epilepsy: a SEEG study. *Neurology.* (2021) 96:e280–93. doi: 10.1212/WNL.0000000000011003
23. Pizzo F, Roehri N, Catenoix H, Medina S, McGonigal A, Giusiano B, et al. Epileptogenic networks in nodular heterotopia: a stereoelectroencephalography study. *Epilepsia.* (2017) 58:2112–23. doi: 10.1111/epi.13919
24. Peltola ME, Trébuchon A, Lagarde S, Scavarda D, Carron R, Metsähonkala L, et al. Anatomoelectroclinical features of SEEG-confirmed pure insular-onset epilepsy. *Epilepsy Behav.* (2020) 105:106964. doi: 10.1016/j.yebeh.2020.106964
25. Bartolomei F, Gavaret M, Hewett R, Valton L, Aubert S, Régis J, et al. Neural networks underlying parietal lobe seizures: a quantified study from intracerebral recordings. *Epilepsy Res.* (2011) 93:164–76. doi: 10.1016/j.eplepsyres.2010.12.005
26. Engel J. *Surgical Treatment of the Epilepsies*. 2nd ed. New York, NY: Raven Press (1993).
27. Pillai A, Ratnathankom A, Ramachandran SN, Udayakumaran S, Subhash P, Krishnadas A. Expanding the spectrum of robotic assistance in cranial neurosurgery. *Oper Neurosurg.* (2019) 17:164–73. doi: 10.1093/ons/opy229
28. Friston KJ, Ashburner J, Kiebel S, Nichols T, Penny WD. *Statistical Parametric Mapping: The Analysis of Functional Brain Images*. Boston, MA; Amsterdam: Elsevier; Academic Press (2007).
29. Medina Villalon S, Paz R, Roehri N, Lagarde S, Pizzo F, Colombet B, et al. EpiTools, A software suite for presurgical brain mapping in epilepsy: Intracerebral EEG. *J Neurosci Methods.* (2018) 303:7–15. doi: 10.1016/j.jneumeth.2018.03.018
30. Cendes F, Theodore WH, Brinkmann BH, Sulc V, Cascino GD. Neuroimaging of epilepsy. In: Masdeu JC, González G, editors. *Handbook of Clinical Neurology*. Elsevier (2016). p. 985–1014. doi: 10.1016/B978-0-444-53486-6.00051-X
31. Niedermeyer E, Silva Lda. *Electroencephalography: Basic Principles, Clinical Applications, and Related Fields*. Philadelphia, PA: Lippincott Williams & Wilkins (2005).
32. McNemar Q. Note on the sampling error of the difference between correlated proportions or percentages. *Psychometrika.* (1947) 12:153–7. doi: 10.1007/BF02295996
33. Barba C, Barbati G, Minotti L, Hoffmann D, Kahane P. Ictal clinical and scalp-EEG findings differentiating temporal lobe epilepsies from temporal "plus" epilepsies. *Brain.* (2007) 130:1957–67. doi: 10.1093/brain/awm108
34. Besson P, Bandt SK, Proix T, Lagarde S, Jirsa VK, Ranjeva JP, et al. Anatomic consistencies across epilepsies: a stereotactic-EEG informed high-resolution structural connectivity study. *Brain.* (2017) 140:2639–52. doi: 10.1093/brain/awx181
35. Proix T, Bartolomei F, Guye M, Jirsa VK. Individual brain structure and modelling predict seizure propagation. *Brain.* (2017) 140:641–54. doi: 10.1093/brain/awx004
36. Basser PJ, Mattiello J, LeBihan D. MR diffusion tensor spectroscopy and imaging. *Biophys J.* (1994) 66:259–67. doi: 10.1016/S0006-3495(94)80775-1
37. Keller CJ, Honey CJ, Entz L, Bickel S, Groppe DM, Toth E, et al. Corticocortical evoked potentials reveal projectors and integrators in human brain networks. *J Neurosci.* (2014) 34:9152–63. doi: 10.1523/JNEUROSCI.4289-13.2014
38. Kellmeyer P, Vry M-S. Euclidean distance as a measure to distinguish ventral and dorsal white matter connectivity in the human brain. *bioRxiv.* (2019). doi: 10.1101/053959
39. Kunieda T, Yamao Y, Kikuchi T, Matsumoto R. New approach for exploring cerebral functional connectivity: review of cortico-cortical evoked potential. *Neurol Med Chir.* (2015) 55:374–82. doi: 10.2176/nmc.ra.2014-0388
40. Zhao C, Liang Y, Li C, Gao R, Wei J, Zuo R, et al. Localization of epileptogenic zone based on cortico-cortical evoked potential (CCEP): a feature extraction and graph theory approach. *Front Neuroinform.* (2019) 13:31. doi: 10.3389/fninf.2019.00031
41. Wendling F, Hernandez A, Bellanger JJ, Chauvel P, Bartolomei F. Interictal to ictal transition in human temporal lobe epilepsy: insights from a computational model of intracerebral EEG. *J Clin Neurophysiol.* (2005) 22:343–56. doi: 10.1016/B978-012373649-9.50026-0
42. Jirsa VK, Proix T, Perdikis D, Woodman MM, Wang H, Bernard C, et al. The virtual epileptic patient: individualized whole-brain models of epilepsy spread. *Neuroimage.* (2017) 145:377–88. doi: 10.1016/j.neuroimage.2016.04.049
43. Lindén H, Tetzlaff T, Potjans TC, Pettersen KH, Grün S, Diesmann M, et al. Modeling the spatial reach of the LFP. *Neuron.* (2011) 72:859–72. doi: 10.1016/j.neuron.2011.11.006
44. Parasuram H, Nair B, D'Angelo E, Hines M, Naldi G, Diwakar S. Computational modeling of single neuron extracellular electric potentials and network local field potentials using LFPsim. *Front Comput Neurosci.* (2016) 10:65. doi: 10.3389/fncom.2016.00065
45. Traub RD. Single-column thalamocortical network model exhibiting gamma oscillations, sleep spindles, and epileptogenic bursts. *J Neurophysiol.* (2004) 93:2194–232. doi: 10.1152/jn.00983.2004
46. Morrell F. Secondary epileptogenesis in man. *Arch Neurol.* (1985) 42:318–35. doi: 10.1001/archneur.1985.04060040028009
47. Morrell F. Varieties of human secondary epileptogenesis. *J Clin Neurophysiol.* (1989) 6:227–75. doi: 10.1097/00004691-198907000-00002
48. Olmi S, Petkoski S, Guye M, Bartolomei F, Jirsa V. Controlling seizure propagation in large-scale brain networks. *PLoS Comput Biol.* (2019) 15:1–23. doi: 10.1371/journal.pcbi.1006805

Conflict of Interest: The authors declare that the research was conducted in the absence of any commercial or financial relationships that could be construed as a potential conflict of interest.

Publisher's Note: All claims expressed in this article are solely those of the authors and do not necessarily represent those of their affiliated organizations, or those of the publisher, the editors and the reviewers. Any product that may be evaluated in this article, or claim that may be made by its manufacturer, is not guaranteed or endorsed by the publisher.

frontiers in Neurology

ORIGINAL RESEARCH
published: 11 November 2021
doi: 10.3389/fneur.2021.705119

Deep Learning of Simultaneous Intracranial and Scalp EEG for Prediction, Detection, and Lateralization of Mesial Temporal Lobe Seizures

*Zan Li[1], Madeline Fields[2], Fedor Panov[2], Saadi Ghatan[2], Bülent Yener[3] and Lara Marcuse[2]**

[1] Department of Electrical, Computer, and Systems Engineering (ECSE), Rensselaer Polytechnic Institute, Troy, NY, United States, [2] Department of Neurology, Icahn School of Medicine at Mount Sinai, New York, NY, United States, [3] Department of Computer Science (CS) and Electrical, Computer, and Systems Engineering (ECSE), Rensselaer Polytechnic Institute, Troy, NY, United States

In people with drug resistant epilepsy (DRE), seizures are unpredictable, often occurring with little or no warning. The unpredictability causes anxiety and much of the morbidity and mortality of seizures. In this work, 102 seizures of mesial temporal lobe onset were analyzed from 19 patients with DRE who had simultaneous intracranial EEG (iEEG) and scalp EEG as part of their surgical evaluation. The first aim of this paper was to develop machine learning models for seizure prediction and detection (i) using iEEG only, (ii) scalp EEG only and (iii) jointly analyzing both iEEG and scalp EEG. The second goal was to test if machine learning could detect a seizure on scalp EEG when that seizure was not detectable by the human eye (surface negative) but was seen in iEEG. The final question was to determine if the deep learning algorithm could correctly lateralize the seizure onset. The seizure detection and prediction problems were addressed jointly by training Deep Neural Networks (DNN) on 4 classes: non-seizure, pre-seizure, left mesial temporal onset seizure and right mesial temporal onset seizure. To address these aims, the classification accuracy was tested using two deep neural networks (DNN) against 3 different types of similarity graphs which used different time series of EEG data. The convolutional neural network (CNN) with the Waxman similarity graph yielded the highest accuracy across all EEG data (iEEG, scalp EEG and combined). Specifically, 1 second epochs of EEG were correctly assigned to their seizure, pre-seizure, or non-seizure category over 98% of the time. Importantly, the pre-seizure state was classified correctly in the vast majority of epochs (>97%). Detection from scalp EEG data alone of surface negative seizures and the seizures with the delayed scalp onset (the surface negative portion) was over 97%. In addition, the model accurately lateralized all of the seizures from scalp data, including the surface negative seizures. This work suggests that highly accurate seizure prediction and detection is feasible using either intracranial or scalp EEG data. Furthermore, surface negative seizures can be accurately predicted, detected and lateralized with machine learning even when they are not visible to the human eye.

Keywords: intracranial and scalp EEG, deep neural networks, LSTM (long short term memory networks), seizure lateralization, seizure prediction, convolutional neural networks, seizure detection

OPEN ACCESS

Edited by:
Sharon Chiang, University of California, San Francisco, United States

Reviewed by:
Afshin Shoeibi, Ferdowsi University of Mashhad, Iran
Jon Kleen, University of California, San Francisco, United States

***Correspondence:**
Lara Marcuse
lara.marcuse@mssm.edu

Specialty section:
This article was submitted to Epilepsy, a section of the journal Frontiers in Neurology

Received: *04 May 2021*
Accepted: *26 August 2021*
Published: *11 November 2021*

Citation:
Li Z, Fields M, Panov F, Ghatan S, Yener B and Marcuse L (2021) Deep Learning of Simultaneous Intracranial and Scalp EEG for Prediction, Detection, and Lateralization of Mesial Temporal Lobe Seizures. Front. Neurol. 12:705119. doi: 10.3389/fneur.2021.705119

INTRODUCTION

Epilepsy is characterized by recurrent and unpredictable seizures. This unpredictability is the core of suffering in the person with epilepsy. Certain actions, like taking medication and getting enough rest, decrease the risk of seizures. However, there is never a guarantee for a seizure free day. The field, and this collection of articles, is working to address this suffering by improving the accuracy of seizure prediction, detection and forecasting. Forecasting differs from prediction by identifying a period of time, lasting hours to days, during which the person is more likely to have seizures based upon their known prior patterns and rhythms (1). The focus of our work is not forecasting but in seizure prediction and detection. In seizure prediction, the goal is to provide a warning that a seizure is about to occur within minutes. For this warning to be useful, it must be accurate with a low false positive and a low false negative rate.

The field of seizure prediction was established in the 1980s, but after >20 years, a comprehensive review published in 2007 concluded that "the current literature allows no definite conclusion as to whether seizures are predictable by prospective algorithms" (2). Nevertheless, in the past decade, several innovations have driven the field forward including the compiling of extensive databases of long-term EEG recordings; the establishment of international seizure prediction competitions; and a prospective trial of a seizure forecasting device that provided convincing evidence that forecasting of seizures is possible (3).

Several reasons can be listed for this problem to evade success including: inadequate amount of data; complexity of data generated by EEG signals (noisy, non-linear, and non-stationary); and lack of labeled data for certain classes. This is partially due to the fact that EEG signal intensity is very small, in μV range, and there are significant sensing difficulties given physiological and non-physiological artifacts.

The nature of data collected by intracranial EEG (iEEG) and scalp EEG differs greatly. Scalp EEG is readily available and is not invasive. However, it is more prone to artifacts introduced by shifting electrodes, muscle interference, and the effects of volume conduction. Intracranial EEG has a better signal-to-noise ratio than scalp EEG and can target specific areas of the brain directly. Most previous work focuses on either scalp or iEEG recordings since data sets that contain simultaneous recordings of scalp and iEEG on the same patient are exceedingly rare. The novelty of the work in this paper rests on a simultaneous iEEG and scalp EEG data sets.

There are recent comprehensive survey papers on both seizure detection and prediction (4–8) While many of the studies for seizure detection are focused on training supervised learning algorithms on EEG signals (4–6, 9), there are also unsupervised algorithms based on multiway tensor analysis of scalp EEG signals (10) and tunable Q factor wavelet transformation (11) or non-negative matrix factorization of iEEG signals (12).

Seizure detection and prediction systems using intracranial or scalp EEG signals rely on moving window analysis on extracted features to generate predictions. One of the main challenges for accurate prediction is extracting and evaluating linear and non-linear univariate and bivariate features from the signal. However, to achieve high sensitivity and a low false prediction rate, many of the previous studies relied on handcraft feature extraction and/or tailored feature extraction, which is performed for each patient independently. This approach, however, is not generalizable, and requires significant modifications (13).

The length of the pre-ictal period during which it is possible to predict the seizure is called the prediction horizon or pre-seizure period. The electrical changes that occur in the brain prior to a seizure are poorly understood and undetectable by the human eye. In the literature, the length of the pre-seizure period has varied from minutes to hours (14), and has often been left as a design choice. Estimates as to the length of the pre-seizure period exist, but the estimates are not shown to be general (14, 15) or they are patient specific (16, 17).

In our prior work, the length of the pre-seizure period was determined as a part of the learning process and optimized using grid search (18) on scalp EEG data. The pre-seizure length was validated by analyzing the extracted features with different pre-ictal lengths to elucidate the phase transition between the interictal and pre-seizure state (18). The length of the horizon was determined from the EEG data to be optimal at 10 min.

From a machine learning perspective, we built on current models and added new methodology. Previously the maximal absolute cross correlation value was defined as a functional connectivity measure and further calculated for each pair of EEG channels to quantify the similarity between any two EEG signals (19). In this work, we used 3 methods to build similarity graphs [Correlation Coefficient, Mutual Information and Waxman model (20)] and used these as input into the deep neural networks (DNN). A similarity graph is denoted by $G = (V, E)$ where the vertex set V is the set of electrodes and the edge set E contains an edge (i, j) between the vertices i and j if they are "similar." Transforming raw EEG signal to a graph representation enables us to capture spatial information as well as frequency and time domain information.

In a seizure detection model (21) using DNNs, raw EEG signal was segmented into 5 second (s) epochs to discriminate the EEG seizure from the background. We expanded on that concept and examined several window sizes ranging from 1 to 6 s and evaluated the impact of this parameter on the accuracy of the results.

For this paper, 102 seizures of mesial temporal lobe onset were analyzed from 19 patients who had simultaneous stereo and scalp EEG as part of their evaluation for drug resistant epilepsy (DRE). The first aim of this paper was to develop machine learning models for seizure prediction and detection (i) using iEEG only, (ii) scalp EEG only and (iii) jointly analyzing both iEEG and scalp EEG. The data sets allowed for a direct comparison of classification accuracy. The second goal was to test if machine learning can detect a seizure on scalp EEG when that seizure was not detectable by the human eye (surface negative) but was seen in iEEG. The final question was to determine if the deep learning algorithm could correctly lateralize the seizure onset. We tested various combinations of machine learning algorithms to

determine the highest accuracy of classifying the EEG data into either non-seizure, pre-seizure or seizure (right vs. left).

MATERIALS AND METHODS

Data Sets

The study was approved by the Icahn School of Medicine Institutional Review Board. Simultaneous iEEG and scalp EEG were collected from patients using a Natus XLTEK 128 or Natus Quantum amplifier (Natus Medical Incorporated, Pleasanton, CA). Nineteen scalp electrodes were used in the standard 10-10 system. Placement of iEEG electrodes was performed by two neurosurgeons (FP, SG) using the robotic stereotactic assistance device ROSA software (Rosa; Medtech Montpellier, France).

Intracranial seizure onset and offset time were determined by the reading epileptologist and confirmed by independent review (LM, MF), who adjusted onset and offset times in rare cases. Scalp EEG onset times were reviewed separately from iEEG to avoid bias. A comparison of seizure detection on intracranial data and scalp data using this data sets was previously published (22).

One hundred and two seizures of mesial temporal lobe onset were analyzed from 19 patients who had simultaneous stereo and scalp EEG as part of their evaluation for their DRE. For all seizures, the integrity of scalp and intracranial electrodes was intact. Movement artifact was not excluded. For the 19 patients included, 7 had normal imaging and 12 had abnormal imaging. Of the 12 with abnormal imaging, only one had prior epilepsy surgery (R mesial temporal laser ablation). Nine of the patients had lesions in the mesial temporal area. Three had lesions that did not localize to the mesial temporal area (cingulate cavernoma, diffuse encephalomacia, and bilateral insular/lateral temporal polymicrogryia). The patient with the polymicrogyria had seizure onsets in the mesial temporal area and arising from the insula and lateral temporal lobe. Only the seizures of mesial temporal lobe onset were included.

All patients had 19 bilateral scalp electrode contacts for analysis, placed using the standard 10-10 system. Of these 102 seizures, 35 were not seen on the scalp EEG and were surface negative. These seizures were either focal aware or subclinical. Of the remaining 67 seizures, 7 had simultaneous scalp and iEEG onset and 60 had a delayed scalp onset. Eighty seizures were of right mesial temporal onset and 22 of the seizures were of left mesial temporal onset. Sixty-eight seizures were focal aware or subclinical, 18 seizures were focal impaired aware seizures, and 16 were focal to bilateral tonic clonic. As the SEEG arrays for each patient could differ in the density of coverage and number of electrodes, a subset of SEEG contacts common to all patients was used. These were selected by visual analysis of both the SEEG and the post-operative CT to ensure electrode integrity and proper anatomic placement. For each hemisphere 24 contacts were used with 4 contacts in each of the following areas: amygdala, lateral anterior temporal, hippocampus, lateral mid temporal, medial orbitofrontal and lateral frontal. Five patients had unilateral studies (24 SEEG contacts) and the remaining 14 patients had bilateral studies (48 SEEG contacts).

Data Processing

Our model was written in Python and run on a Macbook Pro using Spyder with Adam as the optimizer. Adam has a high performance for machine learning with high computational efficiency and little memory requirements. All EEG data was converted to EDF files without bandpass or notch filters.

Prior to running the DNN model, EEG signal segmentations were chosen from non-overlapping EEG data with the sampling rate of 512 Hz. Each similarity graph was calculated from 1 s of EEG data, i.e., the similarity between two EEG channels during 1 s was calculated from 512 data points. For DNN models with a 1 s time series, each sample is a single similarity graph that was calculated from 1 s of EEG. For DNN models using 2 or 6 s time series, each sample is 2 or 6 similarity graphs calculated from 2 or 6 consecutive time series.

Modeling Multichannel EEG by Similarity Graphs and DNN

The relevant parameters and the notation is summarized below:

A_{cc}	Correlation Coefficient similarity graph adjacency matrix
A_{MI}	Mutual Information similarity graph adjacency matrix
A_{waxman}	Waxman similarity graph adjacency matrix
y_{it}	t^{th} sample of the time series measured at channel i
μ_{it}	The mean values of y_{it}
σ_{it}	The standard deviation of y_{it}
$P_{(y_{it}, y_{jt})}$	The joint probability mass function of y_{it} and y_{jt}
$p_{y_{it}}$	The marginal probability mass function of y_{it}
n_{ij}	L_2 norm of y_{it} and y_{jt}.

Samples of non-seizure, pre-seizure and seizure data were randomly extracted from our EEG data sets. The ratio of these three classes were non seizure: pre-seizure: seizure – 4:3:2. The length of time was determined by the length of the seizure. For example, if a seizure was 60 s, then 120 s of non-seizure data and 90 s of pre-seizure data was used to train the model. Based on our prior work, the pre-seizure period was defined as the 10 min prior to seizure onset.

Multi-electrode time series data were quantized into 1 s windows. For each window, a graph where nodes represent the contacts, and pairwise edges indicate a measure of similarity between the contacts was constructed. In addition to using a single second of EEG data, the interaction between consecutive time series was analyzed for 2 and 6 s time series. In order to compare the effect of different similarity metrics, we proposed 3 graph construction models based on computing the pairwise similarity between two electrodes: Correlation Coefficient, Mutual Information and Waxman model. Each graph model was tested against different DNNs to determine the combination that yielded the highest accuracy for correctly classifying EEG data as either not-seizure, pre-seizure or seizure.

Similarity Metrics and Graph Models

Fourteen patients had bilateral SEEG with 48 contacts selected while the remaining 5 had unilateral SEEG with 24 SEEG

contacts. For the unilateral iEEG, the architecture was maintained with 48 contacts, 24 with recorded EEG data and 24 without data. The similarity value between the 24 non-recorded contacts was defined as 0. Similarly, the value between the recorded and the unrecorded contacts was set at 0. The dimensions of the input similarity graph adjacency matrix was *n x n*, where $n = 48$ for iEEG data; $n = 19$ for scalp EEG data and $n = 67$ for combined EEG data (**Figure 1**). The adjacency matrices were then vectorized as the inputs to the DNNs yielding to 2,304 (48×48) for iEEG, 361 (19×19) for scalp EEG, 4,489 (67×67) for joint scalp and iEEG.

Next we formally describe how to compute the similarity metrics. Consider N channels of recorded EEG signals, each channel associated with an observable time series$\{y_{it}\}_{t=1}^{T}$ measured over T time-slots, y_{it} denotes the t^{th} sample of the time series measured at channel *i*, i.e., the EEG recording of channel *i* at t^{th} second.

1) *Correlation Coefficient* based similarity graph $\{A_{CC}\}_{t=1}^{T}$,

the similarity coefficient between channel *i* and channel *j* can given by $\{c_{ij}\}_{t=1}^{T}, i = 1, 2, ..., N, j = 1, 2, ..., N$

$$c_{ijt} = \frac{E[(y_{it} - \mu_{it})(y_{jt} - \mu_{jt})]}{\sigma_{it}\sigma_{jt}} \tag{1}$$

where μ_{it} and μ_{jt} are the mean values of y_{it} and y_{jt}, respectively, σ_{it} and σ_{jt} are the standard deviation of y_{it} and y_{jt}.

2) *Mutual Information* based similarity graph $\{A_{MI}\}_{t=1}^{T}$,

the similarity coefficient between channel *j* and channel *j* can given by

$$\{m_{ij}\}_{t=1}^{T}, i = 1, 2, ..., N, j = 1, 2, ..., N$$

where $P_{(y_{it}, y_{jt})}$ is the joint probability mass function of y_{it} and y_{jt}, respectively, $P_{y_{it}}$ and $P_{y_{jt}}$ are the marginal probability mass functions of y_{it} and y_{jt}.

$$m_{ijt} = I\left(y_{it}; y_{jt}\right) = \sum_{i \in y_{it}} \sum_{j \in y_{jt}} p_{(y_{it}, y_{jt})}\,(i,j)\, log\left(\frac{p_{(y_{it}, y_{jt})}\,(i,j)}{p_{y_{it}}\,(i)\, p_{y_{jt}}\,(j)}\right) \tag{2}$$

3) In *Waxman model* based similarity graph $\{A_{waxman}\}_{t=1}^{T}$,

the similarity coefficient between channel *i* and channel *j* can be given by $\{w_{ij}\}_{t=1}^{T}, i = 1, 2, ..., N, j = 1, 2, ..., N$.

$$w_{ijt} = \beta * exp\left(-n_{ij}\,/\alpha \cdot max\,(n)\right) \tag{3}$$

where $\beta = 0.4$, $\alpha = 0.1$, and $n \in R^{N \times N}$ have $n_{ij} = ||\, y_{it} - y_{jt}\,||_2$, n_{ij} is the L_2 norm of y_{it} and y_{jt} .

Deep Neural Network Architectures for the Joint Problem of Seizure Detection and Prediction

The seizure detection and prediction problems were addressed jointly by training several different types of neural network architectures. One shallow and several deep neural network (DNN) architectures were used. A single layer neural network was constructed as a baseline comparison. For the DNNs, we focused on Convolutional Neural Networks (CNNs) and Long Short-Term Memory (LSTM) and reported the classification accuracy for the 3 class classification problems. **Figure 1** shows the overall DNN architecture used in this study with different layers and input dimensions depending on the data sets being analyzed (intracranial, scalp, or combined). We trained the CNNs by using the Adam optimizer with 0.0005 as the learning rate, and we trained the LSTM by using Adam optimizer with 0.001 as the learning rate.

The Four-Class Classifier System for Lateralizing Seizure Onset Using Scalp EEG

In order to analyze anatomic localization, the 3-class classifier system (non-seizure, pre-seizure, and seizure) was expanded to a 4-class classifier system with the seizure category subdivided into left and right mesial temporal onsets. Compared with the DNN architectures shown in **Figure 1**, we extended the dimension of the output layer to 4×1. For the 4-class classifier system, we trained the CNN (1 s time series) in conjunction with the Waxman graph by using the Adam optimizer with 0.0005 as the learning rate, then presented the classification accuracy using scalp EEG data. Seizures from both the bilateral SEEG and unilateral SEEG studies were included. For the unilateral SEEG, the ground truth onset lateralization was assumed to be the side with the electrodes implanted. In no cases did the scalp data or semiology suggest a different lateralization.

RESULTS

Seizure Detection and Prediction

The data was split into a training set and a testing set in multiple analyses. The training and test sets for each learning model were kept separate to prevent data snooping. Furthermore, we performed 5-fold cross validation to ensure there is no overfitting. Seizure onset time was defined as the time of the onset on iEEG data as the scalp onset was often delayed and in 35 seizures not present at all (surface negative seizures).

In the first analysis, all epochs from 16 patients were used as the training set and all epochs from the remaining 3 patients as the testing set. This process was repeated 5 times (5-fold cross validation) to ensure that the 3 patients in the testing set were different. **Table 1** reports the average accuracy on the testing sets for iEEG data alone, **Table 2** shows the results with the same approach on scalp EEG data alone, and **Table 3** reports the results on the joint iEEG and scalp EEG data sets. Within the training and test data sets epochs are treated as a *bag-of-epochs*.

Classification accuracy was repeated on iEEG data alone using a patient agnostic approach (**Table 4**). For this analysis, all epochs were separated into 5 groups with 4 of those groups used for training and the remaining epochs used for testing. This was performed a total of 5 times (5-fold cross validation) with epochs randomly assigned to one of the 5 groups. **Table 4** reports the

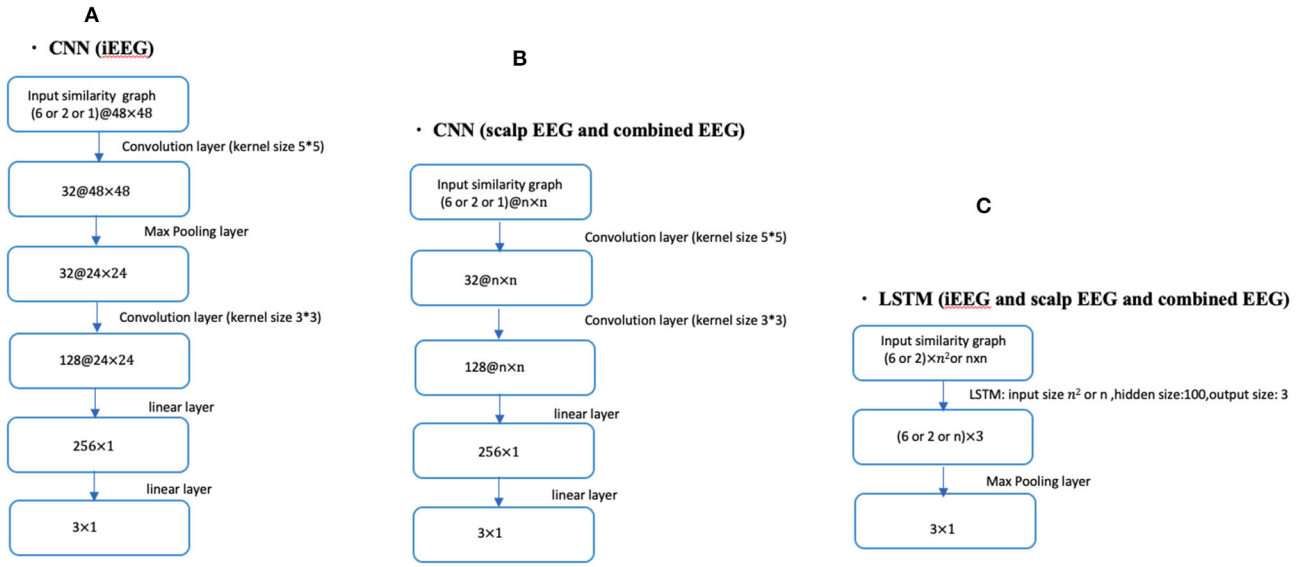

FIGURE 1 | CNN and LSTM architecture using different lengths of time series (1, 2, or 6 s) in conjunction with iEEG, scalp EEG or combined EEG similarity graphs. **(A)** Shows the CNN architecture for iEEG data only. **(B)** Depicts the CNN architecture for both scalp EEG data and the combined input of scalp and iEEG data. **(C)** Shows the LSTM architecture used for all three cases of the input (i.e., iEEG, scalp EEG, and combined EEG recordings). The dimension of input similarity graph adjacency matrix was *n x n*, where $n = 48$ for iEEG data; $n = 19$ for scalp EEG data and $n = 67$ for combined EEG studies. Inputs to DNNs are vectorization of these matrices.

TABLE 1 | Impact of different combinations of similarity graphs with a shallow NN or DNNs on the average accuracy of intracranial EEG classification with 5-fold cross validation using 16 patients in the training set, and 3 patients in the testing set with multiple random splits.

Intracranial EEG	Base line: Shallow NN (1 s time series)	CNN (6 s time series)	CNN (2 s time series)	CNN (1 s time series)	LSTM (6 s time series)	LSTM (2 s time series)	LSTM (1 s time series)
Correlation Coefficient graph	90.14%	97.10%	97.96%	99.14%	90.16%	94.40%	99.27%
Waxman graph	90.48%	97.93%	98.20%	99.38%	93.48%	96.48%	98.61%
Mutual Information graph	88.12%	95.08%	96.19%	97.13%	90.10%	93.30%	96.39%

TABLE 2 | Impact of different combinations of similarity graphs with a shallow NN or DNNs on the overall average accuracy of scalp EEG classification with 5-fold cross validation using 16 patients in the training set, and 3 patients in the testing set with multiple random splits.

Scalp EEG	Base line: Shallow NN (1 s time series)	CNN (6 s time series)	CNN (2 s time series)	CNN (1 s time series)	LSTM (6 s time series)	LSTM (2 s time series)	LSTM (1 s time series)
Correlation Coefficient graph	87.99%	95.66%	96.95%	97.76%	89.32%	93.65%	97.93%
Waxman graph	88.36%	97.08%	97.50%	98.56%	92.54%	95.28%	97.87%
Mutual Information graph	85.42%	90.01%	90.36%	92.14%	89.43%	90.22%	91.23%

TABLE 3 | Impact of different combinations of similarity graphs with a shallow NN or DNNs on the overall average accuracy of iEEG and scalp EEG classification with 5-fold cross validation using 16 patients in the training set, and 3 patients in the testing set with multiple random splits.

Intracranial and Scalp EEG	Base line: Shallow NN (1 s time series)	CNN (6 s time series)	CNN (2 s time series)	CNN (1 s time series)	LSTM (6 s time series)	LSTM (2 s time series)	LSTM (1 s time series)
Correlation Coefficient graph	88.43%	96.69%	98.16%	98.25%	89.96%	94.39%	98.42%
Waxman graph	88.66%	97.45%	98.11%	98.99%	93.15%	96.14%	98.65%
Mutual Information graph	87.95%	94.82%	96.30%	97.21%	90.70%	93.66%	96.10%

TABLE 4 | Impact of different combinations of similarity graphs with DNNs on the overall average accuracy of intracranial EEG classification with 5-fold cross validation based on patient agnostic epochs.

Intracranial EEG	CNN (6 s time series)	CNN (2 s time series)	CNN (1 s time series)	LSTM (6 s time series)	LSTM (2 s time series)	LSTM (1 s time series)
Correlation Coefficient graph	97.07%	98.01%	99.13%	90.10%	94.38%	99.32%
Waxman graph	97.97%	98.21%	99.38%	93.46%	96.51%	98.60%
Mutual Information graph	95.13%	96.27%	97.14%	90.06%	93.32%	96.44%

average accuracy on the testing set. This approach mixed the data from all the patients and treated the data as a *bag-of-epochs*.

The classification accuracy was nearly identical with this patient agnostic approach. The rest of the discussion focuses on the results presented with each patient's data being kept as a whole in either the testing or training set (**Tables 1–3**).

For all EEG data, results were poorest (as expected) when the single layer (shallow) neural network was used. When using the DNNs, for the iEEG data, the least accurate model was the LSTM (6 s time series) with the Mutual Information graph at 90.10% and the highest accuracy was 99.38% using CNN (1 s time series) in conjunction with the Waxman graphs. This latter combination was the most accurate for scalp (98.56%) as well as for the combined data sets (98.99%). While accuracy was high for all EEG subsets, the accuracy was highest for iEEG (99.38%) and lowest for scalp EEG (98.56%). All subsequent analysis is based on CNN (1 s time series) with the Waxman graphs.

A confusion matrix for iEEG, scalp EEG and all EEG (**Figure 2**) demonstrates how many time windows in each class can be correctly classified as well as the specific errors of misclassification. The confusion matrices are obtained by using CNN model with the Waxman graphs constructed in 1 s windows. For example, in **Figures 2A**, **4**, 023 s of IEEG seizure were inputted into the model and classified correctly as seizure for 3,991 s and misclassified as pre-seizure for 32 s.

The misclassification percent was 0.65% for iEEG, 1.40% for scalp, and for combined data it was 1.03%. The model showed a low false positive rate with high classification accuracy for non-seizure EEG (99.47% iEEG, 99.34% scalp, 99.42% all EEG). The pre-seizure EEG epochs were correctly classified 99.27% (iEEG), 97.95% (scalp EEG) and 98.2% (all EEG) of the time. For seizure, the data was classified correctly in 99.20% (iEEG), 98.07% (scalp EEG), 99.19% (all EEG). Interestingly, EEG epochs from seizures were rarely misclassified as pre-seizure but were **never** misclassified as non-seizure.

Seizure Detection From Scalp EEG

This analysis sought to ascertain if the model could detect the seizures or the portions of seizures that were not visible on scalp EEG. Of the 102 seizures analyzed 35 were surface negative (not seen on scalp EEG), 60 were seen on scalp EEG after a delay, and 7 had simultaneous iEEG and scalp onsets. For the surface negative seizures, the CNN model (1 s time series) in conjunction with the Waxman graph detected the seizure 98.47% of the time. For the 60 seizures with a delayed scalp onset, only the scalp EEG prior to a visible seizure was used in this analysis, essentially the surface negative portion of the seizure. The model classified these seizures correctly 97.83% of the time. The seizures with a simultaneous iEEG and scalp EEG onset were classified correctly classified 99.1% of the time. Any misclassifications labeled seizure data as pre-seizure, none as non-seizure, as shown in **Figure 3**.

Lateralization of Seizure Onset From Scalp EEG

For the 4-class classifier system (non-seizure, pre-seizure, left-seizure, right-seizure), the accuracy of the CNN (1 s time series) in conjunction with the Waxman graph was 98.11% with scalp EEG as the input. Seizure detection accuracy was high. For the seizures of left mesial temporal onset, surface negative seizures were classified correctly 95.00%, the surface negative portion of seizures with a delayed onset 96.38% and the simultaneous onset seizures 100%. For the seizures of right mesial temporal onset, surface negative seizures were classified correctly 95.25%, the surface negative portion of seizures with a delayed onset 92.31% and the simultaneous onset seizures 97.49% (**Figure 4**). Importantly, seizures of left brain onset were never misclassified as right brain onset and the reverse is true as well. This finding held firm when analyzing surface negative seizure and the surface negative portion of seizures with delayed scalp onset. All misclassifcation errors occurred with seizure data being mislabeled as pre-seizure data. Seizure data was never misclassified as non-seizure. For surface negative seizures (including the surface negative portion of the seizures with a delayed scalp onset), the model was able to both detect and to lateralize them with very high accuracy, as shown in **Figure 4**.

DISCUSSION

In this paper we re-explore seizure prediction and detection on a unique data sets of simultaneous iEEG and scalp EEG. As part of this work, various combinations of DNNs (both CNNs and LTSM) were tested with different similarity graph models (Correlation Coefficient, Mutual Information, and Waxman) to determine which combination had the highest classification accuracy. Interestingly, the models which used consecutive time series, 2 or 6 s, did not perform as well as the models that used a single second of EEG data for input. This is perhaps because for the longer time series there was some averaging of features which may have impacted accuracy. All models performed quite well, but the CNN (1 s time series) in conjunction with the Waxman

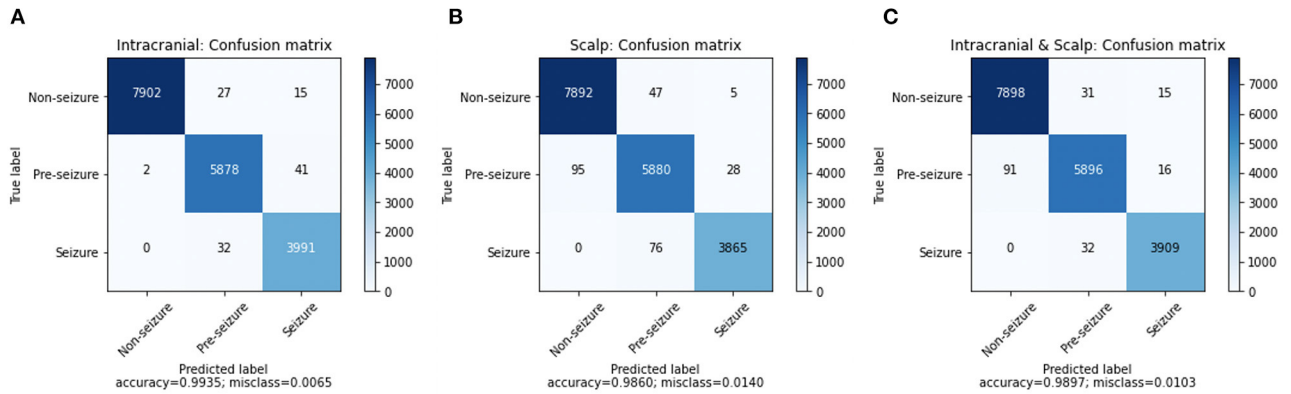

FIGURE 2 | The confusion matrix of CNN (1 s time series) with Waxman graph of **(A)** iEEG data, **(B)** scalp EEG and **(C)** scalp and iEEG data jointly.

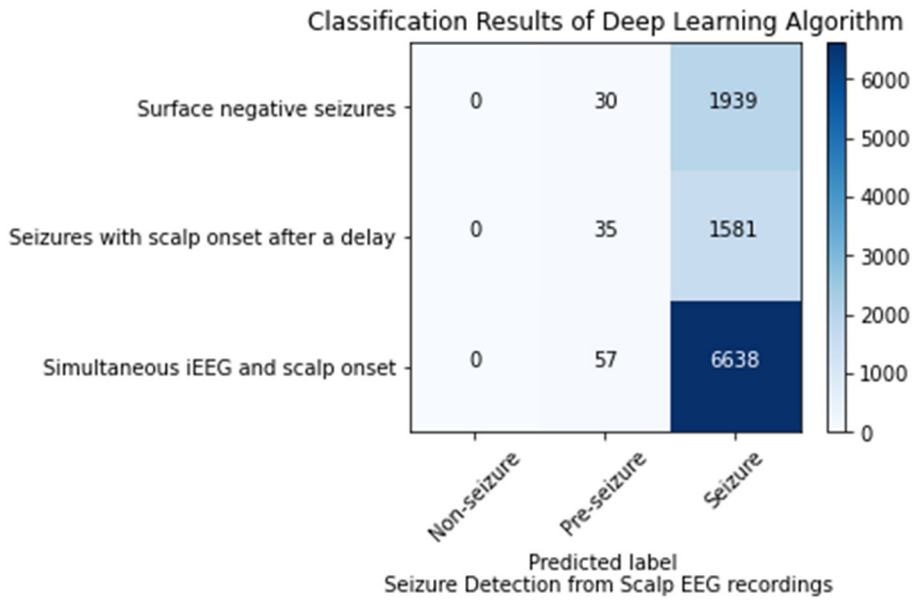

FIGURE 3 | Seizure detection on scalp EEG data for seizures that are surface negative, have an onset after the iEEG onset (only surface negative portion of seizure inputted), and have a simultaneous scalp and iEEG onset.

similarity graph performed the best. This combination became the primary machine learning model in this paper.

The accuracy for correctly classifying EEG data into non-seizure, pre-seizure and seizure was over 98% for iEEG alone, scalp alone and iEEG and scalp combined. This classification system can be used for both prediction and detection. In the field of seizure forecasting and prediction, false positives have the potential to create unnecessary anxiety and intervention. In this model, the false positive rate was very low, with <1% of the non-seizure epochs being classified as seizure or pre-seizure. Further, the results suggest that prediction is indeed possible, as over 97% of EEG epochs from the 10 minutes prior to a seizure were labeled as pre-seizure. This worked best on iEEG data alone (99.27%) and slightly less well on scalp EEG data (97.95%). Correct classification of EEG data into seizure was similarly highly accurate (>98%), demonstrating high efficacy in seizure detection.

It is important to remember that this 10 min pre-seizure period is not different from the non-seizure period to the human eye either intracranially or on scalp. Interestingly, seizure prediction accuracy was not very different than seizure detection accuracy; even though for the experienced epileptologist detecting a seizure is quite easy and predicting a seizure is impossible.

Surface negative seizures are seizures that do not appear electrographically on a scalp EEG but are visible intracranially. These can be clinical or subclinical. If clinical, they are usually

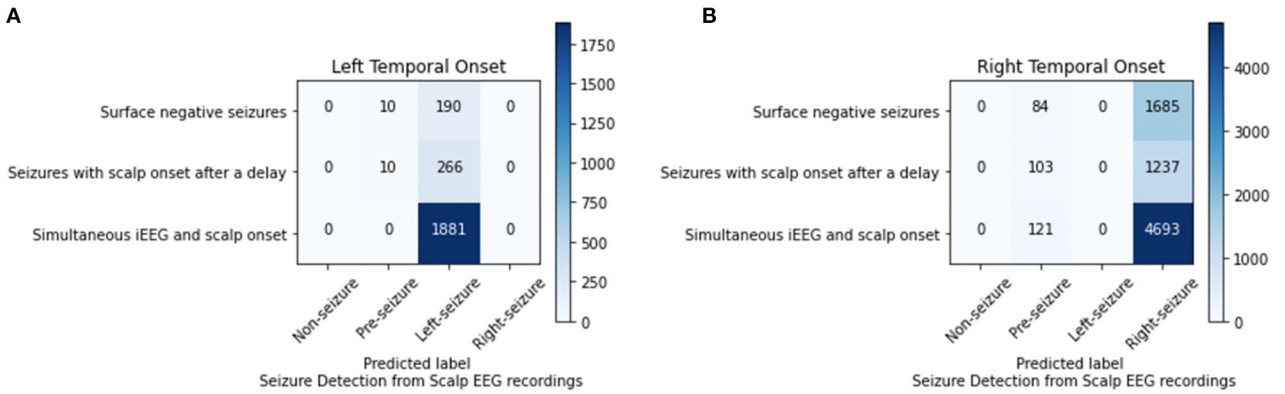

FIGURE 4 | Analysis of left **(A)** and right **(B)** mesial temporal onset seizures using scalp EEG data for seizures that are surface negative, have an onset after the iEEG onset (only surface negative portion of seizure inputted), and have a simultaneous scalp and iEEG onset.

focal aware seizures, like focal motor or a temporal lobe aura. In our previous work with simultaneous scalp and iEEG electrodes, 67% of focal aware and 67% of subclinical seizures had no visible scalp EEG seizure (22). This can occur when the seizure involves <6 cm^2 of cortex and/or when the source is deep. In this work, 35 of the seizures were surface negative and 60 of the seizures had a surface negative portion (intracranial onset occurred first followed by a delayed scalp EEG onset). *The model was able to classify these surface negative seizures accurately as seizures over 97% of the time using scalp EEG data alone.* This suggests that seizure detection is possible using scalp EEG alone, even when the seizure is not visible to the human eye.

Lastly, the model was able to *successfully lateralize scalp EEG data into left and right onset* (all were mesial temporal) with high accuracy, using a 4-class DNN classifier. This is perhaps not surprising for seizures that are visible on scalp. More interesting is that this accuracy held firm for the surface negative seizures and the surface negative portion of the seizures with a delayed scalp onset.

In summary, the contributions of this paper are two-fold. From the neuroscience perspective, we are the first to use machine learning to (i) model, analyze, and evaluate iEEG and scalp EEG jointly, (ii) detect surface negative seizures on the scalp using scalp data, (iii) lateralize seizures using machine learning from scalp EEG data, even those that are not visible on the scalp EEG. This work expands on our previous results reported in (22).

From the machine learning perspective, our contribution is on the spatial, frequency and temporal modeling of EEG data using graph theory. In our previous work we introduced the concept of graph theoretical analysis of scalp EEG recordings for seizure prediction and detection using hand crafted features (19, 21). In this work we (i) introduce and analyze different similarity metrics for graph construction, and (ii) use the graph adjacency matrices as the input to deep learning algorithms (CNN and LSTM) which extract and learn from convoluted graph features. To our knowledge, we are the first to apply the Waxman model to the seizure prediction problem. This model is a method of determining if two nodes on a graph are linked (20) and has been used in communication and data networks. It surprisingly outperformed the other two similarity graphs tested, suggesting future utility in EEG modeling.

Clinical Significance

To our knowledge, this is the first work to provide seizure prediction and detection using machine learning on a combined data sets using simultaneous iEEG and scalp EEG. The iEEG seizure onset time was used as the ground truth. Accuracy for both prediction and detection was high whether or not the input was iEEG data alone or scalp EEG data. This suggests that different devices could be constructed from different sources of EEG data depending on the clinical need. A wearable extracranial seizure prediction device may be of use for a person with rare but dangerous seizures who wishes to do a higher risk activity like hiking. While a permanent intracranial prediction device would be of greater use for people with refractory epilepsy and more frequent seizures.

The ability to detect surface negative seizures from scalp data may provide additional opportunities to non-invasively understand surface negative seizure frequency and impact. Both predicting a seizure before it occurs and detecting seizures at their onset, before they manifest on scalp EEG, suggest a window for intervention. Possible interventions include administration of a fast acting medication or simply getting into a safe position and notifying family.

The model was able to successfully lateralize all seizures, even those that were not visible on scalp EEG. This suggests that it may in the future be possible to detect surface negative seizures in the epilepsy monitoring unit and lateralize them, which has the potential to shorten length of stay. Additionally, accurate lateralization can help guide surgical work-up and management and may give greater detail to the seizure network, the visible and the invisible.

Future Research and Limitations

The study was limited by data that was retrospective and from only 19 patients. Additionally, we purposefully limited this paper to seizures of mesial temporal onset for a more

homogenous group. However, it is not known if these results can be generalized to seizure onsets in other parts of the brain. While this work shows accurate lateralization, a more intensive study of localization using seizures of different onset location would be of value.

In this paper, each 1 s window was treated as independent, but for a real-time deployment of a prediction or detection system, a risk assessment model, which considers the labeling of consecutive 1 s windows, can be developed using conditional probabilities. In other words, if the model assigns a 1 s epoch into a category, the risk assessment model may require several consecutive seconds to be classified similarly before the system makes a categorization determination. This will decrease the false positive rate. The next planned project is to test this program prospectively on patients with simultaneous intracranial and scalp EEG undergoing an epilepsy surgical work-up.

Accurate seizure prediction and detection will enable the creation of wearable and implantable devices. In recent work on seizure prediction using scalp EEG, there have been advancements that will make it easier to deploy within hardware (23–25). A limitation of the paper is that we did not use other algorithms on our data sets for direct comparison. We met our goal with high accuracy of classifying EEG data including demonstrating it is possible to detect seizures on scalp EEG that are not visible. Future research will need to allow for direct comparisons as well as refinement of methods in order to optimize models for use in portable devices.

The work in seizure prediction does indicate a pre-seizure state, during which a seizure is nearly inevitable. However, the transition from non-seizure to pre-seizure is not understood. One avenue of research is to investigate the DNN themselves by creating topographical images of the model, ie saliency maps, to further inform us as to the nature of the pre-seizure state. A very different avenue is to use prediction tools to conduct real time experiments during that pre-seizure period of minutes to understand the biology of the transition into seizure, and the epileptic brain.

DATA AVAILABILITY STATEMENT

The data sets presented in this study can be found in online repositories. The name of the repository and accession number(s) can be found below: Rensselaer Polytechnic Institute (RPI) Data Science Research Center (DSRC), http://dsrc.rpi.edu/?page=databank. Requests to access these data sets should be directed to Daniel Park, parkd5@rpi.edu.

ETHICS STATEMENT

The studies involving human participants were reviewed and approved by Icahn School of Medicine Institutional Review Board. Written informed consent for participation was not required for this study in accordance with the national legislation and the institutional requirements.

AUTHOR CONTRIBUTIONS

ZL, MF, LM, and BY conceived and designed the project. ZL and BY carried out all computational analysis. MF and LM provided the data, domain expertise, ground truth, and interpreted the computational analysis. ZL, BY, MF, LM, FP, and SG contributed to the writing of the manuscript. All authors contributed to the article and approved the submitted version.

REFERENCES

1. Proix T, Truccolo W, Leguia MG, Tcheng TK, King-Stephens D, Rao VR, et al. Forecasting seizure risk in adults with focal epilepsy: a development and validation study. *Lancet Neurol.* (2021) 20:127–35. doi: 10.1016/S1474-4422(20)30396-3
2. Mormann F, Andrzejak RG, Elger CE, Lehnertz K. Seizure prediction: the long and winding road. *Brain.* (2007) 130:314–33. doi: 10.1093/brain/awl241
3. Stirling RE, Cook MJ, Grayden DB, Karoly PJ. Seizure forecasting and cyclic control of seizures. *Epilepsia.* (2021) 62 (Suppl. 1):S2–S14. doi: 10.1111/epi.16541
4. Kuhlmann L, Lehnertz K, Richardson MP, Schelter B, Zaveri HP. Seizure prediction — ready for a new era. *Nat Rev Neurol.* (2018) 14:618–30. doi: 10.1038/s41582-018-0055-2
5. Abbasi B, Goldenholz DM. Machine learning applications in epilepsy. *Epilepsia.* (2019) 60:2037–47. doi: 10.1111/epi.16333
6. Rasheed K, Qayyum A, Qadir J, Sivathamboo S, Kwan P, Kuhlmann L, et al. Machine learning for predicting epileptic seizures using EEG signals: a review. *IEEE Rev Biomed Eng.* (2021) 14:139–55. doi: 10.1109/RBME.2020.3008792
7. Siddiqui MK, Morales-Menendez R, Huang X, Hussain N. A review of epileptic seizure detection using machine learning classifiers. *Brain Inform.* (2020) 7:5. doi: 10.1186/s40708-020-00105-1
8. Shoeibi A, Ghassemi N, Alizadehsani R, Rouhani M, Hosseini-Nejad H, Khosravi A, et al. A comprehensive comparison of handcrafted features and convolutional autoencoders for epileptic seizures detection in EEG signals. *Expert Syst Appl.* (2021) 163:113788. doi: 10.1016/j.eswa.2020.113788
9. Shoeibi A, Khodatars M, Ghassemi N, Jafari M, Moridian P, Alizadehsani R, et al. Epileptic seizure detection using deep learning techniques: a review. *J Environ Res Public Health.* (2020) 18:5780. doi: 10.3390/ijerph18115780
10. Acar E, Aykut-Bingol C, Bingol H, Bro R, Yener B. Multiway analysis of epilepsy tensors. *Bioinformatics.* (2007) 23:i10–8. doi: 10.1093/bioinformatics/btm210
11. Ghassemi N, Shoeibi A, Rouhani M, Hosseini-Nejad H. Epileptic seizures detection in EEG signals using TQWT and ensemble learning. In: *2019 9th International Conference on Computer and Knowledge Engineering (ICCKE)* IEEE (2019). p. 403–8.
12. Stojanović O, Kuhlmann L, Pipa G. Predicting epileptic seizures using nonnegative matrix factorization. *PLoS ONE.* (2020) 15:e0228025. doi: 10.1371/journal.pone.0228025
13. Truong ND, Kuhlmann L, Bonyadi MR, Querlioz D, Zhou L, Kavehei O. Epileptic seizure forecasting with generative adversarial networks. *IEEE Access.* (2019) 7:143999–4009. doi: 10.1109/ACCESS.2019.2944691
14. Bandarabadi M, Rasekhi J, Teixeira CA, Karami MR, Dourado A, et al. On the proper selection of pre-ictal period for seizure prediction. *Epilepsy Behav.* (2015) 46:158–66. doi: 10.1016/j.yebeh.2015.03.010
15. Truong ND, Nguyen AD, Kuhlmann L, Bonyadi MR, Yang J, Ippolito S, et al. Convolutional neural networks for seizure prediction using intracranial and scalp electroencephalogram. *Neural Netw.* (2018) 105:104–11. doi: 10.1016/j.neunet.2018.04.018
16. Freestone DR, Karoly PJ, Cook MJ. A forward-looking review of seizure prediction. *Curr Opin Neurol.* (2017) 30:167–73. doi: 10.1097/WCO.0000000000000429

17. Cook MJ, O'Brien TJ, Berkovic SF, Murphy M, Morokoff A, Fabinyi G, et al. Prediction of seizure likelihood with a long-term, implanted seizure advisory system in patients with drug-resistant epilepsy: a first-in-man study. *Lancet Neurol*. (2013) 12:563–71. doi: 10.1016/S1474-4422(13)70075-9
18. Khan H, Marcuse L, Fields M, Swann K, Yener B. Focal onset seizure prediction using convolutional networks. *IEEE Trans Biomed Eng*. (2018) 65:2109–18. doi: 10.1109/TBME.2017.2785401
19. Dhulekar N, Oztan B, Yener B, Bingol HO, Irim G, Aktekin B, et al. Graph-theoretic analysis of epileptic seizures on scalp EEG recordings. In: *Proceedings of the 5th ACM Conference on Bioinformatics, Computational Biology, and Health Informatics, BCB 2014*. New York, NY: ACM (2014). p. 155–63.
20. Waxman BM. Routing of multipoint connections. *IEEE J Sel Area Commun*. (1988) 6:1617–22.
21. Dhulekar N, Nambirajan S, Oztan B, Yener B. Seizure prediction by graph mining transfer learning and transformation learning. In: *Proc. Int. Conf. Mach. Learn. Data Mining*. (2015). p. 32–52.
22. Casale MJ, Marcuse LV, Young JJ, Jette N, Panov FE, Bender HA, et al. The sensitivity of scalp EEG at detecting seizures-a simultaneous scalp and stereo EEG study. *J Clin Neurophysiol*. (2020) 1–7. doi: 10.1097/WNP.0000000000000739
23. Sadeghzadeh H, Hosseini-Nejad H, Salehi S. (2019). Real-time epileptic seizure prediction based on online monitoring of pre-ictal features. *Medical and biological engineering and computing*. 57(11), 2461–2469.
24. Tsiouris K. M, Pezoulas VC, Zervakis M, Konitsiotis S, Koutsouris DD, Fotiadis DI. A long short-term memory deep learning network for the prediction of epileptic seizures using EEG signals. *Comput Biol Med*. (2018) 99:24–37. doi: 10.1016/j.compbiomed.2018.05.019
25. Daoud H, Williams P, Bayoumi M. IoT based efficient epileptic seizure prediction system using deep learning. In: *2020 IEEE 6th World Forum on Internet of Things (WF-IoT)*. IEEE (2020). p. 1–6.

Conflict of Interest: The authors declare that the research was conducted in the absence of any commercial or financial relationships that could be construed as a potential conflict of interest.

Publisher's Note: All claims expressed in this article are solely those of the authors and do not necessarily represent those of their affiliated organizations, or those of the publisher, the editors and the reviewers. Any product that may be evaluated in this article, or claim that may be made by its manufacturer, is not guaranteed or endorsed by the publisher.

frontiers in Neurology

ORIGINAL RESEARCH
published: 23 December 2021
doi: 10.3389/fneur.2021.718329

The Individual Ictal Fingerprint: Combining Movement Measures With Ultra Long-Term Subcutaneous EEG in People With Epilepsy

Troels W. Kjaer[1,2]*, *Line S. Remvig*[3], *Asbjoern W. Helge*[3] and *Jonas Duun-Henriksen*[3]

[1] Center of Neurophysiology, Department of Neurology, Zealand University Hospital, Roskilde, Denmark, [2] Department of Clinical Medicine, University of Copenhagen, Copenhagen, Denmark, [3] Epilepsy Science, UNEEG medical A/S, Alleroed, Denmark

Background: Epileptic seizures are caused by abnormal brain wave hypersynchronization leading to a range of signs and symptoms. Tools for detecting seizures in everyday life typically focus on cardiac rhythm, electrodermal activity, or movement (EMG, accelerometry); however, these modalities are not very effective for non-motor seizures. Ultra long-term subcutaneous EEG-devices can detect the electrographic changes that do not depend on clinical changes. Nonetheless, this also means that it is not possible to assess whether a seizure is clinical or subclinical based on an EEG signal alone. Therefore, we combine EEG and movement-related modalities in this work. We focus on whether it is possible to define an individual "multimodal ictal fingerprint" which can be exploited in different epilepsy management purposes.

Methods: This study used ultra long-term data from an outpatient monitoring trial of persons with temporal lobe epilepsy obtained with a subcutaneous EEG recording system. Subcutaneous EEG, an EMG estimate and chest-mounted accelerometry were extracted from four persons showing more than 10 well-defined electrographic seizures each. Numerous features were computed from all three modalities. Based on these, the Gini impurity measure of a Random Forest classifier was used to select the most discriminative features for the ictal fingerprint. A total of 74 electrographic seizures were analyzed.

Results: The optimal individual ictal fingerprints included features extracted from all three tested modalities: an acceleration component; the power of the estimated EMG activity; and the relative power in the delta (0.5–4 Hz), low theta (4–6 Hz), and high theta (6–8 Hz) bands of the subcutaneous EEG. Multimodal ictal fingerprints were established for all persons, clustering seizures within persons, while separating seizures across persons.

Conclusion: The existence of multimodal ictal fingerprints illustrates the benefits of combining multiple modalities such as EEG, EMG, and accelerometry in future epilepsy management. Multimodal ictal fingerprints could be used by doctors to get a better understanding of the individual seizure semiology of people with epilepsy. Furthermore, the multimodal ictal fingerprint gives a better understanding of how seizures manifest simultaneously in different modalities. A knowledge that could be used to improve seizure acknowledgment when reviewing EEG without video.

Keywords: subcutaneous EEG, accelerometry, EMG, seizure detection, ictal fingerprint, epilepsy

OPEN ACCESS

Edited by:
Maxime O. Baud,
University Hospital Bern, Switzerland

Reviewed by:
Johannes Sarnthein,
University of Zurich, Switzerland
Ewan Nurse,
Seer Medical, Australia
Benjamin H. Brinkmann,
Mayo Clinic, United States

***Correspondence:**
Troels W. Kjaer
twk@regionsjaelland.dk

Specialty section:
This article was submitted to Epilepsy, a section of the journal Frontiers in Neurology

Received: *31 May 2021*
Accepted: *06 December 2021*
Published: *23 December 2021*

Citation:
Kjaer TW, Remvig LS, Helge AW and Duun-Henriksen J (2021) The Individual Ictal Fingerprint: Combining Movement Measures With Ultra Long-Term Subcutaneous EEG in People With Epilepsy. Front. Neurol. 12:718329. doi: 10.3389/fneur.2021.718329

INTRODUCTION

People with epilepsy (PWE) experience repetitive, unexpected seizure episodes, caused by abnormal brain wave hypersynchronization leading to a range of signs and symptoms—the so-called semiology. Quantitative and qualitative characterization of semiology is the cornerstone in every case of epilepsy management. While seizure types tend to be similar from time to time within an individual PWE, many different seizure types exist in different PWE (1). Therefore, an objective description of the most common individual seizure characteristics for each PWE—the multimodal ictal fingerprint—could have multiple potential uses within epilepsy treatment (e.g., clinical management or seizure detection).

In epilepsy management, automatic device-based seizure detection may be useful for qualitative description of the seizure semiology in daily life. In the clinic, a concise and objective qualitative description of the seizure semiology can add value in the epilepsy diagnostic process for the healthcare professionals. With an ictal fingerprint available, the clinical management and treatment optimization might be less cumbersome. Including movement measures in the ictal fingerprint can potentially add clinical symptoms, which is an important part of the seizure semiology—both during the diagnostic process and treatment optimization.

In the outpatient setting, accurate seizure documentation remains an ongoing challenge. Seizure diaries, the current standard assessment of seizure counts at home, has been shown to be unreliable, potentially leading to over- or under-reporting (2). Both of which might lead to incorrect seizure treatment and complications for PWE (3). Furthermore, unobserved seizures have been associated with increased risk of morbidity and mortality through seizure related accidents, SUDEP etc. Hence, a seizure alarm making another person aware of the seizure may help reduce the risk (4). There exist several seizure alarms, of which most are based on movement (pressure, accelerometry, and EMG). However, focus on other modalities like ECG and EEG seems promising especially in seizures with a limited motor component (5). Many of the current alarm systems have a limited use due to low sensitivity, high false alarm rate, not being body worn or being obtrusive, hence not used (6).

For objective seizure counting and alarms, the need for improved combinations of devices and algorithms that work in everyday life settings is substantial. Novel subcutaneous EEG (sqEEG) devices present an intriguing hardware development which makes EEG recordings possible around the clock (3, 7–10). However, the use of these devices requires automatic algorithms to process the recordings due to the vast amount of data. Two possible approaches for improving these algorithms could be multimodal sensing and detection based on the individual ictal seizure semiology. Multimodal sensing is performed as standard in the epilepsy monitoring unit, but also examples of multimodal home monitoring are published (11). Combining sqEEG sensing with movement sensing is a simple way to capture both the electrographic and clinical motor parts of the seizure semiology during home monitoring. This approach is novel and exactly what is investigated in this study. Hereby the gap between home monitoring and the golden standard video-EEG in the epilepsy monitoring unit is narrowed.

This article presents a multimodal ictal fingerprint based on movement measures and ultra long-term sqEEG recorded in the everyday life of PWE. The aim is to explore if the concept of an ictal fingerprint can be used to describe and better understand the homogeneity of seizures within each PWE and the heterogeneity of seizures across PWEs. If that is the case, multimodal recordings could be used to supply doctors with an improved, subject-specific epilepsy semiology during outpatient monitoring. Furthermore, it could be used to improve seizure detection methods by increasing the knowledge of the heterogeneity of individual seizures.

MATERIALS AND METHODS

Data from an outpatient trial using ultra long-term minimally invasive sqEEG to monitor epileptic seizures constituted the basis for this work. For a detailed account on the study design, data collection procedures and demographics of the participating persons please refer to the initial report of the clinical trial (3).

Study Population

To ensure a representative distribution of seizure data a minimum of 10 well-defined electrographic seizures were required for each participant. This meant that four out of nine participants were included in the present publication. All included persons suffered from medically refractory left temporal lobe epilepsy. **Table 1** depicts person characteristics.

In total, 78 electrographic seizures from the four persons (range: 12–25 seizures/person) were identified from the sqEEG data. All focal to bilateral tonic-clonic seizures (FBTCS) were excluded from the analysis (a total of four seizures from two different persons) to focus on defining the ictal fingerprint of seizures with a smaller motor component. These are the challenging ones to separate as opposed to FBTCS which can be detected using wearable devices (12), and in addition, they constitute most seizures. Thus, 74 electrographic non-FBTCS's constituted the basis for this work.

Data Collection and Characteristics

The sqEEG recorder system (24/7 EEG™ SubQ, UNEEG medical, Lynge, Denmark), referred to as the SubQ solution, consists of an implant and an external device. The implant consists of a 3-contact lead wire (yielding 2-channel bipolar EEG) and a small housing, implanted unilaterally under local anesthesia over the temporal region of interest (see **Figure 1**). The external device connects to the implant housing *via* an inductive link, powering the implant and recording/storing data (sampling rate: 207 Hz). The external device holds a 3-axis accelerometer (applied sampling rate of 10 or 20 Hz). As the external device is typically carried on the shirt as depicted in **Figure 1**, derivative accelerometer measures carry information on the orientation, posture, and movement of the body trunk.

Each person used the SubQ solution for 2–3 months of their everyday life. The total amount of outpatient sqEEG has been reviewed and labeled with "electrographic seizure" by a thorough

TABLE 1 | Epilepsy and data characteristics for each person.

Person ID	Ictal onset zone	Semiology	EEG data (h)	Number of electrographic seizures (*N*)*
B	LT	FAS	1,552	25
E	LT	FIAS	1,147	15
G	LT	Uncertain	1,516	12
I	LT	FIAS	1,605	22

FAS, focal aware seizure; FIAS, focal impaired awareness seizure; LT, left temporal.
**Number of seizures when the four FBTCS's (focal to bilateral tonic-clonic seizures) were excluded.*

FIGURE 1 | The SubQ solution and its placement in this study. *Left*: sagittal view of the head showing the placement of implant at the temporal region, recording 2-channel bipolar temporal sqEEG. *Right*: frontal view of the trunk demonstrating the placement of the external device, recording 3-axis accelerometry of the body trunk.

review process of leading experts from three different institutions (in preparation for publication).

Data Analysis

Of the large amounts of recorded data, ictal, pre-ictal and baseline data was extracted and applied in this study. All electrographic seizures were labeled with seizure onset and duration, defining the ictal period. The baseline and pre-ictal periods were extracted for comparison with the ictal periods to demonstrate that the activity during the ictal periods were different from the remaining signal. The baseline period was defined as a 1-min period ending 5 min before the seizure onset and the pre-ictal period was defined as the minute period preceding the seizure onset. A length of 1 min was deemed sufficient to minimize the influence of inherent signal variance. The first two and the last 2 s of the ictal periods and the last 2 s of the pre-ictal periods were excluded from the analysis to avoid transition phenomena.

In addition to the sqEEG and 3-axis accelerometry, an EMG signal estimate was extracted from the sqEEG, based on the frequency content above 20 Hz. The recording electrodes of the implant span the temporalis muscle, thus, recorded activity above 20 Hz is very likely temporalis activity (13).

To assess a multimodal ictal fingerprint across persons, ∼70 features spanning all three modalities were calculated for the ictal and pre-ictal periods. To find a compact ictal fingerprint, it was decided to remove the redundant features. For this purpose, a Random Forest classifier was trained in a 5-fold cross-validation scheme with nine different hyperparameter settings (14). The hyperparameter settings were a grid search over the number of trees (25, 50, 100) and the minimum number of samples to split a node (2, 4, 6). The remaining hyperparameters were the default parameters used by the Random Forest Classifier function of the python package sklearn (v. 0.24.1). The classification task consisted of separating ictal periods between persons. From the best performing model, a feature importance parameter was extracted based on the internal gini impurity measure, which determines the node splits in each of the decision trees. The five most discriminative features were selected for further analysis (hereafter referred to as the reduced feature space).

A principal component analysis was performed in the reduced feature space to visualize the person-specific, feature-based clusters of seizures. A seizure centroid was computed for each person in the space spanned by the principal components by averaging over all seizures. Then each seizure was assigned to the person with the centroid which was closest measured using Euclidean distance. The accuracy of this simple clustering was calculated.

To illustrate the uniqueness of the multivariate ictal fingerprint, radar charts of the ictal feature medians and interquartile ranges were displayed for each person. All features were Z-score normalized for optimized visualization and comparison.

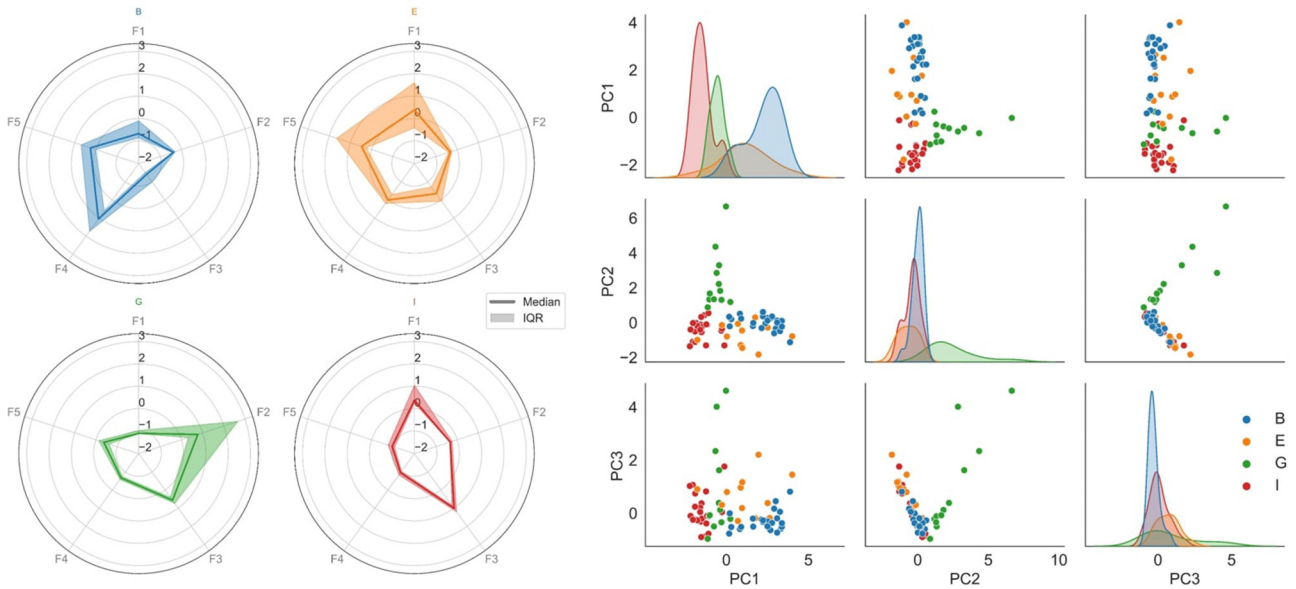

FIGURE 2 | The multimodal ictal fingerprint. Each color represents a separate participant (blue, orange, green, and red are person B, E, G, and I, respectively). *Left:* Radar charts of the ictal feature medians and interquartile ranges for each person. F1: X-axis acceleration component; F2: EMG power proximal; F3: EEG relative delta power; F4: EEG relative low theta power; F5: EEG relative high theta power. The heterogeneity across persons is shown. The ictal fingerprint of person B (blue) is dominated by EEG theta power elevation. The fingerprint of person E (orange) has a partial overlap with elevated theta activity. However, the movement component (F1) is a major contributor for this fingerprint. The movement component is also substantial for person I (red), but with no remarkable theta elevation. The ictal fingerprint of person G (green) is not dominated by either of the mentioned features; instead, elevated EMG activity is the main contributor. *Right:* Pair plot of the first three principal components of the reduced feature space of the ictal periods, where each dot represents a seizure. Scatterplots are shown for each pairing of the principal components, and marginal distributions are plotted along the diagonal (layered kernel density estimates). Within-person clustering and separation across persons are shown. The seizures of each individual could be separated from the rest with an 84.5% accuracy.

To demonstrate that the ictal periods differ from the baseline and pre-ictal periods within persons, a distance-to-ictal-cluster-average vs. distance-to-preictal-cluster-average plot was made for all ictal and pre-ictal periods. Distances were to person-specific cluster averages, calculated as Euclidean norms in the reduced feature space.

RESULTS

Feature Space Reduction

The reduced feature space included one accelerometer-based feature: the x-axis accelerometer component; one estimated EMG feature: the >20 Hz power at the proximal electrode contact point; and three EEG-based features: the relative power in the delta (0.5–4 Hz), low theta (4–6 Hz), and high theta (6–8 Hz) band.

Ictal Clustering

The pair plot of the first three principal components of the reduced feature vectors (right chart of **Figure 2**) shows that the seizures group together in person-specific, feature-based clusters. Using a simple clustering method, the accuracy of separating the seizures of all subjects reached 84.5%. By visual inspection of the figure, it can be observed that B, G, and I were more distinguishable than E and separating only B, G, and I could be done with an accuracy of 93.1%. To some extent, the feature characteristics of person E seem to group with person I. According to **Table 1**, their seizure semiologies are alike, both experiencing focal impaired awareness seizures.

The Ictal Fingerprint

In the left graph of **Figure 2**, radar plots of the ictal feature medians and interquartile ranges demonstrate the heterogeneity across persons. E.g., the ictal period of person G is dominated by high EMG activity, whereas it is not the case for any other person. Likewise, the relative low theta power is elevated for the ictal periods of person B, whereas this does not dominate the ictal fingerprints of the remaining persons.

Baseline and Pre-ictal to Ictal Separation

Figure 3 includes the pre-ictal periods to show pre-ictal to ictal separation and **Table 2** present the statistics of the separation task. The cluster center distances show a separation accuracy of 83.8% for the pre-ictal to ictal separation and 88.1% for the baseline to ictal separation. Thereby, it is indicated that the created ictal fingerprints are truly ictal, and not general person-specific multimodal fingerprints.

DISCUSSION

Seizures can be split up into separate seizure types and the same seizure type can manifest differently for each patient

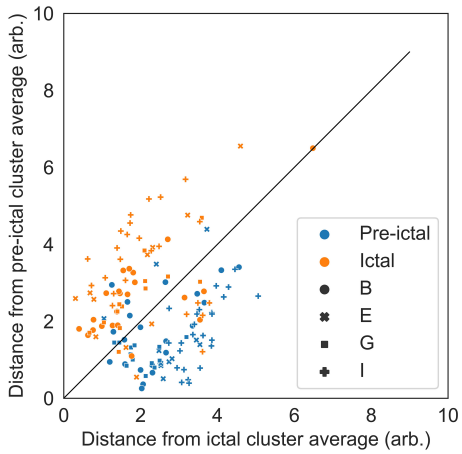

FIGURE 3 | Distance-to-ictal-cluster-average vs. distance-to-preictal-cluster-average for all ictal and pre-ictal periods to illustrate the separation capability. Distances are to person-specific cluster averages, calculated as Euclidean norms in the reduced feature space. The solid black line represents the class separation. The separation accuracy was 83.8%. Period is shown with different colors (blue are pre-ictal periods and orange are ictal periods) and the subject ID is shown with different marker types (circles, crosses, squares and plusses are persons B, E, G, and I, respectively).

TABLE 2 | Accuracy, sensitivity, specificity, positive predictive value, and negative predictive value of separating ictal from pre-ictal periods.

Statistic	Value (%)	Confidence interval (%)
Accuracy	83.8	±6.1
Sensitivity	80.3	±6.5
Specificity	87.3	±5.5
Positive predictive value	86.4	±5.6
Negative predictive value	81.6	±6.4

(15). Here we have demonstrated that the concept of an ictal fingerprint is meaningful when based on data from three different modalities: EEG, EMG, and accelerometry all recorded with the SubQ solution in four different PWE. We have not managed to find previous efforts showing this phenomenon even though previous studies have tried to use multiple modalities in seizure detection algorithms (16). For that reason, the purpose was not to achieve the highest possible separation of seizures in the person-specific, feature-based clusters. Instead, it was to demonstrate that an ictal fingerprint exists defined by easily interpretable features and discuss the advantages of using multiple modalities. Collecting data on individual seizures from multiple modalities has the potential to improve clinical treatment management. The proposed ictal fingerprint supplies information that could give healthcare professionals in the clinic a more detailed description of any specific individual's seizure semiology. Part of this information would allow to distinguish between clinical and subclinical seizures. A task that is not possible with unimodal data because EEG is needed to discover the subclinical seizures and other modalities, such as EMG or accelerometry, are needed to determine whether a seizure is clinical.

PWE need a solution for seizure detection that works in their everyday life, and multiple unimodal setups have been proposed. The performance of EEG based alarms has so far been problematic, potentially challenging clinical utility and user tolerance (17, 18). Most of the studies regarding EEG-based alarms show only moderate sensitivity, tolerable false detection rates and are performed on data obtained under standardized circumstances, e.g., in the hospital and instead of during everyday activities (19). Most commercially available alarms are triggered by movement (accelerometry, EMG), or sympathetic activity (ECG, electrodermal response), requiring either a significant motor component or autonomic component of the seizures to work (20). Often movements, exercise or change in autonomic load cause false detections.

The crucial challenge when designing devices and algorithms for seizure detection is to detect all true seizures while avoiding false alarms, i.e., obtaining high sensitivity and specificity. Achieving this goal requires data in which seizures are separable from background activity. Our findings in four persons with temporal lobe epilepsy show that the modalities which describe the seizures best are different from person to person. Visual inspection makes it clear that the seizures can be grouped into person-specific, feature-based clusters, meaning they are generally more similar within PWEs and more different between PWEs (**Figure 2**).

EEG signals differ from person to person to a degree where EEG has even been proposed as a modality that could be used for biometric recognition (21–23). It was therefore expected that the persons could be distinguished based on multiple modalities incl. EEG. **Figure 3** illustrates that there is not only a multimodal overall fingerprint but also a separate ictal fingerprint as the pre-ictal periods could be separated from the ictal periods.

This study only presents the ictal fingerprint of four PWEs. It is therefore unknown to what degree the proposed ictal fingerprint will overlap between many individuals. While the reduced feature space represents commonly used features from the selected modalities, the proposed ictal fingerprint contains more features than there are PWEs. Separability of the person-specific, feature-based clusters presented in **Figure 2** would be expected to decrease with increasing number of persons. This could lead to a need for a revised model of the ictal fingerprint incorporating other and possibly more features. The approach described in this paper is novel in the way it combines movement and EEG in an everyday life setting. What is also special, is that the accelerometer used in this study is placed on the chest revealing movement of the trunk rather than extremities, which is usually the case for seizure detectors. Finding that body trunk movements can contribute to the ictal fingerprint might be surprising. However, it is advantageous that measurement devices placed on extremities are not required in order to limit the number of devices to be worn by the PWEs.

Introducing the concept of an ictal fingerprint has the potential to improve the PWE's knowledge of their own seizures which might increase their device compliance. The readiness

of PWEs to use wearables in everyday life requires that individual needs are addressed, and expectations are met to better understand their life situation. A device can be perceived by the PWEs as a lifeline to health and access to healthcare professionals (24).

In summary, our findings in four persons with temporal lope epilepsy show that it is possible to create unique individual ictal fingerprints, where the multimodal characteristics describing the ictal periods best, differ from person to person while staying consistent within each person. Individual ictal fingerprints may enhance clinical management, improve seizure acknowledgment and detection algorithms, and lead to better personal healthcare experiences.

DATA AVAILABILITY STATEMENT

The data analyzed in this study is subject to the following licenses/restrictions: the data consists of huge amounts of raw EEG, which are not available to the public. The study where the data was collected is registered in ClinicalTrials.gov (NCT02946151). Requests to access these datasets should be directed to Troels W. Kjaer, twk@regionsjaelland.dk.

ETHICS STATEMENT

The studies involving human participants were reviewed and approved by the Committee of Science Ethics for Region Zealand (SJ-551). The patients/participants provided their written informed consent to participate in this study.

AUTHOR CONTRIBUTIONS

JDH and TK contributed to conception and design of the study where the applied data has been recorded. AH and LR performed the statistical analysis. AH, LR, and TK wrote sections of the manuscript. All authors contributed to manuscript revision, read, and approved the submitted version.

REFERENCES

1. Fisher RS, Cross JH, D'Souza C, French JA, Haut SR, Higurashi N, et al. Instruction manual for the ILAE 2017 operational classification of seizure types. *Epilepsia.* (2017) 58:531–42. doi: 10.1111/epi.13671
2. Blachut B, Hoppe C, Surges R, Elger C, Helmstaedter C. Subjective seizure counts by epilepsy clinical drug trial participants are not reliable. *Epilepsy Behav.* (2017) 67:122–7. doi: 10.1016/j.yebeh.2016.10.036
3. Weisdorf S, Duun-Henriksen J, Kjeldsen MJ, Poulsen FR, Gangstad SW, Kjaer TW. Ultra-long-term subcutaneous home monitoring of epilepsy-490 days of EEG from nine patients. *Epilepsia.* (2019) 60:2204–14. doi: 10.1111/epi.16360
4. Ryvlin P, Ciumas C, Wisniewski I, Beniczky S. Wearable devices for sudden unexpected death in epilepsy prevention. *Epilepsia*, (2018) 59:61–6. doi: 10.1111/epi.14054
5. Qaraqe M, Ismail M, Serpedin E, Zulfi H. Epileptic seizure onset detection based on EEG and ECG data fusion. *Epilepsy Behav.* (2016) 58:48–60. doi: 10.1016/j.yebeh.2016.02.039
6. Bruno E, Viana PF, Sperling MR, Richardson MP. Seizure detection at home: do devices on the market match the needs of people living with epilepsy and their caregivers? *Epilepsia.* (2020) 61(Suppl. 1):S11–24. doi: 10.1111/epi.16521
7. Duun-Henriksen J, Baud M, Richardson MP, Cook M, Kouvas G, Heasman JM, et al. A new era in electroencephalographic monitoring? Subscalp devices for ultra–long-term recordings. *Epilepsia.* (2020) 61:1805–17. doi: 10.1111/epi.16630
8. Viana PF, Duun-Henriksen J, Glasstëter M, Dümpelmann M, Nurse ES, Martins IP, et al. 230 days of ultra long-term subcutaneous EEG: seizure cycle analysis and comparison to patient diary. *Ann Clin Transl Neurol.* (2021) 8:288–93. doi: 10.1002/acn3.51261
9. Viana PF, Remvig LS, Duun-Henriksen J, Glasstetter M, Dümpelmann M, Nurse ES, et al. Signal quality and power spectrum analysis of remote ultra long-term subcutaneous EEG. *MedRxiv.* (2021) 62:1820–8. doi: 10.1111/epi.16969
10. Weisdorf S, Zibrandtsen IC, Kjaer TW. Subcutaneous EEG monitoring reveals AED response and breakthrough seizures. *Case Rep Neurol Med.* (2020) 2020:8756917. doi: 10.1155/2020/8756917
11. van Andel J, Ungureanu C, Arends J, Tan F, Van Dijk J, Petkov G, et al. Multimodal, automated detection of nocturnal motor seizures at home: Is a reliable seizure detector feasible? *Epilepsia Open.* (2017) 2:424–31. doi: 10.1002/epi4.12076
12. Beniczky S, Wiebe S, Jeppesen J, Tatum WO, Brazdil M, Wang Y, et al. Automated seizure detection using wearable devices: a clinical practice guideline of the International League Against Epilepsy and the International Federation of Clinical Neurophysiology. *Epilepsia.* (2021) 62:632–46. doi: 10.1111/epi.16818
13. Whitham EM, Pope KJ, Fitzgibbon SP, Lewis T, Clark CR, Loveless S, et al. Scalp electrical recording during paralysis: Quantitative evidence that EEG frequencies above 20 Hz are contaminated by EMG. *Clin Neurophysiol.* (2007) 118:1877–88. doi: 10.1016/j.clinph.2007.04.027
14. Breiman L. Random forests. *Mach Learn.* (2001) 45:5–32. doi: 10.1023/A:1010933404324
15. Devinsky O, Vezzani A, O'Brien TJ, Jette N, Scheffer IE, de Curtis M, et al. Epilepsy. *Nat Rev Disease Prim.* (2018) 4:18024. doi: 10.1038/nrdp.2018.24
16. Leijten FSS, van Andel J, Ungureanu C, Arends J, Tan F, van Dijk J, et al. Multimodal seizure detection: a review. *Epilepsia.* (2018) 59:42–7. doi: 10.1111/epi.14047
17. Bacher D, Amini A, Friedman D, Doyle W, Pacia S, Kuzniecky R. Validation of an EEG seizure detection paradigm optimized for clinical use in a chronically implanted subcutaneous device. *J Neurosci Methods.* (2021) 358:109220. doi: 10.1016/j.jneumeth.2021.109220
18. Zibrandtsen IC, Kidmose P, Christensen CB, Kjaer TW. Ear-EEG detects ictal and interictal abnormalities in focal and generalized epilepsy - a comparison with scalp EEG monitoring. *Clin Neurophysiol.* (2017) 128:2454–61. doi: 10.1016/j.clinph.2017.09.115
19. Baumgartner C, Koren JP. Seizure detection using scalp-EEG. *Epilepsia.* (2018) 59(Suppl. 1):14–22. doi: 10.1111/epi.14052
20. Regalia G, Onorati F, Lai M, Caborni C, Picard RW. Multimodal wrist-worn devices for seizure detection and advancing research: focus on the Empatica wristbands. *Epilepsy Res.* (2019) 153:79–82. doi: 10.1016/j.eplepsyres.2019.02.007
21. Chan HL, Kuo PC, Cheng CY, Chen YS. Challenges and future perspectives on electroencephalogram-based biometrics in person recognition. *Front Neuroinform.* (2018) 12:e00066. doi: 10.3389/fninf.2018.00066
22. Näpflin M, Wildi M, Sarnthein J. Test-retest reliability of resting EEG spectra validates a statistical signature of persons. *Clin Neurophysiol.* (2007) 118:2519–24. doi: 10.1016/j.clinph.2007.07.022
23. Stassen HH. Computerized recognition of persons by EEG spectral patterns. *Electroencephalogr Clin Neurophysiol.* (1980) 49:190–4. doi: 10.1016/0013-4694(80)90368-5
24. Beck M, Simony C, Zibrandtsen I, Kjaer TW. Readiness among people with epilepsy to carry body-worn monitor devices in everyday life: a qualitative

study. *Epilepsy Behav*. (2020) 112:107390. doi: 10.1016/j.yebeh.2020.107390

Conflict of Interest: TK consults for UNEEG medical A/S. LR, AH, and JDH are employees of UNEEG medical A/S.

Publisher's Note: All claims expressed in this article are solely those of the authors and do not necessarily represent those of their affiliated organizations, or those of the publisher, the editors and the reviewers. Any product that may be evaluated in this article, or claim that may be made by its manufacturer, is not guaranteed or endorsed by the publisher.

frontiers in Neurology

OPINION
published: 11 February 2022
doi: 10.3389/fneur.2022.779551

A Patient Perspective on Seizure Detection and Forecasting

Aria Moss[1], Evan Moss[2], Robert Moss[3], Lisa Moss[3,4], Sharon Chiang[5] and Peter Crino[6]*

[1] Northern Virginia Community College, Alexandria, VA, United States, [2] W. T. Woodson High School, Fairfax, VA, United States, [3] Seizure Tracker, LLC, Springfield, VA, United States, [4] TSC Alliance, Silver Spring, MD, United States, [5] Department of Neurology and Weill Institute for Neurosciences, University of California, San Francisco, San Francisco, CA, United States, [6] Department of Neurology, University of Maryland School of Medicine, Baltimore, MD, United States

Keywords: epilepsy, seizures, forecasting, devices, patient perspective, tuberous sclerosis complex, seizure detection

OPEN ACCESS

Edited by:
Leon D. Iasemidis, Barrow Neurological Institute (BNI), United States

Reviewed by:
Noah Hutson, Barrow Neurological Institute (BNI), United States
Johannes Koren, Clinic Hietzing, Austria
Vinit Shah, Temple University, United States

****Correspondence:***
Aria Moss
aria.moss@gmail.com

Specialty section:
This article was submitted to Epilepsy, a section of the journal Frontiers in Neurology

Received: *19 September 2021*
Accepted: *20 January 2022*
Published: *11 February 2022*

Citation:
Moss A, Moss E, Moss R, Moss L, Chiang S and Crino P (2022) A Patient Perspective on Seizure Detection and Forecasting. Front. Neurol. 13:779551. doi: 10.3389/fneur.2022.779551

INTRODUCTION

My name is Aria Moss. My brother, Evan Moss, was diagnosed with epilepsy when he was 3 months old, and Tuberous Sclerosis Complex (TSC) at 2 years. TSC is a genetic disorder that causes tumor growth in vital organs; Evan has tumors in his brain, kidneys, liver, and skin. At 4 years old, he was having >15 seizures a day and underwent brain surgery, becoming seizure-free for 2 years. Unfortunately, his seizures recurred at age six, as nocturnal status epilepticus. He's since had multiple surgeries and tried >10 medications to treat them. While Evan's seizures are now less frequent, occurring every 2 weeks rather than daily, their unpredictability and impact have remained.

Evan is currently 17 years old. I'm nineteen with hopes of 1 day becoming a doctor. Our parents are both highly involved with the epilepsy community: our mom, Lisa, works for the TSC Alliance, and our dad, Rob, developed the online seizure diary Seizure Tracker.

The following interview, conducted by Evan's neurologist, Dr. Peter Crino, shares the perspective of our family.

DETECTION DEVICE FUNCTIONALITY

The features of detection devices valued by patients as end-users are vital to device design. While important features may vary from user to user, certain features are considered particularly important by the majority of patients. High comfort, low visibility, and high usability are often crucial features for patient uptake (1), whereas uncomfortable or visible devices dramatically limit patient willingness to use them and are weighed against benefit and reliability (2).

Dr. Peter Crino: "Today we're meeting with Evan Moss, along with his parents, Rob and Lisa, and sister, Aria. We'll touch on how Evan and his family deal with the uncertainty of living with seizures and how seizure detection/forecasting carries for their family hope for ultimately improving quality of life. There are many emerging approaches for seizure detection and forecasting that promise individuals with epilepsy a view of when seizures might occur (3, 4). All are exciting but imperfect (5). Evan, what are your experiences with seizure detection devices? What's worked for you, what have you struggled with?"

Evan Moss: "Well, a lot of the devices haven't helped me much. My seizures cycle every two weeks. I can tell on my own when I'm getting close to a seizure, but I don't know exactly when it'll occur. I need to know ahead, and I need precision; I want to know what day it's going to be on."

Dr. Crino: "That's an important observation. As you said, seizure detection and forecasting are distinct. Many individuals with epilepsy have some ability to self-predict, but it's not always reliable, and doesn't work for everyone (6, 7). Alerting devices say when you have a seizure but knowing exactly when seizures will occur would really help you to prepare. You've tried several devices for seizure alerting–a pulse oximeter, heart rate patches, and cameras, for example. What have been your experiences with those?"

Robert Moss: "When we used the pulse oximeter and heart rate patch, they weren't super reliable. Other devices, like EMG, relied on algorithms that required lengthy periods of muscle involvement. Evan's seizures included muscle contractions that were detected by EMG but wouldn't last long enough for it to alert."

Lisa Moss: "There were also challenges wearing the pulse oximeter; when he wore it on his hand or foot, it didn't stay on. The heart rate patches stuck to his chest and were difficult to remove. They'd irritate his skin."

Dr. Crino: "So they were uncomfortable, which led to a lack of functionality."

Rob: "Comfort and reliability have definitely been an issue. The best for us as parents has been video monitoring. We can tell based on motion whether Evan's having a seizure, and run in to treat it."

Evan: "I think there are four features needed for a good device: it needs to be comfortable, easy to use, accurate, and precise. They're different–precision is always hitting the same spot; accuracy is always hitting the bullseye."

PRIVACY AND STIGMA

When using wearable devices, patients often report that a device's visibility and privacy (or lack thereof) negatively impacts their experience, which can be isolating or uncomfortable (1, 2, 8). Here, the Moss family reflects on similar experiences with other seizure detection methods they use.

Dr. Crino: "Evan, what are your thoughts about being monitored on camera for seizures? Is that comfortable for you?"

Evan: "Not at all! There's a camera constantly on in my room. I have a hard time ever feeling that I'm not being watched."

Dr. Crino: "I think most people would be pretty opposed to having a camera in their room, right? We hear this in epilepsy monitoring units; you're live theater, all the time. It serves a function— you all can have eyes on Evan and respond rapidly, which is great, but privacy is an big issue (9). Tangentially—tell me about your experience with Mindy, your seizure alert dog. Is it extra attention you don't want?"

Evan: "It's not that bad for me. At school, everyone knows I have Mindy and love her! I can also choose to leave her at home on small outings."

Lisa: "There are even challenges with having Mindy. You may think everybody knows service dogs are allowed in public spaces but that isn't always the case. We've had to fight to enter restaurants, doctor's offices, even hospitals!"

Dr. Crino: "Really?"

Lisa: "Yes! Life can become confrontational doing basic things, and it can be unsettling. We're a spectacle–everywhere we go, heads turn, people comment. As soon as the vest is on, you get that attention, whether you want it or not."

Rob: "Our community's looking for solutions, but I feel like there's rarely conversation about the unintended consequences. Sometimes the lifestyle changes have an even bigger detrimental effect on quality of life."

Lisa: "I think we were really hoping for independence for Evan, so he could sleep alone without the camera. Mindy alerts two days ahead of a seizure and responds as it happens, but we usually wake up before she does. She's part of our team but doesn't fill all the gaps."

FORECASTING HORIZONS AND PRIORITIES

Many surveys on patient needs with regards to the performance of seizure forecasting algorithms have been conducted. In general, patients have reported that high sensitivity is vital for seizure prediction (10), with the potential morbidity/mortality from false negatives a high concern (11). One survey of 1,168 people with epilepsy found that "detecting all seizures" was rated as the most important priority for detection devices (12). Another survey found that about 60% of people and caregivers of epilepsy required 100% accuracy in detection rates to find devices useful (13). Only 25% (32%) of patients have said they would be very likely to continue using a forecasting tool if it made one false negative (false positive) prediction, respectively (14).

Dr. Crino: "Let's discuss seizure prediction. Recent evidence suggests that when you have a seizure, it's been building up for hours, maybe days (15). There're lots of markers that go up in the blood and brain around the time of seizure activity (16, 17). It's clearly a systemic effect, we just don't have a way to reliably pick it up in advance."

Lisa: "It would be great if there was a way to predict a seizure and treat preventatively so it doesn't occur or you're prepared. If you're going to go out and you're alerted about a likely seizure, maybe plans change. Evan's needs are different since his seizures happen in his sleep."

Rob: "That's why patients have to be involved in developing devices. Electrographic seizures are considered a gold standard in prediction, but as a father I don't want to predict every seizure. I want to know when he'll have a seizure that would require intervention."

Dr. Crino: "There's discussion by developers of what prediction horizons they should aim for. For you, what would be a good prediction horizon?"

Evan: "My seizures are in my sleep, and usually happen early in the morning. If I get an alert too far ahead, like over two hours, I'm going to lie awake, dreading a seizure. But it needs to be far enough ahead to act, at least more than 10 min."

Dr. Crino: "Earlier, Evan gave four important features of a seizure forecasting device–ease of use, comfort, precision, and accuracy. Is there anything else?"

Rob: "It's dependent on the characteristics of each person's epilepsy. There was a switch when Evan went from many small seizures a day to status seizures every two weeks. Until we had to act on those long seizures, we didn't care about predicting the small ones. We already knew he was going to have ten or fifteen seizures the next day."

Aria Moss: "In general, a device has to be able to predict seizures better than the patient or caretaker can–which isn't easy.

But until you can replace their usual detection methods, you're not going to alleviate meaningful burden on the family. Evan has seizures every two weeks, which always go into status and are treated with emergency medication right away, and we often call 911. We can't miss a seizure. If we have a device that works 95% of the time but will still miss 5% of his seizures, that's just not helpful–it's not enough to rely on alone."

Dr. Crino: "That's an interesting point–your family has put together a strategy for 100% catch rate. That's the benchmark for these devices: 100% sensitivity. You really can't miss any seizures; there's morbidity associated with that."

DISCUSSION: THE PATIENT PERSPECTIVE

About a fifth of patients have expressed that existing devices are not effective for their seizure type(s), which causes skepticism about the use of forecasting or detection devices (14). Almost all evidence for devices currently on the market is specific to seizure types with major motor features, and there is little evidence on accuracy for other seizure types (1). Ultimately, in order to develop effective devices, it is vital to ensure patient voices are considered throughout the development process.

Dr. Crino: "I'd like to wrap up with a broader question. What's your perspective on how well the research community is involving patient perspectives?"

Lisa: "I don't think that the patient voice is brought in early enough. The patient is the one to buy the device, follow the method, wear the tool. When patients are involved early on, they share their views, and some aspects might improve. Sometimes a change will evade developers because they're not living it day to day, so it's important to have a diverse population of patients involved in those discussions. This is related to patient-doctor interactions, too; patients need to be viewed as valuable and knowledgeable members of the treatment team and be included in all aspects of care. As parents we've seen our son have thousands of seizures, and that provides expertise. We're experts in Evan's epilepsy and which treatments will improve his quality of life. It's the same when considering a seizure detection device: it's important to recognize the knowledge of the patient community in all stages of development."

Rob: "Epilepsy is a hard disorder to manage and requires strong patient/physician communication to treat effectively. Technology needs to compliment that communication, not replace it. Developing technologies that collect data alongside patient-reported outcomes is a way developers can prioritize both clean data collection and patient interests."

Dr. Crino: "I think you're right–many people think about this problem in terms of removing the patient altogether, but to be honest with you, I don't foresee a future where we can do that. The patient tells us what outcomes matter most. Someday, maybe seizure forecasting will be tied to adjusting the wiring in the brain in real-time (18). We don't have any therapies right now to adjust the wiring in the brain, to really help patients. That's for you to figure out when you're a doctor, Aria."

Aria: "Talking about predicting seizures is amazing; it's a new frontier for epilepsy. When I'm a doctor, I hope we have solutions that go beyond anything we have today. I'm excited to see where we'll be ten, twenty years down the line."

AUTHOR CONTRIBUTIONS

Manuscript conceptualization was developed by SC, AM, and RM. The interview was conducted with PC as interviewer and AM, EM, LM, and RM as interviewees. AM drafted the manuscript. All authors read, refined, and approved the manuscript.

REFERENCES

1. Bruno E, Viana PF, Sperling MR, Richardson MP. Seizure detection at home: do devices on the market match the needs of people living with epilepsy and their caregivers? *Epilepsia.* (2020) 61:S11–24. doi: 10.1111/epi.16521
2. Simblett SK, Biondi A, Bruno E, Ballard D, Stoneman A, Lees S, et al. Patients' experience of wearing multimodal sensor devices intended to detect epileptic seizures: a qualitative analysis. *Epilepsy Behav.* (2020) 102:106717. doi: 10.1016/j.yebeh.2019.106717
3. Mormann F, Andrzejak RG, Elger CE, Lehnertz K. Seizure prediction: the long and winding road. *Brain.* (2007) 130:314–33. doi: 10.1093/brain/awl241
4. Freestone DR, Karoly PJ, Cook MJ. A forward-looking review of seizure prediction. *Curr Opin Neurol.* (2017) 30:167–73. doi: 10.1097/WCO.0000000000000429
5. Bosl WJ, Leviton A, Loddenkemper T. Prediction of seizure recurrence. A note of caution. *Front Neurol.* (2021) 12:675728. doi: 10.3389/fneur.2021.675728
6. Haut SR, Hall CB, Borkowski T, Tennen H, Lipton RB. Modeling seizure self-prediction: an e-diary study. *Epilepsia.* (2013) 54:1960–7. doi: 10.1111/epi.12355
7. Privitera M, Haut SR, Lipton RB, McGinley JS, Cornes S. Seizure self-prediction in a randomized controlled trial of stress management. *Neurology.* (2019) 93:e2021–31. doi: 10.1212/WNL.0000000000008539
8. Olsen LS, Nielsen JM, Simonÿ C, Kjær TW, Beck M. Wearables in real life: a qualitative study of experiences of people with epilepsy who use home seizure monitoring devices. *Epilepsy Behav.* (2021) 125:108398. doi: 10.1016/j.yebeh.2021.108398
9. Hegde M, Chiong W, Rao VR. New ethical and clinical challenges in "closed-loop" neuromodulation. *Neurology.* (2021) 96:799–804. doi: 10.1212/WNL.0000000000011834
10. Schulze-Bonhage A, Sales F, Wagner K, Teotonio R, Carius A, Schelle A, et al. Views of patients with epilepsy on seizure prediction devices. *Epilepsy Behav.* (2010) 18:388–96. doi: 10.1016/j.yebeh.2010.05.008
11. Herrera-Fortin T, Bou Assi E, Gagnon MP, Nguyen DK. Seizure detection devices: a survey of needs and preferences of patients and caregivers. *Epilepsy Behav.* (2021) 114:107607. doi: 10.1016/j.yebeh.2020.107607
12. Patel AD, Moss R, Rust SW, Patterson J, Strouse R, Gedela S, et al. Patient-centered design criteria for wearable seizure detection devices. *Epilepsy Behav.* (2016) 64:116–21. doi: 10.1016/j.yebeh.2016.09.012
13. Van de Vel A, Smets K, Wouters K, Ceulemans B. Automated non-EEG based seizure detection: do users have a say?. *Epilepsy Behav.* (2016) 62:121–8. doi: 10.1016/j.yebeh.2016.06.029
14. Grzeskowiak CL, Dumanis SB. Seizure forecasting: patient and caregiver perspectives. *Front Neurol.* (2021) 12:717428. doi: 10.3389/fneur.2021.717428
15. Baud MO, Kleen JK, Mirro EA, Andrechak JC, King-Stephens D, Chang EF, et al. Multi-day rhythms modulate seizure risk in epilepsy. *Nat Commun.* (2018) 9:88. doi: 10.1038/s41467-017-02577-y

16. Catala A, Grandgeorge M, Schaff J-L, Cousillas H, Hausberger M, Cattet J. Dogs demonstrate the existence of an epileptic seizure odour in humans. *Sci Rep.* (2019) 9:4103. doi: 10.1038/s41598-019-40721-4
17. van Campen JS, Hompe EL, Jansen FE, Velis DN, Otte WM, van de Berg F, et al. Cortisol fluctuations relate to interictal epileptiform discharges in stress sensitive epilepsy. *Brain.* (2016) 139:1673–9. doi: 10.1093/brain/aww071
18. Nagaraj V, Lee ST, Krook-Magnuson E, Soltesz I, Benquet P, Irazoqui PP, et al. Future of seizure prediction and intervention: closing the loop. *J Clin Neurophysiol.* (2015) 32:194–206. doi: 10.1097/WNP.0000000000000139

Conflict of Interest: RM is the cofounder/owner of Seizure Tracker, LLC and reports financial income to Seizure Tracker, LLC, from Neurelis, UCB, Greenwich Biosciences, Neuropace and the Tuberous Sclerosis Complex Alliance. SC is supported by the National Institute of Neurological Disorders and Stroke, National Institutes of Health (5R25NS070680-12).

The remaining authors declare that the research was conducted in the absence of any commercial or financial relationships that could be construed as a potential conflict of interest.

frontiers in Neurology

ORIGINAL RESEARCH
published: 04 March 2022
doi: 10.3389/fneur.2021.703797

A Comparison of Energy-Efficient Seizure Detectors for Implantable Neurostimulation Devices

Farrokh Manzouri[1], Marc Zöllin[2], Simon Schillinger[2,3], Matthias Dümpelmann[1], Ralf Mikut[3], Peter Woias[2], Laura Maria Comella[2] and Andreas Schulze-Bonhage[1,4]*

[1] Epilepsy Center, Department of Neurosurgery, Medical Center — University of Freiburg, Faculty of Medicine, University of Freiburg, Freiburg, Germany, [2] Laboratory for Design of Microsystems, Department of Microsystems Engineering — IMTEK, University of Freiburg, Freiburg, Germany, [3] Institute for Automation and Applied Informatics, Karlsruhe Institute of Technology, Eggenstein-Leopoldshafen, Germany, [4] Faculty of Medicine, Center for Basics in NeuroModulation, University of Freiburg, Freiburg, Germany

Introduction: About 30% of epilepsy patients are resistant to treatment with antiepileptic drugs, and only a minority of these are surgical candidates. A recent therapeutic approach is the application of electrical stimulation in the early phases of a seizure to interrupt its spread across the brain. To accomplish this, energy-efficient seizure detectors are required that are able to detect a seizure in its early stages.

Methods: Three patient-specific, energy-efficient seizure detectors are proposed in this study: (i) random forest (RF); (ii) long short-term memory (LSTM) recurrent neural network (RNN); and (iii) convolutional neural network (CNN). Performance evaluation was based on EEG data ($n = 40$ patients) derived from a selected set of surface EEG electrodes, which mimic the electrode layout of an implantable neurostimulation system. As for the RF input, 16 features in the time- and frequency-domains were selected. Raw EEG data were used for both CNN and RNN. Energy consumption was estimated by a platform-independent model based on the number of arithmetic operations (AOs) and memory accesses (MAs). To validate the estimated energy consumption, the RNN classifier was implemented on an ultra-low-power microcontroller.

Results: The RNN seizure detector achieved a slightly better level of performance, with a median area under the precision-recall curve score of 0.49, compared to 0.47 for CNN and 0.46 for RF. In terms of energy consumption, RF was the most efficient algorithm, with a total of 67k AOs and 67k MAs per classification. This was followed by CNN (488k AOs and 963k MAs) and RNN (772k AOs and 978k MAs), whereby MAs contributed more to total energy consumption. Measurements derived from the hardware implementation of the RNN algorithm demonstrated a significant correlation between estimations and actual measurements.

Discussion: All three proposed seizure detection algorithms were shown to be suitable for application in implantable devices. The applied methodology for a platform-independent energy estimation was proven to be accurate by way of hardware implementation of the RNN algorithm. These findings show that seizure detection can

OPEN ACCESS

Edited by:
Maxime O. Baud,
University Hospital Bern, Switzerland

Reviewed by:
Brittany H. Scheid,
University of Pennsylvania, United States
Janir Ramos Da Cruz,
Wyss Center for Bio and Neuroengineering, Switzerland

****Correspondence:***
Matthias Dümpelmann
matthias.duempelmann@uniklinik-freiburg.de

Specialty section:
This article was submitted to Epilepsy, a section of the journal Frontiers in Neurology

Received: *30 April 2021*
Accepted: *29 November 2021*
Published: *04 March 2022*

Citation:
Manzouri F, Zöllin M, Schillinger S, Dümpelmann M, Mikut R, Woias P, Comella LM and Schulze-Bonhage A (2022) A Comparison of Energy-Efficient Seizure Detectors for Implantable Neurostimulation Devices. Front. Neurol. 12:703797. doi: 10.3389/fneur.2021.703797

be achieved using just a few channels with limited spatial distribution. The methodology proposed in this study can therefore be applied when designing new models for responsive neurostimulation.

Keywords: seizure detection, responsive neurostimulation, low-power hardware implementation, random forest, recurrent neural network, convolutional neural network

INTRODUCTION

Problem Definition

Epilepsy is a brain disorder characterized by recurrent epileptic seizures (1) and is one of the most common neurological diseases, affecting nearly 70 million people worldwide (2). Epileptic seizures are defined as episodes of excessive or abnormal synchronous neuronal activity in the brain, and can be accompanied by clinical neurological symptoms such as abnormal movements, abnormal sensory phenomena, loss of consciousness, or alterations in consciousness. Epilepsy is therefore associated with considerable neurological morbidity. Epileptic seizures can vary in form, not only between different patients but also within a single patient.

Despite advances in the development of medication, about 30% of epilepsy patients are resistant to a treatment with antiepileptic medications (3). Nevertheless, only 7–8% of these patients are surgical candidates (4).

In the case of focal seizures, surgical resection of the brain region(s) generating the seizures may be used to prevent further seizures. Nonetheless, because not all of these patients have a unifocal seizure onset zone (SOZ) and the epileptogenic brain tissue cannot always be resected without significant functional loss, more innovative therapeutic approaches are urgently required.

A recently proposed treatment approach for these patients is electrical stimulation of the epileptic focus during the early phases of a seizure in order to interrupt its spread across the brain (2). This can be accomplished using a closed-loop neurostimulation implant, which records electrical brain activity via a set of electrodes and continuously monitors electroencephalography (EEG) activity applying a seizure detection algorithm. It then triggers electrical stimulation at the SOZ via the same electrodes in the advent of an emerging seizure. This approach requires the early detection of seizures with high accuracy based on EEG. Furthermore, the selected seizure detection algorithm should be computationally efficient to have a low energy consumption for long-term application in an implantable, battery-powered device.

Currently, the only FDA-approved implantable device for clinical applications that applies this principle is the so-called "RNS device" (Neuropace Inc., USA). This device provides electrical stimulation via a generator fixed to the skull, with electrodes within or directly above the cortical region of the epileptic focus (1). Whereas, this device has proven to be efficacious both under short-term and long-term applications (3, 5, 6), its implantation is complex and the risk of infection at the implantation site is high, due to the intracranial placement of the electrodes (4).

In addition, the RNS device suffers from a high number of false detections. As false detection rates (FDRs) of the device are not reported explicitly, they can only be derived from the length of reported stimulation times. According to Heck et al. (3) a mean stimulation period of 5.9 min was applied. With a pulse burst duration of 100 ms, this corresponds to 3,540 stimulations per day and a minimum of 354 detections per day and 10,620 detections per month. At a baseline seizure frequency of 8.7 per month, this corresponds to >1,220 false detections per crisis event. This high number of interventions leads to the question of how much efficacy is related to closed-loop suppression of seizure-related ictal activity, in contrast to long-term depression of seizure probability by neuromodulation. In addition, improved seizure detection algorithms with higher specificity of interventions can lead to a longer neurostimulator battery life, due to the reduced number of stimulations; accordingly, it may lead to fewer side effects of the stimulation.

Previous Studies

The development of seizure detection algorithms based on EEG data began several decades ago (7). The initial objective was to reduce the workload of reviewing continuous long-term recordings in epilepsy monitoring units and presenting the neurologist with intervals of only the highest clinical relevance. In addition, more recent studies have addressed the development of seizure detection algorithms for responsive stimulation to prevent the onset or spread of seizure activity in the early phase of a seizure (8). Such application scenarios require a reliable seizure detector at a reasonable computational load. Furthermore, performing an intervention exactly at the onset of a seizure, requires early detection, which is considered in more recent approaches (9–11). Because of the high variation in EEG patterns that characterize a seizure (12), the large variability in background EEG activity among patients, and the intra-individual fluctuations in EEG activity, the problem of seizure detection remains an active research topic (13–15). While several publications have proposed seizure detection algorithms for either offline or online applications, only a limited number of studies have addressed the limitations of seizure detection for closed-loop applications. One particular limitation is the use of only a few electrodes for seizure detection, which is driven by properties of the neurostimulator. Seizure detection using a low number of electrodes has recently achieved increased interest, as this concept enables mobile seizure monitoring (16–18). In contrast, outpatient monitoring with a complete electrode setup is seen as stigmatizing—as in any application that exposes the patient to the public—and is therefore not feasible in practice. A recent study by Vandecasteele et al. (19) described a seizure

detection algorithm based on a support vector machine classifier using behind-the-ear EEG data derived from only four electrodes. However, although the proposed model had a relatively low FDR, it also had low sensitivity (19). In another recent study, Dan et al. (20) proposed a method for detecting electrographic patterns during absence seizures (short, non-motor generalized onset seizures); this was based on a linear multichannel filter which was precomputed with the spatiotemporal signature of the seizure and the peak interference statistics that could run on a microcontroller. Nevertheless, this particular method requires 20 recording channels. Therefore, the need to develop a seizure detection algorithm that can detect seizures in early stages not only with high sensitivity and specificity, but also with low computational power and a limited number of electrodes has not yet been fulfilled.

Regarding energy estimation of the seizure detection algorithms, several methods have been introduced. García-Martín et al. (21) reviewed the current approaches used to estimate energy consumption in machine learning. They suggested dividing the common methods of energy estimation into three different categories, namely at the software-application level, the software-instruction level, and the hardware level (21). The software categories describe the energy related to the algorithm features, and are based either directly on the application level, or on the underlying instructions. Here, a model links the instructions to the energy demand. The hardware level relates the energy caused by the application to the components in the hardware setup. Among the methods, the instruction level in the software category is most relevant to the scope of this study. At the instruction level in particular, the energy consumption is evaluated on the basis of program-specific instructions. This approach was followed by Rouhani et al. (22), in which the power consumption of a deep neural network (DNN) was estimated using the number of multiply-accumulate (MAC) operations. Likewise, Taghavi et al. (23) estimated the hardware requirements of DNNs and decision tree ensembles in terms of MAC operations and parameters required for the classification model. They compared several studies using energy efficiency, hardware complexity and classification performance as parameters (23). Yang et al. (24) applied this approach to estimate the energy consumption for a CNN algorithm. They constructed the total energy consumption by first extending the model based on MAC operations and model parameters with the number of memory accesses (MAs). Next, they weighted these parameters with measured MAC operations and MA energies to calculate the total energy dissipation (24).

Own Approach

A minimally invasive, implantable neurostimulation approach was recently developed using subgaleally placed stimulation electrodes (EASEE System, Precisis AG, Heidelberg). The subcutaneous system uses electrodes that are placed outside the cranium over the SOZ, and connected to a pulse generator on the trunk (**Figure 1**). For the integration of a seizure detection algorithm into this kind of fully implantable intervention device, several limitations must first be considered. The seizure detection algorithm must perform well despite a low number of electrodes, limited spatial coverage, and low computational power. To address this issue, three patient-specific seizure detection algorithms that only apply four channels each were developed and their performance was evaluated: random forest (RF), convolutional neural network (CNN), and long short-term memory (LSTM) recurrent neuronal network (RNN). In addition, to evaluate their suitability for application in an implantable, responsive neurostimulator, their respective computational load and power consumption were estimated. As in this study, the classification rate is 1 Hz; the estimated energy demand in μJ is equal to the power consumption in μW. To estimate the required computational load, an instruction-level model based on application-specific instructions and MAs was developed and validated.

FIGURE 1 | A minimally invasive electrode setup as a part of an implantable system for focal epilepsy (Copyright © Precisis AG, Heidelberg, Germany).

The quality of subcutaneous recordings was compared to standard surface EEG recordings by Duun-Henriksen et al. (25). They showed that some aspects of the subcutaneous recordings might be similar, or even superior, to surface EEG recordings (25). Likewise, Weisdorf et al. (26) reported a high similarity between EEG data from subcutaneous and proximate scalp electrodes in patients with temporal lobe epilepsy. Accordingly, the seizure detection algorithms developed in the current study were tested on surface EEG data from electrodes configured to resemble the subgaleal electrode placement.

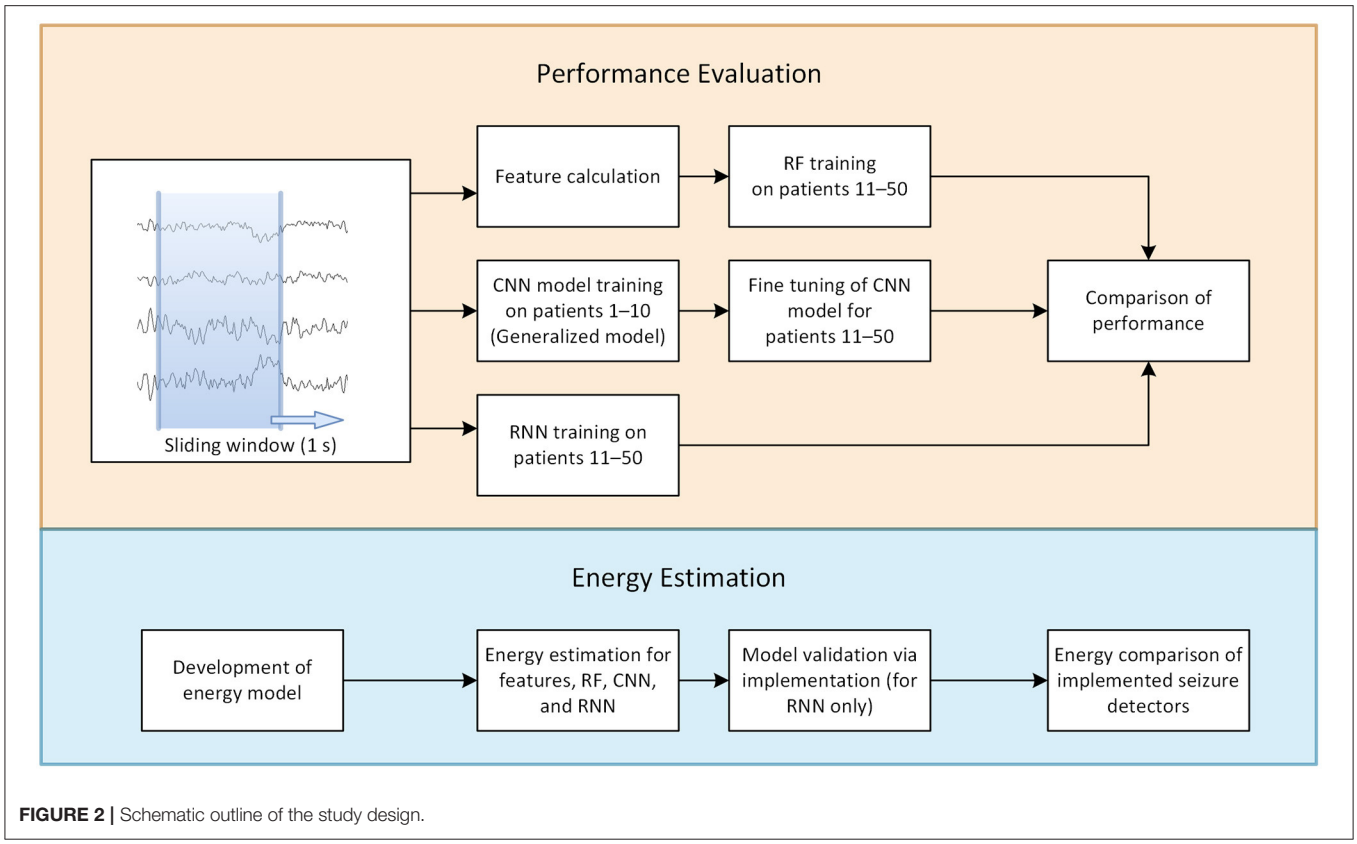

FIGURE 2 | Schematic outline of the study design.

MATERIALS AND METHODS

A schematic outline of the study design is presented in **Figure 2**. In the following sections, the methodology used for evaluating performance and estimating power consumption is described. A more detailed description of the energy estimation method is provided in the **Supplementary Material** section.

Dataset

The dataset consists of surface EEG recordings from 50 patients (23 female; age range, 14–66 years; mean age, 32.5 years) with focal-onset seizures at the Epilepsy Center Freiburg, Germany; the total number of seizures was 357. **Figure 2** demonstrates how the dataset was split for training the different classifiers, i.e., patients 1–10 were selected for pre-training (CNN only), while the remaining 40 patients (11–50) were selected for training and evaluation (all 3 methods). Due to considerable imbalance between the ictal and interictal classes for each seizure, an hour-long time window around each seizure was selected for evaluation and the remaining data were then excluded from analysis. Patients were selected based on long-term video recordings that included at least five seizures, with electrodes positioned over the SOZ according to the 10–10 electrode layout (27). Electrode selection was performed to represent device layout. Expert epileptologists defined the SOZ by visual exploration of the seizure onset electrodes recordings, taking into account the inter-electrode distances. The study was approved by the local Ethics Review Board. Informed consent of the patient covered the in-house use of EEG recordings. EEG data were recorded at a 256 Hz sampling rate on a 256-channel DC amplifier with 24-bit resolution (Compumedics, Abbotsford, Australia). For anti-aliasing, a low-pass filter with a cut-off frequency of 100 Hz was applied. Five electrodes covering the SOZ were selected for seizure detection in each patient.

Data Preprocessing

A small number of preprocessing steps were applied to reduce the effects of noise and artifacts on the performance of the seizure detection algorithms. First, invalid segments of the EEG signals, including segments where the signal was not recorded due to electrode deficiency or during the electrode impedance measurement, were excluded from analysis. Next, to improve the signal quality, a 10th order Chebyshev Type-II IIR (infinite impulse response) bandpass filter with a stopband attenuation of 40 dB and respective stopband frequencies of $f_1 = 0.1\ Hz$, and $f_2 = 48\ Hz$ was applied. The settings were chosen to filter power line noise and reduce the influence of broad-band muscle activity, spanning up to 200 Hz (28). To remove high-amplitude sharp artifactual transients, another artifact rejection step was added in which periods of $T_p = 1\ s$ that contain amplitudes higher than 1 mV were removed. This threshold was set in such a way that allowed amplitudes in the range of 100 μV [typical of EEG signals in healthy subjects (29)], as well as interictal spikes up to ∼140 μV (30) to remain in the data. Moreover, the selected threshold

value allows a good trade-off between excluding artifacts vs. retaining the scarcely represented ictal patterns in the data, so as to avoid further imbalance in the dataset. Finally, to account for the locality of the target electrode configuration, the EEG channels were re-referenced by subtracting the recordings of the centrally positioned electrode from those of each of the peripheral electrodes.

Seizure Detection

Seizure detection can be modeled as a time-series classification in which ictal phases (seizures) and interictal phases (non-seizures) are classified. In this section, the three proposed supervised-learning algorithms for seizure detection are detailed.

Random Forest (RF)

RF is an ensemble-learning method for classification or regression that operates by constructing a group of decision trees in which each tree is grown using binary decisions (each parent node is split into two children) (31). This method combines the "bagging" technique with the random selection of features. The randomness of each tree is accomplished in two ways: first, by random selection of a subset of approximately two thirds of the data for training the tree, and second, by feature selection of the nodes of each tree, which is done using a randomly selected subgroup of features. The remaining one third of the training data is used for out-of-bag error evaluation and performance calibration of the tree. In this study, the number of binary decision trees was set to 100. Entropy was selected as the branching index for growing each decision tree. The best feature (splitter) from the eligible, randomly selected subset of features, which has the highest importance, is used to split the node. In line with the Liaw and Wiener (32) results, the optimal number of randomly selected features at each tree node is sqrt(N), where N is the number of features. In this study, 16 time- and frequency-domain features were calculated from the EEG data as input. The time-domain features were mean, maximum, mean absolute deviation (MAD), variance, skewness, kurtosis, line length and entropy. Frequency-domain features included values for the maximum, mean, and variance of the power spectrum, power in the theta (4–8 Hz), beta (13–30 Hz), and gamma band (30–45 Hz), spectral entropy, and epileptogenicity index, the latter of which is defined as the ratio of power in the higher frequency bands (beta + gamma) vs. the lower frequency bands (theta + alpha) (33). As a result, four features were randomly selected at each decision tree node. To maintain a limited tree size and to confine the required memory for hardware implementation, the maximum depth of the decision tree was limited to 10. Bootstrap samples were used while building the decision trees. The sample weights for each class were adjusted to be inversely proportional to the class frequencies in the training data. A non-overlapping time window of 1 s was selected for seizure detection. For implementation of the RF, the freely available and open source Scikit-learn machine learning library was used (34).

Convolutional Neural Network (CNN)

CNN is a class of DNNs that were inspired by biological processes (35) and are commonly applied for pattern recognition (36). A CNN consists of an input layer, multiple hidden layers, and an output layer. The hidden layers consist of convolutional layers, pooling layers, and potentially fully connected layers. In the convolutional layers, the input is convolved with filters to detect patterns, and the results are conveyed to the activation function which is usually a rectified linear unit (ReLU). In addition, CNNs may include local or global pooling layers that reduce the dimensions of the data. The pooling layer helps to control overfitting by making the pattern representation almost invariant to minor translations of the input. This is accomplished by striding a window over the output of the activation function and pooling the average or maximum value. Subsequently, the results matrix is flattened and fed to the fully connected layers to drive the classification decision.

To create the inputs for the convolutional network, sliding windows of 1 s over the EEG data were processed. First, the data was rescaled by dividing it by the standard deviation of the training data. Next, the data was normalized using an estimation of the hyperbolic tangent function, as shown in the following equation:

$$\hat{x}(t) = \tanh(0.2 \cdot x(t))$$

To facilitate hardware implementation of the hyperbolic tangent function and avoid the need for a lookup table, a linear approximation of the hyperbolic tangent was applied for classification:

$$\text{lintanh(x)} := \begin{cases} x/1.2 & -1.2 \le x \le 1.2 \\ 1 & x > 1.2 \\ -1 & x < -1.2 \end{cases}$$

The architecture of the proposed CNN in this study is shown in **Table 1**. Four channels of simultaneously recorded raw EEG data with a duration of 1 s (256 data points) were selected as the input. In the first convolutional layer, a kernel size that extends over time and all four EEG channels was used to facilitate efficient learning of the spatiotemporal patterns. No padding was applied in the convolutional layers. In all hidden layers, batch normalization was applied after the convolutions were performed (37). The ReLu was selected as the activation function. Dropout regularization was used during training to reduce overfitting and generalization error (38). In the last two layers, two fully connected layers were employed.

Due to the limited amount of available data for each patient, the transfer learning method was applied for training the model. This is generally done by applying the gained knowledge from a learning problem to improve learning on a related problem. Accordingly, the model was first pre-trained with data from 10 patients. For each of the remaining 40 patients, the model was subsequently fine-tuned using patient-specific data. Because the classes (ictal vs. interictal) were imbalanced, the class indices were weighted to balance the weighting of the loss function during the training phase (39). Each model was trained for 500 epochs with a batch size of 512. For weight optimization, an Adam solver (40) with a learning rate of 10^{-3} was used. Binary cross-entropy was selected as the loss function.

TABLE 1 | Architecture of the proposed CNN.

Layer	Operation	Output	Parameters #
	Input (C × 256)	C × 256 × 1	–
1	15 × Conv2D (C × 25)	1 × 232 × 15	1,515
	Batch Normalization	1 × 232 × 15	60
2	MaxPool2D (1 × 4)	1 × 58 × 15	0
	Dropout (0.2)	1 × 58 × 15	0
3	15 × Conv2D (1 × 11)	1 × 48 × 15	2,490
	Batch Normalization	1 × 48 × 15	60
4	MaxPool2D (1 × 4)	1 × 12 × 15	0
	Dropout (0.2)	1 × 12 × 15	0
5	10 × Conv2D (1 × 5)	1 × 8 × 10	760
	Batch Normalization	1 × 8 × 10	40
	Dropout (0.2)	1 × 8 × 10	0
6	Dense (8)	8	648
7	Dense (4)	4	36
8	Sigmoid	1	5

C, Number of channels.

Recurrent Neural Network (RNN)

Recurrent Neural Networks (RNNs) are a class of neural networks with recurrent connections that allow the network to store information over time. RNNs started to gain attention with the introduction of LSTM cells, which significantly improves their performance. The LSTM cell was first introduced by Hochreiter and Schmidhuber (41) to overcome the problem of vanishing gradients in RNNs. With its internal state, the LSTM cell is capable of storing information over time, depending on its input and output values. The flow of information is controlled by the so-called gates that can learn which data in a sequence is important to remember or disregard. Gates can be seen as controlling valves with the ability to let the information pass through by multiplying it by the gate values. These features allow LSTM cells to be used in time-series problems. Combined with other neural network layers, they form an LSTM neural network. Such networks are used across many different applications and are considered especially useful in sequence prediction or sequence classification problems (42).

The proposed RNN architecture is based on the work of Hussein et al. (43) with a few modifications to reduce the complexity of the model. Similar to CNN, four channels of simultaneously recorded raw EEG data with the duration of 1 s (256 data points) were selected as the input. As shown in **Table 2**, the network consists of an LSTM layer containing 20 cells with an input size of 256. Similar to the CNN, a dropout layer is used for regularization. This is followed by a time-distributed dense layer consisting of 20 dense cells with a linear activation function that is computed at every time step. Subsequently, the global average pooling layer averages the dense cell outputs over time. Finally, as this is a binary classification task, an output dense layer with a sigmoid activation function is used that simplifies the calculation.

The classifier performance was investigated with both raw data and its time-derivative for each individual channel. The latter was calculated through the difference of subsequent values for all electrodes and all time steps as:

TABLE 2 | Architecture of the proposed RNN.

Layer	Operation	Output	Parameters #
	Input (C × 256)	C × 256 × 1	–
1	LSTM (20)	256 × 20	2,000
	Dropout (0.1)	256 x 20	0
2	Time-Distributed Dense (20)	256 x 20	420
3	Global Average Pooling 1D	20	0
4	Dense (1)	1	21

C, Number of channels.

$$\Delta x_{c_k} = x_{c_k} - x_{c_{k-1}}$$

where c corresponds to the electrode number and $k \in \{1, \ldots, K\}$ is the sample index with K samples in the corresponding seizure. Next, the training data were prepared by striding a moving window over the sample axis of the input data. For training, a step size of $stride_{inter-ictal} = 16$ was chosen for the interictal class, and a $stride_{ictal} = 1$ was used for the ictal class; this was done both to account for the imbalance and to increase the ictal sample size. For validation, a single seizure that was excluded from the training data was used with the same stride settings as those used for training. The test set was created with a moving window step size of $stride = 256$. Furthermore, early stopping (44) was applied as another regularization technique to prevent overfitting and reduce training time. The patience parameter was set to 10 epochs. It defines the maximum number of epochs than may occur until an improvement in the validation dataset is observed, before stopping the training process. Validation loss was used as the performance metric to decide whether early stopping was necessary. The samples were presented with a mini-batch size of 256. The binary cross entropy was chosen as the loss function and the Adam optimizer chosen to tune the learning rate. Finally, to further improve the classifier performance, the output probabilities were median filtered with a moving median size of three.

Performance Evaluation

For performance evaluation of the seizure detection algorithms, the "leave-one-out" method was used for cross-validation, whereby in every iteration one seizure was selected for testing and all remaining data were used for training. The EEG data from ten patients were used to pre-train the CNN model. Performance evaluation was conducted across the remaining 40 patients (total number of seizures = 286) for each of three proposed classifiers. Evaluation metrics were calculated for each patient separately and then averaged across all the patients. Metrics for the performance evaluation of seizure detection algorithms are either dependent on a threshold-level set for the seizure probability, or are threshold-free. Accepted threshold-dependent metrics for performance evaluation of the seizure detectors are sensitivity, FDR, and average detection delay. For calculation of the sensitivity, a seizure was counted as correctly detected when it was detected at least once

during the ictal phase. Regarding the FDR, false detections within a 5 s window were counted only once, since they generally refer to the same detected pattern. Nevertheless, there is an inevitable trade-off between these threshold-dependent evaluation metrics. For example, a higher sensitivity and lower detection delay can be attained if a higher FDR is accepted. While the use of these metrics facilitates the estimation of seizure detector performance in different application scenarios, the use of threshold-free metrics simplifies the comparison of the classifier performance by combining threshold-dependent metrics into one threshold-free metric. To yield a threshold-free comparison of the classifiers, the area under the curve (AUC) of the receiver operating characteristic (ROC) and precision-recall (PR) curves were selected as performance metrics. For calculating threshold-free metrics, the true and false detections were counted for each time window (1 s), which is different from how the threshold-dependent metrics were calculated. Considering that detection delay is not projected in the AUC, a modified version of the selected metrics was used as additional metrics, denoted as "early seizure AUC." In this case, only those seizures detected within the first 10 s of seizure onset (as determined by the epileptologist) were deemed successfully detected.

Energy Estimation

The energy estimation of the proposed seizure detection algorithms in this study is based on the number of arithmetic, memory read, and store operations. The total energy required was estimated via the energy costs per operation (24). The method in Yang et al. (24) was modified to use the energy estimation per operation based on the findings reported in Horowitz (45), instead of measuring the energy for specific hardware. Additional measurements were performed, and assumptions were made for operations not included in their proposed method. **Table 3** shows an overview of the operations and corresponding energy consumption relevant for the developed model. Horowitz (45) defines the rough energy cost in a 45 nm process technology for the fundamental operations and MAs. In addition, Horowitz included the energy cost of the microprocessor overhead, which deliberately was not taken into account in the current study for the purpose of obtaining a hardware-independent measure. Nevertheless, the proposed model can be adapted to specific hardware if required. In addition, it enables the identification of operations that have a higher impact on energy consumption. Hence, it helps in implementing efficient signal processing algorithms, or aids in selecting the most suitable microprocessor.

The total energy is calculated as $E_{tot} = (N_{load} + N_{store}) \cdot E_m + \sum_x N_x \cdot E_x$, where N_{load} is the number of load operations, N_{store} the number of store operations, E_m the MA energy, N_x and E_x the number of operation x and the corresponding energy defined in **Table 3**.

The following assumptions were additionally made: (1) the energy required for a MAC operation E_{MAC} is defined as $E_{MAC} = E_{add} + E_{mult}$. (2) The energy overhead of the square root function, which is not included in Horowitz (45), corresponds to that of a division operation. This assumption is based on the specification of the ARM Cortex-M4F floating-point unit, which states that the two operations have the same number of execution cycles.

TABLE 3 | Energies assumed for the estimation of the power consumption.

Parameter	Energy
E_m	5 *pJ*
$E_{int32-add}$	0.1 *pJ*
$E_{int32-mult}$	3.1 *pJ*
$E_{float32-add}$	0.9 *pJ*
$E_{float32-mult}$	3.7 *pJ*
$E_{compare}$ [a]	0.9 *pJ*
$E_{float32-divide}$ [b]	26.3 *pJ*
$E_{float32-1-cycle}$ [c]	3.7 *pJ*

E_m is half the cache energy estimated by the energy cost table for 45 nm at 0.9 V from Horowitz (45) for an 8 kB 64-bit wide cache access, as only 32-bit loads are considered in this study. $E_{float32-add}$, $E_{float32-mult}$, $E_{int32-add}$, $E_{int32-mult}$ values are also from Horowitz (45).

[a] As a compare operation can be performed as a subtraction which is basically an addition, the same energy is assumed for the compare operation. [b] A benchmark on the Ambiq Apollo 3 Blue with ARM Cortex M4F processor measured by executing three different measurements with a loop containing float multiply, divide and both instructions to cancel out loop and other overhead, showed a factor of 7.1 of float division energy consumption compared to float multiply energy consumption. [c] Other floating-point operations that take one clock cycle are considered to consume as much as a multiply operation.

Random Forest Energy Estimation

For energy estimation of the RF classifier, the number of required arithmetic and memory operations for the 16 time- and frequency-domain features were first calculated. A 32-Bit floating-point arithmetic was chosen to obtain an energy estimation value comparable to that of the RNN and CNN. Divisions by a constant are considered as multiplications, as their energy consumption is lower compared to a division. Each feature is considered to be computed over the sample or time axis in the input data array $v_{in} \in \mathbb{R}^{N_w \times C}$, for $N_w = F_s \cdot T_w$, where F_s is the sampling frequency and T_w is the length of the window required for an observation. In this section, individual energy considerations are made for a single input channel. Consequently, the total energy is calculated by multiplying the required energy for a single channel with the number of channels C, assuming that all features are calculated for each channel.

Time-Domain Features

To improve computational efficiency and avoid redundant calculations, zero-mean values of the signal and their square values were calculated only once, and then shared along a set of features. The required number of arithmetic operations (AOs) and MAs were estimated based on the number and type of mathematical operations needed to calculate the features. **Table 4** shows the equations that were considered for the calculation of the time-domain features, with x being the vector containing the input samples.

TABLE 4 | Assumed equations for the Time-domain features.

Time-Domain feature	Equation
Maximum	$\max - \text{val} = max(x)$
Mean	$\overline{x} = \frac{1}{N_w} \cdot \sum_{i=1}^{N_w} x_i$
MAD	$MAD = \frac{1}{N_w} \sum_{i=1}^{N_w} \lvert x_i - \overline{x} \rvert$
Variance	$var = \frac{1}{N_w} \sum_{i=1}^{N_w} \left(x_i - \overline{x}\right)^2$
Skewness	$g_m = \frac{1}{N_w \cdot s^3} \sum_{i=1}^{N_w} \left(x_i - \overline{x}\right)^3$
Kurtosis	$w = \frac{1}{N_w \cdot s^4} \sum_{i=1}^{N_w} \left(x_i - \overline{x}\right)^4$
Line Length	$LL = \sum_{k=2}^{N_w} \lvert x_k - x_{k-1} \rvert$
Entropy	$H = -\sum_i p_i \cdot log_2(p_i)$

TABLE 5 | Frequency-domain features and their respective equations that were considered in this work.

Time-Domain feature	Equation
Spectral entropy	$H = -\sum_i p_i \cdot log_2(p_i)$, with $p_i = \frac{P_i}{\sum_{i=0}^{L-1} P_i}$
Mean spectral power	$\overline{P} = \frac{1}{L} \cdot \sum_{i=1}^{L} P_i$
Maximum spectral power	$max_P = \max(P)$
Spectral power variance	$var_P = \frac{1}{L} \sum_{i=1}^{L} \left(P_i - \overline{P}\right)^2$
Band power	$BP = \sum_{i=f_1/\Delta f}^{f_2/\Delta f} P_i$, with $\Delta f = \frac{1}{t_w}$
Epileptogenicity index	$Epi_{index} = \frac{P_\beta + P_\gamma}{P_\theta + P_\alpha}$

P is the power spectrum vector, obtained by the DFT, f_1 the lower band frequency, f_2 the upper band frequency of the band power, and t_w the duration of the sampled window in the time-domain.

Frequency-Domain Features

The calculation of the frequency-domain features is based on the power spectrum $P \in \mathbb{R}^L$, where L is the number of frequency bins. It is obtained using the squared values of the Discrete Fourier Transform (DFT) of the windowed raw time-domain signal $x(t)$. To minimize spectral leakage, a Hanning-window was applied before performing the DFT. The equations of the frequency-domain features are summarized in **Table 5**.

Random Forest Classifier

For the classifier itself, the highest possible energy consumption was considered, whereby all 100 trees are used for classification and the tree branches are developed to the maximum depth, which, in this case, was set to 10.

Convolutional Neural Network and Recurrent Neural Network Energy Estimation

The same scheme was applied for estimating the AOs for the proposed CNN and RNN models, where each processing layer was considered individually. For the CNN model, all the convolutional layers were estimated according to the standard CNN implementation. Batch normalization parameters were incorporated into the CNN filter parameters. The same applies to the RNN, where the original LSTM implementation was considered. For calculation of hyperbolic tangent and sigmoid activation functions, look-up tables with approximated values were used in both architectures. A more detailed description of the individual layers can be found in the **Supplementary Material** section.

Energy Estimation Validation

To validate the feasibility of estimating energy consumption based on the number of MAs, instructions and AOs, the RNN classifier was implemented into an ultra-low-power Apollo 3 Blue microcontroller from Ambiq (Austin, Texas, USA). The energy consumption was measured and compared to the energy calculated.

The energy consumption was measured with the Texas Instrument EnergyTrace™ technology for different numbers of LSTM cells, $N_{LSTM} \in \{2, \ldots, 20\}$. The LSTM cells in the model were decreased stepwise from 20 to 2, and the corresponding classification energy consumption was determined for each step.

The validity of the model was proven by analyzing the correlation between measured and calculated classification energy. For this purpose, a linear ordinary least squares regression was performed using the Statsmodels toolbox, which is a Python module (46). The quality of the fit was investigated by evaluating the residuals of the fit with the adjusted R^2-value (R^2: coefficient of determination). In addition, a *t*-test was conducted to investigate the significance (significance level: 5%) of the estimated coefficients. Pearson correlation coefficients were calculated using SciPy, a free and open-source python library, as measure of correlation between the two values.

RESULTS

In this section, the results are presented in two parts. First, the implemented seizure detectors are compared by using several metrics to evaluate and compare their performance. Using these metrics provides valuable insight into the characteristics of these seizure detectors as well as their suitability for closed-loop applications. In the second part, the results of the power consumption estimation for the proposed seizure detection algorithms are presented. These estimations are based on hardware implementation on the Apollo 3 Blue microcontroller.

Classifier Performance

Boxplots were selected for visualization of the results because they display the spread of the plotted variable and provide an indication of the variable distribution, such as symmetry and skewness. Moreover, boxplots display the outliers, which help in the understanding how often a classifier fails to perform robustly. The AUC-ROC scores of the three seizure detection algorithms are shown in **Figure 3**.

For the RNN classifier, two types of input were used and their performance was evaluated. Application of the time-derivative of the data, in place of using the raw data as inputs to the RNN, improved the mean AUC-ROC across all patients ∼2.5% for normal seizure detection, and 6.4% for early seizure detection, respectively. For this reason, the results of the time-derivative are presented here.

The median (mean) AUC-ROC score was the highest across all patients for the RNN 0.941 (0.910), compared to that of the

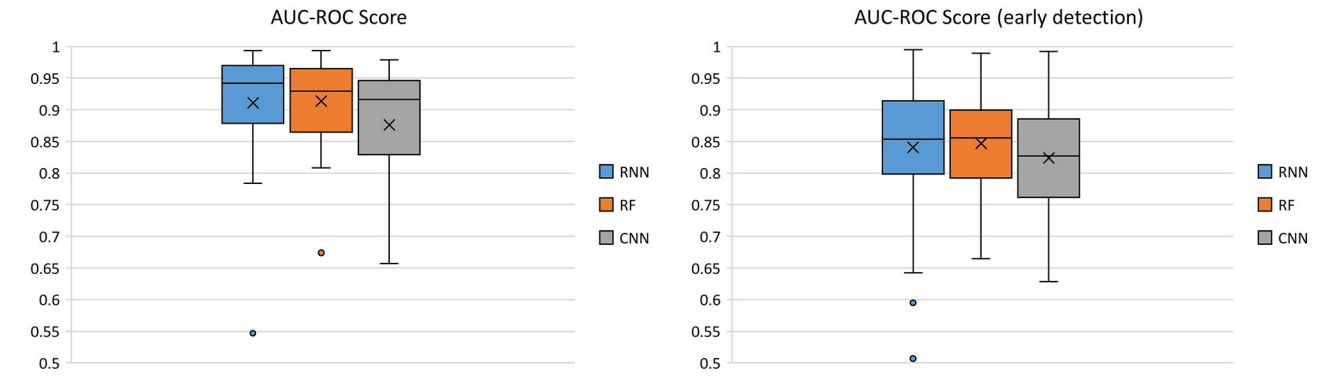

FIGURE 3 | Comparison of the three classifiers across 40 patients using the AUC-ROC score as the performance metric.

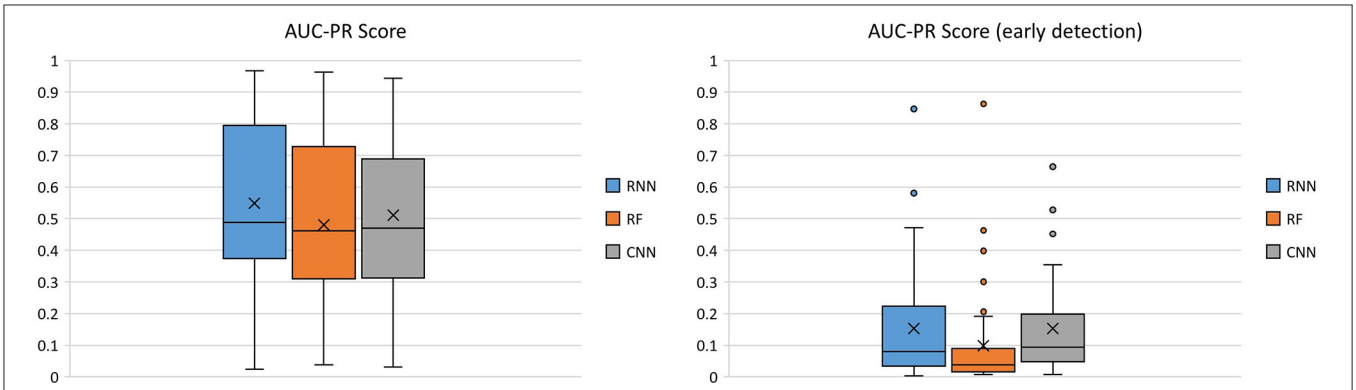

FIGURE 4 | Comparison of the three classifiers across 40 patients using AUC-PR score as the performance metric.

RF 0.929 (0.914) and CNN 0.916 (0.876). The average AUC-ROC score for early seizure detection was similar between the RNN 0.853 (0.840) and the RF 0.855 (0.847), followed by CNN 0.827 (0.824).

Due to the fact that "ictal" and "interictal" classes are very imbalanced, another useful measure of prediction success is the AUC-PR score. The PR curve shows the trade-off between the precision and recall of different thresholds. The AUC-PR score of the three classifiers across 40 patients is shown in **Figure 4**.

The RNN had the highest median (mean) AUC-PR score across all patients [0.487 (0.548)], compared to that of the RF 0.462 (0.481), and the CNN 0.470 (0.511). The average AUC-PR score for early seizure detection was similar between the RNN 0.080 (0.153) and CNN 0.093 (0.152), but lower for the RF 0.038 (0.099).

For a more intuitive representation of seizure detector performance, sensitivity (**Figure 5**), FDR (per hour), and average detection delay (in seconds) for optimized probability thresholds, based on F1-score, were calculated for all seizure detectors across the 40 patients.

Median (mean) sensitivity across all 40 patients were 1.0 (0.90) for the RNN, 1.0 (0.93) for the RF, and 1.0 (0.94) for the CNN. The FDR (per hour) across all patients was 7.77 (12.93) for the RNN, 18.59 (22.49) for RF, and 14.25 (17.89) for CNN. The median (mean) average detection delay (s) across all patients was 8.05 (9.70) for the RNN, 7.65 (8.70) for RF, and 5.60 (6.62) for CNN.

Energy Estimation

The total number of MAs and AOs required for hardware implementation of the proposed seizure detection algorithms is shown in **Figures 6**, **7**. A window size of $t_w = 1s$ was chosen, resulting in a number of samples, $N_w = F_s \cdot t_w = 256$, multiplied by the number of channels, $C = 4$.

Figure 6A shows the number of MAs, AOs, and the resulting energy estimation for the calculated time and frequency domain features of EEG as input for the RF classifier. Thereby, it underlines the difference of energy consumption among the different features. The most energy intense operations are required to calculate the power spectrum, the spectral entropy, and the entropy.

Figure 6B shows the number of MAs, AOs, and corresponding energy for every layer of the CNN. It can be observed that the network consumes most of the energy in the convolutional layers. About 69% of the energy in the convolutional layers relates to MAs.

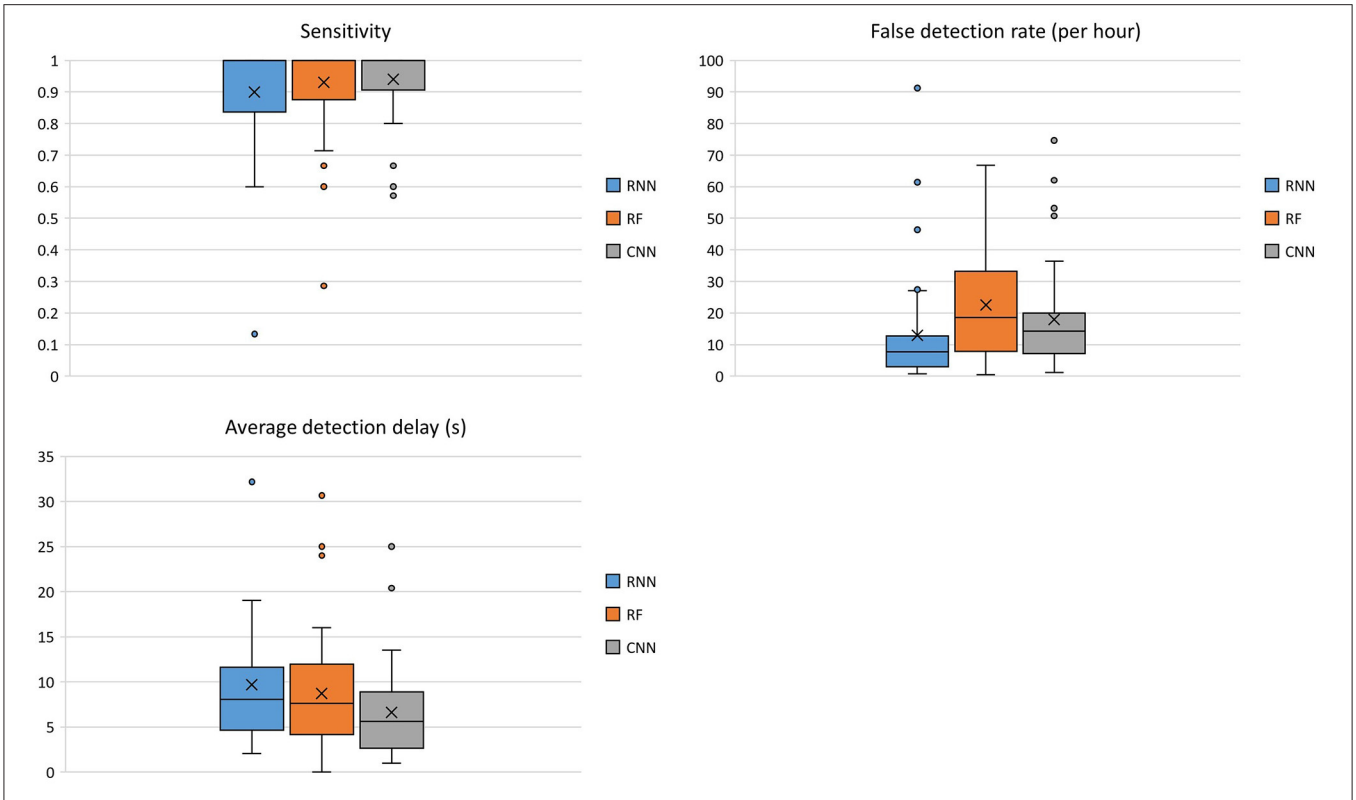

FIGURE 5 | Comparison of the seizure detectors across 40 patients using sensitivity, FDR (per hour), and average detection delay (s) as the performance metrics.

Figure 6C shows that the LSTM layer is by far the most energy intense layer of the RNN. The energy ratio of energy related to MA is about 58% of 6.42 μJ. The Time-Distributed (Dense) layer, however, shows with 69% of 1.55 μJ the same behavior as the convolutional layer in the CNN.

Figure 7 compares the three algorithms and underlines the superiority of the RF classifier over the RNN and the CNN in terms of energy consumption. RNN requires 16.6 times and the CNN 14.5 times more energy than that consumed by the RF.

The total number of AOs required for CNN, RNN, and RF were estimated as denoted in **Table 6**.

Energy Estimation Validation

The energy model was evaluated based on the RNN implementation. The results showed that all the coefficients of the fitted linear regression (as shown in **Figure 8**) are significant.

A linear trend with a slope b_1 of 32.29 and an offset b_0 of 17.06 μJ were observed for the RNN implementation using an Apollo 3 Blue ARM Cortex-M4F microcontroller. The model was proven to be accurate with an adj R^2 value of 0.9990 and a high correlation coefficient r of 0.9995. As b_1 serves as a hardware-dependent scaling factor, it follows that the measured energy consumption for this specific hardware setup is over the estimated energy consumption by this factor. Its high value in this case is due to the instruction overhead, which is not part of the model. Furthermore, the offset b_0 is explained by the hardware-dependent static power consumption in the target system.

An oscillation of the residuals of the linear fit with varying number of LSTM cells can be observed in **Figure 8**. A possible cause of this phenomenon is the loop-unrolling of the pre-compiled ARM DSP-library. A loop unrolling with a factor of 4 is applied to the vector dot-product function that triggers the running of extra loop-overhead code for vectors longer than a multiple of 4.

DISCUSSION

In this study, the development of seizure detection algorithms for integration into responsive neurostimulators was addressed. As such a system needs to be implantable into the patient's body, there are considerable restrictions in terms of computational load and energy consumption. Considering these aspects, three seizure detection algorithms were proposed and their performance, as well as the required energy for their implementation in embedded systems, were estimated and compared. Results of the performance comparison showed that the RNN classifier outperforms the other classifiers. Comparison of the required energy using an energy model based on the respective numbers of specific AOs and MAs revealed that the RF classifier is the most efficient seizure detection algorithm, followed by the CNN and RNN. To evaluate the accuracy of the energy estimation of the seizure detection algorithms, the RNN classifier was implemented on an ultra-low-power microcontroller.

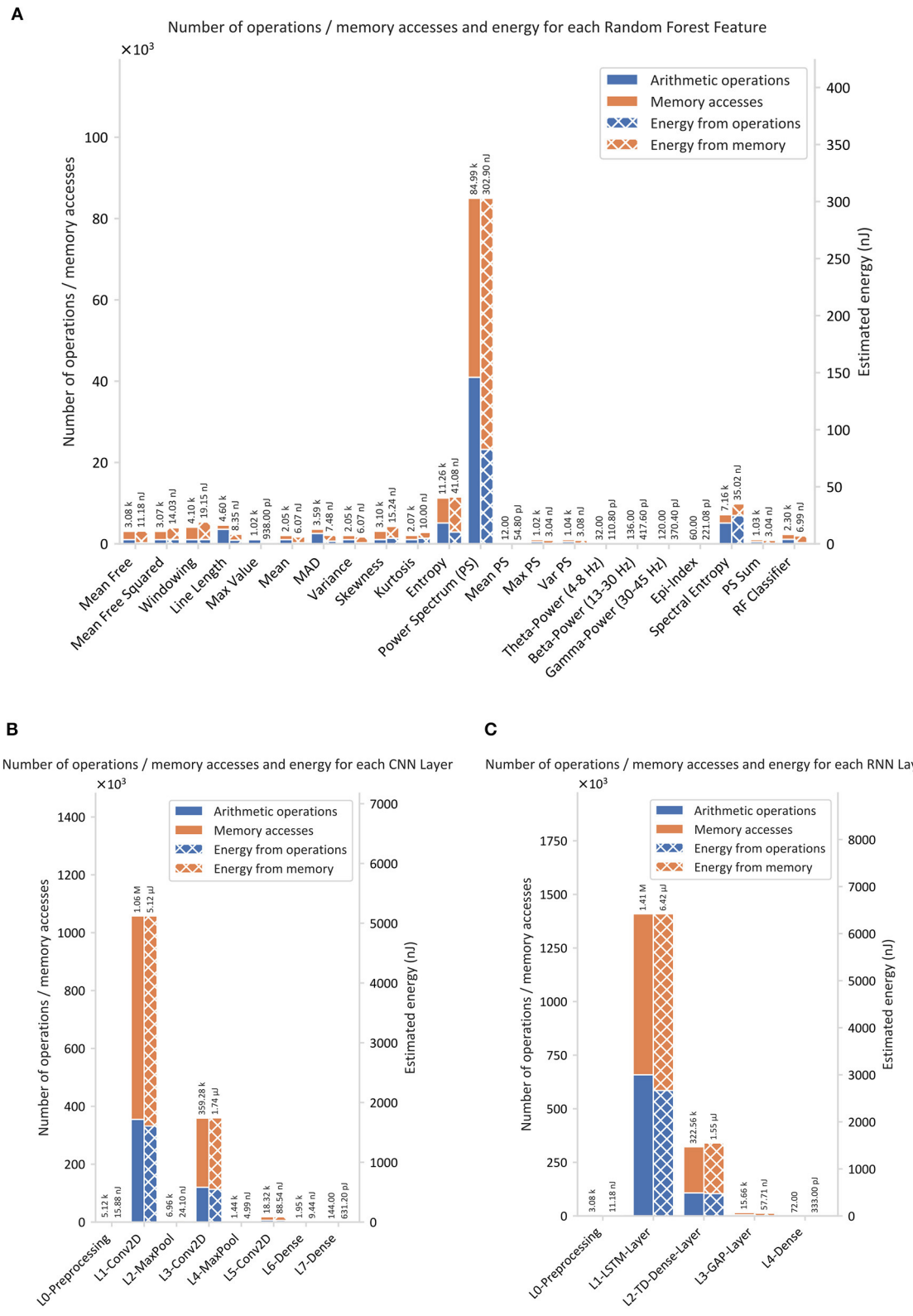

FIGURE 6 | Estimated number of arithmetic operations, memory accesses, and energy using the proposed method: **(A)** RF, **(B)** CNN, and **(C)** RNN.

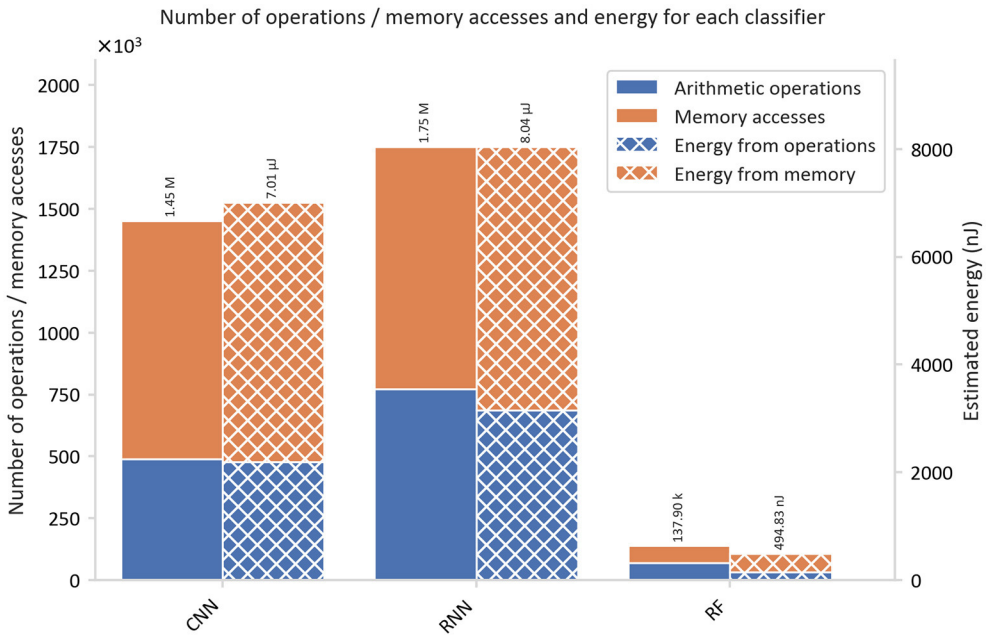

FIGURE 7 | Comparison of the classification energy consumption and the number of operations for the proposed seizure detection classifiers.

TABLE 6 | Estimated energies, number of arithmetic operations, and memory accesses for the CNN, RNN, and RF classifier.

Classifier	Energy (µJ)			Number of operations (×10³)	
	Total	Operations	Memory accesses	Arithmetic operations	Memory accesses
CNN	7.01	2.19	4.81	488	963
RNN	8.04	3.15	4.89	772	978
RF	0.495	0.147	0.348	68.4	69.5

The introduced energy estimation model showed good compliance with the energy measurements of the RNN implementation running on an ARM Cortex-M4F-based microcontroller. This notion was validated for the RNN classifier by a significant constant factor in the linear regression fit of the estimated energy with the measured energy over varying numbers of LSTM cells.

A comparison of energy consumption with the existing "RNS device" (Neuropace Inc., Mountain View, CA, USA) is difficult to perform, since detailed information about the energy consumption of the seizure detection algorithms are missing. Only a rough estimation on the basis of battery capacity and longevity for the whole system, including the required energy for stimulation, can be performed. The overall power for a patient profile with low stimulation frequency is ∼40 µW. Nevertheless, more detailed information is available for some other prototype devices. For example, a modified ActivaPC device from Medtronic (Minneapolis, Minnesota, USA), which was developed for bi-directional brain machine interfaces by Stanslaski et al. (47), offers 8 MB of RAM. It can operate in a time-domain mode, with a power consumption of 100 µW per channel and a spectral mode with a power consumption of 5 µW per channel. A simple classification stage offers a linear support vector machine with a typical power consumption of 5 µW per channel (47). This is comparable to the power consumption of the proposed models in this study based on RNN (68.1 µW per channel), CNN (60.8 µW estimated per channel), and RF (8.3 µW estimated per channel). An interesting comparison between local feature computation (2.1 µW) and external classification (43 µW) with radio transmission of the data (1,733 µW) for external processing is provided in a study by Verma et al. (48), which clearly favors the use of low-power processing on the edge device over transferring the data to a more powerful external device.

RNN classifiers were used for seizure detection in several recent studies. For example, Abbasi et al. (49) proposed a seizure detection algorithm in which an LSTM architecture with double-layered memory units was applied. They reported a sensitivity of 96.7% on the Bonn University dataset (49). Their proposed network consisted of 100 and 128 LSTM cells in the first and second layers, respectively, which results in a considerably higher computational load and a subsequent higher energy cost compared to the proposed architecture in this study. Similarly, Ahmedt-Aristizabal et al. (50) proposed a seizure detection algorithm based on the RNN-LSTM. They used an LSTM-NN architecture with two subsequent LSTM layers (128 and 64 cells) and obtained an AUC-ROC of 98.52% on the dataset from University of Bonn (50). In another study, Hussein et al. (43) introduced an LSTM architecture where raw EEG data in sequences of 23.6 s were passed on to a recurrent layer with 80

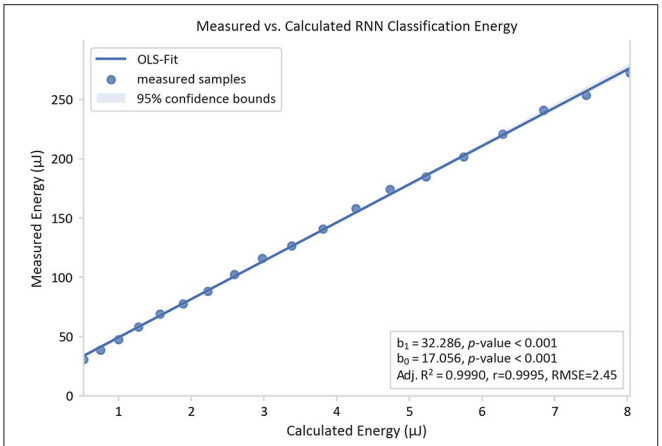

FIGURE 8 | Measured classification energy over the calculated energy and its linear regression curve. The energies are determined by measuring the energy of an RNN implementation on an Apollo 3 Blue ARM Cortex-M4F microcontroller unit under the variation of the number of LSTM cells from 2 to 20.

LSTM cells followed by a fully connected layer with 80 cells, a global average pooling layer and a 2-cell classification layer. They reported this methodology as having 100% accuracy, sensitivity, and specificity on the Bonn University dataset (43). As previously mentioned, the model proposed by Hussein et al. influenced the architecture of the RNN model described in the current study, which was modified to contain just one recurrent layer with 20 LSTM cells. This modification then renders the RNN model a better candidate for application in implantable devices. In addition, the use of a much more comprehensive dataset in the current study enables more precise performance evaluation.

Similar to the RNN, CNN and RF have been recently employed for seizure detection (51, 52). For example, Hugle et al. (53) proposed a CNN model for the early detection of seizures from intracranial EEG signals that was designed for implementation on a low-power microcontroller. They reported a median sensitivity level of 0.96, an FDR of 10.1 per hour, and a detection delay of 3.7 s. In comparison, the present study found median sensitivity level of 1, an FDR of 14.25 per hour, and a detection delay of 5.60 s. As there are differences in the signal characteristics of the applied dataset in these two studies, a direct comparison is not possible. In an earlier study from the current research group, Manzouri et al. (54) proposed a seizure detection algorithm based on RF for efficient hardware implementation in implantable devices. The proposed model was similar to that described in the current study, however; 10 features for classification were applied, and a median AUC-ROC score of 0.89 was obtained, compared to 0.93 in the present study. However, because a dataset of intracranial recordings which have a higher signal-to-noise ratio (55), was used in Manzouri et al. (54), a direct comparison of classifier performance with the present study is not possible.

Regarding power consumption, Liu and Richardson (56) implemented and compared the power consumption of a DNN, CNN, and LSTM-based model on the CHB-MIT database. The median (mean) sensitivity of the suggested DNN, CNN, and LSTM models were 0.857 (0.874), 1.00 (0.967), and 1.00 (0.976), respectively, compared to 1.0 (0.899) for RNN and 1.0 (0.940) for CNN in the present study. Although these values are similar between the two studies, they are not directly comparable due to the use of different datasets. By applying a sliding window-based weighted majority voting algorithm, Liu et al. reduced the FDR and reported values of 0.14 (0.169) 1/h for the DNN, 0.084 (0.102) 1/h for the CNN, and 0.063 (0.071) 1/h for the LSTM (56), all of which are lower than those of the current study. Although the deep learning models applied by Liu et al. showed high performance, they exceed the complexity of the seizure detection models proposed in the current study. The CNN model with the best performance-to-energy trade-off proposed by Liu et al. requires 2.4M MAC operations, whereas the proposed CNN model in the current study requires only 472k. The higher complexity results in a high demand for memory, inference time and power consumption.

Since the dataset used in the study is selected based on the geometry of the suggested subgaleal electrodes and is not yet publicly available, it is not possible to perform a one-to-one comparison with other studies that used public datasets such as the CHB-MIT Scalp EEG database (57) or the EPILEPSIAE database (58). Nevertheless, the results of this study allow a direct comparison between three state-of-the-art algorithms for such an electrode setup, which may have similar properties to future implantable devices. Sub-clinical seizures and their impact on seizure detection algorithm performance were not investigated in this study. Sub-clinical seizures are defined as electrographic seizures with rhythmic ictal discharges that evolve in frequency and space, without any subjective or objective alteration in behavior or consciousness (59). Indeed, the development of more robust seizure detectors may be facilitated by including sub-clinical seizures in the performance analysis of seizure detection algorithms. Another aspect to consider during the evaluation of seizure detection algorithms is the strong imbalance between ictal and inter-ictal classes. Evaluation of the proposed models over longer periods of recordings can provide a more realistic representation of the clinical performance of these models in long-term and ultra-long-term recordings.

Regarding energy estimation, the influence of the code compilation process on energy estimation was not investigated. However, incorporating this aspect into the analysis would give an overview of how different compiler settings influence the energy demand of the implemented algorithm.

Different hardware implementations of the seizure detection algorithms could be conceived by designing application-specific integrated circuits. For example, specialized hardware accelerators could be built to reduce the number of required MAs. In this case, the applicability of the model is limited. Besides, adjustment of the model is necessary because some neural network weights can be preserved in the hardware registers. As a result, less MA overhead is needed. However, the model helps to identify the aspects which are key to the design of ASICs. Moreover, it aids in selecting the right accelerator for the chosen algorithm.

How the energy consumption of the proposed classifiers can be further optimized will be investigated in future studies. One possibility for this is the application of pruning (22) or quantization techniques. The latter allows for the use of single-instruction multiple-data instructions to perform AOs on multiple data, instead of only two operands in a typical microprocessor setup. Horowitz (45) outlined how this method saves energy by decreasing the ratio of instruction overhead for the same number of AOs. He also suggested using integer calculations with small bit-widths to reduce energy consumption. The intensive use of single-instruction multiple-data for neural network applications was proposed by Lai et al. (60) by introducing the CMSIS-NN library from ARM Ltd. (Cambridge, England, UK). A more modern approach is the application of DNN-Accelerators. For microcontroller systems, one possibility was introduced by ARM with the Ethos neural processing unit. Among other things, they improved the memory access of network parameters, which showed significant improvement in inference, speed, and power consumption (61).

The proposed methodology for energy estimation in the current study can be used to verify both the suitability and applicability of the developed seizure detection models for implantable devices, and provides a reliable estimation. Furthermore, the three proposed models in this study are all candidates for utilization in implantable devices and can be selected based on the specific requirements, limitations, and application of the implantable device.

DATA AVAILABILITY STATEMENT

The original contributions presented in the study are included in the article/**Supplementary Material**. Further inquiries can be directed to the corresponding author.

ETHICS STATEMENT

The studies involving human participants were reviewed and approved by Ethics commission of the Albert-Ludwigs-Universität Freiburg, Germany. Written informed consent to participate in this study was provided by the participant or the participant's legal guardian/next of kin. Informed consent of the patient covered the in-house use of EEG recordings.

AUTHOR CONTRIBUTIONS

FM and MZ: writing, conceptualization, algorithm development, and implementation. SS: algorithm development and implementation. MD: conceptualization, data curation, and supervision. RM and LC: conceptualization and supervision. PW and AS-B: conceptualization, supervision, and funding acquisition. All authors contributed to the article and approved the submitted version.

ACKNOWLEDGMENTS

This work was supported by the BMBF, PIMIDES (Patienten Individualisierte Modulation und Intervention durch Epikraniale Stimulation) Project (Grant number: 13GW0269b) and Precisis AG, Heidelberg, Germany. Many thanks to Dr. Sandra Dieni who assisted with the editorial aspects of this work. The article processing charge was funded by the Baden-Württemberg Ministry of Science, Research and Art and the University of Freiburg in the funding programme Open Access Publishing.

SUPPLEMENTARY MATERIAL

The Supplementary Material for this article can be found online at: https://www.frontiersin.org/articles/10.3389/fneur.2021.703797/full#supplementary-material

REFERENCES

1. Sun FT, Morrell MJ. The RNS System: responsive cortical stimulation for the treatment of refractory partial epilepsy. *Expert Rev Med Devices.* (2014) 11:563–72. doi: 10.1586/17434440.2014.947274
2. Ngugi AK, Bottomley C, Kleinschmidt I, Sander JW, Newton CR. Estimation of the burden of active and life-time epilepsy: a meta-analytic approach. *Epilepsia.* (2010) 51:883–90. doi: 10.1111/j.1528-1167.2009.02481.x
3. Heck CN, King-Stephens D, Massey AD, Nair DR, Jobst BC, Barkley GL, et al. Two-year seizure reduction in adults with medically intractable partial onset epilepsy treated with responsive neurostimulation: final results of the RNS System Pivotal trial. *Epilepsia.* (2014) 55:432–41. doi: 10.1111/epi.12534
4. Bergey GK, Morrell MJ, Mizrahi EM, Goldman A, King-Stephens D, Nair D, et al. Long-term treatment with responsive brain stimulation in adults with refractory partial seizures. *Neurology.* (2015) 84:810–7. doi: 10.1212/WNL.0000000000001280
5. Geller EB, Skarpaas TL, Gross RE, Goodman RR, Barkley GL, Bazil CW, et al. Brain-responsive neurostimulation in patients with medically intractable mesial temporal lobe epilepsy. *Epilepsia.* (2017) 58:994–1004. doi: 10.1111/epi.13740
6. Jobst BC, Kapur R, Barkley GL, Bazil CW, Berg MJ, Bergey GK, et al. Brain-responsive neurostimulation in patients with medically intractable seizures arising from eloquent and other neocortical areas. *Epilepsia.* (2017) 58:1005–14. doi: 10.1111/epi.13739
7. Gotman J. Automatic recognition of epileptic seizures in the EEG. *Electroencephalogr Clin Neurophysiol.* (1982) 54:530–40. doi: 10.1016/0013-4694(82)90038-4
8. Mormann F, Andrzejak RG, Elger CE, Lehnertz K. Seizure prediction: the long and winding road. *Brain.* (2007) 130:314–33. doi: 10.1093/brain/awl241
9. Dümpelmann M. Early seizure detection for closed loop direct neurostimulation devices in epilepsy. *J Neural Eng.* (2019) 16:041001. doi: 10.1088/1741-2552/ab094a
10. Talathi S. Deep Recurrent Neural Networks for seizure detection and early seizure detection systems. *arXiv.* (2017) doi: 10.2172/1366924
11. Donos C, Dümpelmann M, Schulze-Bonhage A. Early seizure detection algorithm based on intracranial EEG and random forest classification. *Int J Neural Syst.* (2015) 25:1550023. doi: 10.1142/S0129065715500239
12. Meier R, Dittrich H, Schulze-Bonhage A, Aertsen A. Detecting epileptic seizures in long-term human EEG: a new approach to automatic online and real-time detection and classification of polymorphic seizure patterns. *J Clin Neurophysiol.* (2008) 25:119–31. doi: 10.1097/WNP.0b013e3181775993
13. Ramgopal S, Thome-Souza S, Jackson M, Kadish NE, Sánchez Fernández I, Klehm J, et al. Seizure detection, seizure prediction,

and closed-loop warning systems in epilepsy. *Epilepsy Behav.* (2014) 37:291–307. doi: 10.1016/j.yebeh.2014.06.023
14. Baumgartner C, Koren JP. Seizure detection using scalp-EEG. *Epilepsia.* (2018) 59:14–22. doi: 10.1111/epi.14052
15. Baumgartner C, Koren JP, Rothmayer M. Automatic computer-based detection of epileptic seizures. *Front Neurol.* (2018) 9:639. doi: 10.3389/fneur.2018.00639
16. Qaraqe M, Ismail M, Serpedin E, Zulfi H. Epileptic seizure onset detection based on EEG and ECG data fusion. *Epilepsy Behav.* (2016) 58:48–60. doi: 10.1016/j.yebeh.2016.02.039
17. Herta J, Koren J, Fürbass F, Hartmann M, Gruber A, Baumgartner C. Reduced electrode arrays for the automated detection of rhythmic and periodic patterns in the intensive care unit: frequently tried, frequently failed? *Clin Neurophysiol.* (2017) 128:1524–31. doi: 10.1016/j.clinph.2017.04.012
18. Cogan D, Birjandtalab J, Nourani M, Harvey J, Nagaraddi V. Multi-Biosignal analysis for epileptic seizure monitoring. *Int J Neural Syst.* (2017) 27:1650031. doi: 10.1142/S0129065716500313
19. Vandecasteele K, De Cooman T, Dan J, Cleeren E, Van Huffel S, Hunyadi B, et al. Visual seizure annotation and automated seizure detection using behind-the-ear electroencephalographic channels. *Epilepsia.* (2020) 61:766–75. doi: 10.1111/epi.16470
20. Dan J, Vandendriessche B, Van Paesschen W, Weckhuysen D, Bertrand A, Van Paesschen W, et al. Computationally-efficient algorithm for real-time absence seizure detection in wearable electroencephalography. *Int J Neural Syst.* (2020) 30:2050035. doi: 10.1142/S0129065720500355
21. García-Martín E, Rodrigues CF, Riley G, Grahn H. Estimation of energy consumption in machine learning. *J Parallel Distrib Comput.* (2019) 134:75–88. doi: 10.1016/j.jpdc.2019.07.007
22. Rouhani BD, Mirhoseini A, Koushanfar F. DeLight: adding energy dimension to deep neural networks. In: *Proceedings of the International Symposium on Low Power Electronics and Design.* New York, NY: ACM (2016). p. 112–17.
23. Taghavi M, Shoaran M. Hardware complexity analysis of deep neural networks and decision tree ensembles for real-time neural data classification. In: *International IEEE/EMBS Conference on Neural Engineering, NER.* San Francisco, CA: IEEE Computer Society (2019). p. 407–10.
24. Yang TJ, Chen YH, Sze V. Designing energy-efficient convolutional neural networks using energy-aware pruning. In: *Proceedings - 30th IEEE Conference on Computer Vision and Pattern Recognition, CVPR 2017.* Honolulu, HI: Institute of Electrical and Electronics Engineers Inc. (2016). p. 6071–9.
25. Duun-Henriksen J, Kjaer TW, Looney D, Atkins MD, Sørensen JA, Rose M, et al. signal quality of a subcutaneous recording system compared to standard surface electrodes. *J Sensors.* (2015) 2015:1–9. doi: 10.1155/2015/341208
26. Weisdorf S, Gangstad SW, Duun-Henriksen J, Mosholt KSS, Kjær TW. High similarity between EEG from subcutaneous and proximate scalp electrodes in patients with temporal lobe epilepsy. *J Neurophysiol.* (2018) 120:1451–60. doi: 10.1152/jn.00320.2018
27. Oostenveld R, Praamstra P. The five percent electrode system for high-resolution EEG and ERP measurements. *Clin Neurophysiol.* (2001) 112:713–9. doi: 10.1016/S1388-2457(00)00527-7
28. Goncharova II, McFarland DJ, Vaughan TM, Wolpaw JR. EMG contamination of EEG: spectral and topographical characteristics. *Clin Neurophysiol.* (2003) 114:1580–93. doi: 10.1016/S1388-2457(03)00093-2
29. Aurlien H, Gjerde IO, Aarseth JH, Eldøen G, Karlsen B, Skeidsvoll H, et al. background activity described by a large computerized database. *Clin Neurophysiol.* (2004) 115:665–73. doi: 10.1016/j.clinph.2003.10.019
30. Aanestad E, Gilhus NE, Brogger J. Interictal epileptiform discharges vary across age groups. *Clin Neurophysiol.* (2020) 131:25–33. doi: 10.1016/j.clinph.2019.09.017
31. Breiman L. Random forests. *Mach Learn.* (2001) 45:5–32. doi: 10.1023/A:1010933404324
32. Liaw A, Wiener M. Classification and regression by randomForest. *Newsl R Proj News.* (2002) 2/3:18–22.
33. Bartolomei F, Chauvel P, Wendling F. Epileptogenicity of brain structures in human temporal lobe epilepsy: a quantified study from intracerebral EEG. *Brain.* (2008) 131:1818–30. doi: 10.1093/brain/awn111
34. Varoquaux G, Buitinck L, Louppe G, Grisel O, Pedregosa F, Mueller A. Scikit-learn. *GetMobile Mob Comput Commun.* (2015) 19:29–33. doi: 10.1145/2786984.2786995
35. Fukushima K. Neocognitron: a self-organizing neural network model for a mechanism of pattern recognition unaffected by shift in position. *Biol Cybern.* (1980) 36:193–202. doi: 10.1007/BF00344251
36. Valueva MV, Nagornov NN, Lyakhov PA, Valuev GV, Chervyakov NI. Application of the residue number system to reduce hardware costs of the convolutional neural network implementation. *Math Comput Simul.* (2020) 177:232–43. doi: 10.1016/j.matcom.2020.04.031
37. Ioffe S, Szegedy C. *Batch Normalization: Accelerating Deep Network Training by Reducing Internal Covariate Shift*. PMLR (2015). Available online at: http://proceedings.mlr.press/v37/ioffe15.html (accessed April 14, 2021).
38. Hugle M, Heller S, Watter M, Blum M, Manzouri F, Dumpelmann M, et al. Early seizure detection with an energy-efficient convolutional neural network on an implantable microcontroller. In: *Proceedings of the International Joint Conference on Neural Networks*. Rio de Janeiro (2018).
39. King G, Zeng L. Logistic regression in rare events data. *Polit Anal.* (2001) 9:137–63. doi: 10.1093/oxfordjournals.pan.a004868
40. Kingma DP, Ba JL. Adam: a method for stochastic optimization. In: *3rd International Conference on Learning Representations, ICLR 2015 - Conference Track Proceedings.* (2014). Available online at: http://arxiv.org/abs/1412.6980 (accessed November 13, 2020).
41. Hochreiter S, Schmidhuber J. Long short-term memory. *Neural Comput.* (1997) 9:1735–80. doi: 10.1162/neco.1997.9.8.1735
42. Van Houdt G, Mosquera C, Nápoles G. A review on the long short-term memory model. *Artif Intell Rev.* (2020) 53:5929–55. doi: 10.1007/s10462-020-09838-1
43. Hussein R, Palangi H, Wang ZJ, Ward R. Robust detection of epileptic seizures using deep neural networks. In: *ICASSP, IEEE International Conference on Acoustics, Speech and Signal Processing – Proceedings.* Calgary, AB: Institute of Electrical and Electronics Engineers Inc. (2018). p. 2546–50.
44. Prechelt L. Automatic early stopping using cross validation: quantifying the criteria. *Neural Networks.* (1998) 11:761–7. doi: 10.1016/S0893-6080(98)00010-0
45. Horowitz M. 1.1 Computing's energy problem (and what we can do about it). In: *Digest of Technical Papers - IEEE International Solid-State Circuits Conference.* San Francisco, CA (2014). p. 10–14.
46. Seabold S, Perktold J. *Statsmodels: Econometric and Statistical Modeling With Python.* (2010). Available online at: http://statsmodels.sourceforge.net/ (accessed April 9, 2021).
47. Stanslaski S, Afshar P, Cong P, Giftakis J, Stypulkowski P, Carlson D, et al. Design and validation of a fully implantable, chronic, closed-loop neuromodulation device with concurrent sensing and stimulation. *IEEE Trans Neural Syst Rehabil Eng.* (2012) 20:410–21. doi: 10.1109/TNSRE.2012.2183617
48. Verma N, Shoeb A, Bohorquez J, Dawson J, Guttag J, Chandrakasan AP, et al. micro-power EEG acquisition SoC with integrated feature extraction processor for a chronic seizure detection system. *IEEE J Solid State Circuits.* (2010) 45:804–16. doi: 10.1109/JSSC.2010.2042245
49. Abbasi MU, Rashad A, Basalamah A, Tariq M. Detection of epilepsy seizures in neo-natal EEG using LSTM architecture. *IEEE Access.* (2019) 7:179074–85. doi: 10.1109/ACCESS.2019.2959234
50. Ahmedt-Aristizabal D, Fookes C, Nguyen K, Sridharan S. Deep classification of epileptic signals. In: *Proceedings of the Annual International Conference of the IEEE Engineering in Medicine and Biology Society, EMBS.* Honolulu, HI: Institute of Electrical and Electronics Engineers Inc. (2018). p. 332–5.
51. Baldassano SN, Brinkmann BH, Ung H, Blevins T, Conrad EC, Leyde K, et al. Crowdsourcing seizure detection: algorithm development and validation on human implanted device recordings. *Brain.* (2017) 140:1680–91. doi: 10.1093/brain/awx098
52. Shoeibi A, Khodatars M, Ghassemi N, Jafari M, Moridian P, Alizadehsani R, et al. Epileptic seizures detection using deep learning techniques: a review. *Int J Environ Res Public Heal.* (2021) 18:5780. doi: 10.3390/ijerph18115780
53. Hugle M, Heller S, Watter M, Blum M, Manzouri F, Dumpelmann M, et al. Early seizure detection with an energy-efficient convolutional neural network on an implantable microcontroller. In: *2018 International Joint Conference on Neural Networks (IJCNN).* Rio de Janeiro: IEEE (2018). p. 1–7.
54. Manzouri F, Heller S, Dümpelmann M, Woias P, Schulze-Bonhage A. A Comparison of machine learning classifiers for energy-efficient implementation of seizure detection. *Front Syst Neurosci.* (2018) 12:1–11. doi: 10.3389/fnsys.2018.00043

55. Ball T, Kern M, Mutschler I, Aertsen A, Schulze-Bonhage A. Signal quality of simultaneously recorded invasive and non-invasive EEG. *Neuroimage.* (2009) 46:708–16. doi: 10.1016/j.neuroimage.2009.02.028
56. Liu X, Richardson AG. Edge deep learning for neural implants: a case study of seizure detection and prediction. *J Neural Eng.* (2021) 18:046034. doi: 10.1088/1741-2552/abf473
57. Shoeb A, Edwards H, Connolly J, Bourgeois B, Ted Treves S, Guttag J. Patient-specific seizure onset detection. *Epilepsy Behav.* (2004) 5:483–98. doi: 10.1016/j.yebeh.2004.05.005
58. Klatt J, Feldwisch-Drentrup H, Ihle M, Navarro V, Neufang M, Teixeira C, et al. The EPILEPSIAE database: an extensive electroencephalography database of epilepsy patients. *Epilepsia.* (2012) 53:1669–76. doi: 10.1111/j.1528-1167.2012.03564.x
59. Sperling MR, O'Connor MJ. Auras and subclinical seizures: characteristics and prognostic significance. *Ann Neurol.* (1990) 28:320–8. doi: 10.1002/ana.410280304
60. Lai L, Suda N, Chandra V. CMSIS-NN: Efficient Neural Network Kernels for Arm Cortex-M CPUs. *ArXiv* (2018), abs/1801.06601.
61. Skillman A, Edso T. A technical overview of cortex-M55 and ethos-U55: arm's most capable processors for endpoint AI. In: *2020 IEEE Hot Chips 32 Symposium, HCS 2020.* Palo Alto, CA: Institute of Electrical and Electronics Engineers Inc. (2020) p. 1–20.

Conflict of Interest: The authors declare that the research was conducted in the absence of any commercial or financial relationships that could be construed as a potential conflict of interest.

Publisher's Note: All claims expressed in this article are solely those of the authors and do not necessarily represent those of their affiliated organizations, or those of the publisher, the editors and the reviewers. Any product that may be evaluated in this article, or claim that may be made by its manufacturer, is not guaranteed or endorsed by the publisher.

Advantages of publishing in Frontiers

OPEN ACCESS
Articles are free to read for greatest visibility and readership

FAST PUBLICATION
Around 90 days from submission to decision

HIGH QUALITY PEER-REVIEW
Rigorous, collaborative, and constructive peer-review

TRANSPARENT PEER-REVIEW
Editors and reviewers acknowledged by name on published articles

Frontiers
Avenue du Tribunal-Fédéral 34
1005 Lausanne | Switzerland

Visit us: www.frontiersin.org
Contact us: frontiersin.org/about/contact

REPRODUCIBILITY OF RESEARCH
Support open data and methods to enhance research reproducibility

DIGITAL PUBLISHING
Articles designed for optimal readership across devices

FOLLOW US
@frontiersin

IMPACT METRICS
Advanced article metrics track visibility across digital media

EXTENSIVE PROMOTION
Marketing and promotion of impactful research

LOOP RESEARCH NETWORK
Our network increases your article's readership